METHODS AND APPLICATION IN CARDIOVASCULAR AND SMOOTH MUSCLE PHARMACOLOGY: 2021

EDITED BY: Ahmed F. El-Yazbi, Khaled S. Abd-Elrahman, Ali H. Eid, Fouad Antoine Zouein and Asad Zeidan

PUBLISHED IN: Frontiers in Pharmacology

frontiers Research Topics

frontiers

ISSN 1664-8714
ISBN 978-2-83250-703-2
DOI 10.3389/978-2-83250-703-2

About Frontiers

Frontiers is more than just an open-access publisher of scholarly articles: it is a pioneering approach to the world of academia, radically improving the way scholarly research is managed. The grand vision of Frontiers is a world where all people have an equal opportunity to seek, share and generate knowledge. Frontiers provides immediate and permanent online open access to all its publications, but this alone is not enough to realize our grand goals.

Frontiers Journal Series

The Frontiers Journal Series is a multi-tier and interdisciplinary set of open-access, online journals, promising a paradigm shift from the current review, selection and dissemination processes in academic publishing. All Frontiers journals are driven by researchers for researchers; therefore, they constitute a service to the scholarly community. At the same time, the Frontiers Journal Series operates on a revolutionary invention, the tiered publishing system, initially addressing specific communities of scholars, and gradually climbing up to broader public understanding, thus serving the interests of the lay society, too.

Dedication to Quality

Each Frontiers article is a landmark of the highest quality, thanks to genuinely collaborative interactions between authors and review editors, who include some of the world's best academicians. Research must be certified by peers before entering a stream of knowledge that may eventually reach the public - and shape society; therefore, Frontiers only applies the most rigorous and unbiased reviews.
Frontiers revolutionizes research publishing by freely delivering the most outstanding research, evaluated with no bias from both the academic and social point of view. By applying the most advanced information technologies, Frontiers is catapulting scholarly publishing into a new generation.

What are Frontiers Research Topics?

Frontiers Research Topics are very popular trademarks of the Frontiers Journals Series: they are collections of at least ten articles, all centered on a particular subject. With their unique mix of varied contributions from Original Research to Review Articles, Frontiers Research Topics unify the most influential researchers, the latest key findings and historical advances in a hot research area! Find out more on how to host your own Frontiers Research Topic or contribute to one as an author by contacting the Frontiers Editorial Office: frontiersin.org/about/contact

METHODS AND APPLICATION IN CARDIOVASCULAR AND SMOOTH MUSCLE PHARMACOLOGY: 2021

Topic Editors:
Ahmed F. El-Yazbi, Alexandria University, Egypt
Khaled S. Abd-Elrahman, University of Ottawa, Canada
Ali H. Eid, Qatar University, Qatar
Fouad Antoine Zouein, American University of Beirut, Lebanon
Asad Zeidan, American University of Beirut, Lebanon

Citation: El-Yazbi, A. F., Abd-Elrahman, K. S., Eid, A. H., Zouein, F. A., Zeidan, A., eds. (2022). Methods and Application in Cardiovascular and Smooth Muscle Pharmacology: 2021. Lausanne: Frontiers Media SA.
doi: 10.3389/978-2-83250-703-2

Table of Contents

frontiers | Frontiers in Pharmacology

TYPE Editorial
PUBLISHED 21 October 2022
DOI 10.3389/fphar.2022.1049022

OPEN ACCESS

EDITED AND REVIEWED BY
Alessandro Cannavo,
University of Naples Federico II, Italy

*CORRESPONDENCE
Ahmed F. El-Yazbi,
ahmed.fawzy.aly@alexu.edu.eg

SPECIALTY SECTION
This article was submitted to Cardiovascular and Smooth Muscle Pharmacology, a section of the journal Frontiers in Pharmacology

RECEIVED 20 September 2022
ACCEPTED 10 October 2022
PUBLISHED 21 October 2022

CITATION
El-Yazbi AF, Eid AH, Zouein FA and Abd-Elrahman KS (2022), Editorial: Methods and application in cardiovascular and smooth muscle pharmacology: 2021.
Front. Pharmacol. 13:1049022.
doi: 10.3389/fphar.2022.1049022

Editorial: Methods and application in cardiovascular and smooth muscle pharmacology: 2021

Ahmed F. El-Yazbi[1,2]*, Ali H. Eid[3], Fouad A. Zouein[4,5,6,7] and Khaled S. Abd-Elrahman[1,8,9]

[1]Department of Pharmacology and Toxicology, Faculty of Pharmacy, Alexandria University, Alexandria, Egypt, [2]Faculty of Pharmacy, Alamein International University, Al Alamein, Egypt, [3]Department of Basic Medical Sciences, College of Medicine, QU Health, Qatar University, Doha, Qatar, [4]Department of Pharmacology and Toxicology, Faculty of Medicine, American University of Beirut, Beirut, Lebanon, [5]Department of Signaling and Cardiovascular Pathophysiology, UMR-S 1180, Inserm, Université Paris-Saclay, Paris-Saclay, France, [6]The Cardiovascular Renal and Metabolic Diseases Research Center of Excellence, American University of Beirut Medical Center, Beirut, Lebanon, [7]Department of Pharmacology and Toxicology, School of Medicine, University of Mississippi Medical Center, Jackson, MS, United States, [8]Department of Cellular and Molecular Medicine, Faculty of Medicine, University of Ottawa, Ottawa, ON, Canada, [9]Department of Pharmacology and Therapeutics, College of Medicine and Health Sciences, Khalifa University, Abu Dhabi, United Arab Emirates

KEYWORDS

cardiovasclar disease, biomarkers, natural products, biomedical research, disease outcome

Editorial on the Research Topic
Methods and application in cardiovascular and smooth muscle pharmacology: 2021

Despite significant advances in basic, translational, and clinical research tackling heart disease, cardiovascular pathologies remain among the leading causes of mortality and morbidity worldwide, being responsible for one-third of global deaths as estimated by the WHO (Organization, 2021). The complexity of risk factors and pathways underlying the development of cardiovascular disorders (CVDs) limits the efficacy of a given therapeutic intervention and necessitates combined pharmacological approaches, as well as lifestyle modification to provide a reasonable health impact (Arnett et al., 2019). Be that as it may, there remains a considerable room for scientific inquiry in pursuit of novel and more refined avenues to prevent, diagnose, mitigate, and reverse different forms of cardiovascular ailment, as well as optimize patient management. Indeed, such a need for research in this field was even further emphasized as the world faced heightened health challenges during the COVID-19 pandemic with cardiovascular complications being among the most serious consequences of SARS-CoV-2 infection (Wehbe et al., 2020).

In the current Research Topic in Frontiers in Pharmacology, we aimed to shed light on the latest experimental techniques and methods used to investigate fundamental questions in Cardiovascular and Smooth Muscle Pharmacology. The topic features several

articles that span the spectrum of cardiovascular research from natural product and drug action, including their underlying mechanisms in functional disorders of the heart and blood vessels, to mathematical and machine learning models for diagnosis and prediction of therapy outcomes of CVDs. The article assortment also includes discussion of cutting-edge research on diagnostic markers, therapeutic targets, and treatment technologies.

Indeed, natural product pharmacology received significant attention in this topic. Chen et al. explored the potential mechanism of polydatin glycosides on pulmonary hypertension by modulating endothelial-to-mesenchymal transition. In related studies, Zhao et al. and Deng et al. investigated the effect of astragaloside and nuciferine, the principal component of Lotus leaf extract, on the chronic intermittent hypoxia-induced endothelial dysfunction and endothelium-dependent vasodilation, respectively. Along the same lines, Shao et al. provide an in-depth discussion of the protective and therapeutic effect of Taohong Siwu on ischemic myocardial injury. On the other hand, small molecule drug pharmacology was also tackled in this issue, where Mustafa et al. review the available data describing the molecular pathways underlying the impact of sacubitril/valsartan on cardiac remodeling in heart failure. On the same premise, Yuan et al. propose gut microbiota as a target for the modulation of diabetic cardiomyopathy.

From a different perspective, Fares et al. offer new insight on the role mathematical processing of heart rate and blood pressure signals as predictors of early cardiovascular dysfunction associated with metabolic disease. Relatedly, in their study, Jia et al. explored the clinical implications and the sex differences in the role of circulating PCSK-9 in the development of atherosclerosis and as a biomarker for the severity of cardiovascular and metabolic disease. Significantly, the current topic is not lacking in contributions addressing advances in biomedical technology. Whereas Marei et al. highlight recent innovations in strategies for biofunctionalization of stents to reduce stent thrombosis in diabetes, Dai et al. explored the use of internet-based medical services and machine learning models to improve clinical outcomes of anticoagulant therapy. In the review article by Marei et al., the authors discuss how thrombosis is one of the leading causes of stent failure in patients undergoing percutaneous coronary intervention (PCI). Stent thrombosis is primarily caused by impaired endothelialization of the stent lumen. Marei et al. discuss the mounting evidence supporting the use of circulating endothelial progenitor cells as a potential source for *in situ* endothelialization to prevent thrombosis and stent failure. This approach can have major implications in the treatment of coronary artery disease especially in type 2 diabetic patients who often presents with suboptimal outcomes following PCI or revascularization. Together, this research topic features novel developments in predicting cardiovascular dysfunction and provides insights into innovative interventions to alleviate cardiovascular insults that can pave the way for better diagnostic and therapeutic tools for CVDs.

Author contributions

AE-Y wrote the first draft of the manuscript. All authors contributed to the review and editing. All authors have read the manuscript and agree to the content.

Conflict of interest

The authors declare that the research was conducted in the absence of any commercial or financial relationships that could be construed as a potential conflict of interest.

Publisher's note

Reference

Arnett, D. K., Blumenthal, R. S., Albert, M. A., Buroker, A. B., Goldberger, Z. D., Hahn, E. J., et al. (2019). 2019 ACC/AHA guideline on the primary prevention of cardiovascular disease: A report of the American college of cardiology/American heart association task force on clinical practice guidelines. *Circulation* 140 (11), e596–e646. doi:10.1161/CIR.0000000000000678

Organization, W. H. (2021). *Cardiovascular diseases fact sheet*. Available at: https://www.who.int/news-room/fact-sheets/detail/cardiovascular-diseases-(cvds)#:~:text=Key%20facts,to%20heart%20attack%20and%20stroke.

Wehbe, Z., Hammoud, S., Soudani, N., Zaraket, H., El-Yazbi, A., and Eid, A. H. (2020). Molecular insights into SARS COV-2 interaction with cardiovascular disease: Role of RAAS and MAPK signaling. *Front. Pharmacol.* 11, 836. doi:10.3389/fphar.2020.00836

frontiers in Pharmacology

REVIEW
published: 26 January 2022
doi: 10.3389/fphar.2022.816347

Effects and Mechanisms of Taohong Siwu Decoction on the Prevention and Treatment of Myocardial Injury

Chang-Le Shao[1,2], *Guo-Hong Cui*[3]* and *Hai-Dong Guo*[1,2]*

[1]Academy of Integrative Medicine, Shanghai University of Traditional Chinese Medicine, Shanghai, China, [2]Department of Anatomy, School of Basic Medicine, Shanghai University of Traditional Chinese Medicine, Shanghai, China, [3]Department of Neurology, Shanghai No. 9 People's Hospital, Shanghai Jiaotong University School of Medicine, Shanghai, China

Taohong Siwu decoction (THSWD) is one of the classic prescriptions for promoting blood circulation and removing blood stasis. With the continuous in-depth excavation in basic and clinical research, it has been found that THSWD has made greater progress in the prevention and treatment of cardiovascular diseases. Mechanisms of the current studies have shown that it could prevent and treat the myocardial injury by inhibiting inflammatory reaction, antioxidant stress, inhibiting platelet aggregation, prolonging clotting time, anti-fibrosis, reducing blood lipids, anti-atherosclerosis, improving hemorheology and vascular pathological changes, regulating related signal pathways and other mechanisms to prevent and treat the myocardial injury, so as to protect cardiomyocytes and improve cardiac function. Many clinical studies have shown that THSWD is effective in the prevention and treatment of cardiovascular diseases related to myocardial injuries, such as coronary heart disease angina pectoris (CHD-AP), and myocardial infarction. In clinical practice, it is often used by adding and subtracting prescriptions, the combination of compound prescriptions and combinations of chemicals and so on. However, there are some limitations and uncertainties in both basic and clinical research of prescriptions. According to the current research, although the molecular biological mechanism of various active ingredients needs to be further clarified, and the composition and dose of the drug have not been standardized and quantified, this study still has exploration for scientific research and clinical practice. Therefore, this review mainly discusses the basic mechanisms and clinical applications of THSWD in the prevention and treatment of the myocardial injury caused by CHD-AP and myocardial infarction. The authors hope to provide valuable ideas and references for researchers and clinicians.

Keywords: taohong siwu decoction, cardiovascular diseases, myocardial injury, cardiomyocytes protection, mechanisms and applications

OPEN ACCESS

Edited by:
Ali H. Eid,
Qatar University, Qatar

Reviewed by:
Guosheng Cao,
Hubei University of Chinese Medicine, China
Yuanli Chen,
Hefei University of Technology, China

***Correspondence:**
Guo-Hong Cui
gh_cui@qq.com
Hai-Dong Guo
hdguo@shutcm.edu.cn

Specialty section:
This article was submitted to Cardiovascular and Smooth Muscle Pharmacology, a section of the journal Frontiers in Pharmacology

Received: *16 November 2021*
Accepted: *10 January 2022*
Published: *26 January 2022*

Citation:
Shao C-L, Cui G-H and Guo H-D (2022) Effects and Mechanisms of Taohong Siwu Decoction on the Prevention and Treatment of Myocardial Injury. Front. Pharmacol. 13:816347. doi: 10.3389/fphar.2022.816347

INTRODUCTION

Due to the change of people's lifestyle and the improvement of living standards, the incidence of metabolic diseases, cardiovascular diseases and many other diseases is gradually increasing and showing a trend of youthfulness. Among them, cardiovascular diseases is the number one killer endangering human life and health (Chen and Gao, 2016; Benjamin et al., 2018). Myocardial injury (MI) can be caused by a variety of causes, resulting in the occurrence and development of

many diseases, among which coronary heart disease angina pectoris (CHD-AP) and myocardial ischemia-reperfusion injury (MIRI) are the most common cardiovascular diseases leading to MI in clinical practice.

A series of traumatic changes such as myocardial ultrastructure, energy metabolism, cardiac function and electrophysiology caused by MIRI during ischemia are more prominent after vascular recanalization (Kalogeris et al., 2012; Kalogeris et al., 2016), and severe arrhythmias can lead to sudden death. At present, it is considered that the mechanisms of MIRI are mainly related to the production of a large number of oxygen free radicals, calcium overload, leukocyte inflammation and the lack of high-energy phosphate compounds (Sanada et al., 2011; Raedschelders et al., 2012; Jennings, 2013; Xu, 2014; Wang and Zhang, 2018; Xia and Dong, 2019; Gao et al., 2020). Coronary heart disease (CHD, coronary atherosclerotic heart disease) is a heart disease caused by myocardial ischemia, hypoxia and even necrosis (Kachur et al., 2017). CHD is a common and frequently-occurring disease among the middle and old aged people. However, its incidence is getting younger in recent years, which seriously threatens to human health and life. With the development of atherosclerotic plaque of CHD, the coronary artery will be blocked gradually, resulting in decline of cardiac functions, adaptive changes and even damage of cardiomyocytes. Moreover, stable angina pectoris (SAP) is easy to develop into unstable angina pectoris (UAP) and acute myocardial infarction clinically (Tegn et al., 2016).

Chinese medicine (CM) is a valuable natural resource in China's drug inventory. Its multi-component, multi-pathway and multi-target characteristics have shown unique advantages in the prevention and treatment of MI (Li et al., 2021). Although the chemical composition of CM is very complex (there may be dozens or even hundreds of kinds), their characteristic is the material basis of its effect on the prevention and treatment of diseases (Zhang and Li, 2015). Under the guidance of the holistic concept of Traditional Chinese Medicine (TCM), the comprehensive pharmacological effects of multi-pathways and multi-targets shown by the effective components of CM (Jiang and Gao, 2018), correspond to the occurrence mechanism of the disease to a certain extent. CM can improve multiple links of myocardial ischemic injury and reperfusion injury at the same time, as well as protect undamaged tissues, which is the greatest advantage of TCM in the prevention and treatment of cardiovascular disease. In addition, CM and its compound prescription also have the characteristics of outstanding curative effect, small side effect, good economy and low cost, which provides the possibility for the popularization, standardization and internationalization of TCM. This review mainly discusses the basic mechanisms and clinical applications of Taohong Siwu decoction in the prevention and treatment of MI caused by CHD-AP and myocardial infarction, hoping to provide valuable ideas and references for researchers and clinicians.

TAOHONG SIWU DECOCTION

Taohong Siwu decoction (THSWD) was initially used exclusively as a basic prescription for gynecological menstruation regulation, then gradually expanded to other clinical treatments (**Figure 1**). Now it is widely used in internal medicine, surgery, gynecology, pediatrics, ophthalmology, otorhinolaryngology, and other clinical departments (Nie and Cheng, 2020). It can prevent and treat CHD-AP, myocardial infarction, stroke, migraine, epilepsy, chronic glomerulonephritis, diabetic peripheral neuropathy, functional uterine bleeding, dysmenorrhea, female climacteric syndrome, thromboangiitis obliterans, pediatric thrombocytopenic purpura, urticaria, fundus hemorrhage and other cardiovascular diseases, cerebral and renal vascular, blood and neurological diseases (Lian and Qin, 2010; Zhang and Peng, 2011; Zhang, 2014a; Deng, 2021).

THSWD, also known as Jiawei Siwu decoction, as one of the classic prescriptions for promoting blood circulation and nourishing blood, comes from the Heart Tips of Yizong Jinjian Gynecology (Volume 44) written by Wu Qian (Qing Dynasty) (Qian, 1980). The original article states that "if there are many lumps of blood, purple and sticky, there is blood stasis inside, with Siwu decoction (*Chuanxiong Rhizoma, Angelicae sinensis radix, Paeoniae radix alba, Rehmanniae radix praeparata*) plus *Persicae semen, Carthami flos* broken, which is called Taohong Siwu Decoction." Modern pharmacological studies have shown that many active ingredients in THSWD have the effects of anti-inflammation (Mao, 2016; Liu, 2019a), improving hemorheology and microcirculation (Xie and Luo, 2008; Yi and Peng, 2011), reducing blood lipids, anti-atherosclerosis (Zhou, 2003; Xie and Luo, 2008), anti-myocardial ischemia, improving cardiac function, relaxing blood vessels, and inhibiting platelet aggregation (Han et al., 2010; Han and Peng, 2010), prolonging clotting time, anti-fibrosis (Tan et al., 2021), anti-hypoxia, anti-oxidation (Luo et al., 2019), anti-aging, anti-tumor, immunomodulatory, anti-fatigue (Li et al., 2012), anti-shock, anti-allergy, and supplement of trace elements (Wu, 2011; Zhang and Wang, 2011; Li and Guo, 2016; Wang, 2021; Xiang and Shi, 2021). The general clinical dosage of THSWD is 5–10 g *Persicae semen*, 3–10 g *Carthami flos*, 3–10 g *Chuanxiong Rhizoma*, 6–12 g *Angelicae sinensis radix*, 6–15 g *Paeoniae radix alba*, and 9–15 g *Rehmanniae radix praeparata* (Chinese Pharmacopoeia Commission, 2015; Ji and Lian, 2016; Gao and Zhang, 2017), but the specific dosage of medicinal ingredients needs to be determined according to specific symptoms of the disease (**Figure 1**).

MECHANISMS OF TAOHONG SIWU DECOCTION IN PREVENTION AND TREATMENT OF MI

The mechanisms of THSWD in prevention and treatment of MI inluding anti-inflammation, anti-oxidation, improving hemorheology and vascular pathology, anti-fibrosis, reducing blood lipids and anti-atherosclerosis, inhibiting platelet

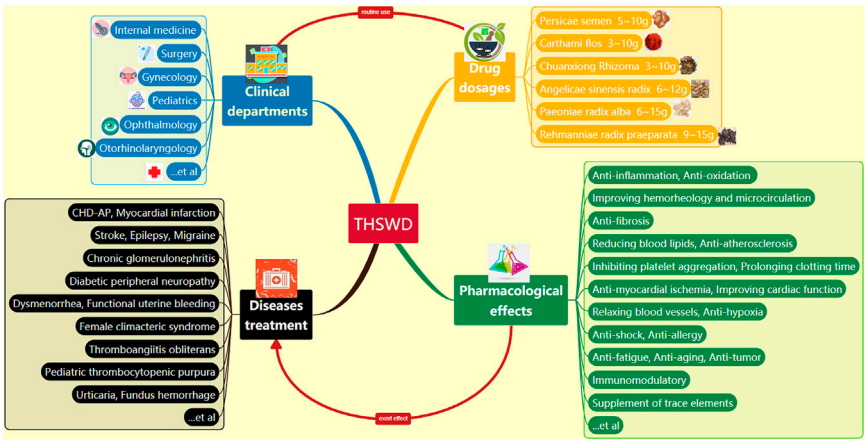

FIGURE 1 | Clinical applications and pharmacological effects of THSWD (THSWD: Tao Hong Siwu decoction).

aggregation and prolonging clotting time, and regulting some signal pathways (**Figure 2**).

Anti-Inflammation

Excessive inflammatory reaction is harmful to the human body. The inflammatory reaction is caused by the action of inflammatory factors on the body, resulting in local tissue and cell damage, even degeneration and necrosis. Among the many inflammatory cytokines, tumor necrosis factor-α (TNF-α), interleukin-1β (IL-1β), interleukin-6 (IL-6), interleukin-8 (IL-8) and so on play a major role in MI. THSWD can down-regulate the levels of serum inflammatory factors such as IL-6 and TNF-α (Liu, 2019a). The main mechanisms may be to inhibit the uncontrolled release of TNF-α and IL-6, remove inflammatory mediators, reduce inflammatory exudation, promote inflammatory absorption, thus inhibiting the progress of inflammatory reaction. The experiment showed that the serum-containing THSWD could significantly inhibit the increase of the content of reactive oxygen species (ROS) and the mRNA expression of TNF-α, IL-1β and monocyte chemoattractant protein-1 (MCP-1) induced by lipopolysaccharide (LPS) (Zhang, 2014b). Paeoniflorin, an intrinsic component of *Paeoniae radix alba*, can not only inhibit the expression of the above mRNA, but also reduce the LPS induced neutrophil/leukocyte infiltration (Zhou et al., 2013; Chen et al., 2015; Zhai and Guo, 2016). In addition, Kaempferol is a main component of *Carthami flos*, which could ameliorate inflammatory response in hyperglycemia-induced cardiac injury (Chen et al., 2018a). Oral adminstration of *Carthami flos* could induce macrophage activation (Choi et al., 2007), and baicalin, an ingredient of *Carthami flos*, could regulate macrophages polarization, thereby alleviating MIRI and inflammation (Xu et al., 2020).

Besides, inflammatory reaction significantly affects the formation and development of atherosclerosis (AS) plaques, and determines the formation speed and stability of plaques (Conti and Shaik-Dasthagirisaeb, 2015). Serum hypersensitive C-reactive protein (hs-CRP) is the most commonly used inflammatory marker in the clinical (Yayan, 2013). CRP can not only reflect the occurrence and development of AS, but also damage vascular endothelial cells through direct infiltration or indirect production of cytokines, and activate complements to aggravate myocardial injury (TIu et al., 2013; Zang and He, 2015). The study showed that the serum hs-CRP of the observation group decreased significantly after treatment with THSWD (Chu and Sun, 2014; Haoli, 2018; Lujuan and Wang, 2018), indicating that the inflammatory reaction was alleviated, but its mechanism is not clear. Furthermore, THSWD can enhance the activity of superoxide dismutase (SOD) (Luo and Zhou, 2014), inhibit the synthesis and release of prostaglandins (PG) and other inflammatory factors, thus improving inflammatory response, and preventing and repairing cell and tissue damage.

Anti-Oxidation

Oxidative stress refers to the state of imbalance between oxidation and anti-oxidation *in vivo*, which tends to oxidation, resulting in inflammatory infiltration of neutrophils, increased secretion of protease, and the production of a large number of oxidation intermediates. Oxidative stress is a negative effect produced by free radicals in the body, and is considered to be an important factor in aging and diseases. Reactive oxygen species (ROS), including free radicals and non-free radical oxygen intermediates, play a key role in vascular endothelial dysfunction, low-density lipoprotein (LDL) oxidation, and inflammatory events in the initiation and development of atherosclerotic lesions (Negre-Salvayre et al., 2020).

Compared with the control group, the THSWD group significantly reduced the division of mitochondria and the production of mitochondrial ROS (Luo et al., 2019), and both its ethanol extract and water extract had a scavenging effect on 1,1-diphenyl-2-picrylhydrazyl radical (Yang et al., 2011), thus inhibiting the oxidative stress reaction and reducing the damage of myocardial cells (Liu et al., 2011; Yu and Hong, 2016). THSWD can decrease the levels of serum creatine kinase (CK) and lactate dehydrogenase (LDH) in myocardial tissue during acute myocardial ischemia (Zhu and Zhang, 2003; Luo and Zhou,

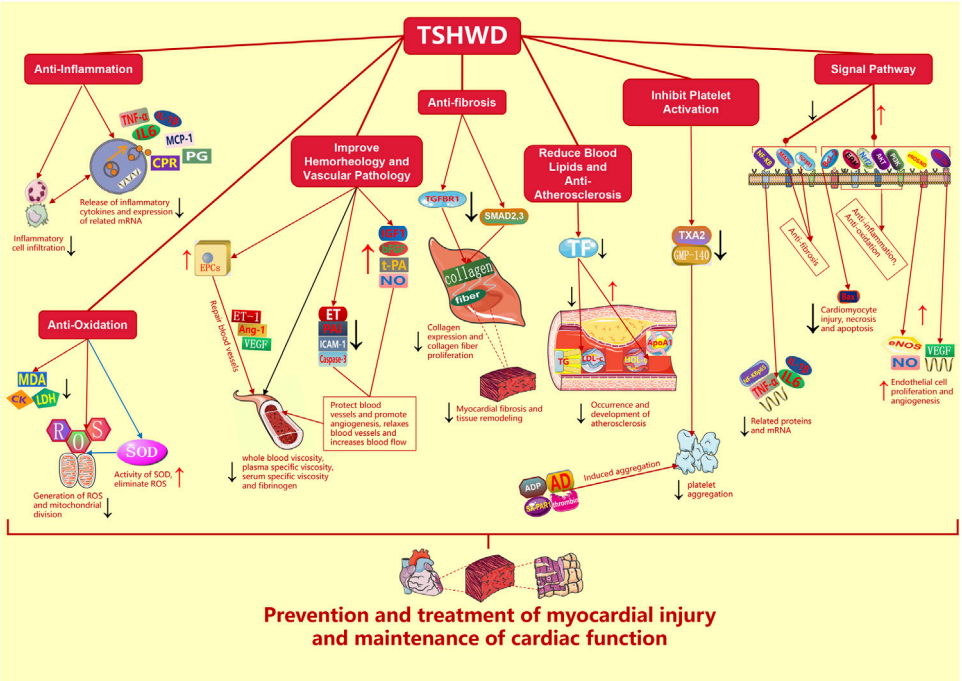

FIGURE 2 | Mechanisms of THSWD in prevention and treatment of MI (THSWD: Taohong Siwu decoction, MI: myocardial injury, TNF-α: tumor necrosis factor-α, IL-1β: interleukin-1β, IL-6: interleukin-6, IL-8: interleukin-8, ROS: reactive oxygen species, MCP-1: monocyte chemoattractant protein-1, LPS: lipopolysaccharide, NF-κB: nuclear factor-κβ, hs-CRP: hypersensitive C-reactive protein, SOD: superoxide dismutase, PG: prostaglandins, LDL: low density lipoprotein, CK: creatine kinase, LDH: lactate dehydrogenase, MDA: malondialdehyde, bFGF: basic fibroblast growth factor, IGF-1: insulin-like growth factor-1, EPCs: endothelial progenitor cells, ET-1: endothelin-1, Ang-1: angiopoietin-1, VEGF: vascular endothelial growth factor, PAI: plasminogen activator inhibitor, ICAM-1: intercellular adhesion molecule-1, t-PA: tissue plasminogen activator, Caspase-3: cysteine aspartate protease-3, TGFBR1: transforming growth factor 1 receptor, SMAD2, 3: the phosphorylation of signal transduction protein 2,3, TC: total cholesterol, TG: triglyceride, LDL-c: low density lipoprotein-C, HDL-c: high density lipoprotein-C, TF: tissue factor, ApoA1: apolipoprotein A1, PLT: platelets, ADP: adenosine diphosphate, AD: adrenaline, TXA2: thromboxane A2, GMP-140: granule membrane protein-140, SA-PAR1: selective agonists of protease-activated receptor-1, HIF-1α: hypoxia inducible factor-1α, eNOS/NO: endothelial nitric oxide synthase/nitric oxide, Bcl-2: B lymphocyte tumor-2, Bax: Bcl-2-associated X protein, Nrf2: NF-E2 related factor 2, PI3K: phosphatidylinositol 3-kinase, ERK: extracellular regulated protein kinases, MAPK: mitogen-activated protein kinase).

2014), thus reducing myocardial cell necrosis. Meanwhile, its effective component paeoniflorin can reduce the content of malondialdehyde (MDA) and enhance the activity of SOD (Zhang and Zhu, 2003; Liu, 2018; Wu et al., 2020a; He and Wang, 2020). SOD has a strong antioxidant capacity, can quickly decompose excessive oxygen free radicals in the human body, eliminate lipid peroxidation in tissues and cells, and then prevent the injury of cardiomyocytes.

Furthermore, the study reveals that kaempferol could protect the mouse heart and H9c2 cells from pathological oxidative stress via antioxidant activity (Zhou et al., 2015; Feng et al., 2017). Luteolin from *Carthami flos* could improve cardiac function, alleviate mitochondrial injury, decrease oxidative stress (Luo et al., 2017), inhibited cardiac apoptosis and enhanced autophagy (Wu et al., 2020b). Quercetin from *Carthami flos* also appeared to affect heart mitochondrial function (Ruiz et al., 2015), and could relieve cardiac oxidative stress, so as to exhibit cardioprotective effects (Roslan et al., 2017). β-Sitosterol is widely found in *Persicae semen*, *Carthami flos*, *Angelicae sinensis radix*, *Paeoniae radix alba*, *Rehmanniae radix praeparata*. β-Sitosterol pretreatment could cause an increase in superoxide dismutase and glutathione activities and a decrease in malondialdehyde levels in the heart (Koc et al., 2021), indicating its cardioprotective effects were related to anti-oxidative stress. Moreover, β-Sitosterol produced an up-regulation of cellular glutathione redox cycling and protected against hypoxia/reoxygenation-induced apoptosis in H9c2 cells (Wong et al., 2014).

Improve Hemorheology and Vascular Pathology

Hemorheology includes the rheology of blood vessels, the fluidity, viscosity, deformability and coagulability of blood. THSWD can decrease the whole blood viscosity (Xie and Luo, 2008; Liu et al., 2014; Luo and Zhou, 2014; Zhou and Shu, 2017; Wang and Wang, 2018; Jinxia et al., 2021), plasma specific viscosity, serum specific viscosity and fibrinogen (Han and Xu, 2007; Lujuan and Wang, 2018), and significantly increase the expression of basic fibroblast growth factor (bFGF) and insulin-like growth factor-1 (IGF-1) (Luo et al., 2019). These cytokines can promote neovascularization and protect the activity of cardiomyocytes. Studies have shown that the decrease of the above-mentioned

indexes may be due to the pharmacological effect of *Carthamus tinctorius* lutein (Li et al., 2009). Moreover, *Chuanxiong Rhizoma* and *Angelicae sinensis radix* had evident angiogenic effects by promoting the endothelial cell proliferation and stimulating quantity of vessels (Meng et al., 2008). The changes in hemorheology and the formation of neovascularization improve the microcirculation of the heart and the microenvironment of cardiomyocytes, which provide potential possibilities for the prevention and treatment of cardiomyocyte injury.

THSWD promotes the expression of IGF-1 (Luo et al., 2019). IGF-1 can dilate blood vessels, reduces vascular resistance and increase blood flow to the heart, thus protecting cardiomyocytes and improving cardiac function. In addition, the left ventricular end-systolic volume of the model rats was significantly decreased after 4 weeks of THSWD treatment, which increased the cardiac ejection fraction, and improved the left ventricular short-axis shortening rate and left ventricular systolic function (Zhu and Zhang, 2003; Luo et al., 2019). Its internal mechanism may be that paeoniflorin, one of its active components, alleviates the decline of cardiac function caused by myocardial ischemia (Zhai and Guo, 2016), and studies have shown that paeoniflorin can significantly attenuates chamber dilatation and dysfunction of left ventricle caused by pressure overload (Zhou et al., 2013).

In terms of vascular protection, since endothelial progenitor cells (EPCs) can repair the injury of vascular endothelium (Hunting et al., 2005; Briasoulis et al., 2011; Toya and Malik, 2012; Zhang et al., 2014; Hu et al., 2019; Leal et al., 2019), the researchers found that THSWD can reduce the damage of vascular endothelial cells and maintain the normal secretory function of blood vessels by improving the functional activity and increasing the number of EPCs (Li et al., 2014; Li et al., 2015; Wang and Jiang, 2019). The mechanism of vascular protection and repair may be related to regulation of endothelin-1 (ET-1), angiopoietin-1 (Ang-1), and vascular endothelial growth factor (VEGF) in serum (Wang and Han, 2017). It was found that the contents of ET with vasoconstriction, plasminogen activator inhibitor (PAI) and intercellular adhesion molecule-1 (ICAM-1) with fibrinolysis inhibition were decreased, while the contents of NO with vasodilation and tissue plasminogen activator (t-PA) with fibrinolysis promotion were increased after treating endothelial cells with serum of Modified THSWD (Wu et al., 2014). This suggests that Modified THSWD can obviously improve the dyssecretion of vascular endothelial cells caused by blood stasis and promote the migration of vascular endothelial cells, thus protecting the morphology and function of blood vessels. Furthermore, the serum containing THSWD can protect human umbilical vein endothelial cells from hydrogen peroxide damage and reduce the apoptosis rate of endothelial cells, and its mechanism of inhibiting apoptosis may be related to the decreased expression of cysteine aspartate protease-3 (Caspase-3) (Liu et al., 2013).

Anti-Fibrosis

Fibrosis can occur in various tissues and organs, and its main pathological changes are the increase of fibrous connective tissue and the decrease of parenchymal cells. Continuous progress can lead to the destruction of organ structure, functional decline and even exhaustion, which seriously threatens human health and life. For the treatment of myocardial fibrosis after myocardial infarction, the latest researches have shown that THSWD can significantly reduce myocardial fibrosis and ensure stable cardiac function by inhibiting transforming growth factor 1 receptor (TGFBR1) (Yayan, 2013), reducing collagen deposition and inhibiting fibrosis proliferation (Luo et al., 2019). The underlying mechanism may be that paeoniflorin and other effective substances reduce the expression of collagen, inhibit the TGFBR1 signaling pathway and the phosphorylation of signal transduction protein 2,3 (SMAD2,3) (Zhou et al., 2013; Liu et al., 2019a; Tan et al., 2021). However, the overexpression of TGFBR1 can reduce or even reverse the anti-fibrosis effect of THSWD (Tan et al., 2021). In addition, the research has shown that THSWD can reduce myocardial interstitial collagen remodeling by inhibiting myocardial interstitial collagen fiber proliferation and collagen expression after myocardial infarction, and reducing the ratio of myocardial Ⅰ/Ⅲ collagen in a non-infarcted area (Zhou and Liu, 2011). Moreover, paeoniflorin not only could improve ventricular remodeling *via* inhibiting BNP, IL-6, TNF-α and increasing IL-10 levels (Chen et al., 2018b), but also could attenuate cardiac hypertrophy and cardiac fibrosis (Liu et al., 2019b).

Reduce Blood Lipids and Anti-Atherosclerosis

The basic pathological process of CHD is that coronary artery fixed stenosis or increased microvascular resistance leads to decreased coronary blood flow, unstable atherosclerotic plaque rupture, erosion or bleeding, secondary platelet aggregation or thrombosis, resulting in a sharp increase in the degree of coronary artery stenosis or closure, and/or coronary artery functional changes (such as spasm), causing in myocardial ischemia and hypoxia injury. However, the increase of serum lipid level is one of the independent risk factors of CHD (Bragg and Walling, 2015). AS is the appearance of yellow substances such as cholesterol and lipids in the intima of large and middle arteries, which is mostly caused by fat metabolism disorders and neurovascular dysfunctions, and often leads to thrombosis, blood supply disorders and so on. Studies have shown that THSWD plays a certain role in reducing total cholesterol (TC), triglyceride (TG), low-density lipoprotein-C (LDL-c), LDL-c/TC ratio, and increasing high-density lipoprotein-C (HDL-c), HDL-c/TC ratio (Chen and Wang, 2005; Xie and Luo, 2008; Luo and Zhou, 2014; Liu, 2015a; Haoli, 2018; Chen et al., 2019; Li and Yan, 2020). One of the mechanisms may be that peach kernel oil significantly downregulates the protein expression of tissue factor (TF) (Hao et al., 2019), thereby inhibiting the formation of atherosclerotic plaques. Moreover, THSWD could significantly decrease the ratio of serum TG/HDL-c and increase the content of serum apolipoprotein A1 (ApoA1) (Zhou, 2003). The decrease of TC, TG, LDL-c, and the increase of LDL-c, ApoA1 help to reduce blood lipids, thus inhibiting the occurrence and development of AS. In addition, baicalin could ameliorate

atherosclerotic lesion progression via lipid modulation in ApoE−/− mice with high-cholesterol diet (Liao et al., 2014). A kind of active ingredients from *Chuanxiong rhizoma*, tetramethylpyrazine (Ligustrazine) also exhibited cardioprotective effects on atherosclerosis and MIRI (Guo et al., 2016).

Inhibit Platelet Aggregation and Prolong Clotting Time

The main functions of platelets (PLT) are coagulation, hemostasis and repair of damaged blood vessels. Since the surface sugar coating of platelets can absorb plasma proteins and coagulation factor Ⅲ, platelet granules also contain substances related to coagulation. Platelet activation consists of three steps: adhesion, aggregation and release. Activated platelets form platelet thrombus, which can cause thrombotic diseases such as acute myocardial infarction and ischemic stroke.

Studies have shown that THSWD can effectively reduce platelet adhesion rate in rats in a dose-dependent manner, and can inhibit platelet aggregation induced by adenosine diphosphate (ADP) and adrenaline (AD), and its effect is similar to that of aspirin (Han et al., 2010). Under the action of ADP (Liu et al., 2016), AD and other inducers, platelets can release a series of active substances, such as thromboxane A2 (TXA2), platelet granule membrane protein-140 (GMP-140), β-thromboglobulin, and platelet factor-4 to promote platelet aggregation (Liu and Yin, 2014). However, THSWD can significantly decrease the levels of plasma TXA2 and GMP-140 in rats (Han et al., 2010), thereby inhibiting platelet aggregation. In addition, within the range of 0.5–2.5 mg/ml, THSWD could inhibit platelet aggregation induced by thrombin and selective agonists of protease-activated receptor-1 (SA-PAR1) in a dose-dependent manner (Yin and Yang, 2012). The research has shown that THSWD can prolong thrombosis time and clotting time in rats (Liu and Yin, 2014), in which the prothrombin time is prolonged with the increase of the dose of *Carthamus tinctorius* lutein (Yin and Yang, 2012), showing an obvious anticoagulant effect. To sum up, THSWD can play a certain role in the three key links of platelet activation, and play the role of anti-platelet and prolonging clotting time.

Signal Pathway

It has been found that THSWD can inhibit inflammatory reaction by regulating the NF-kB signaling pathway, and its internal mechanism may be to inhibit the expression of NF-kBp65, TNF-α protein, and its mRNA in myocardial tissue, and reduce the contents of IL-1β and IL-6 in serum (Shen and Shi, 2019), thus effectively protecting the structure and function of the myocardium. Moreover, THSWD can protect human brain microvascular endothelial cells from ischemic injury, which may enhance the expression of VEGF and the ability of cell antioxidation through hypoxia-inducible factor-1α (HIF-1α) signal pathway (Zhaojie and Han, 2018). It can also promote endothelial cell proliferation by up-regulating endothelial nitric oxide synthase/nitric oxide (eNOS/NO) mediated signal pathway (Xiaoxia, 2010), since eNOS/NO is an important factor in promoting angiogenesis (Yasuda, 2008). Through activating Nrf2 mediated HIF-1α pathway, baicalin can protect cardiomyocytes from apoptosis induced by hypoxia (Yu et al., 2019). Besides, THSWD can increase the expression of B lymphocyte tumor-2 (Bcl-2) gene, decrease the expression of Bcl-2-associated X protein (Bax), alleviate cardiomyocyte injury, inhibit cardiomyocyte necrosis and apoptosis (Li and Wang, 2009), thus preventing the pathological changes of myocardial ischemia and maintain cardiac function.

In studies of the effective components of THSWD, ferulic acid can activate the signal pathways of transcription factor NF-E2 related factor 2 (Nrf2), phosphatidylinositol 3- kinase (PI3K) and extracellular regulated protein kinases (ERK) to play an antioxidant role, thus protecting vascular endothelial cells from oxidative damage (Ma et al., 2010). Cardioprotective potential of amygdalin from *Persicae semen* could inhibit cardiac hypertrophy, oxidative stress and inflammatory responses through modulation of Nrf2 and NF-κB activation (Kung et al., 2021). Paeoniflorin can also reduce the expression of related mRNA (Zhou et al., 2013; Chen et al., 2015), inhibit NF-kB signaling pathway and activate PI3K/Akt signaling pathway (Zhai and Guo, 2016), thereby exerting anti-inflammatory and anti-oxidation effects. Luteolin and quercetin could protect diabetic cardiomyopathy against inflammation and oxidative stress injury *via* NF-kB pathway inhibition (Patel et al., 2018; Li et al., 2019; Chen et al., 2020). Moreover, the findings demonstrated that cardioprotective effects of lactone component from Ligusticum chuanxiong were related to restoration of autophagic flux through the activation of PI3K/Akt/mTOR signaling pathway (Wang et al., 2018a), and ligustrazine from *Chuanxiong rhizoma could* exert cardio protection through multiple signaling pathways in MIRI (Zheng et al., 2018).

Paeoniforin could attenuate myocardial fibrosis and improve cardiac function in CHF rats by down-regulating the p38 MAPK signaling pathway (Liu et al., 2020). Hydroxysafflor yellow A (HSYA) in *Carthami flos* has a protective effect on vascular endothelial injury induced by hypoxia. It may be that HSYA can increase the level of NO under hypoxia, up-regulate the ratio of Bcl-2/bax, the expression of eNOS-mRNA and VEGF-mRNA and its protein, enhance the accumulation of HIF-1α protein and its transcriptional activity (Ji et al., 2008; Ji et al., 2009), thus improving the viability of vascular endothelial cells under hypoxia and promoting endothelial cell proliferation and angiogenesis through VEGF/VEGF receptor (Song et al., 2005).

CLINICAL APPLICATIONS OF TAOHONG SIWU DECOCTION IN PREVENTION AND TREATMENT OF MI

In the clinical prevention and treatment of myocardial injury related diseases, THSWD can decrease serum TC, increase coronary blood flow, reduce myocardial oxygen consumption, resist myocardial ischemia, inhibit platelet aggregation and enhance the activity of the fibrinolytic enzyme system (Yang, 2007). It can also effectively reduce blood viscosity and the level of

TABLE 1 | Clinical applications of THSWD in prevention and treatment of MI.

	Drugs/Prescriptions	Diseases	Pharmacological effects	References
Application of combined chemicals	Sodium ozagrel	UAP	Improve microcirculation and myocardial ischemia	Jing and Wang (2009), Renhua and Li (2017)
	Shuxuening			Wang and Wang (2008)
	Salvia miltiorrhiza injection			Yu (2012)
	Agkistrodon halys antithrombotic enzyme			Rui (2002)
	Metoprolol	AP of qi deficiency and blood stasis syndrome	Regulate of hemorheology, improve left ventricular systolic function	Wang et al. (2018b), Wang and Wang (2018), Wang and Jiang (2019)
	Diltiazem	Coronary spasm AP	Improve the level of blood lipids	Song et al. (2005)
	Low molecular heparin calcium	ACS	Prevention and treatment of myocardial infarction	Zhu et al. (2011)
	Rosuvastatin	AP	Reduce blood lipid, improve myocardial blood supply and heart function	Haoli (2018)
	Isosorbide mononitrate			Yan et al. (2012)
	Atorvastatin	CHD	Improve efficacy and reduce side effects	Wang (2018)
Use of combined prescriptions	Zhenwu decoction	CSHF	Increase LVEF, delay the ventricular remodeling	Joung et al. (2003); Xiao and Chen. (2015); Xiao and Gao. (2017)
	Shenfu decoction		Increase LVEF	Wang and Li, (2017)
	Baoyuan decoction	AP of qi deficiency and blood stasis type	Dilate coronary artery, improve microcirculation	Song. (2010), Li and Zhang. (2018), Zhang. (2019)
	Gualou Xiebai banxia decoction	SAP of phlegm and blood stasis type	Improve myocardial ischemia and the high viscosity and hypercoagulable state of hemorheology	Xiong. (2014), Li and Muhati. (2016), Wang and Zhai. (2016), Zhou and Shu. (2017), Zhao. (2018)
	Shexiang baoxin pill	AP of qi and blood stasis type	Prevent myocardial injury	Yue (2014)
Add and subtract THSWD alone	—	SAP complicated with heart failure	Improve serology, hemorheology and cardiac function, reduce the level of blood lipids and alleviates inflammatory reaction, delay the progress of heart failure	Jiang. (2009), Wang et al. (2020)
	Astragalus membranaceus	UAP	Maintain the function of vascular endothelium, regulate blood lipids	Zheng et al. (2010)
	Ginseng	CHD-AP	Improve heart function and blood lipid status	Hunting et al. (2005)

serum inflammation, thus improving the clinical effect (Lujuan and Wang, 2018). In addition, THSWD can inhibit the level of serum ET-1 in patients with coronary spastic AP of qi stagnation and blood stasis type, and its improvement of AP may be related to the decrease of ET-1 level and the improvement of vascular endothelial function (Chen, 2013). However, the efficacy of THSWD will decrease with the increase of the degree of AP, and it may only have a certain curative effect on mild and moderate AP (Yang, 2007). Moreover, the current clinical practical applications are mostly carried out in the way of combination formulas and combined chemical drugs, and there are fewer examples of THSWD alone (**Table 1**).

Application of Combined Chemicals

Clinical research has shown that THSWD combined with conventional chemical drugs can decrease the levels of serum TC, TG and LDL in patients with UAP (He et al., 2011), thus playing a role in reducing blood lipid and preventing AS. In chemical drugs combination therapy, modified THSWD combined with sodium ozagrel for injection (Jing and Wang, 2009; Renhua and Li, 2017), or Shuxuening (Wang and Wang, 2008), *Salvia miltiorrhiza* injection (Yu, 2012), Agkistrodon halys antithrombotic enzyme (Rui, 2002), which can effectively improve microcirculation and myocardial ischemia, alleviate the symptoms of AP and prevent the occurrence of myocardial infarction in patients with UAP, and there are no obvious adverse reactions and toxic and side effects. For patients with SAP with qi deficiency and blood stasis syndrome (Liu and Zhang, 2014; Dai and Wu, 2017; Zhang, 2018; Yang, 2019; Wu and Su, 2020), integrated traditional Chinese and Western medicine has a clear therapeutic effect, which can obviously improve the treatment efficiency and the quality of life of patients, reduce the level of blood lipid and the degree and frequency of AP attack, so as to accelerate the relief of clinical symptoms and improve cardiac function. Studies have shown that THSWD combined with Baoyuan Decoction and Metoprolol can treat patients with AP of qi deficiency and blood stasis syndrome (Wang and Wang, 2018), relieve symptoms and improve left ventricular systolic function (Wang et al., 2018b; Wang and Jiang, 2019). The mechanism may be related to the regulation of hemorheology and the levels of N-terminal pro-brain natriuretic peptide (NT-proBNP) (Xiao et al., 2016), serum troponin I and MCP-1. Furthermore, THSWD combined with diltiazem has outstanding clinical efficacy in the treatment of

coronary spasm AP, and which can significantly improve the level of blood lipid indexes compared with the control group (Liu, 2015a).

Besides, the researchers believe that on the basis of routine use of chemical drugs for anti-angina pectoris, THSWD combined with Gualou Xiebai Banxia Decoction is used to treat chest arthralgia of phlegm and blood stasis type (Yang et al., 2014; Wang, 2016), and THSWD combined with Chaihu Shugan Powder is added to treat UAP of qi stagnation and blood stasis type (Yuan and Fan, 2019), which has significant clinical efficacy, thus further controlling the attack of AP and improving the quality of life, reflecting the concept of prevention and treatment of both symptoms and root causes of disease in TCM. The combined prescription may have the effects of dilating blood vessels, anti-inflammation, reducing blood lipids, anti-shock, regulating immune function and reducing blood viscosity (Li et al., 2008), so as to relieve AP and protect myocardium. For the prevention and treatment of acute coronary syndrome (ACS includes UAP and myocardial infarction), the curative effect of THSWD combined with Gualou Xiebai Banxia Decoction plus low molecular heparin calcium (Zhu et al., 2011), and THSWD combined with Sini Powder plus conventional chemical drugs is more significant than that of chemical drugs alone (Gao, 2014). Other studies have found that Ginseng plus THSWD combined with rosuvastatin (Haoli, 2018), or Shengmai Powder combined with THSWD and isosorbide mononitrate in preventing and treating AP (Yan et al., 2012), can not only improve myocardial blood supply and heart function, but also reduce blood lipid, thereby alleviating the damage of myocardial cells. In addition, on the basis of routine chemicals treatment, THSWD combined with Shixiao Powder can improve the ischemic electrocardiogram (ECG) performance of chest obstruction caused by blood stasis (Liu, 2015b; Yu, 2015), THSWD combined with Zhishi Xiebai Guizhi decoction can alleviate the clinical manifestations of myocardial ischemia in chronic CHD (Chen, 2018; Cheng, 2019), and only taking THSWD also can improve the TCM syndrome and the quality of life of patients (Wang and Fu, 2017; Chen and Xia, 2018; Dong, 2018; Liu, 2019b; Jia, 2020). The clinical use of atorvastatin alone in the treatment of CHD has poor efficacy and large side effects, while adding THSWD and Xiebai Banxia Decoction can avoid these adverse reactions (Wang, 2018).

The above research showed that the integrated traditional Chinese and western medicine therapy may be superior to the single chemicals therapy in improving the pathological changes and clinical manifestations of cardiovascular diseases related to myocardial injury to a certain extent (Yu, 2015), (Huang, 2012; Yu, 2015; Yang et al., 2019; Yang and Zhou, 2019), but the specific mechanism needs to be further clarified.

Use of Combined Prescriptions

THSWD combined with Zhenwu decoction can reduce left ventricular end-diastolic and end-systolic diameter, plasma levels of brain natriuretic peptide (BNP) and matrix metalloproteinase-9 (MMP-9), increase left ventricular ejection fraction (LVEF) and tissue inhibitor of metalloproteinase-1 (TIMP-1) (Joung et al., 2003; Xiao and Chen, 2015; Xiao and Gao, 2017). It can improve the symptoms and signs of patients with chronic systolic heart failure (CSHF is the heart failure caused by SAP in ischemic heart disease) of yang deficiency and blood stasis, and suppresses the degradation of extracellular matrix (ECM) to delay the occurrence of ventricular remodeling. Among them, MMP-9 and TIMP-1 play an important role in the occurrence and development of ventricular remodeling and heart failure (Siwik et al., 2000). MMP-9 is a marker reflecting the degradation of myocardial ECM and ventricular remodeling (Martos et al., 2009). Under normal circumstances, TIMP-1 inhibits the activity of MMP-9 in a state of dynamic balance, and if unbalanced, ventricular remodeling will be aggravated (Chesler et al., 1999; Bradham et al., 2002; Fedak et al., 2004; Kassiri et al., 2005). In addition, clinical observation of CSHF with yang deficiency and blood stasis showed that Shenfu decoction combined with THSWD could significantly relieve symptoms such as palpitation, shortness of breath, wheezing, dyspnea and chest pain, increase LVEF and decrease the contents of NT-proBNP and BNP in plasma (Wang and Li, 2017).

Moreover, many researchers believe that THSWD combined with Baoyuan Decoction can significantly improve the clinical symptoms of patients with AP of qi-deficiency and blood-stasis type with higher safety (Song, 2010; Li and Zhang, 2018; Zhang, 2019). The pharmacological study of the combined prescription confirmed part of the action mechanism of Baoyuan decoction combined with THSWD (Li and Zhang, 2018), including coronary artery dilation, improvement of microcirculation, protection of damaged myocardium, enhancement of myocardial contractility, anti-platelet aggregation, inhibition of thrombosis and so on. In the treatment of SAP of phlegm and blood stasis type with THSWD combined with Gualou Xiebai Banxia decoction, several studies have shown that the combined prescription can improve myocardial ischemia and the high viscosity and hypercoagulable state of hemorheology (Xiong, 2014; Li et al., 2015; Li and Muhati, 2016; Wang and Zhai, 2016; Zhao, 2018), so as to protect cardiomyocytes from further injury. In addition, research has confirmed that THSWD combined with Shexiang Baoxin Pill has a certain prevention and therapeutic effect on AP of qi and blood stasis type (Yue, 2014).

In the clinical study of combined prescriptions, THSWD combined with other prescriptions has significant clinical effect in the treatment of cardiovascular disease, which can improve the TCM syndrome of patients and their quality of life. However, there are few cases in these clinical studies, and there is a lack of research and analysis of large clinical samples and standardization of syndrome types. Secondly, due to the limited observation time, there are few objective indicators selected in the study, so the inferences of results need to be further verified.

Add and Subtract Taohong Siwu Decoction

Early studies showed that after GE's THSWD was used for SAP, the pain and ECG were obviously improved. Although there was no statistically significant difference compared with the chemicals control group, the improvement of clinical symptoms of the

TABLE 2 | The main active ingredients from THSWD in protection of cardiomyocytes.

Chinese medicine	Ingredients	Pharmacological effects	References
Persicae semen *Carthami flos* *Angelicae sinensis radix* *Paeoniae radix alba* *Rehmanniae radix praeparata*	β-sitosterol	Anti-oxidative stress	Wong et al. (2014), Koc et al. (2021)
Chuanxiong rhizoma	Tetramethylpyrazine (Ligustrazine)	Anti-atherosclerosis, anti-oxidation, anti-inflammation	Guo et al. (2016)
	Lactone component from *Ligusticum chuanxiong*	Regulate autophagy	Wang et al. (2018a)
Persicae semen	Amygdalin	Anti-inflammation, anti-oxidation	Kung et al. (2021)
Carthami flos	Hydroxysafflor yellow A	Protect vascular endothelium, Promote endothelial cell proliferation and angiogenesis	Ji et al. (2008), Ji et al. (2009)
	Baicalin	Cardiomyocytes protection, Macrophages polarization, lipid modulation	Liao et al., 2014, Yu et al. (2019), Xu et al. (2020)
	Quercetin	Anti-inflammation, anti-oxidation, mitochondrial function regulation, Cardiomyocytes protection	Ruiz et al. (2015), Roslan et al. (2017), Patel et al. (2018), Chen et al. (2020)
	Luteolin	Anti-inflammation, anti-oxidation, autophagy regulation	Luo et al. (2017), Li et al. (2019), Wu et al. (2020b)
	Kaempferol	Cardiomyocytes protection, inhibit inflammatory responses and oxidative stress	Zhou et al. (2015), Feng et al. (2017), Chen et al. (2018a)
Paeoniae radix alba	Paeoniflorin	improve ventricular remodeling, attenuate cardiac hypertrophy, anti-inflammation, anti-fibrosis, anti-oxidative stress	Zhang et al. (2012), Zhou et al. (2013), Chen et al. (2015), Chen et al. (2018b), Qian et al. (2015), Zhai and Guo. (2016), Liu et al. (2019a), Liu et al. (2019b), Liu et al. (2020), Wu et al. (2020a)

treatment group was better than that in the control group (Jiang, 2009). Moreover, THSWD can improve the clinical efficacy of conventional chemical drugs in the treatment of SAP complicated with heart failure, and further improve the indexes of serology, hemorheology and cardiac function in patients (Wang et al., 2020). At the same time, it also lowers blood lipids and alleviates inflammatory reactions, thus delaying the progress of heart failure. THSWD combined with *Astragalus membranaceus* were used to enhance the efficacy of routine drugs in the treatment of UAP (Zheng et al., 2010), by maintaining the function of vascular endothelium, regulating blood lipids and reducing the levels of plasma ET and hs-CRP, to improve ECG and clinical manifestation of the patients. Research have shown that Ginseng combined with THSWD in the treatment of AP patients with CHD can further increase the curative effect, improve the heart function and blood lipid status of patients and higher safety (Chen et al., 2019). Although the use of THSWD alone can improve the prevention and treatment of the MI caused by cardiovascular disease, there are few clinical studies, and there are still many internal mechanisms that are not clear.

SUMMARY AND DISCUSSION

As one of the classic prescriptions for promoting blood circulation and removing blood stasis, THSWD has certain effects on the prevention and treatment of cardiovascular diseases (CHD, myocardial infarction, etc.). On the whole, it aims to control or delay the progression of CHD, alleviate the symptoms and frequency of myocardial ischemia and AP, thereby improving the quality of life, preventing myocardial infarction and prolonging life (Montalescot et al., 20132013).

At present, many studies have shown that THSWD can protect cardiomyocytes and improve cardiac function by inhibiting inflammatory reaction, antioxidant stress, inhibiting platelet aggregation, prolonging clotting time, anti-fibrosis, reducing blood lipids, anti-atherosclerosis, improving hemorheology and vascular lesions, regulating related signal pathways and so on. These possible mechanisms not only provide some research paths for researchers, but also provide clinicians with beneficial choices in the prevention and treatment of cardiovascular diseases, which is also a kind of welfare and hope for patients with cardiovascular diseases!

However, there are still some limitations and uncertainties in the research of prescriptions. According to the current research, THSWD contains many active ingredients (Wu, 2011; Li and Guo, 2016; Wang and Peng, 2017; WangChen and Han, 2019; Zhao and Liu, 2019; Nie and Cheng, 2020), including ligustilide, catalpol, paeoniflorin (Zhang et al., 2012; Zhou et al., 2013; Chen et al., 2015; Chen et al., 2018b; Qian et al., 2015; Zhai and Guo, 2016; Liu et al., 2019b; Liu et al., 2020), paeonional lactonine, amygdalin (Kung et al., 2021), kaempferol (Zhou et al., 2015; Feng et al., 2017; Chen et al., 2018a), quercetin (Ruiz et al., 2015; Roslan et al., 2017; Patel et al., 2018; Chen et al., 2020), paeonol, ferulic acid (Dai and Wu, 2017), benzoic acid, coumaric acid,

caffeic acid, gallic acid, and hydroxysafflor yellow A (Song et al., 2005; Ji et al., 2008; Ji et al., 2009), etc., (**Table 2**). However, the molecular biological mechanism of which or several components play a role needs to be further studied and elucidated. Moreover, there are still many unknown ingredients in THSWD that have not been discovered and studied, and the pharmacological effects and mechanisms of these ingredients still need to be explored. In addition, although there are many clinical studies on the prevention and treatment of cardiovascular disease with THSWD, due to the blind sampling selection, short-term follow-up time and drop-out, the long-term effect of the study cannot be determined. Moreover, due to the lack of clear mechanisms of action, the combined use of THSWD with other prescriptions and chemical drugs is ambiguous and confusing to some extent, and there is still a lack of clear systematic evaluation of its efficacy and safety in the prevention and treatment of cardiovascular diseases. In addition, the dosage of each Chinese medicine component of THSWD in the literature research was inconsistent, and the quality of TCM was uneven, which may adversely affect the results of the study. Therefore, the results of the study may have a certain degree of psychological comfort tendency, which is not universal, and as the drug composition and dose are not standardized and quantified, the conclusion may have errors.

To sum up, THSWD has shown a broad prospect in the prevention and treatment of myocardial injury caused by cardiovascular diseases, but there are still many uncertainties. In the basic research of prescriptions and drugs, scientific research institutions should strengthen the quality control of drugs and further clarify the molecular biological mechanism of prevention and treatment of myocardial injury. In clinical research, clinical researchers should carry out multicenter, large sample prospective cohort studies to fully clarify its clinical efficacy and safety, providing sufficient and reliable theoretical and practical basis for the clinical application of THSWD in the prevention and treatment of myocardial injury. After thousands of years of traditional Chinese medicine practice challenges, the preservation of THSWD is inseparable from its practical value and historical significance. THSWD deserves further exploration by more researchers, so as to provide more potential utility for the prevention and treatment of other diseases besides myocardial injury, creating social value and ensuring people's health, and realizing standardization, quantification and internationalization.

AUTHOR CONTRIBUTIONS

C-LS collated and analyzed literatures, and wrote the manuscript. G-HC edited the manuscript. H-DG provided design and concept.

FUNDING

This work was supported by grants from the National Natural Science Foundation of China (Grant No. 82174120), Natural Science Foundation of Shanghai (No. 21ZR1463100) and Shanghai Talent Development Funding Scheme (No. 2019090).

REFERENCES

Benjamin, E. J., Virani, S. S., Callaway, C. W., Chamberlain, A. M., Chang, A. R., Cheng, S., et al. (2018). Heart Disease and Stroke Statistics-2018 Update: A Report from the American Heart Association. *Circulation* 137 (12), e67–e492. doi:10.1161/CIR.0000000000000558

Bradham, W. S., Bozkurt, B., Gunasinghe, H., Mann, D., and Spinale, F. G. (2002). Tumor Necrosis Factor-Alpha and Myocardial Remodeling in Progression of Heart Failure: a Current Perspective. *Cardiovasc. Res.* 53 (4), 822–830. doi:10.1016/s0008-6363(01)00503-x

Bragg, D. A., and Walling, A. (2015). Metabolic Syndrome: Hyperlipidemia. *FP Essent.* 435, 17–23.

Briasoulis, A., Tousoulis, D., Antoniades, C., Papageorgiou, N., and Stefanadis, C. (2011). The Role of Endothelial Progenitor Cells in Vascular Repair after Arterial Injury and Atherosclerotic Plaque Development. *Cardiovasc. Ther.* 29 (2), 125–139. doi:10.1111/j.1755-5922.2009.00131.x

Chen, Bo. (2013). *To Explore the Clinical Effect of Taohongsiwu Soup against Coronary Artery Spasm (CAS) Patients and the Influence on Endothelin-1 (ET-1) [D]*. Heilongjiang University of Chinese Medicine. [In Chinese].

Chen, C., Du, P., and Wang, J. (2015). Paeoniflorin Ameliorates Acute Myocardial Infarction of Rats by Inhibiting Inflammation and Inducible Nitric Oxide Synthase Signaling Pathways. *Mol. Med. Rep.* 12 (3), 3937–3943. doi:10.3892/mmr.2015.3870

Chen, D. (2018). Clinical Experience of Taohong Siwu Decoction and Zhishi Xie Bai Guizhi Decoction in Treating 30 Cases of Chronic Coronary Heart Disease with Myocardial Ischemia. *World Latest Med. Inf.* 18 (89), 146+182. [In Chinese].

Chen, D., and Wang, Z. (2005). Clinical Observation on Modified Taohong Siwu Decoction in Treating 60 Cases of Hyperlipemia with Qi Stagnation and Blood Stasis Syndrome. *Jilin J. Chin. Med.* (03), 24–25. [In Chinese].

Chen, H., Dong, Y., He, X., Li, J., and Wang, J. (2018). Paeoniflorin Improves Cardiac Function and Decreases Adverse Postinfarction Left Ventricular Remodeling in a Rat Model of Acute Myocardial Infarction. *Drug Des. Devel Ther.* 12, 823–836. doi:10.2147/DDDT.S163405

Chen, J., Wang, J., and Zeng, M. (2019). Effect of Ginseng Combined with Taohong Siwu Decoction on Cardiac Function and Blood Lipid in Patients with Coronary Heart Disease and Angina Pectoris. *China Med. Herald* 16 (24), 135–138. [In Chinese].

Chen, S., and Xia, Z. (2018). The Clinical Effect of Taohong Siwu Decoction in the Treatment of Stable Coronary Heart Disease with Blood Stasis Type. *J. China Prescription Drug* 16 (04), 105–106. [In Chinese].

Chen, T., Zhang, X., Zhu, G., Liu, H., Chen, J., Wang, Y., et al. (2020). Quercetin Inhibits TNF-α Induced HUVECs Apoptosis and Inflammation via Downregulating NF-kB and AP-1 Signaling Pathway *In Vitro*. *Medicine (Baltimore)* 99 (38), e22241. doi:10.1097/MD.0000000000022241

Chen, W., and Gao, R. (2016). Summary of the Chinese Cardiovascular Disease Report 2015. *Chin. Circ. J.* 31 (06), 521–528. [In Chinese].

Chen, X., Qian, J., Wang, L., Li, J., Zhao, Y., Han, J., et al. (2018). Kaempferol Attenuates Hyperglycemia-Induced Cardiac Injuries by Inhibiting Inflammatory Responses and Oxidative Stress. *Endocrine* 60 (1), 83–94. doi:10.1007/s12020-018-1525-4

Cheng, Q. (2019). Clinical Effect Observation on 192 Cases of Chronic Coronary Heart Disease Myocardial Ischemia Treated by Taohong Siwu Decoction and Zhishi Xiebai Guizhi Decoction. *World Latest Med. Inf.* 19 (74), 176+178. [In Chinese].

Chesler, N. C., Ku, D. N., and Galis, Z. S. (1999). Transmural Pressure Induces Matrix-Degrading Activity in Porcine Arteries *Ex Vivo*. *Am. J. Physiol.* 277 (5), H2002–H2009. doi:10.1152/ajpheart.1999.277.5.H2002

Chinese Pharmacopoeia Commission (2015). *Pharmacopoeia of the People's Republic of China [S]*. Beijing: China Medical Science Press. [In Chinese].

Choi, Y. H., Do, J. S., Seo, H. J., Hwang, J. K., Kim, J. H., Song, E. J., et al. (2007). Oral Administration of Aqueous Extract of Carthami Flos Induces Macrophage Activation and Preferentially Potentiates Type 1 Helper T-Cell Response *In Vivo*. *Immunopharmacol Immunotoxicol* 29 (2), 187–200. doi:10.1080/08923970701511892

Chu, L., and Sun, M. (2014). Effect of Taohong Siwu Decoction on Hypersensitive C-Reactive Protein in Patients with Coronary Heart Disease. *Inner Mongolia J. Traditional Chin. Med.* 33 (3), 36–37. [In Chinese].

Conti, P., and Shaik-Dasthagirisaeb, Y. (2015). Atherosclerosis: a Chronic Inflammatory Disease Mediated by Mast Cells. *Cent. Eur. J. Immunol.* 40 (3), 380–386. doi:10.5114/ceji.2015.54603

Dai, S., and Wu, Z. (2017). Clinical Study on Treatment of Stable Angina Pectoris with Qi Deficiency and Blood Stasis Syndrome by Integrated Traditional Chinese and Western Medicine. *J. Pract. Traditional Chin. Med.* 33 (06), 647–648. [In Chinese].

Deng, J. (2021). Based on Network Pharmacology and Molecular Docking to Explore Mechanism of Classic Prescription Taohong Siwu Decoction in Treating Different Diseases Simultaneously. *Chin. Traditional Herbal Drugs* 52 (10), 3018–3029. [In Chinese].

Dong, W. (2018). Clinical Value of Treating Stable Coronary Heart Disease of Heart-Blood Stasis Type by Combining Routine Western Medicine with Taohong Siwu Decoction. *Cardiovasc. Dis. Electron. J. Integrated Traditional Chin. West. Med.* 6 (01), 165. [In Chinese].

Fedak, P. W., Smookler, D. S., Kassiri, Z., Ohno, N., Leco, K. J., Verma, S., et al. (2004). TIMP-3 Deficiency Leads to Dilated Cardiomyopathy. *Circulation* 110 (16), 2401–2409. doi:10.1161/01.CIR.0000134959.83967.2D

Feng, H., Cao, J., Zhang, G., and Wang, Y. (2017). Kaempferol Attenuates Cardiac Hypertrophy via Regulation of ASK1/MAPK Signaling Pathway and Oxidative Stress. *Planta Med.* 83 (10), 837–845. doi:10.1055/s-0043-103415

Gao, Q., Dong, X., and Deng, C. (2020). Progress in Myocardial Ischemia and Reperfusion Injury. *South China J. Cardiovasc. Dis.* 26 (01), 107–109. [In Chinese].

Gao, Xin (2014). 40 Cases of Acute Myocardial Infarction Treated by Taohong Siwu Decoction and Sini Powder Combined with Western Medicine. *Shaanxi J. Traditional Chin. Med.* 35 (06), 655–656. [In Chinese].

Gao, X., and Zhang, T. (2017). *Chinese Materia Medica [M]*. Beijing: China Press of Traditional Chinese Medicine. [In Chinese].

Guo, M., Liu, Y., and Shi, D. (2016). Cardiovascular Actions and Therapeutic Potential of Tetramethylpyrazine (Active Component Isolated from Rhizoma Chuanxiong): Roles and Mechanisms. *Biomed. Res. Int.* 2016, 2430329. doi:10.1155/2016/2430329

Han, L., Peng, D., Xu, F., Wang, N., Liu, Q., Dai, M., et al. (2010). Studies on Anti-platelet Activation Effect and Partial Mechanisms of Taohong Siwu Decoction. *Zhongguo Zhong Yao Za Zhi* 35 (19), 2609–2612. [In Chinese].

Han, L., and Peng, D. (2010). Studies on Antithrombotic Effects of Taohong Siwu Decoction. *J. Anhui Univ. Chin. Med.* 29 (01), 47–49. [In Chinese].

Han, L., and Xu, V. (2007). Experimental Study of Taohong Siwu Decoction on Promoting Blood Circulation and Removing Blood Stasis. *J. Anhui Univ. Chin. Med.* (01), 36–38. [In Chinese].

Hao, E., Pang, G., Du, Z., Lai, Y. H., Chen, J. R., Xie, J., et al. (2019). Peach Kernel Oil Downregulates Expression of Tissue Factor and Reduces Atherosclerosis in ApoE Knockout Mice. *Int. J. Mol. Sci.* 20 (2), 405. doi:10.3390/ijms20020405

Haoli, F. (2018). Effect of Ginseng and Taohong Siwu Decoction Combined with Rosuvastatin on Cardiac Function and Blood Lipid in Patients with Coronary Heart Disease and Angina Pectoris. *Chin. J. Integr. Med. Cardio-Cerebrovascular Dis.* 16 (21), 3177–3179. [In Chinese].

He, X., and Wang, J. (2020). Effects and Mechanism of Erchen Decoction and Taohong Siwu Decoction on the Regulation of p53/SLC7A11 Mediated Oxidative Damage and Ferroptosis on Atherosclerosis. *China J. Traditional Chin. Med. Pharm.* 35 (05), 2344–2348. [In Chinese].

He, Y., Zhu, Z., and Wang, H. (2011). Clinical Observation and Nursing Care of 30 Cases of Unstable Angina Pectoris Treated by Taohong Siwu Decoction. *China Pharmaceuticals* 20 (12), 76–77. [In Chinese].

Hu, Z., Wang, H., Fan, G., Zhang, H., Wang, X., Mao, J., et al. (2019). Danhong Injection Mobilizes Endothelial Progenitor Cells to Repair Vascular Endothelium Injury via Upregulating the Expression of Akt, eNOS and MMP-9. *Phytomedicine* 61, 152850. doi:10.1016/j.phymed.2019.152850

Huang, Zezi. (2012). Clinical Observation of Taohong Siwu Decoction Combined with Yinxingdamo Injection in the Treatment of Angina Pectoris of Coronary Heart Disease. *Guide China Med.* 10 (16), 272–273. [In Chinese].

Hunting, C. B., Noort, W. A., and Zwaginga, J. J. (2005). Circulating Endothelial (Progenitor) Cells Reflect the State of the Endothelium: Vascular Injury, Repair and Neovascularization. *Vox Sang* 88 (1), 1–9. doi:10.1111/j.1423-0410.2005.00589.x

Jennings, R. B. (2013). Historical Perspective on the Pathology of Myocardial Ischemia/reperfusion Injury. *Circ. Res.* 113 (4), 428–438. doi:10.1161/CIRCRESAHA.113.300987

Ji, D. B., Zhang, L. Y., Li, C. L., Ye, J., and Zhu, H. B. (2009). Effect of Hydroxysafflor Yellow A on Human Umbilical Vein Endothelial Cells under Hypoxia. *Vascul Pharmacol.* 50 (3-4), 137–145. doi:10.1016/j.vph.2008.11.009

Ji, D. B., Zhu, M. C., Zhu, B., Zhu, Y. Z., Li, C. L., Ye, J., et al. (2008). Hydroxysafflor Yellow A Enhances Survival of Vascular Endothelial Cells under Hypoxia via Upregulation of the HIF-1 Alpha-VEGF Pathway and Regulation of Bcl-2/Bax. *J. Cardiovasc. Pharmacol.* 52 (2), 191–202. doi:10.1097/FJC.0b013e318181fb02

Ji, Li., and Lian, J. (2016). *Chinese Medicinal Formulas [M]*. Beijing: China Press of Traditional Chinese Medicine. [In Chinese].

Jia, L. (2020). Therapeutic Analysis of Taohong Siwu Decoction in the Treatment of Stable Coronary Heart Disease with Heart and Blood Stasis. *Guide China Med.* 18 (07), 185–186. [In Chinese].

Jiang, X. (2009). Analysis of the Effect of Taohong Siwu Decoction on the Treatment of Angina Pectoris of Coronary Heart Disease. *Chin. J. Mod. Drug Appl.* 3 (23), 116–117. [In Chinese].

Jiang, Z., and Gao, Z. (2018). Characteristics of TCM Prevention and Treatment of Stable Coronary Heart Disease. *Chin. J. Integr. Med. Cardio-Cerebrovascular Dis.* 16 (02), 243–245. [In Chinese].

Jing, X., and Wang, X. (2009). Therapeutic Effect of Taohong Siwu Decoction Combined with Ozagrel Sodium in the Treatment of Unstable Angina Pectoris. *Hebei J. Traditional Chin. Med.* 31 (08), 1193+1203. [In Chinese].

Jinxia, L. I., Xiaoqing, Z. H. O. U., Caixing, Z. H. E. N. G., Lina, L. A. I., and Ling, L. I. (2021). Comparison of Mechanisms and Efficacies of Five Formulas for Improving Blood Circulation and Removing Blood Stasis. *Digital Chin. Med.* 4 (2), 144–158. doi:10.1016/j.dcmed.2021.06.007

Joung, B. Y., Park, B. E., Kim, D. S., Hong, B. K., Kim, D. Y., Cho, Y. H., et al. (2003). B-type Natriuretic Peptide Predicts Clinical Presentations and Ventricular Overloading in Patients with Heart Failure. *Yonsei Med. J.* 44 (4), 623–634. doi:10.3349/ymj.2003.44.4.623

Kachur, S., Chongthammakun, V., Lavie, C. J., De Schutter, A., Arena, R., Milani, R. V., et al. (2017). Impact of Cardiac Rehabilitation and Exercise Training Programs in Coronary Heart Disease. *Prog. Cardiovasc. Dis.* 60 (1), 103–114. doi:10.1016/j.pcad.2017.07.002

Kalogeris, T., Baines, C. P., Krenz, M., and Korthuis, R. J. (2012). Cell Biology of Ischemia/reperfusion Injury. *Int. Rev. Cel Mol Biol* 298, 229–317. doi:10.1016/B978-0-12-394309-5.00006-7

Kalogeris, T., Baines, C. P., Krenz, M., and Korthuis, R. J. (2016). Ischemia/Reperfusion. *Compr. Physiol.* 7 (1), 113–170. doi:10.1002/cphy.c160006

Kassiri, Z., Oudit, G. Y., Sanchez, O., Dawood, F., Mohammed, F. F., Nuttall, R. K., et al. (2005). Combination of Tumor Necrosis Factor-Alpha Ablation and Matrix Metalloproteinase Inhibition Prevents Heart Failure after Pressure Overload in Tissue Inhibitor of Metalloproteinase-3 Knock-Out Mice. *Circ. Res.* 97 (4), 380–390. doi:10.1161/01.RES.0000178789.16929.cf

Koc, K., Geyikoglu, F., Cakmak, O., Koca, A., Kutlu, Z., Aysin, F., et al. (2021). The Targets of β-sitosterol as a Novel Therapeutic against Cardio-Renal Complications in Acute Renal Ischemia/reperfusion Damage. *Naunyn Schmiedebergs Arch. Pharmacol.* 394 (3), 469–479. doi:10.1007/s00210-020-01984-1

Kung, Y. L., Lu, C. Y., Badrealam, K. F., Kuo, W. W., Shibu, M. A., Day, C. H., et al. (2021). Cardioprotective Potential of Amygdalin against Angiotensin II Induced Cardiac Hypertrophy, Oxidative Stress and Inflammatory Responses through Modulation of Nrf2 and NF-Kb Activation. *Environ. Toxicol.* 36 (5), 926–934. doi:10.1002/tox.23094

Leal, V., Ribeiro, C. F., Oliveiros, B., António, N., and Silva, S. (2019). Intrinsic Vascular Repair by Endothelial Progenitor Cells in Acute Coronary Syndromes: an Update Overview. *Stem Cel Rev Rep* 15 (1), 35–47. doi:10.1007/s12015-018-9857-2

Li, B., Chen, H., and Li, L. (2008). *Practical Traditional Chinese Medicine Prescriptions and Clinical Remedies [M]*. Beijing: Scientific and Technical Documentation Press, 374. [In Chinese].

Li, H. X., Han, S. Y., Wang, X. W., Ma, X., Zhang, K., Wang, L., et al. (2009). Effect of the Carthamins Yellow from Carthamus tinctorius L. On Hemorheological Disorders of Blood Stasis in Rats. *Food Chem. Toxicol.* 47 (8), 1797–1802. doi:10.1016/j.fct.2009.04.026

Li, J., and Wang, D. (2009). The Expermental Research of Activating Blood and Removing Stasis Decoctions on Myocardial Cellular Apoptosis and Expression of Bcl-2 and Bax in Acute Experimental Ischemic Myocardium. *Chin. J. Integr. Med. Cardio-Cerebrovascular Dis.* 7 (03), 295–296. [In Chinese].

Li, L., Luo, W., Qian, Y., Zhu, W., Qian, J., Li, J., et al. (2019). Luteolin Protects against Diabetic Cardiomyopathy by Inhibiting NF-Kb-Mediated Inflammation and Activating the Nrf2-Mediated Antioxidant Responses. *Phytomedicine* 59, 152774. doi:10.1016/j.phymed.2018.11.034

Li, M., and Zhang, Y. (2018). Therapeutic Effect of Baoyuan Decoction and Taohong Siwu Decoction on Qi Deficiency and Blood Stasis Type of Chest Arthralgia and Heartache. *World Latest Med. Inf.* 18 (45), 218–219. [In Chinese].

Li, R. S., Li, D. Y., Chen, W. N., Ma, X. D., Zhang, Y., and Li, X. J. (2014). Taohong Siwu Decoction Regulated Functions of Endothelial Cells and Treated Arteriosclerosis Obliterans: an Experimental Study. *Zhongguo Zhong Xi Yi Jie He Za Zhi* 34 (02), 191–196. [In Chinese].

Li, S., and Guo, C. (2016). Advances on Chemical Constituents and Pharmacological Effects of Taohongsiwu Decoction. *Acta Neuropharmacologica* 6 (04), 42–49. [In Chinese].

Li, S. S., Chen, Z. C., and Zhang, C. H. (2012). Effect of tao-hong-si-Wu-tang, a Traditional Chinese Herbal Medicine Formula, on Physical Fatigue in Mice. *Afr. J. Tradit Complement. Altern. Med.* 10 (1), 60–65. doi:10.4314/ajtcam.v10i1.10

Li, X., Li, D. Y., Chen, W. N., Zhang, Y., Liu, B. Q., Li, S. Z., et al. (2015). Effect of ASO Blood Stasis Syndrome Serum on Vascular Endothelial Cell Injury and Regulation of Taohong Siwu Decoction on it. *Zhongguo Zhong Xi Yi Jie He Za Zhi* 35 (11), 1373–1377. [In Chinese].

Li, Y., and Yan, L. (2020). Effect of Modified Yuquanwan Combined with Taohong Siwutang on Major Cardiovascular Risk Factors of Patients with Type 2 Diabetes. *Chin. J. Exp. Traditional Med. Formulae* 26 (19), 177–182. [In Chinese].

Li, Y., and Muhati, G. (2016). Gualou Xiebai Banxia Decoction Combined with Taohong Siwu Decoction in the Treatment of 100 Cases of Thoracic Obstruction. *Inner Mongolia J. Traditional Chin. Med.* 35 (13), 13. [In Chinese].

Li, Y. Y., Li, J. J., Ge, F. X., Ma, X. J., Li, C., Ai, X. N., et al. (2021). Research Progress on *In Vitro* Models of Cardiomyocyte Injury. *Zhongguo Zhong Yao Za Zhi* 46 (13), 3257–3269. [In Chinese]. doi:10.19540/j.cnki.cjcmm.20210311.601

Lian, H., and Qin, Z. R. (2010). Research Survey of the Clinical Application and Experimental Studies of Taohongsiwutang. *Chin. Arch. Traditional Chin. Med.* 28 (09), 1868–1870. [In Chinese].

Liao, P., Liu, L., Wang, B., Li, W., Fang, X., and Guan, S. (2014). Baicalin and Geniposide Attenuate Atherosclerosis Involving Lipids Regulation and Immunoregulation in ApoE-/- Mice. *Eur. J. Pharmacol.* 740, 488–495. doi:10.1016/j.ejphar.2014.06.039

Liu, G., and Zhang, Z. (2014). Integrative Interventions Stable Angina Syndrome of Blood Stasis Due to Qi Deficiency Clinical Efficacy. *Chin. Arch. Traditional Chin. Med.* 32 (11), 2616–2619. [In Chinese].

Liu, J. (2019). Effect of Taohong Siwu Decoction on Serum Levels of IL-6 and TNF-α in a Rat Model of Acute Deep Venous Thrombosis. *J. Hunan Univ. Chin. Med.* 39 (01), 32–34. [In Chinese].

Liu, J. (2019). Observation on Therapeutic Effect of Taohong Siwu Decoction in Treating Stable Coronary Heart Disease of Blood Stasis Type. *J. North Pharm.* 16 (04), 44–45. [In Chinese].

Liu, L., Duan, J., Tang, Y., Ma, H., Su, S., and Li, X. (2011). Study on Antioxidant Effect and Chemical Constituents of Taohong Siwu Decoction. *Zhongguo Zhong Yao Za Zhi* 36 (12), 1591–1595. [In Chinese]. doi:10.4268/cjcmm20111209

Liu, L., Duan, J. A., Su, S. L., Liu, P., Tang, Y. P., and Qian, D. W. (2016). Effect of Different Fractions of Taohong Siwu Decoction on ADP-Induced Platelet Aggregation and Thrombin Activity. *Zhongguo Zhong Yao Za Zhi* 41 (04), 716–721. [In Chinese]. doi:10.4268/cjcmm20160429

Liu, L. (2018). The Influence of TCM Comprehensive Therapy on Cardiac Function and Myocardial Ischemia-Reperfusion in Patients with Coronary Heart Disease after Percutaneous Coronary Intervention. *Henan Traditional Chin. Med.* 38 (10), 1511–1514. [In Chinese].

Liu, M., Ai, J., Feng, J., Zheng, J., Tang, K., Shuai, Z., et al. (2019). Effect of Paeoniflorin on Cardiac Remodeling in Chronic Heart Failure Rats through the Transforming Growth Factor β1/Smad Signaling Pathway. *Cardiovasc. Diagn. Ther.* 9 (3), 272–280. doi:10.21037/cdt.2019.06.01

Liu, M., Feng, J., Du, Q., Ai, J., and Lv, Z. (2020). Paeoniflorin Attenuates Myocardial Fibrosis in Isoprenaline-Induced Chronic Heart Failure Rats via Inhibiting P38 MAPK Pathway. *Curr. Med. Sci.* 40 (2), 307–312. doi:10.1007/s11596-020-2178-0

Liu, X., Chen, K., Zhuang, Y., Huang, Y., Sui, Y., Zhang, Y., et al. (2019). Paeoniflorin Improves Pressure Overload-Induced Cardiac Remodeling by Modulating the MAPK Signaling Pathway in Spontaneously Hypertensive Rats. *Biomed. Pharmacother.* 111, 695–704. doi:10.1016/j.biopha.2018.12.090

Liu, Y., Li, D., and Li, X. (2014). Study of Taohong Siwu Decoction Regulating Blood Flow for Arteriosclerosis Obliterans Model Rat. *Chin. Arch. Traditional Chin. Med.* 32 (04), 761–763. [In Chinese].

Liu, Y. (2015). Clinical Observation of Diltiazem Combined with Taohong Siwu Decoction in Treating Coronary Artery Spasm Angina Pectoris. *J. Community Med.* 13 (07), 29–30+72. [In Chinese].

Liu, Y., and Yin, H. (2014). The Use of Chinese Medicinal Herbs and Formulas that Activate Blood Circulation and Antiplatelet Therapies. *Chin. Sci. Bull.* 59 (08), 647–655. [In Chinese].

Liu, Y. (2015). Observation on the Therapeutic Effect of Taohong Siwu Decoction and Shixiao Powder in Treating Thoracic Obstruction and Heartache. *Cardiovasc. Dis. Electron. J. Integrated Traditional Chin. West. Med.* 3 (18), 53+55. [In Chinese].

Liu, Z. Q., Yin, D. K., Han, L., Li, B. K., and Peng, D. Y. (2013). Protective Effect of Medicated Serum Prepared with Taohong Siwu Tang on Hydrogen Peroxide-Induced Human Umbilical Vein Endothelial Cells. *Zhongguo Zhong Yao Za Zhi* 38 (03), 402–406. [In Chinese].

Lujuan, W. M., and Wang, P. (2018). Effect of Taohong Siwu Decoction on Serum Hs-CRP and Hemorheology in Patients with Coronary Heart Disease and Angina Pectoris. *Hainan Med. J.* 29 (22), 3129–3131. [In Chinese].

Luo, W., and Zhou, X. (2014). Qualitative and Quantitative Study of Blood Stasis Pathological and Huoxue Huayu Decoctions. *Lishizhen Med. Materia Med. Res.* 25 (02), 509–512. [In Chinese].

Luo, Y., Shang, P., and Li, D. (2017). Luteolin: A Flavonoid that Has Multiple Cardio-Protective Effects and its Molecular Mechanisms. *Front. Pharmacol.* 8, 692. doi:10.3389/fphar.2017.00692

Luo, Z. R., Li, H., Xiao, Z. X., Shao, S. J., Zhao, T. T., Zhao, Y., et al. (2019). Taohong Siwu Decoction Exerts a Beneficial Effect on Cardiac Function by Possibly Improving the Microenvironment and Decreasing Mitochondrial Fission after Myocardial Infarction. *Cardiol. Res. Pract.* 2019, 5198278. doi:10.1155/2019/5198278

Ma, Z. C., Hong, Q., Wang, Y. G., Tan, H. L., Xiao, C. R., Liang, Q. D., et al. (2010). Ferulic Acid Protects Human Umbilical Vein Endothelial Cells from Radiation Induced Oxidative Stress by Phosphatidylinositol 3-kinase and Extracellular Signal-Regulated Kinase Pathways. *Biol. Pharm. Bull.* 33 (1), 29–34. doi:10.1248/bpb.33.29

Mao, H. (2016). Research Progress on the Mechanism of Taohong Siwu Decoction in the Treatment of Coronary Atherosclerotic Heart Disease. *Glob. Traditional Chin. Med.* 9 (09), 1145–1148. [In Chinese].

Martos, R., Baugh, J., Ledwidge, M., O'Loughlin, C., Murphy, N. F., Conlon, C., et al. (2009). Diagnosis of Heart Failure with Preserved Ejection Fraction: Improved Accuracy with the Use of Markers of Collagen Turnover. *Eur. J. Heart Fail.* 11 (2), 191–197. doi:10.1093/eurjhf/hfn036

Meng, H., Guo, J., Sun, J. Y., Pei, J. M., Wang, Y. M., Zhu, M. Z., et al. (2008). Angiogenic Effects of the Extracts from Chinese Herbs: Angelica and

Chuanxiong. *Am. J. Chin. Med.* 36 (3), 541–554. doi:10.1142/S0192415X08005965

Task Force MembersMontalescot, G., Sechtem, U., Achenbach, S., Andreotti, F., Arden, C., Budaj, A., et al. (20132013). 2013 ESC Guidelines on the Management of Stable Coronary Artery Disease: the Task Force on the Management of Stable Coronary Artery Disease of the European Society of Cardiology. *Eur. Heart J.* 34 (38), 2949–3003. doi:10.1093/eurheartj/eht296

Negre-Salvayre, A., Guerby, P., Gayral, S., Laffargue, M., and Salvayre, R. (2020). Role of Reactive Oxygen Species in Atherosclerosis: Lessons from Murine Genetic Models. *Free Radic. Biol. Med.* 149, 8–22. doi:10.1016/j.freeradbiomed.2019.10.011

Nie, X., and Cheng, Y. (2020). Review of Chemical Constituents,Pharmacological Effects and Clinical Applications of Taohong Siwutang and Predictive Analysis of its Quality Marker. *Chin. J. Exp. Traditional Med. Formulae* 26 (04), 226–234. [In Chinese].

Patel, R. V., Mistry, B. M., Shinde, S. K., Syed, R., Singh, V., and Shin, H. S. (2018). Therapeutic Potential of Quercetin as a Cardiovascular Agent. *Eur. J. Med. Chem.* 155, 889–904. doi:10.1016/j.ejmech.2018.06.053

Qian, G. Q., Ding, J., Zhang, X., Yin, X., Gao, Y., and Zhao, G. P. (2015). Preconditioning with Glycyrrhizic, Ferulic, Paeoniflorin, Cinnamic Prevents Rat Hearts from Ischemia/reperfusion Injury via Endothelial Nitric Oxide Pathway. *Pharmacogn Mag.* 11 (42), 292–296. doi:10.4103/0973-1296.153081

Qian, Q. D·W. (1980). *The Golden Mirror of Medicine [M]*. Beijing: People's Medical Publishing House, 13. [In Chinese].

Raedschelders, K., Ansley, D. M., and Chen, D. D. (2012). The Cellular and Molecular Origin of Reactive Oxygen Species Generation during Myocardial Ischemia and Reperfusion. *Pharmacol. Ther.* 133 (2), 230–255. doi:10.1016/j.pharmthera.2011.11.004

Renhua, N., and Li, Y. (2017). Therapeutic Effect of Taohong Siwu Decoction and Ozagrel Sodium in the Treatment of Angina Pectoris (Instability). *Biped and Health* 26 (12), 173–174. [In Chinese].

Roslan, J., Giribabu, N., Karim, K., and Salleh, N. (2017). Quercetin Ameliorates Oxidative Stress, Inflammation and Apoptosis in the Heart of Streptozotocin-Nicotinamide-Induced Adult Male Diabetic Rats. *Biomed. Pharmacother.* 86, 570–582. doi:10.1016/j.biopha.2016.12.044

Rui, Y. (2002). Taohong Siwu Decoction Combined with Venomin Antiembolic Enzyme in the Treatment of Non-stable Heart Pain. *Liaoning J. Traditional Chin. Med.* (11), 674–675. [In Chinese].

Ruiz, L. M., Salazar, C., Jensen, E., Ruiz, P. A., Tiznado, W., Quintanilla, R. A., et al. (2015). Quercetin Affects Erythropoiesis and Heart Mitochondrial Function in Mice. *Oxid Med. Cel Longev* 2015, 836301. doi:10.1155/2015/836301

Sanada, S., Komuro, I., and Kitakaze, M. (2011). Pathophysiology of Myocardial Reperfusion Injury: Preconditioning, Postconditioning, and Translational Aspects of Protective Measures. *Am. J. Physiol. Heart Circ. Physiol.* 301 (5), H1723–H1741. doi:10.1152/ajpheart.00553.2011

Shen, A., and Shi, H. (2019). Regulation of NF-kB Signal Pathway and protection of Cardiac Structure and Function of Type 2 Diabetes Mellitus Rat by Treating with Taohong Siwu Decoction. *China J. Traditional Chin. Med. Pharm.* 34 (04), 1359–1362. [In Chinese].

Siwik, D. A., Chang, D. L., and Colucci, W. S. (2000). Interleukin-1beta and Tumor Necrosis Factor-Alpha Decrease Collagen Synthesis and Increase Matrix Metalloproteinase Activity in Cardiac Fibroblasts *In Vitro*. *Circ. Res.* 86 (12), 1259–1265. doi:10.1161/01.res.86.12.1259

Song, H. (2010). Treatment of 60 Cases of Qi Deficiency and Blood Stasis Syndrome with Baoyuan Decoction and Taohong Siwu Decoction. *J. Traditional Chin. Med.* 51 (12), 1107–1108. [In Chinese].

Song, Y., Zhang, L., and Qu, K. (2005). Hydroxysafflor Yellow A Promotes Vascular Endothelial Cell Proliferation via VEGF/VEGF Receptor. *J. Chin. Pharm. Sci.* 14 (3), 181–185.

Tan, Z., Jiang, X., Zhou, W., Deng, B., Cai, M., Deng, S., et al. (2021). Taohong Siwu Decoction Attenuates Myocardial Fibrosis by Inhibiting Fibrosis Proliferation and Collagen Deposition via TGFBR1 Signaling Pathway. *J. Ethnopharmacol* 270, 113838. doi:10.1016/j.jep.2021.113838

Tegn, N., Abdelnoor, M., Aaberge, L., Endresen, K., Smith, P., Aakhus, S., et al. (2016). Invasive versus Conservative Strategy in Patients Aged 80 Years or Older with Non-ST-elevation Myocardial Infarction or Unstable Angina Pectoris (After Eighty Study): an Open-Label Randomised Controlled Trial. *Lancet* 387 (10023), 1057–1065. doi:10.1016/S0140-6736(15)01166-6

TIu, S., Grigor'ev, A. M., and Ivanov, S. V. (2013). The Dynamics of C-Reactive Protein in the Process of Coronary Artery Bypass Grafting in Patients with Ischemic Heart Disease. *Klin Lab. Diagn.* 33 (3), 3–6.

Toya, S. P., and Malik, A. B. (2012). Role of Endothelial Injury in Disease Mechanisms and Contribution of Progenitor Cells in Mediating Endothelial Repair. *Immunobiology* 217 (5), 569–580. doi:10.1016/j.imbio.2011.03.006

Wang, F., and Han, L. (2017). Effect of Taohong Siwutang on Contents of ET-1,Ang-1 and VEGF in Serum of Cerebral Ischemia Rats. *Chin. J. Exp. Traditional Med. Formulae* 23 (01), 101–106. [In Chinese].

Wang, G., Dai, G., Song, J., Zhu, M., Liu, Y., Hou, X., et al. (2018). Lactone Component from Ligusticum Chuanxiong Alleviates Myocardial Ischemia Injury through Inhibiting Autophagy. *Front. Pharmacol.* 9, 301. doi:10.3389/fphar.2018.00301

Wang, G., and Wang, Y. (2008). Taohong Siwu Decoction Combined with Shuxuening in Treating Unstable Angina Pectoris. *China Med. Herald* (12), 49. [In Chinese].

Wang, H. (2018). Effect of Taohong Siwu Decoction and Xiebai Banxia Decoction Combined with Atorvastatin in Treating 63 Cases of Coronary Heart Disease. *J. Electrocardiogram(Electronic Edition)* 7 (04), 109–110. [In Chinese].

Wang, H., Luo, Y., and Wang, Y. (2018). Effect of Taohong Siwu Decoction and Baoyuan Decoction in Treating Patients of Qi-Deficiency and Blood-Stasis Syndrome Coronary Heart Disease after PCI with Left Ventricular Systolic Dysfunction. *Clin. J. Traditional Chin. Med.* 30 (12), 2274–2277. [In Chinese].

Wang, H., and Peng, D. (2017). Identification of Effective Constituents of Taohong Siwu Decoction in Rat Plasma by Liquid Chromatography-Tandem Mass Spectrometry. *J. Anhui Univ. Chin. Med.* 36 (03), 69–73. [In Chinese].

Wang, J., and Li, Z. (2017). Clinical Effect Observation of Shenfu Decoction Combine with Taohong Siwu Decoction in Treating Chronic Cardiac Failure and the Syndrome of Deficiency of Heart Yang and Blood Stasis. *Clin. J. Traditional Chin. Med.* 29 (11), 1887–1889. [In Chinese].

Wang, S., and Zhai, J. (2016). Observation on the Effect of Taohong Siwu Decoction and Gualou Xiebai Banxia Decoction in Patients with Angina Pectoris. *Cardiovasc. Dis. Electron. J. Integrated Traditional Chin. West. Med.* 4 (23), 16–17. [In Chinese].

Wang, S. (2016). Randomized Parallel Contrast Study of Joint Effect of Gualou Xiebai Banxia Decoction and Taohong Siwu Decoction as Well as Western Medicine on Phlegm Turbid-Blood Stasis Thoracic Obstruction. *J. Pract. Traditional Chin. Intern. Med.* 30 (07), 52–54. [In Chinese].

Wang, X., and Jiang, H. (2019). Time-dose Effects of Taohong Siwu Decoction on Number and Functional Activity of Peripheral Blood Endothelial Progenitor Cells. *Chin. J. Tissue Eng. Res.* 23 (09), 1354–1358. [In Chinese].

Wang, Y., Zhang, J., and Liu, L. (2020). Effect of Taohong Siwu Decoction on Stable Angina Pectoris with Heart Failure. *Shaanxi J. Traditional Chin. Med.* 41 (05), 625–628. [In Chinese].

Wang, Y., and Wang, S. (2018). Clinical Research on Baoyuan Decoction, Taohong Siwu Decoction and Metoprolol in the Treatment of Angina Pectoris Due to Coronary Heart Disease with Qi Deficiency and Blood Stasis Syndrome. *Chin. J. Integr. Med. Cardio-Cerebrovascular Dis.* 16 (18), 2652–2656. [In Chinese].

Wang, Z., and Fu, D. (2017). Clinical Effects of Taohong-Siwu Decoction on Stable Coronary Heart Disease with Blood Stasis Type. *Hebei J. Traditional Chin. Med.* 39 (04), 506–510. [In Chinese].

Wang, Z., and Zhang, L. (2018). Progress in Myocardial Ischemia and Reperfusion Injury. *Chin. J. Gerontol.* 38 (06), 1532–1535. [In Chinese].

Wang, Z. (2021). Research Progress on Pharmacological Action of Taohong Siwu Decoction. *Mod. Traditional Chin. Med.* 41 (02), 22–28. [In Chinese].

WangChen, J., and Han, L. (2019). Content Determination of Six Index Components in Taohong Siwu Decoction. *J. Anhui Univ. Chin. Med.* 38 (02), 80–85. [In Chinese].

Wong, H. S., Chen, N., Leong, P. K., and Ko, K. M. (2014). β-Sitosterol Enhances Cellular Glutathione Redox Cycling by Reactive Oxygen Species Generated from Mitochondrial Respiration: protection against Oxidant Injury in H9c2 Cells and Rat Hearts. *Phytother Res.* 28 (7), 999–1006. doi:10.1002/ptr.5087

Wu, B., Song, H., Fan, M., You, F., Zhang, L., Luo, J., et al. (2020). Luteolin Attenuates Sepsis-induced M-yocardial injury by E-nhancing A-utophagy in M-ice. *Int. J. Mol. Med.* 45 (5), 1477–1487. doi:10.3892/ijmm.2020.4536

Wu, F., Ye, B., Wu, X., Lin, X., Li, Y., Wu, Y., et al. (2020). Paeoniflorin on Rat Myocardial Ischemia Reperfusion Injury of Protection and Mechanism Research. *Pharmacology* 105 (5-6), 281–288. doi:10.1159/000503583

Wu, H., Qi, Y., and Li, W. (2014). Effect of Serum Containing Modified Taohong Siwu Decoction on Function of Vascular Endothelial Cells in Rat Model of Atherosclerosis and Blood Stasis Syndrome. *Hunan J. Traditional Chin. Med.* 30 (09), 142–145. [In Chinese].

Wu, M., and Su, W. (2020). Clinical Study on Treatment of Stable Angina Pectoris with Qi Deficiency and Blood Stasis Syndrome by Integrated Traditional Chinese and Western Medicine. *Med. Diet Health* 18 (10), 26–27. [In Chinese].

Wu, Y. (2011). Progress in Chemical Composition and Pharmacological Action of Taohong Siwu Decoction. *Chin. Traditional Patent Med.* 33 (11), 1965–1968. [In Chinese].

Xia, J., and Dong, Li (2019). Advances in Myocardial Ischemia-Reperfusion Injury. *Chin. J. Integr. Med. Cardio-Cerebrovascular Dis.* 17 (21), 3329–3334. [In Chinese].

Xiang, Y., and Shi, L. (2021). Basic and Clinical Research Progress of Taohong Siwu Decoction in the Treatment of Cardiovascular Diseases. *Hunan J. Traditional Chin. Med.* 37 (05), 179–181. [In Chinese].

Xiao, X., and Chen, Z. (2015). Zhenwu Decoction and Taohongsiwu Decoction on Yang Deficiency and Blood Stasis of Blood BNP in Patients with Chronic Congestive Heart Failure. *J. Changchun Univ. Chin. Med.* (6), 1186–1188. [In Chinese].

Xiao, X., Gao, Z., and Ma, Z. (2016). The Influence of Peach Kernel and Carthamus Four Substances Decoction on NT-Pro-BNP of Syndrome of Blood Stasis Due to Chronic Heart Failure. *Henan Traditional Chin. Med.* 36 (06), 996–998. [In Chinese].

Xiao, X., and Gao, Z. (2017). The Influence of True Warrior Decoction Combined with Four Substances Decoction on Myocardial Remodeling of Chronic Congestive Heart Failure with Syndrome of Yang Deficiency and Blood Stasis. *Henan Traditional Chin. Med.* 37 (10), 1746–1748. [In Chinese].

Xiaoxia, C. (2010). Taohong Siwu Decoction Induces Endothelial Cells Proliferation and its Premiliary Mechanisms. *Strait Pharm. J.* 22 (01), 39–41. [In Chinese].

Xie, H., and Luo, W. (2008). Effect of Xuefu Zhuyu Decoction and its Parts on Serum Lipid and Hemodynamics in Rabbits with Experimental Atherosclerosis. *J. Hunan Univ. Chin. Med.* (02), 13–15. [In Chinese].

Xiong, Y. (2014). White Peach Siwu Decoction and Fructus Scallions Pinellia Soup Treatment of Coronary Heart Disease (CHD) and 40 Cases of Clinical Observation. *J. Pract. Traditional Chin. Intern. Med.* 28 (01), 46–47. [In Chinese].

Xu, M., Li, X., and Song, L. (2020). Baicalin Regulates Macrophages Polarization and Alleviates Myocardial Ischaemia/reperfusion Injury via Inhibiting JAK/STAT Pathway. *Pharm. Biol.* 58 (1), 655–663. doi:10.1080/13880209.2020.1779318

Xu, M. (2014). Research on Main Mechanisms of MIRI and Related Drug Therapy. *Pract. Pharm. Clin. Remedies* 17 (08), 1052–1056. [In Chinese].

Yan, J., Zhang, Y., and Wang, D. (2012). Clinical Observation at Shengmai Powder Taohong Siwu Decoction Combined with Western Medicine in the Treatment of Angina Pectoris of Coronary Heart Disease(CHD). *J. Pract. Traditional Chin. Intern. Med.* 26 (08), 34–35. [In Chinese].

Yang, H., Wang, K., and Liu, Y. (2019). Effects of Taohong Siwu Decoction and Ginkgo Biloba Damo on Hemorheology and Serum Inflammatory Factor in Patients with Angina Pectoris of Heart Blood Stasis Type. *J. Basic Chin. Med.* 25 (03), 340–343. [In Chinese].

Yang, H., Hu, Y., and Guo, C. (2011). Determination of Total Phenolic Acid Content in Ethanol Extract and Water Extract of Taohong Siwu Decoction and Removal of DPPH Free Radical Activity. *Lishizhen Med. Materia Med. Res.* 22 (06), 1439–1440. [In Chinese].

Yang, J. (2007). Therapeutic Effect Observation of 154 Cases of Coronary Artery Disease Angina Using Taohongsiwutang (THSW). *China J. Mod. Med.* (18), 2268–2269+2275. [In Chinese].

Yang, L. (2019). To Observe the Clinical Efficacy of Taohong Siwu Decoction Combined with Conventional Western Medicine in the Treatment of Angina Pectoris of Coronary Heart Disease. *World Latest Med. Inf.* 19 (64), 192+194. [In Chinese].

Yang, W., Chen, Q., and Yang, L. (2014). Clinical Observation on 78 Cases of Angina Pectoris Treated with Taohong Siwu Decoction and Gualou Xiebai Banxia Decoction. *Pract. Clin. J. Integrated Traditional Chin. West. Med.* 14 (09), 8–9. [In Chinese].

Yang, Y., and Zhou, J. (2019). Evaluation of Anti-platelet Efficacy of Taohong Siwu Decoction and Clopidogrel in Patients with Stable Coronary Heart Disease after Percutaneous Coronary Intervention. *Chin. J. Integr. Med. Cardio-Cerebrovascular Dis.* 17 (23), 3649–3653. [In Chinese].

Yasuda, H. (2008). Solid Tumor Physiology and Hypoxia-Induced Chemo/radio-Resistance: Novel Strategy for Cancer Therapy: Nitric Oxide Donor as a Therapeutic Enhancer. *Nitric Oxide* 19 (2), 205–216. doi:10.1016/j.niox.2008.04.026

Yayan, J. (2013). Emerging Families of Biomarkers for Coronary Artery Disease: Inflammatory Mediators. *Vasc. Health Risk Manag.* 9, 435–456. doi:10.2147/VHRM.S45704

Yi, L., and Peng, D. (2011). Progress in Pharmacological of Taohong Siwu Decoction. *Anhui Med. Pharm. J.* 15 (05), 529–531. [In Chinese].

Yin, D., and Yang, Y. (2012). Effect of Taohong Siwu Decoction on VEGF and Endostatin Release from Platelet by Proteinase-Activated Receptors Agonist. *Chin. Traditional Patent Med.* 34 (09), 1631–1635. [In Chinese].

Yu, H., Chen, B., and Ren, Q. (2019). Baicalin Relieves Hypoxia-Aroused H9c2 Cell Apoptosis by Activating Nrf2/HO-1-Mediated HIF1α/BNIP3 Pathway. *Artif. Cell Nanomed Biotechnol* 47 (1), 3657–3663. doi:10.1080/21691401.2019.1657879

Yu, S. (2015). Clinical Research on Peach Kernel and Carthamus Four Substances Decoction Combined with Conventional Western Medicine for Treating Angina Pectoris in Coronary Heart Disease. *Henan Traditional Chin. Med.* 35 (07), 1527–1529. [In Chinese].

Yu, Y. (2012). Clinical Observation of Taohong Siwu Decoction Combined with Danshen Injection in the Treatment of Angina Pectoris of Coronary Heart Disease. *Chin. Foreign Med. Res.* 10 (09), 114. [In Chinese].

Yu, Y., and Hong, B. (2016). Taohongsiwu Decoction Combined with Trimetazidine on Patients with Type 2 Diabetic Cardiomyopathy of Yin Deficiency and Blood Stasis Syndrome and Oxidative Stress. *Jilin J. Chin. Med.* 36 (02), 131–135. [In Chinese].

Yuan, L., and Fan, L. (2019). Clinical Observation of Addition and Subtraction Therapy of Taohong Siwutang Combined with Chaihu Shugansan to Unstable Angina Pectoris with Type A Behavior Pattern. *Chin. J. Exp. Traditional Med. Formulae* 25 (18), 89–94. [In Chinese].

Yue, C. (2014). Taohong Siwu Decoction and Shexiang Baoxin Pills in the Treatment of 70 Cases of Qi and Blood Stasis Type of Chest Arthralgia and Heartache. *China Pharmaceuticals* 23 (10), 84–85. [In Chinese].

Zang, G., and He, J. (2015). Serum Hcy Level in Patients with Angina and its Relationship with Coronary Artery Lesions Degree, Serum Inflammatory Cytokines Levels. *Hainan Med. J.* 26 (22), 3301–3303. [In Chinese].

Zhai, J., and Guo, Y. (2016). Paeoniflorin Attenuates Cardiac Dysfunction in Endotoxemic Mice via the Inhibition of Nuclear Factor-Kb. *Biomed. Pharmacother.* 80, 200–206. doi:10.1016/j.biopha.2016.03.032

Zhang, B. (2014). Effect of Medicated Serum Prepared with Taohong Siwu Decoction on Expressions of TNF-A, MCP-1 and IL-1B of Human Umbilical Vein Endothelial Cells Treated with Lipopolysaccharide. *Liaoning J. Traditional Chin. Med.* 41 (11), 2280–2283. [In Chinese].

Zhang, D. (2014). Clinical Application of Taohong Siwu Decoction. *J. Liaoning Univ. Traditional Chin. Med.* 16 (11), 217–219. [In Chinese].

Zhang, G., and Zhu, W. (2003). Experimental Study of Taohong Siwu Decoction on Anti-acute Myocardial Ischemia. *Chin. Arch. Traditional Chin. Med.* (09), 1425–1451. [In Chinese].

Zhang, H., and Wang, H. (2011). Effects and Mechanism Explore of Taohong Siwu Decoction. *Clin. J. Chin. Med.* 3 (18), 51–52. [In Chinese].

Zhang, J., and Li, S. (2015). Advantages of Traditional Chinese Medicine in Treating Myocardial No-Reflow after Acute Myocardial Infarction/reperfusion. *Chin. J. New Drugs* 24 (03), 276–280. [In Chinese].

Zhang, J. Y., Li, P., and Li, Y. K. (2012). Protective Effects of Paeonol, Paeoniflorin and Their Compatibility on *In Vitro* Cultured Cardiomyocytes Suffering from Hypoxia-Reoxygenation Injury. *Zhongguo Zhong Xi Yi Jie He Za Zhi* 32 (04), 510–514. [In Chinese].

Zhang, M., Malik, A. B., and Rehman, J. (2014). Endothelial Progenitor Cells and Vascular Repair. *Curr. Opin. Hematol.* 21 (3), 224–228. doi:10.1097/MOH.0000000000000041

Zhang, Y. (2019). Therapeutic Evaluation of Baoyuan Decoction and Taohong Siwu Decoction on Qi Deficiency and Blood Stasis of Chest Obstruction

and Heart Pain. *Inner Mongolia J. Traditional Chin. Med.* 38 (04), 14–15. [In Chinese].

Zhang, Z. (2018). Clinical Observation on the Treatment of Stable Angina Pectoris of Coronary Heart Disease with Qi Deficiency and Blood Stasis Syndrome by Integrated Traditional Chinese and Western Medicine. *Yunnan J. Traditional Chin. Med. Materia Med.* 39 (02), 29–30. [In Chinese].

Zhang, Z., and Peng, D. (2011). Clinical Application of Taohong Siwu Decoction. *Anhui Med. Pharm. J.* 15 (09), 1162–1165. [In Chinese].

Zhao, Q. (2018). Clinical Analysis of Taohong Siwu Decoction and Gualou Xiebai Banxia Decoction in the Treatment of Patients with Angina Pectoris. *Electron. J. Clin. Med. Lit.* 5 (41), 165. [In Chinese].

Zhao, Z., and Liu, Q. (2019). Research Progress on the Effective Material Basis and Quality Control Methods of Taohong Siwu Decoction. *J. Chin. Med. Mater.* 42 (11), 2730–2735. [In Chinese].

Zhaojie, J., and Han, L (2018). Protective Effect and Mechanism of Taohong Siwutang on OGD-Induced Injury of Human Brain Microvascular Endothelial Cells. *Chin. J. Exp. Traditional Med. Formulae* 24 (07), 95–100. [In Chinese].

Zheng, G., Wang, J., and Li, J. (2010). Therapeutic Effect of Taohong Siwu Decoction and Astragalus Membranaceus on Unstable Angina Pectoris. *Chin. J. Traditional Med. Sci. Tech.* 17 (04), 357–358. [In Chinese].

Zheng, Q., Huang, Y. Y., Zhu, P. C., Tong, Q., Bao, X. Y., Zhang, Q. H., et al. (2018). Ligustrazine Exerts Cardioprotection in Animal Models of Myocardial Ischemia/Reperfusion Injury: Preclinical Evidence and Possible Mechanisms. *Front. Pharmacol.* 9, 729. doi:10.3389/fphar.2018.00729

Zhou, H., Yang, H. X., Yuan, Y., Deng, W., Zhang, J. Y., Bian, Z. Y., et al.(2013). Paeoniflorin Attenuates Pressure Overload-Induced Cardiac Remodeling via Inhibition of TGFβ/Smads and NF-Kb Pathways. *J. Mol. Histol.* 44 (3), 357–367. doi:10.1007/s10735-013-9491-x

Zhou, M., Ren, H., Han, J., Wang, W., Zheng, Q., and Wang, D. (2015). Protective Effects of Kaempferol against Myocardial Ischemia/Reperfusion Injury in Isolated Rat Heart via Antioxidant Activity and Inhibition of Glycogen Synthase Kinase-3β. *Oxid Med. Cel Longev* 2015, 481405. doi:10.1155/2015/481405

Zhou, X. (2003). Effect of the Five Recipes for Promoting Blood Circulation for Removing Blood Stasis on Serum Lipid and Apoprotein in Experimental Acheriosclerosis Rabbits. *Chin. J. Inf. Traditional Chin. Med.* (04), 29–31. [In Chinese].

Zhou, Y., and Liu, B. (2011). Influence of Taohong Siwu Decoction on Myocardium Interstitial Collagen Reconstitution after Acute Myocardial Infarction in Rats. *Chin. J. Exp. Traditional Med. Formulae* 17 (13), 152–155. [In Chinese].

Zhou, Y., and Shu, J. (2017). Observation on Curative Effect of Gualou Xiebai Banxia Decoction and Taohong Siwu Decoction in Treating Stable Angina Pectoris of Phlegm Blocking and Blood Stasis. *J. Guangxi Univ. Chin. Med.* 20 (02), 5–6. [In Chinese].

Zhu, W., and Zhang, G. (2003). Experimental Study of Taohong Siwu Decoction on Anti-acute Myocardial Ischemia. *J. Shanxi Univ. Chin. Med.* (02), 20–21. [In Chinese].

Zhu, X., Ying, L., and Jia, J. (2011). Treatment of 40 Cases of Acute Coronary Syndrome with Gualou Xiebai Banxia Decoction and Taohong Siwu Decoction. *Shaanxi J. Traditional Chin. Med.* 32 (06), 649–651. [In Chinese].

Conflict of Interest: The authors declare that the research was conducted in the absence of any commercial or financial relationships that could be construed as a potential conflict of interest.

Publisher's Note: All claims expressed in this article are solely those of the authors and do not necessarily represent those of their affiliated organizations, or those of the publisher, the editors and the reviewers. Any product that may be evaluated in this article, or claim that may be made by its manufacturer, is not guaranteed or endorsed by the publisher.

frontiers in Pharmacology

ORIGINAL RESEARCH
published: 18 March 2022
doi: 10.3389/fphar.2022.862017

Polydatin Glycosides Improve Monocrotaline-Induced Pulmonary Hypertension Injury by Inhibiting Endothelial-To-Mesenchymal Transition

Xing Chen[1,2]*, *Yao He*[1,2], *Zhijie Yu*[1,2], *Jianli Zuo*[1,2], *Yan Huang*[1,2], *Yi Ruan*[1,2], *Xiaoyuan Zheng*[1,2]* and *Yu Ma*[3]*

[1]Pharmacy Department, Chongqing Emergency Medical Center, Chongqing, China, [2]Pharmacy Department, Chongqing University Central Hospital, Chongqing, China, [3]Chongqing Emergency Medical Center, Chongqing, China

OPEN ACCESS

Edited by:
Ali H. Eid,
Qatar University, Qatar

Reviewed by:
Rajamma Mathew,
New York Medical College, United States
Gianfranco Pintus,
University of Sharjah, United Arab Emirates

***Correspondence:**
Xing Chen
729159845@qq.com
Xiaoyuan Zheng
XiaoyuanZheng20@126.com
Yu Ma
492972575@qq.com

Specialty section:
This article was submitted to Cardiovascular and Smooth Muscle Pharmacology, a section of the journal Frontiers in Pharmacology

Received: 25 January 2022
Accepted: 21 February 2022
Published: 18 March 2022

Citation:
Chen X, He Y, Yu Z, Zuo J, Huang Y, Ruan Y, Zheng X and Ma Y (2022) Polydatin Glycosides Improve Monocrotaline-Induced Pulmonary Hypertension Injury by Inhibiting Endothelial-To-Mesenchymal Transition. Front. Pharmacol. 13:862017. doi: 10.3389/fphar.2022.862017

Objective: To study the effect of polydatin on the injury of pulmonary arterial hypertension (PAH) induced by monocrotaline (MCT).

Methods: SD rats were induced to develop PAH injury by a single subcutaneous injection of MCT (60 mg/kg). From the second day, rats in the administration group were orally given sildenafil (20 mg/kg) and polydatin (30 or 60 mg/kg) for 3 weeks. At the end of the experiment, right ventricular hypertrophy (RVH) index of SD rats was calculated, pathological damage was assessed by HE staining, transcription levels of target genes were detected by RT-PCR and Elisa, and expression levels of Endothelial-to-mesenchymal transition (EndMT) related proteins were detected by immunohistochemistry (IHC) and immunofluorescence (IF). Finally, molecular docking analysis was used to verify the interaction of polydatin on the main targets.

Results: Polydatin could significantly restore the body function, reduce MCT-induced PAH injury, reduce serum biochemical indices; polydatin could effectively inhibit EndMT process by decreasing the expression of N-cadherin, β-catenin and vimentin; polydatin could down-regulate TAGLN expression and increase PECAM1 expression to reduce pulmonary vascular remodeling. The interaction between polydatin and EndMT target was confirmed by molecular docking operation.

Conclusion: Pharmacological experiments combined with Combining molecular docking was first used to clarify that polydatin can reduce the pulmonary endothelial dysfunction and pulmonary vascular remodeling induced by MCT by inhibiting EndMT. The results of the study provide new ideas for the further treatment of PAH injury.

Keywords: polydatin, pulmonary arterial hypertension, EndMT, HIF-2α, Arg1

INTRODUCTION

Pulmonary hypertension (PAH) is still a progressive disease that seriously threatens the lives of patients. The initial symptoms of PAH are shortness of breath, fatigue and angina. With the increase of pulmonary vascular resistance, the load of right ventricle (RV) increases, which is pathologically manifested as right ventricular hypertrophy, pulmonary endothelial dysfunction and pulmonary vascular remodeling, and ultimately leads to right ventricular failure and death (del Valle and DuBrock, 2021). According to the latest global epidemiological research, the incidence of PAH are crudely estimated at 5 cases per million adults (Hoeper et al., 2016). Current therapeutic drugs, such as prostacyclin, endothelin, and nitric oxide pathways, mainly focus on improving vasodilator properties and improving cardiopulmonary function, but cannot prevent or reverse the development of PAH. The 1-year, 3-years, and 5-years survival rates of PAH patients receiving drug therapy are 85, 68, and 57%, respectively (Benza et al., 2012; Zheng et al., 2020). Therefore, exploring and elucidating the pharmacotherapy of PAH injury has profound significance for greatly reducing the incidence of PAH.

Within the settings of cardiovascular biology, Endothelial-mesenchymal transition (EndMT) plays a role in various diseases, including valvular heart disease, myocardial fibrosis, myocardial infarction and atherosclerosis. EndMT is also gradually implicated in the development and progression of PAH. Long-term chronic pressure and the internal environment of inflammatory mediators can trigger EndMT of endothelial cells. Specifically, it obtains mesenchymal cell markers, loses endothelial marker proteins (VE-cadherin, PECAM1, TIE1, and TIE2), and gains migration and invasion capabilities, ultimately contributing to the formation of obstructive intimal lesions (Good et al., 2015; Ranchoux et al., 2015). Vascular remodeling caused by endothelial cell proliferation disorder, endothelial barrier destruction and enhanced inflammatory cell infiltration are common features of PAH (Xue et al., 2020). A large number of studies have emphasized the important role of EndMT in the pathology of PAH, including human PAH and PAH experimental models (Van et al., 2014; Xue et al., 2020). The presence of transitional EndMT cells in the pulmonary vasculature of PAH patients, underscoring their important contribution to vascular remodeling and fibrosis (Thuan et al., 2018). Therefore, improving endothelial dysfunction and inhibiting EndoMT may become a new direction for research and treatment of PAH.

Polydatin, a natural stilbene compound extracted from the root of polygonum cuspidatum, possesses many pharmacological activities, such as antioxidant, anti-inflammatory and improvement of microcirculation, and it has significant protective effects on lung, liver, nervous system and cardiovascular system (Zou et al., 2018; Fakhri et al., 2021; Gu et al., 2021). A large number of studies have confirmed that polydatin can play a direct vascular therapeutic role by reducing atherosclerotic vascular damage and inflammation (Peng et al., 2019; Wu et al., 2020), and it also reduce PAH in rats and improve pulmonary vascular hemodynamics against hypobaric and hypoxic PAH (Qing et al., 2009; Meng et al., 2009). Noteworthy, the latest experiments confirmed that polydatin can reduce the expression of c-Myc in human cervical cancer, inhibit cell migration and invasion, and partially reverse the EndMT of cervical cancer cells (Bai et al., 2021), and polydatin can reduce ROS and EndMT in cells exposed to high glucose, which play a therapeutic role in diabetic retinopathy (Giordo et al., 2021). Based on these findings, there is a hypothesis and tested whether polydatin can play a beneficial role in MCT-induced PAH in rats by inhibiting EndoMT and improving endothelial function (**Figure 1**).

METHODS

Animals

Specified pathogen-free (SPF) male Sprague-Dawley rats (180 ± 20 g) were purchased from Weitong Lihua Laboratory Animal Technology Co., Ltd. (Beijing, China). Rats were adaptively reared in groups of 8 per cage for 1 week under certain conditions (temperature: 25 ± 0.5°C, humidity: 55 ± 5%, 12 h: 12 h light-dark cycle), and freely available food and water were provided. The animal experiment procedures in this study were carried out in strict accordance with the guidelines of the "Guidelines for the Care and Use of Laboratory Animals" of the Ministry of Science and Technology of China.

Experimental Reagents

Endotoxin-free polydatin (**Figure 2A**, Purity ≧ 95%, CAS wkq21052105) purchased from Vikki Biotechnology Co., Ltd. (Sichuan, China). Monocrotaline (MCT) was purchased from Vikki Biotechnology Co., Ltd. (Sichuan, China). Sildenafil was purchased from Jinheng Pharmaceutical Co., Ltd. (Jilin, China). All reagents was dissolved in sodium chloride injection (NS 0.9%) and diluted to the corresponding concentration for subsequent treatment of SD rats.

Animal Model and Experimental Protocol

The rats were randomly divided into a control group, a model group, and an intervention group. Except the control group, the other rats were injected with MCT (60 mg/kg, ig) dissolved in normal saline to induce PAH injury (Jundong et al., 2011). From the second day, rats in each group were given corresponding drugs once a day. Specifically, the control group and model group were given normal saline 2 ml/kg, the positive drug group was given sildenafil 20 mg/kg, and the paeoniflorin low-dose group Paeoniflorin was given 30 mg/kg, and the paeoniflorin high-dose group was given paeoniflorin 60 mg/kg for 3 weeks. The rats eat and drink freely throughout the experiment, and record the weight change and growth status of the rats once a week, and comprehensively evaluate the degree of the model and the therapeutic effect after the last intragastric administration. After confirming the success of the experiment, the rats were injected with 10% chloral hydrate for euthanasia, and blood samples, lungs and heart tissues were collected.

Histopathological Examination

The isolated lungs were fixed and stored in 10% neutral formalin buffer, then embedded in paraffin to prepared into 5 μm thick sections. Hematoxylin-eosin (H&E) staining was performed according to standard procedures to assess the degree of pathological damage, then calculated the Ratio of Pulmonary Vascular Remodeling (PVR) = Vascular Wall area/total vascular area.

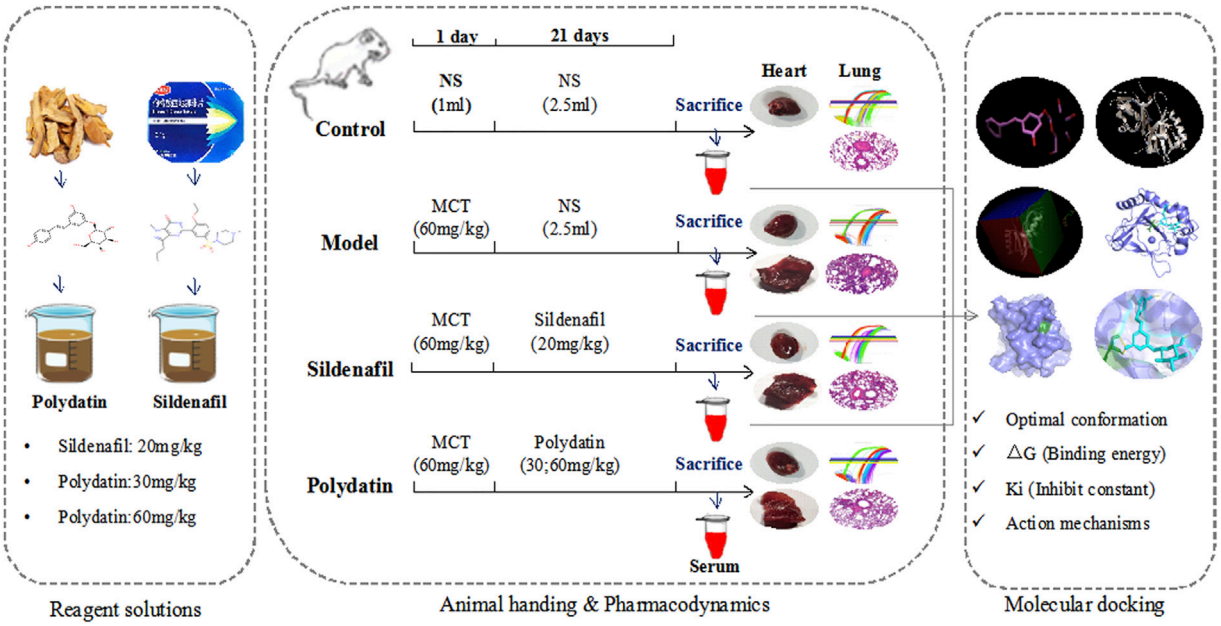

FIGURE 1 | Scheme of the study.

Right Ventricular Hypertrophy Detection

The isolated rat heart retains the ventricular tissue after removing the atrium. Separate the right ventricle and the left ventricle + septum along the interventricular groove, and after the filter paper absorbs the water, weigh the right ventricle (RV), left ventricle (LV), and diaphragm (S) respectively, and calculate the right ventricle hypertrophy index (RVHI) = RV/(LV + S).

Real-Time Quantitative PCR for mRNA Expressions

RNA extracts from frozen rat stomach tissues were used for microarray analysis. According to the manufacturer's protocol, total RNA was isolated using TRIzol reagent (Nordic Bioscience, Beijing,China) and converted into cDNA using a reverse transcription kit (Promega, Madison,United States). The primer sequences of BMPR2, PHD2, HIF-2α, Arginine1 (Arg1) are shown in **Table 1**. Add SYBR Green PCR Master Mix (Nordic Bioscience, Beijing,China) to the sample and perform RT-PCR analysis on the 7,500 fast real-time PCR system (Applied Biosystems, Foster City, CA, United States). Using GAPDH as the endogenous reference, calculate the relative amount of mRNA based on $2^{-\Delta\Delta}$CT.

Immunohistochemistry and Immunofluorescence

Paraffin sections of lung tissue were stained with polyclonal anti-N-cadherin, anti-β-catenin, anti-vimentin, anti-PECAM1 and anti-TAGLN (**Table 2**). Use NIS Elements imaging software version 4.0 (Olympus, Japan) to shoot and collect images at 100×, 200× magnification.

Enzyme-Linked Immunosorbent Assay

According to the ELISA kit (MLBIO biotechnology Co., Ltd., Shanghai, China) manufacturer's instructions, Synergy H1 Hybrid Reader (Biotech, United States) was used to determine the concentration of HIF-2α, Arg1 in rat serum. The indicated ligand concentration in the serum is calculated as pg of the ligand or ng/mL serum.

Molecular Docking Analysis

The 3D structures of the target protein and ligand are downloaded from the PDB database (https://www.rcsb.org/) and the ZINC database (https://zinc.docking.org/).Import AutoDockTools-1.5.6 to carry out the hydrogenation of the target protein and the removal of the water base of the ligand, and convert it into the PDBQT format. Use AutoDock vina software for molecular docking. The smaller the ΔG (Gibbs free binding energy) and Ki (Inhibit constant) values, the stronger the binding ability to the receptor. ΔG < -1.2 kcal/mol or ΔG < -5kj/mol indicates good binding affinity. Choose the model with the lowest free energy and use PyMOL for visual analysis.

Statistical Analysis

All measurement data were expressed as mean ± standard deviation (S.D.). One-way analysis of variance (ANOVA) was used for analysis in the SPSS software program (version 17.0; SPSS Inc., Chicago, IL, United States). The significance of the results was evaluated by the Bonferroni method. Specifically, $p < 0.05$ was considered statistically significant, and $p < 0.01$ was considered very significant. All results were visualized in GraphPad Prism software (version 6.02; Inc., San Diego, United States).

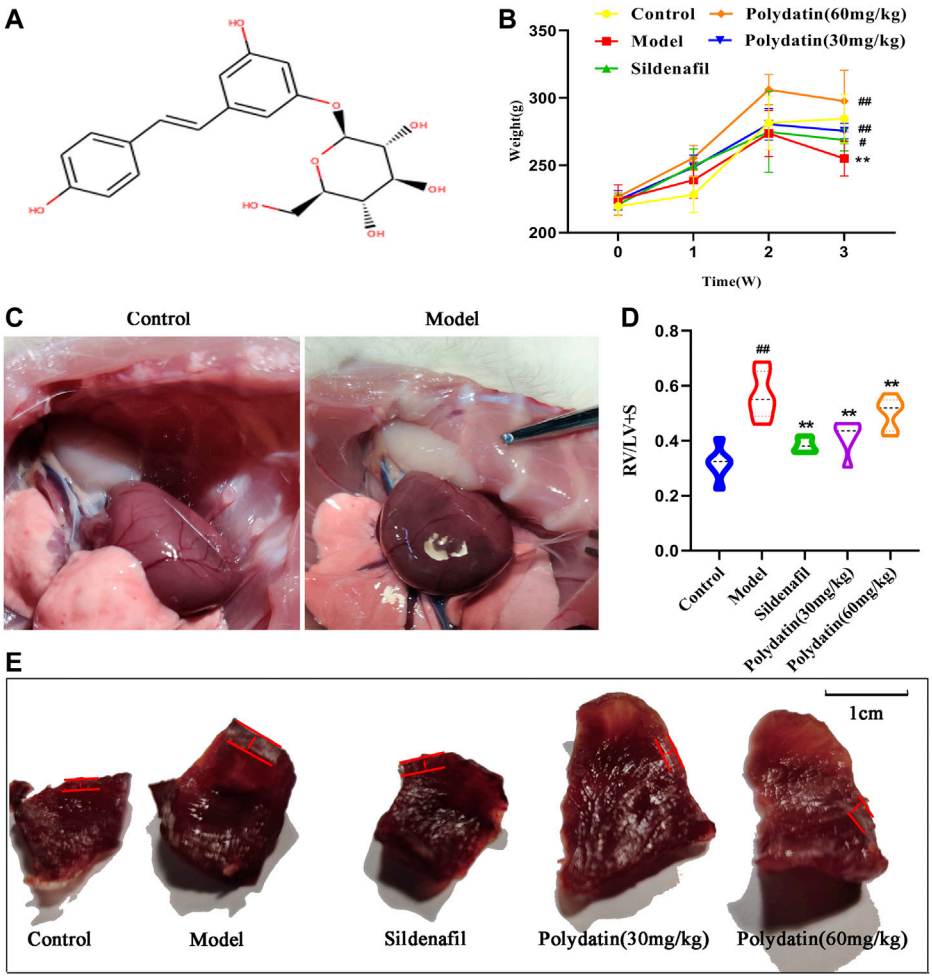

FIGURE 2 | Polydatin alleviates right ventricular hypertrophy induced by MCT in SD rats. **(A)** Chemical structure of Polydatin. **(B)** Weight of SD rats (n = 6). **(C)** Morphology of rat heart. **(D)** the ratio of RV/(LV + S) (n = 6). **(E)** Morphology of right ventricular hypertrophy. Data correspond to mean values ±standard error. Groups were compared using One-way ANOVA adjusted with Dunnett's test. $^{*}p < 0.05$ and $^{**}p < 0.01$ versus control group. $^{\#}p < 0.05$ and $^{\#\#}p < 0.01$ versus model group.

TABLE 1 | Primers sequences.

Gene	Forward primer (5-3′)	Reverse primer (5-3′)
Rat BMPR2	CAAAGCCCAGAAGAGCACAGAGG	TTGCCATCCTGCGTTGACTCAC
Rat PHD2	TCCGTCACGTCGATAACCCAAATG	CGAAGAATACCTCCGCTCACCTTG
Rat HIF-2α	ACTGAGACACCTGCCACCTTCC	CTTGCCACTCCTGACCCCTTTTG
Rat Arg1	AGACCACAGTATGGCAATTGGAAGC	TTGTCAGCGGAGTGTTGATGTCAG
Rat CXCL12	CGCTCTGCATCAGTGACGGTAAG	AAGGGCACAGTTTGGAGTGTTGAG
Rat CXCR4	CAGCCTGTGGATGGTGGTGTTC	CTTGCCACTCCTGACCCCTTTTG

RESULTS

Polydatin Alleviates Right Ventricular Hypertrophy Induced by MCT in SD Rats

Right ventricular hypertrophy is a typical early injury of PAH. Previous studies have shown that one-time injection of MCT is an effective means to induce PAH injure in SD rats, and the disease will progress to severe stage by the third week. Therefore, the drug intervention was initiated in the administration group on the second day after MCT injection, and tested the disease model in the third week. During the whole experiment, MCT injection resulted in decreased activity and slow weight gain in SD rats (**Figure 2B**); the apex of the rat heart tissue was significantly rounded, and the right ventricular funnel was obviously bulged and congested (**Figure 2C**). Then, right ventricle and left ventricle + diaphragm were separated, and calculated the right ventricular hypertrophy index. The results

TABLE 2 | Antibodies and other reagents.

Antibodies and reagents	Dilution	Manufacturers
For immunohistochemical staining		
Rabbit anti-human/Rat N-cadherin	1/5,000–1/20,000	Abcam
For Immunofluorescence		
Rabbit anti-Rat β-catenin	1/500	Abcam
Rabbit anti-Rat vimentin	1/250–1/1,000	Abcam
Rabbit anti-human/Rat PECAM1	1/2000	Abcam
Rabbit anti-Rat TAGLN	1/100–1/1,000	Abcam
Mouse anti-human/Rat GAPDH	1:50,000	Proteintech
Goat anti-rabbit IgG (H + L)	1:20,000	ZSGB-BIO
Goat anti-mouse IgG (H + L)	1:20,000	ZSGB-BIO

showed that MCT injection caused right ventricular remodeling in rats; sildenafil and polydatin could effectively reduce right heart hypertrophy index (**Figures 2D,E**), suggesting that polydatin can significantly reduce the damage of PAH to heart, and enhance the self-regulation and protection of heart under pathological conditions, which is of great significance for maintaining circulatory function of the body.

Polydatin Ameliorates the Pathological Damage of PAH Induced by MCT in Rats

Consistent with clinical patients, progressive damage from PAH eventually accumulates in the lungs. In this study, injection of mct resulted in the formation of pleural and ascites in some rats, and the lungs were accompanied by congestive star spots (**Figure 3A**), indicating that MCT injection caused significant lung injury in SD rats. HE staining showed that the inner elastic membrane of the small pulmonary arteries of the model group was wavy, the distance between the inner and outer elastic fiber membranes was obviously widened, the thickness of the tube wall increased, the diameter of the blood vessel became smaller, and the inflammatory cells around the blood vessel showed significant Infiltration, indicating that MCT causes pulmonary vascular endothelial damage in rats, and the ratio of PVR in the model group was higher; after the intervention of sildenafil and polydatin, vascular remodeling and inflammatory cell infiltration were significantly relieved compared with the model group, and pulmonary vascular remodeling was effectively improved (**Figure 3B**), suggesting that polydatin can reduce the lung tissue damage induced by MCT in rats with PAH.

Inflammation also plays an important role in the process of MCT induced PAH. MCT induced pathological observation of the model showed that there were a large number of inflammatory cells infiltrated in the lung tissue after modeling, mainly distributed around the blood vessels. The pro-inflammatory factor CXCL12 and its receptor CXCR4 were significantly increased, similar to the performance of vascular inflammation. After treatment with positive drugs and polydatin, inflammatory cell infiltration and inflammatory factors were significantly improved (**Figures 3C,D**), indicating that polydatin can effectively alleviate the vascular inflammation induced by MCT.

Polydatatin Inhibits MCT-Induced Activation of HIF-2α/Arg1 Signaling Pathway

BMPR2 is the one that has been studied and found to be most related to PAH among all genes belonging to the TGF-β family, including familial primary PAH (Rol et al., 2018). BMPR2 counteracts the abnormal activation of HIF-2α, and the activity of HIF-2α is regulated by the degradation of proline-4-hydroxylase domain (PHD) protein (Kapitsinou et al., 2016; Morikawa et al., 2019). The active HIF-2α/Arg1 axis means the development of pulmonary vascular resistance and PAH (Cowburn et al., 2016). The results showed that MCT reduced the expression of BMPR2 and PHD2 (**Figures 4A,B**), while the mRNA expressions of HIF-2α and Arg1 were significantly increased (**Figures 4C,D**). In order to verify the experimental hypothesis, the expression and release detection of HIF-2α and Arg1 in SD rat serum were further tested. The results showed that compared with the control group, MCT caused up-regulation of HIF-2α levels (**Figures 4A,E** similar increase in Arg1protein release (**Figure 4F**), suggesting a significant enhancement of HIF-2α/Arg1 signaling. The intervention of sildenafil and polydatin can restore the normal expression of BMPR2 and PHD2, and block the HIF-2α/Arg1 dependent progress of PAH.

Polydatin Improves Lung Endothelial Cell Dysfunction Induced by MCT

Endothelial dysfunction induced by EndMT is a contributing factor to the progression of PAH. The occurrence of EndMT breaks the tight connections between cells, causing them to lose their original stability and polarity, presenting the characteristics of loosely arranged mesenchymal cells. The results of this study showed that MCT enhanced the expression of mesenchymal cell markers in the lung tissue of the model group. For example, the expression of N-cadherin was up-regulated (**Figures 5A,B**), β-catenin (**Figures 5C,D**) and vimentin (**Figures 5E,F**) also showed similar strong fluorescence, suggesting endothelium the expression of intercellular connexin was inhibited. Attenuated endothelial barrier function supports higher cell migration. (Good et al., 2015). However sildenafil group and polydatin group could inhibit the expression of these mentioned mesenchymal cell markers to regain epithelial connexin, thereby preventing the migration and invasion of endothelial cells.

Polydatin Improves Pulmonary Vascular Remodeling Induced by MCT

EndMT is an important mechanism of pulmonary vascular remodeling in animal PAH models and human PAH patients. Injured pulmonary vessels can trigger endothelial cell muscularization, which further leads to pulmonary arterial wall thickening and even the formation of occlusive neointima, representing an irreversible stage in the pathology of pulmonary hypertension. PECAM (ECs) cell

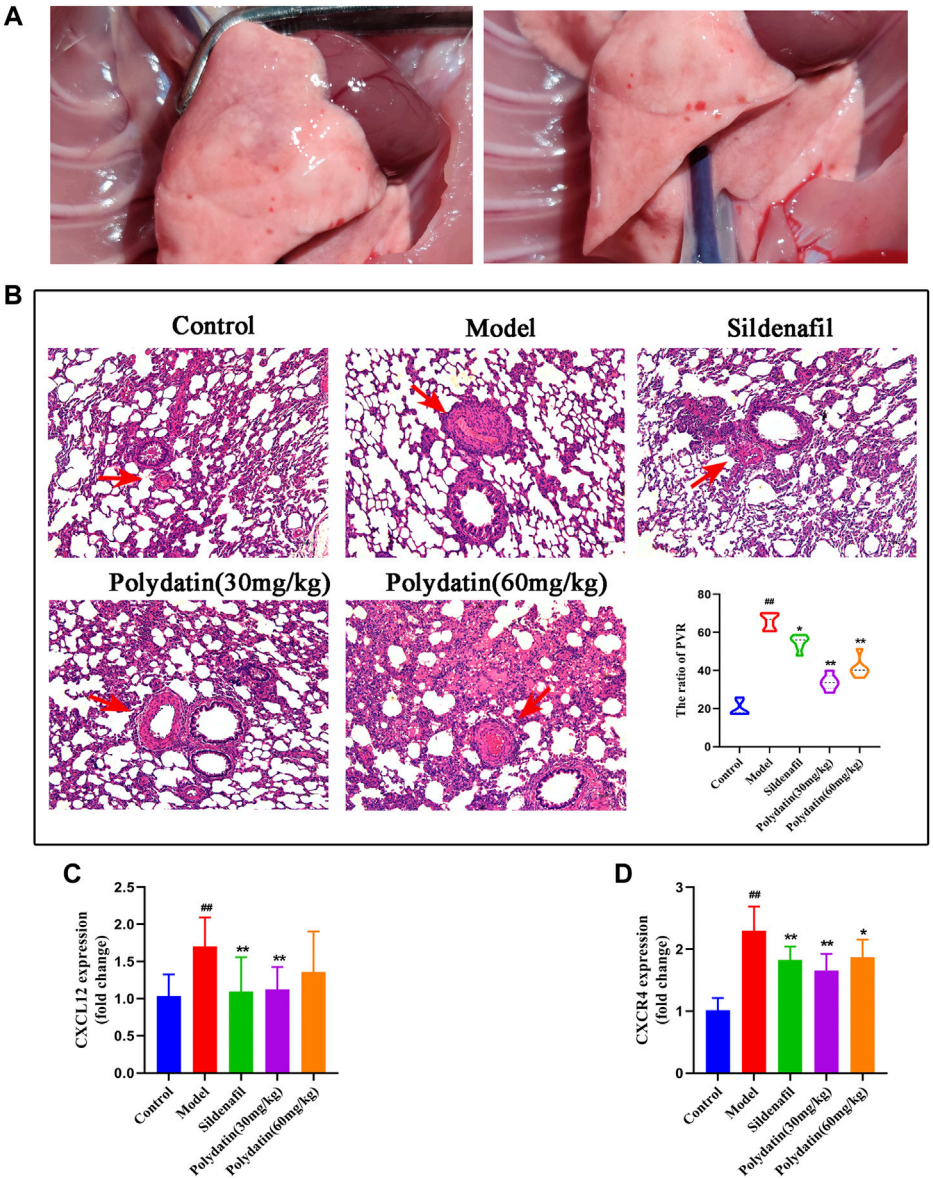

FIGURE 3 | Polydatin ameliorates the pathological damage of PAH induced by MCT in SD rats. **(A)** Morphology of rat lung. **(B)** HE staining of rat lung tissue, Scale bar = 20 μm. **(C–D)** The mRNA expression levels of CXCL12 and CXCR4 (n = 6). Data correspond to mean values ±standard error. Groups were compared using One-way ANOVA adjusted with Dunnett's test. $^{*}p < 0.05$ and $^{**}p < 0.01$ versus control group. $^{\#}p < 0.05$ and $^{\#\#}p < 0.01$ versus model group.

marke and TAGLN (SMC marker) have been used to assess reendothelialization rate of endothelial cells in several cardiovascular disease studies (Hutter et al., 2003; Ouyang et al., 2021). This study showed that MCT-induced EndMT further promoted the increase in the expression of TAGLN in intraluminal obstruction in model group (**Figures 6A,B**), while the expression of PECAM1 (CD31) decreased or even lost (**Figures 6C,D**), suggesting the formation of pulmonary artery muscle tissue and neointima in model group; while the sildenafil and polydatin maintained the above-mentioned protein expression at a normal level, indicating that polydatin can effectively alleviate the pulmonary vascular remodeling induced by MCT.

Molecular Docking Analysis of Polydatin to Key Targets of PAH

Pharmacological studies have shown that polydatin can inhibit EndMT triggered pulmonary endothelial dysfunction and pulmonary vascular remodeling, which may be mediated by inhibiting upstream targets. Therefore, molecular docking of polydatin with BMPRR2, PHD2, HIF-2α and Arg1 was

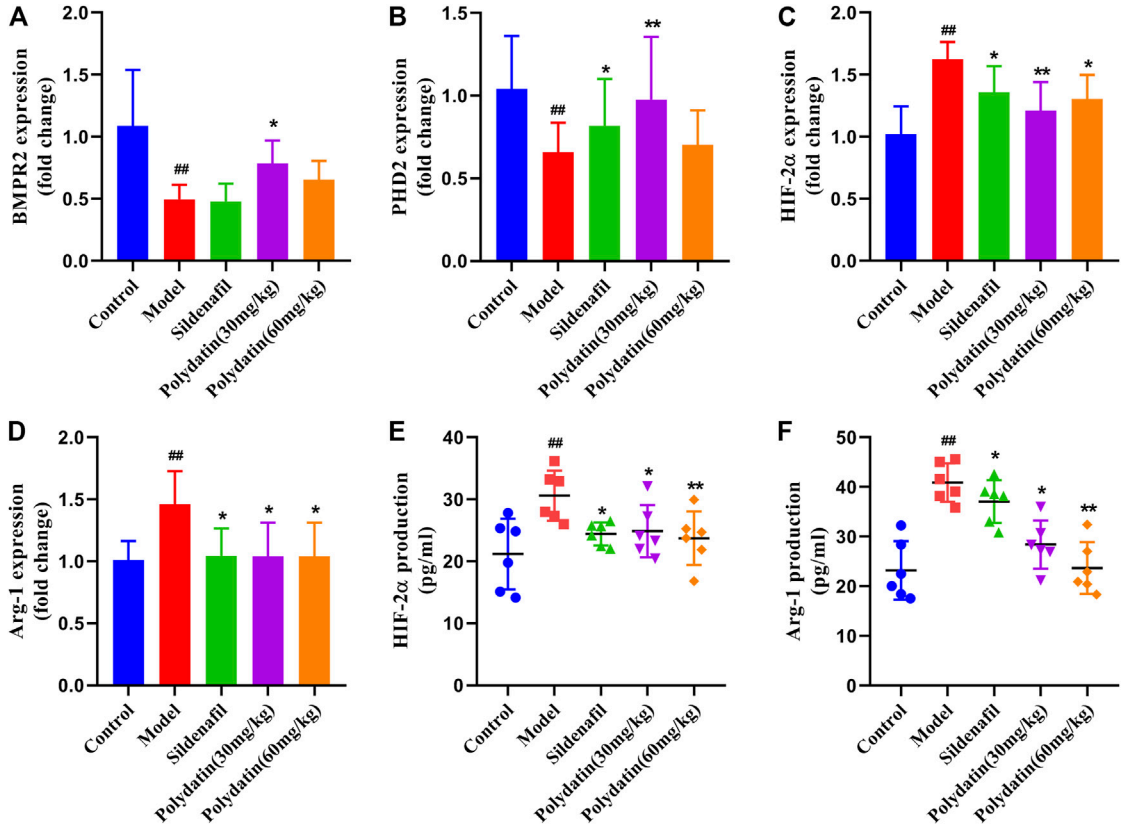

FIGURE 4 | Polydatin inhibits MCT-induced activation of HIF-2α/Arg1 signaling pathway. **(A–D)** The mRNA expression levels of BMPR2, PHD2, HIF-2α and Arg1 (n = 6). **(E–F)** HIF-2α and Arg1 expression and production was measured by ELISA (n = 6). Data correspond to mean values ±standard error. Groups were compared using One-way ANOVA adjusted with Dunnett's test. $^{*}p < 0.05$ and $^{**}p < 0.01$ versus control group. $^{\#}p < 0.05$ and $^{\#\#}p < 0.01$ versus model group.

performed to investigate whether polydatin is an effective inhibitor of PAH disease progression.

Figure 7 shows the conformation of the molecular docking experiment. Only the optimal docking between the compound and the active center site of the protein was screened and labeled. The hydrogen bonds were highlighted by yellow dotted lines, and dark green represented the amino acid residues closely linked to the compound in the active site of the protein, and finally marked the interatomic distance. Molecular docking calculation showed that VAL-100 of BMPR2 interacted with polydatin via hydrogen bond (△G = -9.08 kcal/mol Ki = 221.04 nM) (**Figure 7A**). ASP-254 of PHD2 interacts with polydine through hydrogen bond (△G = -7.84 kcal/mol Ki = 1.79 uM) (**Figure 7B**). THR 445, GLN-322 and GLN-447 of HIF-2α interact with polydatin via hydrogen bond (△G = −9.33 kcal/mol Ki = 145.91 nM) (**Figure 7C**). Lys-191 and ILe-58 of Arg1 interact with polydine through hydrogen bonds (△G = −8.02 kcal/mol Ki = 1.33 uM) (**Figure 7D**). The four protein targets showed good docking results with polydatin (△G < −1.2 kcal/mol). The Ki value of BMPR2 and HIF-2α docking with polydatin was lower than that of PHD2 and Arg 1, and even reached nanomolar level. Therefore, BMPR2, PHD2, HIF-2α and Arg1 proteins may be the main targets of polydatin against PAH injury.

DISCUSSION

Polydatin is the product of the combination of resveratrol and glucose, also known as resveratrol glycosides. Polydatin and resveratrol have similar pharmacological effects, and they can be interconverted *in vivo* (Wang and Zhang, 2017). Polydatin tends to be more abundant than resveratrol in nature (Song et al., 2019). Therefore, many studies have been devoted to the conversion of polydatin to resveratrol, but the functional properties of polydatin with stronger antioxidant effects and metabolic stability have been ignored (Platella et al., 2019). Among the numerous pharmacological effects, antioxidant effect is undoubtedly the most important, and vascular damage caused by reactive oxygen species (ROS) also plays an important role in cardiovascular diseases (Krzemińska et al., 2022). Therefore, the biological properties and various pharmacological effects of polydatin make it have high research and application value, and it is expected to become a characteristic new drug for the prevention and treatment of cardiovascular diseases. This study confirmed for the first time that resveratrol glycosides can inhibit HIF-2α/Arg1 signaling by inhibiting the protein expression of BMPR2 and PHD2, thereby improving MCT-induced pulmonary endothelial dysfunction and pulmonary vascular remodeling (**Figure 8**). It is worth

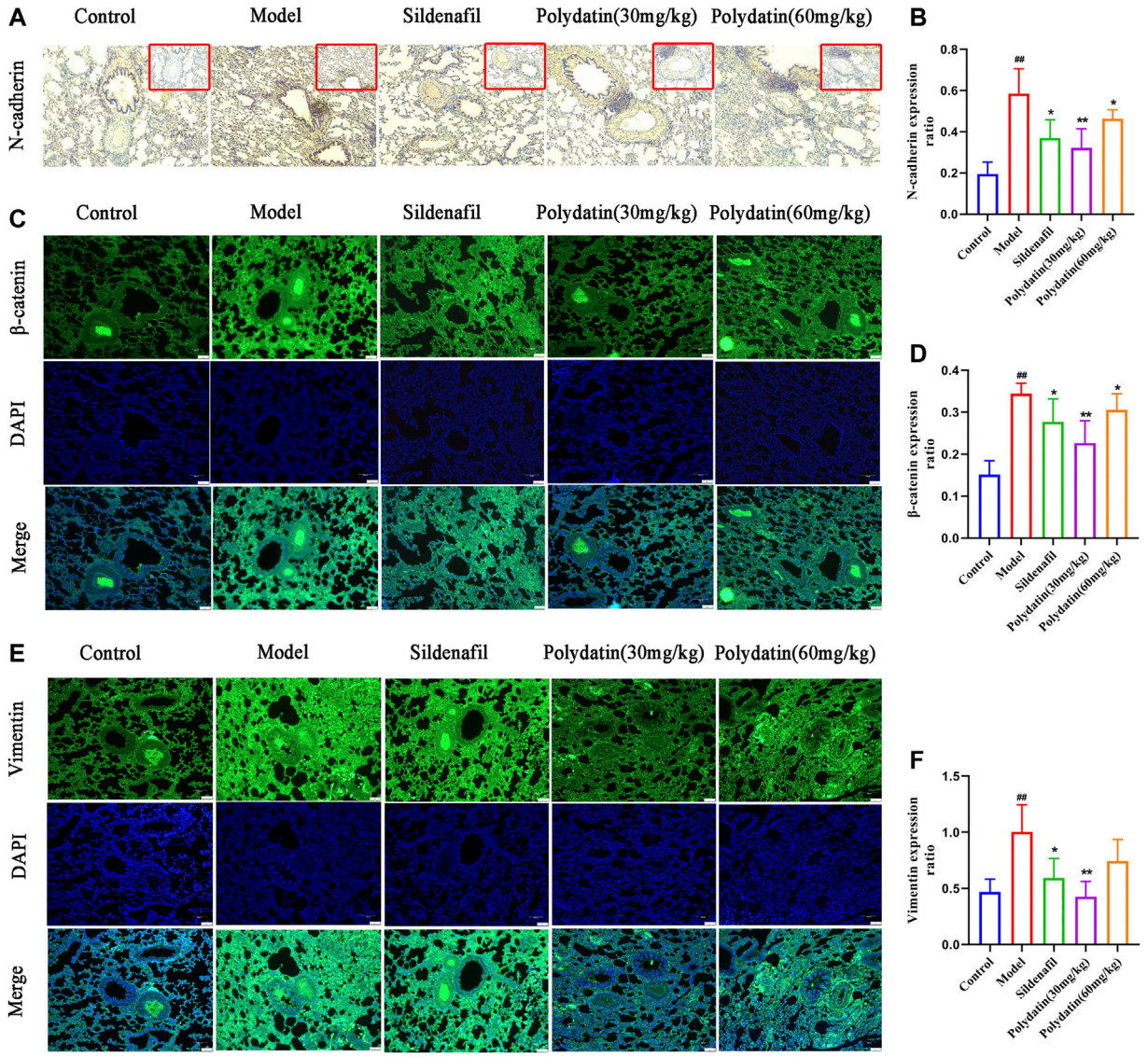

FIGURE 5 | Polydatin improves lung endothelial cell dysfunction induced by MCT. **(A–B)** Representative immunohistochemical staining (100 × magnification) and gray mean values of N-cadherin expression in lung tissues. **(C–D)** Representative immunofluorescence staining (100 × magnification) and gray mean values of β-catenin expression in lung tissues. **(E–F)** Representative immunofluorescence staining (100 × magnification) and gray mean values of vimentin expression in lung tissues. Data correspond to mean values ±standard error. Groups were compared using One-way ANOVA adjusted with Dunnett's test. $^{*}p < 0.05$ and $^{**}p < 0.01$ versus control group. $^{\#}p < 0.05$ and $^{\#\#}p < 0.01$ versus model group.

noting that the effect of high dose of polydatin in improving the pathological damage of PAH is inferior to that of low dose, and it has a slight pro-fibrotic effect. It is possible that polydatin at high concentration activates the pro-fibrosis factor (Liu et al., 2019), which damages its anti-fibrosis effect and aggravates lung injury induced by MCT. Therefore, the benefits of polydatin are varied and highly dose-dependent, but the mechanism by which high doses promote pulmonary fibrosis remains to be explored.

BMPR2 mutation is a key risk factor for hereditary pulmonary arterial hypertension (hPAH), and about 20% of carriers will get the disease (Thomson et al., 2000). The importance of BMPR2 dysfunction in PAH is supported by research in transgenic mice, and human patients also show more severe pulmonary vascular remodeling (Stacher et al., 2012). HIF is a key regulator of transcription factors and molecular responses to hypoxia. HIF-2α, as the direct target of BMPR2, is the mediating hub that regulates pulmonary vascular response. Transcription analysis of PAH-related gene expression suggests that HIF-2α mediates the differential expression of a large number of genes (Zhu et al., 2021). Prolyl hydroxylase domain protein (PHD) is the most

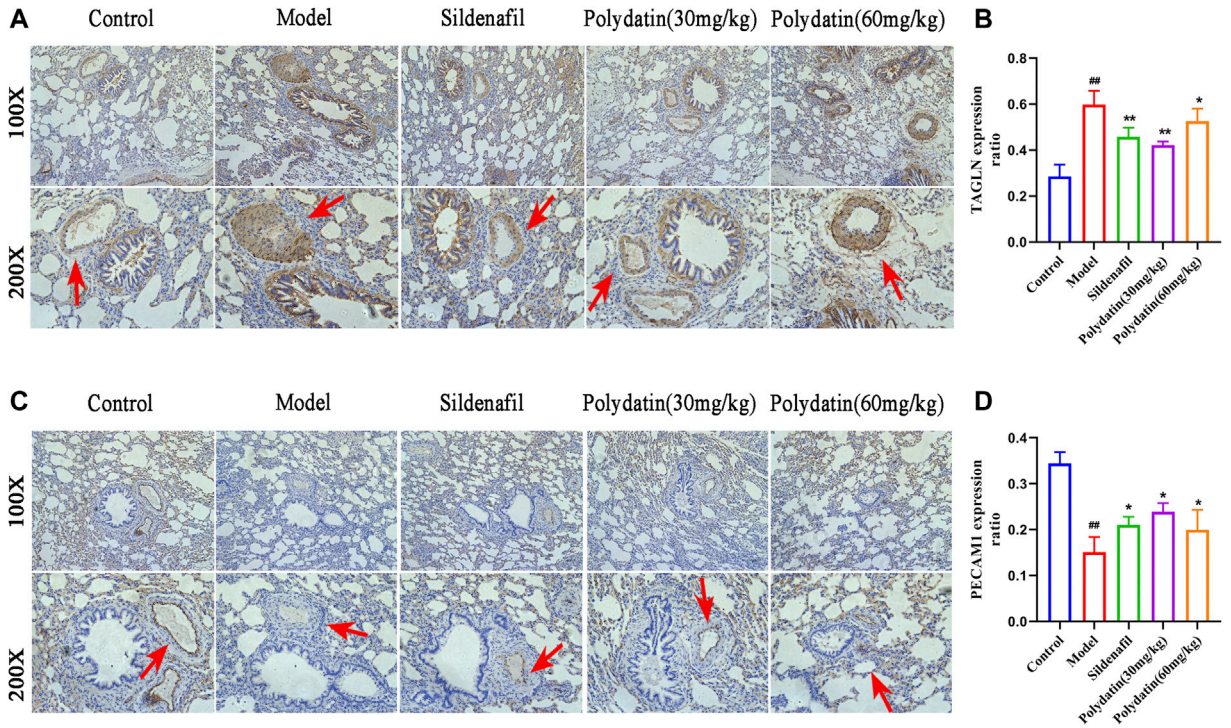

FIGURE 6 | Polydatin improves pulmonary vascular remodeling induced by MCT. **(A–B)** Representative immunohistochemical staining (100 × and 200 × magnification) and gray mean values of TAGLN expression in lung tissues. **(C–D)** Representative immunofluorescence staining (100 × and 200 × magnification) and gray mean values of PECAM1 expression in lung tissues. Data correspond to mean values ±standard error. Groups were compared using One-way ANOVA adjusted with Dunnett's test. $^{*}p < 0.05$ and $^{**}p < 0.01$ versus control group. $^{\#}p < 0.05$ and $^{\#\#}p < 0.01$ versus model group.

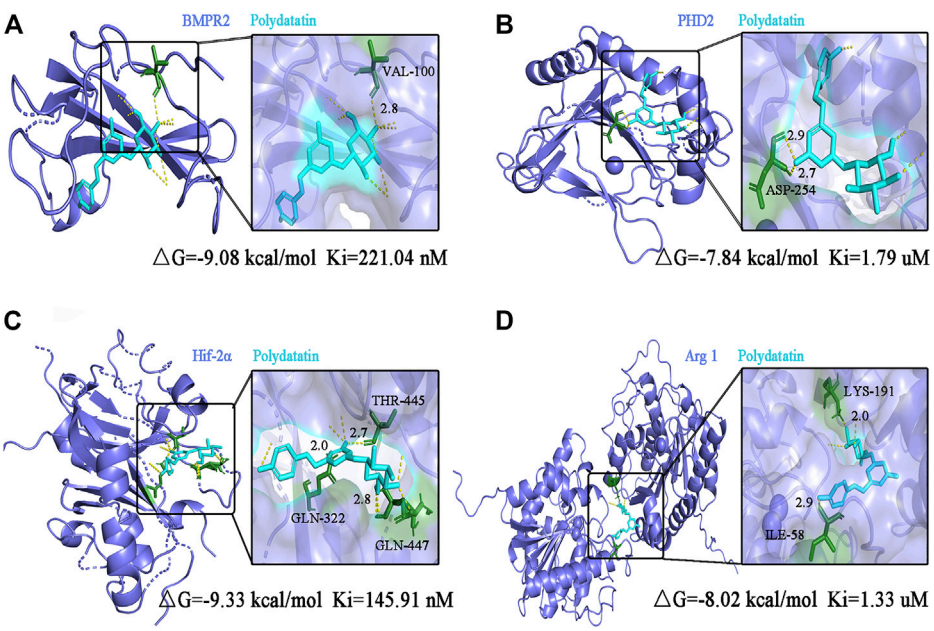

FIGURE 7 | Molecular docking analysis of polydatin to key targets of PAH induced by MCT. **(A–D)** Complex model of polydatin to human BMPR2 **(A)**, PHD2 **(B)**, HIF-2α **(C)** and Arg1 **(D)** rendered in backbone cartoon (left) or in molecular surface (right).

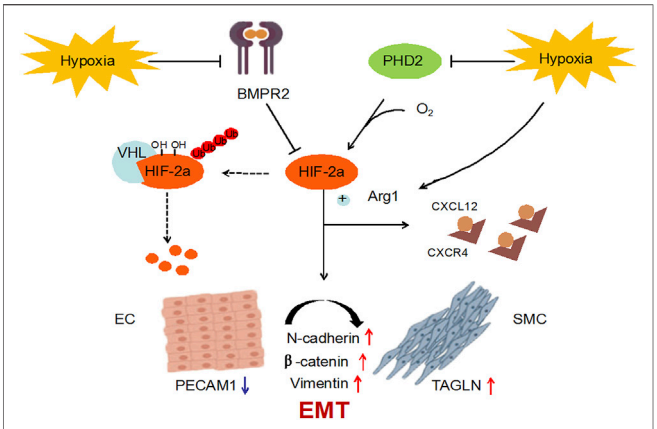

FIGURE 8 | Polydatin improves MCT-induced PAH by inhibiting EndMT.

important isoenzyme under normoxic conditions and is involved in a variety of hypoxic stress processes, such as angiogenesis and cardiac function. PHD2 can hydroxylate the conserved proline residues in HIF-2α and further mediate the degradation of the complex between von Hippel-Lindau protein (VHL) and HIF-2α. Therefore, BMPR2 and PHD2 together affect the protein abundance and activity of HIF-2α. Arg1, a HIF-2α dependent gene, is down-regulated in HIF-2α pulmonary endothelial mutants, leading to a reduction in NOS source and NO formation (Cowburn et al., 2016). In this study, the expression of PAH-related genes was abnormal after injection of MCT in SD rats, which indicated that MCT caused progressive damage to PAH in rats; After the intervention of polydatin, the expression levels of the above genes could be significantly recovered, suggesting that polydatin could resist MCT induced lung disease injury.

A complete pulmonary endothelial barrier is indispensable for maintaining vascular homeostasis. EndMT is an important process for cells to acquire mesenchymal properties and movement, and plays a key role in the progression of the disease. N-cadherin and vimentin are considered to be typical mesenchymal markers, which are usually used to reflect the progress of EndMT (Ranchoux et al., 2015). β-catenin binds and dissociates cytoskeleton proteins to promote cell migration by regulating cytoskeleton and intercellular co-adhesion (Zhang et al., 2017). In this study, MCT induced up-regulation of N-cadherin, vimentin and β-catenin in lung tissue of SD rats, suggesting that endothelial injury triggered endothelial cell proliferation and migration to restore endothelial barrier integrity and vascular homeostasis. Polydatin could effectively maintain the integrity of the cell-cell connection complex and reduce the expression of mesenchymal markers.

Progressive pulmonary vascular remodeling is one of the main causes of disease progression in almost all PAH patients. A series of studies relying on autopsy samples of severe PAH have emphasized pulmonary vascular alterations, showing pulmonary endothelial cell growth disorder, leading to plexiform lesions (Wagenvoort et al., 1970; Zhang et al., 2017). Muscularization after endothelial cell injury is an important factor in determining the size of neovascularization (Tuder et al., 2007). In this study, MCT induced pulmonary vascular endothelial cells (EC) to undergo EndMT, which showed that EC cells acquired the smooth muscle cell (SMC) marker (up-regulated in TAGLN expression) and lost the EC marker (down-regulated in PECAM1 expression), suggesting that PAH-related stress promoted the formation of pulmonary vascular neointima in SD rats. As expected, polydatin effectively prevented phenotypic transformation of pulmonary endothelial cells and reversed PAH-associated pulmonary vascular remodeling.

Perivascular inflammation also plays an important role in vascular remodeling and ultimately drives the progression of PAH (Rabinovitch et al., 2014). CXCL12, also known as stromal cell-derived factor 1 (SDF1), is an angiogenic chemokine that acts by binding to its homologous receptor CXCR4 or CXCR7. CXCL12 promotes the formation of new blood vessels in multiple organs, including the development of skeletal muscle and heart arteries, while promotes tumor and leukemia progression and accelerates atherosclerosis under pathological conditions (McCullagh et al., 2015; Yi et al., 2021). Earlier studies showed that CXCL12 was elevated in plasma and CXCR4 was significantly upregulated in hypoxia-induced PAH rats, and the same trend was observed in clinical samples; pharmacological inhibition of CXCR4 reversed RV hypertrophy, pulmonary artery middle layer hypertrophy and pulmonary vascular remodeling in PAH rats (Xu et al., 2021). In this study, CXCL12 was highly expressed in MCT injected SD rats, and CXCR4 was also significantly upregulated. However, CXCL12/CXCR4 was significantly inhibited after 3 weeks of treatment with polydatin, suggesting that polydatin can effectively improve perivascular inflammation induced by MCT in SD rats.

Next, molecular docking analysis confirmed the interaction of polydatin with key targets of PAH. Abnormal expression of BMPR2 and PHD2 has been included in the progression of EndMT - related diseases in early studies (Sun et al., 2020; Guan et al., 2021), which together regulated the abundance and activity of HIF-2α protein. Targeting HIF2α/AGR1 is considered as a novel treatment strategy for PAH, and Arg1 overexpression has been reported to be positively correlated with the viability and invasion ability of hepatocellular carcinoma cells (You et al., 2018; Macias et al., 2021). Therefore, it is reasonable to believe that focusing on improving the EndMT process can help prevent the progression of PAH disease. The results of molecular docking operations confirmed that polydatin could deeply bound to BMPR2, PHD2, HIF-2α and Arg1 protein, and established a strong interaction network on the HIF2α/Arg1 signal axis, which effectively inhibited EndMT process and ameliorated MCT-induced PAH progressive damage.

At present, no toxicological and safety reports of polydatin have been found in literature search. More importantly, polydatin can be fully absorbed by human body through passive diffusion and active transport (Yee, 1997). Lv et al. (2006) confirmed that Wistar rats could be rapidly absorbed into the blood after orally taking 50 mg/kg of resveratrol glycoside, reaching the maximum concentration in most tissues within 10 min, and reaching the peak content in the heart

30 min later. These studies laid a foundation for the protective effect of polydatin on cardiovascular system and provided guidance for clinical practice. To investigate the ameliorative effect of polydatin on PAH injury, this study established MCT-induced PAH related injury, including right ventricular compensatory hypertrophy, CXCL12/CXCR4 dominated pro-inflammatory environment, impairment of HIF-2α/Arg1 pathway, endothelial dysfunction, and vascular remodeling. Interestingly, clear associations have been reported between these disease-related states and EndMT. Next, the infection of individuals who routinely ingest polydatin from natural or supplementary sources is simulated. Data showed that polydatin significantly inhibited EndMT process, ultimately improved perivascular and interstitial inflammatory infiltration, blocked HIF-2α/Arg1 signaling pathway, improved pulmonary endothelial dysfunction and alleviated pulmonary vascular remodeling.

CONCLUSION

In summary, the present study supported that polydatin exerted protective effect on on MCT-induced PAH injury. Polydatin attenuates MCT-induced right ventricular compensatory hypertrophy and CXCL12/CXCR4 related inflammatory response, improves pulmonary endothelial dysfunction and inhibits pulmonary vascular remodeling. The underlying mechanism may involve inhibition of EndoMT by blocking HIF-2α/Arg1 signaling. Overall, these experimental data indicate suggest that polydatin has great potential and specific therapeutic value for the development of innovative drugs to ameliorate PAH related injury.

DATA AVAILABILITY STATEMENT

The original contributions presented in the study are included in the article/Supplementary Materials, further inquiries can be directed to the corresponding authors.

ETHICS STATEMENT

The animal study was reviewed and approved by the Pharmacy department, Chongqing Emergency Medicie Center, Chongqing.

AUTHOR CONTRIBUTIONS

All authors have made important contributions to the writing of the manuscript, and all authors have confirmed the final manuscript. Conceptualization: XC. Methodology: YH and ZY. Investigation: JZ, YH, and YR. Writing—original draft: XC. Writing—review and editing: XC. Funding acquisition: XZ and YM.

FUNDING

Appreciate the financial support of Chongqing Clinical Pharmacy Key Specialties Construction Project and the Science and Technology Planning Project of Chongqing Yuzhong District (No. 20170132).

REFERENCES

Bai, L., Ma, Y., Wang, X., Feng, Q., Zhang, Z., Wang, S., et al. (2021). Polydatin Inhibits Cell Viability, Migration, and Invasion through Suppressing the C-Myc Expression in Human Cervical Cancer. *Front. Cel Dev. Biol.* 9 (undefined), 587218. doi:10.3389/fcell.2021.587218

Benza, R. L., Miller, D. P., Barst, R. J., Badesch, D. B., Frost, A. E., and McGoon, M. D. (2012). An Evaluation of Long-Term Survival from Time of Diagnosis in Pulmonary Arterial Hypertension from the REVEAL Registry. *Chest* 142 (2), 448–456. doi:10.1378/chest.11-1460

Cowburn, A. S., Crosby, A., Macias, D., Branco, C., Colaço, R. D., Southwood, M., et al. (2016). HIF2α-arginase axis Is Essential for the Development of Pulmonary Hypertension. *Proc. Natl. Acad. Sci. U S A.* 113, 8801–8806. doi:10.1073/pnas.1602978113

del Valle, K., and DuBrock, H. M. (2021). Hepatopulmonary Syndrome and Portopulmonary Hypertension: Pulmonary Vascular Complications of Liver Disease. *Compr. Physiol.* 11 (4), 1–22. doi:10.1002/cphy.c210009

Fakhri, S., Gravandi, M. M., Abdian, S., Akkol, E. K., Farzaei, M. H., and Sobarzo-Sánchez, E. (2021). The Neuroprotective Role of Polydatin: Neuropharmacological Mechanisms, Molecular Targets, Therapeutic Potentials, and Clinical Perspective. *Molecules* 26 (19). undefined, 5985. doi:10.3390/molecules26195985

Giordo, R., Nasrallah, G. K., Posadino, A. M., Galimi, F., Capobianco, G., Eid, A. H., et al. (2021). Resveratrol-Elicited PKC Inhibition Counteracts NOX-Mediated Endothelial to Mesenchymal Transition in Human Retinal Endothelial Cells Exposed to High Glucose. *Antioxidants (Basel)* 10 (2), 224. . Published 2021 Feb 2. doi:10.3390/antiox10020224

Good, R. B., Gilbane, A. J., Trinder, S. L., Denton, C. P., Coghlan, G., Abraham, D. J., et al. (2015). Endothelial to Mesenchymal Transition Contributes to Endothelial Dysfunction in Pulmonary Arterial Hypertension. *Am. J. Pathol.* 185 (7), 1850–1858. doi:10.1016/j.ajpath.2015.03.019

Gu, Z., Li, L., Li, Q., Tan, H., Zou, Z., Chen, X., et al. (2021). Polydatin Alleviates Severe Traumatic Brain Injury Induced Acute Lung Injury by Inhibiting S100B Mediated NETs Formation. *Int. Immunopharmacology* 98 (undefined), 107699. doi:10.1016/j.intimp.2021.107699

Guan, D., Li, C., Li, Y., Li, Y., Wang, G., Gao, F., et al. (2021). The DpdtbA Induced EMT Inhibition in Gastric Cancer Cell Lines Was through Ferritinophagy-Mediated Activation of P53 and PHD2/hif-1α Pathway. *J. Inorg. Biochem.* 218, 111413. doi:10.1016/j.jinorgbio.2021.111413

Hoeper, M. M., Humbert, M., Souza, R., Idrees, M., Kawut, S. M., Sliwa-Hahnle, K., et al. (2016). A Global View of Pulmonary Hypertension. *Lancet Respir. Med.* 4 (4), 306–322. doi:10.1016/S2213-2600(15)00543-3

Hutter, R., Sauter, B. V., Reis, E. D., Roque, M., Vorchheimer, D., Carrick, F. E., et al. (2003). Decreased Reendothelialization and Increased Neointima Formation with Endostatin Overexpression in a Mouse Model of Arterial Injury. *Circulation* 107 (12), 1658–1663. doi:10.1161/01.CIR.0000058169.21850.CE

Jundong, W., Dakuan, Y., Zhigang, L., and Shude, L. (2011). Establishment of Pulmonary Hypertension Model Induced by Monocrotaline in Rats[J]. *Chin. Tissue Eng. Res. Clin. Rehabil.* 15 (28), 5237–5240. doi:10.3969/j.issn.1673-8225.2011.28.027

Kapitsinou, P. P., Rajendran, G., Astleford, L., Michael, M., Schonfeld, M. P., Fields, T., et al. (2016). The Endothelial Prolyl-4-Hydroxylase Domain 2/Hypoxia-Inducible Factor 2 Axis Regulates Pulmonary Artery Pressure in Mice. *Mol. Cel Biol* 36 (10), 1584–1594. doi:10.1128/MCB.01055-15

Krzemińska, J., Wronka, M., Młynarska, E., Franczyk, B., and Rysz, J. (2022). Arterial Hypertension-Oxidative Stress and Inflammation. *Antioxidants (Basel)* 11 (1), 172. undefined. doi:10.3390/antiox11010172

Liu, S., Zhao, M., Zhou, Y., Wang, C., Yuan, Y., Li, L., et al. (2019). Resveratrol Exerts Dose-dependent Anti-fibrotic or Pro-fibrotic Effects in Kidneys: A

Potential Risk to Individuals with Impaired Kidney Function. *Phytomedicine* 57 (undefined), 223–235. doi:10.1016/j.phymed.2018.12.024

Lv, C., Zhang, L., Wang, Q., Liu, W., Wang, C., Jing, X., et al. (2006). Determination of Piceid in Rat Plasma and Tissues by High-Performance Liquid Chromatographic Method with UV Detection. *Biomed. Chromatogr.* 20, 1260–1266. doi:10.1002/bmc.693

Macias, D., Moore, S., Crosby, A., Southwood, M., Du, X., Tan, H., et al. (2021). Targeting HIF2α-ARNT Hetero-Dimerisation as a Novel Therapeutic Strategy for Pulmonary Arterial Hypertension. *Eur. Respir. J.* 57, 1902061. undefined. doi:10.1183/13993003.02061-2019

McCullagh, B. N., Costello, C. M., Li, L., O'Connell, C., Codd, M., Lawrie, A., et al. (2015). Elevated Plasma CXCL12α Is Associated with a Poorer Prognosis in Pulmonary Arterial Hypertension. *PLoS One* 10 (4), e0123709. Published 2015 Apr 9. doi:10.1371/journal.pone.0123709

Meng, W. (2009). The protection and herapeutic effects of polydatin an experimental high altitude pulmonary edema model of rats and its mechanism [D].Fourth military medical University, 1–97. (In Chinese).

Morikawa, M., Mitani, Y., Holmborn, K., Kato, T., Koinuma, D., Maruyama, J., et al. (2019). The ALK-1/SMAD/ATOH8 axis Attenuates Hypoxic Responses and Protects against the Development of Pulmonary Arterial Hypertension. *Sci. Signal.* 12 (607), eaay4430. undefined. doi:10.1126/scisignal.aay4430

Ouyang, C., Li, J., Zheng, X., Mu, J., Torres, G., Wang, Q., et al. (2021). Deletion of Ulk1 Inhibits Neointima Formation by Enhancing KAT2A/GCN5-Mediated Acetylation of TUBA/α-tubulin *In Vivo*. *Autophagy* 17 (12), 4305–4322. doi:10.1080/15548627.2021.1911018

Peng, Y., Xu, J., Zeng, Y., Chen, L., and Xu, X. L. (2019). Polydatin Attenuates Atherosclerosis in Apolipoprotein E-Deficient Mice: Role of Reverse Cholesterol Transport. *Phytomedicine* 62 (undefined), 152935. doi:10.1016/j.phymed.2019.152935

Platella, C., Raucci, U., Rega, N., D'Atri, S., Levati, L., Roviello, G. N., et al. (2020). Shedding Light on the Interaction of Polydatin and Resveratrol with G-Quadruplex and Duplex DNA: A Biophysical, Computational and Biological Approach. *Int. J. Biol. Macromol.* 151, 1163–1172. doi:10.1016/j.ijbiomac.2019.10.160

Qing, M., Siwang, W., Jianbo, W., Shan, M., Jiyuan, S., and Huayan, X. (2009). Preventive Effect of Polydatin on Hypoxic Pulmonary Hypertension in Rats and Preliminary Mechanism[J]. *Chin. J. New Drugs* 18 (19), 1872–1876. doi:10.1088/1674-1056/18/7/023

Rabinovitch, M., Guignabert, C., Humbert, M., and Nicolls, M. R. (2014). Inflammation and Immunity in the Pathogenesis of Pulmonary Arterial Hypertension. *Circ. Res.* 115 (1), 165–175. doi:10.1161/CIRCRESAHA.113.301141

Ranchoux, B., Antigny, F., Rucker-Martin, C., Hautefort, A., Péchoux, C., Bogaard, H. J., et al. (2015). Endothelial-to-mesenchymal Transition in Pulmonary Hypertension. *Circulation* 131 (11), 1006–1018. doi:10.1161/CIRCULATIONAHA.114.008750

Rol, N., Kurakula, K. B., Happé, C., Bogaard, H. J., and Goumans, M. J. (2018). TGF-β and BMPR2 Signaling in PAH: Two Black Sheep in One Family. *Int. J. Mol. Sci.* 19 (9), 2585. undefined. doi:10.3390/ijms19092585

Song, X., Cui, L., Li, J., Yan, H., Li, L., Wen, L., et al. (2019). A Novel Bioreactor for Highly Efficient Biotransformation of Resveratrol from Polydatin with High-Speed Counter-current Chromatography. *Lwt* 103, 192–198. doi:10.1016/j.lwt.2018.12.057

Stacher, E., Graham, B. B., Hunt, J. M., Gandjeva, A., Groshong, S. D., McLaughlin, V. V., et al. (2012). Modern Age Pathology of Pulmonary Arterial Hypertension. *Am. J. Respir. Crit. Care Med.* 186, 261–272. doi:10.1164/rccm.201201-0164OC

Sun, Z., Liu, C., Jiang, W. G., and Ye, L. (2020). Deregulated Bone Morphogenetic Proteins and Their Receptors Are Associated with Disease Progression of Gastric Cancer. *Comput. Struct. Biotechnol. J.* 18, 177–188. doi:10.1016/j.csbj.2019.12.014

Thomson, J. R., Machado, R. D., Pauciulo, M. W., Morgan, N. V., Humbert, M., Elliott, G. C., et al. (2000). Sporadic Primary Pulmonary Hypertension Is Associated with Germline Mutations of the Gene Encoding BMPR-II, a Receptor Member of the TGF-Beta Family. *J. Med. Genet.* 37 (10), 741–745. doi:10.1136/jmg.37.10.741

Thuan, D. T. B., Zayed, H., Eid, A. H., Abou-Saleh, H., Nasrallah, G. K., Mangoni, A. A., et al. (2018). A Potential Link between Oxidative Stress and Endothelial-To-Mesenchymal Transition in Systemic Sclerosis. *Front. Immunol.* 9, 1985. doi:10.3389/fimmu.2018.01985

Tuder, R. M., Marecki, J. C., Richter, A., Fijalkowska, I., and Flores, S. (2007). Pathology of Pulmonary Hypertension. *Clin. Chest Med.* 28 (1), 23. doi:10.1016/j.ccm.2006.11.010

Van Hung, T., Emoto, N., Vignon-Zellweger, N., Nakayama, K., Yagi, K., Suzuki, Y., et al. (2014). Inhibition of Vascular Endothelial Growth Factor Receptor under Hypoxia Causes Severe, Human-like Pulmonary Arterial Hypertension in Mice: Potential Roles of Interleukin-6 and Endothelin. *Life Sci.* 118 (2), 313–328. doi:10.1016/j.lfs.2013.12.215

Wagenvoort, C. A., and Wagenvoort, N. (1970). Primary Pulmonary Hypertension. *Circulation* 42, 1163–1184. doi:10.1161/01.cir.42.6.1163

Wang, Y., and Zhang, Q. (2017). Knotweed of Pharmacological Activity Research Progress [J]. *J. Med. Rev.* 23 (5), 989–991996. doi:10.3969/j.iSSN.1006-2084.2017.05.034

Wu, M., Li, X., Wang, S., Yang, S., Zhao, R., Xing, Y., et al. (2020). Polydatin for Treating Atherosclerotic Diseases: A Functional and Mechanistic Overview. *Biomed. Pharmacother.* 128 (undefined), 110308. doi:10.1016/j.biopha.2020.110308

Xu, J. J., Li, X. N., Zhou, S. Q., Wang, R., Wu, M., Tan, C., et al. (2021). Inhibition of CXCR4 Ameliorates Hypoxia-Induced Pulmonary Arterial Hypertension in Rats. *[J] .Am J. Transl Res.* 13, 1458–1470.

Xue, C., Senchanthisai, S., Sowden, M., Pang, J., White, R. J., and Berk, B. C. (2020). Endothelial-to-Mesenchymal Transition and Inflammation Play Key Roles in Cyclophilin A-Induced Pulmonary Arterial Hypertension. *Hypertension* 76 (4), 1113–1123. doi:10.1161/HYPERTENSIONAHA.119.14013

Yee, S. (1997). *In Vitro* permeability across Caco-2 Cells (Colonic) Can Predict *In Vivo* (Small Intestinal) Absorption in Man-Ffact or Myth. *Pharm. Res.* 14, 763–766. doi:10.1023/a:1012102522787

Yi, D., Liu, B., Wang, T., Liao, Q., Zhu, M. M., Zhao, Y. Y., et al. (2021). Endothelial Autocrine Signaling through CXCL12/CXCR4/FoxM1 Axis Contributes to Severe Pulmonary Arterial Hypertension. *Int. J. Mol. Sci.* 22, 3182. undefined. doi:10.3390/ijms22063182

You, J., Chen, W., Chen, J., Zheng, Q., Dong, J., and Zhu, Y. (2018). The Oncogenic Role of ARG1 in Progression and Metastasis of Hepatocellular Carcinoma. *Biomed. Res. Int.* 2018, 2109865. doi:10.1155/2018/2109865

Zhang, J.-H., Jiao, L.-Y., Li, T.-J., Zhu, Y. Y., Zhou, J. W., and Tial, J. (2017). In vitroGSK-3β Suppresses HCC Cell Dissociation by Upregulating Epithelial junction Proteins and Inhibiting Wnt/β-Catenin Signaling pathway[J]. *J. Cancer* 8, 1598–1608. doi:10.7150/jca.18744

Zheng, W., Wang, Z., Jiang, X., Zhao, Q., and Shen, J. (2020). Targeted Drugs for Treatment of Pulmonary Arterial Hypertension: Past, Present, and Future Perspectives. *J. Med. Chem.* 63 (24), 15153–15186. doi:10.1021/acs.jmedchem.0c01093

Zhu, J., Zhao, L., Hu, Y., Cui, G., Luo, A., Bao, C., et al. (2021). Hypoxia-Inducible Factor 2-Alpha Mediated Gene Sets Differentiate Pulmonary Arterial Hypertension.[J]. *Front Cel Dev Biol* 9, 701247. doi:10.3389/fcell.2021.701247

Zou, J., Yang, Y., Yang, Y., and Liu, X. (2018). Polydatin Suppresses Proliferation and Metastasis of Non-small Cell Lung Cancer Cells by Inhibiting NLRP3 Inflammasome Activation via NF-Kb Pathway. *Biomed. Pharmacother.* 108 (undefined), 130–136. doi:10.1016/j.biopha.2018.09.051

Conflict of Interest: The authors declare that the research was conducted in the absence of any commercial or financial relationships that could be construed as a potential conflict of interest.

Publisher's Note: All claims expressed in this article are solely those of the authors and do not necessarily represent those of their affiliated organizations, or those of the publisher, the editors and the reviewers. Any product that may be evaluated in this article, or claim that may be made by its manufacturer, is not guaranteed or endorsed by the publisher.

frontiers | Frontiers in Pharmacology

ORIGINAL RESEARCH
published: 24 June 2022
doi: 10.3389/fphar.2022.902582

Predictive Capacity of Beat-to-Beat Blood Pressure Variability for Cardioautonomic and Vascular Dysfunction in Early Metabolic Challenge

Souha A. Fares[1,2], *Nour-Mounira Z. Bakkar*[1,3] *and Ahmed F. El-Yazbi*[3,4,5]*

[1]Rafic Hariri School of Nursing, American University of Beirut, Beirut, Lebanon, [2]Department of Biostatistics and Informatics, Colorado University Anschutz Medical Campus, Aurora, Colorado, [3]Department of Pharmacology and Toxicology, Faculty of Medicine, American University of Beirut, Beirut, Lebanon, [4]Department of Pharmacology and Toxicology, Faculty of Pharmacy, Alexandria University, Alexandria, Egypt, [5]Faculty of Pharmacy, Alamein International University, Alalamein, Egypt

OPEN ACCESS

Edited by:
Abdel Abdel-Rahman, East Carolina University, United States

Reviewed by:
Mohamed Fouda, Simon Fraser University, Canada
Soheb Anwar Mohammed, University of Pittsburgh, United States
Ibrahim M. Salman, Case Western Reserve University, United States

***Correspondence:**
Ahmed F. El-Yazbi
ahmed.fawzy.aly@alexu.edu.eg

Specialty section:
This article was submitted to Cardiovascular and Smooth Muscle Pharmacology, a section of the journal Frontiers in Pharmacology

Received: *23 March 2022*
Accepted: *13 May 2022*
Published: *24 June 2022*

Citation:
Fares SA, Bakkar N-MZ and El-Yazbi AF (2022) Predictive Capacity of Beat-to-Beat Blood Pressure Variability for Cardioautonomic and Vascular Dysfunction in Early Metabolic Challenge. Front. Pharmacol. 13:902582. doi: 10.3389/fphar.2022.902582

Diabetic patients present established cardiovascular disease at the onset of diagnostic metabolic symptoms. While premature autonomic and vascular deterioration considered risk factors for major cardiovascular complications of diabetes, present in initial stages of metabolic impairment, their early detection remains a significant challenge impeding timely intervention. In the present study, we examine the utility of beat-to-beat blood pressure variability (BPV) parameters in capturing subtle changes in cardiac autonomic and vascular control distinguishing between various risk categories, independent of the average BP. A rat model of mild hypercaloric (HC) intake was used to represent the insidious cardiovascular changes associated with early metabolic impairment. Invasive hemodynamics were used to collect beat-to-beat BP time series in rats of either sex with different durations of exposure to the HC diet. Linear (standard deviation and coefficient of variation) and nonlinear (approximate entropy, ApEn, and self-correlation of detrended fluctuation analysis, α) BPV parameters were calculated to assess the impact of early metabolic impairment across sexes and feeding durations. HC-fed male, but not female, rats developed increased fat:lean ratio as well as hyperinsulinemia. Unlike linear parameters, multivariate analysis showed that HC-fed rats possessed lower ApEn and higher α, consistent with early changes in heart rate variability and blunting of parasympathetic baroreceptor sensitivity, particularly in males. Moreover, logistic regression demonstrated the superiority of nonlinear parameters of diastolic BPV in predicting a prediabetic disease state. Our findings support the use of nonlinear beat-to-beat BPV for early detection of cardiovascular derangements in the initial stages of metabolic impairment.

Keywords: blood pressure variability, approximate entropy, self-correlation, metabolic challenge, autonomic dysfunction

INTRODUCTION

Average blood pressure (BP) values have long been used to characterize overt changes in vascular function and BP control mechanisms associated with hypertension. However, a recent understanding of cardiovascular signals emphasizes variability in cardiovascular parameters as an indicator of the cardiovascular and autonomic control of hemodynamics (Parati et al., 2013a). BP spontaneously fluctuates in the long, short, and very short term conferring week-to-week, diurnal and beat-to-beat BP variability (BPV), respectively (Parati et al., 2013b). Significantly, abnormal long- and short-term BPV are reported to detect hidden and early changes in various pathophysiological states, establish risk stratification within the same condition, and predict prognosis independent of mean systolic (SBP) and diastolic BP (DBP) (Hsu et al., 2016; Chowdhury et al., 2018; Palatini et al., 2019).

Continuous BPV captures the intricacies of BP dynamics which are not otherwise collected by intermittent BP monitoring (Webb and Rothwell, 2014; Wei et al., 2014; Webb et al., 2018). Linear and nonlinear parameters describe different aspects of beat-to-beat BPV. Linear time-domain parameters are mainly measures of dispersion frequently reported to increase in pathological conditions (Parati and Ochoa, 2019). Indeed, aberrant beat-to-beat BPV is associated with end-organ damage related to excursions in perfusion (Wei et al., 2014). Alternatively, nonlinear parameters quantify complexity and regularity that decreases and increases in disease states, respectively (Bakkar et al., 2021). Despite the value of linear parameters of variability, fluctuations of the cardiovascular system are described as nonhomogeneous, that is, different parts of the signal exhibit distinctive scaling properties, and are thus believed to be better quantified using nonlinear parameters (Ivanov et al., 2001). Indeed, entropy and detrended fluctuation analysis of the beat-to-beat BP time series are shown to possess superior power of discriminating among patient groups compared to conventional parameters of variability and average BP (Bakkar et al., 2021).

Research on beat-to-beat BPV remains a relatively new field with a potential early diagnostic value for premature changes prior to overt symptomatic manifestations (Wu et al., 2017). Particularly, studies of beat-to-beat BPV in the context of metabolic diseases remain limited (Bakkar et al., 2021), with previous studies, not directly measuring beat-to-beat BPV, in adults with metabolic syndrome, indicating possible changes in these parameters (Chang et al., 2016). Hence, it is prudent to study continuous BPV in transition states like prediabetes (Chang et al., 2016) and prehypertension (Pal et al., 2015) and its sex-specific evolution over time.

In this regard, we demonstrated in our previous work that 12 weeks of mild hypercaloric (HC) feeding led to subtle metabolic impairment characterized by hyperinsulinemia, hyperlipidemia, and altered body composition in the absence of hyperglycemia, hypertension, and increased body weight recapitulating the early stages of prediabetes (Al-Assi et al., 2018; Alaaeddine et al., 2019; Elkhatib et al., 2019; Fakih et al., 2020; Hammoud et al., 2021a). Such metabolic alterations were associated with cardiac-, renal-, and cerebral-vascular dysfunction as well as cardiac autonomic deterioration only discernible upon considerably invasive hemodynamic interventions. Nevertheless, our results demonstrated the ability of nonlinear metrics of beat-to-beat BPV to describe the progression from prediabetes to type 2 diabetes with worsening of baroreflex function (Bakkar et al., 2020). We also showed the ability of nonlinear metrics to discriminate between hypertensive and nonhypertensive rats switching from low- to high-salt diet while linear parameters remained unchanged across groups and experimental conditions (Fares et al., 2016).

Our present study aimed to examine the role of BPV as a novel cardiovascular risk factor discriminating between subjects as to the presence or absence of a subtle underlying vascular pathology. For this purpose, we utilized our established model of mild metabolic challenge as a representation of the transition state of early cardiometabolic dysfunction to offer the much-needed pathophysiological insight. An implied hypothesis is that rats exposed to the mild HC challenge will exhibit different BPV profiles evolving disparately with sex over time, irrespective of mean BP. We also aimed to compare the powers of linear and nonlinear BPV parameters in predicting this early altered metabolic state.

METHODS

Ethical Approval

Experimental procedures were performed according to a protocol approved by the Institutional Animal Care and Use Committee at the American University of Beirut in accordance with the Guide for Care and Use of Laboratory Animals of the Institute for Laboratory Animal Research of the National Academy of Sciences (National Research Council (US) Committee for the Update of the Guide for the Care and Use of Laboratory Animals, 2011).

Experimental Design

Beat-to-beat BP time series were derived from two groups of Sprague–Dawley rats: a control group ($N = 28$) fed with a normal chow containing 3 kcal/g and HC-fed group ($N = 23$) receiving a HC diet providing 4.035 kcal/g. The normal chow contained 32% of calories from protein, 14% from fat (0.9% of weight saturated fat), and 54% from carbohydrates, while the HC diet was prepared in-house, as described previously, to contain 15.66% of calories from protein (15.8% by weight), 38.68% from fat (18.06% by weight of which 5% was saturated fat), and 45.73% from carbohydrates (46.13% by weight) (Al-Assi et al., 2018; Alaaeddine et al., 2019; Elkhatib et al., 2019; Fakih et al., 2020; Hammoud et al., 2021a). Rats of both sexes (24 males and 27 females) were received at 5 weeks of age, housed individually at standard temperature and humidity conditions with a 12-h dark/light cycle, and randomly divided into control and HC groups fed the corresponding diet *ad libitum* for a duration of either 12 weeks (22 rats) or 24 weeks (29 rats). The selection of feeding duration was based on our previous results where the end of week 12 was the earliest time point at which manifestations of metabolic dysfunction, which mimic prediabetes, started to

appear in our rat model (Elkhatib et al., 2019). Particularly, hyperinsulinemia and dyslipidemia as well as perivascular adipose tissue inflammation started at week 12 (Al-Assi et al., 2018; Elkhatib et al., 2019). Signs of early cardiovascular (Alaaeddine et al., 2019; Elkhatib et al., 2019), cerebrovascular (Fakih et al., 2020), renovascular (Hammoud et al., 2020; Al-Saidi et al., 2021) deteriorations, as well as cardiac autonomic neuropathy (Al-Assi et al., 2018), were also evident at 12 weeks. No signs of overt cardiac or vascular dysfunction manifested up to 12 weeks of HC feeding, as indicated by echocardiography and noninvasive blood pressure monitoring performed biweekly starting from baseline (Al-Assi et al., 2018). Starting week 24, our data showed that fasting and random blood glucose as well as HbA1C levels begin to rise gradually, possibly marking the progression to type 2 diabetes (Elkhatib et al., 2019; Fakih et al., 2020). As such, we have chosen these two time points to represent compensated versus decompensated metabolic disease states in an attempt to assess the diagnostic, and rather discriminatory, capacity of beat-to-beat BPV parameters in this context (Bakkar et al., 2020).

Our experimental design targeted a typical group size of 5–7 animals shown to yield enough statistical power and an allocation strategy described in detail in our previous work (Elkhatib et al., 2019). The number of control female rats fed for 24 weeks was exceptionally duplicated due to an ordering error that occurred during the period of pandemic-related lockdowns. To avoid potential selection bias, their results were added. At the end of the designated feeding duration, the control group comprised 12 male rats (six 12-week and six 24-week) and 16 female rats (five 12-week and eleven 24-week), while the HC group had 12 male rats (six 12-week and six 24-week) and 11 female rats (five 12-week and six 24-week). Calorie intake was determined for each rat based on the amount of food consumed daily. Anesthetized rats were sacrificed by decapitation after 12 (age = 17 weeks) or 24 weeks (age = 29 weeks) of feeding (Dwaib et al., 2020).

Echocardiography

In order to assess the heart structure and function, echocardiography along the parasternal long axis M- and B-modes was performed 1 day before sacrifice using SonixTouch Q+ ultrasound (BK ultrasound, Peabody, MA, United States) on rats sedated with a mixture of ketamine and xylazine (80% of 1.5 mg/ml/kg of ketamine followed by 80% 0.375 mg/ml/kg of xylazine for complete sedation). Images were acquired at a probe frequency of 20.0 MHz. For structural left ventricular (LV) parameters, interventricular septum thickness (during systole and diastole), posterior wall thickness (during systole and diastole), and LV diameters (during systole and diastole) were measured. LV end systolic volume, end diastolic volume, as well as LV mass were automatically estimated based on experts' recommendations (Belenkie et al., 1973; Gibson, 1973; Teichholz et al., 1976; Oh et al., 2006). All structural indices were normalized to body weight and tibia length. As for functional parameters, the device automatically calculates ejection fraction (EF), fractional shortening, and stroke volume, according to standard formulas from Terry Reynold's *The Echocardiographer's Pocket Reference*.

Body Composition Analysis, Blood Glucose Levels, and Serum Insulin Concentrations

The rat fat:lean ratio was measured using the LF10 Minispec nuclear magnetic resonance (NMR) machine (Bruker, MA, United States) detecting different tissue densities as previously described (Fakih et al., 2020). On the other hand, similar to our previous work (Bakkar et al., 2020), random blood glucose levels (BGLs) were measured using an Accu-Chek glucometer (Roche Diagnostics, Basel, Switzerland) by lateral tail vein puncture on the day of sacrifice, before anesthesia induction for the surgical procedure. Serum insulin concentrations were measured using ELISA kit (Cat. no. ERINS), according to the manufacturer's protocol (Thermo Scientific, Walter, MA, United States).

Invasive Hemodynamic Recording in Anesthetized Rats

Rats were anesthetized and instrumented for invasive hemodynamic monitoring as previously described (Al-Assi et al., 2018; Bakkar et al., 2020). Briefly, rats were intraperitoneally injected with thiopental (50 mg/kg) to induce light anesthesia, followed by phenobarbital (10 mg/kg) for maintenance. A paw pinch test was performed prior to surgical intervention to confirm total loss of sensation. A similar dose of barbiturate was shown to preserve mechanisms of cardiovascular modulation, like BPV, HRV, vasopressor and vasodepressor responses, as well as baroreceptor sensitivity (BRS) (Yang et al., 1996; Bencze et al., 2013). It is thus believed to be suitable for use in hemodynamic experiments (Kuo et al., 2005; Bencze et al., 2013). Importantly, such a level of anesthesia was shown to maintain BP levels within the same range previously recorded invasively in conscious rats of the same model using the same experimental setup (Elkhatib et al., 2019). Prior to carotid catheterization, tracheostomy was performed in order to facilitate ventilation and prevent overaccumulation of respiratory secretions (Yang et al., 1996; Kuo et al., 2005). BP signals were obtained using a pressure transducer (SP844, Cat. no. 32030, MEMSCAP, Norway) connected to the carotid catheter. Acquiring beat-to-beat BP signals under such conditions (carotid catheterization of anesthetized rats) is an alternative to a more complex and elaborate procedure (involving tunneling and femoral catheterization) requiring extensive manipulation. While the effect of anesthesia on beat-to-beat BPV cannot be underestimated, the latter puts the rat under increased stress and infection risk, two factors which might affect beat-to-beat BPV and introduce confounders to its analysis.

PowerLab (Model ML870, AD Instruments Ltd., Dunedin, New Zealand) was used for data acquisition and LabChart Pro 8 (AD Instruments Ltd., Dunedin, New Zealand) software for recording. After stabilization and prior to BRS assessment, 25 min of signal acquisition was conducted. Then, SBP and DBP recordings for a stable 5-min time series were acquired at a sampling rate of 1,000 Hz corresponding to approximately 300,000 data points. At such a sampling rate, every heart beat would be represented by 150–200 data points. BP time series were then extracted and downsampled by 20× (50 Hz) to obtain approximately 15,100 data points (8–10 data points/heart beat) for beat-to-beat BPV analysis.

Baroreceptor Sensitivity

BRS was determined using the vasoactive method as described previously (Al-Assi et al., 2018; Bakkar et al., 2020). After 30 min of signal stabilization, rats were intravenously (through a catheterized jugular vein) injected with increasing doses of the vasopressor, phenylephrine (ICN Biochemicals) (PE 0.25, 0.5, 0.75, 1, and 2 μg), followed by increasing doses of the vasodepressor, sodium nitroprusside (Sigma-Aldrich, 228710-5G) (SNP 0.5, 1, 2, 4, and 8 μg), in order to assess the functionality of the parasympathetic and the sympathetic arms of BRS in decreasing and increasing HR, respectively. Changes in the heart rate (ΔHR) were plotted as a function of the corresponding changes in mean arterial pressure (ΔMAP) in response to the vasoactive drugs. GraphPad Prism for Mac OS version 8 was used to calculate the BRS of the parasympathetic and sympathetic nervous system (PSNS and SNS, respectively) as the best-fit slope of the linear regression of ΔHR vs. ΔMAP in response to PE and SNP, respectively.

Linear Beat-to-Beat HRV and BPV Measures

The standard deviation (SD) and coefficient of variation (CV) of beat-to-beat HR and BP values were calculated. SD was determined as a measure of dispersion around the mean, while CV was used to reduce the dependence of SD on the mean value (Di Rienzo et al., 1983; Jinadasa et al., 2018).

Approximate Entropy Analysis

Approximate entropy (ApEn) was computed using a MATLAB (Mathworks, Natick, MA, United States) code derived in our laboratory. ApEn was determined as a measure reflecting system complexity or self-similarity in a time series (Bakkar et al., 2020). By definition, ApEn is the negative natural logarithm of the conditional probability that a sequence similar for m values remains similar at the next point within a tolerance r (Pincus, 1991; Pincus and Goldberger, 1994). ApEn was calculated for m = 2 and r = 0.2, where r is conventionally recommended to be in the range of (0.1–0.25) times the standard deviation of the given time series (Pincus, 1991; Chon et al., 2009). In our control rats, the SD of the systolic and diastolic BP time series ranged from ~1.5 to 4, thus implicating a potential r value ranging from 0.15 to 1. Based on our previous work (Fares et al., 2016), we expected a decrease in entropy measures in disease states, and thus we opted for an r value toward the lower end of the range (0.2) to maximize ApEn value and increase the sensitivity of detection of differences among different groups. Importantly, at a heart rate of approximately 300 BPM, a series length of L = 1,500 cardiac beats and N = 15,100 data points were used for ApEn calculations. It is worth mentioning that the use of such a lengthy time series overcomes the potential "bias toward regularity" associated with ApEn (Bakkar et al., 2021). Indeed, as mentioned by Porta et al. (2007), the bias of counting self-matches is particularly a concern in short signals consisting of a "few hundreds of samples" or around 300 beat-to-beat samples (Porta et al., 2007), which is far below the number of samples we are considering. As such, the contribution of self-matches becomes minimal.

Detrended Fluctuation Analysis

Detrended fluctuation analysis (DFA) is a measure of system correlation (Peng et al., 1995) on varying ranges (short- and long-term) (Fares et al., 2016). Briefly, the original time series is integrated and detrended and the root mean square fluctuation of the detrended time series is calculated over different box sizes (n). A correlation coefficient, α, is then calculated as the linear slope of the logarithm of root mean square fluctuation versus the logarithm of box size (n). α quantifies fractal scaling of beat-to-beat signals and reflects long-term self-correlation in multicomponent systems (Goldberger et al., 2002). In fact, fractal scaling emerges from complex and rather nonlinear coupling processes (Goldberger et al., 2002). As such, the fractal scaling exponent, α, assesses temporal characteristics, that is, correlations, of a time series with nonlinear control mechanisms (Ivanov et al., 2001). Thus, while α in itself might not be a nonlinear value, it rather depicts changes in nonlinear processes, the assessment of which in the context of early metabolic disease was the intent of the present study. DFA correlations were computed, for the same series length of 1,500 cardiac beats (5×300BPM) sampled at 50 Hz (15,100 data points), using a MATLAB code developed in our laboratory (Fares et al., 2016).

Statistical Analysis

Normality was tested using the Shapiro–Wilk test. Continuous variables and variability metrics were summarized using means and standard errors (SEs) and were compared univariately across groups using the independent samples t-test or the Mann–Whitney U test. Three-way ANOVA was used for subgroup analysis to compare the changes in different parameters across dietary groups for different sexes and feeding durations. Sidak's multiple comparison test was used for *post hoc* comparisons. Bootstrap multivariable linear regression models were conducted to determine the adjusted associations among sex, diet type and duration, and average BP and BPV metrics to test their interactions with independent variables irrespective of the average BP. Due to the small sample size, the nonparametric bootstrap technique was used to estimate SEs, 95% confidence intervals (CIs), and p-values for the regression coefficients. In the bootstrap analysis, 1,000 samples of the same size as the original sample were drawn, with replacement from the original data set. Logistic regression was carried out to determine and compare the powers of BPV parameters in predicting disease state, represented by the presence or absence of HC feeding. Odds ratio (OR), SEs, and 95% CIs were reported. All tests were two-tailed, and p-values < 0.05 were considered significant. Statistical analyses were performed using Stata version 13.1 for Windows and GraphPad Prism for iOS.

RESULTS

Metabolic Impact of HC Feeding

As expected, HC feeding for different durations was associated with increased caloric intake compared to the corresponding

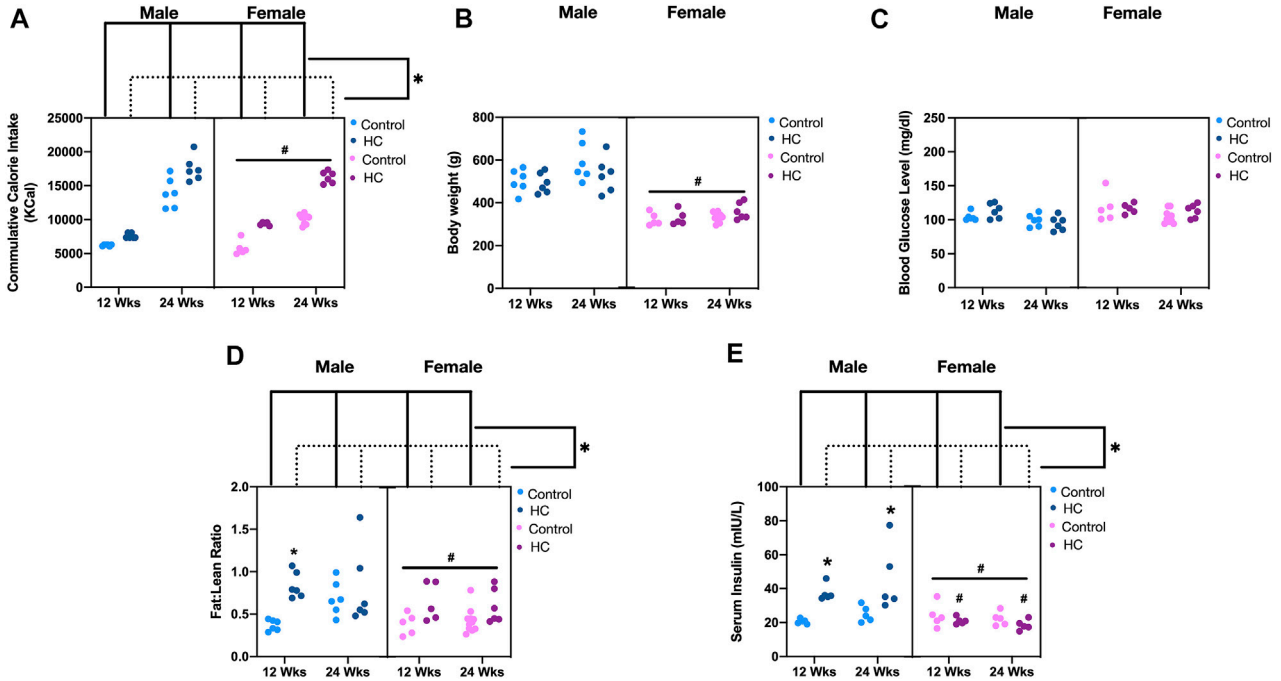

FIGURE 1 | Metabolic parameters of different rat groups. Cumulative calorie intake **(A)**, body weight **(B)**, blood glucose level **(C)**, fat:lean ratio **(D)**, and serum insulin concentration **(E)** in control and hypercaloric diet (HC)-fed rats of either sex in different feeding duration groups. Statistical analysis was performed by three-way ANOVA followed by Sidak's multiple comparison test. * denotes $p < 0.05$ vs. control group of the same sex and feeding duration group (control vs. HC), while # denotes $p < 0.05$ vs. the corresponding male group (males vs. females).

rat group receiving control diet, albeit being generally less in female compared to male rats (**Figure 1A**). Similar to our previous results (Al-Assi et al., 2018; Elkhatib et al., 2019; Fakih et al., 2020; Hammoud et al., 2021a), the increased calorie intake in HC-fed rats was not associated with an increase in neither body weight (**Figure 1B**) nor random blood glucose level (**Figure 1C**), yet HC-fed rats generally showed altered body composition as depicted by an increased fat:lean ratio across sexes and along different feeding durations (**Figure 1D**) confirming the occurrence of the previously demonstrated metabolic impairment. Interestingly, commensurate with the lower caloric intake in female rats, both their body weight and fat:lean ratio were lower than those of the male rat groups (**Figures 1B,D**). On the other hand, HC feeding was globally associated with hyperinsulinemia, mainly driven by significant increases in serum insulin levels in male rats fed HC diet for 12 or 24 weeks compared to their NC-fed counterparts (**Figure 1E**). Importantly, HC-fed female rats exhibited significantly lower serum insulin levels than their male counterparts.

Gross Myocardial and Cardiac Autonomic Function Changes

Similar to our previous studies (Al-Assi et al., 2018; Bakkar et al., 2020), no changes were detected in baseline hemodynamics and myocardial structure or function across different diet groups. Indeed, **Figure 2A** shows the representative echocardiographic images without alteration in ejection fraction (**Figure 2B**). Similarly, there was no difference in MAP among control and HC rats of either sex or feeding duration group, albeit with female rats showing a lower MAP (**Figure 2C**). Significantly, an impaired cardiac autonomic activity, particularly on the parasympathetic side, was revealed following a hemodynamic challenge using a vasopressor agent. This was observed as a reduced parasympathetic BRS following HC feeding in both 12-week and 24-week male rats, but not in female rats (**Figure 2D**), and not in the sympathetic arm of baroreflex (**Figure 2E**). Consistently, a significant interaction appeared between sex and diet ($p = 0.0003$), whereby males were more prone to the effect of diet on parasympathetic BRS.

Linear and Nonlinear Heart Rate Variability Indices

Examination of beat-to-beat HR tracing revealed that female rats collectively exhibited significantly lower average HR than males (**Figure 3A**). Particularly, healthy female rats demonstrated significantly lower average HR than their male counterparts (NC-fed for 12 weeks). Regarding HRV, no significant differences in linear fluctuations of HR, assessed by SD and CV, were observed among rats from either sex, on either diet for the different feeding durations (**Figure 3B**). Interestingly, alterations in nonlinear parameters of beat-to-beat HRV were exclusively observed in male rats on HC diet for 12 weeks, reflected by a decrease in ApEn and an increase in α of DFA

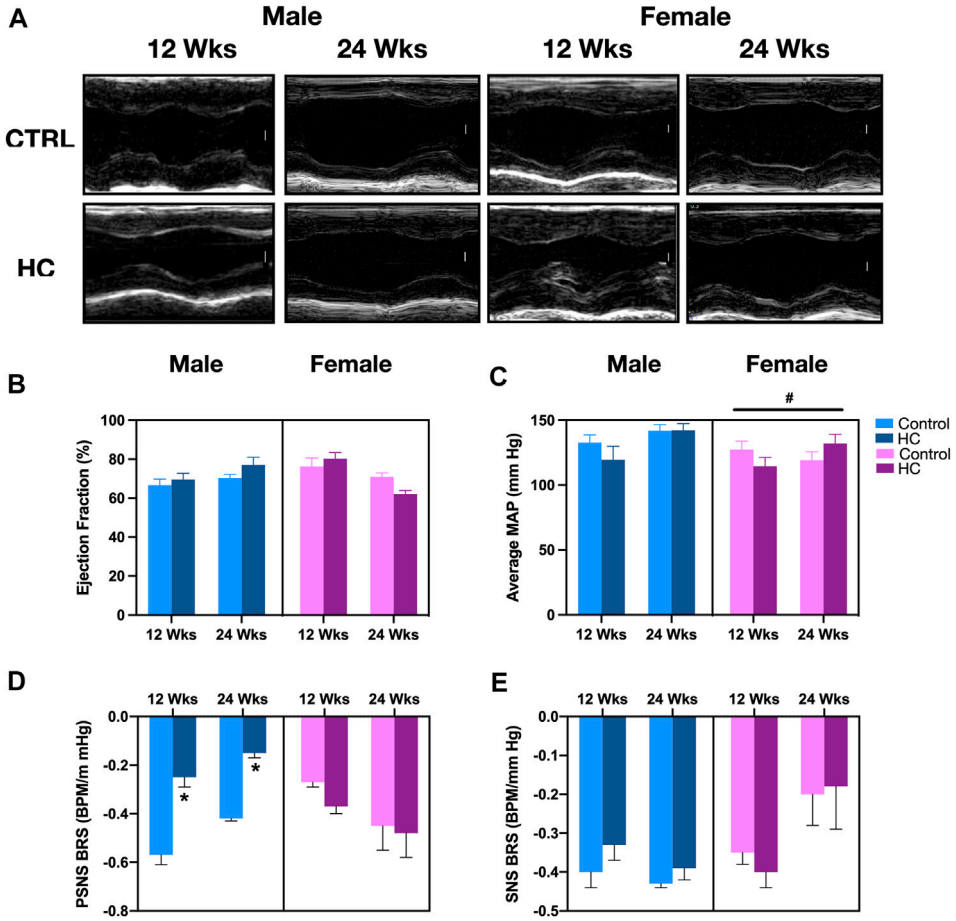

FIGURE 2 | Gross myocardial, hemodynamic, and cardiac autonomic functions in response to HC-feeding as a function of feeding duration and sex. **(A)** Representative electrocardiograms of M-mode images (scale bar corresponds to 1 mm), **(B)** ejection fraction (EF) assessed by echocardiography, **(C)** average mean arterial pressure (MAP) assessed by invasive carotid artery catheterization, and slope of the best-fit linear regression of reflex bradycardic responses to a rise in mean arterial pressure (MAP) following increasing doses of phenylephrine (PE) or sodium nitroprusside (SNP) reflecting **(D)** parasympathetic nervous system (PSNS) or **(E)** sympathetic nervous system (SNS) activity, respectively, of control and hypercaloric diet (HC)-fed rats of either sex in different feeding duration groups. Statistical analysis was performed by three-way ANOVA followed by Sidak's multiple comparison test. * denotes a $p < 0.05$ vs. control of the same sex and feeding duration group (control vs. HC), while # denotes a $p < 0.05$ vs. the corresponding male group (males vs. females).

with respect to their NC-fed counterparts (**Figures 3C,D**, respectively). Additionally, HC-fed rats collectively exhibited higher α of DFA than those fed an NC diet (**Figure 3D**). Importantly, significant interactions existed between feeding duration and diet for ApEn ($p = 0.0004$) and α ($p = 0.014$) of HR, indicating a more pronounced decrease and increase, respectively, in 12-week HC-fed rats. Another significant interaction was found between sex and feeding duration for α of HR ($p = 0.027$), reflecting a stronger effect of feeding duration on males.

Linear Beat-to-Beat Blood Pressure Variability Indices

Figure 4 depicts BP tracings of the raw (**Figures 4A,B**) and downsampled signals (**Figures 4C,D**). Examination of beat-to-beat BP tracings revealed that despite equal average BP values, rats from different groups might demonstrate disparate variability patterns (**Figure 4**). Whereas female rats had lower average and linear BPV parameters for SBP, univariate analysis showed that the average beat-to-beat SBP, SD, and CV did not differ with respect to diet type and duration (**Table 1**). Other than an increased SD of DBP in HC-fed rats, no differences were observed in average DBP or CV for DBP by univariate analysis across sexes or with diet type or duration (**Table 1**). While further subgroup analysis using three-way ANOVA confirmed the broad changes across sexes for SBP parameters, 24-week control female rats had lower average SBP and 12-week HC-fed female rats showed lower values for SD and CV than their male counterparts (**Figures 5A,C,E**). No differences were observed for the average DBP or SD and CV values for DBP across sexes, diet type, or duration (**Figures 5B,D,F**).

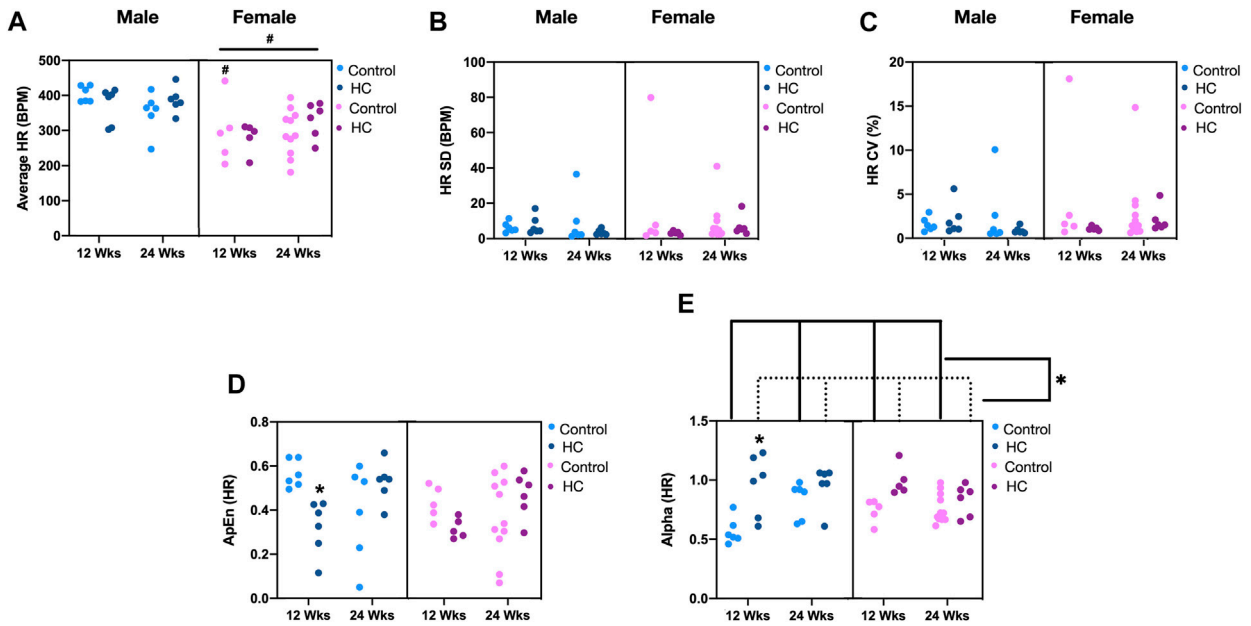

FIGURE 3 | Impact of HC feeding on average HR and linear and nonlinear parameters of beat-to-beat HRV in rats of either sex in different feeding duration groups. **(A)** Average, **(B)** standard deviation (SD), **(C)** coefficient of variation (CV), **(D)** approximate entropy (ApEn), and **(E)** α of detrended fluctuation analysis of HR in control and HC-fed rats of either sex in different feeding duration groups. Statistical analysis was performed by three-way ANOVA followed by Sidak's multiple comparison test. * denotes a $p < 0.05$ vs. control of the same feeding duration and sex (control vs. HC), while # denotes a $p < 0.05$ vs. the corresponding male group (males vs. females).

Nonlinear Beat-to-Beat Blood Pressure Variability Indices

Univariate examination of nonlinear BPV indices revealed a lower ApEn for SBP and α for both SBP and DBP in female rats compared to their male counterparts (**Table 2**). Moreover, a reduction and an increase in ApEn and α for DBP, respectively, were observed in HC-fed rats compared to those receiving the control chow (**Table 2**). Subgroup analysis confirmed a lower ApEn for SBP and α for both SBP and DBP in female rats (**Figures 6A,C,D**). For ApEn, while HC-feeding reduced the values for DBP across sex and feeding duration groups, 12-week HC-fed rats were particularly vulnerable to that effect for both SBP and DBP (**Figures 6A,B**). Indeed, there was a significant interaction between feeding duration and diet for ApEn of both SBP and DBP ($p = 0.0041$ and $p = 0.01$, respectively). On the other hand, α for DBP was increased for HC-fed rats across sex and feeding duration groups without a specific trend in one subgroup over the other (**Figure 6D**).

Adjusted Associations Between Study Variables and Linear Parameters of BPV Based on Bootstrap Linear Regression

Bootstrap multivariable linear regression models were conducted to determine the adjusted associations between average BP, sex, diet type and duration, and BPV metrics. Interactions among sex, and diet type and duration were examined to determine whether the associations with BPV metrics vary across the different rat categories, while that with average BP was performed to examine whether these parameters are affected by baseline BP. For the linear parameters, average SBP ($B_{SBP} = 0.03$, $p < 0.001$) and sex ($B_{SBP} = 0.63$, $p = 0.014$) were significantly associated with SD of the SBP and resulted in an adjusted R^2 of 0.3. As expected by the subgroup analysis, significantly higher values of SD were found in rats with higher average SBP and in males (**Figures 5A,C**), while no such associations were found with SD of the DBP. On the other hand, CV of the SBP series showed a significant interaction with feeding duration and sex resulting in an increase in CV in males only in the 12-week rats ($B_{SBP} = 0.74$, $p = 0.008$), possibly driven by the lower CV values observed in young HC-fed females (**Figure 5E**). The model, however, had an adjusted R^2 of 0.19 only. Average SBP was not associated with CV of the SBP. Alternatively, CV of the DBP was associated with average DBP ($B_{DBP} = -0.42$, $p = 0.01$) with an adjusted R^2 of 0.4. Surprisingly, a decrease in mean DBP was associated with an increase in CV.

Adjusted Associations Between Study Variables and Nonlinear Parameters of BPV Based on Bootstrap Linear Regression

As opposed to findings related to SD for SBP, no association was observed for any of the nonlinear parameters with average BP. For ApEn regression models, significant interactions were found with diet type and duration for both SBP and DBP series ($p = 0.005$ and $p = 0.005$, respectively). Adjusted R^2 for the overall models with these interactions were 0.39 for SBP and 0.43 for

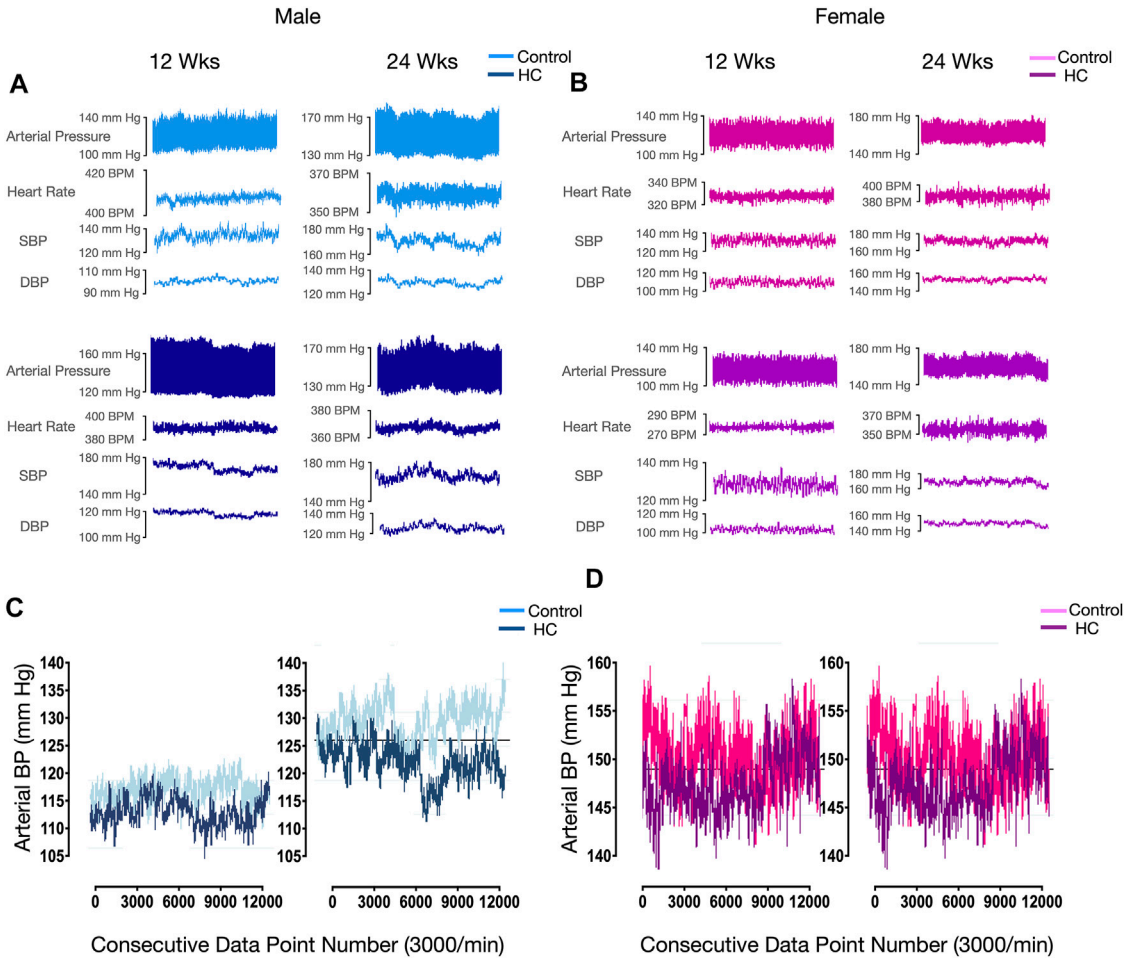

FIGURE 4 | Representative beat-to-beat blood pressure and heart rate tracings of selected rats. Raw arterial pressure, heart rate, and systolic and diastolic blood pressure recordings in 12-week and 24-week control and HC-fed **(A)** male and **(B)** female rats. **(C)** Downsampled beat-to-beat diastolic blood pressure (BP) tracing of control and HC-fed male rats of different feeding duration groups showing equal average, SD, and CV values for all groups with reduced ApEn values in 12-week HC-fed rats. **(D)** Beat-to-beat systolic blood pressure (BP) tracing of control and HC-fed female rats of different feeding duration groups showing equal average, SD, and CV values for all groups with reduced ApEn and α values compared to male rats.

TABLE 1 | Univariate analysis of linear variability parameters of beat-to-beat systolic blood pressure(SBP) and diastolic blood pressure (DBP) time series across different rat groups. Statistical analysis was determined using *t*-test or Mann–Whitney *U* test based on the results of the Shapiro–Wilk test of normality. *denotes $p < 0.05$ for 12 weeks vs. 24 weeks, males vs. females, or control vs. HC.

Variable (*n*)		Mean		SD		CV	
		SBP	DBP	SBP	DBP	SBP	DBP
Feeding	12 weeks (22)	142.39 ± 3.29	114.34 ± 4.54	3.32 ± 0.26	2.50 ± 0.22	2.31 ± 0.16	2.43 ± 0.39
Duration	24 weeks (29)	146.9 ± 4.07	123.44 ± 3.57	3.28 ± 0.17	2.68 ± 0.20	2.21 ± 0.08	2.21 ± 0.18
Sex	Male (24)	155.44 ± 3.42	123.24 ± 4.16	3.91 ± 0.24	2.87 ± 0.28	2.51 ± 0.14	2.55 ± 0.40
	Female (27)	136.65 ± 3.23*	116.20 ± 3.91	2.75 ± 0.12*	2.37 ± 0.10	2.03 ± 0.075*	2.09 ± 0.11
Diet	Control (28)	144.45 ± 3.88	120.36 ± 3.56	3.16 ± 0.16	2.46 ± 0.21	2.18 ± 0.09	2.09 ± 0.19
	HC (23)	145.58 ± 3.81	118.48 ± 4.73	3.47 ± 0.27	2.77 ± 0.20*	2.35 ± 0.15	2.57 ± 0.37

SD, standard deviation; CV, coefficient of variation.

DBP. After running separate models for 12-week and 24-week rats, ApEn was found to decrease in 12-week HC-fed rats only ($B_{SBP} = -0.08$, $p = 0.005$ and $B_{DBP} = -0.1$, $p < 0.001$) similar to observations in subgroup analyses (**Figures 6A,B**). No changes in ApEn across diets and sex were observed in the 24-week rats. No significant interactions were found with α of both BP series.

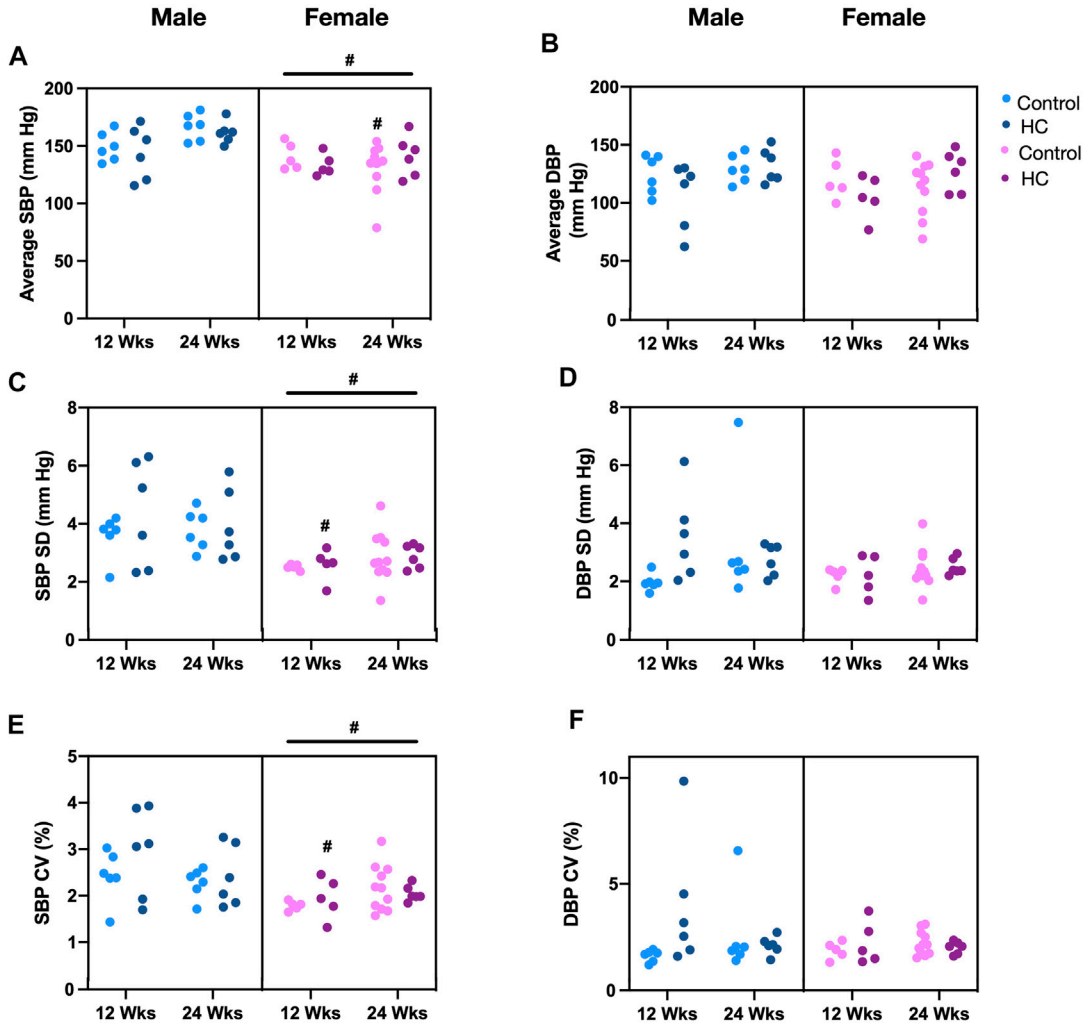

FIGURE 5 | Impact of HC-feeding on average and linear parameters of beat-to-beat systolic and diastolic blood pressure (SBP and DBP, respectively) in rats of either sex in different feeding duration groups. **(A,B)** Average, **(C,D)** standard deviation (SD), and **(E,F)** coefficient of variation (CV) of SBP and DBP, respectively, in control and HC-fed rats of either sex in different feeding duration groups. Statistical analysis was performed by three-way ANOVA followed by Sidak's multiple comparisons test. * denotes a $p < 0.05$ vs. control of the same feeding duration and sex (control vs. HC), while # denotes a $p < 0.05$ vs. the corresponding male group (males vs. females).

TABLE 2 | Univariate analysis of nonlinear variability parameters of beat-to-beat systolic and diastolic blood pressure (SBP and DBP, respectively) time series across different rat groups. Statistical analysis was determined using *t*-test or Mann–Whitney *U* test based on the results of the Shapiro–Wilk test of normality. *denotes $p < 0.05$ for 12 vs. 24 weeks, males vs. females, or control vs. HC.

Variable (*n*)		ApEn		α	
		SBP	DBP	SBP	DBP
Feeding	12 weeks (22)	0.39 ± 0.017	0.28 ± 0.02	0.94 ± 0.03	0.96 ± 0.03
Duration	24 weeks (29)	0.37 ± 0.01	0.29 ± 0.01	0.91 ± 0.02	0.92 ± 0.02
Sex	Male (24)	0.41 ± 0.02	0.29 ± 0.02	1.00 ± 0.02	1.00 ± 0.29
	Female (27)	0.35 ± 0.01*	0.27 ± 0.1	0.85 ± 0.017*	0.88 ± 0.02*
Diet	Control (28)	0.39 ± 0.02	0.31 ± 0.01	0.90 ± 0.03	0.90 ± 0.03
	HC (23)	0.37 ± 0.01	0.25 ± 0.02*	0.96 ± 0.02	0.98 ± 0.02*

ApEn, approximate entropy; α, alpha of detrended fluctuation analysis.

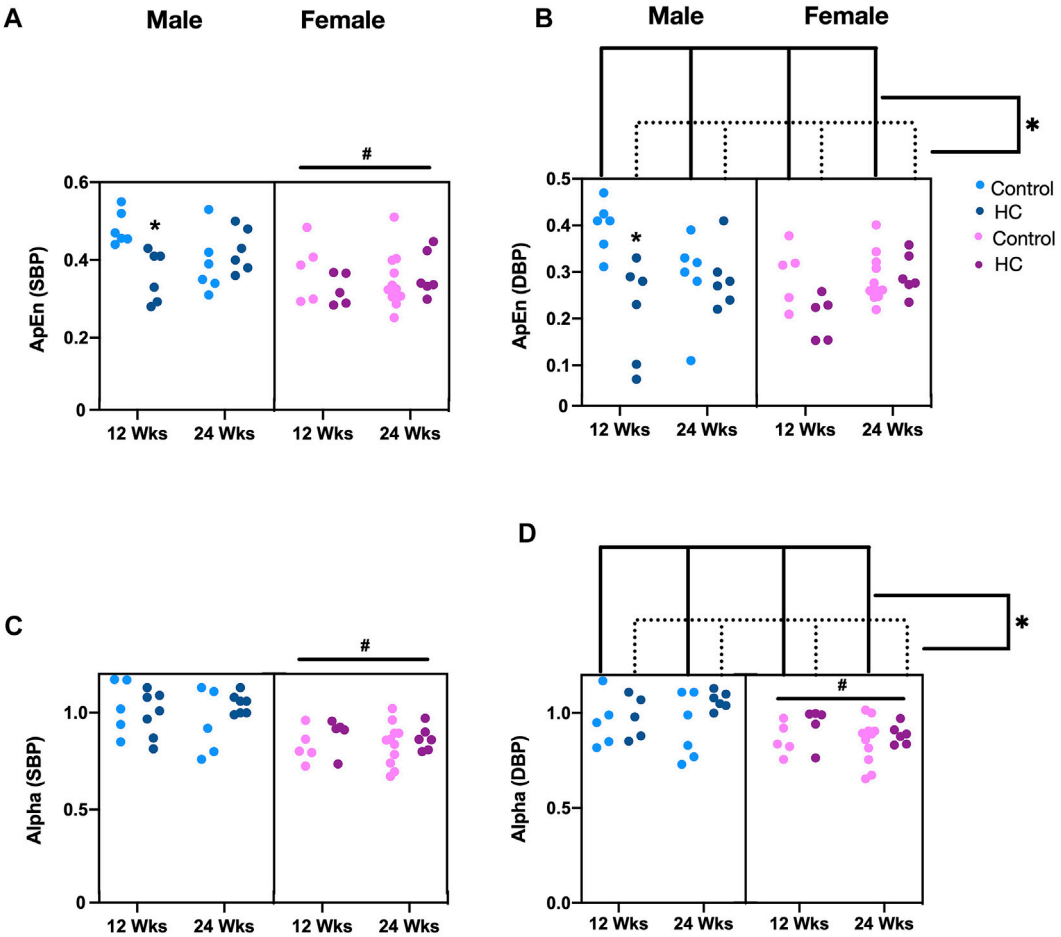

FIGURE 6 | Impact of HC-feeding on nonlinear parameters of beat-to-beat systolic and diastolic blood pressure (SBP and DBP, respectively) in rats of either sex in different feeding duration groups. **(A,B)** Approximate entropy (ApEn) and **(C,D)** α of detrended fluctuation analysis of SBP and DBP, respectively, in control and HC-fed rats of either sex in different feeding duration groups. Statistical analysis was performed by three-way ANOVA followed by Sidak's multiple comparisons test. * denotes a $p < 0.05$ vs. control of the same feeding duration and sex (control vs. HC), while # denotes a $p < 0.05$ vs. the corresponding male group (males vs. females).

Adjusted R^2 for the overall models were 0.36 for SBP and 0.23 for DBP. α was higher in males in both series ($B_{SBP} = 0.13$, $p = 0.001$ and $B_{DBP} = 0.12$, $p = 0.001$) (**Figures 6C,D**) and in DBP for HC-fed rats ($B_{DBP} = 0.07$, $p = 0.039$) (**Figure 6D**) similar to what was concluded from the subgroup analysis.

BPV Parameters in Predicting Early Disease State

Since ApEn and α for DBP were found in subgroup analysis and bootstrap regression to consistently decrease and increase, respectively, in different rat groups following HC-feeding, logistic regression was carried out to determine and compare the powers of BPV parameters in predicting a prediabetic disease state induced by HC feeding and associated with subtle yet significant cardiovascular and autonomic impairment. The overall logistic regression model was significant (p-value = 0.0159, Pseudo R^2 = 17.4%). As expected, a 0.1 unit increase in ApEn or α of DBP was associated with an OR of 0.27 ± 0.16 (CI: 0.09–0.85, $p = 0.026$) or 1.69 ± 0.43 (CI: 1.03–2.79, $p = 0.040$), respectively, for the incidence of early cardiovascular involvement and metabolic impairment associated with HC feeding (**Table 3**). Linear parameters of DBP, SD and CV, did not significantly predict disease stage with ORs of 1.2 ± 0.77 (CI: 0.34–4.25, $p = 0.773$) and 0.7 ± 0.44 (CI: 0.21–2.4, $p = 0.574$) for a 0.1 unit increase in SD and CV of DBP, respectively.

DISCUSSION

Despite significant advances in care for diabetic patients in the past decade, evidence has long indicated that glycemic control was not sufficient to reduce cardiovascular complications (Giorgino et al., 2013; Hayward et al., 2015; Barer et al., 2018). Indeed, the deleterious process culminating in overt cardiovascular dysfunction as diabetic patients progress along the course of the disease appears to start much earlier than the initial diagnosis of hyperglycemia, extending the elevated

TABLE 3 | Odds ratio reflecting the potential predictive capacity of linear and nonlinear diastolic blood pressure variability parameters for early cardiovascular dysfunction associated with a mild metabolic challenge triggered by HC-feeding.

	Based on a 1-unit increase in ApEn and α		Based on a 0.1-unit increase in ApEn and α			
BPV parameter	**OR**	**SE**	**OR**	**SE**	***p*-value**	**95% CI**
ApEn	2×10^{-6}	1.2×10^{-5}	0.27	0.16	0.026	(0.09–0.85)
α	192.44	492.19	1.69	0.43	0.040	(1.03–2.79)
SD	1.20	0.77	1.20	0.77	0.773	(0.34–4.25)
CV	0.70	0.44	0.70	0.44	0.574	(0.21–2.40)

OR, odds ratio; SE, standard error; CI, confidence interval; ApEn, approximate entropy, α, alpha of detrended fluctuation analysis; SD, standard deviation; CV, coefficient of variation.

cardiovascular risk to the prediabetic stage (Fowler, 2008; DeFronzo and Abdul-Ghani, 2011; Wasserman et al., 2018). In this regard, one of the greatest challenges would be the detection of changes in cardiovascular function triggered by early metabolic impairment leading to increased risk of morbidity and mortality, especially since many of these changes are subtle or asymptomatic, and an onset point of metabolic impairment lacks an unequivocal definition. Here, we propose the use of nonlinear BPV parameters as potential predictors of the earliest signs of cardiovascular involvement in the course of metabolic disease. To the best of our knowledge, ours is the first study to assess the impact of early metabolic challenge on linear as well as nonlinear parameters of beat-to-beat BPV in a nonobese prediabetic model. While our experimental method collected BP data series using an invasive technique, calculation of such parameters is equally feasible using noninvasive recording methods (Bakkar et al., 2021).

In this context, we measured linear and nonlinear BPV parameters in control and HC-fed rats of either sex exposed to different feeding durations. Indeed, 12 weeks of mild hypercaloric challenge were shown to induce an early state of nonobese metabolic dysfunction characterized by hyperinsulinemia associated with increased fat:lean ratio and localized adipose tissue inflammation in male rats, while lacking hyperglycemia and signs of systemic inflammation (Al-Assi et al., 2018; Alaaeddine et al., 2019; Elkhatib et al., 2019; Fakih et al., 2020; Hammoud et al., 2021a). While these rats lacked signs of gross cardiovascular dysfunction, with no hypertension or cardiac remodeling seen with echocardiography, renal and vascular endothelial, cerebrovascular, and parasympathetic cardiac autonomic dysfunction demonstrated as suppressed measures of time-domain and frequency-domain parameters of heart rate variability (HRV) together with reduced BRS, as well as markers of cardiovascular oxidative stress and inflammation, were seen upon molecular profiling (Al-Assi et al., 2018; Alaaeddine et al., 2019; Elkhatib et al., 2019; Fakih et al., 2020; Hammoud et al., 2021a). Thus, we believe that HC-fed rats would serve as a reasonable model for mild metabolic impairment with early cardiovascular involvement lacking baseline gross diagnostic signs.

Importantly, the association between metabolic syndrome and cardiac autonomic dysfunction is well documented and thought to underlie the increased risk of incidence of other cardiovascular disorders (Fowler, 2008). In this regard, the study of the considerable and characteristic degree of change associated with various physiological signals such as heart rate (HR) and BP due to the competitive interaction between different reflex control mechanisms might offer a means of detecting autonomic dysfunction. While cardiorespiratory and baroreceptor reflexes reflect as variability in both HR and BP, a main advantage of BPV over HRV analysis is its capacity to depict an integrative view of vascular and autonomic control. Specifically, vascular properties like reactivity (Xu et al., 2017), elasticity, and compliance (Webb and Rothwell, 2014; Xia et al., 2017), together with autonomic input through BRS, were shown to affect beat-to-beat BP dynamics (DeBoer et al., 1987; Grilletti et al., 2018). As such, it became prudent to investigate the capacity of BPV parameters to reflect and predict early cardiovascular dysfunction in a prediabetic disease state (Chang et al., 2016).

Univariate analysis of our present results showed that changes in nonlinear BPV parameters indicative of cardiovascular pathology occurred in HC-fed rats more so than those in linear parameters. Indeed, a reduction in DBP beat-to-beat signal complexity, manifested as a lower ApEn, and increased self-correlation, measured as a higher α for DBP, were observed in HC-fed rats of either sex at different feeding durations. Only an increased beat-to-beat DBP SD was observed for HC-fed rats. Interestingly, multivariate subgroup analyses revealed that these changes persisted only for the nonlinear parameters, ApEn and α, but not for SD. Moreover, adjusted bootstrap analysis confirmed that, unlike linear parameters, nonlinear BPV parameters appeared to be affected by intake of HC diet and hence early metabolic impairment. Our results are in line with observations from different human studies revealing that various pathological conditions are associated with a similar trend of beat-to-beat BP aberrations (Bakkar et al., 2021).

Despite the fact that HRV is believed to be more complex owing to cardiac parasympathetic innervation and antagonistic firing (Porta et al., 2012), the paradigm of pathological increase in signal predictability, reflected by migration of ApEn and α to lower and higher values, respectively, typically observed with HRV (Goldberger et al., 2002), seems to hold for BPV. In fact, although beat-to-beat BPV is essentially under sympathetic control, vagal activity was found to have an indirect effect on BPV by modulating HRV. For example, Castiglioni et al. (2011) showed that parasympathetic outflow alters BP scaling exponents by increasing white noise in HR time series. As such, beat-to-beat BPV analysis is complementary to HRV assessment (Porta et al.,

2012). Indeed, our study reveals similar HC-induced changes in nonlinear HRV and BPV in 12-week-fed male rats.

Interestingly, neither ApEn nor α seemed to be affected by BP as opposed to SD for SBP. Given the lack of difference in BP among control and HC-fed rats observed in our present as well as previous studies (Al-Assi et al., 2018; Alaaeddine et al., 2019; Elkhatib et al., 2019; Fakih et al., 2020; Hammoud et al., 2021a), this latter finding suggests that nonlinear parameters might be a more reliable reflection of the cardiovascular status in early metabolic impairment. Indeed, the values of α of DFA remained approximately equal to 1 in HC-fed rats indicating the presence of pink noise which typically describes healthy time series that are essentially complex with a degree of long-term self-correlation (Peng et al., 1995; Goldberger et al., 2002). However, slight yet significant differences in α of BPV were observed between the different groups according to their propensity to early cardiovascular impairment.

Significantly, logistic regression indicated a solid ability of nonlinear diastolic BPV parameters to predict the cardiovascular status associated with the mild metabolic impairment triggered by the HC diet. A 0.1 unit decrease or increase in DBP ApEn or α corresponded to an increased risk of such a state by 73% or 69%, respectively. This was not the case with DBP SD or CV as linear parameters of BPV. Such an outcome would not be surprising since nonlinear parameters are based on the postulation that erratic cardiovascular processes stem from competitive autonomic signals, which feed into a system whose components do not sum up to the whole (Subramaniam et al., 2014). In this regard, it is plausible that the altered sympathovagal balance observed in HC-fed rats (Al-Assi et al., 2018), together with the impaired endothelial function (Alaaeddine et al., 2019; Fakih et al., 2020) and increased sensitivity to vasoconstrictors (Elkhatib et al., 2019), have interacted to confer these changes in ApEn and α. Indeed, these latter observations suggest that HC-fed rats are prone to furnish an increased peripheral vascular resistance commonly reflected by DBPV as a surrogate measure (Carrara et al., 2018).

From a different perspective, the results of the present study showed that females exhibited a more favorable beat-to-beat BPV profile compared to males reflecting the sex-based disparity where females are postulated to require a more profound metabolic deterioration prior to significant cardiovascular risk involvement (de Ritter et al., 2020). Consistently, female rats seemed resistant to diet-induced hyperinsulinemia and fat accumulation and thus had preserved BRS and HRV. Univariate analysis revealed that females possessed lower average and linear fluctuations (SD and CV) of SBP and a lesser degree of self-correlation in SBP and DBP time series. Particularly, on subgroup comparisons, 24-week control female rats were shown to possess lower average SBP than males of the same group. Such observations could be possibly attributed to vascular and/or autonomic sex-specific characteristics. On the vascular level, α-adrenergic vasoconstriction was shown to be masked by β-adrenergic vasodilation in females (Hart et al., 2012). Additionally, vagal activity was found to predominate in females as opposed to sympathetic firing in males (Dart et al., 2002; Du et al., 2006).

On the other hand, sex segregation revealed that HC-induced alterations in beat-to-beat BPV were more pronounced in males. Along the same lines, diet-induced sympathovagal imbalance in response to HC feeding (Al-Assi et al., 2018; Hammoud et al., 2021b) can possibly explain sex differences in propensity to aberrations in vascular dynamics (Laitinen et al., 1999). Indeed, augmented sympathetic activity is associated with increased total peripheral resistance in men but not in women (Hart et al., 2012). The latter is concordant with the observation that changes in diastolic BPV significantly predicted prediabetic disease state. Consistent with our results, such a discrepancy was related to differential fat distribution along with less variable glucose homeostasis and kidney function in women (Barajas Martínez et al., 2021).

Women are more likely to store fat subcutaneously and on their lower extremities, whereas men are more likely to store fat in the abdominal region (Power and Schulkin, 2008). Not only is visceral adiposity associated with worse metabolic outcomes (Karelis et al., 2004), but it was also correlated to increased pro-inflammatory cytokine production (Beasley et al., 2009) potentially suggesting a worsened inflammatory-driven cardiovascular outcome in males. Significantly, estrogen receptor α deletion in mice was shown to increase diet-induced adipose inflammation, to which control mice were relatively resistant (Ribas et al., 2010). Moreover, estrogen signaling was found to produce antiadipogenic and anti-inflammatory effects in perivascular adipose tissues which were associated with amelioration of endothelial function (Sun et al., 2020).

Interestingly, diet-induced changes in BPV parameters appeared to be driven mainly by 12-week male rats despite a similar decrease in parasympathetic BRS in 24-week male rats compared to their control counterparts. This suggests that while BRS reflects cardiovascular involvement in prediabetic metabolic dysfunction, it correlates weakly with beat-to-beat BP dynamics with increasing age. This could be attributed to age-dependent increases and decreases in vascular stiffness and reactivity, respectively, which are stronger determinants of beat-to-beat BPV.

Results from our study show that different linear and nonlinear parameters of beat-to-beat BPV possess varying sensitivities to sex and early metabolic impairment. Indeed, nonlinear parameters of beat-to-beat BPV, namely ApEn and α, are superior in predicting the early signs of cardiovascular and autonomic dysfunction. These results support the use of beat-to-beat BPV assessment as a screening tool for insidious autonomic and vascular dysfunction in early stages of metabolic conditions including prediabetes. Interestingly, our previous work indicates worsening control of beat-to-beat BPV on establishment of type 2 diabetes in the same rat model (Bakkar et al., 2020).

Significantly, a limitation of the present study is that the results reflect the processing of data collected by invasive techniques from anesthetized rats. Future work using telemetry recording methods has the potential to reveal more details on the diurnal changes of these parameters in early metabolic dysfunction and thus further highlight these differences. Additionally, direct assessment of sympathetic nerve activity has the capacity to provide insight into the pathophysiological determinants of beat-to-beat BPV changes in early metabolic disease (Kuo et al., 2005). Yet, the resilience of the detected differences in face of anesthesia emphasizes the potential diagnostic value of the nonlinear BPV metrics. Indeed, the availability of noninvasive methods to monitor beat-to-beat BP in patients, such as finger plethysmography and tonometry (Kemmotsu et al., 1991),

makes the utility of beat-to-beat BPV attractive, especially in the light of studies indicating the validity of noninvasive techniques in comparison to invasive methods (Gibson et al., 2019).

Moreover, the discrepant effect of anesthesia in rats with different fat:lean ratios secondary to HC diet feeding cannot be precluded. Distribution of anesthesia into fat tissues can alter the final effective concentration in HC-fed rats (Brandon and Baggot, 1981). However, in our hands, rats from the different groups reached the same sedative levels before the surgical procedure. It is worth mentioning that studies have indicated that invasive, perioperative beat-to-beat BPV assessment under similar conditions (anesthesia and arterial catheterization) provides valuable information for risk appraisal, making such an assessment reasonably acceptable (Subramaniam et al., 2014; Jinadasa et al., 2018; Putowski et al., 2022). Extensive future work will be required for the appropriate translation of such findings to clinical practice.

DATA AVAILABILITY STATEMENT

The original contributions presented in the study are included in the article/Supplementary Material; further inquiries can be directed to the corresponding author.

ETHICS STATEMENT

The animal study was reviewed and approved by the Faculty of Medicine Institutional Animal Care and Use Committee, the American University of Beirut.

AUTHOR CONTRIBUTIONS

AE-Y and SF conceived and designed the research; N-MB performed experiments and acquired data; SF, N-MB, and AE-Y analyzed the data; SF, N-MB, and AE-Y interpreted the results of the experiments; SF, N-MB, and AE-Y prepared the figures; N-MB and AE-Y drafted the manuscript; AE-Y edited and revised the manuscript; SF, N-MB, and AE-Y approved the final version of the manuscript.

FUNDING

This work was supported by grants to AE-Y and SF from the American University of Beirut, Faculty of Medicine, Medical Practice Plan #320148 and #320162, respectively.

REFERENCES

Al-Assi, O., Ghali, R., Mroueh, A., Kaplan, A., Mougharbil, N., Eid, A. H., et al. (2018). Cardiac Autonomic Neuropathy as a Result of Mild Hypercaloric Challenge in Absence of Signs of Diabetes: Modulation by Antidiabetic Drugs. *Oxidative Med. Cell. Longev.* 2018, 9389784. doi:10.1155/2018/9389784

Al-Saidi, A. M., Abdallah, S., Hammoud, S., Mougharbil, N., and El-Yazbi, A. (2021). Interruption of Perirenal Adipose Tissue Thromboinflammation Reverses Prediabetic Kidney Impairment. *Circulation* 144, A10233. doi:10.1161/circ.144.suppl_1.10233

Alaaeddine, R., Elkhatib, M. A. W., Mroueh, A., Fouad, H., Saad, E. I., El-Sabban, M. E., et al. (2019). Impaired Endothelium-Dependent Hyperpolarization Underlies Endothelial Dysfunction During Early Metabolic Challenge: Increased ROS Generation and Possible Interference with NO Function. *J. Pharmacol. Exp. Ther.* 371, 567–582. doi:10.1124/jpet.119.262048

Bakkar, N.-M. Z., El-Yazbi, A. F., Zouein, F. A., and Fares, S. A. (2021). Beat-to-Beat Blood Pressure Variability: An Early Predictor of Disease and Cardiovascular Risk. *J. Hypertens.* 39, 830–845. doi:10.1097/hjh.0000000000002733

Bakkar, N. Z., Mougharbil, N., Mroueh, A., Kaplan, A., Eid, A. H., Fares, S., et al. (2020). Worsening Baroreflex Sensitivity on Progression to Type 2 Diabetes: Localized vs. Systemic Inflammation and Role of Antidiabetic Therapy. *Am. J. Physiol. Endocrinol. Metab.* 319, E835–E851. doi:10.1152/ajpendo.00145.2020

Barajas Martínez, A., Ibarra-Coronado, E. G., Fossion, R. Y. M., Toledo-Roy, J. C., Martínez Garcés, V., López-Rivera, J. A., et al. (2021). Sex Differences in the Physiological Network of Healthy Young Subjects. *Front. physiology* 12, 608. doi:10.3389/fphys.2021.678507

Barer, Y., Cohen, O., and Cukierman-Yaffe, T. (2018). Effect of Glycaemic Control on Cardiovascular Disease in Individuals with Type 2 Diabetes with Pre-Existing Cardiovascular Disease: A Systematic Review and Meta-Analysis. *Diabetes, Obes. Metabolism* 21, 732–735. doi:10.1111/dom.13581

Beasley, L. E., Koster, A., Newman, A. B., Javaid, M. K., Ferrucci, L., Kritchevsky, S. B., et al. (2009). Inflammation and Race and Gender Differences in Computerized Tomography-Measured Adipose Depots. *Obes. (Silver Spring)* 17, 1062–1069. doi:10.1038/oby.2008.627

Belenkie, I., Nutter, D. O., Clark, D. W., McCraw, D. B., and Raizner, A. E. (1973). Assessment of Left Ventricular Dimensions and Function by Echocardiography. *Am. J. Cardiol.* 31, 755–762. doi:10.1016/0002-9149(73)90011-8

Bencze, M., Behuliak, M., and Zicha, J. (2013). The Impact of Four Different Classes of Anesthetics on the Mechanisms of Blood Pressure Regulation in Normotensive and Spontaneously Hypertensive Rats. *Physiol. Res.* 62, 471–478. doi:10.33549/physiolres.932637

Brandon, R. A., and Baggot, J. D. (1981). The Pharmacokinetics of Thiopentone. *J. Vet. Pharmacol. Ther.* 4, 79–85. doi:10.1111/j.1365-2885.1981.tb00714.x

Carrara, M., Bollen Pinto, B., Baselli, G., Bendjelid, K., and Ferrario, M. (2018). Baroreflex Sensitivity and Blood Pressure Variability Can Help in Understanding the Different Response to Therapy During Acute Phase of Septic Shock. *Shock* 50, 78–86. doi:10.1097/SHK.0000000000001046

Castiglioni, P., Parati, G., Di Rienzo, M., Carabalona, R., Cividjian, A., and Quintin, L. (2011). Scale Exponents of Blood Pressure and Heart Rate During Autonomic Blockade as Assessed by Detrended Fluctuation Analysis. *J. Physiol.* 589, 355–369. doi:10.1113/jphysiol.2010.196428

Chang, Y. W., Hsiu, H., Yang, S. H., Fang, W. H., and Tsai, H. C. (2016). Characteristics of Beat-To-Beat Photoplethysmography Waveform Indexes in Subjects with Metabolic Syndrome. *Microvasc. Res.* 106, 80–87. doi:10.1016/j.mvr.2016.04.001

Chon, K., Scully, C. G., and Lu, S. (2009). Approximate Entropy for All Signals. *IEEE Eng. Med. Biol. Mag.* 28, 18–23. doi:10.1109/MEMB.2009.934629

Chowdhury, E. K., Wing, L. M. H., Jennings, G. L. R., Beilin, L. J., and Reid, C. M. (2018). Visit-to-Visit (Long-Term) and Ambulatory (Short-Term) Blood Pressure Variability to Predict Mortality in an Elderly Hypertensive Population. *J. Hypertens.* 36, 1059–1067. doi:10.1097/HJH.0000000000001652

Dart, A. M., Du, X. J., and Kingwell, B. A. (2002). Gender, Sex Hormones and Autonomic Nervous Control of the Cardiovascular System. *Cardiovasc Res.* 53, 678–687. doi:10.1016/s0008-6363(01)00508-9

de Ritter, R., de Jong, M., Vos, R. C., van der Kallen, C. J. H., Sep, S. J. S., Woodward, M., et al. (2020). Sex Differences in the Risk of Vascular Disease Associated with Diabetes. *Biol. Sex. Differ.* 11, 1. doi:10.1186/s13293-019-0277-z

DeBoer, R. W., Karemaker, J. M., and Strackee, J. (1987). Hemodynamic Fluctuations and Baroreflex Sensitivity in Humans: A Beat-To-Beat Model. *Am. J. Physiol.* 253, H680–H689. doi:10.1152/ajpheart.1987.253.3.H680

DeFronzo, R. A., and Abdul-Ghani, M. (2011). Assessment and Treatment of Cardiovascular Risk in Prediabetes: Impaired Glucose Tolerance and Impaired Fasting Glucose. *Am. J. Cardiol.* 108, 3B–24B. doi:10.1016/j.amjcard.2011.03.013

Di Rienzo, M., Grassi, G., Pedotti, A., and Mancia, G. (1983). Continuous vs Intermittent Blood Pressure Measurements in Estimating 24-Hour Average Blood Pressure. *Hypertension* 5, 264–269. doi:10.1161/01.hyp.5.2.264

Du, X. J., Fang, L., and Kiriazis, H. (2006). Sex Dimorphism in Cardiac Pathophysiology: Experimental Findings, Hormonal Mechanisms, and Molecular Mechanisms. *Pharmacol. Ther.* 111, 434–475. doi:10.1016/j.pharmthera.2005.10.016

Dwaib, H. S., Taher, M. F., Mougharbil, N., Obeid, O. F., and El-Yazbi, A. F. (2020). Therapeutic Fasting Mitigates Metabolic and Cardiovascular Dysfunction in a Prediabetic Rat Model: Possible Role of Adipose Inflammation. *FASEB J.* 34, 1. doi:10.1096/fasebj.2020.34.s1.05510

Elkhatib, M. A. W., Mroueh, A., Rafeh, R. W., Sleiman, F., Fouad, H., Saad, E. I., et al. (2019). Amelioration of Perivascular Adipose Inflammation Reverses Vascular Dysfunction in a Model of Nonobese Prediabetic Metabolic Challenge: Potential Role of Antidiabetic Drugs. *Transl. Res.* 214, 121–143. doi:10.1016/j.trsl.2019.07.009

Fakih, W., Mroueh, A., Salah, H., Eid, A. H., Obeid, M., Kobeissy, F., et al. (2020). Dysfunctional Cerebrovascular Tone Contributes to Cognitive Impairment in a Non-Obese Rat Model of Prediabetic Challenge: Role of Suppression of Autophagy and Modulation by Anti-Diabetic Drugs. *Biochem. Pharmacol.* 178, 114041. doi:10.1016/j.bcp.2020.114041

Fares, S. A., Habib, J. R., Engoren, M. C., Badr, K. F., and Habib, R. H. (2016). Effect of Salt Intake on Beat-To-Beat Blood Pressure Nonlinear Dynamics and Entropy in Salt-Sensitive versus Salt-Protected Rats. *Physiol. Rep.* 4, e12823. doi:10.14814/phy2.12823

Fowler, M. J. (2008). Microvascular and Macrovascular Complications of Diabetes. *Clin. Diabetes* 26, 77–82. doi:10.2337/diaclin.26.2.77

Gibson, D. G. (1973). Estimation of Left Ventricular Size by Echocardiography. *Br. Heart J.* 35, 128–134. doi:10.1136/hrt.35.2.128

Gibson, L. E., Henriques, T. S., Costa, M. D., Davis, R. B., Mittleman, M. A., Mathur, P., et al. (2019). Comparison of Invasive and Noninvasive Blood Pressure Measurements for Assessing Signal Complexity and Surgical Risk in Cardiac Surgical Patients. *Anesth. Analgesia* 130, 1653–1660. doi:10.1213/ANE.0000000000003894

Giorgino, F., Leonardini, A., and Laviola, L. (2013). Cardiovascular Disease and Glycemic Control in Type 2 Diabetes: Now that the Dust Is Settling from Large Clinical Trials. *Ann. N. Y. Acad. Sci.* 1281, 36–50. doi:10.1111/nyas.12044

Goldberger, A. L., Peng, C. K., and Lipsitz, L. A. (2002). What Is Physiologic Complexity and How Does it Change with Aging and Disease? *Neurobiol. Aging* 23, 23–26. doi:10.1016/s0197-4580(01)00266-4

Grilletti, J. V. F., Scapini, K. B., Bernardes, N., Spadari, J., Bigongiari, A., Mazuchi, F. A. E. S., et al. (2018). Impaired Baroreflex Sensitivity and Increased Systolic Blood Pressure Variability in Chronic Post-Ischemic Stroke. *Clin. (Sao Paulo)* 73, e253. doi:10.6061/clinics/2018/e253

Hammoud, S., AlZaim, I., Bekdash, A., Mougharbil, N., Itani, H. A., and El-Yazbi, A. F. (2021). Abstract 9725: Autonomic Modulation Mitigates Perivascular and Perirenal Adipose Inflammation and Consequent Cardiorenal Involvement in Prediabetes. *Circulation* 144, A9725. doi:10.1161/circ.144.suppl_1.9725

Hammoud, S. H., AlZaim, I., Mougharbil, N., Koubar, S., Eid, A. H., Eid, A. A., et al. (2021). Peri-Renal Adipose Inflammation Contributes to Renal Dysfunction in a Non-Obese Prediabetic Rat Model: Role of Anti-Diabetic Drugs. *Biochem. Pharmacol.* 186, 114491. doi:10.1016/j.bcp.2021.114491

Hammoud, S. H., Koubar, S., Mougharbil, N. H., Eid, A. H., and El-Yazbi, A. F. (2020). Peri-Renal Adipose Tissue Inflammation Possibly Underlies Mild Renal Dysfunction in Early Metabolic Challenge. *FASEB J.* 34, 1. doi:10.1096/fasebj.2020.34.s1.05464

Hart, E. C., Joyner, M. J., Wallin, B. G., and Charkoudian, N. (2012). Sex, Ageing and Resting Blood Pressure: Gaining Insights from the Integrated Balance of Neural and Haemodynamic Factors. *J. Physiol.* 590, 2069–2079. doi:10.1113/jphysiol.2011.224642

Hayward, R. A., Reaven, P. D., Emanuele, N. V., Bahn, G. D., Reda, D. J., Ge, L., et al. (2015). Follow-Up of Glycemic Control and Cardiovascular Outcomes in Type 2 Diabetes. *N. Engl. J. Med.* 373, 978–2206. doi:10.1056/NEJMc1508386

Hsu, P. F., Cheng, H. M., Wu, C. H., Sung, S. H., Chuang, S. Y., Lakatta, E. G., et al. (2016). High Short-Term Blood Pressure Variability Predicts Long-Term Cardiovascular Mortality in Untreated Hypertensives but Not in Normotensives. *Am. J. Hypertens.* 29, 806–813. doi:10.1093/ajh/hpw002

Ivanov, P. C., Nunes Amaral, L. A., Goldberger, A. L., Havlin, S., Rosenblum, M. G., Stanley, H. E., et al. (2001). From 1/f Noise to Multifractal Cascades in Heartbeat Dynamics. *Chaos* 11, 641–652. doi:10.1063/1.1395631

Jinadasa, S. P., Mueller, A., Prasad, V., Subramaniam, K., Heldt, T., Novack, V., et al. (2018). Blood Pressure Coefficient of Variation and its Association with Cardiac Surgical Outcomes. *Anesth. Analg.* 127, 832–839. doi:10.1213/ANE.0000000000003362

Karelis, A. D., St-Pierre, D. H., Conus, F., Rabasa-Lhoret, R., and Poehlman, E. T. (2004). Metabolic and Body Composition Factors in Subgroups of Obesity: What Do We Know? *J. Clin. Endocrinol. Metab.* 89, 2569–2575. doi:10.1210/jc.2004-0165

Kemmotsu, O., Ueda, M., Otsuka, H., Yamamura, T., Winter, D. C., and Eckerle, J. S. (1991). Arterial Tonometry for Noninvasive, Continuous Blood Pressure Monitoring During Anesthesia. *Anesthesiology* 75, 333–340. doi:10.1097/00000542-199108000-00023

Kuo, T. B., Lai, C. J., Huang, Y. T., and Yang, C. C. (2005). Regression Analysis Between Heart Rate Variability and Baroreflex-Related Vagus Nerve Activity in Rats. *J. Cardiovasc Electrophysiol.* 16, 864–869. doi:10.1111/j.1540-8167.2005.40656.x

Laitinen, T., Hartikainen, J., Niskanen, L., Geelen, G., and Länsimies, E. (1999). Sympathovagal Balance Is Major Determinant of Short-Term Blood Pressure Variability in Healthy Subjects. *Am. J. Physiol.* 276, H1245–H1252. doi:10.1152/ajpheart.1999.276.4.H1245

National Research Council (US) Committee for the Update of the Guide for the Care and Use of Laboratory Animals (2011). *Guide for the Care and Use of Laboratory Animals*. Washington: National Academies Press.

Oh, J. K., Seward, J. B., and Tajik, A. J. (2006). *The Echo Manual*. Pennsylvania, United States: Lippincott Williams & Wilkins.

Pal, G. K., Chandrasekaran, A., Pal, P., Nivedita, N., Indumathy, J., and Sirisha, A. (2015). Prehypertension Status, Cardiometabolic Risks, and Decreased Baroreflex Sensitivity Are Linked to Sympathovagal Imbalance in Salt-Preferring Individuals. *Clin. Exp. Hypertens.* 37, 609–615. doi:10.3109/10641963.2015.1036059

Palatini, P., Saladini, F., Mos, L., Fania, C., Mazzer, A., Cozzio, S., et al. (2019). Short-Term Blood Pressure Variability Outweighs Average 24-h Blood Pressure in the Prediction of Cardiovascular Events in Hypertension of the Young. *J. Hypertens.* 37, 1419–1426. doi:10.1097/HJH.0000000000002074

Parati, G., Ochoa, J. E., Lombardi, C., and Bilo, G. (2013). Assessment and Management of Blood-Pressure Variability. *Nat. Rev. Cardiol.* 10, 143–155. doi:10.1038/nrcardio.2013.1

Parati, G., Ochoa, J. E., Salvi, P., Lombardi, C., and Bilo, G. (2013). Prognostic Value of Blood Pressure Variability and Average Blood Pressure Levels in Patients with Hypertension and Diabetes. *Diabetes care* 36 (Suppl 2), S312–S324. doi:10.2337/dcS13-2043

Parati, G., and Ochoa, J. E. (2019). *Blood Pressure Variability, Prehypertension and Cardiometabolic Syndrome*. Berlin, Germany: Springer, 395–417. doi:10.1007/978-3-319-75310-2_28

Peng, C. K., Havlin, S., Stanley, H. E., and Goldberger, A. L. (1995). Quantification of Scaling Exponents and Crossover Phenomena in Nonstationary Heartbeat Time Series. *Chaos* 5, 82–87. doi:10.1063/1.166141

Pincus, S. M. (1991). Approximate Entropy as a Measure of System Complexity. *Proc. Natl. Acad. Sci. U. S. A.* 88, 2297–2301. doi:10.1073/pnas.88.6.2297

Pincus, S. M., and Goldberger, A. L. (1994). Physiological Time-Series Analysis: what Does Regularity Quantify? *Am. J. Physiol.* 266, H1643–H1656. doi:10.1152/ajpheart.1994.266.4.H1643

Porta, A., Castiglioni, P., Di Rienzo, M., Bari, V., Bassani, T., Marchi, A., et al. (2012). Short-term Complexity Indexes of Heart Period and Systolic Arterial Pressure Variabilities Provide Complementary Information. *J. Appl. Physiol. (1985)* 113, 1810–1820. doi:10.1152/japplphysiol.00755.2012

Porta, A., Gnecchi-Ruscone, T., Tobaldini, E., Guzzetti, S., Furlan, R., and Montano, N. (2007). Progressive Decrease of Heart Period Variability Entropy-Based Complexity during Graded Head-Up Tilt. *J. Appl. Physiol. (1985)* 103, 1143–1149. doi:10.1152/japplphysiol.00293.2007

Power, M. L., and Schulkin, J. (2008). Sex Differences in Fat Storage, Fat Metabolism, and the Health Risks from Obesity: Possible Evolutionary Origins. *Br. J. Nutr.* 99, 931–940. doi:10.1017/S0007114507853347

Putowski, Z., Czok, M., and Krzych, Ł. J. (2022). The Impact of Intraoperative Blood Pressure Variability on the Risk of Postoperative Adverse Outcomes in Non-Cardiac Surgery: A Systematic Review. *J. Anesth.* 36, 316–322. doi:10.1007/s00540-022-03035-w

Ribas, V., Nguyen, M. T., Henstridge, D. C., Nguyen, A. K., Beaven, S. W., Watt, M. J., et al. (2010). Impaired Oxidative Metabolism and Inflammation Are Associated with Insulin Resistance in ERalpha-Deficient Mice. *Am. J. Physiol. Endocrinol. Metab.* 298, E304–E319. doi:10.1152/ajpendo.00504.2009

Subramaniam, B., Khabbaz, K. R., Heldt, T., Lerner, A. B., Mittleman, M. A., Davis, R. B., et al. (2014). Blood Pressure Variability: Can Nonlinear Dynamics Enhance Risk Assessment During Cardiovascular Surgery? *J. Cardiothorac. Vasc. Anesth.* 28, 392–397. doi:10.1053/j.jvca.2013.11.014

Sun, B., Yang, D., Yin, Y. Z., and Xiao, J. (2020). Estrogenic and Anti-Inflammatory Effects of Pseudoprotodioscin in Atherosclerosis-Prone Mice: Insights into Endothelial Cells and Perivascular Adipose Tissues. *Eur. J. Pharmacol.* 869, 172887. doi:10.1016/j.ejphar.2019.172887

Teichholz, L. E., Kreulen, T., Herman, M. V., and Gorlin, R. (1976). Problems in Echocardiographic Volume Determinations: Echocardiographic-Angiographic Correlations in the Presence of Absence of Asynergy. *Am. J. Cardiol.* 37, 7–11. doi:10.1016/0002-9149(76)90491-4

Wasserman, D. H., Wang, T. J., and Brown, N. J. (2018). The Vasculature in Prediabetes. *Circ. Res.* 122, 1135–1150. doi:10.1161/CIRCRESAHA.118.311912

Webb, A. J., and Rothwell, P. M. (2014). Physiological Correlates of Beat-To-Beat, Ambulatory, and Day-To-Day Home Blood Pressure Variability after Transient Ischemic Attack or Minor Stroke. *Stroke* 45, 533–538. doi:10.1161/STROKEAHA.113.003321

Webb, A. J. S., Mazzucco, S., Li, L., and Rothwell, P. M. (2018). Prognostic Significance of Blood Pressure Variability on Beat-To-Beat Monitoring after Transient Ischemic Attack and Stroke. *Stroke* 49, 62–67. doi:10.1161/strokeaha.117.019107

Wei, F. F., Li, Y., Zhang, L., Xu, T. Y., Ding, F. H., Wang, J. G., et al. (2014). Beat-to-beat, Reading-To-Reading, and Day-To-Day Blood Pressure Variability in Relation to Organ Damage in Untreated Chinese. *Hypertension* 63, 790–796. doi:10.1161/HYPERTENSIONAHA.113.02681

Wu, D., Xu, L., Abbott, D., Hau, W. K., Ren, L., Zhang, H., et al. (2017). Analysis of Beat-To-Beat Blood Pressure Variability Response to the Cold Pressor Test in the Offspring of Hypertensive and Normotensive Parents. *Hypertens. Res.* 40, 581–589. doi:10.1038/hr.2017.4

Xia, Y., Liu, X., Wu, D., Xiong, H., Ren, L., Xu, L., et al. (2017). Influence of Beat-To-Beat Blood Pressure Variability on Vascular Elasticity in Hypertensive Population. *Sci. Rep.* 7, 8394. doi:10.1038/s41598-017-08640-4

Xu, C., Xiong, H., Gao, Z., Liu, X., Zhang, H., Zhang, Y., et al. (2017). Beat-to-Beat Blood Pressure and Two-Dimensional (Axial and Radial) Motion of the Carotid Artery Wall: Physiological Evaluation of Arterial Stiffness. *Sci. Rep.* 7, 42254. doi:10.1038/srep42254

Yang, C. C., Kuo, T. B., and Chan, S. H. (1996). Auto- and Cross-Spectral Analysis of Cardiovascular Fluctuations during Pentobarbital Anesthesia in the Rat. *Am. J. Physiol.* 270, H575–H582. doi:10.1152/ajpheart.1996.270.2.H575

Conflict of Interest: The authors declare that the research was conducted in the absence of any commercial or financial relationships that could be construed as a potential conflict of interest.

Publisher's Note: All claims expressed in this article are solely those of the authors and do not necessarily represent those of their affiliated organizations, or those of the publisher, the editors and the reviewers. Any product that may be evaluated in this article, or claim that may be made by its manufacturer, is not guaranteed or endorsed by the publisher.

frontiers | Frontiers in Pharmacology

TYPE Original Research
PUBLISHED 02 August 2022
DOI 10.3389/fphar.2022.920977

OPEN ACCESS

EDITED BY
Ali H. Eid,
Qatar University, Qatar

REVIEWED BY
Maria Luisa Del Moral,
University of Jaén, Spain
David A. Tulis,
East Carolina University, United States
Fernanda Priviero,
University of South Carolina,
United States

*CORRESPONDENCE
Hongxin Wang,
hongxinwang@jzmu.edu.cn
Meili Lu,
lumeili@jzmu.edu.cn

SPECIALTY SECTION
This article was submitted to Cardiovascular and Smooth Muscle Pharmacology, a section of the journal Frontiers in Pharmacology

RECEIVED 15 April 2022
ACCEPTED 27 June 2022
PUBLISHED 02 August 2022

CITATION
Zhao F, Meng Y, Wang Y, Fan S, Liu Y, Zhang X, Ran C, Wang H and Lu M (2022), Protective effect of Astragaloside IV on chronic intermittent hypoxia-induced vascular endothelial dysfunction through the calpain-1/SIRT1/AMPK signaling pathway. *Front. Pharmacol.* 13:920977. doi: 10.3389/fphar.2022.920977

Protective effect of Astragaloside IV on chronic intermittent hypoxia-induced vascular endothelial dysfunction through the calpain-1/SIRT1/AMPK signaling pathway

Fang Zhao, Yan Meng, Yue Wang, Siqi Fan, Yu Liu, Xiangfeng Zhang, Chenyang Ran, Hongxin Wang* and Meili Lu*

Key Laboratory of Cardiovascular and Cerebrovascular Drug Research of Liaoning Province, Jinzhou Medical University, Jinzhou, China

Vascular endothelial dysfunction (VED) is linked with the pathogenesis of obstructive sleep apnea (OSA) comorbidities, such as cardiovascular disease. Astragaloside IV (As-IV) has exhibited significant improvement for endothelial dysfunction. Nonetheless, the protective mechanism is not clear. Therefore, the present study investigated the potential mechanism of As-IV on VED. Calpain-1 knockout and wild-type C57BL/6 mice exposed to chronic intermittent hypoxia (CIH) were established and treated with As-IV (40, 80 mg/kg) for 4 weeks. Human coronary artery endothelial cells (HCAECs) subjected to CIH exposure were pretreated with As-IV, MDL-28170 (calpain-1 inhibitor) and SRT1720 (SIRT1 activator) for 48 h *in vitro*. The endothelial function, inflammation, oxidative stress and mitochondrial function were measured to evaluate VED. Our data revealed that As-IV treatment ameliorated CIH-induced endothelial-dependent vasomotion and augmented nitric oxide (NO) production. As-IV administration suppressed the secretion of inflammation, oxidative stress and mitochondrial dysfunction. As-IV treatment reduced the expression of calpain-1 and restored the downregulated expression of SIRT1 and Thr^{172} AMPK and Ser^{1177} eNOS phosphorylation. The effects of calpain-1 knockout and SRT1720 were similar to the effect of As-IV on VED. These findings demonstrated that As-IV ameliorated VED induced by chronic intermittent hypoxia via the calpain-1/SIRT1/AMPK signaling pathway.

KEYWORDS

Astragaloside IV, chronic intermittent hypoxia, vascular endothelial dysfunction, oxidative stress, calpain-1

Introduction

Obstructive sleep apnea (OSA) is a sleep breathing disorder that is manifested as the partial or complete collapse of the upper airway during sleep (Baltzis et al., 2016). OSA affects 14% and 5% of adult males and females in the US, respectively (Chang et al., 2020), and it is an independent and significant factor of cerebrovascular and cardiovascular disease (CVD). Previous studies showed that chronic intermittent hypoxia (CIH) was the major pathophysiological characteristic of vascular endothelial dysfunction (VED) in OSA, which may lead to CVD by initiating nitric oxide (NO) unavailability, oxidative stress and vascular inflammation (Feng et al., 2012). As the first-line treatment of OSA patients, continuous positive airway pressure (CPAP) has a low compliance rate and poor prevention effect on cardiovascular events (Mcevoy et al., 2016; Arnaud et al., 2020). Therefore, there is an urgent need for other treatments to acquire an improvement in preventing cardiovascular complications and quality of life of OSA patients.

SIRT1 is an NAD^+-dependent deacetylase that has crucial role in mediating inflammation, oxidative stress and mitochondrial function (Mihanfar et al., 2021). SIRT1 is involved in maintaining vascular endothelial homeostasis and protecting VED (Ministrini et al., 2021). SIRT1 and AMPK stimulate NO production by increasing endothelial NO synthase (eNOS) activity (Xia et al., 2014). Calpain is a conserved family of calcium-activated cysteine proteases that widely exist in mammals. Calpain-1, is the major isoform, and it is primarily expressed in endothelial cells and participates in many pathophysiological processes (Liu et al., 2020). Early studies showed that VED was associated with calpain overactivation in chronic vascular diseases (Miyazaki and Miyazaki, 2018). Calpain-1 also contributes to oxidative stress, inflammation and adhesiveness to leukocytes (Xu C. et al., 2021). Calpain is involved in the AMPK/eNOS signaling pathway in VED (Etwebi et al., 2018). Although previous studies demonstrated that activation of calpains caused a reduction in SIRT1 protein levels (Biel et al., 2016), whether the calpain-1/SIRT1/AMPK signaling pathway is a major factor of VED was not reported.

Astragaloside IV (As-IV) is a major natural molecule compound isolated from *Astragalus* membranaceus that exerts diverse cardiovascular pharmacological activities, including anti-inflammatory, anti-fibrosis, anti-oxidative stress and immune regulation activities (Chen et al., 2021; Deng et al., 2022). Our previous studies demonstrated that As-IV protected against hyperglycemia-induced VED by inhibiting calpain-1 overactivation (Nie et al., 2019). As-IV also attenuates CIH-induced myocardial injury and inflammation (Chen et al., 2020; Jiang et al., 2020). However, the potential mechanism of As-IV activity against CIH-induced VED is not clear. Therefore, we used calpain-1 knockout *in vivo* and *in vitro* to further study the effect of As-IV on CIH-induced VED and the potential mechanism.

Materials and methods

Reagents

As-IV were obtained from Nanjing Jingzhu Biotechnology Co. Ltd. (Nanjing, China). Assay kits for Cell Counting Kit-8, NO nitrate reductase, dihydroethidium (DHE), GSH-px, MDA, SOD, JC-1, DAF-FM diacetate (DAF-FM DA) and MitoSOX were obtained from Beyotime Biotechnology (Shanghai, China). Calpain-1, SIRT1 and β-actin were obtained from Proteintech (Wuhan, China). Ser^{1177} eNOS phosphorylation, total endothelial nitric oxide (eNOS), Thr^{172} AMPK phosphorylation, total 5' AMP activated protein kinase (t-AMPK), vascular cell adhesion molecule 1 (VCAM-1) and intracellular adhesion molecule 1 (ICAM-1) were obtained from ABclonal (Wuhan, China). Phenylephrine (PE) and acetylcholine (Ach) were obtained from Sigma Aldrich (Shanghai, China). MDL-28170, SRT1720 and L-NAME were obtained from Selleck (Houston, TX, United States).

Animal experiments

Eight-to twelve-week-old male wild-type mice (Liaoning Changsheng Biotechnology Co. Ltd.) and mice deficient in calpain-1 (Capn1 $EK684^{-/-}$, Cyagen Biosciences Inc.) with a mean body weight of 25 g were used. Both wild-type and $Capn1^{-/-}$ mice are the C57BL/6 background, and the same strain. All mice were grown in a normal environment at a controlled temperature (25 ± 2°C) under a 12-h light/dark cycle. The Animal Ethics Committee of Jinzhou Medical University approved all animal procedures. Wild-type mice were randomly divided into four groups (n = 10): control group (Con), chronic intermittent hypoxia group (CIH), CIH + As-IV 40 mg/kg/d (AL) and CIH + As-IV 80 mg/kg/d (AH). $Capn1^{-/-}$ mice were also divided randomly into two groups (n = 10): the control group (CK) and the chronic intermittent hypoxia group (MK). The model of CIH exposure established in this study was reported previously (Jiang et al., 2020). Briefly, the mice were exposed to cages of automated, computer-controlled O_2 concentration exchange systems (Proox-100, Shanghai Tow-Int Tech Ltd.) to achieve a similar oxyhemoglobin saturation (SpO_2) nadir (50~60%) in moderate to severe patients based on previous studies (Zhou et al., 2014; Hu et al., 2021; Li et al., 2021). The mice were exposed to 20 hypoxic events/h (90 s of 21% O_2 and 90 s of 10% O_2) for 8 h/day for 4 weeks. The control mice breathing normal gas were housed in the same environment. During the CIH interval, mice received a gastric injection of As-IV (dissolved in 5% sodium carboxymethyl cellulose) at 40 or 80 mg/kg per day for 4 weeks. The special gavage needle for mice is used for intragastric administration of mice, and the volume of intragastric administration does not exceed 0.2 ml. After

4 weeks, corresponding samples (thoracic aortas and serum) were collected for subsequent experiments.

Cell culture

Human coronary artery endothelial cells (HCAECs) were purchased from BLUEFBIO and grown in DMEM supplemented with 15% fetal bovine serum (HyClone, Logan, Utah, United States) in a CO_2 incubator as described previously (Lv et al., 2019). The model of CIH in HCAECs was implemented by alternating cycles of 1% O_2 for 5 min followed by 20% O_2 for 5 min (3 cycles/h) at 37°C for 24 h in a chamber through automated, computer-controlled O_2 concentration exchange systems (GC-CT, Heilongjiang MAWORDE Industry and Trade Ltd.) as described previously (Jiang et al., 2020; Xu H. et al., 2021; Yan et al., 2021). Cells were incubated with As-IV (100 μM), MDL-28170 (calpain-1 inhibitor, 20 μM) and SRT1720 (SIRT1 activator, 4 μM) for 48 h before CIH exposure.

Vascular reactivity

After sacrifice, the thoracic aorta was fully exposed, quickly removed and placed in ice-cold physiological salt solution (PSS) that included the following: NaCl (130 mM), KCl (4.7 mM), KH_2PO_4 (1.18 mM), $MgSO_4$ (1.17 mM), $CaCl_2$ (1.16 mM), $NaHCO_3$ (14.9 mM), EDTA (0.026 mM), and glucose (11.1 mM). The thoracic aorta was cut into rings approximately 2 mm in length without fat and connective tissue under a microscope. Changes in the tension of rings were measured using DMT (720 M, Danish Myotechnology, AÅrhus, Denmark). The rings of all groups were incubated in chambers with 95% O_2 and 5% CO_2 at 37 °C. Before the formal experiment, we used K-PSS (60 mM KCl in PSS solution; equimolar substitution of KCl for NaCl) to activate the rings. If the difference change in tension of rings was less than 10%, the vasoconstriction was considered relatively stable and rings were used in subsequent experiments. The rings were precontracted with PE (10^{-5} M), and ACh was added after the contraction was stable in the range of concentration (10^{-8} M - 10^{-5} M). The endothelium-dependent relaxation (EDR) response to ACh is expressed as the percentage of maximal contraction amplitude induced by PE. To test the effect of NO on vascular relaxation, the aortic rings of all groups were incubated with the nitric oxide synthase inhibitor NG-nitro-L-arginine (L-NAME, 100 μM) for 30 min before PE-induced constriction. To verify the role of SIRT1 on VED, the rings from the control group and the CIH group were incubated with SRT1720 (4 μM, dissolved in DMSO) for 24 h in chambers with 95% O_2 and 5% CO_2 at 37°C. DMSO (0.1% v/v) did not modify agonist-induced responses. Following incubation, the rings were used to measure vascular reactivity as mentioned above.

Determination of intracellular ROS production and NO imaging

The level of intracellular ROS in aortas and HCAECs was detected using DHE staining. Frozen sections of aortas (embedded in OCT and 5 μm thick) and cells were incubated with 5 μM DHE for 30 min at room temperature in the dark. Rosup was used as a positive control to detect intracellular ROS expression. The sections and cells were stained with Hoechst 33342 for 4 min and washed 3 times with PBS. NO imaging experiments in aortas and cells were performed as described previously (Lee et al., 2020). Briefly, frozen sections of aortas and cells were incubated with 20 μM DAF-FM DA for 20 min at 37°C. The sections were stained with Hoechst 33342 for 4 min. Images were viewed under a Leica DMI3000B fluorescence microscope, and the relative fluorescence intensity was analyzed using ImageJ software.

Immunofluorescence staining

Four% paraformaldehyde-fixed, paraffin-embedded aortic tissues were cut into 5-μm thick slices. Then the slices were deparaffinized, rehydrated, and incubated in 5% BSA for 1 h. The slices were incubated with primary antibodies against calpain-1 (1:100) and SIRT1 (1:100) at 4°C overnight. The relative secondary antibody was incubated with the slices for 1 h at 37°C in the dark. Nuclei were marked using Hoechst 33342. Quantification of the images was analyzed by ImageJ Software from each group.

Western blot

The collected sample proteins were homogenized in lysis buffer, and the concentration of total proteins was measured using the BCA method. The prepared samples were separated using 8%–10% SDS–PAGE then transferred to PVDF membranes. Membranes were blocked with 1% BSA for 1.5 h and subsequently incubated with calpain-1 (1:1,000), SIRT1 (1:4,000), t-AMPK (1:1,000), Thr^{172} phosphorylated AMPK (1:1,000), eNOS (1:1,000), ICAM-1 (1:1,000), VCAM-1 (1:1,000), Ser^{1177} phosphorylated eNOS (1:1,000) and β-actin (1:10,000) overnight at 4°C. After washing with TBST, membranes were incubated with HRP-conjugated secondary antibody for 2 h at room temperature. The intensity of the bands was determined using ImageJ software.

Measurements of SOD, MDA, GSH-px

MDA, SOD, and GSH-px assay kits were used to measure MDA and GSH-px levels and SOD activity in the

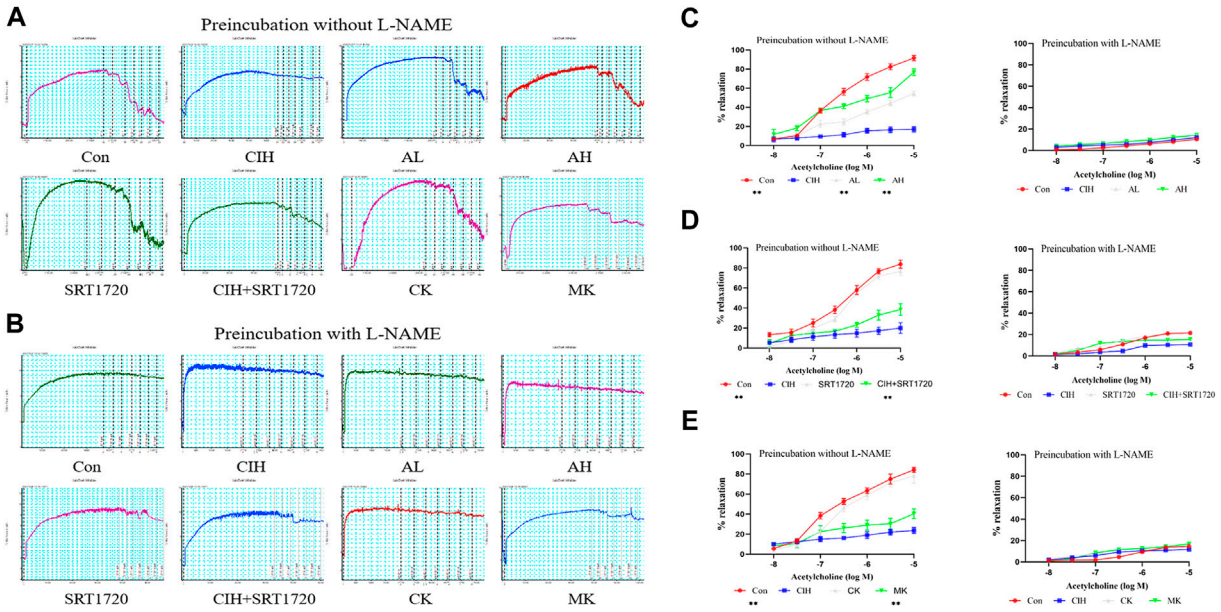

FIGURE 1
Effects of As-IV, Capn1 knockout and SRT1720 on VED in mice exposed to CIH. **(A,B)** The reactivity of PE-preconstricted aortic rings from all groups to ACh-mediated relaxation with or without L-NAME **(C)** The effect of As-IV treatment on ACh-induced vasodilation in aortas of CIH-exposed (90 s of 21% O_2 and 90 s of 10% O_2) mice (n = 5). **(D)** The effect of SRT1720 (4 μM) incubation on ACh-induced vasodilation in aortas of CIH-exposed mice (n = 5). **(E)** The effect of Capn1 knockout treatment on ACh-induced vasodilation in aortas of CIH-exposed mice (n = 5). Data are presented as the means ± SD, $^{**}p < 0.01$, vs. CIH group.

serum and culture supernatant according to the manufacturer's protocol. The NO levels in serum and culture supernatant were tested using the nitrate reductase method according to the manufacturer's protocol.

Enzyme-linked immunosorbent assay

The levels of IL-6 and TNF-α in serum and culture supernatant were analyzed using ELISA kits according to the manufacturer's instructions.

Cell viability assay

The cell viability of HCAECs was assessed using a Cell Counting Kit-8 (CCK-8 kit) as previously described (Yan et al., 2021). Briefly, HCAECs under the indicated times and different conditions were seeded in 96-well plates at the density of 2×10^4 cells/well and were added with 10 μl CCK-8 reagent for 1 h. The absorbance at 450 nm was measured with a microplate reader (BioRad, United States). Cell viability was calculated based on the percentage of the optical density relative to that of untreated controls.

Assessment of mitochondrial function

The cells were incubated with 10 μg/ml JC-1 and 5 μM MitoSOX. The mitochondrial membrane potential was determined using JC-1 staining as previously described (Umbaugh et al., 2021). Briefly, the cells were incubated with JC-1 at 10 μg/ml for 15 min at 37°C, CCCP was set as the positive control of mitochondrial membrane potential decline, and then the images were observed by fluorescence microscopy. Increased monomer (green) fluorescence levels and decreased J-aggregate (red) fluorescence levels indicate mitochondrial membrane potential collapse. All images were analyzed by ImageJ software. Mitochondrial reactive oxygen species (mitoROS) were determined using MitoSOX as previously described (Zhou et al., 2021). Briefly, the cells were incubated with 5 μM MitoSOX for 10 min at 37°C in the dark. Then the images were captured using fluorescence microscopy and analyzed using ImageJ software.

Statistical analysis

All the data are represented as the means ± standard deviation (SD) and analyzed by SPSS 26.0 software. Statistical analyses of all data were performed using One-way analysis of variance (ANOVA) followed by Duncan's LSD. $p < 0.05$ was considered statistically significant.

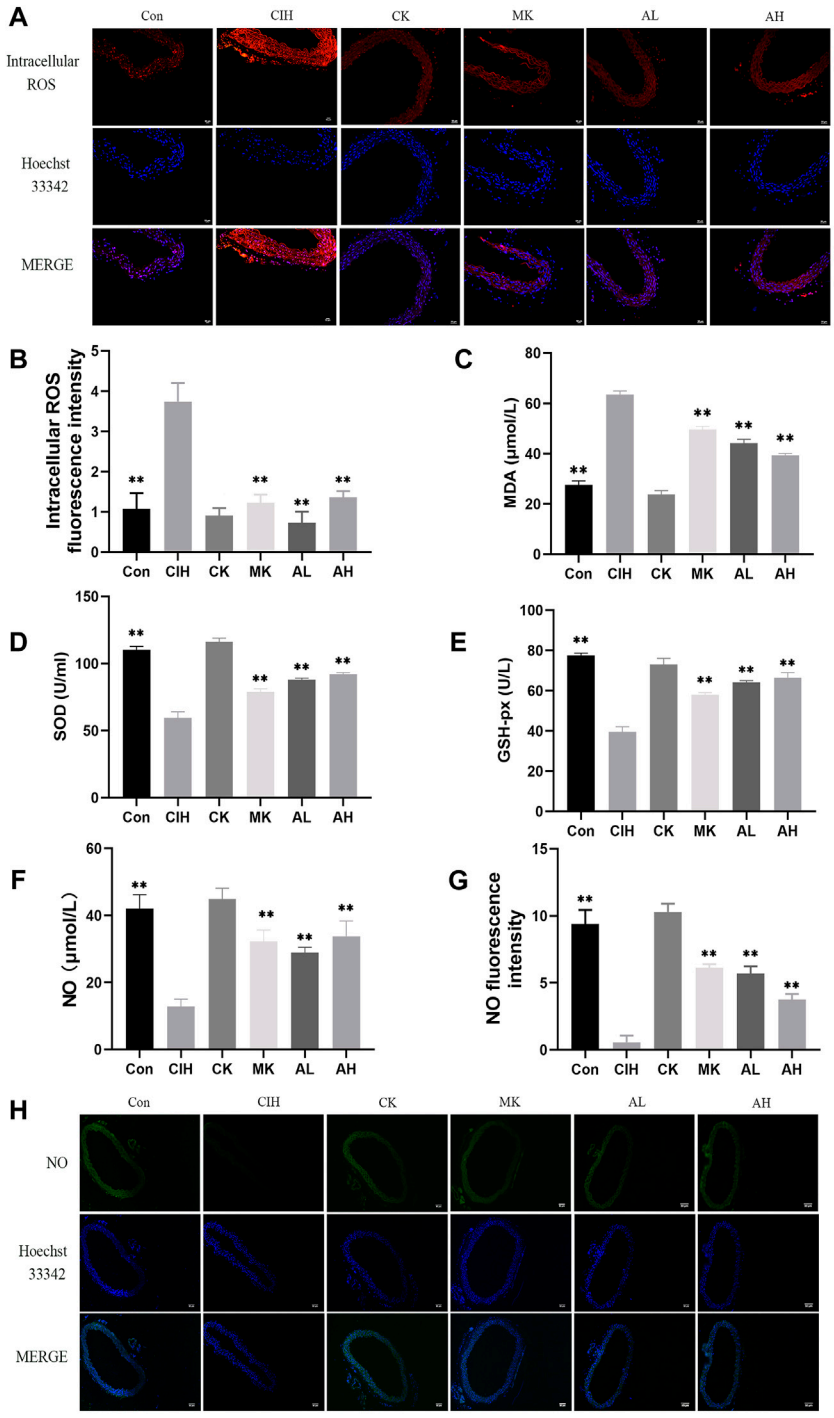

FIGURE 2
Effects of As-IV and Capn1 knockout on CIH-induced oxidative stress and NO levels. **(A,B)** The level of intracellular ROS in aortas was measured using DHE staining (×200 magnification; $n = 3$). DHE dye (red), Hoechst 33342 (blue). **(C–E)** The activity of SOD and the levels of MDA and GSH-px in serum were determined using kits ($n = 8$). **(F)** NO production in serum was evaluated using the nitrate reductase method ($n = 8$). **(G,H)** The level of NO in aortas was measured using DAF-FM DA fluorescence staining (×100 magnification; $n = 3$). DAF-FM DA dye (green), Hoechst 33342 (blue). Data are presented as means ± SD. ns. $^{**}p < 0.01$, vs. CIH group.

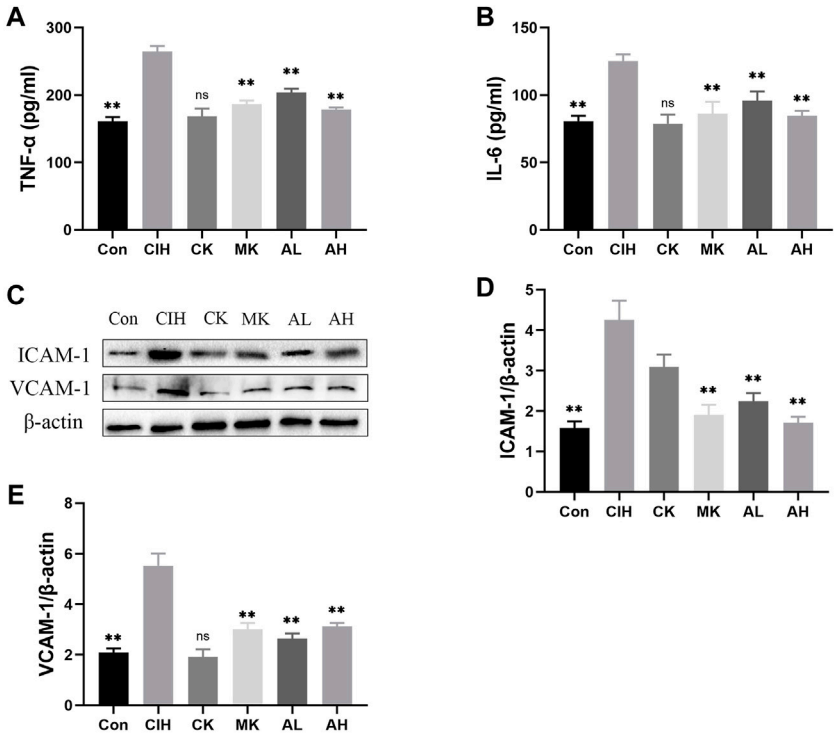

FIGURE 3
Effects of As-IV and Capn1 knockout on CIH-induced inflammation. **(A,B)** The levels of TNF-α and IL-6 were detected using ELISA (n = 8). **(C–E)** Quantitative Western blot analysis of the protein levels of VCAM-1 and ICAM-1 (n = 3). Data are presented as means ± SD. $^{**}p < 0.01$, vs. CIH group.

Results

Effects of As-IV, Capn1 knockout and SRT1720 on VED in mice exposed to CIH

EDR is the most widely used assay for the assessment of VED (Figures 1A, B). The reactivity of isolated thoracic aortic rings to ACh was evaluated in CIH-exposed mice after treatment with As-IV for 4 weeks. As shown in Figure 1C, As-IV attenuated the damaged ACh-induced EDR in isolated thoracic aortic rings of mice exposed to CIH. To determine the effect of SIRT1 on CIH-induced VED, aortic rings from the control group and CIH group were incubated with SRT1720 (4 μM) for 24 h *in vitro*. Our studies showed that SRT1720 ameliorated relaxation to ACh in CIH-exposed mice (Figure 1D). To investigate the role of calpain-1 on CIH-induced VED, we detected ACh-induced dilation after PE preconstriction in the CK group and MK group. Our data indicated that the aortic rings from Capn1$^{-/-}$ mice slightly but statistically improved CIH-induced VED compared to CIH-exposed mice (Figure 1E). And vascular relaxation to ACh was completely abolished by eNOS inhibitor L-NAME in all groups.

Effects of As-IV and Capn1 knockout on CIH-induced oxidative stress and NO levels

To verify the effect of As-IV on VED in mice exposed to CIH, DHE staining, MDA, SOD, and GSH-px assay kits and the nitrate reductase method were performed. Compared to the control group, the levels of intracellular ROS and MDA were increased, the activity of SOD and the levels of GSH-px and NO were significantly inhibited in the CIH group. After treatment with As-IV (40 or 80 mg/kg) for 4 weeks, the activity of SOD and the production of NO and GSH-px were higher than the CIH group. The levels of intracellular ROS and MDA were lower than the CIH group. The effect of Capn1 knockout mice was similar to the above effect of As-IV (Figure 2).

Effects of As-IV and Capn1 knockout on CIH-induced inflammation

Inflammation and adhesion molecules, such as VCAM-1 and ICAM-1, are vital for the development of VED. Our data indicated that the contents of TNF-α and IL-6 were

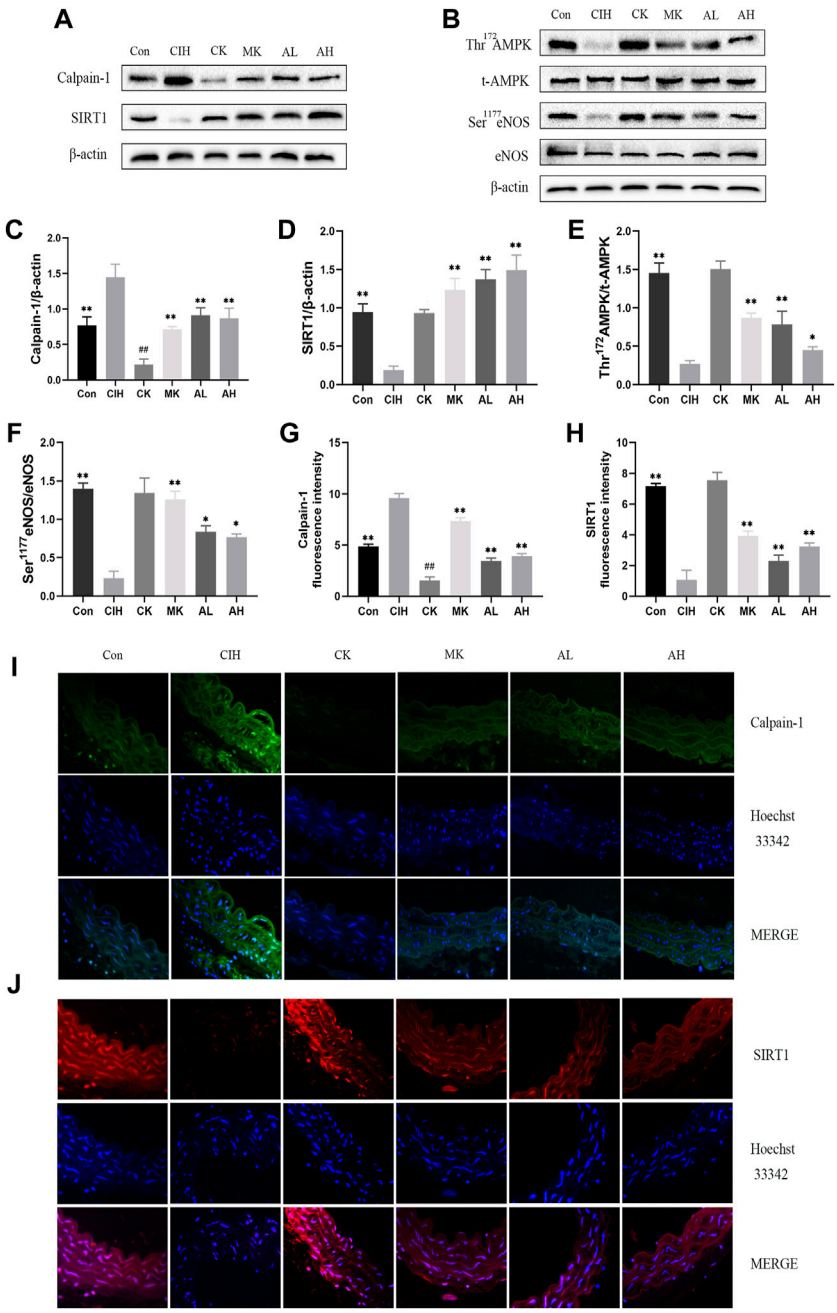

FIGURE 4
Effects of As-IV and Capn1 knockout on the SIRT1/AMPK/eNOS signaling pathway in CIH-induced mice. **(A–F)** Western blot analysis of calpain-1, SIRT1, Thr^{172} AMPK phosphorylation, t-AMPK, Ser^{1177} eNOS phosphorylation and eNOS protein expression in all groups with quantification (n = 3). **(G–J)** Representative fluorescence images and fluorescence intensity of calpain-1 and SIRT1 in all groups of aortic sections (×400 magnification; n = 3). Calpain-1 (green), SIRT1 (red), Hoechst 33342 (blue). Data are presented as means ± SD. #P < 0.05, vs. Con group, **p < 0.01, *P < 0.05, vs. CIH group.

enhanced in the CIH group, and As-IV and Capn1 knockout inhibited the levels of inflammation (Figures 3A, B). The mice exposed to CIH showed high expression of VCAM-1 and ICAM-1, and As-IV treatment and Capn1 knockout significantly abolished these changes at the protein level (Figures 3C-E).

Effects of As-IV and Capn1 knockout on calpain-1, SIRT1, AMPK, and eNOS protein expression in CIH-induced mice

To investigate whether calpain-1 regulates VED via the SIRT1/AMPK/eNOS signaling pathway in mice exposed to CIH, western

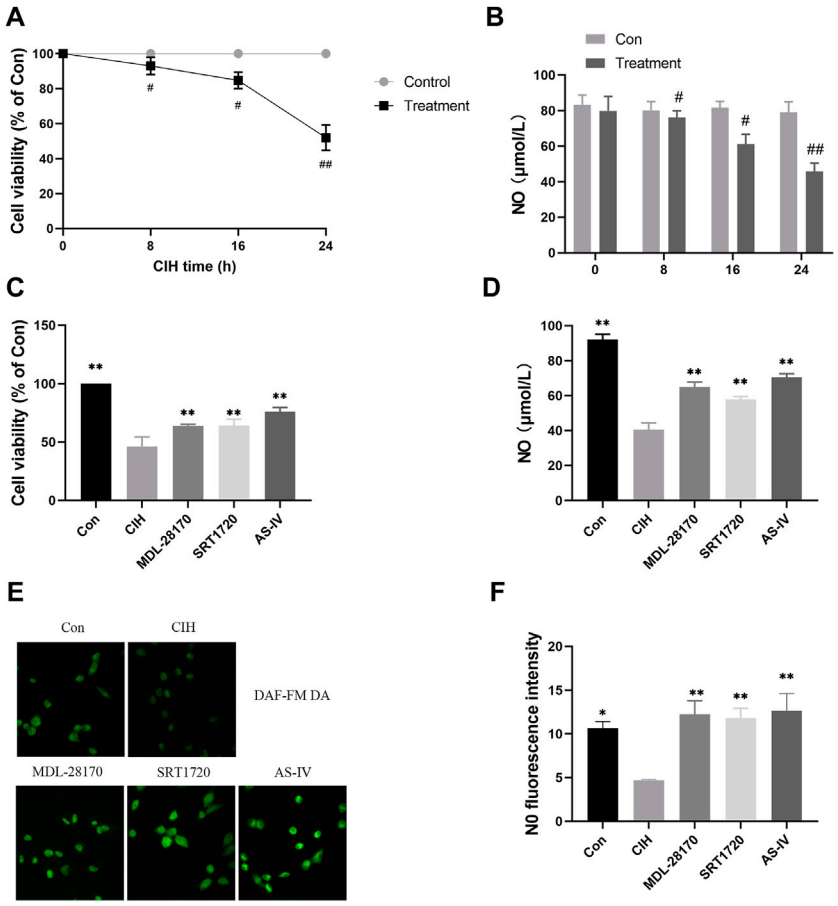

FIGURE 5
Effects of As-IV, MDL-28170 and SRT1720 on HCAEC viability and the production of NO. **(A)** Cell viability of HCAECs subjected to CIH (1% O_2 for 5 min–20% O_2 for 5 min) at the indicated times at the indicated times (n = 5). **(B)** NO level in HCAEC supernatant subjected to CIH at the indicated times (n = 8). **(C)** Cell viability of HCAECs in different groups (n = 5). **(D)** NO levels in HCAEC supernatants from different groups (n = 8). **(E,F)** Representative images and fluorescence intensity of NO in HCAECs of different groups (×200 magnification; n = 3). DAF-FM DA dye (green). Data are presented as means ± SD. $^{\#\#}p < 0.01$, $^{\#}P < 0.05$, vs. Con group, $^{**}p < 0.01$, $^{*}P < 0.05$, vs. CIH group.

blot analysis and immunofluorescence staining were conducted. Our findings revealed that compared with the control group, the expression level of calpain-1 was only reduced in the CK group, the other indexes were not statistically significant. CIH resulted in higher levels of calpain-1 and lower levels of SIRT1, Thr^{172} AMPK phosphorylation and Ser^{1177} eNOS phosphorylation. In contrast, treatment with As-IV and Capn1 knockout downregulated the level of calpain-1 and upregulated the levels of SIRT1, Thr^{172} AMPK phosphorylation and Ser^{1177} eNOS phosphorylation (Figure 4).

Effects of As-IV, MDL-28170 and SRT1720 on VED in HCAECs subjected to CIH

To test the effect of As-IV on VED, we measured the viability of HCAECs under normoxia or CIH exposure for the indicated times. Compared to the control group, cell viability decreased with prolonged CIH administration (Figure 5A). The NO level in the HCAEC supernatant after CIH exposure was also reduced in a time-dependent manner (Figure 5B). However, the As-IV, MDL-28170 and SRT1720 groups exhibited increased cell viability and NO levels in HCAECs compared to the CIH group (Figures 5C–F).

Effects of As-IV, MDL-28170 and SRT1720 on oxidative stress in HCAECs exposed to CIH

Oxidative stress is an indispensable element of the earlier periods of endothelial damage. Our data indicated that compared to the control group, CIH exposure facilitated

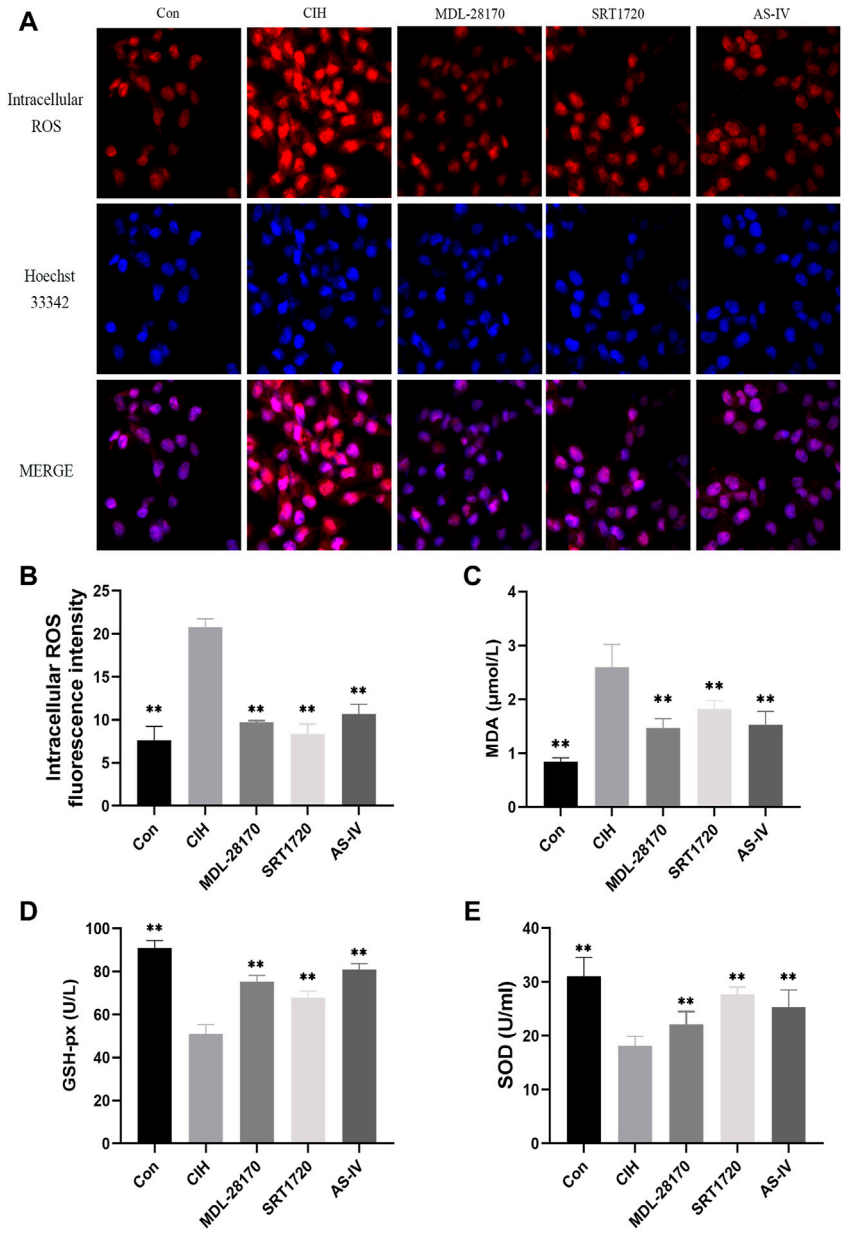

FIGURE 6
Effects of As-IV, MDL-28170 and SRT1720 on oxidative stress in HCAECs exposed to CIH. **(A,B)** Representative fluorescence images and fluorescence intensity of intracellular ROS in HCAECs of different groups (×200 magnification; $n = 3$). DHE dye (red), Hoechst 33342 (blue). **(C–E)** The activity of SOD and the levels of MDA and GSH-px in HCAEC supernatant were detected using kits ($n = 8$). Data are presented as means ± SD. $^{**}p < 0.01$, vs. CIH group.

the levels of intracellular ROS and MDA in HCAECs and decreased the level of GSH-px and the activity of SOD. The administration of AS-IV suppressed the levels of intracellular ROS and MDA in HCAECs compared to the CIH group and enhanced the activity of SOD and the level of GSH-px. The effect of AS-IV on oxidative stress was similar to MDL-28170 and SRT1720 (Figure 6).

Effects of As-IV, MDL-28170 and SRT1720 on mitochondrial dysfunction in HCAECs exposed to CIH

Mitochondria are the primary producers of intracellular ROS. To test whether As-IV ameliorated CIH-induced mitochondrial dysfunction, JC-1 and MitoSOX staining were conducted. The

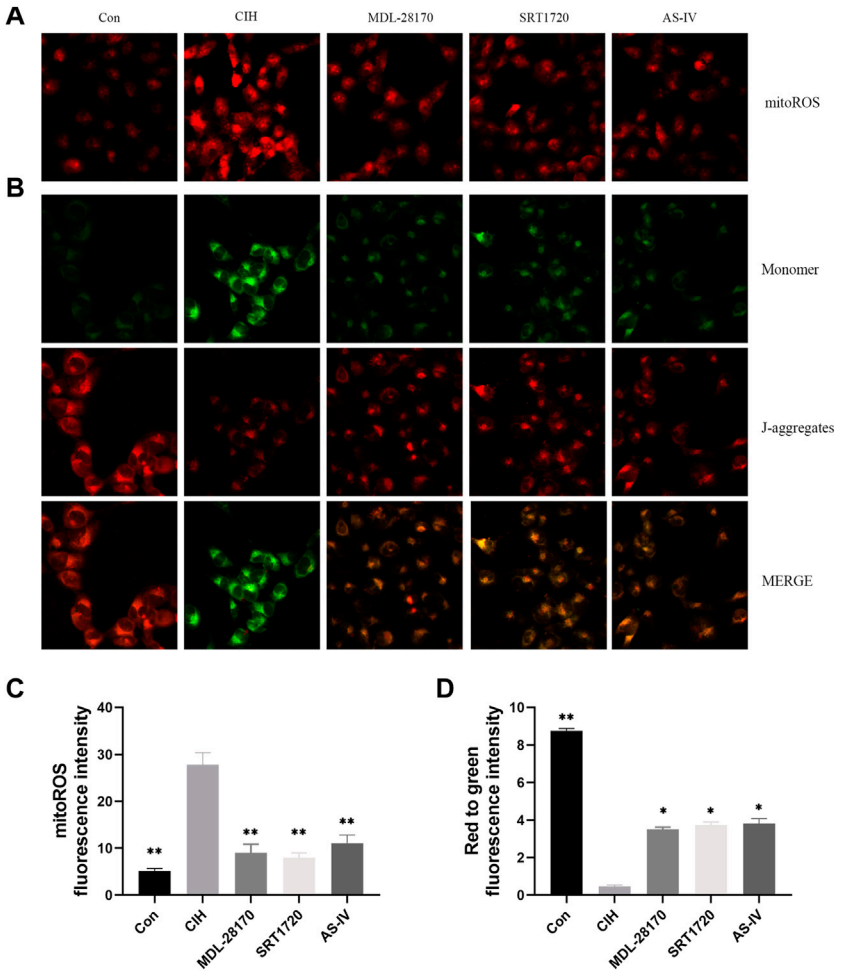

FIGURE 7
Effects of As-IV, MDL-28170 and SRT1720 on mitochondrial dysfunction in HCAECs exposed to CIH. **(A,C)** Representative fluorescence images and fluorescence intensity of mitoROS in HCAECs of different groups (×200 magnification; $n = 3$). MitoSOX dye (red). **(B,D)** Representative fluorescence images of JC-1 staining indicating the mitochondrial membrane potential in HCAECs of different groups (×200 magnification; $n = 3$). Monomer (green), J-aggregates (red). Data are presented as means ± SD. $^{**}p < 0.01$, $^{*}P < 0.05$, vs. CIH group.

results showed an apparent increase in the level of mitoROS and a decline in the membrane potential of HCAECs exposed to CIH compared to the control group. As-IV, MDL-28170 and SRT1720 treatment restored the increased level of mitoROS and the reduced membrane potential (Figure 7).

Effects of As-IV, MDL-28170 and SRT1720 on inflammation in HCAECs exposed to CIH

To evaluate the effect of As-IV, MDL-28170 and SRT1720 on inflammation, ELISA and Western blot experiments were performed. ELISA indicated that the levels of TNF-α and IL-6 was increased in the supernatants of HCAECs subjected to CIH, and As-IV, MDL-28170 and SRT1720 treatment reduced the secretion of inflammatory factors (Figures 8A, B). The levels of VCAM-1 and ICAM-1 protein were enhanced by CIH exposure compared to the control, and the administration of As-IV, MDL-28170 and SRT1720 partially abolished the upregulated secretion of inflammatory factors in HCAECs exposed to CIH (Figures 8C–E).

Effects of As-IV, MDL-28170 and SRT1720 administration on calpain-1, SIRT1, AMPK, and eNOS protein expression in HCAECs

To verify the effects of As-IV, MDL-28170 and SRT1720 administration on calpain-1, SIRT1, AMPK, and

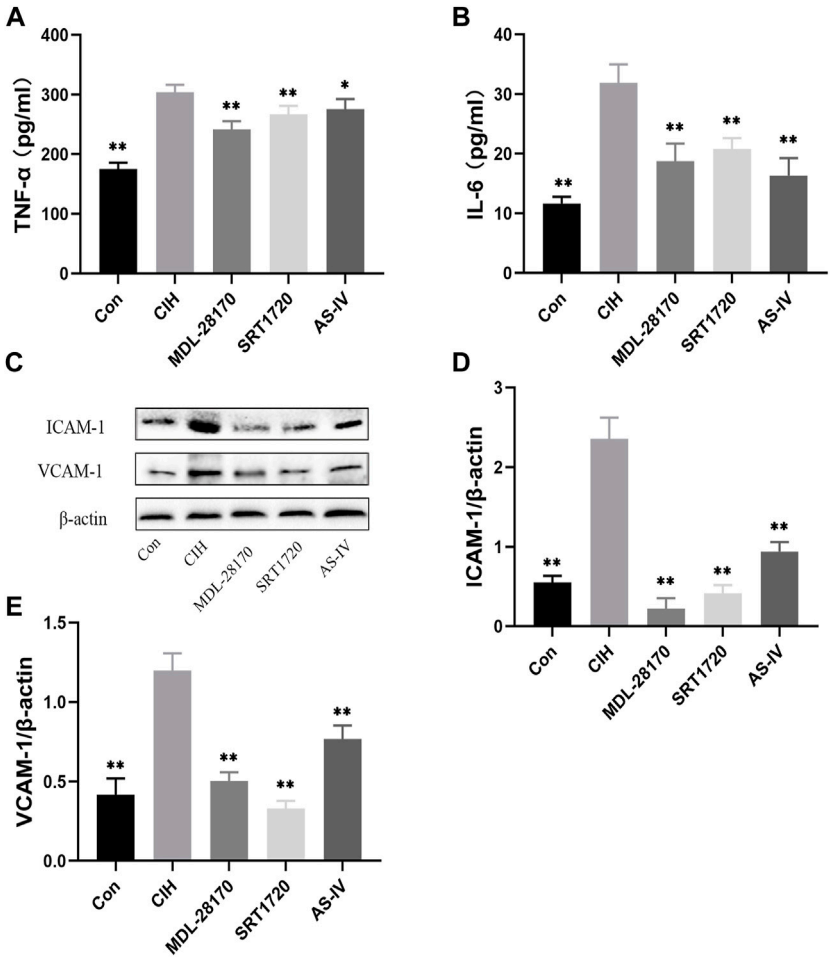

FIGURE 8
Effects of As-IV, MDL-28170 and SRT1720 on inflammation in HCAECs. **(A,B)** The levels of TNF-α and IL-6 was detected using ELISA (n = 8). **(C–E)** The levels of VCAM-1 and ICAM-1 were measured using Western blot (n = 3). Data are presented as means ± SD. $^{**}p < 0.01$, vs. CIH group.

eNOS protein expression in HCAECs, Western blot experiments were performed. The data indicated that the expression level of calpain-1 protein was increased and the levels of SIRT1 protein expression, Thr^{172} AMPK phosphorylation and Ser^{1177} eNOS phosphorylation were reduced in HCAECs after CIH exposure. Treatment with As-IV, MDL-28170 and SRT1720 reversed the protein expression levels (Figure 9).

Discussion

The vascular endothelium is formed from a monolayer of endothelial cells that regulate vascular hemostasis, maintains permeability and controls vascular tone. VED is linked with reduced nitric oxide (NO) production or bioavailability and damaged endothelial-dependent vasomotion (Cyr et al., 2020; Xu S. et al., 2021). OSA characterized by intermittent hypoxemia, is a main independent and important risk factor for the occurrence of cardiovascular disease (CVD). Numerous studies demonstrated that VED played a key role in the pathogenesis of OSA comorbidities, such as cardiovascular and metabolic diseases (Baltzis et al., 2016). After 4 weeks of exposure to intermittent hypoxemia in mice, we found that CIH decreased endothelial-dependent vasomotion to ACh, and As-IV reversed this response. CIH inhibited relative viability, Ser^{1177} eNOS phosphorylation and NO production in HCAECs, and As-IV rescued these changes. HCAECs were used in the current study since coronary endothelium expresses a pathologic gene pattern compared to aortic endothelium, and were commonly used in cell model of CIH (Dancu and Tarbell, 2007; Zychowski et al., 2016). However, this is also the limitation of this study. The differences between different species and tissues should be taken into account in future studies. These results suggested that As-IV ameliorated CIH-induced VED via the NO

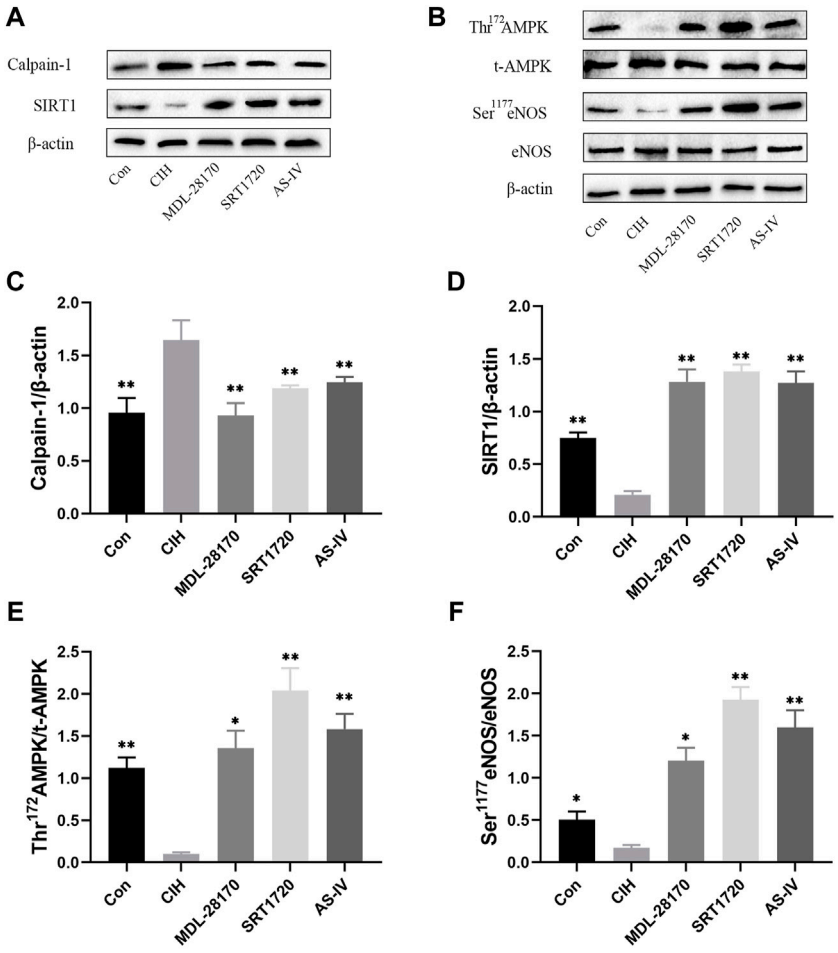

FIGURE 9
Effects of As-IV, MDL-28170 and SRT1720 administration on calpain-1, SIRT1, AMPK, and eNOS protein expression in HCAECs. **(A–F)** The protein expression levels of calpain-1, SIRT1, Thr^{172} AMPK phosphorylation, t-AMPK, Ser^{1177} eNOS phosphorylation and eNOS were analyzed using Western blots (n = 3). Data are presented as means ± SD. $^{**}p < 0.01$, $^{*}P < 0.05$, vs. CIH group.

pathway. OSA is associated with the excessive generation of inflammatory mediators and the overproduction of adhesion molecules in the development of VED (Baltzis et al., 2016). Previous studies indicated that increased levels of the inflammatory factors TNF-α and IL-6 are primarily responsible for inflammatory responses in OSA patients (Kiernan et al., 2016). The upregulation of adhesion molecules, such as ICAM-1 and VCAM-1, stimulates endothelial activation by promoting leukocyte adhesion to endothelial cells when inflammation occurs (Sun et al., 2019). An activated endothelium results in decreased NO bioavailability and impaired vascular tone, which further cause VED. Intermittent hypoxia accelerated the activation of ICAM-1 and VCAM-1, which was demonstrated in human endothelial cells and animal models (Feng et al., 2012). The overactivation of ROS and mitochondrial dysfunction, which result in oxidative stress, play a crucial role in producing VED and ultimately increases cardiovascular risk in OSA (Baltzis et al., 2016; Incalza et al., 2018). According to previous studies, the increased production of ROS correlates with higher interaction with NO and ROS, which form peroxynitrite in one of the earlier periods of endothelial damage (Badran et al., 2014). Mitochondrial dysfunction is associated with the loss of mitochondrial membrane potential and excess production of mitochondrial reactive oxygen species (mitoROS) (Rizwan et al., 2020). Previous studies demonstrated that oxidative stress biomarkers (SOD, GSH-px, and MDA) were increased in rats exposed to CIH (Joseph et al., 2020). Our data confirmed these effects and indicated that As-IV suppressed the activation of inflammation, oxidative stress and mitochondrial dysfunction.

SIRT1 is one of the most extensively studied and vital members of the sirtuin family, and it is an NAD$^+$-dependent deacetylase that is highly expressed in endothelial cells (Kida and Goligorsky, 2016). Many studies showed that SIRT1 activators degraded the expression of inflammatory factors and leukocyte adhesion in the

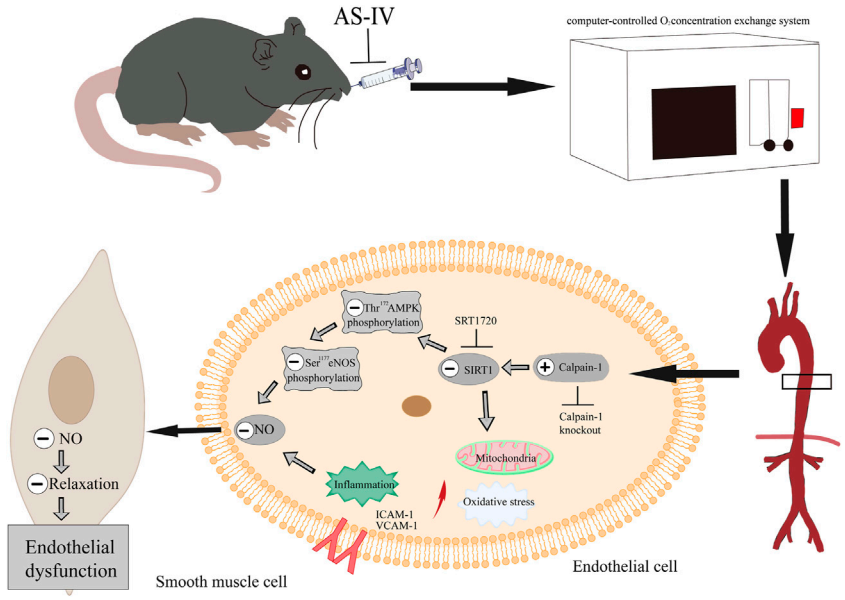

FIGURE 10
As-IV ameliorates endothelial dysfunction induced by chronic intermittent hypoxia through the calpain-1/SIRT1/AMPK signaling pathway.

aortas of mice and consequently improved VED in cardiovascular diseases (Kida and Goligorsky, 2016; Parsamanesh et al., 2021). SIRT1 also could suppress the development of oxidative stress and mitochondrial dysfunction in endothelial cells (Yuan et al., 2016). A number of recent findings mentioned that SIRT1 mediates eNOS expression via the SIRT1/AMPK pathway (Liu et al., 2016). Our data demonstrated that CIH reduced the level of SIRT1 protein and Thr^{172} AMPK and Ser^{1177} eNOS phosphorylation in the aortas of mice and HCAECs, which were restored by As-IV treatment. To investigate whether SIRT1 was involved in the development of VED, we used isolated aortic rings from control and CIH-exposed mice to measure changes in vascular tension with or without incubation using the SIRT1 activator SRT1720. Treatment with SRT1720 attenuated the impaired EDR to ACh in CIH-exposed aortic rings, and increased the production of NO in HCAECs. SRT1720 treatment also reversed Thr^{172} AMPK and Ser^{1177} eNOS phosphorylation in CIH-treated HCAECs, and the protein expression of total AMPK and eNOS remained unchanged. SRT1720 treatment restrained the increase in inflammatory factors, the activation of oxidative stress and mitochondrial dysfunction in the CIH environment. These results suggested that As-IV suppressed inflammation, oxidative stress and mitochondrial dysfunction via the SIRT1/AMPK/eNOS signaling pathway and eventually ameliorated CIH-induced VED. Calpain-1 is a Ca^{2+}-sensitive intracellular cysteine protease that widely exists in endothelial cells (Tang et al., 2015). The overactivation of calpain is involved in VED via the AMPK/eNOS signaling pathway (Miyazaki and Miyazaki, 2018). Convincing evidence revealed that calpains regulate SIRT1 depletion (Biel et al., 2016). Calpain-1 contributes to oxidative stress, mitochondrial dysfunction, inflammation and adhesiveness to leukocytes (Xia et al., 2014; Liu et al., 2020; Dang et al., 2022). Our laboratory and other laboratories reported that calpain-1 aggravated diabetes-induced and arsenic-induced VED (Cai et al., 2019; Nie et al., 2019). However, sufficient evidence to determine whether calpain-1 is participated in CIH-induced VED is lacking. Our study indicated that the expression level of calpain-1 was enhanced in aortas and HCAECs subjected to CIH, and As-IV decreased calpain-1 expression. To test the role of calpain-1 in CIH-induced VED, the thoracic aortic rings in control and CIH-exposed mice with Capn1 knockout were placed in standard organ chambers for isometric tension recording. The results demonstrated that Capn1 knockout improved the EDR impairment induced by CIH. Capn1 knockout reversed NO levels, SIRT1 protein expression and Thr^{172} AMPK and Ser^{1177} eNOS phosphorylation. Notably, Capn1 knockout suppressed the secretion of inflammatory factors, oxidative stress and mitochondrial dysfunction. Taken together, our studies indicated that As-IV ameliorated VED induced by CIH via the calpain-1/SIRT1/AMPK signaling pathway.

Conclusion

In conclusion, these findings confirmed that As-IV ameliorated VED induced by CIH via the calpain-1/SIRT1/

AMPK signaling pathway, which suppressed inflammation, oxidative stress and mitochondrial dysfunction, and ultimately protected against the impaired EDR (Figure 10). Our results further provide a novel understanding of AS-IV as a potential treatment for OSA-associated VED.

Data availability statement

The original contributions presented in the study are included in the article/supplementary material, further inquiries can be directed to the corresponding authors.

Ethics statement

The animal study was reviewed and approved by The Animal Ethics Committee of Jinzhou Medical University.

Author contributions

FZ contributed conception and design of the study. YM, YW, SF, and YL participated in experiments at both animal and cellular level of the study. XZ and CR participated in western blot experiment of the study. HW and ML read and revised the entire manuscript. All authors contributed to manuscript revision, read, and approved the submitted version.

Funding

This study was supported by grant from National Natural Science Foundation of China (Nos:81973553), and Guide Planned Project of Liaoning Province (JYTJCZR2020077).

Conflict of interest

The authors declare that the research was conducted in the absence of any commercial or financial relationships that could be construed as a potential conflict of interest.

Publisher's note

All claims expressed in this article are solely those of the authors and do not necessarily represent those of their affiliated organizations, or those of the publisher, the editors and the reviewers. Any product that may be evaluated in this article, or claim that may be made by its manufacturer, is not guaranteed or endorsed by the publisher.

References

Arnaud, C., Bochaton, T., Pepin, J. L., and Belaidi, E. (2020). Obstructive sleep apnoea and cardiovascular consequences: Pathophysiological mechanisms. *Arch. Cardiovasc. Dis.* 113 (5), 350–358. doi:10.1016/j.acvd.2020.01.003

Badran, M., Ayas, N., and Laher, I. (2014). Cardiovascular complications of sleep apnea: Role of oxidative stress. *Oxid. Med. Cell. Longev.* 2014, 985258. doi:10.1155/2014/985258

Baltzis, D., Bakker, J. P., Patel, S. R., and Veves, A. (2016). Obstructive sleep apnea and vascular diseases. *Compr. Physiol.* 6 (3), 1519–1528. doi:10.1002/cphy.c150029

Biel, T. G., Lee, S., Flores-Toro, J. A., Dean, J. W., Go, K. L., Lee, M. H., et al. (2016). Sirtuin 1 suppresses mitochondrial dysfunction of ischemic mouse livers in a mitofusin 2-dependent manner. *Cell Death Differ.* 23 (2), 279–290. doi:10.1038/cdd.2015.96

Cai, Z., Zhang, Y., Zhang, Y., Miao, X., Li, S., Yang, H., et al. (2019). Use of a mouse model and human umbilical vein endothelial cells to investigate the effect of arsenic exposure on vascular endothelial function and the associated role of calpains. *Environ. Health Perspect.* 127 (7), 77003. doi:10.1289/EHP4538

Chang, H. P., Chen, Y. F., and Du, J. K. (2020). Obstructive sleep apnea treatment in adults. *Kaohsiung J. Med. Sci.* 36 (1), 7–12. doi:10.1002/kjm2.12130

Chen, J. K., Guo, M. K., Bai, X. H., Chen, L. Q., Su, S. M., Li, L., et al. (2020). Astragaloside IV ameliorates intermittent hypoxia-induced inflammatory dysfunction by suppressing MAPK/NF-κB signalling pathways in Beas-2B cells. *Sleep. Breath.* 24 (3), 1237–1245. doi:10.1007/s11325-019-01947-8

Chen, T., Yang, P., and Jia, Y. (2021). Molecular mechanisms of astragalosideIV in cancer therapy (Review). *Int. J. Mol. Med.* 47 (3), 13. doi:10.3892/ijmm.2021.4846

Cyr, A. R., Huckaby, L. V., Shiva, S. S., and Zuckerbraun, B. S. (2020). Nitric oxide and endothelial dysfunction. *Crit. Care Clin.* 36 (2), 307–321. doi:10.1016/j.ccc.2019.12.009

Deng, H., Tian, X., Sun, H., Liu, H., Lu, M., Wang, H., et al. (2022). Calpain-1 mediates vascular remodelling and fibrosis via HIF-1α in hypoxia-induced pulmonary hypertension. *J. Cell. Mol. Med.* 26 (10), 2819–2830. doi:10.1111/jcmm.17295

Dancu, M. B., and Tarbell, J. M. (2007). Coronary endothelium expresses a pathologic gene pattern compared to aortic endothelium: Correlation of asynchronous hemodynamics and pathology *in vivo*. *Atherosclerosis* 192 (1), 9–14. doi:10.1016/j.atherosclerosis.2006.05.042

Dang, D. S., Stafford, C. D., Taylor, M. J., Buhler, J. F., Thornton, K. J., Matarneh, S. K., et al. (2022). Ultrasonication of beef improves calpain-1 autolysis and caspase-3 activity by elevating cytosolic calcium and inducing mitochondrial dysfunction. *Meat Sci.* 183, 108646. doi:10.1016/j.meatsci.2021.108646

Etwebi, Z., Landesberg, G., Preston, K., Eguchi, S., and Scalia, R. (2018). Mechanistic role of the calcium-dependent protease calpain in the endothelial dysfunction induced by MPO (myeloperoxidase). *Hypertension* 71 (4), 761–770. doi:10.1161/HYPERTENSIONAHA.117.10305

Feng, J., Zhang, D., and Chen, B. (2012). Endothelial mechanisms of endothelial dysfunction in patients with obstructive sleep apnea. *Sleep. Breath.* 16 (2), 283–294. doi:10.1007/s11325-011-0519-8

Hu, C., Wang, P., Yang, Y., Li, J., Jiao, X., Yu, H., et al. (2021). Chronic intermittent hypoxia participates in the pathogenesis of atherosclerosis and perturbs the formation of intestinal microbiota. *Front. Cell. Infect. Microbiol.* 11, 560201. doi:10.3389/fcimb.2021.560201

Incalza, M. A., D'Oria, R., Natalicchio, A., Perrini, S., Laviola, L., Giorgino, F., et al. (2018). Oxidative stress and reactive oxygen species in endothelial dysfunction associated with cardiovascular and metabolic diseases. *Vasc. Pharmacol.* 100, 1–19. doi:10.1016/j.vph.2017.05.005

Jiang, S., Jiao, G., Chen, Y., Han, M., Wang, X., Liu, W., et al. (2020). Astragaloside IV attenuates chronic intermittent hypoxia-induced myocardial injury by modulating Ca(2+) homeostasis. *Cell biochem. Funct.* 38 (6), 710–720. doi:10.1002/cbf.3538

Joseph, V., Laouafa, S., Marcouiller, F., Roussel, D., Pialoux, V., Bairam, A., et al. (2020). Progesterone decreases apnoea and reduces oxidative stress induced by

chronic intermittent hypoxia in ovariectomized female rats. *Exp. Physiol.* 105 (6), 1025–1034. doi:10.1113/EP088430

Kida, Y., and Goligorsky, M. S. (2016). Sirtuins, cell senescence, and vascular aging. *Can. J. Cardiol.* 32 (5), 634–641. doi:10.1016/j.cjca.2015.11.022

Kiernan, E. A., Smith, S. M., Mitchell, G. S., and Watters, J. J. (2016). Mechanisms of microglial activation in models of inflammation and hypoxia: Implications for chronic intermittent hypoxia. *J. Physiol.* 594 (6), 1563–1577. doi:10.1113/JP271502

Lee, G. H., Hoang, T. H., Jung, E. S., Jung, S. J., Han, S. K., Chung, M. J., et al. (2020). Anthocyanins attenuate endothelial dysfunction through regulation of uncoupling of nitric oxide synthase in aged rats. *Aging Cell* 19 (12), e13279. doi:10.1111/acel.13279

Li, M. M., Zheng, Y. L., Wang, W. D., Lin, S., and Lin, H. L. (2021). Neuropeptide Y: An update on the mechanism underlying chronic intermittent hypoxia-induced endothelial dysfunction. *Front. Physiol.* 12, 712281. doi:10.3389/fphys.2021.712281

Liu, S., Xu, J., Fang, C., Shi, C., Zhang, X., Yu, B., et al. (2016). Over-expression of heat shock protein 70 protects mice against lung ischemia/reperfusion injury through SIRT1/AMPK/eNOS pathway. *Am. J. Transl. Res.* 8 (10), 4394–4404.

Liu, Z., Ji, J., Zheng, D., Su, L., Peng, T., Tang, J., et al. (2020). Protective role of endothelial calpain knockout in lipopolysaccharide-induced acute kidney injury via attenuation of the p38-iNOS pathway and NO/ROS production. *Exp. Mol. Med.* 52 (4), 702–712. doi:10.1038/s12276-020-0426-9

Lv, X., Wang, K., Tang, W., Yu, L., Cao, H., Chi, W., et al. (2019). miR-34a-5p was involved in chronic intermittent hypoxia-induced autophagy of human coronary artery endothelial cells via Bcl-2/beclin 1 signal transduction pathway. *J. Cell. Biochem.* 120 (11), 18871–18882. doi:10.1002/jcb.29207

Mcevoy, R. D., Antic, N. A., Heeley, E., Luo, Y., Ou, Q., Zhang, X., et al. (2016). CPAP for prevention of cardiovascular events in obstructive sleep apnea. *N. Engl. J. Med.* 375 (10), 919–931. doi:10.1056/NEJMoa1606599

Mihanfar, A., Akbarzadeh, M., Ghazizadeh, D. S., Sadighparvar, S., and Majidinia, M. (2021). SIRT1: A promising therapeutic target in type 2 diabetes mellitus. *Arch. Physiol. Biochem.*, 1–16. doi:10.1080/13813455.2021.1956976

Ministrini, S., Puspitasari, Y. M., Beer, G., Liberale, L., Montecucco, F., Camici, G. G., et al. (2021). Sirtuin 1 in endothelial dysfunction and cardiovascular aging. *Front. Physiol.* 12, 733696. doi:10.3389/fphys.2021.733696

Miyazaki, T., and Miyazaki, A. (2018). Dysregulation of calpain proteolytic systems underlies degenerative vascular disorders. *J. Atheroscler. Thromb.* 25 (1), 1–15. doi:10.5551/jat.RV17008

Nie, Q., Zhu, L., Zhang, L., Leng, B., and Wang, H. (2019). Astragaloside IV protects against hyperglycemia-induced vascular endothelial dysfunction by inhibiting oxidative stress and Calpain-1 activation. *Life Sci.* 232, 116662. doi:10.1016/j.lfs.2019.116662

Parsamanesh, N., Asghari, A., Sardari, S., Tasbandi, A., Jamialahmadi, T., Xu, S., et al. (2021). Resveratrol and endothelial function: A literature review. *Pharmacol. Res.* 170, 105725. doi:10.1016/j.phrs.2021.105725

Rizwan, H., Pal, S., Sabnam, S., and Pal, A. (2020). High glucose augments ROS generation regulates mitochondrial dysfunction and apoptosis via stress signalling cascades in keratinocytes. *Life Sci.* 241, 117148. doi:10.1016/j.lfs.2019.117148

Sun, H., Zhang, H., Li, K., Wu, H., Zhan, X., Fang, F., et al. (2019). ESM-1 promotes adhesion between monocytes and endothelial cells under intermittent hypoxia. *J. Cell. Physiol.* 234 (2), 1512–1521. doi:10.1002/jcp.27016

Tang, F., Chan, E., Lu, M., Zhang, X., Dai, C., Mei, M., et al. (2015). Calpain-1 mediated disorder of pyrophosphate metabolism contributes to vascular calcification induced by oxLDL. *PLoS One* 10 (6), e0129128. doi:10.1371/journal.pone.0129128

Umbaugh, D. S., Nguyen, N. T., Jaeschke, H., and Ramachandran, A. (2021). Mitochondrial membrane potential drives early change in mitochondrial morphology after acetaminophen exposure. *Toxicol. Sci.* 180 (1), 186–195. doi:10.1093/toxsci/kfaa188

Xia, N., Forstermann, U., and Li, H. (2014). Resveratrol and endothelial nitric oxide. *Molecules* 19 (10), 16102–16121. doi:10.3390/molecules191016102

Xu, C., Xu, J., Zou, C., Li, Q., Mao, S., Shi, Y., et al. (2021a). Chronic intermittent hypoxia regulates CaMKII-dependent MAPK signaling to promote the initiation of abdominal aortic aneurysm. *Oxid. Med. Cell. Longev.* 2021, 2502324. doi:10.1155/2021/2502324

Xu, H., Zhang, L., Xu, D., Deng, W., Yang, W., Tang, F., et al. (2021b). Knockout of calpain-1 protects against high-fat diet-induced liver dysfunction in mouse through inhibiting oxidative stress and inflammation. *Food Sci. Nutr.* 9 (1), 367–374. doi:10.1002/fsn3.2002

Xu, S., Ilyas, I., Little, P. J., Li, H., Kamato, D., Zheng, X., et al. (2021c). Endothelial dysfunction in atherosclerotic cardiovascular diseases and beyond: From mechanism to pharmacotherapies. *Pharmacol. Rev.* 73 (3), 924–967. doi:10.1124/pharmrev.120.000096

Yan, Y. R., Zhang, L., Lin, Y. N., Sun, X. W., Ding, Y. J., Li, N., et al. (2021). Chronic intermittent hypoxia-induced mitochondrial dysfunction mediates endothelial injury via the TXNIP/NLRP3/IL-1β signaling pathway. *Free Radic. Biol. Med.* 165, 401–410. doi:10.1016/j.freeradbiomed.2021.01.053

Yuan, Y., Shi, M., Li, L., Liu, J., Chen, B., Chen, Y., et al. (2016). Mesenchymal stem cell-conditioned media ameliorate diabetic endothelial dysfunction by improving mitochondrial bioenergetics via the Sirt1/AMPK/PGC-1α pathway. *Clin. Sci.* 130 (23), 2181–2198. doi:10.1042/CS20160235

Zhou, L., Zhang, Y. F., Yang, F. H., Mao, H. Q., Chen, Z., Zhang, L., et al. (2021). Mitochondrial DNA leakage induces odontoblast inflammation via the cGAS-STING pathway. *Cell Commun. Signal.* 19 (1), 58. doi:10.1186/s12964-021-00738-7

Zhou, S., Wang, Y., Tan, Y., Cai, X., Cai, L., Cai, J., et al. (2014). Deletion of metallothionein exacerbates intermittent hypoxia-induced oxidative and inflammatory injury in aorta. *Oxid. Med. Cell. Longev.*, 141053. doi:10.1155/2014/141053

Zychowski, K. E., Sanchez, B., Pedrosa, R. P., Lorenzi-Filho, G., Drager, L. F., Polotsky, V. Y., et al. (2016). Serum from obstructive sleep apnea patients induces inflammatory responses in coronary artery endothelial cells. *Atherosclerosis* 254, 59–66. doi:10.1016/j.atherosclerosis.2016.09.017

frontiers | Frontiers in Pharmacology

TYPE Review
PUBLISHED 08 August 2022
DOI 10.3389/fphar.2022.892460

OPEN ACCESS

EDITED BY
Fouad Antoine Zouein,
American University of Beirut, Lebanon

REVIEWED BY
Mark C. Chappell,
Wake Forest School of Medicine, United States
Vincenzo Quagliariello,
G. Pascale National Cancer Institute Foundation (IRCCS), Italy

*CORRESPONDENCE
Yusof Kamisah,
kamisah_y@yahoo.com,
kamisah_y@ppukm.ukm.edu.my

SPECIALTY SECTION
This article was submitted to Cardiovascular and Smooth Muscle Pharmacology, a section of the journal Frontiers in Pharmacology

RECEIVED 09 March 2022
ACCEPTED 11 July 2022
PUBLISHED 08 August 2022

CITATION
Mustafa NH, Jalil J, Zainalabidin S, Saleh MSM, Asmadi AY and Kamisah Y (2022), Molecular mechanisms of sacubitril/valsartan in cardiac remodeling.
Front. Pharmacol. 13:892460.
doi: 10.3389/fphar.2022.892460

Molecular mechanisms of sacubitril/valsartan in cardiac remodeling

Nor Hidayah Mustafa[1], Juriyati Jalil[1], Satirah Zainalabidin[2], Mohammed S.M. Saleh[3], Ahmad Yusof Asmadi[4] and Yusof Kamisah[3]*

[1]Centre for Drug and Herbal Research Development, Faculty of Pharmacy, Universiti Kebangsaan Malaysia, Kuala Lumpur, Malaysia, [2]Program of Biomedical Science, Centre of Applied and Health Sciences, Faculty of Health Sciences, Universiti Kebangsaan Malaysia, Kuala Lumpur, Malaysia, [3]Department of Pharmacology, Faculty of Medicine, Universiti Kebangsaan Malaysia, Kuala Lumpur, Malaysia, [4]Unit of Pharmacology, Faculty of Medicine and Defence Health, Universiti Pertahanan Nasional Malaysia, Kuala Lumpur, Malaysia

Cardiovascular diseases have become a major clinical burden globally. Heart failure is one of the diseases that commonly emanates from progressive uncontrolled hypertension. This gives rise to the need for a new treatment for the disease. Sacubitril/valsartan is a new drug combination that has been approved for patients with heart failure. This review aims to detail the mechanism of action for sacubitril/valsartan in cardiac remodeling, a cellular and molecular process that occurs during the development of heart failure. Accumulating evidence has unveiled the cardioprotective effects of sacubitril/valsartan on cellular and molecular modulation in cardiac remodeling, with recent large-scale randomized clinical trials confirming its supremacy over other traditional heart failure treatments. However, its molecular mechanism of action in cardiac remodeling remains obscure. Therefore, comprehending the molecular mechanism of action of sacubitril/valsartan could help future research to study the drug's potential therapy to reduce the severity of heart failure.

KEYWORDS

sacubitril, valsartan, LCZ696, neprilysin inhibitor, fibrosis, cardiac function, cardiomyopathy, entresto

1 Introduction

Heart failure following long-standing uncontrolled hypertension and myocardial infarction (MI) remains a significant public health problem worldwide. Hypertrophic cardiomyopathy can also evolve into heart failure (Brieler et al., 2017). Despite emerging medical advancements in the therapy of cardiovascular disease, death and disability due to heart failure have raised enormously (Bhattacharya and Sil, 2018). Cardiac remodeling is generally accepted as a determinant of the clinical course of heart failure, and is now recognized as an important aspect of cardiovascular disease progression that is therefore emerging as a therapeutic target in heart failure of all etiologies (Mann, 2005).

10.3389/fphar.2022.892460

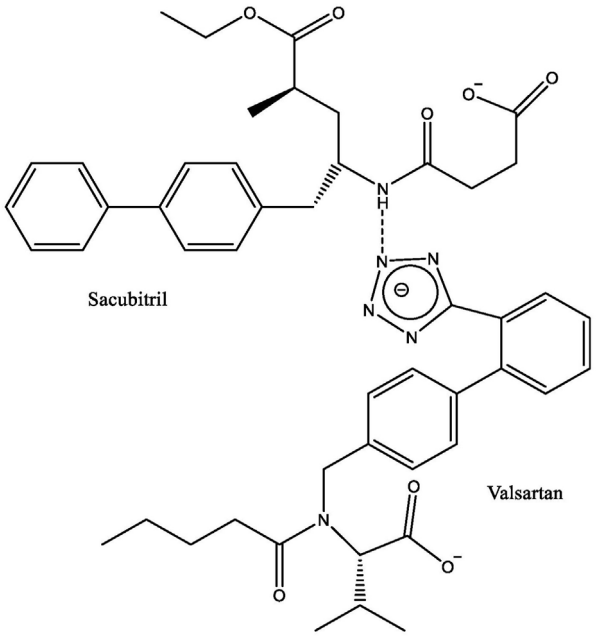

FIGURE 1
Chemical structure of sacubitril/valsartan.

Cardiac remodeling is a complex structural transformation marked by changes in the size and shape of myocardium. At the beginning, remodeling is an adaptive response to preserve normal heart function in circumstances such as chronic hypertension and MI (Nakamura and Sadoshima, 2018). Continuous remodeling is maladaptive, however, resulting in left ventricular dilation, hypertrophy, and dysfunction, involving molecular and cellular alterations such as cardiomyocyte hypertrophy, fibrosis, changes in cardiac extracellular matrix, and gene expression. These alterations within the myocyte are followed by cell death induced by apoptosis or necrosis, while in progressed compensated hypertrophy to dilated heart failure, the alterations result in myocyte lengthening, extracellular matrix remodeling, chamber dilation, and impaired systolic or diastolic functions (Gajarsa and Kloner, 2011).

Many pharmacological therapies have been used to treat and decrease the severity of heart failure for patients with reduced ejection fraction (HFrEF). Among them angiotensin-converting enzyme (ACE) inhibitors, β-blockers, mineralocorticoid receptor antagonists, and angiotensin receptor blockers, as well as two new classes of drugs—angiotensin receptor-neprilysin inhibitor (ARNI) and sodium-glucose co-transporter 2 (SGLT2) inhibitors (Burnett et al., 2017; Balan et al., 2021). Analysis has suggested that ARNI monotherapy is more effective than angiotensin receptor blockers or ACE inhibitors monotherapy (Burnett et al., 2017). Currently, sacubitril/valsartan (Figure 1), formerly known as LCZ696, and marketed by Novartis International AG as Entresto®, is the only drug that belongs to the ARNI group (Hubers and Brown, 2016).

Sacubitril is a neprilysin inhibitor, while valsartan is an angiotensin II (Ang II) type 1 receptor (AT_1R) blocker. Neprilysin is an enzyme involved in the breakdown of circulating natriuretic peptides that have a blood pressure-lowering property (Vilela-Martin, 2016). Therefore, the combination drug acts by simultaneously maintaining circulating natriuretic peptides and blocking the renin-angiotensin-aldosterone system (RAAS) (Cuthbert et al., 2020). Studies have revealed that inhibition of neprilysin by sacubitril alone failed to improve the prognosis of heart failure. This is likely due to its counterbalance effect (Cleland and Swedberg, 1998; Greenberg, 2020; Sutanto et al., 2021), resulting from an accumulation of vasoconstrictors Ang II and endothelin-1, which are also broken down by neprilysin (Vilela-Martin, 2016). Both vasoconstrictors could promote the development of cardiac hypertrophy (Miyauchi and Sakai, 2019; Siti et al., 2021a). Simultaneous inhibition of RAAS and neprilysin produces more effective neurohormonal modulation, preventing clinical deterioration in patients with heart failure (Choi and Shin, 2020; Książczyk and Lelonek, 2020).

Sacubitril/valsartan is the first drug with a double-acting pharmaceutical design conveying two pharmacological effects synchronously (Abumayyaleh et al., 2020). It was approved by the European Medicine Agency and the United States Food and Drug Administration in 2015 (Vilela-Martin, 2016; Chrysant and Chrysant, 2018), and was included a year later as a Class I recommendation, indicated for chronic heart failure patients with HFrEF (Kaplinsky, 2016). The drug is tolerated well and linked to a low incidence of angioedema due to a smaller increase in bradykinin in patients as compared with ACE inhibitors such as enalapril (Desai et al., 2015; McCormack, 2016; Yandrapalli et al., 2017; Myhre et al., 2019; Tanase et al., 2019). The drug is reported to be superior to enalapril in decreasing the risk of mortality in patients with heart failure (Desai et al., 2015). Moreover, omapatrilat, the first dual inhibitor of both neprilysin and ACE, produced a higher incidence of potentially life-threatening angioedema than enalapril, despite its greater efficacy in reducing blood pressure. Hence, further development of omapatrilat as an antihypertensive was terminated (Greenberg 2020; Pascual-Figal et al., 2021).

In addition to neprilysin inhibition and AT_1R blockade, sacubitril/valsartan inhibits multiple targets such as signaling pathways involved in cardiac fibrosis, matrix remodeling, and apoptosis. This review provides updates on the molecular mechanisms of sacubitril/valsartan in cardiac remodeling modulation, with the goals of better understanding the drug combination's role in the management of patients with heart failure and promoting future studies.

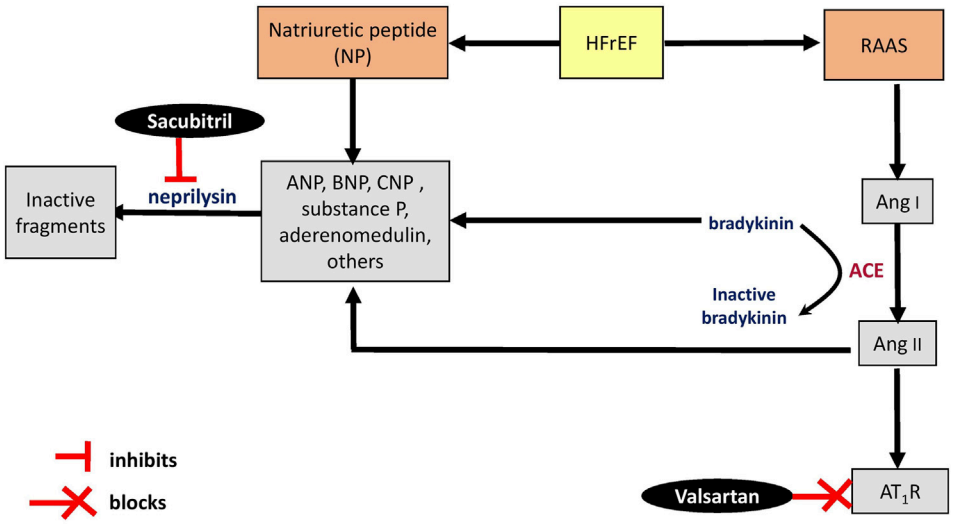

FIGURE 2
Schematic representation of mechanisms of sacubitril/valsartan on renin-angiotensin-aldosterone system and natriuretic peptide system. ACE, angiotensin converting enzyme; Ang, angiotensin; ANP, atrial natriuretic peptide; ARB, angiotensin receptor blocker; ARNI, angiotensin receptor-neprilysin inhibitor; AT_1R, angiotensin type 1 receptor; BNP, B-type natriuretic peptide; CNP, C-type natriuretic peptide; HFrEF, heart failure with reduced ejection fraction; NP natriuretic peptide; RAAS, renin-angiotensin-aldosterone system; ↑, increase.

2 Effects of sacubitril/valsartan on renin-angiotensin-aldosterone system and the natriuretic peptide system

Neprilysin, a component of RAAS, is predominantly expressed in the kidneys, lungs, heart, and brain (Bellis et al., 2020; Nalivaeva et al., 2020). Even though the kidneys execute an important role in regulating the enzyme in systemic circulation (Pavo et al., 2020), the heart is the main origin of soluble circulating neprilysin (Arrigo et al., 2018). Surprisingly, myocardial expression of the enzyme decreased in heart failure (Pavo et al., 2020) and following repeated episodes of heart ischemia-reperfusion (Pavo et al., 2017) in animal experiments. To the best of our knowledge, the expression of the enzyme in a failing human heart has not been reported. Augmenting the natriuretic peptide system is the rationale for inhibiting circulating neprilysin in patients with HFrEF (Singh et al., 2017). As previously mentioned, sacubitril/valsartan simultaneously inhibits neprilysin and RAAS. Circulating natriuretic peptides—atrial (ANP), B-type (BNP) and C-type (CNP) natriuretic peptides (Kuwahara, 2021)—as well as Ang II and endothelin-1 levels are increased following neprilysin inhibition (Ferro et al., 1998; Khder et al., 2017; Pavo et al., 2020) by sacubitril (Figure 2). However, the detrimental efffects of Ang II on the heart and vascular system are blocked by valsartan (Kaplinsky, 2016). Sacubitril/valsartan was also reported to decrease the expresssion of hepatic endothelin-1 (Hsu et al., 2020) and its plasma level (Clements et al., 2019) in hypertensive rats. The inhibition of neprilysin was confirmed by a significant time-dependent reduction in plasma activity of soluble neprilysin as well as an elevation of ANP levels in patients with chronic heart failure after receiving sacubitril/valsartan for 30 and 90 days. BNP and N-terminal pro-BNP (NT-pro-BNP)—a prohormone of BNP with a longer half-life than BNP—levels remained stable in these patients (Nougué et al., 2019). Unlike BNP, NT-pro-BNP is not a substrate of neprilysin (Haynes et al., 2018).

Additionally, the apelinergic system (composed of apelin and elabela as well as APJ receptors) is believed to be a promising target for the treatment of cardiovascular disease. Both apelin and elabela possess inodilator properties (Sainsily et al., 2021). However, the effects of sacubitril/valsartan on apelin and elabela have not been studied. Neprilysin cleaves apelin (McKinnie et al., 2016). Therefore, it could be hypothesized that the drug would increase the level of apelin. Apelin promotes ACE2 expression—in other words, it stimulates formation of vasodilating substrates—and antagonizes Ang II (Chatterjee et al., 2020). These properties of apelin would be beneficial for patients with heart failure.

Even though sacubitril/valsartan exerts beneficial effects in the management of cardiovascular disease, there is a concern regarding its effects on Alzheimer's disease. Neprilysin is known to be involved in the degradation of β-amyloid peptide in the brain. Therefore, inhibition of the enzyme would promote deposition of β-amyloid peptide, a hallmark pathology in Alzheimer's disease diagnosis (Murphy and LeVine, 2010; Nalivaeva et al., 2020). Possible effects of sacubitril/valsartan

TABLE 1 The effects of sacubitril/valsartan on cardiac function in human studies.

Subjects (*n*)	Dose and duration of sacubitril/valsartan	Findings	References
Patients with HFrEF (n = 99)	Target dose of 97/103 mg b.i.d. for median follow-up of 6.2 months	↓ SBP, ↑ LVEF, ↑ VO_2, ↓VE/VCO_2 slope	Vitale et al. (2019)
Patients with HFrEF (n = 149)	24/26, 49/51, 97/103 mg for 316 days mean duration	↓ SBP, ↓ DBP, sPAP, ↑ LVEF	Morillas-Climent et al. (2019)
Patients with HFrEF (n = 654)	24/26, 49/51 and 97/103 mg for 12 months	↑ LVEF, ↓ LVEDV, ↓ LVESV, ↓ LAVI, ↓ E/e'	Januzzi et al. (2019)
Patients with HFrEF (n = 192)	50, 100, 200, 400 mg/day for 12 months	↑ LVEF	Hsiao et al. (2020)
Cancer patients with HFrEF (n = 67)	Titrated to 200 mg b.i.d. for median follow up of 4.6 months	↑ LVEF, ↓ LVEDV, ↓ LVESV	Martín-Garcia et al. (2020)
Patients with HFrEF (n = 90)	97/103 mg b.i.d. for 6 months	↑ LVEF, ↓ LVESV, and ↓ sPAP	Polito et al. (2020)
Patients with HFrEF (n = 69)	24/26 or 49/51 mg b.i.d. for 12 months	↓ LVEDV, ↓ LVESV, ↓ sPAP, ↓ MR	Villani et al. (2020)
Patients with advanced HF (n = 37)	Titrated to 97/103 mg b.i.d. for 12 months	↑ VO_2, ↓VE/VCO_2 slope, ↓ SBP, E/e', ↓ DBP	Cacciatore et al. (2020)
Patients with HFrEF (n = 163)	24/26, 49/51, and 97/103 mg b.i.d. for 2 years	↑ LVEF, ↓ LVEDV, ↓ LVESV, ↓ LAV, ↓ PCWP, ↑ TAPSE, ↑ peak systolic S wave, ↓ PASP, ↓ mPAP, ↑ RV-PA coupling	Masarone et al. (2020)
Patients with ST-elevation MI after pPCI (n = 79)	Not stated (titrated according to patient's condition) for 6 months	↑ LVEF ↓ infarct size	Zhang et al. (2021b)
Patients with LV systolic dysfunction (n = 68)	Titrated to 97/103 mg b.i.d. for 24 weeks	↑ LVEF, ↓ LVESV, ↓ wall motion sore index	Wang and Fu (2021)
Patients with HFrEF (n = 150)	24/26, 49/51 or 97/103 mg b.i.d. for 6 months	↓ NT-proBNP, ↓ mPAP, ↓ RV-MPI, ↑ LVEF, ↑ TAPSE, ↑ RV-FAC	Yenerçağ et al. (2021)
Patients with chronic heart failure (n = 35)	Titrated to 97/103 mg b.i.d. for 6 months	↑ LVEF, ↓ global longitudinal strain, ↓ mechanical dispersion, ↑ myocardial constructive work, ↑ myocardial work index, ↑ myocardial work efficiency, ↓ LAV, ↓ RAV	Valentim Gonçalves et al. (2019); Valentim Gonçalves et al. (2020a)

b.i.d., twice daily; DBP, diastolic blood pressure; E/e', ratio peak early diastolic mitral velocity to mitral annulus early diastolic velocity; HFrEF, heart failure with ejection fraction; LAV, left atrial volume; LVEF, left ventricular ejection fraction; LVEDV, left ventricle end diastolic volume, LVESV; left ventricle end systolic volume; mPAP, mean pulmonary artery pressure; MR, mitral regurgitation; PCWP, pulmonary capillary wedges pressure; pPCI, primary percutaneous coronary intervention; RAV, right atrial volume; RV-FAC, right ventricle-functional area change; RV-MPI, right ventricle-myocardial performance index; RV-PA, right ventricle-pulmonary artery SBP, systolic blood pressure; sPAP, systolic pulmonary arterial pressure; TAPSE, tricuspid annular plane systolic excursion; VE/VCO_2, relationship between ventilation and CO_2 production; ↓, decrease; ↑, increase.

in patients with heart failure and Alzheimer's disease should be investigated further.

3 Mechanistic roles of sacubitril/valsartan in cardiac remodeling

3.1 Effects on cardiac function

In heart failure patients, left ventricular ejection fraction (LVEF) and left ventricular volumes reflect global left ventricular systolic performance and are associated with left ventricular remodeling. Initiation of sacubitril/valsartan therapy in these patients has been shown to induce reverse remodeling of left ventricle, with a significant improvement of ventricular volume overload and dimension indices which subsequently resulting in an augmented LVEF (Liu L. W. et al., 2020; Hu et al., 2020; Karagodin et al., 2020; Mazzetti et al., 2020; Rezq et al., 2021). The improvement was observed with the reduction in left ventricular end-diastolic (LVEDV) and end-systolic (LVESV) volume, left atrial volume index, and estimated mean pulmonary capillary wedge pressure (PCWP) (Januzzi et al., 2019; Martín-Garcia et al., 2020; Masarone et al., 2020). Sacubitril/valsartan also exerts beneficial effects on right ventricular function, marked by increases in peak systolic S wave and tricuspid anular plane systolic excursion (TAPSE), as well as decreases in medium pulmonary artery pressure (mPAP) and pulmonary artery systolic pressure (PASP) (Masarone et al., 2020; Yenerçağ et al., 2021) (Table 1).

In terms of diastolic function, diastolic dysfunction alters the relationship between early diastolic filling velocity (E) and late left ventricular filling (A). E/A ratio is defined as the ratio of peak velocity blood flow from left ventricular relaxation in early diastole to peak velocity flow in late diastole caused by atrial contraction. Sacubitril/valsartan improved E/A ratio in patients with HFrEF (Romano et al., 2019; Nakou et al., 2020; Russo et al., 2020). However, the use of ratio of mitral inflow velocity to mitral annular relaxation velocity (E/E') ratio is more sensitive than E/A

TABLE 2 The effects of sacubitril/valsartan on cardiac function in animal studies.

Type of model	Treatment, dose, route of administration and duration	Findings	References
Left anterior descending ligation-induced MI in rats	Post-treatment 60 mg/kg/day, orally for 4 weeks	↓ LVESV, ↓ LVFS, ↑ diastolic wall strain, ↑ ESPV relationship, ↓ EDPV, ↑ preload recruitable stroke work, ↓ tau logistic, ↑ dP/dt_{max}	Kompa et al. (2018)
Balloon implantation-induced MI followed by reperfusion in rabbits	Post-treatment 10 mg/kg, orally for 10 weeks	↑ LVEF	Torrado et al. (2018)
Isoproterenol-induced cardiac hypertrophy	Concurrent treatment 60 mg/kg/day, orally for 7 days	↓ LVEDP, ↓ dP/dt	Miyoshi et al. (2019)
Spontaneously hypertensive rats	60 mg/kg/day for 12 weeks	↓ SBP, ↑ LVEF, ↑ LVFS	Zhao et al. (2019)
Aortic valve insufficiency (AVI)-induced HF in rats	Post-treatment 68 mg/kg/day, orally 8 weeks	↑ total arterial compliance, ↑ LVEF, ↑ dP/dt_{max}, Ees of LV contractility	Maslov et al. (2019a)
Coronary artery ligation- induced MI in rats	Post-treatment 68 mg/kg/day, orally for 4 weeks	↑ LVEF, ↓ LVESV, ↑ LVFS, ↓ VERP	Chang et al. (2019)
Spontaneous hypertensive rats	300 mg/kg, orally for 2 weeks	↑ DT_E	Sung et al. (2020)
Coronary artery ligation-induced MI in rabbits	Post-treatment 60 mg/kg/day for 4 weeks	↑ LVEF	Chang et al. (2020)
Aortic banding-induced cardiac pressure overload in rats	Post-treatment 68 mg/kg/day orally for 8 weeks	Improved diastolic dysfunction by restoring E/e'SR	Nordén et al. (2021)
Pulmonary hypertension-induced RV failure in rats	Post-treatment 60 mg/kg/day, orally for 5 weeks	↓ RVSP, ↓ RVEDV, ↓ RVESV	Andersen et al. (2019)
Obesity-associated diastolic function in Zucker obese rats	68 mg/kg/day, orally for 10 weeks	↓ IVCT, ↓ IVRT, ↑ e'/a'	Aroor et al. (2021)
Pulmonary hypertension-induced RV failure in rats	Post-treatment 68 mg/kg/d, orally for 21 days	↓ RV maximum pressure, ↓ dP/dt_{max}, ↑ dP/dt_{min}	Sharifi Kia et al. (2020)
Ligated-induced MI in rats	Post-treatment 60 mg/kg, orally for 4 weeks	↑ LVEF, ↑ LVFS, ↑ E/A, ↑ E'/A'	Liu et al. (2021b)

ANP, atrial natriuretic peptide; BW, body weight; cTnT, cardiac troponin; E/e'SR, early mitral inflow velocity to global diastolic strain rate ratio; e'/a', ratio of early and late septal wall velocity during diatole; ESPV, end-systolic pressure volume; EDPV, end-diastolic pressure volume; IVCT, isovolumic contraction time; IVRT, isovolumic relaxation time; LVFS, left ventricular fractional shortening; HFrEF, heart failure with ejection fraction; HW, heart weight; LVEF, left ventricular ejection fraction; LVESV, left ventricle end systolic volume; LVM, left ventricular mass; LVEDP, left ventricular end-diastolic pressure; dP/dt, the rate of rise and decline of left ventricular pressure; β-MHC, β-myosin heavy chain; MI, myocardial infarction; RV, right ventricle; RVEDV, right ventricular end-diastolic volume; RVESV, right ventricular end-systolic volume; RVSP, right ventricular systolic pressure; VERP, ventricular effective refractory period; ↓, decrease; ↑, increase; ↔, no effect.

ratio for measuring left ventricular diastolic function. A significant improvement in E/E' ratio was seen with sacubitril/valsartan therapy in heart failure patients (Kang et al., 2019; Hu et al., 2020; Nakou et al., 2020). Measurement of myocardial performance index (Tei index) provides an evaluation of both systolic and diastolic function simultaneously, as does global longitudinal strain, a relatively novel measure of myocardial contractility which is superior to LVEF in predicting cardiovascular outcomes (Ashish et al., 2019). Therapy with sacubitril/valsartan was shown to improve Tei index (Gokhroo et al., 2021) and global longitudinal strain in heart failure patients (Valentim Gonçalves et al., 2019; Valentim Gonçalves et al., 2020a; Mirić et al., 2021). In addition, sacubitril/valsartan improves fractional shortening, cardiac output, load-dependent indices of left ventricular contractility (dp/dt_{max}), and relaxation (dp/dt_{min}) in animal heart failure models (Maslov et al., 2019b; Ge et al., 2020; Liu Y. et al., 2021; Raj et al., 2021) (Table 2).

Combination therapy of sacubitril/valsartan therapy with SGLT2 inhibitors—originally developed as anti-diabetic drugs—has shown additional benefits in patients with diabetic cardiomyopathy (Kim et al., 2021; Karabulut et al., 2022). The combination exhibits synergistic effects through independent mechanisms that offer greater prominent improvements in cardiac function, observed with the augmented LVEF and reduction in E/E' ratio, as well as a decrease in the risk of cardiovascular death. Additional cardiovascular benefits observed in the patients are suggested to be conferred by SGLT2 inhibitors *via* their natriuretic and osmotic diuretic effects, along with an amelioration of myocardial bioenergetics (Kim et al., 2021; Lin et al., 2022). However, two other clinical trials reported no significant combinatory effects of SGLT2 inhibitors (dapagliflozin or empagliflozin) and sacubitril/valsartan in patients with heart failure, even though the effect magnitudes were numerically bigger than in those receiving SGLT2 inhibitor alone (Solomon et al., 2020; Packer et al., 2021). One possible reason could be small sample size (508 and 727 patients, respectively). Further studies are needed to achieve a conclusive finding. To the best of our knowledge, no clinical trial has been performed to investigate possible

combinatory effects of other antidiabetic drugs and sacubitril/valsartan on heart failure.

Calcium levels regulate myocardial contraction in cardiomyocytes, which is significantly altered in failing hearts. Na^+/K^+-ATPase, Na^+/Ca^{2+} exchanger (NCX), ryanodine receptor 2 (RyR2), and sarcoplasmic/endoplasmic reticulum calcium ATPase (SERCA) are among the calcium regulators (Salim et al., 2020). Sacubitril/valsartan increased LVEF without affecting the expressions of NCX, RyR2 or SERCA, but downregulated phosphorylated calmodulin-dependent protein kinase II (CaMKII-p) expression in a MI-heart failure rabbit model (Chang et al., 2020). Increased intracellular calcium activates CaMKII, resulting in phosphorylation of the L-type calcium channel and increases in SERCA calcium cycling. CaMKII is upregulated in heart failure (Beckendorf et al., 2018). A study by Eiringhaus et al. (2020) demonstrated that sacubitril/valsartan diminished diastolic calcium-spark frequency (limited sarcoplasmic reticulum calcium release events) and sarcoplasmic reticulum calcium leaks in isolated mouse cardiomyocytes that were exposed to catecholaminergic stress, as well as in human left ventricular cardiomyocytes isolated from explanted hearts of patients with end-stage heart failure. Similar effects were also observed in cardiomyocytes treated with sacubitril alone, but they were lacking when valsartan was used alone, suggesting the direct effects of sacubitril on improving calcium homeostasis in failing cardiomyocytes. The study also reported that sacubitril did not compromise systolic calcium release, sarcoplasmic reticulum calcium transient kinetic and load, as well as SERCA activity (Eiringhaus et al., 2020). Therefore, the findings convey that sacubitril/valsartan promotes cardiac function partly by improving myocardial calcium homeostasis.

Collectively, therapy with sacubitril/valsartan has shown beneficial effects on systolic and diastolic function in patients with heart failure and in animal studies, likely *via* improvement of myocardial contractility, leading to increased ejection fraction. The role of the drug on calcium handling such as Na^+/K^+-ATPase in other heart failure models should be studied further. Certain genes that play a role in the progression of hypertrophy—SUZ12/PRC2-MEF2A, EZH2-CaMKI, and miR-675-CaMKIId (Liu L. et al., 2020)—should also be explored. Sarcomere is the "motor" of cardiomyocyte mechanotransduction that generates force transmission. Cysteine rich protein 3 (also known as muscle LIM protein) and titin are the proteins that participate in force transmission within sarcomere (Lyon et al., 2015); sacubitril/valsartan may modulate these proteins.

3.2 Effects on cardiac structure and hypertrophy

Cardiac hypertrophy is an adaptive and compensatory mechanism (characterized by an increase in cardiomyocyte size and thickening of ventricular walls) that involves alterations in cell structure and protein synthesis (Zhang et al., 2003; Siti et al., 2020). The development of pathological cardiac hypertrophy is usually accompanied by increased expression of typical cardiac genes ANP and BNP (Tham et al., 2015; Siti et al., 2021b). Thus, the plasma level of these peptides are measured as indicators for cardiac dysfunction, including cardiac hypertrophy (Moyes and Hobbs, 2019). Other than these peptides, NT-pro-BNP and cardiac troponin T are more routinely used to assess cardiac function (Berardi et al., 2020).

The effectiveness of sacubitril/valsartan therapy in patients with HFrEF has been appraised in many studies. The drug reduced plasma levels of NT-proBNP, high-sensitivity cardiac troponin T (hs-cTnT), and soluble suppressor of tumorigenicity 2 (sST2) in the patients, high levels of which reflect ventricular wall stress and myocardial injury (Nougué et al., 2019; Murphy et al., 2021) (Table 3). NT-proBNP level and left ventricular mass are positively correlated, and this fact is useful for identifying patients with cardiac hypertrophy (Morillas et al., 2008; Kahveci et al., 2009).

The beneficial effects of sacubitril/valsartan were also demonstrated in animal models. Its administration has resulted in decreased heart weight to body weight ratio in spontaneous hypertensive rats and in rats with induced cardiac hypertrophy (Chang et al., 2019; Zhao et al., 2019; Nordén et al., 2021). It inhibited left ventricular hypertrophy in various models of cardiac hypertrophy, which was confirmed echocardiographically and histologically. Echocardiographic analysis revealed that sacubitril/valsartan decreased left ventricular wall thickness as shown by decreased interventricular septum thickness diameter, left ventricular posterior diastolic wall thickness, left ventricular mass, and left ventricular end-systolic diameter (Chang et al., 2019; Zhao et al., 2019; Tashiro et al., 2020), leading to improved cardiac geometry (Sung et al., 2020). Meanwhile, histological analysis showed that the increases in cardiomyocyte size induced by Ang II was significantly attenuated by the treatment (Tashiro et al., 2020). However, a detailed molecular mechanism of sacubitril/valsartan inhibition on left ventricular hypertrophy was not fully characterized. Table 4 summarizes the findings of sacubitril/valsartan on cardiac structure and biomarkers of cardiac hypertrophy in animal studies.

Sacubitril/valsartan administration lowers blood pressure in patients with chronic HFrEF, primarily by reducing blood volume and enhancing natriuresis (Böhm et al., 2017). However, studies have indicated that the antihypertrophic effects of sacubitril/valsartan were independent of blood pressure. Tashiro et al. (2020) exhibited that the fewest hypertrophic changes—interventricular septum thickness diameter, left ventricular posterior wall thickness diameter and cardiomyocyte cross-sectional area—took place in the sacubutril/valsartan-treated mice treated with Ang II, despite the similar blood pressure-lowering effect of sacubitril/valsartan, enalapril, and valsartan (Tashiro et al., 2020). A similar finding was also noted in a rat model of heart failure with preserved ejection

TABLE 3 The effects of sacubitril/valsartan on cardiac structure and biomarkers of cardiac hypertrophy in clinical studies.

Subjects (*n*)	Dose and duration of sacubitril/valsartan	Findings	References
Patients with HFrEF and acute decompensated HF (*n* = 342)	Titrated to 97/103 mg b.i.d. for 8 weeks	↓ hs-cTnT, ↓ sST2	Morrow et al. (2019)
Patients with HFrEF (*n* = 149)	24/26, 49/51, and 97/103 mg for mean duration of 316 days	↓NT-proBNP, ↓ LVEDD	Morillas-Climent et al. (2019)
Patients with HFrEF (*n* = 654)	24/26, 49/51, and 97/103 mg for 12 months	↓ NT-proBNP	Januzzi et al. (2019)
Patients with HFpEF (*n* = 2407)	Titrated to 97/103 mg b.i.d. for 1 year	↓ NT-proBNP	McMurray et al. (2020)
Patients with HFpEF (*n* = 4796)	49/51 and 97/103 mg b.i.d. for 48 weeks	↓ NT-proBNP	Cunningham et al. (2020b)
Patients with HFrEF (*n* = 367)	Titrated to 97/103 mg, b.i.d. for 12 weeks	↓ NT-proBNP	Myhre et al. (2022)
Patients with HFrEF (*n* = 440)	Not stated (titrated according to patient's condition) for 8 weeks	↓ NT-proBNP	Ambrosy et al. (2020)
Acute decompensated HF patients (*n* = 199)	24/26, 49/51, and 97/103 mg b.i.d. for 8 weeks	↓ NT-proBNP	Berg et al. (2020)
Patients with HFrEF (*n* = 106)	24/26, 49/51, and 97/103 mg for 3 months	↓ NT-proBNP, ↓ CRP	Dereli et al. (2020)
Acute decompensated HF patients (*n* = 881)	Not stated (titrated according to patient's condition) for 8 weeks	↓ NT-proBNP, ↓ hs-cTnT	Berardi et al. (2020)
Acute decompensated HF patients (*n* = 417)	97/103 mg b.i.d. for 12 weeks	↓ NT-proBNP	DeVore et al. (2020)
Patients with HFrEF (*n* = 192)	50, 100, 200, and 400 mg/day for 12 months	↓ BNP, ↓ LV size	Hsiao et al. (2020)
Cancer patients with HFrEF (*n* = 67)	Titrated to 200 mg b.i.d. for a median follow-up of 4.6 months	↓NT-proBNP	Martín-Garcia et al. (2020)
Patients with HFrEF (*n* = 69)	24/26 or 49/51 mg b.i.d. for 12 months	↓ NT-proBNP,	Villani et al. (2020)
Patients with advanced HF (*n* = 37)	Titrated to 97/103 mg b.i.d. for 12 months	↓ NT-proBNP,	Cacciatore et al. (2020)
Patients with HFrEF (*n* = 163)	24/26, 49/51, and 97/103 mg b.i.d. for 2 years	↓ LVEDD, ↓ LVESD	Masarone et al. (2020)
Patients with HFrEF (*n* = 42)	Titrated to 97/103 mg b.i.d. for 6 months	↓ CRP	Valentim Goncalves et al. (2020b)
Patients with ST-elevation MI after primary percutaneous coronary intervention (*n* = 79)	Not stated (titrated according to patient's condition) for 6 months	↓ NT-proBNP, ↓ infarct size	Zhang et al. (2021b)
Outpatients with HFrEF (*n* = 96)	Not stated (titrated according to patient's condition) for 6 months	↓ NT-proBNP	Chalikias et al. (2021)
Outpatients with HFrEF (*n* = 454)	Titrated to 97/103 b.i.d. for 6 months	↓ NT-proBNP	Jariwala et al. (2021)
Patients with HFrEF (*n* = 111)	Titrated to 200 mg b.i.d. for 8 weeks	↓ NT-proBNP	Tsutsui et al. (2021)
Acute anterior wall MI patients with LV systolic dysfunction (*n* = 68)	Titrated to 97/103 mg b.i.d. for 24 weeks	↓NT-proBNP, ↓ sST2	Wang and Fu (2021)
Patients with HFrEF (*n* = 150)	24/26, 49/51, and 97/103 mg b.i.d. for 6 months	↓ NT-proBNP	Yenerçağ et al. (2021)
Patients with chronic heart failure (*n* = 35)	Titrated to 97/103 mg b.i.d. for 6 months	↓ LVEDD, ↓ LVESD	Valentim Gonçalves et al. (2019); Valentim Gonçalves et al. (2020a)

b.i.d., twice daily; ANP, atrial natriuretic peptide; BNP, brain natriuretic peptide; BW, body weight; CaMKII, calmodulin-dependent protein kinase II; CRP, C-reactive protein; cTnT, cardiac troponin; HFrEF, heart failure with reduced ejection fraction; hs-cTnT, high-sensitivity cardiac troponin; HW, heart weight; IVSTd, interventricular septum thickness diameter; β-MHC, β-myosin heavy chain; LV, left ventricle; LVDd, left ventricular internal dimension in diastole LVEDD, left ventricle end-diastolic diameter; LVESD, left ventricle end-systolic diameter; LVPw, left ventricular posterior diastolic wall thickness; LVPWd, left ventricular posterior wall thickness diameter; NT-proBNP, N-terminal (NT)-pro hormone BNP; ↓, decrease; sST2, soluble suppressor of tumorigenicity 2; ↑, increase; ↔, no effect.

fraction (HFpEF) (Nordén et al., 2021). In the study, sacubitril/valsartan had no significant effect on mean arterial pressure in the rats exposed to cardiac pressure overload, as opposed to reduced effect by valsartan. However, the left ventricular weight of the former group was significantly lower than the latter and vehicle-treated groups (Nordén et al., 2021). The findings of both studies suggest that sacubitril/valsartan provides a direct cardioprotection against hypertrophic changes.

Sacubitril/valsartan also demonstrated a potential to inhibit right ventricular hypertrophy in a rat model of pulmonary hypertension. In studies, oral sacubitril/valsartan (34 and 68 mg/kg/day) was administered for 21 (Sharifi Kia et al., 2020) or 42 days (Clements et al., 2019) in rats induced with pulmonary hypertension, resulting in a reduction of right ventricular hypertrophy with reduced right ventricular longitudinal and circumferential stiffness as well as reduced

TABLE 4 The effects of sacubitril/valsartan on cardiac structure and biomarkers of cardiac hypertrophy in animal studies.

Models	Dose and duration of sacubitril/valsartan	Findings	References
Left anterior descending ligation-induced MI in rats	Post-treatment 60 mg/kg/days, orally, 4 weeks	↓ myocyte hypertrophy, ↓ LVPw, ↓ LV mass, ↓ ANP, ↓ β-MHC	Kompa et al. (2018)
Balloon implantation-induced MI followed by reperfusion in rabbits	Post-treatment 10 mg/kg, orally for 10 weeks	↓ infarct size, ↓ cTnT,	Torrado et al. (2018)
Spontaneously hypertensive rats	60 mg/kg/day for 12 weeks	↓ HW/BW, ↓ LV posterior wall thickness, ↓ LV mass,	Zhao et al. (2019)
Coronary artery ligation- induced MI in rats	Post-treatment 68 mg/kg/day, orally for 4 weeks	↓ HW, ↓ HW/BW, ↓ LVESD	Chang et al. (2019)
Spontaneous hypertensive rats	300 mg/kg, orally for 2 weeks	↓ RWT, ↓ IVRT, Improved cardiac geometry, ↓ NT-proBNP	Sung et al. (2020)
Aortic banding-induced HFpEF in rats	Post-treatment 68 mg/kg/day orally for 8 weeks	↓ LV weight	Nordén et al. (2021)
Ang II-induced cardiac hypertrophy in mice	Post-treatment 60 mg/kg/d, orally for 2 weeks	↓ LV mass, ↓ IVSTd, ↓ LVPWd	Tashiro et al. (2020)
Salt-loaded hypertensive rats	Concurrent treatment 6 mg/kg, orally for 6 months.	Concurrent: ↓ VW/BW	Hamano et al. (2019)
	Post-treatment 6 mg/kg, orally for 6 months	Post-treatment: ↔ VW/BW Both types of treatment had no effect on echocardiographic findings	
Pulmonary hypertension-induced RV failure in rats	34 and 68 mg/kg/day, orally for 42 days	↓ RV hypertrophy	Clements et al. (2019)
Pulmonary hypertension-induced RV failure in rats	Post-treatment 68 mg/kg/d, orally for 21 days	↓ RVFW thickness ↓ RV myofiber stiffness ↓ RV longitudinal stiffness, ↓ RV circumferential stiffness	Sharifi Kia et al. (2020)
Ligated-induced MI in rats	Post-treatment 60 mg/kg, orally for 4 weeks	↓ LV mass, ↓ LVEDD	Liu et al. (2021b)

ANP, atrial natriuretic peptide; BNP, brain natriuretic peptide; BW, body weight; CRP, C-reactive protein; cTnT, cardiac troponin; DTE, deceleration time of mitral E wave; HFrEF, heart failure with reduced ejection fraction; hs-cTnT, high-sensitivity cardiac troponin; HW, heart weight; IVRT, isovolumetric relaxation time; IVSTd, interventricular septum thickness diameter; β-MHC, β-myosin heavy chain; LV, left ventricle; LVDd, left ventricular internal dimension in diastole; LVEDD, left ventricle end-diastolic diameter; LVESD, left ventricle end-systolic diameter; LVPw, left ventricular posterior diastolic wall thickness; LVPWd, left ventricular posterior wall thickness diameter; NT-proBNP, N-terminal (NT)-pro hormone BNP; RV, right ventricle; RVFW, right ventricular free wall; RWT, relative wall thickness; VW/BW, ventricular weight to body weight ratio; ↓, decrease; ↑, increase; ↔, no effect.

right ventricular free wall thickness. The protective effect was possibly owing to a mitigation of pulmonary artery pressure which subsequently improved right ventricular afterload, leading to regression in right ventricular hypertrophy (Clements et al., 2019). Collectively, post-treatment of sacubitril/valsartan decreases left and right ventricular hypertrophy and cardiac associated release of biomarkers. The findings are confirmative of the therapeutic effects of the drug on cardiac hypertrophy, as seen in patients with HFrEF.

Studies have further explored the possible mechanism of the protective effects of sacubitril/valsartan on cardiac hypertrophy. Its effect on extracellular signal-regulated kinase (ERK) was investigated in mice with pregnancy-associated cardiomyopathy (PAC) treated with lentiviruses stably transfected with sh-ERK for silencing ERK. This treatment resulted in reduced expression of ERK compared to its negative control group (treated with sh-NC) and was associated with a lower heart size (Wang et al., 2019a). However, ERK silencing had no effect on phosphorylated ERK (pERK). Sacubitril/valsartan did not affect ERK expression in PAC mice that were treated with sh-NC, but it did reduce pERK, whereas in the groups given sh-ERK, the drug significantly reduced the expression of both ERK and pERK. Mice that were treated with the drug had smaller hearts than the control group, regardless of whether they were treated with sh-NC or sh-ERK. However, sacubitril/valsartan further reduced heart size in the group given sh-ERK, compared to the group treated with the drug and sh-NC. Other hypertrophic markers were also inhibited (Wang et al., 2019a). Similar findings were also observed in cardiomyocytes that were transfected with sh-ERK and exposed to Ang II to induce hypertrophy before treatment with sacubitril/valsartan. In the same study, it was also noted that the drug increased the expression of ACE-2 in the Ang II-treated cells (Wang et al., 2019a). ACE2 converts Ang II into Ang 1–7, a heptapeptide which has antiremodeling and cardioprotective properties, by suppressing the synthesis of cardiac fibroblast extracellular matrix and release of hypertrophic growth factors (Iwata et al., 2011; Arendse et al., 2019). However, the possible role of the drug on the peptide level has not been reported. In summary, the findings suggest that role of ERK in the

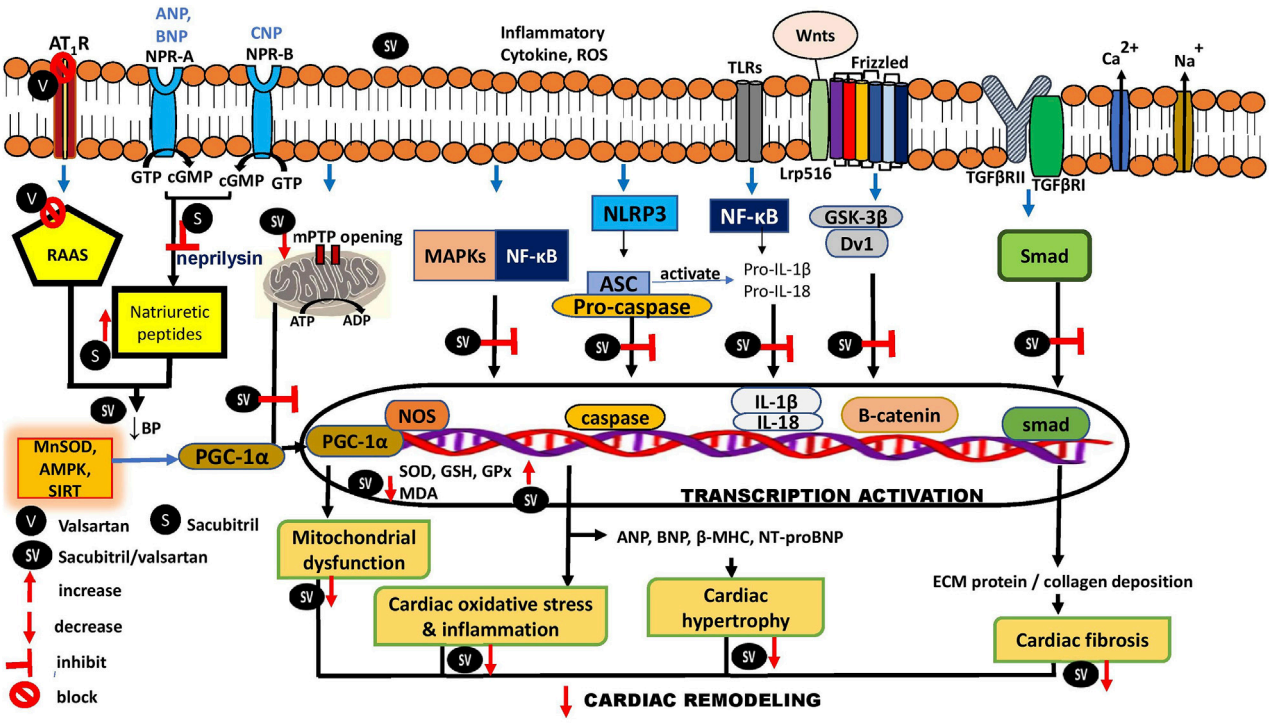

FIGURE 3
Schematic regulatory mechanisms for sacubitril/valsartan during cardiac remodeling. AMPK, AMP-activated protein kinase; ANP, atrial natriuretic peptide; ASC, apoptosis-associated speck-like protein containing a caspase; ATP, adenosine triphosphate; BNP, B-type natriuretic peptide; BP, blood pressure; cGMP, cyclic guanosine monophosphate; CNP, C-type natriuretic peptide; CTGF, connective tissue growth factor; Drp1, Dynamin-related protein one; Dv1, signal transduction molecule disheveled; ECM, extracellular matrix; ERK, extracellular signal-regulated kinase; GPx, glutathione peroxidase; GSH, glutathione; GTP, guanosine triphosphate; IL, interleukin; JNK, c-Jun N-terminal kinases; MAPK, mitogen-activated protein kinase; MDA, malondialdehyde; MFN2, Mitofusin-2; β-MHC, β-myosin heavy chain; MMPs, matrix metalloproteinases; MnSOD, manganese suoeroxide dismutase; mPTP, mitochondrial permeability transition pore; NF-κB, nulear factor-κB; NLRP3, NOD-like receptor protein three; NOS, nitric oxide synthases; NPR-A, natriuretic peptide receptor A; NPR-B, natriuretic peptide receptor B; PGC-1α, peroxisome proliferator-activated-receptor-1α; NT-proBNP, N-terminal pro-BNP; RAAS, renin-angiotensin-aldosterone system; SIRT, mitochondria sirtuin; TGF-βR, transforming growth factor β receptor, TLRs, Toll-like receptors.

pathogenesis of cardiac hypertrophy is crucial and sacubitril/valsartan protects the heart by blocking the activation of ERK and inhibiting the Ang II receptor pathway (Figure 3).

3.3 Effects on cardiac fibrosis and matrix remodeling

Cardiac fibrosis is one of the features in cardiac remodeling underlying the progression of heart failure. It occurs due to an imbalance in extracellular matrix production and degradation in the myocardium, and arises from pathological attempts to repair tissue injury in various cardiac diseases including MI and diabetic hypertrophic cardiomyopathy (Hinderer and Schenke-Layland, 2019; Siti et al., 2020). It involves increased synthesis of matrix metalloproteinases (MMP) and collagen that occurs during inflammation, resulting in fibrosis (Nattel, 2017). Fibrotic tissues become stiffer and less compliant, thus predisposed to the progression of cardiac dysfunction. Therefore, the balance between extracellular matrix synthesis and degeneration is crucial for maintaining cardiac structural integrity (Ma et al., 2018).

The effects of sacubitril/valsartan on cardiac fibrosis through the regulation of transforming growth factor-β1/small mothers against decapentaplegic (TGF-β/Smad) signaling pathways were investigated using numerous animal models and cardiac fibroblast cells (Table 5). TGF-β1 is a molecular mediator that plays a role in the development of cardiac fibrosis (Khan et al., 2014; Yue et al., 2017). It is activated following a cardiac injury (Annes et al., 2003) *via* Smad proteins after binding to its receptor, leading to the recruitment and activation of downstream mediators, mainly Smad2 and Smad3 (Ma et al., 2018). The effects of sacubitril/valsartan on collagen synthesis, TGF-β1, and phosphorylated Smad3 (p-Smad3) expressions were consistent in various animal models on cardiac failure such as streptozotocin-induced diabetic cardiomyopathy

TABLE 5 The effects of sacubitril/valsartan on myocardial fibrosis in animal studies.

Type of model	Treatment, dose, route of administration and duration	Findings	References
Left anterior descending ligation-induced MI in rats	Post-treatment 60 mg/kg/day, orally for 4 weeks (1 week after surgery)	↓ cardiac fibrosis, ↓ collagen I, ↓ TIMP-2	Kompa et al. (2018)
Isoproterenol-induced cardiac hypertrophy	Concurrent treatment 60 mg/kg/day, orally for 7 days	↓ interstitial fibrosis area, ↓TGFβ1, ↓ collagen 1a1	Miyoshi et al. (2019)
Spontaneously hypertensive rats	60 mg/kg/day for 12 weeks	↓ nNos, ↓ eNos, ↓ TGF-β, ↓ RAS components	Zhao et al. (2019)
Aortic valve insufficiency (AVI)-induced HF in rats	Post-treatment 68 mg/kg/day, orally for 8 weeks	↓ myocardial fibrosis	Maslov et al. (2019a)
Spontaneous hypertensive rats	300 mg/kg, orally for 2 weeks	↓ fibrosis area	Sung et al. (2020)
Pulmonary hypertension-induced RV failure in rats	Post-treatment 60 mg/kg/day for 5 weeks	↓ fibrosis volume density, ↓ total fibrosis volume	Andersen et al. (2019)
Obesity-associated diastolic dysfunction in Zucker obese rats	68 mg/kg/day, orally for 10 weeks	↓ LV myocardial interstitial fibrosis, ↓ LV periarterial fibrosis	Aroor et al. (2021)
Ligated-induced MI in rats	Post-treatment 60 mg/kg, orally for 4 weeks	↓ fibrotic area, ↓ α-SMA level and area, ↓ TGF-β mRNA level	Liu et al. (2021b)

eNOS, endothelial nitric oxide synthase; LV, left ventricle; MI, myocardial infarction; nNOS, neuronal nitric oxide synthase; RAS, renin-angiotensin system; TIMP, tissue inhibitor of matrix metalloproteinase; α-SMA, highly contractile protein α-smooth muscle actin; TGFβ1, transforming growth factor β1; ↓, decrease; ↑, increase; ↔, no effect.

(Ai et al., 2021) and left anterior descending (LAD) coronary artery ligation-induced MI (Wu M. et al., 2021) rat models. Sacubitril/valsartan effectively decreased protein expression of TGF-β1 and p-Smad3 in infarcted areas and myocardial types I and III collagen in these models (Ai et al., 2021; Wu M. et al., 2021). Apart from that, the drug (10^{-7}–10^{-5} M) also inhibited cell proliferation and collagen synthesis in neonatal rat myocardial fibroblast cells exposed to hypoxia and TGF-β1 to induce collagen synthesis (Wu M. et al., 2021). Histologically, oral administration of 68 mg/kg/day sacubitril/valsartan for 5 weeks in LAD coronary artery ligation-induced MI rats significantly decreased myocardial interstitial fibrosis accompanied by reduced connective tissue growth factor (CTGF) expression, a known mediator of TGF-β activity during fibrosis (Pfau et al., 2019). Clinically, patients with chronic HFpEF and HFrEF who were treated with sacubitril/valsartan had significantly lower plasma profibrotic biomarkers assessed by the levels of aldosterone, MMP-9, sST2, tissue inhibitor of metalloproteinase-1 (TIMP-1), N-terminal propeptide of collagen I (PINP), and N-terminal propeptide of collagen III (PIIINP) after 8 and 12 months. The effects of sacubitril/valsartan on the profibrotic biomarkers were superior to that of valsartan or enalapril (Zile et al., 2019; Cunningham et al., 2020a).

The antifibrotic effect of sacubitril/valsartan was also demonstrated in other cardiac fibrosis rat models induced by doxorubicin toxicity (Boutagy et al., 2020) and high-salt diet-induced HFpEF (Zhang et al., 2021a). In these models, concurrent oral administration of sacubitril/valsartan (68 mg/kg) with doxorubicin for 6 weeks attenuated MMP activity and highly contractile protein α-smooth muscle actin (α-SMA) expression (Boutagy et al., 2020), while intragastric administration of sacubitril/valsartan (68 mg/kg/day) for 4 weeks mitigated cardiac fibrosis, associated with decreases in types I and III collagen protein and mRNA expressions, as well as MMP-2 protein expression (Zhang et al., 2021a). Tissue inhibitor of metalloproteinase-2 (TIMP-2) and Smad7 expression—an inhibitory regulator of TGF-β (Ma et al., 2018)—were increased in the rats (Zhang et al., 2021a), suggestive of a strong suppressive effect of the drug on myocardial fibrosis production.

There is considerable evidence that shows that the secreted frizzled-related protein 1 (sFRP-1)/Wnt/β-catenin signaling pathway plays a role in TGF-β-mediated fibrosis in cardiac remodeling (Akhmetshina et al., 2012; McMurray et al., 2014). Wnt proteins bind to frizzled receptors to activate signal transduction molecule disheveled (Dvl), which curbs glycogen synthase kinase-3β (GSK-3β) and increases β-catenin expressions (Piersma et al., 2015). Post-treatment of oral sacubitril/valsartan (60 mg/kg) for 4 weeks alleviated myocardial fibrosis by inhibiting the Wnt/β-catenin signal transduction pathway in a mouse model of MI. A mitigation of the expression of β-catenin and Dvl-1, along with overexpression of its inhibitor, sFRP-1, was observed in the sacubitril/valsartan-treated mice (Liu J. et al., 2021). This modulation in turn attenuated cardiac fibrosis by reducing the fibrotic area, α-SMA, TGF-β, types I and III collagen (Figure 3). As expected, treatment of sacubitril/valsartan (30 μmol/L) in primary myocardial fibroblasts stimulated with Ang II produced similar results (Liu J. et al., 2021).

Taken together, the findings suggest that sacubitril/valsartan attenuates cardiac fibrosis by inhibiting the TGF-β1/Smad3 and Wnt/β-catenin signaling pathways. Sacubitril/valsartan may also modulate the phosphatidylinositol 3-kinase/protein kinase B/

glycogen synthase kinase-3β (PI3K/Akt/GSK-3β) and hypoxia-induced mitogenic actor (HIMF)-IL-6 signaling pathways, and this aspect should be studied further. These pathways play a role in regulating cardiac fibrosis. Activation of the PI3K/Akt/GSK-3β pathway results in diminished cell growth and proliferation (Syamsunarno et al., 2021), while HIMF-IL6 promotes the opposite effect, leading to fibrosis (Kumar et al., 2018).

3.4 Effects on myocardial mitochondrial function and apoptosis

Bioenergetic reserve capacity (also known as spare respiratory capacity) can abruptly increase mitochondrial respiration to a maximum for synthesizing more ATP to maintain cellular functions (Sansbury et al., 2011). Impaired mitochondrial activity decreases its energy production, leading to mitochondrial dysfunction which plays an important role in the development of cardiac remodeling and heart failure (Ramaccini et al., 2021). Oral administration of sacubitril/valsartan (68 mg/kg/day) for 10 weeks increased mitochondrial maximal respiration capacity and spare respiration capacity in rats with left ventricular pressure overload, suggesting a beneficial effect of the drug on mitochondrial bioenergetics (Li et al., 2021). A similar finding was also noted in dogs with intracoronary microembolization-induced chronic heart failure following oral doses of sacubitril/valsartan (100 mg) for 3 months. Myocardial bioenergetics was improved in the dogs' failing myocardium, likely due to improved mitochondrial function, evidenced by marked increases in mitochondrial maximal rate of ATP synthesis and membrane potential, as well as decreased opening of the permeability transition pore (mPTP) (Sabbah et al., 2020). Alterations in mitochondrial structure and function in a remodeled heart disrupt mitochondrial membrane integrity and potential. These events trigger the opening of mPTP, leading to ATP depletion (Sharov et al., 2000; Sharov et al., 2007; Sabbah et al., 2020; Yeh et al., 2021b).

In experimental heart failure, mitochondrial complex I and IV activities involved in ATP synthesis were inhibited. Post-treatment with sacubitril/valsartan (100 mg, twice daily) for 3 months restored the activities of these complexes, thus improving oxidative phosphorylation. The drug also normalized the levels of nitric oxide synthase (NOS) isoforms—endothelial NOS (eNOS) and inducible NOS—and peroxisome proliferator-activated receptor coactivator-1α (PGC-1α), proteins involved in regulation of mitochondrial biogenesis and respiration (Sabbah et al., 2020) (Figure 3). eNOS generates nitric oxide which then activates guanylate cyclase to produce cyclic guanosine monophosphate (cGMP). cGMP transmits signals to the nucleus that lead to an induction of PGC-1α gene transcription and mitochondrial biogenesis (Jornayvaz and Shulman, 2010).

Peng et al. (2020) demonstrated that post-treatment with sacubitril/valsartan (20 mg/kg/day) for 4 weeks in mice with pressure overload-induced heart failure distinctly reversed the downregulation of manganese superoxide dismutase (MnSOD), sirtuin-3 (SIRT3), and phosphorylated 5' adenosine monophosphate-activated protein kinase (p-AMPK) expression. The protective effect of sacubitril/valsartan on MnSOD and p-AMK was abolished in SIRT3 deficiency, indicating it was *via* a SIRT3-dependent pathway. SIRT3 has a prominent role in mitochondrial metabolism, thus it is profoundly present in tissues with high energy metabolisms, like the heart (Cao et al., 2022). The activation of PGC-1α indirectly enhances SIRT3 expression that promotes mitochondrial function, thus protecting the organelle against damage (Brandauer et al., 2015), while MnSOD is a deacetylation target of SIRT3, which also controls its expression (Koentges et al., 2016).

Similar effects of sacubitril/valsartan were also exhibited in an obesity-related metabolic heart disease model. The administration of the drug at 100 mg/kg/day for 4 months improved cardiac energetics reflected by an elevation of rate pressure product (RPP), indicative of increased cardiac energy reserve (an index of myocardial oxygen consumption), as well as a decrease in the slope of decline phosphocreatine normalized for ATP (PCr/ATP) relative to RPP in isolated beating hearts of C57BL/6J mice (Croteau et al., 2020). The slope of change in PCr/ATP relative to RPP measures energetic expense of raised contractile conduct (Croteau et al., 2020).

Apoptosis plays a major role in mitochondrial function, the elevation of which increases mitochondrial death. Sacubitril/valsartan (60 mg/kg/day for 4 weeks) administration in mice attenuated doxorubicin-induced dilated cardiomyopathy, observed by a curb on apoptosis that preserved mitochondrial function *via* the dynamin-related protein 1 (Drp1)-mediated pathway (Xia et al., 2017; Yeh et al., 2021a) (Figure 3). The significant reduction in Drp1 and its phosphorylated Ser-616 expression—the activated form—observed in the study was associated with the improvement in cardiac mitochondrial functional capacity. This was evident from the increased mitochondrial respiration complex I activity and ATP content (Xia et al., 2017). Drp1 plays a key role in stimulating mitochondrial disintegration and death (Wu Q. R. et al., 2021).

Sacubitril/valsartan treatment decreased pro-apoptotic markers—cleaved caspase-3, B-cell lymphoma 2 (Bcl-2), and Bcl-2 associated X protein (Bax)—in various models of cardiomyopathy (Ge et al., 2019; Sorrentino et al., 2019; Yeh et al., 2021a; Bai et al., 2021; Dindaş et al., 2021) (Table 6). A similar reduction in apoptosis was also noted in sacubitril/valsartan-pretreated (20 μM for 30 min) H9c2 cells exposed to doxorubicin (Xia et al., 2017) and phenylephrine (Peng et al., 2020) to induce cardiomyocyte hypertrophy. Moreover, it is believed that sustained phosphorylated c-Jun N-terminal kinase (JNK) and p38 mitogen-activated protein kinase

TABLE 6 The effects of sacubitril/valsartan on myocardial mitochondrial function and apoptosis in animal studies.

Type of model	Treatment, dose and duration	Findings	References
5/6 nephrectomy rats-induced chronic kidney disease	Post-treatment 60 mg/kg for 8 weeks	↑ cardiac mitochondrial proteins (ATP synthase β, Porin 1)	Suematsu et al. (2018)
Chemogenetic rats model of persistent cardiac redox stress	Post-treatment 68 mg/kg orally for 4 weeks	↑ isocitrate dehydrogenase 2 expression ↓ caspase 3	Sorrentino et al. (2019)
Doxorubicin-induced dilated cardiomyopathy in rats	Post-treatment 30 mg/kg/day/orally for 47 days	↓ cytosolic cytochrome C expression, ↓ cyclophilin-D expression ↓ Drp1 expression ↓ Mfn2 expression ↓ electron transport chain complex subunits (I, II, III, and V) expression ↓ mitochondrial Bax expression ↓ cleaved caspase 3 expression ↓ cleaved caspase 9 expression ↓ percentage early and late apoptosis cells	Yeh et al. (2021a)
H_2O_2-induced cell apoptosis in H9C2 cells	Pretreatment 12.5 μM	↑ mitochondrial-membrane potential, ↓ mitochondrial damage ↓ p-Drp1 expression ↓ Mfn2 expression	Yeh et al. (2021b)
Cardiorenal syndrome rats fed with high-protein diet	Post-treatment 100 mg/kg/day, orally for 28 days	↑ mitochondrial cytochrome C expression ↓ cytosolic cytochrome C expression ↓ cyclophilin-D expression ↓ DRP1 expression ↓ Mfn2 expression ↓ PGC-1α expression ↑ electron transport chain complex subunits (I,II, III, and V) expression ↓ mitochondrial Bax protein expression ↓ cleaved caspase 3 protein expression ↓ cleaved Poly ADP-ribose polymerase ↓ apoptosis signal-regulating kinase I ↓ p-MMK4, ↓ p-MMK7, ↓ p-ERK, ↓ p-c-Jun	Yeh et al. (2021b)
Simultaneous heart and kidney I/R-induced injury in rats	Post-treatment 10 mg/kg, orally at 30 min/followed by days 1–5 twice daily	↑ mitochondrial cytochrome C expression ↓ cytosolic cytochrome C expression ↓ mitochondrial Bax expression ↓ cleaved caspase 3 expression ↓ cleaved Poly ADP-ribose polymerase expression	Sung et al. (2022)
Doxorubicin-induced cardiotoxicity in mice	Concurrent treatment 80 mg/kg orally for 9 days	↓ caspase 3	Dindaş et al. (2021)
ox-LDL-induced inflammation and apoptosis in HUVECs	Pretreatment 10^{-4} μM	↓ apoptosis rate (%) ↓ cleaved caspase-3/caspase-3 expression ↓ Bax expression ↑ Bcl-2 expression	Bai et al. (2021)
High-fat diet and streptozotocin induced-diabetic cardiomyopathy in rats	Post-treatment 68 mg/kg/day, gastric gavage for 8 weeks	↓ cleaved caspase-3 protein and mRNA expression ↓ Bax protein expression ↑ Bcl-2 protein expression ↓ Bax/Bcl-2 mRNA ratio	Belali et al. (2022)
Doxorubicin-induced cardiotoxicity in rats	Concurrent treatment 60 mg/kg/day for 6 weeks	↓ apoptosis in the myocardium ↓ Bax protein expression ↓ caspase 3 protein expression	Kim et al. (2022)

ATP, adenosine triphosphate; Bcl-2/Bax; B cell lymphoma 2/Bcl-2-associated X ratio; Drp1, dynamin-related protein one; HUVECs, human umbilical vein endothelial cells; I/R, ischemia reperfusion; p-ERK, phosphorylated extracellular signal-regulated kinase; p-c-Jun, phosphorylated c-Jun; PGC-1α, peroxisome proliferator-activated receptor coactivator-1α; mfn2, mitofusin two; p-MMK4, phosphorylated mitogen-activated protein kinase kinase four; MMK7, phosphorylated mitogen-activated protein kinase kinase seven; ox-LDL, oxidized low-density lipoprotein; ↓, decrease; ↑, increase.

(MAPK), and nuclear factor kappa-light-chain-enhancer of activated B cells (NF-κB)—a proinflammatory factor (Mustafa et al., 2018)—translocations are also involved in high-glucose-induced apoptosis in H9c2 cardiomyocytes (Ge et al., 2019). Treatment with sacubitril/valsartan in the cells mitigated apoptosis by downregulating MAPK kinases (MKK), MAPKs, NF-κB, and mitofusin 2 (Mfn2) expressions (Ge et al., 2019; Yeh et al., 2021b) (Figure 3).

Collectively, these findings suggest that sacubitril/valsartan improves mitochondrial energy production, leading to increased myocardial contractile performance, possibly *via* a SIRT3-dependent pathway. Future studies can explore the effects of sacubitril/valsartan on nuclear respiratory factor-1 (NRF-1) and -2 (NRF-2) as well as mitochondrial transcription factor A (MTF-A; also abbreviated as TFAM). NRF-1 and NRF-2 are downstream targets for PGC-1α, while MTF-A is importantly involved in mitochondrial replication and transcription (Javadov et al., 2006). Optic atrophy 1 (OPA1), which participates in mitochondrial fusion, and fission 1 (FIS1), which participates in mitochondrial fission, could also be explored to understand the mechanistic effects of the drug on mitochondrial biogenesis. The expression of these proteins were significantly attenuated (except for FIS1, which was upregulated) in a murine model of heart failure (He et al., 2021). The effects of the drug on survivor activating factor enhancement (SAFE) signaling pathway, which participates in promoting cardiomyocyte survival (Hadebe et al., 2018) can also be investigated.

3.5 Effects on cardiac oxidative stress and inflammation

Oxidative stress and inflammation are the culprits in almost all diseases including heart failure. Sacubitril/valsartan mitigates oxidative stress and inflammation in *vivo* (Yang et al., 2019; Raj et al., 2021) and *in vitro* (Peng et al., 2020) models of heart failure as well as in patients with the disease (Acanfora et al., 2020; Bunsawat et al., 2021; Pang et al., 2021). The drug diminished production of intracellular reactive oxygen species (ROS), oxidative products such as malondialdehyde, and inflammatory factors (tumor necrosis factor-α, TNF-α; interleukins IL-6 and IL-1β) in the models. Sacubitril/valsartan restored the loss in antioxidant enzymes in the myocardium, namely superoxide dismutase, glutathione peroxidase, catalase, glutathione reductase, and glutathione S-transferase levels, as well as glutathione content in an isoprenaline-induced MI rat model, which correlated with a reduction in myocardial infarcted area (Imran et al., 2019). In a streptozotocin-induced diabetic cardiomyopathy mouse model, treatment of sacubitril/valsartan at 60 mg/kg/day for 16 weeks decreased inflammation by downregulating the expressions of NF-κB and MAPKs (JNK and p38), which in turn upregulated antioxidant expression, namely glutathione (GSH), and inhibited pro-inflammatory cytokines (IL-6, IL-1β, and TNF-α), in line with improvement in cardiac structure and function (Ge et al., 2019) (Figure 3). MAPKs play a key role in a range of fundamental cellular processes including cell growth, proliferation, death, and differentiation, which crosstalk with other pathways such as NF-κB (Yahfoufi et al., 2018). JNK and p38 play a role in the inflammatory and apoptotic response (Cargnello and Roux, 2011; Gui et al., 2019). Sacubitril/valsartan (68 mg/kg, orally, 4 weeks) also reduced 8-hydroxy guanosine (8-OHG) levels, a marker of oxidative damage, in rats with chemogenetic model of persistent cardiac redox stress that resembled experimental heart failure (Sorrentino et al., 2019).

Nucleotide-binding domain leucine-rich repeat family pyrin domain containing receptor 3 (NLRP3) inflammasome also acts as an essential mediator by inducing inflammation which could promote the profibrotic pathway (Wang et al., 2019b; Li et al., 2019). Oral administration of sacubitril/valsartan (60 mg/kg/day) for 4 weeks attenuated cardiac fibrosis, as evidenced by a reduction in the percentage of collagen volume fraction and its profibrotic factors—TGF-β, collagen I, MMP-2 and α-SMA-positive area—in mice with post-aortic debanding-induced pressure overload (Li et al., 2020). Sacubitril/valsartan inhibited cardiac inflammation and fibrosis *via* suppression on NF-κB and inhibition of NLRP3 inflammasome activation signaling pathways (Figure 3). The suppression of the inflammatory pathway was noted by the reduced inflammasome mediators CD45, NLRP3, and NF-κB positive-stained areas, TNF, NF-κB, caspase 1, IL-1βo-NF, and phospho-NF-κB/NF-κB expressions (Li et al., 2020).

Owing to its cardioprotective and antioxidant properties, the effects of sacubitril/valsartan on doxorubicin-induced cardiotoxicity were also investigated. Doxorubicin is a chemotherapy drug that causes an overproduction of IL-1β, IL-8, and IL-6 as well as oxidative stress in the heart leading to cardiotoxicity as an adverse effect (Quagliariello et al., 2019), with ferroptosis—accumulation of mitochondrial iron and lipid peroxides—being the underlying mechanism (Li et al., 2022). Sacubitril/valsartan was demonstrated to ameliorate doxorubicin-induced cardiotoxicity *in vivo* and *in vitro*, possibly by alleviating iron-induced mitochondrial and endoplasmic reticulum oxidative stress (Dindaş et al., 2021; Kim et al., 2022; Miyoshi et al., 2022), thereby reducing cardiac damage. It also improved LVEF in rats administered doxorubicin (Boutagy et al., 2020). Significant favorable effects of sacubitril/valsartan on cardiac function were also noted in patients with cancer therapy-related cardiac dysfunction (Sheppard and Anwar 2019; Gregorietti et al., 2020; Martín-Garcia et al., 2020; Frey et al., 2021; Xi et al., 2022).

The antihypertrophic effects of sacubitril/valsartan are frequently attributable to its capacities to reduce excessive oxidative stress and inflammation response which eventually attenuate the remodeling process. However, detailed mechanistic insights into sacubitril/valsartan's mitigative

effects on cardiac remodeling *via* oxidative stress and inflammation are still lacking. Modulative effects of the drug on nuclear factor erythroid 2-related factor 2 (Nrf2)/antioxidant responsive element (Nrf2/ARE) signaling pathway, as well as Kelch-like ECH-associated protein 1 (Keap1) have not been extensively studied. Keap1 forms a complex with Nrf2—a gene involved in oxidative stress regulation—to repress the transcriptional activity of the latter. After its dissociation from Keap1, Nrf2 translocates into the nucleus and establishes a complex with ARE to upregulate heme oxygenase-1 expression, which then inhibits proinflammatory genes (Syamsunarno et al., 2021). The potential role of sacubitril/valsartan in a calcineurin-nuclear factor of activated T cells (NFAT) inflammatory signaling pathway should also be of interest. In cardiac hypertrophy, calcineurin expression is elevated, while phosphorylated NFAT is downregulated (Zhou et al., 2022).

Low antioxidant status in patients is associated with the development of atrial fibrillation and cardiac remodeling (Bas et al., 2017; Gorbunova et al., 2018). Low plasma vitamin C level has been reported to increase the risk of cardiovascular disease (Berretta et al., 2020). Antioxidant supplementation comprising vitamin C (1 g), vitamin E (600 I.U.), and α-lipoic acid (0.6 g) for 30 days exerted beneficial effects on macrovascular function in patients with HFrEF (Bunsawat et al., 2020). A recent meta-analysis also revealed that vitamin C administration augmented LVEF in heart failure patients (Hemilä et al., 2022). The findings suggest that supplemental vitamin C may afford synergistic effects with sacubitril/valsartan if given together in patients with heart failure. However, oral intake of vitamin C (4 g/day) for 4 weeks posed a risk in skeletal muscle damage in patients with chronic heart failure despite improvement in vascular function (Nightingale et al., 2007), possibly due to its higher dose. Thus, studies in animals and clinical trials should be conducted to better understand the interaction between the vitamin and sacubitril/valsartan.

4 Conclusion and direction of future research

Accumulating evidence demonstrates that sacubitril/valsartan improves cardiac function and has beneficial effects on various events involved in cardiac remodeling, such as altered mitochondria function, apoptosis, oxidative stress and inflammation, fibrosis, and matrix remodeling. Thus, sacubitril/valsartan shows promising potential to be authenticated as an antihypertrophic drug particularly for heart disease. Nevertheless, future research needs to be executed to better understand its cardioprotective mechanisms. Figure 3 outlines the mechanistic sites of action of sacubitril/valsartan in cardiac remodeling. Further studies should explore the antihypertrophic effects of the drug on its possible molecular mechanisms. Insulin resistance has been reported in heart failure (Nakamura and Sadoshima, 2018). The role of insulin-like growth factor 1 (IGF1) and its modulation by sacubitril/valsartan should be investigated. IGFI is a molecule structurally similar to insulin that regulates a vast spectrum of cellular processes in the heart, including increased collagen synthesis in cardiac remodeling. Various transcription factors in cardiac remodeling such as CCAAT/enhancer binding protein-β (C/EBPβ), GATA-binding protein 4 (GATA4), and CBP/p300-interacting transactivator 4 (CITED4) could also be probed. C/EBPβ curbs proliferation and growth of cardiomyocytes; thus, its augmented expression indicates cardiomyocyte hypertrophy (Wang et al., 2022). CITED4 regulates the mammalian target of rapamycin (mTOR) and thereby protects against cardiac pathological remodeling (Lerchenmüller et al., 2020). GATA4, on the other hand, promotes cardiac hypertrophic growth (Chen et al., 2022).

Author contributions

NM drafted the manuscript. JJ, SZ, and YK supervised the work. MS, JJ, SZ, AA, and YK critically revised the manuscript.

Funding

The study was funded by the Ministry of Higher Education of Malaysia (FRGS-1-2019-SKK10-UKM-02-1).

Conflict of interest

The authors declare that the research was conducted in the absence of any commercial or financial relationships that could be construed as a potential conflict of interest.

Publisher's note

References

Abumayyaleh, M., El-Battrawy, I., Behnes, M., Borggrefe, M., and Akin, I. (2020). Current evidence of sacubitril/valsartan in the treatment of heart failure with reduced ejection fraction. *Future Cardiol.* 16 (4), 227–236. doi:10.2217/fca-2020-0002

Acanfora, D., Scicchitano, P., Acanfora, C., Maestri, R., Goglia, F., Incalzi, R. A., et al. (2020). Early initiation of sacubitril/valsartan in patients with chronic heart failure after acute decompensation: A case series analysis. *Clin. Drug Investig.* 40 (5), 493–501. doi:10.1007/s40261-020-00908-4

Ai, J., Shuai, Z., Tang, K., Li, Z., Zou, L., Liu, M., et al. (2021). Sacubitril/valsartan alleviates myocardial fibrosis in diabetic cardiomyopathy rats. *Hell. J. Cardiol.* 62 (5), 389–391. doi:10.1016/j.hjc.2021.04.004

Akhmetshina, A., Palumbo, K., Dees, C., Bergmann, C., Venalis, P., Zerr, P., et al. (2012). Activation of canonical Wnt signalling is required for TGF-β-mediated fibrosis. *Nat. Commun.* 3, 735. doi:10.1038/ncomms1734

Ambrosy, A. P., Braunwald, E., Morrow, D. A., DeVore, A. D., McCague, K., Meng, X., et al. (2020). Angiotensin receptor-neprilysin inhibition based on history of heart failure and use of renin-angiotensin system Antagonists. *J. Am. Coll. Cardiol.* 76 (9), 1034–1048. doi:10.1016/j.jacc.2020.06.073

Andersen, S., Axelsen, J. B., Ringgaard, S., Nyengaard, J. R., Hyldebrandt, J. A., Bogaard, H. J., et al. (2019). Effects of combined angiotensin II receptor antagonism and neprilysin inhibition in experimental pulmonary hypertension and right ventricular failure. *Int. J. Cardiol.* 293, 203–210. doi:10.1016/j.ijcard.2019.06.065

Annes, J. P., Munger, J. S., and Rifkin, D. B. (2003). Making sense of latent TGFbeta activation. *J. Cell. Sci.* 116 (2), 217–224. doi:10.1242/jcs.00229

Arendse, L. B., Danser, A., Poglitsch, M., Touyz, R. M., Burnett, J. C., Jr, Llorens-Cortes, C., et al. (2019). Novel therapeutic approaches targeting the renin-angiotensin system and associated peptides in hypertension and heart failure. *Pharmacol. Rev.* 71 (4), 539–570. doi:10.1124/pr.118.017129

Aroor, A. R., Mummidi, S., Lopez-Alvarenga, J. C., Das, N., Habibi, J., Jia, G., et al. (2021). Sacubitril/valsartan inhibits obesity-associated diastolic dysfunction through suppression of ventricular-vascular stiffness. *Cardiovasc. Diabetol.* 20 (1), 80. doi:10.1186/s12933-021-01270-1

Arrigo, M., Vodovar, N., Nougué, H., Sadoune, M., Pemberton, C. J., Ballan, P., et al. (2018). The heart regulates the endocrine response to heart failure: Cardiac contribution to circulating neprilysin. *Eur. Heart J.* 39 (20), 1794–1798. doi:10.1093/eurheartj/ehx679

Ashish, K., Faisaluddin, M., Bandyopadhyay, D., Hajra, A., and Herzog, E. (2019). Prognostic value of global longitudinal strain in heart failure subjects: A recent prototype. *Int. J. Cardiol. Heart Vasc.* 22, 48–49. doi:10.1016/j.ijcha.2018.11.009

Bai, W., Huo, T., Chen, X., Song, X., Meng, C., Dang, Y., et al. (2021). Sacubitril/valsartan inhibits ox-LDL-induced MALAT1 expression, inflammation and apoptosis by suppressing the TLR4/NF-κB signaling pathway in HUVECs. *Mol. Med. Rep.* 23 (6), 402. doi:10.3892/mmr.2021.12041

Balan, I., Khayo, T., Sultanova, S., and Lomakina, Y. (2021). Overview of sodium-glucose Co-transporter 2 (SGLT2) inhibitors for the treatment of non-diabetic heart failure patients. *Cureus* 13 (8), e17118. doi:10.7759/cureus.17118

Bas, H. A., Aksoy, F., Icli, A., Varol, E., Dogan, A., Erdogan, D., et al. (2017). The association of plasma oxidative status and inflammation with the development of atrial fibrillation in patients presenting with ST elevation myocardial infarction. *Scand. J. Clin. Lab. Invest.* 77 (2), 77–82. doi:10.1080/00365513.2016.1244857

Beckendorf, J., van den Hoogenhof, M., and Backs, J. (2018). Physiological and unappreciated roles of CaMKII in the heart. *Basic Res. Cardiol.* 113 (4), 29. doi:10.1007/s00395-018-0688-8

Belali, O. M., Ahmed, M. M., Mohany, M., Belali, T. M., Alotaibi, M. M., Al-Hoshani, A., et al. (2022). LCZ696 protects against diabetic cardiomyopathy-induced myocardial inflammation, ER stress, and apoptosis through inhibiting AGEs/NF-κB and PERK/CHOP signaling pathways. *Int. J. Mol. Sci.* 23 (3), 1288. doi:10.3390/ijms23031288

Bellis, A., Mauro, C., Barbato, E., Di Gioia, G., Sorriento, D., Trimarco, B., et al. (2020). The rationale of neprilysin inhibition in prevention of myocardial ischemia-reperfusion injury during ST-elevation myocardial infarction. *Cells* 9 (9), 2134. doi:10.3390/cells9092134

Berardi, C., Braunwald, E., Morrow, D. A., Mulder, H. S., Duffy, C. I., O'Brien, T. X., et al. (2020). Angiotensin-neprilysin inhibition in black Americans: Data from the PIONEER-HF trial. *JACC. Heart Fail.* 8 (10), 859–866. doi:10.1016/j.jchf.2020.06.019

Berg, D. D., Braunwald, E., DeVore, A. D., Lala, A., Pinney, S. P., Duffy, C. I., et al. (2020). Efficacy and safety of sacubitril/valsartan by dose level achieved in the PIONEER-HF trial. *JACC. Heart Fail.* 8 (10), 834–843. doi:10.1016/j.jchf.2020.06.008

Berretta, M., Quagliariello, V., Maurea, N., Di Francia, R., Sharifi, S., Facchini, G., et al. (2020). Multiple effects of ascorbic acid against chronic diseases: Updated evidence from preclinical and clinical studies. *Antioxidants (Basel)* 9 (12), 1182. doi:10.3390/antiox9121182

Bhattacharya, S., and Sil, P. C. (2018). "Promising natural cardioprotective agents in drug-and toxin-induced pathophysiology," in *Cardioprotective natural products: Promises and hopes*. Editor G. Brahmachari (India: Visva-Bharati University), 47–120. doi:10.1142/9789813231160_0003

Böhm, M., Young, R., Jhund, P. S., Solomon, S. D., Gong, J., Lefkowitz, M. P., et al. (2017). Systolic blood pressure, cardiovascular outcomes and efficacy and safety of sacubitril/valsartan (LCZ696) in patients with chronic heart failure and reduced ejection fraction: Results from PARADIGM-HF. *Eur. Heart J.* 38 (15), 1132–1143. doi:10.1093/eurheartj/ehw570

Boutagy, N. E., Feher, A., Pfau, D., Liu, Z., Guerrera, N. M., Freeburg, L. A., et al. (2020). Dual angiotensin receptor-neprilysin inhibition with sacubitril/valsartan attenuates systolic dysfunction in experimental doxorubicin-induced cardiotoxicity. *JACC. CardioOncol.* 2 (5), 774–787. doi:10.1016/j.jaccao.2020.09.007

Brandauer, J., Andersen, M. A., Kellezi, H., Risis, S., Frøsig, C., Vienberg, S. G., et al. (2015). AMP-activated protein kinase controls exercise training- and AICAR-induced increases in SIRT3 and MnSOD. *Front. Physiol.* 6, 85. doi:10.3389/fphys.2015.00085

Brieler, J., Breeden, M. A., and Tucker, J. (2017). Cardiomyopathy: An overview. *Am. Fam. Physician* 96 (10), 640–646.

Bunsawat, K., Ratchford, S. M., Alpenglow, J. K., Park, S. H., Jarrett, C. L., Stehlik, J., et al. (2020). Chronic antioxidant administration restores macrovascular function in patients with heart failure with reduced ejection fraction. *Exp. Physiol.* 105 (8), 1384–1395. doi:10.1113/EP088686

Bunsawat, K., Ratchford, S. M., Alpenglow, J. K., Park, S. H., Jarrett, C. L., Stehlik, J., et al. (2021). Sacubitril-valsartan improves conduit vessel function and functional capacity and reduces inflammation in heart failure with reduced ejection fraction. *J. Appl. Physiol.* 130 (1), 256–268. doi:10.1152/japplphysiol.00454.2020

Burnett, H., Earley, A., Voors, A. A., Senni, M., McMurray, J. J., Deschaseaux, C., et al. (2017). Thirty years of evidence on the efficacy of drug treatments for chronic heart failure with reduced ejection fraction: A network meta-analysis. *Circ. Heart Fail.* 10 (1), e003529. doi:10.1161/CIRCHEARTFAILURE.116.003529

Cacciatore, F., Amarelli, C., Maiello, C., Pratillo, M., Tosini, P., Mattucci, I., et al. (2020). Effect of sacubitril-valsartan in reducing depression in patients with advanced heart failure. *J. Affect. Disord.* 272, 132–137. doi:10.1016/j.jad.2020.03.158

Cao, M., Zhao, Q., Sun, X., Qian, H., Lyu, S., Chen, R., et al. (2022). Sirtuin 3: Emerging therapeutic target for cardiovascular diseases. *Free Radic. Biol. Med.* 180, 63–74. doi:10.1016/j.freeradbiomed.2022.01.005

Cargnello, M., and Roux, P. P. (2011). Activation and function of the MAPKs and their substrates, the MAPK-activated protein kinases. *Microbiol. Mol. Biol. Rev.* 75 (1), 50–83. doi:10.1128/MMBR.00031-10

Chalikias, G., Kikas, P., Thomaidis, A., Rigopoulos, P., Pistola, A., Lantzouraki, A., et al. (2021). Effect of Sacubitril/Valsartan on Circulating Catecholamine Levels During a 6-Month Follow-Up in Heart Failure Patients. Timeo Danaos et dona ferentes? *Acta Cardiol.* 76 (4), 396–401. doi:10.1080/00015385.2020.1746094

Chang, P. C., Lin, S. F., Chu, Y., Wo, H. T., Lee, H. L., Huang, Y. C., et al. (2019). LCZ696 therapy reduces ventricular tachyarrhythmia inducibility in a myocardial infarction-induced heart failure rat model. *Cardiovasc. Ther.* 6032631. doi:10.1155/2019/6032631

Chang, P. C., Wo, H. T., Lee, H. L., Lin, S. F., Chu, Y., Wen, M. S., et al. (2020). Sacubitril/valsartan therapy ameliorates ventricular tachyarrhythmia inducibility in a rabbit myocardial infarction model. *J. Card. Fail.* 26 (6), 527–537. doi:10.1016/j.cardfail.2020.03.007

Chatterjee, P., Gheblawi, M., Wang, K., Vu, J., Kondaiah, P., Oudit, G. Y., et al. (2020). Interaction between the apelinergic system and ACE2 in the cardiovascular system: Therapeutic implications. *Clin. Sci.* 134 (17), 2319–2336. doi:10.1042/CS20200479

Chen, H., Zhou, J., Chen, H., Liang, J., Xie, C., Gu, X., et al. (2022). Bmi-1-RING1B prevents GATA4-dependent senescence-associated pathological cardiac hypertrophy by promoting autophagic degradation of GATA4. *Clin. Transl. Med.* 12 (4), e574. doi:10.1002/ctm2.574

Choi, H. M., and Shin, M. S. (2020). Angiotensin receptor-neprilysin inhibitor for the treatment of heart failure: A review of recent evidence. *Korean J. Intern. Med.* 35 (3), 498–513. doi:10.3904/kjim.2020.105

Chrysant, S. G., and Chrysant, G. S. (2018). Sacubitril/valsartan: A cardiovascular drug with pluripotential actions. *Cardiovasc. Diagn. Ther.* 8 (4), 543–548. doi:10.21037/cdt.2018.05.10

Cleland, J. G., and Swedberg, K. (1998). Lack of efficacy of neutral endopeptidase inhibitor ecadotril in heart failure. The international ecadotril multi-centre dose-ranging study investigators. *Lancet* 35 (9116), 1657–1658. doi:10.1016/s0140-6736(05)77712-6

Clements, R., Vang, A., Fernandez-Nicolas, A., Kue, N. R., Mancini, T. J., Morrison, A. R., et al. (2019). Treatment of pulmonary hypertension with angiotensin II receptor blocker and neprilysin inhibitor sacubitril/valsartan. *Circ. Heart Fail.* 12 (11), e005819. doi:10.1161/CIRCHEARTFAILURE.119.005819

Croteau, D., Qin, F., Chambers, J. M., Kallick, E., Luptak, I., Panagia, M., et al. (2020). Differential effects of sacubitril/valsartan on diastolic function in mice with obesity-related metabolic heart disease. *JACC. Basic Transl. Sci.* 5 (9), 916–927. doi:10.1016/j.jacbts.2020.07.006

Cunningham, J. W., Claggett, B. L., O'Meara, E., Prescott, M. F., Pfeffer, M. A., Shah, S. J., et al. (2020a). Effect of sacubitril/valsartan on biomarkers of extracellular matrix regulation in patients with HFpEF. *J. Am. Coll. Cardiol.* 76 (5), 503–514. doi:10.1016/j.jacc.2020.05.072

Cunningham, J. W., Vaduganathan, M., Claggett, B. L., Zile, M. R., Anand, I. S., Packer, M., et al. (2020b). Effects of sacubitril/valsartan on N-terminal pro-B-type natriuretic peptide in heart failure with preserved ejection fraction. *JACC. Heart Fail.* 8 (5), 372–381. doi:10.1016/j.jchf.2020.03.002

Cuthbert, J. J., Pellicori, P., and Clark, A. L. (2020). Cardiovascular outcomes with sacubitril-valsartan in heart failure: Emerging clinical data. *Ther. Clin. Risk Manag.* 16, 715–726. doi:10.2147/TCRM.S234772

Dereli, S., Kılınçel, O., Çerik, İ., and Kaya, A. (2020). Impact of sacubitril/valsartan treatment on depression and anxiety in heart failure with reduced ejection fraction. *Acta Cardiol.* 75 (8), 774–782. doi:10.1080/00015385.2020.1730577

Desai, A. S., McMurray, J. J., Packer, M., Swedberg, K., Rouleau, J. L., Chen, F., et al. (2015). Effect of the angiotensin-receptor-neprilysin inhibitor LCZ696 compared with enalapril on mode of death in heart failure patients. *Eur. heart J.* 36 (30), 1990–1997. doi:10.1093/eurheartj/ehv186

DeVore, A. D., Braunwald, E., Morrow, D. A., Duffy, C. I., Ambrosy, A. P., Chakraborty, H., et al. (2020). Initiation of angiotensin-neprilysin inhibition after acute decompensated heart failure: Secondary analysis of the open-label extension of the PIONEER-HF trial. *JAMA Cardiol.* 5 (2), 202–207. doi:10.1001/jamacardio.2019.4665

Dindaş, F., Güngör, H., Ekici, M., Akokay, P., Erhan, F., Doğduş, M., et al. (2021). Angiotensin receptor-neprilysin inhibition by sacubitril/valsartan attenuates doxorubicin-induced cardiotoxicity in A pretreatment mice model by interfering with oxidative stress, inflammation, and caspase 3 apoptotic pathway. *Anatol. J. Cardiol.* 25 (11), 821–828. doi:10.5152/AnatolJCardiol.2021.356

Eiringhaus, J., Wünsche, C. M., Tirilomis, P., Herting, J., Bork, N., Nikolaev, V. O., et al. (2020). Sacubitrilat reduces pro-arrhythmogenic sarcoplasmic reticulum Ca^{2+} leak in human ventricular cardiomyocytes of patients with end-stage heart failure. *Esc. Heart Fail.* 7 (5), 2992–3002. doi:10.1002/ehf2.12918

Ferro, C. J., Spratt, J. C., Haynes, W. G., and Webb, D. J. (1998). Inhibition of neutral endopeptidase causes vasoconstriction of human resistance vessels *in vivo*. *Circulation* 97 (23), 2323–2330. doi:10.1161/01.cir.97.23.2323

Frey, M. K., Arfsten, H., Pavo, N., Han, E., Kastl, S., Hülsmann, M., et al. (2021). Sacubitril/valsartan is well tolerated in patients with longstanding heart failure and history of cancer and improves ventricular function: Real-world data. *Cardiooncology.* 7 (1), 35. doi:10.1186/s40959-021-00121-y

Gajarsa, J. J., and Kloner, R. A. (2011). Left ventricular remodeling in the post-infarction heart: A review of cellular, molecular mechanisms, and therapeutic modalities. *Heart fail. Rev.* 16 (1), 13–21. doi:10.1007/s10741-010-9181-7

Ge, Q., Zhao, L., Liu, C., Ren, X., Yu, Y. H., Pan, C., et al. (2020). LCZ696, an angiotensin receptor-neprilysin inhibitor, improves cardiac hypertrophy and fibrosis and cardiac lymphatic remodeling in transverse aortic constriction model mice. *Biomed. Res. Int.* 2020, 7256862. doi:10.1155/2020/7256862

Ge, Q., Zhao, L., Ren, X. M., Ye, P., and Hu, Z. Y. (2019). LCZ696, an angiotensin receptor-neprilysin inhibitor, ameliorates diabetic cardiomyopathy by inhibiting inflammation, oxidative stress and apoptosis. *Exp. Biol. Med.* 244 (12), 1028–1039. doi:10.1177/1535370219861283

Gokhroo, R. K., Anushri, K., Tarik, M. T., Kailash, C., Rajesh, N., Ashish, K., et al. (2021). 1 year follow up results of "ARTIM HF TRIAL" (angiotensin receptor neprilysin inhibitor effect on TEI index & left ventricular mass in heart failure). *Indian Heart J.* 73 (2), 205–210. doi:10.1016/j.ihj.2021.01.010

Gorbunova, O., Panova, T., Chernysheva, E., and Popov, E. (2018). The level of protection from oxidative stress and three-year dynamics of structural and functional changes of the myocardium in chronic ischemic heart disease in men. *Georgian Med. News* 285, 63–69.

Greenberg, B. (2020). Angiotensin receptor-neprilysin inhibition (ARNI) in heart failure. *Int. J. Heart Fail.* 2 (2), 73. doi:10.36628/ijhf.2020.0002

Gregorietti, V., Fernandez, T. L., Costa, D., Chahla, E. O., and Daniele, A. J. (2020). Use of sacubitril/valsartan in patients with cardio toxicity and heart failure due to chemotherapy. *Cardiooncology.* 6 (1), 24. doi:10.1186/s40959-020-00078-4

Gui, J. S., Jalil, J., Jubri, Z., and Kamisah, Y. (2019). *Parkia speciosa* empty pod extract exerts anti-inflammatory properties by modulating NFκB and MAPK pathways in cardiomyocytes exposed to tumor necrosis factor-α. *Cytotechnology* 71 (1), 79–89. doi:10.1007/s10616-018-0267-8

Hadebe, N., Cour, M., and Lecour, S. (2018). The SAFE pathway for cardioprotection: Is this a promising target? *Basic Res. Cardiol.* 113 (2), 9. doi:10.1007/s00395-018-0670-5

Hamano, G., Yamamoto, K., Takami, Y., Takeshita, H., Shimosato, T., Moritani, T., et al. (2019). Effects of low-dose sacubitril/valsartan on different stages of cardiac hypertrophy in salt-loaded hypertensive rats. *J. Cardiovasc. Pharmacol.* 73 (5), 282–289. doi:10.1097/FJC.0000000000000662

Haynes, R., Judge, P. K., Staplin, N., Herrington, W. G., Storey, B. C., Bethel, A., et al. (2018). Effects of sacubitril/valsartan versus irbesartan in patients with chronic kidney disease. *Circulation* 138 (15), 1505–1514. doi:10.1161/CIRCULATIONAHA.118.034818

He, H., Li, C., Lu, X., Li, Y., Li, X., Sun, X., et al. (2021). RNA-seq profiling to investigate the mechanism of qishen granules on regulating mitochondrial energy metabolism of heart failure in rats. *Evid. Based. Complement. Altern. Med.* 2021, 5779307. doi:10.1155/2021/5779307

Hemilä, H., Chalker, E., and de Man, A. (2022). Vitamin C may improve left ventricular ejection fraction: A meta-analysis. *Front. Cardiovasc. Med.* 9, 789729. doi:10.3389/fcvm.2022.789729

Hinderer, S., and Schenke-Layland, K. (2019). Cardiac fibrosis - a short review of causes and therapeutic strategies. *Adv. Drug Deliv. Rev.* 146, 77–82. doi:10.1016/j.addr.2019.05.011

Hsiao, F. C., Wang, C. L., Chang, P. C., Lu, Y. Y., Huang, C. Y., Chu, P. H., et al. (2020). Angiotensin receptor neprilysin inhibitor for patients with heart failure and reduced ejection fraction: Real-world experience from taiwan. *J. Cardiovasc. Pharmacol. Ther.* 25 (2), 152–157. doi:10.1177/1074248419872958

Hsu, S. J., Huang, H. C., Chuang, C. L., Chang, C. C., Hou, M. C., Lee, F. Y., et al. (2020). Dual angiotensin receptor and neprilysin inhibitor ameliorates portal hypertension in portal hypertensive rats. *Pharmaceutics* 12 (4), 320. doi:10.3390/pharmaceutics12040320

Hu, J., Wu, Y., Zhou, X., Wang, X., Jiang, W., Huo, J., et al. (2020). Beneficial effects of sacubitril/valsartan at low doses in an asian real-world heart failure population. *J. Cardiovasc. Pharmacol.* 76 (4), 445–451. doi:10.1097/FJC.0000000000000873

Hubers, S. A., and Brown, N. J. (2016). Combined angiotensin receptor antagonism and neprilysin inhibition. *Circulation* 133 (11), 1115–1124. doi:10.1161/CIRCULATIONAHA.115.018622

Imran, M., Hassan, M. Q., Akhtar, M. S., Rahman, O., Akhtar, M., Najmi, A. K., et al. (2019). Sacubitril and valsartan protect from experimental myocardial infarction by ameliorating oxidative damage in wistar rats. *Clin. Exp. Hypertens.* 41 (1), 62–69. doi:10.1080/10641963.2018.1441862

Iwata, M., Cowling, R. T., Yeo, S. J., and Greenberg, B. (2011). Targeting the ACE2-ang-(1-7) pathway in cardiac fibroblasts to treat cardiac remodeling and heart failure. *J. Mol. Cell. Cardiol.* 51 (4), 542–547. doi:10.1016/j.yjmcc.2010.12.003

Januzzi, J. L., Jr, Prescott, M. F., Butler, J., Felker, G. M., Maisel, A. S., McCague, K., et al. (2019). Association of change in N-terminal pro–B-type natriuretic peptide following initiation of sacubitril-valsartan treatment with cardiac structure and function in patients with heart failure with reduced ejection fraction. *JAMA* 322 (11), 1085–1095. doi:10.1001/jama.2019.12821

Jariwala, P., Punjani, A., Boorugu, H., and Madhawar, D. B. (2021). A clinical experience of Indian patients with heart failure with reduced left ventricular ejection fraction using an angiotensin receptor-neprilysin inhibitor [ARNI] on an outpatient basis. *Indian Heart J.* 73 (2), 211–213. doi:10.1016/j.ihj.2021.01.002

Javadov, S., Purdham, D. M., Zeidan, A., and Karmazyn, M. (2006). NHE-1 inhibition improves cardiac mitochondrial function through regulation of mitochondrial biogenesis during postinfarction remodeling. *Am. J. Physiol. Heart Circ. Physiol.* 291 (4), H1722–H1730. doi:10.1152/ajpheart.00159.2006

Jornayvaz, F. R., and Shulman, G. I. (2010). Regulation of mitochondrial biogenesis. *Essays Biochem.* 47, 69–84. doi:10.1042/bse0470069

Kahveci, G., Bayrak, F., Mutlu, B., and Basaran, Y. (2009). Determinants of elevated NT-proBNP levels in patients with hypertrophic cardiomyopathy: An echocardiographic study. *Heart Lung Circ.* 18 (4), 266–270. doi:10.1016/j.hlc.2008.11.001

Kang, D. H., Park, S. J., Shin, S. H., Hong, G. R., Lee, S., Kim, M. S., et al. (2019). Angiotensin receptor neprilysin inhibitor for functional mitral regurgitation. *Circulation* 139 (11), 1354–1365. doi:10.1161/CIRCULATIONAHA.118.037077

Kaplinsky, E. (2016). Sacubitril/valsartan in heart failure: Latest evidence and place in therapy. *Ther. Adv. Chronic Dis.* 7 (6), 278–290. doi:10.1177/2040622316665350

Karabulut, U., Keskin, K., Karabulut, D., Yiğit, E., and Yiğit, Z. (2022). Effect of sacubitril/valsartan combined with dapagliflozin on long-term cardiac mortality in heart failure with reduced ejection fraction. *Angiology* 73 (4), 350–356. doi:10.1177/00033197211047329

Karagodin, I., Kalantari, S., Yu, D. B., Kim, G., Sayer, G., Addetia, K., et al. (2020). Echocardiographic evaluation of the effects of sacubitril-valsartan on vascular properties in heart failure patients. *Int. J. Cardiovasc. Imaging* 36 (2), 271–278. doi:10.1007/s10554-019-01708-4

Khan, S., Joyce, J., Margulies, K. B., and Tsuda, T. (2014). Enhanced bioactive myocardial transforming growth factor-β in advanced human heart failure. *Circ. J.* 78 (11), 2711–2718. doi:10.1253/circj.cj-14-0511

Khder, Y., Shi, V., McMurray, J., and Lefkowitz, M. P. (2017). Sacubitril/valsartan (LCZ696) in heart failure. *Handb. Exp. Pharmacol.* 243, 133–165. doi:10.1007/164_2016_77

Kim, B. S., Park, I. H., Lee, A. H., Kim, H. J., Lim, Y. H., Shin, J. H., et al. (2022). Sacubitril/valsartan reduces endoplasmic reticulum stress in A rat model of doxorubicin-induced cardiotoxicity. *Arch. Toxicol.* 96, 1065–1074. doi:10.1007/s00204-022-03241-1

Kim, H. M., Hwang, I. C., Choi, W., Yoon, Y. E., and Cho, G. Y. (2021). Combined effects of arni and Sglt2 inhibitors in diabetic patients with heart failure with reduced ejection fraction. *Sci. Rep.* 11 (1), 22342. doi:10.1038/s41598-021-01759-5

Koentges, C., Bode, C., and Bugger, H. (2016). SIRT3 in cardiac physiology and disease. *Front. Cardiovasc. Med.* 3, 38. doi:10.3389/fcvm.2016.00038

Kompa, A. R., Lu, J., Weller, T. J., Kelly, D. J., Krum, H., von Lueder, T. G., et al. (2018). Angiotensin receptor neprilysin inhibition provides superior cardioprotection compared to angiotensin converting enzyme inhibition after experimental myocardial infarction. *Int. J. Cardiol.* 258, 192–198. doi:10.1016/j.ijcard.2018.01.077

Książczyk, M., and Lelonek, M. (2020). Angiotensin receptor/neprilysin inhibitor-A breakthrough in chronic heart failure therapy: Summary of subanalysis on PARADIGM-HF trial findings. *Heart fail. Rev.* 25, 393–402. doi:10.1007/s10741-019-09879-x

Kumar, S., Wang, G., Liu, W., Ding, W., Dong, M., Zheng, N., et al. (2018). Hypoxia-induced mitogenic factor promotes cardiac hypertrophy via calcium-dependent and hypoxia-inducible factor-1α mechanisms. *Hypertension* 72 (2), 331–342. doi:10.1161/HYPERTENSIONAHA.118.10845

Kuwahara, K. (2021). The natriuretic peptide system in heart failure: Diagnostic and therapeutic implications. *Pharmacol. Ther.* 227, 107863. doi:10.1016/j.pharmthera.2021.107863

Lerchenmüller, C., Rabolli, C. P., Yeri, A., Kitchen, R., Salvador, A. M., Liu, L. X., et al. (2020). CITED4 protects against adverse remodeling in response to physiological and pathological stress. *Circ. Res.* 127 (5), 631–646. doi:10.1161/CIRCRESAHA.119.315881

Li, X., Braza, J., Mende, U., Choudhary, G., and Zhang, P. (2021). Cardioprotective effects of early intervention with sacubitril/valsartan on pressure overloaded rat hearts. *Sci. Rep.* 11 (1), 16542. doi:10.1038/s41598-021-95988-3

Li, X., Geng, J., Zhao, J., Ni, Q., Zhao, C., Zheng, Y., et al. (2019). Trimethylamine N-oxide exacerbates cardiac fibrosis via activating the NLRP3 inflammasome. *Front. Physiol.* 10, 866. doi:10.3389/fphys.2019.00866

Li, X., Liang, J., Qu, L., Liu, S., Qin, A., Liu, H., et al. (2022). Exploring the role of ferroptosis in the doxorubicin-induced chronic cardiotoxicity using a murine model. *Chem. Biol. Interact.* 363, 110008. doi:10.1016/j.cbi.2022.110008

Li, X., Zhu, Q., Wang, Q., Zhang, Q., Zheng, Y., Wang, L., et al. (2020). Protection of sacubitril/valsartan against pathological cardiac remodeling by inhibiting the NLRP3 inflammasome after relief of pressure overload in mice. *Cardiovasc. Drugs Ther.* 34 (5), 629–640. doi:10.1007/s10557-020-06995-x

Lin, Y., Zhang, H., Zhao, S., Chen, L., Li, J., Wang, X., et al. (2022). The efficacy and safety of the combined therapy of sodium-glucose Co-Transporter-2 inhibitors and angiotensin receptor-neprilysin inhibitor in patients with heart failure with reduced ejection fraction: A meta-analysis of the emperor-reduced and dapa-Hf sub-analysis. *Front. Cardiovasc. Med.* 9, 882089. doi:10.3389/fcvm.2022.882089

Liu, J., Zheng, X., Zhang, C., Zhang, C., and Bu, P. (2021b). Lcz696 alleviates myocardial fibrosis after myocardial infarction through the sFRP-1/Wnt/β-Catenin signaling pathway. *Front. Pharmacol.* 12, 724147. doi:10.3389/fphar.2021.724147

Liu, L. W., Wu, P. C., Chiu, M. Y., Tu, P. F., and Fang, C. C. (2020a). Sacubitril/valsartan improves left ventricular ejection fraction and reverses cardiac remodeling in Taiwanese patients with heart failure and reduced ejection fraction. *Acta Cardiol. Sin.* 36 (2), 125–132. doi:10.6515/ACS.202003_36(2).20190812A

Liu, L., Zhang, D., and Li, Y. (2020b). LncRNAs in cardiac hypertrophy: From basic science to clinical application. *J. Cell. Mol. Med.* 24 (20), 11638–11645. doi:10.1111/jcmm.15819

Liu, Y., Fan, Y., Li, J., Chen, M., Chen, A., Yang, D., et al. (2021a). Combination of LCZ696 and ACEI further improves heart failure and myocardial fibrosis after acute myocardial infarction in mice. *Biomed. Pharmacother.* 133, 110824. doi:10.1016/j.biopha.2020.110824

Lyon, R. C., Zanella, F., Omens, J. H., and Sheikh, F. (2015). Mechanotransduction in cardiac hypertrophy and failure. *Circ. Res.* 116 (8), 1462–1476. doi:10.1161/CIRCRESAHA.116.304937

Ma, Z. G., Yuan, Y. P., Wu, H. M., Zhang, X., and Tang, Q. Z. (2018). Cardiac fibrosis: New insights into the pathogenesis. *Int. J. Biol. Sci.* 14 (12), 1645–1657. doi:10.7150/ijbs.28103

Mann, D. L. (2005). Cardiac remodeling as therapeutic target: Treating heart failure with cardiac support devices. *Heart fail. Rev.* 10 (2), 93–94. doi:10.1007/s10741-005-4635-z

Martín-Garcia, A., López-Fernández, T., Mitroi, C., Chaparro-Muñoz, M., Moliner, P., Martin-Garcia, A. C., et al. (2020). Effectiveness of sacubitril-valsartan in cancer patients with heart failure. *Esc. Heart Fail.* 7 (2), 763–767. doi:10.1002/ehf2.12627

Masarone, D., Errigo, V., Melillo, E., Valente, F., Gravino, R., Verrengia, M., et al. (2020). Effects of sacubitril/valsartan on the right ventricular arterial coupling in patients with heart failure with reduced ejection fraction. *J. Clin. Med.* 9 (10), 3159. doi:10.3390/jcm9103159

Maslov, M. Y., Foianini, S., Mayer, D., Orlov, M. V., and Lovich, M. A. (2019a). Interaction between sacubitril and valsartan in preventing heart failure induced by aortic valve insufficiency in rats. *J. Card. Fail.* 25 (11), 921–931. doi:10.1016/j.cardfail.2019.09.008

Maslov, M. Y., Foianini, S., Mayer, D., Orlov, M. V., and Lovich, M. A. (2019b). Synergy between sacubitril and valsartan leads to hemodynamic, antifibrotic, and exercise tolerance benefits in rats with preexisting heart failure. *Am. J. Physiol. Heart Circ. Physiol.* 316 (2), H289–H297. doi:10.1152/ajpheart.00579.2018

Mazzetti, S., Scifo, C., Abete, R., Margonato, D., Chioffi, M., Rossi, J., et al. (2020). Short-term echocardiographic evaluation by global longitudinal strain in patients with heart failure treated with sacubitril/valsartan. *Esc. Heart Fail.* 7 (3), 964–972. doi:10.1002/ehf2.12656

McCormack, P. L. (2016). Sacubitril/valsartan: A review in chronic heart failure with reduced ejection fraction. *Drugs* 76 (3), 387–396. doi:10.1007/s40265-016-0544-9

McKinnie, S. M., Fischer, C., Tran, K. M., Wang, W., Mosquera, F., Oudit, G. Y., et al. (2016). The metalloprotease neprilysin degrades and inactivates apelin peptides. *Chembiochem* 17 (16), 1495–1498. doi:10.1002/cbic.201600244

McMurray, J., Jackson, A. M., Lam, C., Redfield, M. M., Anand, I. S., Ge, J., et al. (2020). Effects of sacubitril-valsartan versus valsartan in women compared with men with heart failure and preserved ejection fraction: Insights from PARAGON-HF. *Circulation* 141 (5), 338–351. doi:10.1161/CIRCULATIONAHA.119.044491

McMurray, J. J., Packer, M., Desai, A. S., Gong, J., Lefkowitz, M. P., Rizkala, A. R., et al. (2014). Angiotensin-neprilysin inhibition versus enalapril in heart failure. *N. Engl. J. Med.* 371 (11), 993–1004. doi:10.1056/NEJMoa1409077

Mirić, D., Baković, D., Eterović, D., Sorić, T., Čapkun, V., Vuković, I., et al. (2021). Left-ventricular function after 3 Months of sacubitril-valsartan in acute decompensated heart failure. *J. Cardiovasc. Transl. Res.* 14 (2), 290–298. doi:10.1007/s12265-020-10041-4

Miyauchi, T., and Sakai, S. (2019). Endothelin and the heart in health and diseases. *Peptides* 111, 77–88. doi:10.1016/j.peptides.2018.10.002

Miyoshi, T., Nakamura, K., Amioka, N., Hatipoglu, O. F., Yonezawa, T., Saito, Y., et al. (2022). Lcz696 ameliorates doxorubicin-induced cardiomyocyte toxicity in rats. *Sci. Rep.* 12 (1), 4930. doi:10.1038/s41598-022-09094-z

Miyoshi, T., Nakamura, K., Miura, D., Yoshida, M., Saito, Y., Akagi, S., et al. (2019). Effect of LCZ696, A dual angiotensin receptor neprilysin inhibitor, on isoproterenol-induced cardiac hypertrophy, fibrosis, and hemodynamic change in rats. *Cardiol. J.* 26 (5), 575–583. doi:10.5603/CJ.a2018.0048

Morillas, P., Castillo, J., Quiles, J., Nuñez, D., Guillén, S., Maceira, A., et al. (2008). Usefulness of NT-proBNP level for diagnosing left ventricular hypertrophy in hypertensive patients. A cardiac magnetic resonance study. *Rev. Espanola Cardiol.* 61 (9), 972–975. doi:10.1016/S1885-5857(08)60259-5

Morillas-Climent, H., Seller-Moya, J., Vicedo-López, Á., Galcerá-Jornet, E., Alania-Torres, E., Rodríguez-Pichardo., et al. (2019). Evolution of functional Class, biochemical and echocardiographic parameters and clinical outcomes after sacubitril/valsartan initiation in daily practice. *J. Comp. Eff. Res.* 8 (9), 685–697. doi:10.2217/cer-2019-0014

Morrow, D. A., Velazquez, E. J., DeVore, A. D., Prescott, M. F., Duffy, C. I., Gurmu, Y., et al. (2019). Cardiovascular biomarkers in patients with acute decompensated heart failure randomized to sacubitril-valsartan or enalapril in the PIONEER-HF trial. *Eur. Heart J.* 40 (40), 3345–3352. doi:10.1093/eurheartj/ehz240

Moyes, A. J., and Hobbs, A. J. (2019). C-Type natriuretic peptide: A multifaceted paracrine regulator in the heart and vasculature. *Int. J. Mol. Sci.* 20 (9), 2281. doi:10.3390/ijms20092281

Murphy, M. P., and LeVine, H., 3rd. (2010). Alzheimer's disease and the amyloid-beta peptide. *J. Alzheimers Dis.* 19 (1), 311–323. doi:10.3233/JAD-2010-1221

Murphy, S. P., Prescott, M. F., Maisel, A. S., Butler, J., Piña, I. L., Felker, G. M., et al. (2021). Association between angiotensin receptor-neprilysin inhibition, cardiovascular biomarkers, and cardiac remodeling in heart failure with reduced ejection fraction. *Circ. Heart Fail.* 14 (6), e008410. doi:10.1161/CIRCHEARTFAILURE.120.008410

Mustafa, N. H., Ugusman, A., Jalil, J., and Kamisah, Y. (2018). Anti-inflammatory property of *Parkia speciosa* empty pod extract in human umbilical vein endothelial cells. *J. Appl. Pharm. Sci.* 8 (1), 152–158. doi:10.7324/JAPS.2018.8123

Myhre, P. L., Prescott, M. F., Murphy, S. P., Fang, J. C., Mitchell, G. F., Ward, J. H., et al. (2022). Early B-type natriuretic peptide change in HFrEF patients treated with sacubitril/valsartan: A pooled analysis of EVALUATE-HF and PROVE-HF. *JACC. Heart Fail.* 10 (2), 119–128. doi:10.1016/j.jchf.2021.09.007

Myhre, P. L., Vaduganathan, M., Claggett, B., Packer, M., Desai, A. S., Rouleau, J. L., et al. (2019). B-Type natriuretic peptide during treatment with sacubitril/valsartan: The PARADIGM-HF trial. *J. Am. Coll. Cardiol.* 73 (11), 1264–1272. doi:10.1016/j.jacc.2019.01.018

Nakamura, M., and Sadoshima, J. (2018). Mechanisms of physiological and pathological cardiac hypertrophy. *Nat. Rev. Cardiol.* 15 (7), 387–407. doi:10.1038/s41569-018-0007-y

Nakou, E. S., Marketou, M. E., Patrianakos, A., Protonotarios, A., Vardas, P. E., Parthenakis, F. I., et al. (2020). Short-term effects of angiotensin receptor-neprilysin inhibitors on diastolic strain and tissue Doppler parameters in heart failure patients with reduced ejection fraction: A pilot trial. *Hell. J. Cardiol.* 61 (6), 415–418. doi:10.1016/j.hjc.2019.12.003

Nalivaeva, N. N., Zhuravin, I. A., and Turner, A. J. (2020). Neprilysin expression and functions in development, ageing and disease. *Mech. Ageing Dev.* 192, 111363. doi:10.1016/j.mad.2020.111363

Nattel, S. (2017). Molecular and cellular mechanisms of atrial fibrosis in atrial fibrillation. *JACC. Clin. Electrophysiol.* 3 (5), 425–435. doi:10.1016/j.jacep.2017.03.002

Nightingale, A. K., Crilley, J. G., Pegge, N. C., Boehm, E. A., Mumford, C., Taylor, D. J., et al. (2007). Chronic oral ascorbic acid therapy worsens skeletal muscle metabolism in patients with chronic heart failure. *Eur. J. Heart Fail.* 9 (3), 287–291. doi:10.1016/j.ejheart.2006.06.006

Nordén, E. S., Bendiksen, B. A., Andresen, H., Bergo, K. K., Espe, E. K., Hasic, A., et al. (2021). Sacubitril/valsartan ameliorates cardiac hypertrophy and preserves diastolic function in cardiac pressure overload. *Esc. Heart Fail.* 8 (2), 918–927. doi:10.1002/ehf2.13177

Nougué, H., Pezel, T., Picard, F., Sadoune, M., Arrigo, M., Beauvais, F., et al. (2019). Effects of sacubitril/valsartan on neprilysin targets and the metabolism of natriuretic peptides in chronic heart failure: A mechanistic clinical study. *Eur. J. Heart Fail.* 21 (5), 598–605. doi:10.1002/ejhf.1342

Packer, M., Anker, S. D., Butler, J., Filippatos, G., Ferreira, J. P., Pocock, S. J., et al. (2021). Influence of neprilysin inhibition on the efficacy and safety of empagliflozin in patients with chronic heart failure and a reduced ejection fraction: The EMPEROR-reduced trial. *Eur. Heart J.* 42 (6), 671–680. doi:10.1093/eurheartj/ehaa968

Pang, Z., Pan, C., Yao, Z., Ren, Y., Tian, L., Cui, J., et al. (2021). A study of the sequential treatment of acute heart failure with sacubitril/valsartan by recombinant human brain natriuretic peptide: A randomized controlled trial. *Medicine* 100 (16), e25621. doi:10.1097/MD.0000000000025621

Pascual-Figal, D., Bayés-Genis, A., Beltrán-Troncoso, P., Caravaca-Pérez, P., Conde-Martel, A., Crespo-Leiro, M. G., et al. (2021). Sacubitril-valsartan, clinical benefits and related mechanisms of action in heart failure with reduced ejection fraction. *A Rev. Front. cardiovasc. Med.* 8, 754499. doi:10.3389/fcvm.2021.754499

Pavo, I. J., Pavo, N., Kastner, N., Traxler, D., Lukovic, D., Zlabinger, K., et al. (2020). Heart failure with reduced ejection fraction is characterized by systemic NEP downregulation. *JACC. Basic Transl. Sci.* 5 (7), 715–726. doi:10.1016/j.jacbts.2020.05.011

Pavo, N., Lukovic, D., Zlabinger, K., Zimba, A., Lorant, D., Goliasch, G., et al. (2017). Sequential activation of different pathway networks in ischemia-affected and non-affected myocardium, inducing intrinsic remote conditioning to prevent left ventricular remodeling. *Sci. Rep.* 7, 43958. doi:10.1038/srep43958

Peng, S., Lu, X. F., Qi, Y. D., Li, J., Xu, J., Yuan, T. Y., et al. (2020). LCZ696 ameliorates oxidative stress and pressure overload-induced pathological cardiac remodeling by regulating the sirt3/MnSOD pathway. *Oxid. Med. Cell. Longev.* 2020, 9815039. doi:10.1155/2020/9815039

Pfau, D., Thorn, S. L., Zhang, J., Mikush, N., Renaud, J. M., Klein, R., et al. (2019). Angiotensin receptor neprilysin inhibitor attenuates myocardial remodeling and improves infarct perfusion in experimental heart failure. *Sci. Rep.* 9 (1), 5791. doi:10.1038/s41598-019-42113-0

Piersma, B., Bank, R. A., and Boersema, M. (2015). Signaling in fibrosis: TGF-β, WNT, and YAP/TAZ converge. *Front. Med.* 2, 59. doi:10.3389/fmed.2015.00059

Polito, M. V., Silverio, A., Rispoli, A., Vitulano, G., Auria, F., De Angelis, E., et al. (2020). Clinical and echocardiographic benefit of sacubitril/valsartan in A real-world population with HF with reduced ejection fraction. *Sci. Rep.* 10 (1), 6665. doi:10.1038/s41598-020-63801-2

Quagliariello, V., Coppola, C., Mita, D. G., Piscopo, G., Iaffaioli, R. V., Botti, G., et al. (2019). Low doses of bisphenol a have pro-inflammatory and pro-oxidant effects, stimulate lipid peroxidation and increase the cardiotoxicity of doxorubicin in cardiomyoblasts. *Environ. Toxicol. Pharmacol.* 69, 1–8. doi:10.1016/j.etap.2019.03.006

Raj, P., Sayfee, K., Parikh, M., Yu, L., Wigle, J., Netticadan, T., et al. (2021). Comparative and combinatorial effects of resveratrol and sacubitril/valsartan alongside valsartan on cardiac remodeling and dysfunction in MI-induced rats. *Molecules* 26 (16), 5006. doi:10.3390/molecules26165006

Ramaccini, D., Montoya-Uribe, V., Aan, F. J., Modesti, L., Potes, Y., Wieckowski, M. R., et al. (2021). Mitochondrial function and dysfunction in dilated cardiomyopathy. *Front. Cell. Dev. Biol.* 8, 624216. doi:10.3389/fcell.2020.624216

Rezq, A., Saad, M., and El Nozahi, M. (2021). Comparison of the efficacy and safety of sacubitril/valsartan versus ramipril in patients with ST-segment elevation myocardial infarction. *Am. J. Cardiol.* 143, 7–13. doi:10.1016/j.amjcard.2020.12.037

Romano, G., Vitale, G., Ajello, L., Agnese, V., Bellavia, D., Caccamo, G., et al. (2019). The effects of sacubitril/valsartan on clinical, biochemical and echocardiographic parameters in patients with heart failure with reduced ejection fraction: The "hemodynamic recovery. *J. Clin. Med.* 8 (12), 2165. doi:10.3390/jcm8122165

Russo, V., Bottino, R., Rago, A., Papa, A. A., Liccardo, B., Proietti, R., et al. (2020). The effect of sacubitril/valsartan on device detected arrhythmias and electrical parameters among dilated cardiomyopathy patients with reduced ejection fraction and implantable cardioverter defibrillator. *J. Clin. Med.* 9 (4), 1111. doi:10.3390/jcm9041111

Sabbah, H. N., Zhang, K., Gupta, R. C., Xu, J., and Singh-Gupta, V. (2020). Effects of angiotensin-neprilysin inhibition in canines with experimentally induced cardiorenal syndrome. *J. Card. Fail.* 26 (11), 987–997. doi:10.1016/j.cardfail.2020.08.009

Sainsily, X., Coquerel, D., Giguère, H., Dumont, L., Tran, K., Noll, C., et al. (2021). Elabela protects spontaneously hypertensive rats from hypertension and cardiorenal dysfunctions exacerbated by dietary high-salt intake. *Front. Pharmacol.* 12, 709467. doi:10.3389/fphar.2021.709467

Salim, S. M., Yunos, N. M., Jauri, M. H., and Kamisah, Y. (2020). Cardiotonic effects of cardiac glycosides from plants of Apocynaceae family. *Chula. Med. J.* 64 (4), 449–456. doi:10.14456/clmj.2020.58

Sansbury, B. E., Jones, S. P., Riggs, D. W., Darley-Usmar, V. M., and Hill, B. G. (2011). Bioenergetic function in cardiovascular cells: The importance of the reserve capacity and its biological regulation. *Chem. Biol. Interact.* 191 (1-3), 288–295. doi:10.1016/j.cbi.2010.12.002

Sharifi Kia, D., Benza, E., Bachman, T. N., Tushak, C., Kim, K., Simon, M. A., et al. (2020). Angiotensin receptor-neprilysin inhibition attenuates right ventricular remodeling in pulmonary hypertension. *J. Am. Heart Assoc.* 9 (13), e015708. doi:10.1161/JAHA.119.015708

Sharov, V. G., Todor, A., Khanal, S., Imai, M., and Sabbah, H. N. (2007). Cyclosporine A attenuates mitochondrial permeability transition and improves mitochondrial respiratory function in cardiomyocytes isolated from dogs with heart failure. *J. Mol. Cell. Cardiol.* 42 (1), 150–158. doi:10.1016/j.yjmcc.2006.09.013

Sharov, V. G., Todor, A. V., Silverman, N., Goldstein, S., and Sabbah, H. N. (2000). Abnormal mitochondrial respiration in failed human myocardium. *J. Mol. Cell. Cardiol.* 32 (12), 2361–2367. doi:10.1006/jmcc.2000.1266

Sheppard, C. E., and Anwar, M. (2019). The use of sacubitril/valsartan in anthracycline-induced cardiomyopathy: A mini case series. *J. Oncol. Pharm. Pract.* 25 (5), 1231–1234. doi:10.1177/1078155218783238

Singh, J., Burrell, L. M., Cherif, M., Squire, I. B., Clark, A. L., Lang, C. C., et al. (2017). Sacubitril/Valsartan: Beyond natriuretic peptides. *Heart* 103 (20), 1569–1577. doi:10.1136/heartjnl-2017-311295

Siti, H. N., Jalil, J., Asmadi, A. Y., and Kamisah, Y. (2021b). *Parkia speciosa* Hassk. Empty pod extract alleviates angiotensin II-induced cardiomyocyte hypertrophy in H9c2 cells by modulating the Ang II/ROS/NO Axis and MAPK pathway. *Front. Pharmacol.* 12, 741623. doi:10.3389/fphar.2021.741623

Siti, H. N., Jalil, J., Asmadi, A. Y., and Kamisah, Y. (2020). Roles of rutin in cardiac remodeling. *J. Funct. Foods* 64, 103606. doi:10.1016/j.jff.2019.103606

Siti, H. N., Jalil, J., Asmadi, A. Y., and Kamisah, Y. (2021a). Rutin modulates MAPK pathway differently from quercetin in angiotensin II-induced H9c2 cardiomyocyte hypertrophy. *Int. J. Mol. Sci.* 22 (10), 5063. doi:10.3390/ijms22105063

Solomon, S. D., Jhund, P. S., Claggett, B. L., Dewan, P., Køber, L., Kosiborod, M. N., et al. (2020). Effect of dapagliflozin in patients with HFrEF treated with sacubitril/valsartan: The DAPA-HF trial. *JACC. Heart Fail.* 8 (10), 811–818. doi:10.1016/j.jchf.2020.04.008

Sorrentino, A., Steinhorn, B., Troncone, L., Saravi, S., Badole, S., Eroglu, E., et al. (2019). Reversal of heart failure in a chemogenetic model of persistent cardiac redox stress. *Am. J. Physiol. Heart Circ. Physiol.* 317 (3), H617–H626. doi:10.1152/ajpheart.00177.2019

Suematsu, Y., Jing, W., Nunes, A., Kashyap, M. L., Khazaeli, M., Vaziri, N. D., et al. (2018). LCZ696 (Sacubitril/Valsartan), an angiotensin-receptor neprilysin inhibitor, attenuates cardiac hypertrophy, fibrosis, and vasculopathy in a rat model of chronic kidney disease. *J. Card. Fail.* 24 (4), 266–275. doi:10.1016/j.cardfail.2017.12.010

Sung, P. H., Chai, H. T., Yang, C. C., Chiang, J. Y., Chen, C. H., Chen, Y. L., et al. (2022). Combined levosimendan and sacubitril/valsartan markedly protected the heart and kidney against cardiorenal syndrome in rat. *Biomed. Pharmacother.* 148, 112745. doi:10.1016/j.biopha.2022.112745

Sung, Y. L., Lin, T. T., Syu, J. Y., Hsu, H. J., Lin, K. Y., Liu, Y. B., et al. (2020). Reverse electromechanical modelling of diastolic dysfunction in spontaneous hypertensive rat after sacubitril/valsartan therapy. *Esc. Heart Fail.* 7 (6), 4040–4050. doi:10.1002/ehf2.13013

Sutanto, H., Dobrev, D., and Heijman, J. (2021). Angiotensin receptor-neprilysin inhibitor (ARNI) and cardiac arrhythmias. *Int. J. Mol. Sci.* 22 (16), 8994. doi:10.3390/ijms22168994

Syamsunarno, M. R. A., Safitri, R., and Kamisah, Y. (2021). Protective effects of *Caesalpinia sappan* Linn. And its bioactive compounds on cardiovascular organs. *Front. Pharmacol.* 12, 725745. doi:10.3389/fphar.2021.725745

Tanase, D. M., Radu, S., Al Shurbaji, S., Baroi, G. L., Florida Costea, C., Turliuc, M. D., et al. (2019). Natriuretic peptides in heart failure with preserved left ventricular ejection fraction: From molecular evidences to clinical implications. *Int. J. Mol. Sci.* 20 (11), 2629. doi:10.3390/ijms20112629

Tashiro, K., Kuwano, T., Ideishi, A., Morita, H., Idemoto, Y., Goto, M., et al. (2020). Sacubitril/valsartan inhibits cardiomyocyte hypertrophy in angiotensin II-induced hypertensive mice independent of a blood pressure-lowering effect. *Cardiol. Res.* 11 (6), 376–385. doi:10.14740/cr1137

Tham, Y. K., Bernardo, B. C., Ooi, J. Y., Weeks, K. L., and McMullen, J. R. (2015). Pathophysiology of cardiac hypertrophy and heart failure: Signaling pathways and novel therapeutic targets. *Arch. Toxicol.* 89 (9), 1401–1438. doi:10.1007/s00204-015-1477-x

Torrado, J., Cain, C., Mauro, A. G., Romeo, F., Ockaili, R., Chau, V. Q., et al. (2018). Sacubitril/valsartan averts adverse post-infarction ventricular remodeling and preserves systolic function in rabbits. *J. Am. Coll. Cardiol.* 72 (19), 2342–2356. doi:10.1016/j.jacc.2018.07.102

Tsutsui, H., Momomura, S. I., Saito, Y., Ito, H., Yamamoto, K., Sakata, Y., et al. (2021). Efficacy and safety of sacubitril/valsartan in Japanese patients with chronic heart failure and reduced ejection fraction - results from the PARALLEL-HF study. *Circ. J.* 85 (5), 584–594. doi:10.1253/circj.CJ-20-0854

Valentim Gonçalves, A., Galrinho, A., Pereira-da-Silva, T., Branco, L., Rio, P., Timóteo, A. T., et al. (2020a). Myocardial work improvement after sacubitril-valsartan therapy: A new echocardiographic parameter for A new treatment. *J. Cardiovasc. Med.* 21 (3), 223–230. doi:10.2459/JCM.0000000000000932

Valentim Gonçalves, A., Pereira-da-Silva, T., Galrinho, A., Rio, P., Moura Branco, L., Soares, R., et al. (2019). Antiarrhythmic effect of sacubitril-valsartan: Cause or consequence of clinical improvement? *J. Clin. Med.* 8 (6), 869. doi:10.3390/jcm8060869

Valentim Goncalves, A., Pereira-da-Silva, T., Galrinho, A., Rio, P., Moura Branco, L., Soares, R., et al. (2020b). C-reactive protein reduction with sacubitril-valsartan treatment in heart failure patients. *Am. J. Cardiovasc. Dis.* 10 (3), 174–181.

Vilela-Martin, J. F. (2016). Spotlight on valsartan–sacubitril fixed-dose combination for heart failure: The evidence to date. *Drug Des. devel. Ther.* 10, 1627–1639. doi:10.2147/DDDT.S84782

Villani, A., Ravaro, S., Cerea, P., Caravita, S., Ciambellotti, F., Branzi, G., et al. (2020). Do the remodeling effects of sacubitril/valsartan treatment depend upon heart failure duration? *J. Cardiovasc. Med.* 21 (9), 682–687. doi:10.2459/JCM.0000000000001000

Vitale, G., Romano, G., Di Franco, A., Caccamo, G., Nugara, C., Ajello, L., et al. (2019). Early effects of sacubitril/valsartan on exercise tolerance in patients with heart failure with reduced ejection fraction. *J. Clin. Med.* 8 (2), 262. doi:10.3390/jcm8020262

Wang, H., and Fu, X. (2021). Effects of sacubitril/valsartan on ventricular remodeling in patents with left ventricular systolic dysfunction following acute anterior wall myocardial infarction. *Coron. Artery Dis.* 32 (5), 418–426. doi:10.1097/MCA.0000000000000932

Wang, L., Wang, P., Xu, S., Li, Z., Duan, D. D., Ye, J., et al. (2022). The cross-talk between PARylation and SUMOylation in C/EBPβ at K134 site participates in pathological cardiac hypertrophy. *Int. J. Biol. Sci.* 18 (2), 783–799. doi:10.7150/ijbs.65211

Wang, Y., Guo, Z., Gao, Y., Liang, P., Shan, Y., He, J., et al. (2019a). Angiotensin II receptor blocker LCZ696 attenuates cardiac remodeling through the inhibition of the ERK signaling pathway in mice with pregnancy-associated cardiomyopathy. *Cell. Biosci.* 9, 86. doi:10.1186/s13578-019-0348-1

Wang, Y., Li, H., Li, Y., Zhao, Y., Xiong, F., Liu, Y., et al. (2019b). Coriolus versicolor alleviates diabetic cardiomyopathy by inhibiting cardiac fibrosis and NLRP3 inflammasome activation. *Phytother. Res.* 33 (10), 2737–2748. doi:10.1002/ptr.6448

Wu, M., Guo, Y., Wu, Y., Xu, K., and Lin, L. (2021a). Protective effects of sacubitril/valsartan on cardiac fibrosis and function in rats with experimental myocardial infarction involves inhibition of collagen synthesis by myocardial fibroblasts through downregulating TGF-β1/smads pathway. *Front. Pharmacol.* 12, 696472. doi:10.3389/fphar.2021.696472

Wu, Q. R., Zheng, D. L., Liu, P. M., Yang, H., Li, L. A., Kuang, S. J., et al. (2021b). High glucose induces drp1-mediated mitochondrial fission via the Orai1 calcium channel to participate in diabetic cardiomyocyte hypertrophy. *Cell. Death Dis.* 12 (2), 216. doi:10.1038/s41419-021-03502-4

Xi, Q., Chen, Z., Li, T., and Wang, L. (2022). Time to switch angiotensin-converting enzyme inhibitors/angiotensin receptor blockers to sacubitril/valsartan in patients with cancer therapy-related cardiac dysfunction. *J. Int. Med. Res.* 50 (1), 3000605211067909. doi:10.1177/03000605211067909

Xia, Y., Chen, Z., Chen, A., Fu, M., Dong, Z., Hu, K., et al. (2017). LCZ696 improves cardiac function via alleviating drp1-mediated mitochondrial dysfunction in mice with doxorubicin-induced dilated cardiomyopathy. *J. Mol. Cell. Cardiol.* 108, 138–148. doi:10.1016/j.yjmcc.2017.06.003

Yahfoufi, N., Alsadi, N., Jambi, M., and Matar, C. (2018). The immunomodulatory and anti-inflammatory role of polyphenols. *Nutrients* 10 (11), 1618. doi:10.3390/nu10111618

Yandrapalli, S., Aronow, W. S., Mondal, P., and Chabbott, D. R. (2017). The evolution of natriuretic peptide augmentation in management of heart failure and the role of sacubitril/valsartan. *Arch. Med. Sci.* 13 (5), 1207–1216. doi:10.5114/aoms.2017.68813

Yang, C. C., Chen, Y. T., Chen, C. H., Li, Y. C., Shao, P. L., Huang, T. H., et al. (2019). The therapeutic impact of Entresto on protecting against cardiorenal syndrome-associated renal damage in rats on high protein diet. *Biomed. Pharmacother.* 116, 108954. doi:10.1016/j.biopha.2019.108954

Yeh, J. N., Sung, P. H., Chiang, J. Y., Sheu, J. J., Huang, C. R., Chu, Y. C., et al. (2021a). Early treatment with combination of SS31 and Entresto effectively preserved the heart function in doxorubicin-induced dilated cardiomyopathic rat. *Biomed. Pharmacother.* 141, 111886. doi:10.1016/j.biopha.2021.111886

Yeh, J. N., Yue, Y., Chu, Y. C., Huang, C. R., Yang, C. C., Chiang, J. Y., et al. (2021b). Entresto protected the cardiomyocytes and preserved heart function in cardiorenal syndrome rat fed with high-protein diet through regulating the oxidative stress and mfn2-mediated mitochondrial functional integrity. *Biomed. Pharmacother.* 144, 112244. doi:10.1016/j.biopha.2021.112244

Yenerçağ, M., Arslan, U., Dereli, S., Çoksevim, M., Doğduş, M., Kaya, A., et al. (2021). Effects of angiotensin receptor neprilysin inhibition on pulmonary arterial stiffness in heart failure with reduced ejection fraction. *Int. J. Cardiovasc. Imaging* 37 (1), 165–173. doi:10.1007/s10554-020-01973-8

Yue, Y., Meng, K., Pu, Y., and Zhang, X. (2017). Transforming growth factor beta (TGF-β) mediates cardiac fibrosis and induces diabetic cardiomyopathy. *Diabetes Res. Clin. Pract.* 133, 124–130. doi:10.1016/j.diabres.2017.08.018

Zhang, W., Elimban, V., Nijjar, M. S., Gupta, S. K., and Dhalla, N. S. (2003). Role of mitogen-activated protein kinase in cardiac hypertrophy and heart failure. *Exp. Clin. Cardiol.* 8 (4), 173–183.

Zhang, W., Liu, J., Fu, Y., Ji, H., Fang, Z., Zhou, W., et al. (2021a). Sacubitril/valsartan reduces fibrosis and alleviates high-salt diet-induced HFpEF in rats. *Front. Pharmacol.* 11, 600953. doi:10.3389/fphar.2020.600953

Zhang, Y., Wu, Y., Zhang, K., Ke, Z., Hu, P., Jin, D., et al. (2021b). Benefits of early administration of sacubitril/valsartan in patients with ST-elevation myocardial infarction after primary percutaneous coronary intervention. *Coron. Artery Dis.* 32 (5), 427–431. doi:10.1097/MCA.0000000000000955

Zhao, Y., Ma, R., Yu, X., Li, N., Zhao, X., Yu, J., et al. (2019). AHU377+Valsartan (LCZ696) modulates renin-angiotensin system (RAS) in the cardiac of female spontaneously hypertensive rats compared with valsartan. *J. Cardiovasc. Pharmacol. Ther.* 24 (5), 450–459. doi:10.1177/1074248419838503

Zhou, H., Xia, C., Yang, Y., Warusawitharana, H. K., Liu, X., Tu, Y., et al. (2022). The prevention role of theaflavin-3, 3'-digallate in angiotensin II induced pathological cardiac hypertrophy via CaN-NFAT signal pathway. *Nutrients* 14 (7), 1391. doi:10.3390/nu14071391

Zile, M. R., O'Meara, E., Claggett, B., Prescott, M. F., Solomon, S. D., Swedberg, K., et al. (2019). Effects of sacubitril/valsartan on biomarkers of extracellular matrix regulation in atients with HFrEF. *J. Am. Coll. Cardiol.* 73 (7), 795–806. doi:10.1016/j.jacc.2018.11.042

frontiers | Frontiers in Pharmacology

TYPE Review
PUBLISHED 26 August 2022
DOI 10.3389/fphar.2022.963672

OPEN ACCESS

EDITED BY
Ali H. Eid,
Qatar University, Qatar

REVIEWED BY
Leigang Jin,
The University of Hong Kong, Hong Kong SAR, China
Milena Veskovic,
University of Belgrade, Serbia
Elena Rampanelli,
Amsterdam University Medical Center, Netherlands

*CORRESPONDENCE
Jian Feng,
jerryfeng@swmu.edu.cn

†These authors have contributed equally to this work

SPECIALTY SECTION
This article was submitted to Cardiovascular and Smooth Muscle Pharmacology, a section of the journal Frontiers in Pharmacology

RECEIVED 07 June 2022
ACCEPTED 04 August 2022
PUBLISHED 26 August 2022

CITATION
Yuan S, Cai Z, Luan X, Wang H, Zhong Y, Deng L and Feng J (2022), Gut microbiota: A new therapeutic target for diabetic cardiomyopathy. *Front. Pharmacol.* 13:963672. doi: 10.3389/fphar.2022.963672

Gut microbiota: A new therapeutic target for diabetic cardiomyopathy

Suxin Yuan[1†], Zhengyao Cai[1†], Xingzhao Luan[2†], Haibo Wang[3], Yi Zhong[1], Li Deng[4] and Jian Feng[1*]

[1]Department of Cardiology, The Affiliated Hospital of Southwest Medical University, Luzhou, Sichuan, China, [2]Department of Neurosurgery, The Affiliated Hospital of Southwest Medical University, Luzhou, Sichuan, China, [3]Department of Cardiology, Gulin People's Hospital, Luzhou, Sichuan, China, [4]Department of Rheumatology, The Affiliated, Hospital of Southwest Medical University, Luzhou, Sichaun, China

Diabetic cardiomyopathy seriously affects quality of life and even threatens life safety of patients. The pathogenesis of diabetic cardiomyopathy is complex and multifactorial, and it is widely accepted that its mechanisms include oxidative stress, inflammation, insulin resistance, apoptosis, and autophagy. Some studies have shown that gut microbiota plays an important role in cardiovascular diseases. Gut microbiota and its metabolites can affect the development of diabetic cardiomyopathy by regulating oxidative stress, inflammation, insulin resistance, apoptosis, and autophagy. Here, the mechanisms of gut microbiota and its metabolites resulting in diabetic cardiomyopathy are reviewed. Gut microbiota may be a new therapeutic target for diabetic cardiomyopathy.

KEYWORDS

diabetic cardiomyopathy, gut microbiota, oxidative stress, inflammation, apoptosis, autophagy

Introduction

Diabetic cardiomyopathy (DCM) refers to the existence of abnormal myocardial structure and performance in individuals with diabetes mellitus (DM) in the absence of other cardiac risk factors such as hypertension, coronary artery disease and significant valvular disease (Jia et al., 2018a). DCM is a pathophysiological condition that is associated with DM and can lead to heart failure (Dillmann, 2019), which is initially characterized by remodeling, myocardial fibrosis, and associated diastolic dysfunction, which is followed by systolic dysfunction, and ultimately by clinical heart failure (Jia et al., 2018a). The pathophysiological factors in patients with diabetes that drive the development of cardiomyopathy include oxidative stress (Tang et al., 2019), insulin resistance, inflammation (Jia et al., 2018a), autophagy (Dewanjee et al., 2021), cell apoptosis (Zhang et al., 2016), and pyroptosis (Shi et al., 2021). Cardiovascular diseases (CVD) are the leading cause of death with DCM among diabetes mellitus regardless previous risks for coronary disease, and the CVD risk of cardiomyopathy is 2–5 times higher than in non-diabetic patients (Kannel et al., 1974). Therefore, it is highly important to find a new target for the treatment of DCM.

Gut microbiota creates a unique ecosystem. It is considered an endocrine organ (Brown and Hazen, 2015). Recent studies have demonstrated that gut microbiota plays a significant role in human health and in diseases such as CVD, atherosclerosis, hypertension, chronic kidney disease, obesity, and type 2 diabetes mellitus (Tang et al., 2017). Interestingly, recent studies have shown that the gut microbiota is closely linked to mechanisms that influence the development of DCM. In this review, the roles of gut microbiota in DCM are discussed and a theoretical basis for the gut microbiota as a new therapeutic target for DCM is provided.

Gut microbiota and its metabolites

The gut microbiota is a complex microbial community in the gut, consisting of 1,014 species of bacteria, viruses, archaea, fungi, and rotifers (Rajilić-Stojanović et al., 2012; Palm et al., 2015). Most of them belong to *Firmicutes*, *Actinobacteria*, *Bacteroidetes*, *Proteobacteria*, and *Microflora verrucose* families (Koren et al., 2012; Tremaroli and Bäckhed, 2012; Goodrich et al., 2014). Dysregulation of the gut microbiota has been linked to a variety of diseases, such as the metabolic syndrome, atherosclerosis, hypertension, heart failure, chronic kidney disease, obesity, cancer, and diabetes (Bäckhed et al., 2004; Turnbaugh et al., 2006; Jackson and Theiss, 2020). Changes in the composition of gut microbes and their corresponding products, such as lipopolysaccharide (LPS), trimethylamine N-oxide (TMAO), and lactic acid, are associated with risk of diabetes (Yuan et al., 2019). According to Luedde et al. (2017), the microbiome diversity of 20 patients with heart failure and reduced ejection fraction was lower than that of the control group, especially in those with obesity or type 2 diabetes. Reduced diversity of gut microbiota is associated with insulin resistance, dyslipidemia, and inflammatory phenotypes (Le Chatelier et al., 2013). Close attention has been paid to the relationship between cardiovascular diseases (including coronary heart disease, hypertension, and DCM) and gut microbiota in numerous studies. However, findings were inconsistent, gut microbiota has both protective and negative effects on cardiovascular disease. Some studies have shown that the presence of *Enterobacteraceae*, *Ruminococcus gnavus*, and *Eggerthella lenta* increased significantly in the atherosclerosis group compared with the control group, whereas the presence of *butyrate-tensteria nestialis* and *Faecalibacterium prausnitzii* decreased significantly (Jie et al., 2017). In heart failure patients, the level of pathogenic bacteria and *Candida* species (Pasini et al., 2016), increased, and the level of anti-inflammatory bacteria, such as *Faecalibacterium prausnitzii*, *Lact. Fermentum*, *Lactobacillus Shirota*, and *F. Prau snitzii* decreased.

Cardiac dysfunction is associated with a variety of changes in microbiota and bacterial metabolite secretion (Bastin and Andreelli, 2020). Some gut bacterial metabolites such as short-chain fatty acids (SCFAs) and trimethylamine (TMA)/TMAO (Brown and Hazen, 2015) also play an important role in cardiovascular disease. However, their role in the heart may

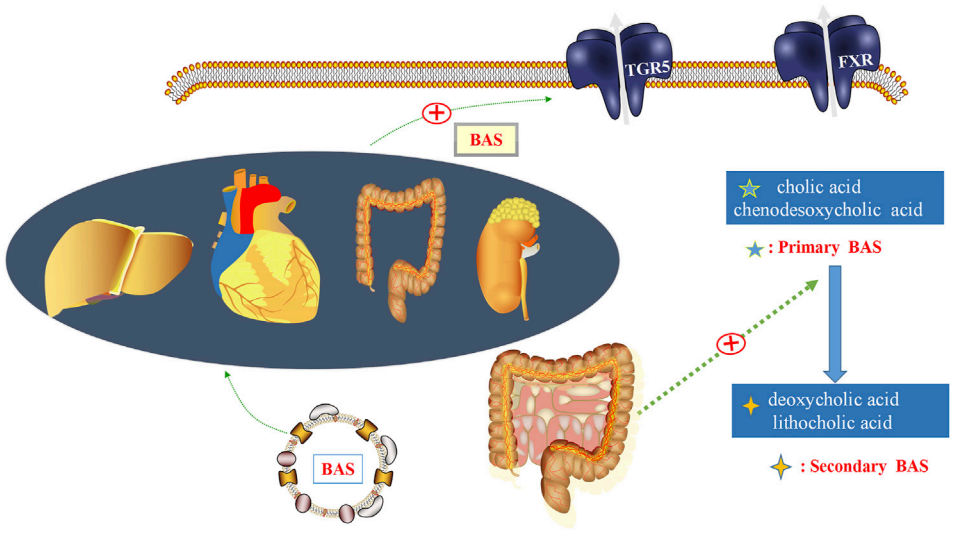

FIGURE 1
Gut microbiota and bile acids (BAs). In the gut, BAs are a detergent required for the formation of mixed micelles, dissolution, and digestion. BAs regulate metabolic homeostasis by activating BA receptors, such as G protein-coupled bile acid receptor 1 (TGR5), which are expressed in the intestinal tract, heart, liver, kidney, and other organs. Primary bile acids, such as cholic acid and chenodesoxycholic acid, could be converted into secondary BAs, including deoxycholic acid and lithocholic acid, under the regulation of gut microbiota.

be two-sided. On the one hand, TMA plays a role in increasing cardiometabolic risk and is produced from phosphatidylcholine, choline, carnitine, and food through the enzymatic action of the microbiome. TMAO, which has been shown to increase not only the cardiovascular risk, but also the risk of developing cardiac insufficiency, is formed by oxidation of TMA in the liver (Tang et al., 2019). TMAO can induce myocardial hypertrophy and fibrosis in rats with aortic contraction (Li et al., 2019). In addition, TMAO can induce inflammatory responses through SIRT3-SOD2-mtROS (sirtuin-3-superoxide dismutase 2-mitochondrial reactive oxygen species) pathway and nuclear factor κ-light-chain-enhancer of activated B cells (NF-kB) pathway (Seldin et al., 2016; Chen et al., 2017). On the other hand, SCFAs have a protective effect on the heart due to anti-inflammatory properties. This can be explained by different effects of bacteria and metabolites on the host. In case of a maladjusted gut microbiota in an organism, the microbiota may induce a series of changes such as abnormal glucose metabolism, oxidative stress, inflammatory response and apoptosis, all of which are important factors causing DCM. (The roles of these bacteria and their metabolites in oxidative stress, inflammatory response, and other mechanisms is elaborated below) (Table 1).

G protein-coupled bile acid receptor 1 (TGR5) is a bile acid (BA) specific receptor, which is part of the G protein coupled receptors family. TGR5 is highly expressed in immune cells and gut tissues, as well as in organs such as heart, liver and kidney. TGR5 can be activated by decoupled and coupled BAs (Baars et al., 2015) (Figure 1). BA is an important component of bile. Primary BAs are converted to secondary BAs by microbiota, and changes in the composition of BA pools also affect the distribution of gut microbiota (Sayin et al., 2013). Thus, gut microbiota and its metabolites can influence BA metabolism. The exact role of TGR5 in BA metabolism remains to be clarified. However, circulating BA levels were reduced in TGR5 KO mice compared with WT mice, suggesting that TGR5 plays a role in BA homeostasis (Li et al., 2011). Deng et al. (2019) have confirmed that activation of the TGR5 has a cardioprotective effect against mice myocardial cell damage induced by high glucose. Therefore, BA metabolism may play an important role in linking TGR5 closely to gut microbiota.

Oxidative stress

Oxidative stress in DCM

Oxidative stress can induce insulin resistance and β-cell dysfunction, which is a potential culprit in diabetes (Zhang et al., 2020). Oxidative stress has been implicated in the pathogenesis and progression of diabetic vascular complications, including CVD, neuropathy, nephropathy, and retinopathy (Rurali et al., 2013) etc. Studies have shown that DCM increases oxidative stress, and oxidative stress can also accelerate the DCM process (Jia et al., 2018b). In addition, sustained hyperglycemia and the signaling pathway involved in β-oxidation is impaired can lead to reactive oxygen species (ROS) overproduction by disrupting mitochondrial function, increasing mitochondrial oxygen consumption, or activating NOX (an evolutionarily conserved ROS-producing enzyme) (Jia et al., 2016; Zhang and Hu, 2020). Increased ROS levels further induce mitochondrial dysfunction and reduce the oxidative capacity of fatty acids, leading to oxidative stress and inflammation in the heart (Jia et al., 2016). Increased oxidative stress and inflammation in the heart leads to cardiac lipid accumulation, fibrosis, diastolic and systolic dysfunction, and resulting heart failure in patients with diabetes (Jia et al., 2018a).

Gut microbiota and oxidative stress

It is well known that increased ROS production can induce cardiac mitochondrial dysfunction, and ultimately lead to clinical heart failure in patients with diabetes. Thus, reducing oxidative

TABLE 1 The influence of different gut microbiota and related products associated with diabetic cardiomyopathy.

	The influence for diabetic cardiomyopathy	
	Positive	**Negative**
Gut Microbiota	Faecalibacterium prausnitzii	Enterobacteraceae
	Lact. Fermentum	Ruminococcus gnavus
	Lactobacillus Shirota	Eggerthella lenta
	Bifidobacterium (BIF)	*candida*
	Bacteroides fragilis (*B. fragilis*)	*Vibrio* proteolyticus (VPRH)
Related products associated with Gut Microbiota	Short-chain fatty acid (SCFA)	Trimethylamine (TMA)
	Bile acids (BAs)	Trimethylamine N-oxide (TMAO)
	Butyrate	Branched chain amino acids (BCAA)
	Butyric acid	Lipopolysaccharide (LPS)

TABLE 2 Summary of findings in clinical, cell and animal studies.

Mechanisms and diseases	Animal/Clinical/ Cell studies	Summary of findings	References
CVD	Clinical	the CVD risk of cardiomyopathy is 2–5 times higher than in non-diabetic patients	Kannel et al. (1974)
Heart failure	Clinical	The microbiome diversity in those with obesity or type 2 diabetes was lower	Luedde et al. (2017)
Heart failure	Clinical	the level of pathogenic bacteria and *Candida* species increased, the level of anti-inflammatory bacteria decreased	Pasini et al. (2016)
Atherosclerosis	Clinical	Enterobacteraceae, Ruminococcus gnavus, and Eggerthella lenta increased, butyrate-tensteria nestialis and Faecalibacterium prausnitzii decreased	Jie et al. (2017)
CVD	Animal	TMAO can induce myocardial hypertrophy and fibrosis in rats with aortic contraction	Li et al. (2019b)
Inflammation	Animal	TMAO can induce inflammatory responses through SIRT3-SOD2-mtROS pathway and NF-kB pathway	Chen et al. (2017)
		circulating BA levels were reduced in TGR5 KO mice, suggesting that TGR5 plays a role in BA homeostasis	Li et al. (2011)
DCM	Cell	TGR5 has a cardioprotective effect against myocardial cell damage induced by high glucose	Deng et al. (2019)
Oxidative stress	Cell	physiological levels of oxidative stress can be generated by the gut epithelial lining	Dumitrescu et al. (2018)
Autophagy	Cell	PI3K/Akt/mTOR pathway can be significantly attenuated by the exposure of cells to cell-free supernatant of Lact. Fermentum	Kumar et al. (2020)
Insulin resistance	Animal	In diet-induced obese mice, supplementation with SCFAs improved insulin resistance and reduced obesity	Perry et al. (2016)
Insulin resistance	Animal	butyric-producing bacteria reduced insulin resistance	Tolhurst et al. (2012)
Inflammation	Animal	Butyrate inhibits proinflammatory factors in gut macrophages by inhibition of histone deacetylase	Chang et al. (2014)
Inflammation	Cell	inflammation induced by TMAO can lead to endothelial dysfunction in human umbilical vein endothelial cells	Sun et al. (2016)
Inflammation	Cell	TMAO can activate the release of the inflammatory cytokines IL-18 and IL-1β	Yue et al. (2017)
Autophagy	Animal	Cardiac dysfunction and abnormalities can cause autophagy injury in diabetic hearts	Xiao et al., 2018; Wu et al., 2020
Autophagy	Animal	Autophagy damage by AMPK suppression can lead to dyslipidemia in the diabetic environment	Zhang et al. (2014)
Autophagy	Cell	BIF improved TNF-α-induced autophagy in Caco-2 cells by inhibiting p62 levels and expression of autophagy-related markers	Nie et al. (2020)
Autophagy	Cell	SCFAs can induce autophagy in hepatocytes through the UCP2	Iannucci et al. (2016)
Autophagy	Cell	sodium butyrate promoted the decrease of α-synuclein by regulating the autophagy pathway	Qiao et al. (2020)
Cell apoptosis	Cell	A long-term hyperglycemic state induces apoptosis by activating caspase apoptosis, which leads to myocardial injury and dysfunction	Wei et al. (2018)
Cell apoptosis	Animal	lncRNA MIAT can modulate myocardial cell apoptosis in DCM through miR-22-3p	Zhou et al. (2017)
Pyroptosis	Animal and Cell	Abnormal pyroptosis of cardiac fibroblasts can induce cardiac dysfunction and collagen deposition, thus aggravating the development of diabetic myocardial fibrosis	Shi et al. (2021)
Cell apoptosis	Animal and Cell	*Bacteroides fragilis* (*B. fragilis*) had a protective effect on the apoptosis of HT29 cells induced by Shiga toxin	Saito et al. (2019)
Pyroptosis	Animal and Cell	TMAO promotes the pyroptosis of vascular endothelial cells through the production of ROS, which leads to the development of atherosclerosis	Cohen et al. (2020)
Pyroptosis	Cell	sodium butyrate has an antipyroptosis effect on glomerular endothelial cells and protects them from damage caused by high glucose	Gu et al. (2019)
Oxidative stress	Cell	gut microbiota can reduce myocardial damage by alleviating oxidative stress	Finamore et al. (2018)
Insulin resistance	Animal	FMT prevented weight gain, reduced local TNF-α expression in the ileum and ascending colon, and ameliorated insulin resistance in diabetic mice	Bastos et al. (2022)
Insulin resistance	Cell	The improvement in peripheral insulin sensitivity of male metabolic syndrome recipients after receiving heterogenous gut microbiota from lean donors is attributed to an increased diversity in gut microbiota	Vrieze et al. (2012)
FMT	Clinical	a major disadvantage of FMT is that viruses are also transplanted	Chehoud et al. (2016)

Abbreviations: CVD, cardiovascular diseases; SIRT3-SOD2-mtROS, sirtuin-3-superoxide dismutase 2-mitochondrial reactive oxygen species; TMAO, trimethylamineN-oxide; NF-kB, nuclear factor κ-light-chain-enhancer of activated B cells; DCM, diabetic cardiomyopathy; TGR5, G protein-coupled bile acid receptor 1; PI3K, phosphatidylinositol 3-kinase; Akt, protein kinase B; mTOR, mammalian target of rapamycin; SCFAs, short-chain fatty acids; IL, interleukin; AMPK, AMP-activated protein kinase; BIF, Bifidobacterium; UCP2, uncoupling protein 2; MIAT, myocardial infarction associated transcript; lncRNA, long non-coding RNA; ROS, reactive oxygen species; miR, microRNA; FMT, fecal microbiota transplantation.

stress by regulating gut microbiota will be an important mean to treat DCM. The effect of gut microbiota on oxidative stress remains controversial. Recent research shows that physiological levels of oxidative stress can be generated by the gut epithelial lining (Dumitrescu et al., 2018). Gram-negative bacteria could increase lipopolysaccharide (LPS) levels (Lee and Hüttemann, 2014; Mafra et al., 2019), which could produce a large number of ROS, mainly from macrophages and infiltrating neutrophils (Sah et al., 2011). Moreover, Yang and Zhang (2021) proved that TMAO could promote oxidative stress by mediating inositol-requiring enzyme 1α (IRE1α)/X-box binding protein 1 (XBP-1) pathway. However, some researchers have suggested that the gut microbiota can mitigate oxidative stress. For example, a recent report by Kumar et al. (2020) has shown that *Lactobacillus fermentum* (*Lact. fermentum*) significantly attenuated hydrogen peroxide (H_2O_2)-induced ROS production in 3T3-L1 preadipocytes. Meanwhile, another study showed that *Lactobacillus Shirota* can protect gut cell-like epithelial cells from 2, 2′-azobis (2-amidinopropane) dihydrochloride-induced oxidative and inflammatory stress by regulating the expression of antioxidant enzymes (Finamore et al., 2018). This contradiction may be explained by differences in the richness and composition of the gut microbiota. Therefore, the most critical issue is to maintain the ecological stability of gut microbiota and improve the types of beneficial bacterias for the host in gut microbiota, which will be a major breakthrough in the treatment of DCM.

Insulin resistance

Impaired insulin metabolism and cardiac insulin resistance in DCM

Impaired insulin metabolic signaling in the heart plays a key role in the pathogenesis of DCM (Jia et al., 2018b). Cardiac insulin signaling regulates intracellular stability by regulating substrate use, protein synthesis, and cell survival (Jia et al., 2018a). In advanced DCM, the PPARγ coactivator 1α (PGC-1α)/AMP-activated protein kinase (AMPK) signaling pathway involved in β-oxidation is impaired, leading to further mitochondrial dysfunction (Jia et al., 2016). In skeletal muscle, liver, and adipose and heart tissues, glucose transport is mediated by the glucose transporter 4 (GLUT4) (Jia et al., 2016). Under normal physiological conditions, the phosphatidylinositol 3-kinase (PI3K)/protein kinase B (PKB; also called Akt) signaling pathway stimulates the translocation of GLUT4 to the membrane in cardiomyocytes, resulting in glucose uptake of cells in the heart (Jia et al., 2016). In addition, cardiac insulin receptor knockout models showed reduced cardiac glucose uptake, induced mitochondrial dysfunction, and increased cardiac ROS production. In case of dual knockout of insulin receptor substrate-1/2 (IRS-1/2), the ATP content in cardiomyocytes was reduced, cardiomyocyte contractility and function were impaired, and the incidence of fibrosis and heart failure was increased (Bugger et al., 2012; Qi et al., 2013). When the PI3K/protein kinase B (Akt)/mammalian target of rapamycin (mTOR) pathway is activated by insulin signaling, not only protein synthesis is stimulated, but autophagy is also inhibited (Figure 2), which could accelerate the DCM process (Mizushima, 2005; Meijer and Codogno, 2006).

Gut microbiota and cardiac insulin resistance

A healthy gut microbiota can decrease insulin resistance (Saad et al., 2016). It has been suggested that the response of bacterial SCFAs production levels to nutrient-lipid intake plays a key role in the gut microbiota's ability to regulate energy balance and metabolism (Kimura et al., 2013; Cani, 2014). Moreover, it was shown that an altered intestinal barrier and a dysregulated gut microbiota cause increased levels of branched chain amino acids (BCAA), secondary Bas, and LPS production, all of which can result in insulin resistance (Saad et al., 2016).

In diet-induced obese mice, supplementation with SCFAs improved insulin resistance and reduced obesity (Perry et al., 2016). In other animal studies, butyric-producing bacteria, such as *F. Prau snitzii*, induces colon L cells to secrete glucagon-like peptide 1 (GLP-1) *via* discrete sampling of the free fatty acid receptor 2(FFAR2), resulting in reduced insulin resistance (Tolhurst et al., 2012; Christiansen et al., 2018). BAs-induced activation of TGR5 promotes the release of GLP-1 by intestinal cells and indirectly affects the secretion of insulin by pancreatic β-cells, thereby affecting insulin sensitivity (Duboc et al., 2014). Therefore, TGR5 may be an important target to offset insulin resistance and reduce damage caused by diabetes.

Inflammation

It is generally accepted that an inflammatory response accelerates the development of DCM. The Nucleotide-binding oligomerization domain-like receptor pyrin domains-containing 3 (NLRP3) inflammasome, a new molecular marker of DCM, is activated by impaired insulin metabolic signaling, high FFA levels, and hyperglycemia (Pal et al., 2017). Upon NLRP3 activation, increased migration of monocytes/macrophages through the coronary endothelium occurs, resulting in an increased number of resident cardiac macrophages. When ROS is increased and bioavailable nitric oxide (NO) is reduced, monocytes/macrophages can be polarized into the proinflammatory M1 phenotype (Jia et al., 2016). In a recent study, it was shown that the anti-inflammatory response of M2 macrophages is repressed, whereas the pro-inflammatory polarization of M1 macrophages is upregulated in diabetic heart tissues (Figure 3) (Jia et al., 2015).

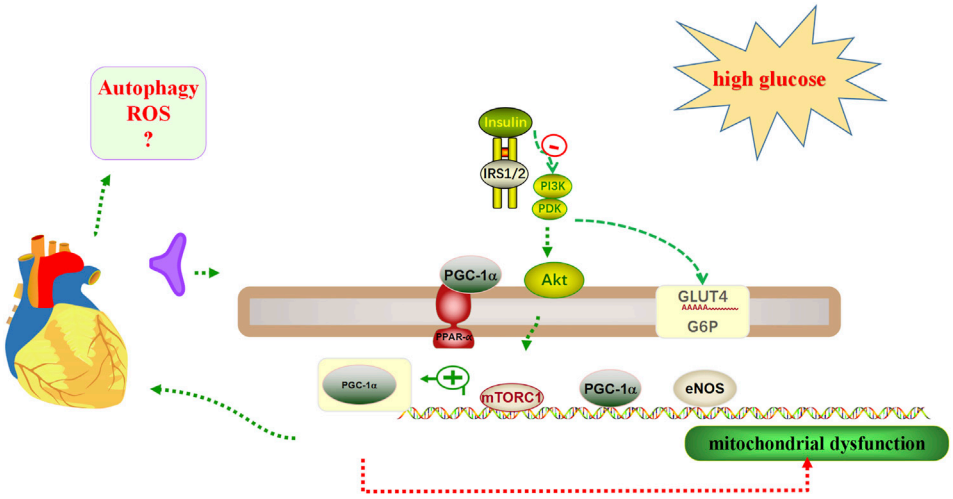

FIGURE 2
Insulin mechanisms in cardiac glucose regulation. 1) Insulin resistance may occur when cardiomyocytes are exposed to high glucose. 2) The phosphatidylinositol 3-kinase (PI3K)/protein kinase B (Akt) signaling pathway stimulates the translocation of glucose transporter type 4 (GLUT4) to the membrane, thereby resulting in glucose uptake to cells of the heart. However, in a knockout model of the cardiac insulin receptor, cardiac glucose uptake is reduced, resulting in mitochondrial dysfunction, and increased cardiac reactive oxygen species (ROS) production. 3) Mitochondrial dysfunction occurs when the PPARγ coactivator 1α (PGC-1α)/AMP-activated protein kinase (AMPK) signaling pathway is impaired. 4) The level of autophagy may be reduced when the phosphatidylinositol 3-kinase (PI3K)/protein kinase B (Akt)/mammalian target of rapamycin1 (mTORC1) pathway is activated.

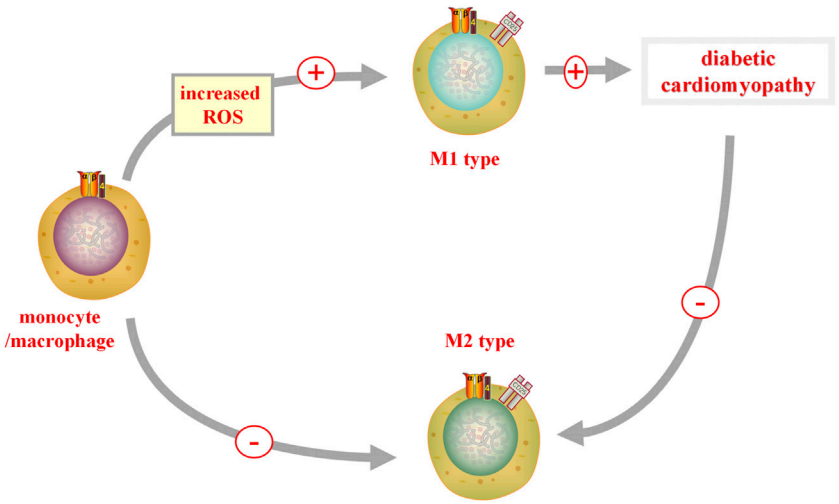

FIGURE 3
M1 and M2 in DCM. When reactive oxygen species (ROS) is increased, monocytes/macrophages can polarize into a pro-inflammatory M1 phenotype, promoting the occurrence of diabetic cardiomyopathy (DCM). In diabetic heart tissue, the pro-inflammatory polarization of M2 macrophages is inhibited, while the pro-inflammatory polarization of M1 macrophages is upregulated. M1, classically activated macrophages; M2, alternatively activate anti-inflammatory macrophages.

Recently, Bartolomaeus et al. (2019) confirmed the anti-inflammatory effects of SCFAs. SCFAs are produced by the fermentation of fibers in the colon and include three main products, namely, propionate, acetate, and butyrate (Chang et al., 2014). Butyrate inhibits proinflammatory factors in gut macrophages, including interleukin-6, interleukin-12, and NO,

by inhibition of histone deacetylase (HDAC) (Chang et al., 2014). Besides, propionate has been shown to significantly reduce cardiovascular damage by reducing the number of T-helper 17 cells and effector memory T cells (Bartolomaeus et al., 2019).

However, gut microbiota and its bacterial products not only have anti-inflammatory effects, but also pro-inflammatory effects. For example, Sun et al. (2016) suggested that inflammation induced by TMAO can lead to endothelial dysfunction in human umbilical vein endothelial cells through activation of the inflammasome ROS- thioredoxin interacting protein (TXNIP)-NLRP3. According to Yue et al. (2017), TMAO can activate the release of the inflammatory cytokines interleukin (IL)-18 and IL-1β in the NLRP3 inflammation. TMAO markedly increased inflammatory markers, such as ICAM1, IL-6, E-selectin, and cyclooxygenase-2(COX-2), through activation of the mitogen-activated protein kinase (MAPK) and NF-κB signaling pathways, which then led to vascular inflammation (Seldin et al., 2016). This contradiction may be explained by differences in composition of gut microbiota. It is generally accepted that the inflammatory response is an important pathogenic mechanism of DCM. Together, the data indicate that interfering with the composition of the gut microbiota to increase the number of anti-inflammatory bacteria may result in new ways to treat DCM.

Autophagy

Autophagy is a highly conserved catabolic process that involves the malformation of proteins, degradation of long-lived proteins, and injury of organelles through the actions of lysosomes (Li et al., 2016). Autophagy occurs in many cells of the cardiovascular system, including vascular smooth muscle cells, myocytes, macrophages, fibroblasts, and endothelial cells (Lavandero et al., 2015). In preclinical trials, autophagy disorders have been observed in diabetic hearts (Kobayashi and Liang, 2015; Jia et al., 2018a). Interestingly, autophagy has two-sided effects. Several investigators have revealed the pathogenic and protective role of autophagy in patients with DCM in type 1 and type 2 diabetes (Dewanjee et al., 2021). This contradiction may be explained by differences in the degree of autophagy. On the one hand, Autophagy is an adaptive protective response of cardiomyocytes to cellular stresses including hyperglycemia, hyperlipidemia, malnutrition, hypoxia, and redox stress (Mellor et al., 2011; Chen et al., 2020). Autophagy also could help restore plasticity in the heart (Lavandero et al., 2015). Besides, autophagy can enhance the antioxidant capacity of cells by activating the nuclear factor erythroid 2-related factor 2 (Nrf2) (Wible and Bratton, 2018). On the other hand, autophagy damage can lead to heart damage (Orogo and Gustafsson Å, 2015). Cardiac dysfunction and abnormalities can cause autophagy injury in diabetic hearts (Xiao et al., 2018; Wu et al., 2020). Autophagy damage by AMP-activated protein kinase (AMPK) suppression can lead to dyslipidemia in the diabetic environment (Zhang et al., 2014), and dyslipidemia can further inhibit cardiac autophagy by enhancing mechanistic target of rapamycin kinase (mTOR) signaling of cardiomyocytes (Glazer et al., 2009). In addition, the myocardial inflammation in diabetic heart can also occur and establish by damaging cardiac autophagy (Zhang et al., 2016). Lavandero et al. (2015) suggested that autophagy hyperactivation may be a cause of heart failure. Autophagy overactivation in the diabetic heart can lead to self-digestion and enhanced ROS production, which are potential contributors to DCM (Xu et al., 2019). Thus, both inhibition and overactivation of cardiac autophagy can have pathological effects on DCM.

Different scholars have different views on the role of gut microbiota in regulating autophagy. Nie et al. (2020) showed that *Bifidobacterium* (BIF) ameliorated tumor necrosis factor alpha (TNF-α)-induced autophagy in colorectal adenocarcinoma cell line (Caco-2) cells by inhibiting p62 levels and expression of autophagy-related markers such as microtubule-associated protein 1 light chain 3- II (LC3II) and Beclin1. Lannucci and colleagues have shown that SCFAs can induce autophagy in hepatocytes through the uncoupling protein 2 (UCP2) (Iannucci et al., 2016). Furthermore, sodium butyrate promoted the decrease of α-synuclein both by inhibiting the autophagy pathway of PI3K/Akt/mTOR and enhancing autophagy-mediated by autophagy-related gene 5 (Atg5) (Qiao et al., 2020). Thus, different bacterias in the gut microbiota have different roles in regulating autophagy.

Combining all, with the emergence of new findings, autophagy has been regarded as a crucial player in regulating DCM. It is well known that gut microbiota can regulate the degree of autophagy through PI3K/Akt/mTOR pathway (Qiao et al., 2020). In addition, PI3K/Akt/mTOR pathway plays an important role in the regulation of autophagy in DCM(Zhao et al., 2020). Therefore, the PI3K/Akt/mTOR pathway may be an important bridge between gut microbiota and DCM in autophagy. In addition, different kinds of bacterias in the gut microbiota also have different effects on autophagy, if we can adjust the gut microbiota to maintain autophagy in a favorable state for the body, it will bring benefits to patients with DCM. However, at present, there is no method to detect the autophagy state in the human heart (Dewanjee et al., 2021). Therefore, in order to find more treatments for DCM, it is very urgent for us to find a way to monitor the exact state of autophagy regulated by bacteria.

Cell apoptosis and pyroptosis

Cell apoptosis in DCM

A long-term hyperglycemic state in diabetic patients induces apoptosis by activating caspase apoptosis, which

leads to myocardial injury and dysfunction (Wei et al., 2018). It has been shown that long non-coding RNA (lncRNA) can modulate functions in DCM (Yang et al., 2018b; Pant et al., 2018). For example, Zhou et al. (2017) have shown that lncRNA myocardial infarction associated transcript (MIAT) can modulate myocardial cell apoptosis in DCM through microRNA (miR)-22-3p. Also, the modulation of the growth arrest-specific 5(Gas5)/miR-320-3p/transcription factor 3 (Tcf3) pathway in nuclear management coactivator (NMC) and nuclear receptor coactivator (NRC) apoptosis was detected. Moreover, it was demonstrated that Tcf3-activated lncRNA Gas5 modulated the apoptosis of NMC in DCM (Su et al., 2020). However, to date, there is no reported explanation for the low rate of apoptosis in patients with late-stage diabetes and severe cardiac dysfunction (Gu et al., 2018), which needs more experiments to explore it.

Pyroptosis in DCM

Pyroptosis is defined as programmed cell death associated with inflammation, and characterized by pore formation, cell swelling and destruction of the plasma membrane (Wan et al., 2020). Pyroptosis plays a role in the process of DCM (Yang et al., 2018a). Abnormal pyroptosis of cardiac fibroblasts can induce cardiac dysfunction and collagen deposition, thus aggravating the development of diabetic myocardial fibrosis (Shi et al., 2021). Shi et al. (2021) demonstrated that miR-21–3p can promote myocardial fibroblasts pyroptosis induced by high glucose (HG) *via* enhancing NLRP3 and caspase-1 expression. Recently, another data have shown that the regulation of miRs plays an important role in cell pyroptosis and fibrosis (Li et al., 2019), which bearing out Shi et al. (2021)'s research.

Gut microbiota affects the development of DCM by regulating apoptosis and pyroptosis

Apoptosis is one of the most studied type of programmed cell death. It is characterized by the formation of unique apoptotic bodies. It is common in patients with heart failure, myocardial infarction and other vascular damage (Zhou et al., 2020). According to the study of Saito et al. (2019), *Bacteroides fragilis* (*B. fragilis*) had a protective effect on the apoptosis of HT29 cells induced by Shiga toxin. However, gut microbiota also has pro-apoptotic effects. Nie et al. (2020) showed that BIF improved TNF-α-induced apoptosis of Caco-2 cells. Li and Elsasser (2005) suggested that butyric acid induced apoptosis and cell cycle arrest in renal epithelial cells.

Pyrodeath, characterized by cell swelling, the release of cytokines, and damage to subcellular organelles, is a type of pro-inflammatory cell death (Liu et al., 2019). Data have shown that TMAO promotes the pyroptosis of vascular endothelial cells through the production of ROS, which leads to the development of atherosclerosis (Cohen et al., 2020). According to the study of Cohen et al. (2020) the gram-negative bacteria *Vibrio proteolyticus* (*VPRH*) from the gut tract of borers induced pyroptosis by activating the NLRP3 inflammasome and caspase-1, resulting in the secretion of IL-1β. By contrast, another study demonstrated that sodium butyrate has an antipyroptosis effect on glomerular endothelial cells and protects them from damage caused by high glucose (Gu et al., 2019).

In summary, gut microbiota has apoptosis, anti-apoptosis, pyroptosis, and anti-pyroptosis effects in host cells. The role of bacterial metabolites of gut microbiota in apoptosis and pyroptosis is still controversial. This controversy may be explained by differences in the composition and species of gut microbiota and its metabolites.

Gut microbiota and the level of calcium ions

High glucose levels increase Ca^{2+} levels in cardiac myocytes (Cheng et al., 2019). Calcium ions are the key regulator of cardiac hypertrophy; the Ca^{2+}-calcineurin-nuclear factor of activated T cells (NFAT) cascade is the main pathway resulting in cardiac hypertrophy (Fiedler and Wollert, 2004). Gut microbiota are the primary source of SCFAs in the plasma (Vinolo et al., 2011). SCFA can regulate the contraction of airway smooth muscle by regulating calcium channels (Mizuta et al., 2020).

Gut microbiota and its metabolites can affect the development of pyroptosis, oxidative stress, inflammation, insulin resistance, and autophagy in the host through the regulation TGR5, BA metabolism, and the PI3K/Akt/mTOR, ROS- TXNIP-NLRP3, and MAPK-NF-κB pathways, among others. Therefore, gut microbiota can affect the development of DCM (Figure 4).

The therapeutic prospect of DCM

The pathogenesis of DCM is various, and it is generally believed that oxidative stress, inflammation, insulin resistance, cell apoptosis and autophagy are closely related to DCM. In recent years, a large number of scholars have found some new methods to prevent and treat DCM by targeting these mechanisms. For example, Gu et al. (2018) have experimently confirmed that inhibition of p53 could prevent DCM by preventing early-stage apoptosis. At present, gut microbiota has been applied to some clinical diseases, such as inflammatory bowel disease (IBD), obesity and some other

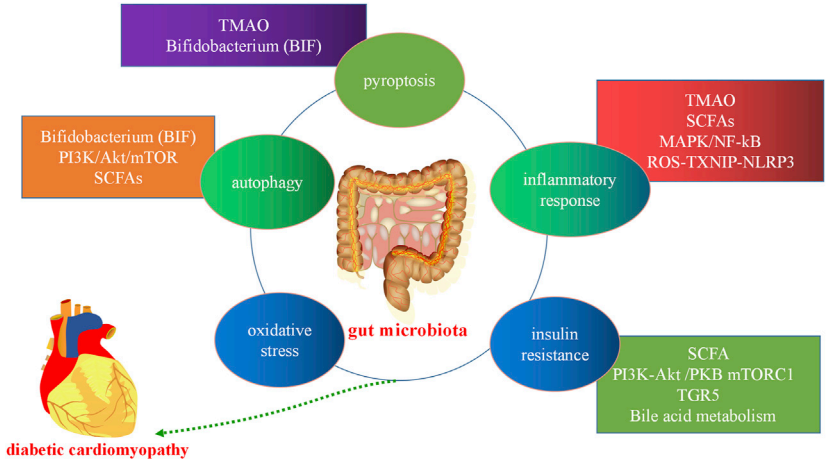

FIGURE 4
Gut microbiota in diabetic cardiomyopathy. Gut microbiota and its metabolites can affect the development of host cell autophagy, the inflammatory response, oxidative stress, apoptosis, pyroptosis, and insulin resistance through the short-chain fatty acids (SCFAs) metabolic pathway, bile acid (BA) metabolism, and the trimethylamine N-oxide (TMAO) metabolic, mitogen-activated protein kinase (MAPK), and PI3K/Akt/mTOR pathways, among others. PI3K:phosphatidylinositol 3-kinase; Akt, protein kinase B, mTORC: mammalian target of rapamycin.

metabolic diseases (Patterson et al., 2016). The widespread use of probiotics in clinical practice is a good proof. Interestingly, numerous studies have found that the gut microbiota is associated with the pathogenesis of DCM. However, up to now, the role of gut microbiota in DCM is still controversial. Some scholars believe that gut microbiota can reduce myocardial damage in patients with DM by alleviating oxidative stress (Finamore et al., 2018), while others think that gut microbiota can also increase the harmful risk to DCM *via* increasing inflammatory response and insulin resistance (Sun et al., 2016). The contradiction of the two-sided effects of the gut microbiota can mainly be explained by the difference of the bacterial species present in the gut microbiota. It might be possible to reduce oxidative stress, inflammation response, insulin resistance and maintain appropriate levels of autophagy by intervening with the composition of the gut microbiota to increase the species richness of the bacterias which are beneficial for the host in gut microbiota, thereby reducing diabetic myocardial injury. However, it is very difficult for us to intervene with the composition of gut microbiota due to the limited technology available. If we can solve this thorny problem, it will bring a major breakthrough in the treatment of DCM in the future.

Fortunately, there are possibly three ways to modify the composition of the gut microbiota to treat DCM. First, dietary interventions are a good therapeutic option. Experimental studies have shown that dietary modifications for 5 days (short term) can change the number of bacteria in and species of gut microbiota (David et al., 2014). Second, probiotics may be used for the clinical treatment of DCM in the future. Probiotic bacteria mainly derive from the genera *Bifidobacterium* and *Lactobacillus*. Probiotics supplementation has been found to restore the gut microbiota after it had been disrupted. Besides, probiotics supplementation induces changes in the composition of undisrupted gut microbiota. Recent evidence suggests that probiotics affect BA metabolism by altering the microbiota (Baars et al., 2015). Therefore, the probiotics may reduce myocardial injury in DCM by affecting BA metabolism, thereby activating TGR5 expression. Third, fecal microbiota transplantation (FMT) may be a future treatment. FMT is a treatment for patients with gut microecological imbalance. Bacteria or metabolites are introduced from donor feces to the diseased recipient (Cammarota et al., 2014). Bastos et al. (2022) showed that FMT is a safe treatment, they found that FMT prevented weight gain, reduced local TNF-α expression in the ileum and ascending colon, and ameliorated insulin resistance in diabetic mice. The improvement in peripheral insulin sensitivity of male metabolic syndrome recipients after receiving heterogenous gut microbiota from lean donors is attributed to an increased diversity in gut microbiota, including those associated with butyrate production (Vrieze et al., 2012). FMT alone is not sufficient to control glycemic levels effectively. Thus, the regulation of gut microbiota should be combined with other established classical therapies, which can obtain better metabolic parameters (Vallianou et al., 2019; Zhang and Hu, 2020). However, the effectiveness of FMT is challenged by several factors, such as delivery route, number of transplants, fecal volume per sample, disease burden, and target impact (Napolitano and Covasa, 2020). Therefore, FMT is highly difficult to implement and its possibility of success is low. Besides, a major disadvantage of FMT is that viruses are also transplanted (Chehoud et al., 2016) (Table 2). The problem of the

balance between the advantages and disadvantages of FMT treatment is still unsolved. In the future, there will be more treatments for DCM by regulating the gut microbiota.

Conclusion

DCM has a serious impact on people's quality of life, and even threatens lives of patients. Therefore, it is very important to find new therapeutic targets to treat DCM. The pathogenesis of DCM is complex and diverse. It is generally accepted that the mechanisms include oxidative stress, inflammation, insulin resistance, and cell apoptosis. In recent years, it has been suggested that the development of DCM is closely related to autophagy and cell pyroptosis.

The gut microbiota has become topic of interest in research. Some studies have shown that gut microbiota plays an important role in cardiovascular disease. However, the role of gut microbiota in DCM may be two-sided. On the one side, some bacteria can reduce myocardial damage by reducing the inflammatory response, while others can aggravate myocardial damage by increasing the oxidative stress response. This contradiction can mainly be explained by the difference in the composition of gut microbiota in patients. Therefore, finding an effective way to intervene with the composition of gut microbiota and regulate the metabolism of gut microbes will be a major breakthrough in the clinical treatment of DCM.

Author contributions

SY, ZC, XL, and JF created the contents of this review article. XL, HW, and YZ conducted the initial search of studies and prepared the figures. SY drafted the manuscript. LD and JF revised the manuscript. All authors read and approved the final manuscript.

Funding

This research was funded by the Key Laboratory of Medical Electrophysiology (KeyME-KeyME-2020-004), the Collaborative Innovation Center for Prevention and Treatment of Cardiovascular Disease of Sichuan Province (xtcx2019-13), the Luzhou Municipal People's Government - Southwest Medical University Science and Technology Strategic Cooperation (2021LZXNYD-J33), and the Southwest Medical University, Teaching reform project of Southwest Medical University (2020XSJG-C01-19).

Acknowledgments

We thank International Science Editing (http://www.internationalscienceediting.com) for editing this manuscript.

Conflict of interest

The authors declare that the research was conducted in the absence of any commercial or financial relationships that could be construed as a potential conflict of interest.

Publisher's note

References

Baars, A., Oosting, A., Knol, J., Garssen, J., and Van Bergenhenegouwen, J. (2015). The gut microbiota as a therapeutic target in IBD and metabolic disease: A role for the bile acid receptors FXR and TGR5. *Microorganisms* 3, 641–666. doi:10.3390/microorganisms3040641

Bäckhed, F., Ding, H., Wang, T., Hooper, L. V., Koh, G. Y., Nagy, A., et al. (2004). The gut microbiota as an environmental factor that regulates fat storage. *Proc. Natl. Acad. Sci. U. S. A.* 101, 15718–15723. doi:10.1073/pnas.0407076101

Bartolomaeus, H., Balogh, A., Yakoub, M., Homann, S., Markó, L., Höges, S., et al. (2019). Short-chain fatty acid propionate protects from hypertensive cardiovascular damage. *Circulation* 139, 1407–1421. doi:10.1161/circulationaha.118.036652

Bastin, M., and Andreelli, F. (2020). The gut microbiota and diabetic cardiomyopathy in humans. *Diabetes Metab.* 46, 197–202. doi:10.1016/j.diabet.2019.10.003

Bastos, R. M. C., Simplício-Filho, A., Sávio-Silva, C., Oliveira, L. F. V., Cruz, G. N. F., Sousa, E. H., et al. (2022). Fecal microbiota transplant in a pre-clinical model of type 2 diabetes mellitus, obesity and diabetic kidney disease. *Int. J. Mol. Sci.* 23, 3842. doi:10.3390/ijms23073842

Brown, J. M., and Hazen, S. L. (2015). The gut microbial endocrine organ: bacterially derived signals driving cardiometabolic diseases. *Annu. Rev. Med.* 66, 343–359. doi:10.1146/annurev-med-060513-093205

Bugger, H., Riehle, C., Jaishy, B., Wende, A. R., Tuinei, J., Chen, D., et al. (2012). Genetic loss of insulin receptors worsens cardiac efficiency in diabetes. *J. Mol. Cell. Cardiol.* 52, 1019–1026. doi:10.1016/j.yjmcc.2012.02.001

Cammarota, G., Ianiro, G., and Gasbarrini, A. (2014). Fecal microbiota transplantation for the treatment of *Clostridium difficile* infection: a systematic review. *J. Clin. Gastroenterol.* 48, 693–702. doi:10.1097/mcg.0000000000000046

Cani, P. D. (2014). Metabolism in 2013: The gut microbiota manages host metabolism. *Nat. Rev. Endocrinol.* 10, 74–76. doi:10.1038/nrendo.2013.240

Chang, P. V., Hao, L., Offermanns, S., and Medzhitov, R. (2014). The microbial metabolite butyrate regulates intestinal macrophage function via histone deacetylase inhibition. *Proc. Natl. Acad. Sci. U. S. A.* 111, 2247–2252. doi:10.1073/pnas.1322269111

Chehoud, C., Dryga, A., Hwang, Y., Nagy-Szakal, D., Hollister, E. B., Luna, R. A., et al. (2016). Transfer of viral communities between human individuals during fecal microbiota transplantation. *mBio* 7, e00322. doi:10.1128/mBio.00322-16

Chen, M. L., Zhu, X. H., Ran, L., Lang, H. D., Yi, L., and Mi, M. T. (2017). Trimethylamine-N-Oxide induces vascular inflammation by activating the NLRP3 inflammasome through the SIRT3-SOD2-mtROS signaling pathway. *J. Am. Heart Assoc.* 6, e006347. doi:10.1161/jaha.117.006347

Chen, Y., Hua, Y., Li, X., Arslan, I. M., Zhang, W., and Meng, G. (2020). Distinct types of cell death and the implication in diabetic cardiomyopathy. *Front. Pharmacol.* 11, 42. doi:10.3389/fphar.2020.00042

Cheng, K. C., Chang, W. T., Kuo, F. Y., Chen, Z. C., Li, Y., and Cheng, J. T. (2019). TGR5 activation ameliorates hyperglycemia-induced cardiac hypertrophy in H9c2 cells. *Sci. Rep.* 9, 3633. doi:10.1038/s41598-019-40002-0

Christiansen, C. B., Gabe, M. B. N., Svendsen, B., Dragsted, L. O., Rosenkilde, M. M., and Holst, J. J. (2018). The impact of short-chain fatty acids on GLP-1 and PYY secretion from the isolated perfused rat colon. *Am. J. Physiol. Gastrointest. Liver Physiol.* 315, G53–g65. doi:10.1152/ajpgi.00346.2017

Cohen, H., Baram, N., Edry-Botzer, L., Munitz, A., Salomon, D., and Gerlic, M. (2020). Vibrio pore-forming leukocidin activates pyroptotic cell death via the NLRP3 inflammasome. *Emerg. Microbes Infect.* 9, 278–290. doi:10.1080/22221751.2020.1720526

David, L. A., Maurice, C. F., Carmody, R. N., Gootenberg, D. B., Button, J. E., Wolfe, B. E., et al. (2014). Diet rapidly and reproducibly alters the human gut microbiome. *Nature* 505, 559–563. doi:10.1038/nature12820

Deng, L., Chen, X., Zhong, Y., Wen, X., Cai, Y., Li, J., et al. (2019). Activation of TGR5 partially alleviates high glucose-induced cardiomyocyte injury by inhibition of inflammatory responses and oxidative stress. *Oxid. Med. Cell. Longev.* 2019, 6372786. doi:10.1155/2019/6372786

Dewanjee, S., Vallamkondu, J., Kalra, R. S., John, A., Reddy, P. H., and Kandimalla, R. (2021). Autophagy in the diabetic heart: A potential pharmacotherapeutic target in diabetic cardiomyopathy. *Ageing Res. Rev.* 68, 101338. doi:10.1016/j.arr.2021.101338

Dillmann, W. H. (2019). Diabetic cardiomyopathy. *Circ. Res.* 124, 1160–1162. doi:10.1161/circresaha.118.314665

Duboc, H., Taché, Y., and Hofmann, A. F. (2014). The bile acid TGR5 membrane receptor: from basic research to clinical application. *Dig. Liver Dis.* 46, 302–312. doi:10.1016/j.dld.2013.10.021

Dumitrescu, L., Popescu-Olaru, I., Cozma, L., Tulbă, D., Hinescu, M. E., Ceafalan, L. C., et al. (2018). Oxidative stress and the microbiota-gut-brain Axis. *Oxid. Med. Cell. Longev.* 2018, 2406594. doi:10.1155/2018/2406594

Fiedler, B., and Wollert, K. C. (2004). Interference of antihypertrophic molecules and signaling pathways with the Ca2+-calcineurin-NFAT cascade in cardiac myocytes. *Cardiovasc. Res.* 63, 450–457. doi:10.1016/j.cardiores.2004.04.002

Finamore, A., Ambra, R., Nobili, F., Garaguso, I., Raguzzini, A., and Serafini, M. (2018). Redox role of Lactobacillus casei Shirota against the cellular damage induced by 2, 2'-azobis (2-amidinopropane) dihydrochloride-induced oxidative and inflammatory stress in enterocytes-like epithelial cells. *Front. Immunol.* 9, 1131. doi:10.3389/fimmu.2018.01131

Glazer, H. P., Osipov, R. M., Clements, R. T., Sellke, F. W., and Bianchi, C. (2009). Hypercholesterolemia is associated with hyperactive cardiac mTORC1 and mTORC2 signaling. *Cell Cycle* 8, 1738–1746. doi:10.4161/cc.8.11.8619

Goodrich, J. K., Waters, J. L., Poole, A. C., Sutter, J. L., Koren, O., Blekhman, R., et al. (2014). Human genetics shape the gut microbiome. *Cell* 159, 789–799. doi:10.1016/j.cell.2014.09.053

Gu, J., Huang, W., Zhang, W., Zhao, T., Gao, C., Gan, W., et al. (2019). Sodium butyrate alleviates high-glucose-induced renal glomerular endothelial cells damage via inhibiting pyroptosis. *Int. Immunopharmacol.* 75, 105832. doi:10.1016/j.intimp.2019.105832

Gu, J., Wang, S., Guo, H., Tan, Y., Liang, Y., Feng, A., et al. (2018). Inhibition of p53 prevents diabetic cardiomyopathy by preventing early-stage apoptosis and cell senescence, reduced glycolysis, and impaired angiogenesis. *Cell Death Dis.* 9, 82. doi:10.1038/s41419-017-0093-5

Iannucci, L. F., Sun, J., Singh, B. K., Zhou, J., Kaddai, V. A., Lanni, A., et al. (2016). Short chain fatty acids induce UCP2-mediated autophagy in hepatic cells. *Biochem. Biophys. Res. Commun.* 480, 461–467. doi:10.1016/j.bbrc.2016.10.072

Jackson, D. N., and Theiss, A. L. (2020). Gut bacteria signaling to mitochondria in intestinal inflammation and cancer. *Gut Microbes* 11, 285–304. doi:10.1080/19490976.2019.1592421

Jia, G., Demarco, V. G., and Sowers, J. R. (2016). Insulin resistance and hyperinsulinaemia in diabetic cardiomyopathy. *Nat. Rev. Endocrinol.* 12, 144–153. doi:10.1038/nrendo.2015.216

Jia, G., Habibi, J., Demarco, V. G., Martinez-Lemus, L. A., Ma, L., Whaley-Connell, A. T., et al. (2015). Endothelial mineralocorticoid receptor deletion prevents diet-induced cardiac diastolic dysfunction in females. *Hypertension* 66, 1159–1167. doi:10.1161/hypertensionaha.115.06015

Jia, G., Hill, M. A., and Sowers, J. R. (2018a). Diabetic cardiomyopathy: An update of mechanisms contributing to this clinical entity. *Circ. Res.* 122, 624–638. doi:10.1161/circresaha.117.311586

Jia, G., Whaley-Connell, A., and Sowers, J. R. (2018b). Diabetic cardiomyopathy: a hyperglycaemia- and insulin-resistance-induced heart disease. *Diabetologia* 61, 21–28. doi:10.1007/s00125-017-4390-4

Jie, Z., Xia, H., Zhong, S. L., Feng, Q., Li, S., Liang, S., et al. (2017). The gut microbiome in atherosclerotic cardiovascular disease. *Nat. Commun.* 8, 845. doi:10.1038/s41467-017-00900-1

Kannel, W. B., Hjortland, M., and Castelli, W. P. (1974). Role of diabetes in congestive heart failure: the framingham study. *Am. J. Cardiol.* 34, 29–34. doi:10.1016/0002-9149(74)90089-7

Kimura, I., Ozawa, K., Inoue, D., Imamura, T., Kimura, K., Maeda, T., et al. (2013). The gut microbiota suppresses insulin-mediated fat accumulation via the short-chain fatty acid receptor GPR43. *Nat. Commun.* 4, 1829. doi:10.1038/ncomms2852

Kobayashi, S., and Liang, Q. (2015). Autophagy and mitophagy in diabetic cardiomyopathy. *Biochim. Biophys. Acta* 1852, 252–261. doi:10.1016/j.bbadis.2014.05.020

Koren, O., Goodrich, J. K., Cullender, T. C., Spor, A., Laitinen, K., Bäckhed, H. K., et al. (2012). Host remodeling of the gut microbiome and metabolic changes during pregnancy. *Cell* 150, 470–480. doi:10.1016/j.cell.2012.07.008

Kumar, R., Sharma, A., Gupta, M., Padwad, Y., and Sharma, R. (2020). Cell-free culture supernatant of probiotic Lactobacillus fermentum protects against H(2)O(2)-induced premature senescence by suppressing ROS-akt-mTOR Axis in murine preadipocytes. *Probiotics Antimicrob. Proteins* 12, 563–576. doi:10.1007/s12602-019-09576-z

Lavandero, S., Chiong, M., Rothermel, B. A., and Hill, J. A. (2015). Autophagy in cardiovascular biology. *J. Clin. Invest.* 125, 55–64. doi:10.1172/jci73943

Le Chatelier, E., Nielsen, T., Qin, J., Prifti, E., Hildebrand, F., Falony, G., et al. (2013). Richness of human gut microbiome correlates with metabolic markers. *Nature* 500, 541–546. doi:10.1038/nature12506

Lee, I., and Hüttemann, M. (2014). Energy crisis: the role of oxidative phosphorylation in acute inflammation and sepsis. *Biochim. Biophys. Acta* 1842, 1579–1586. doi:10.1016/j.bbadis.2014.05.031

Li, C. J., and Elsasser, T. H. (2005). Butyrate-induced apoptosis and cell cycle arrest in bovine kidney epithelial cells: involvement of caspase and proteasome pathways. *J. Anim. Sci.* 83, 89–97. doi:10.2527/2005.83189x

Li, J., Xue, J., Wang, D., Dai, X., Sun, Q., Xiao, T., et al. (2019a). Regulation of gasdermin D by miR-379-5p is involved in arsenite-induced activation of hepatic stellate cells and in fibrosis via secretion of IL-1β from human hepatic cells. *Metallomics.* 11, 483–495. doi:10.1039/c8mt00321a

Li, L., Xu, J., He, L., Peng, L., Zhong, Q., Chen, L., et al. (2016). The role of autophagy in cardiac hypertrophy. *Acta Biochim. Biophys. Sin.* 48, 491–500. doi:10.1093/abbs/gmw025

Li, T., Holmstrom, S. R., Kir, S., Umetani, M., Schmidt, D. R., Kliewer, S. A., et al. (2011). The G protein-coupled bile acid receptor, TGR5, stimulates gallbladder filling. *Mol. Endocrinol.* 25, 1066–1071. doi:10.1210/me.2010-0460

Li, Z., Wu, Z., Yan, J., Liu, H., Liu, Q., Deng, Y., et al. (2019b). Gut microbe-derived metabolite trimethylamine N-oxide induces cardiac hypertrophy and fibrosis. *Lab. Invest.* 99, 346–357. doi:10.1038/s41374-018-0091-y

Liu, J., Wang, Y., Meng, H., Yu, J., Lu, H., Li, W., et al. (2019). Butyrate rather than LPS subverts gingival epithelial homeostasis by downregulation of intercellular junctions and triggering pyroptosis. *J. Clin. Periodontol.* 46, 894–907. doi:10.1111/jcpe.13162

Luedde, M., Winkler, T., Heinsen, F. A., Rühlemann, M. C., Spehlmann, M. E., Bajrovic, A., et al. (2017). Heart failure is associated with depletion of core intestinal microbiota. *ESC Heart Fail.* 4, 282–290. doi:10.1002/ehf2.12155

Mafra, D., Borges, N. A., Lindholm, B., and Stenvinkel, P. (2019). Mitochondrial dysfunction and gut microbiota imbalance: An intriguing relationship in chronic kidney disease. *Mitochondrion* 47, 206–209. doi:10.1016/j.mito.2018.11.006

Meijer, A. J., and Codogno, P. (2006). Signalling and autophagy regulation in health, aging and disease. *Mol. Asp. Med.* 27, 411–425. doi:10.1016/j.mam.2006.08.002

Mellor, K. M., Bell, J. R., Young, M. J., Ritchie, R. H., and Delbridge, L. M. (2011). Myocardial autophagy activation and suppressed survival signaling is associated with insulin resistance in fructose-fed mice. *J. Mol. Cell. Cardiol.* 50, 1035–1043. doi:10.1016/j.yjmcc.2011.03.002

Mizushima, N. (2005). The pleiotropic role of autophagy: from protein metabolism to bactericide. *Cell Death Differ.* 12, 1535–1541. doi:10.1038/sj.cdd.4401728

Mizuta, K., Sasaki, H., Zhang, Y., Matoba, A., Emala, C. W., and Sr, . (2020). The short-chain free fatty acid receptor FFAR3 is expressed and potentiates contraction in human airway smooth muscle. *Am. J. Physiol. Lung Cell. Mol. Physiol.* 318, L1248–l1260. doi:10.1152/ajplung.00357.2019

Napolitano, M., and Covasa, M. (2020). Microbiota transplant in the treatment of obesity and diabetes: Current and future perspectives. *Front. Microbiol.* 11, 590370. doi:10.3389/fmicb.2020.590370

Nie, N., Bai, C., Song, S., Zhang, Y., Wang, B., and Li, Z. (2020). Bifidobacterium plays a protective role in TNF-α-induced inflammatory response in Caco-2 cell through NF-κB and p38MAPK pathways. *Mol. Cell. Biochem.* 464, 83–91. doi:10.1007/s11010-019-03651-3

Orogo, A. M., and Gustafsson Å, B. (2015). Therapeutic targeting of autophagy: potential and concerns in treating cardiovascular disease. *Circ. Res.* 116, 489–503. doi:10.1161/circresaha.116.303791

Pal, P. B., Sonowal, H., Shukla, K., Srivastava, S. K., and Ramana, K. V. (2017). Aldose reductase mediates NLRP3 inflammasome-initiated innate immune response in hyperglycemia-induced Thp1 monocytes and male mice. *Endocrinology* 158, 3661–3675. doi:10.1210/en.2017-00294

Palm, N. W., De Zoete, M. R., and Flavell, R. A. (2015). Immune-microbiota interactions in health and disease. *Clin. Immunol.* 159, 122–127. doi:10.1016/j.clim.2015.05.014

Pant, T., Dhanasekaran, A., Fang, J., Bai, X., Bosnjak, Z. J., Liang, M., et al. (2018). Current status and strategies of long noncoding RNA research for diabetic cardiomyopathy. *BMC Cardiovasc. Disord.* 18, 197. doi:10.1186/s12872-018-0939-5

Pasini, E., Aquilani, R., Testa, C., Baiardi, P., Angioletti, S., Boschi, F., et al. (2016). Pathogenic gut flora in patients with chronic heart failure. *JACC. Heart Fail.* 4, 220–227. doi:10.1016/j.jchf.2015.10.009

Patterson, E., Ryan, P. M., Cryan, J. F., Dinan, T. G., Ross, R. P., Fitzgerald, G. F., et al. (2016). Gut microbiota, obesity and diabetes. *Postgrad. Med. J.* 92, 286–300. doi:10.1136/postgradmedj-2015-133285

Perry, R. J., Peng, L., Barry, N. A., Cline, G. W., Zhang, D., Cardone, R. L., et al. (2016). Acetate mediates a microbiome-brain-β-cell axis to promote metabolic syndrome. *Nature* 534, 213–217. doi:10.1038/nature18309

Qi, Y., Xu, Z., Zhu, Q., Thomas, C., Kumar, R., Feng, H., et al. (2013). Myocardial loss of IRS1 and IRS2 causes heart failure and is controlled by p38α MAPK during insulin resistance. *Diabetes* 62, 3887–3900. doi:10.2337/db13-0095

Qiao, C. M., Sun, M. F., Jia, X. B., Shi, Y., Zhang, B. P., Zhou, Z. L., et al. (2020). Sodium butyrate causes α-synuclein degradation by an Atg5-dependent and PI3K/Akt/mTOR-related autophagy pathway. *Exp. Cell Res.* 387, 111772. doi:10.1016/j.yexcr.2019.111772

Rajilić-Stojanović, M., Heilig, H. G., Tims, S., Zoetendal, E. G., and De Vos, W. M. (2012). Long-term monitoring of the human intestinal microbiota composition. *Environ. Microbiol.* 15, 1146–1159. doi:10.1111/1462-2920.12023

Rurali, E., Noris, M., Chianca, A., Donadelli, R., Banterla, F., Galbusera, M., et al. (2013). ADAMTS13 predicts renal and cardiovascular events in type 2 diabetic patients and response to therapy. *Diabetes* 62, 3599–3609. doi:10.2337/db13-0530

Saad, M. J., Santos, A., and Prada, P. O. (2016). Linking gut microbiota and inflammation to obesity and insulin resistance. *Physiol. (Bethesda)* 31, 283–293. doi:10.1152/physiol.00041.2015

Sah, S. P., Tirkey, N., Kuhad, A., and Chopra, K. (2011). Effect of quercetin on lipopolysaccharide induced-sickness behavior and oxidative stress in rats. *Indian J. Pharmacol.* 43, 192–196. doi:10.4103/0253-7613.77365

Saito, K., Suzuki, R., Koyanagi, Y., Isogai, H., Yoneyama, H., and Isogai, E. (2019). Inhibition of enterohemorrhagic *Escherichia coli* O157:H7 infection in a gnotobiotic mouse model with pre-colonization by Bacteroides strains. *Biomed. Rep.* 10, 175–182. doi:10.3892/br.2019.1193

Sayin, S. I., Wahlström, A., Felin, J., Jäntti, S., Marschall, H. U., Bamberg, K., et al. (2013). Gut microbiota regulates bile acid metabolism by reducing the levels of tauro-beta-muricholic acid, a naturally occurring FXR antagonist. *Cell Metab.* 17, 225–235. doi:10.1016/j.cmet.2013.01.003

Seldin, M. M., Meng, Y., Qi, H., Zhu, W., Wang, Z., Hazen, S. L., et al. (2016). Trimethylamine N-oxide promotes vascular inflammation through signaling of mitogen-activated protein kinase and nuclear factor-κb. *J. Am. Heart Assoc.* 5, e002767. doi:10.1161/jaha.115.002767

Shi, P., Zhao, X. D., Shi, K. H., Ding, X. S., and Tao, H. (2021). MiR-21-3p triggers cardiac fibroblasts pyroptosis in diabetic cardiac fibrosis via inhibiting androgen receptor. *Exp. Cell Res.* 399, 112464. doi:10.1016/j.yexcr.2020.112464

Su, D., Ju, Y., Han, W., Yang, Y., Wang, F., Wang, T., et al. (2020). Tcf3-activated lncRNA Gas5 regulates newborn mouse cardiomyocyte apoptosis in diabetic cardiomyopathy. *J. Cell. Biochem.* 121, 4337–4346. doi:10.1002/jcb.29630

Sun, X., Jiao, X., Ma, Y., Liu, Y., Zhang, L., He, Y., et al. (2016). Trimethylamine N-oxide induces inflammation and endothelial dysfunction in human umbilical vein endothelial cells via activating ROS-TXNIP-NLRP3 inflammasome. *Biochem. Biophys. Res. Commun.* 481, 63–70. doi:10.1016/j.bbrc.2016.11.017

Tang, S.-G., Liu, X.-Y., Wang, S.-P., Wang, H.-H., Jovanović, A., and Tan, W. (2019a). Trimetazidine prevents diabetic cardiomyopathy by inhibiting Nox2/TRPC3-induced oxidative stress. *J. Pharmacol. Sci.* 139, 311–318. doi:10.1016/j.jphs.2019.01.016

Tang, W. H., Kitai, T., and Hazen, S. L. (2017). Gut microbiota in cardiovascular health and disease. *Circ. Res.* 120, 1183–1196. doi:10.1161/circresaha.117.309715

Tang, W. H. W., Li, D. Y., and Hazen, S. L. (2019b). Dietary metabolism, the gut microbiome, and heart failure. *Nat. Rev. Cardiol.* 16, 137–154. doi:10.1038/s41569-018-0108-7

Tolhurst, G., Heffron, H., Lam, Y. S., Parker, H. E., Habib, A. M., Diakogiannaki, E., et al. (2012). Short-chain fatty acids stimulate glucagon-like peptide-1 secretion via the G-protein-coupled receptor FFAR2. *Diabetes* 61, 364–371. doi:10.2337/db11-1019

Tremaroli, V., and Bäckhed, F. (2012). Functional interactions between the gut microbiota and host metabolism. *Nature* 489, 242–249. doi:10.1038/nature11552

Turnbaugh, P. J., Ley, R. E., Mahowald, M. A., Magrini, V., Mardis, E. R., and Gordon, J. I. (2006). An obesity-associated gut microbiome with increased capacity for energy harvest. *Nature* 444, 1027–1031. doi:10.1038/nature05414

Vallianou, N. G., Stratigou, T., and Tsagarakis, S. (2019). Metformin and gut microbiota: their interactions and their impact on diabetes. *Horm. (Athens)* 18, 141–144. doi:10.1007/s42000-019-00093-w

Vinolo, M. A., Rodrigues, H. G., Nachbar, R. T., and Curi, R. (2011). Regulation of inflammation by short chain fatty acids. *Nutrients* 3, 858–876. doi:10.3390/nu3100858

Vrieze, A., Van Nood, E., Holleman, F., Salojärvi, J., Kootte, R. S., Bartelsman, J. F., et al. (2012). Transfer of intestinal microbiota from lean donors increases insulin sensitivity in individuals with metabolic syndrome. *Gastroenterology* 143, 913–916. doi:10.1053/j.gastro.2012.06.031

Wan, P., Su, W., Zhang, Y., Li, Z., Deng, C., Li, J., et al. (2020). LncRNA H19 initiates microglial pyroptosis and neuronal death in retinal ischemia/reperfusion injury. *Cell Death Differ.* 27, 176–191. doi:10.1038/s41418-019-0351-4

Wei, X., Yang, Y., Jiang, Y. J., Lei, J. M., Guo, J. W., and Xiao, H. (2018). Relaxin ameliorates high glucose-induced cardiomyocyte hypertrophy and apoptosis via the Notch1 pathway. *Exp. Ther. Med.* 15, 691–698. doi:10.3892/etm.2017.5448

Wible, D. J., and Bratton, S. B. (2018). Reciprocity in ROS and autophagic signaling. *Curr. Opin. Toxicol.* 7, 28–36. doi:10.1016/j.cotox.2017.10.006

Wu, Q. Q., Liu, C., Cai, Z., Xie, Q., Hu, T., Duan, M., et al. (2020). High-mobility group AT-hook 1 promotes cardiac dysfunction in diabetic cardiomyopathy via autophagy inhibition. *Cell Death Dis.* 11, 160. doi:10.1038/s41419-020-2316-4

Xiao, Y., Wu, Q. Q., Duan, M. X., Liu, C., Yuan, Y., Yang, Z., et al. (2018). TAX1BP1 overexpression attenuates cardiac dysfunction and remodeling in STZ-induced diabetic cardiomyopathy in mice by regulating autophagy. *Biochim. Biophys. Acta. Mol. Basis Dis.* 1864, 1728–1743. doi:10.1016/j.bbadis.2018.02.012

Xu, T., Ding, W., Ji, X., Ao, X., Liu, Y., Yu, W., et al. (2019). Oxidative stress in cell death and cardiovascular diseases. *Oxid. Med. Cell. Longev.* 2019, 9030563. doi:10.1155/2019/9030563

Yang, F., Qin, Y., Lv, J., Wang, Y., Che, H., Chen, X., et al. (2018a). Silencing long non-coding RNA Kcnq1ot1 alleviates pyroptosis and fibrosis in diabetic cardiomyopathy. *Cell Death Dis.* 9, 1000. doi:10.1038/s41419-018-1029-4

Yang, F., Qin, Y., Wang, Y., Li, A., Lv, J., Sun, X., et al. (2018b). LncRNA KCNQ1OT1 mediates pyroptosis in diabetic cardiomyopathy. *Cell. Physiol. Biochem.* 50, 1230–1244. doi:10.1159/000494576

Yang, G., and Zhang, X. (2021). TMAO promotes apoptosis and oxidative stress of pancreatic acinar cells by mediating IRE1α-XBP-1 pathway. *Saudi J. Gastroenterol.* 27, 361–369. doi:10.4103/sjg.sjg_12_21

Yuan, T., Yang, T., Chen, H., Fu, D., Hu, Y., Wang, J., et al. (2019). New insights into oxidative stress and inflammation during diabetes mellitus-accelerated atherosclerosis. *Redox Biol.* 20, 247–260. doi:10.1016/j.redox.2018.09.025

Yue, C., Yang, X., Li, J., Chen, X., Zhao, X., Chen, Y., et al. (2017). Trimethylamine N-oxide prime NLRP3 inflammasome via inhibiting ATG16L1-induced autophagy

in colonic epithelial cells. *Biochem. Biophys. Res. Commun.* 490, 541–551. doi:10.1016/j.bbrc.2017.06.075

Zhang, J., Cheng, Y., Gu, J., Wang, S., Zhou, S., Wang, Y., et al. (2016). Fenofibrate increases cardiac autophagy via FGF21/SIRT1 and prevents fibrosis and inflammation in the hearts of Type 1 diabetic mice. *Clin. Sci.* 130, 625–641. doi:10.1042/cs20150623

Zhang, L., Ding, W. Y., Wang, Z. H., Tang, M. X., Wang, F., Li, Y., et al. (2016). Early administration of trimetazidine attenuates diabetic cardiomyopathy in rats by alleviating fibrosis, reducing apoptosis and enhancing autophagy. *J. Transl. Med.* 14, 109. doi:10.1186/s12967-016-0849-1

Zhang, P., Li, T., Wu, X., Nice, E. C., Huang, C., and Zhang, Y. (2020). Oxidative stress and diabetes: antioxidative strategies. *Front. Med.* 14, 583–600. doi:10.1007/s11684-019-0729-1

Zhang, Q., and Hu, N. (2020). Effects of metformin on the gut microbiota in obesity and type 2 diabetes mellitus. *Diabetes Metab. Syndr. Obes.* 13, 5003–5014. doi:10.2147/dmso.S286430

Zhang, Z., Wang, S., Zhou, S., Yan, X., Wang, Y., Chen, J., et al. (2014). Sulforaphane prevents the development of cardiomyopathy in type 2 diabetic mice probably by reversing oxidative stress-induced inhibition of LKB1/AMPK pathway. *J. Mol. Cell. Cardiol.* 77, 42–52. doi:10.1016/j.yjmcc.2014.09.022

Zhao, G., Zhang, X., Wang, H., and Chen, Z. (2020). Beta carotene protects H9c2 cardiomyocytes from advanced glycation end product-induced endoplasmic reticulum stress, apoptosis, and autophagy via the PI3K/Akt/mTOR signaling pathway. *Ann. Transl. Med.* 8, 647. doi:10.21037/atm-20-3768

Zhou, W., Cheng, Y., Zhu, P., Nasser, M. I., Zhang, X., and Zhao, M. (2020). Implication of gut microbiota in cardiovascular diseases. *Oxid. Med. Cell. Longev.* 2020, 5394096. doi:10.1155/2020/5394096

Zhou, X., Zhang, W., Jin, M., Chen, J., Xu, W., and Kong, X. (2017). lncRNA MIAT functions as a competing endogenous RNA to upregulate DAPK2 by sponging miR-22-3p in diabetic cardiomyopathy. *Cell Death Dis.* 8, e2929. doi:10.1038/cddis.2017.321

frontiers | Frontiers in Pharmacology

TYPE Review
PUBLISHED 07 September 2022
DOI 10.3389/fphar.2022.953845

OPEN ACCESS

EDITED BY
Ahmed F. El-Yazbi,
Alexandria University, Egypt

REVIEWED BY
Haneen S. Dwaib,
American University of Beirut, Lebanon
Serena Del Turco,
National Research Council (CNR), Italy

*CORRESPONDENCE
Cong Xue,
xuecongme1@126.com
Jian-Jun Li,
lijianjun938@126.com

SPECIALTY SECTION
This article was submitted to Cardiovascular and Smooth Muscle Pharmacology, a section of the journal Frontiers in Pharmacology

RECEIVED 26 May 2022
ACCEPTED 08 August 2022
PUBLISHED 07 September 2022

CITATION
Jia F, Fei S-F, Tong D-B, Xue C and Li J-J (2022), Sex difference in circulating PCSK9 and its clinical implications. *Front. Pharmacol.* 13:953845. doi: 10.3389/fphar.2022.953845

Sex difference in circulating PCSK9 and its clinical implications

Fang Jia[1], Si-Fan Fei[1], De-Bing Tong[1], Cong Xue[1]* and Jian-Jun Li[2]*

[1]Department of Cardiology, The Third Affiliated Hospital of Soochow University, Changzhou, China, [2]Cardio-Metabolic Center, Fu Wai Hospital, Chinese Academy of Medical Sciences, Peking Union Medical College, Beijing, China

Proprotein convertase subtilisin kexin type 9 (PCSK9) is a proprotein convertase that increases plasma low-density lipoprotein cholesterol (LDL-C) levels by triggering the degradation of LDL receptors (LDLRs). Beyond the regulation of circulating LDL-C, PCSK9 also has direct atherosclerotic effects on the vascular wall and is associated with coronary plaque inflammation. Interestingly, emerging data show that women have higher circulating PCSK9 concentrations than men, suggesting that the potential roles of PCSK9 may have different impacts according to sex. In this review, we summarize the studies concerning sex difference in circulating levels of PCSK9. In addition, we report on the sex differences in the relations of elevated circulating PCSK9 levels to the severity and prognosis of coronary artery disease, the incidence of type 2 diabetes mellitus, and neurological damage after cardiac arrest and liver injury, as well as inflammatory biomarkers and high-density lipoprotein cholesterol (HDL-C). Moreover, sex difference in the clinical efficacy of PCSK9 inhibitors application are reviewed. Finally, the underlying mechanisms of sex difference in circulating PCSK9 concentrations and the clinical implications are also discussed.

KEYWORDS

proprotein convertase subtilisin kexin type 9, sex difference, estrogen, coronary artery disease, PCSK9 inhibitor

Introduction

Major differences exist between men and women in the epidemiology, pathophysiology, and outcomes of cardiovascular diseases (CVDs) (Group et al., 2016). Significant variations in the prevention, clinical manifestations and treatment effects of CVDs according to sex persist worldwide, despite improvements in diagnostic and therapeutic interventions. Compared to men, women with acute coronary syndrome (ACS) are more likely to present with a range of atypical symptoms, including dyspnea, fatigue, and dizziness or weakness, instead of the classic symptoms of chest pain (An et al., 2019). In addition, women are characterized by a higher burden of cardiometabolic risk factors (Gerdts and Regitz-Zagrosek, 2019), a higher prevalence of nonobstructive coronary artery disease (CAD) on angiography (Bairey Merz et al., 2006; DeFilippis

et al., 2020), and a higher prevalence of coronary microvascular dysfunction compared to men (Waheed et al., 2020). The nonspecific chest pain and nonobstructive CAD often observed in women do not confer a lower risk for recurrent acute myocardial infarction (AMI) and mortality, and the prognosis in these women is not benign (Robinson et al., 2008; Kenkre et al., 2017). Moreover, women with established atherosclerotic cardiovascular disease (ASCVD) are less likely to use specific guideline-directed medications for secondary prevention than men (Xia et al., 2020). Several studies have demonstrated less favorable outcomes in women with ACS than in men and worse all-cause mortality following primary percutaneous coronary intervention (PCI) after ST-elevation myocardial infarction (STEMI) (Pagidipati and Peterson, 2016; Rathod et al., 2021).

Sex differences in CVD are due to differences in gene expression and the regulation of sex hormones that lead to differences in various cardiovascular functions, for example, in nitric oxide (NO) signaling, myocardial remodeling under stress, glucose regulation and lipid metabolism (Group et al., 2016). Preclinical evidence on sex differences and pathophysiological clarification may contribute to the development of sex-specific therapeutic strategies. Deciphering sex-specific differences in biomarkers may improve our understanding of the associated biological mechanisms. The circulating level of proprotein convertase subtilisin kexin type 9 (PCSK9), which is associated with the severity and outcomes of patients with CAD, has been described as a new risk marker of CAD (Bae et al., 2018; Panahi et al., 2019; Peng et al., 2020; Kajingulu et al., 2022). An animal model evaluating the sex-specific distribution of low-density lipoprotein receptors (LDLRs) shows that the absence of PCSK9 results in a sex- and tissue-specific subcellular distribution of LDLRs, suggesting that PCSK9 and estrogen may act as molecular regulators of cholesterol homeostasis, and PCSK9 inhibitors may have different effects in women than in men (Roubtsova et al., 2015). The range of circulating PCSK9 concentrations is broad and differs between sexes. The current review focuses on sex difference in circulating PCSK9 levels and the potential mechanisms and clinical implications for these observed sex-based differences.

Methods

This systematic review examined sex difference in circulating PCSK9 levels and the underlying mechanisms and clinical implications of these sex differences. The selected studies included cross-sectional, case-control and prospective studies. There were no language or time restrictions for eligible studies. The PubMed electronic database was used. The following search terms were used: “proprotein convertase subtilisin kexin type 9” OR “PCSK9” AND “sex difference” AND “estrogen” OR “estradiol” AND “coronary artery diseases” OR “type 2 diabetes mellitus” OR “neurological damage after cardiac arrest” OR “liver injury” OR “inflammatory biomarkers” OR “HDL-C” OR “PCSK9 inhibitor”.

Sex difference in circulating PCSK9 concentrations

Increasing evidence shows that PCSK9 is a well-known therapeutic target in the prevention and treatment of atherosclerosis. PCSK9 is an important enzyme in cholesterol metabolism that regulates serum low-density lipoprotein cholesterol (LDL-C) levels through the degradation of LDLRs. PCSK9 inhibitors could lead to significant LDL-C reductions in high-risk patients, and they have shown a favorable safety profile in recent clinical trials (Robinson et al., 2015; Sabatine et al., 2017). Beyond the regulation of circulating LDL-C levels, PCSK9 also has direct atherogenic effects on the vascular wall and is associated with coronary plaque inflammation (Gencer et al., 2016; Tang et al., 2017; Liu and Frostegard, 2018). PCSK9 can interfere with the underlying molecular mechanisms in atherosclerosis, from endothelial dysfunction to smooth muscle cell migration and the activation of inflammatory pathways (Ding et al., 2015; Ferri et al., 2016; Liu et al., 2020). All these findings consistently indicate that PCSK9 plays a significant role in every step of the development and progression of coronary plaque.

Although the potential role of PCSK9 still remains to be elucidated, many studies in humans have shown that there is a significant sex difference in circulating levels of PCSK9. PCSK9 levels have been measured in many studies, which have shown a broad range of concentrations. The PCSK9 level was significantly higher in women than in men (331 ± 105 ng/ml vs. 290 ± 109 ng/ml) in the IMPROVE cohort study, a large-scale multicenter study encompassing several European countries with the centralized measurement of PCSK9 (Ferri et al., 2020). The effect of sex on PCSK9 concentrations was also observed in a population-based prospective study conducted among 4,205 Chinese participants with prediabetes (average age 56.1 ± 7.5 years), as circulating PCSK9 levels were higher in females than in males (289.62 ± 98.80 ng/ml vs. 277.50 ± 97.57 ng/ml, $p < 0.001$) (Shi et al., 2020). Although the clinical implications of elevated circulating PCSK9 levels are still unclear in AMI patients, circulating PCSK9 are higher in women than in men not only for all admitted AMI patients, but also for patients with STEMI (Zhang et al., 2019). Many studies concerning PCSK9 levels have been conducted in elderly people with high ASCVD risk or established ASCVD; however, it is notable that sex difference in circulating levels of PCSK9 also exists in young people (Levenson et al., 2017). Levenson’s study showed that PCSK9 levels in young men were lower than those in young women, which was consistent with findings in elderly individuals. As listed in Table 1, these studies have demonstrated

TABLE 1 Demographic features and PCSK9 levels in the observational studies comparing circulating PCSK9 levels between women and men.

Author, year	Study design	Number of participants (women vs. men)	Location	Age (y)	PCSK9 levels (women vs. men)	Hr (95%CI)
Ferri et al. (2020)	Prospective	1929 vs. 1774	Five European countries: Finland, Sweden, the Netherlands, France, and Italy	54 to 79	331 ± 105 vs. 290 ± 109 ng/ml	$p < 0.0001$
Shi et al. (2020)	Prospective	2,817 vs. 1,388	China	56.1 ± 7.5	289.62 ± 98.80 ng/ml vs. 277.50 ± 97.57 ng/ml	$p < 0.001$
Zhang et al. (2019)	Prospective	61 vs. 220	China	Males: 58.53 ± 12.83; Females: 68.64 ± 8.97	325.1 (247.5–445.3) vs. 273.6 (215.6–366.8) ng/ml	$p = 0.0136$
Levenson et al. (2017)	Cross-sectional analysis	167 vs. 119	United States	15 to 26	—	$p = 0.03$
Simeone et al. (2021)	Observational	67 vs. 99	Italy	68	308 (251–394) vs. 267 (231–340) ng/ml	$p = 0.005$
Jeenduang. (2019)	Cross-sectional analysis	284 vs. 152	Thailand	52.50 ± 13.56	87.38 ± 26.49 vs. 79.15 ± 25.51 ng/ml	$p = 0.002$

similar findings that PCSK9 levels are higher in women than in men.

Potential mechanisms

Circulating PCSK9 appears to be produced mainly by the liver, and its expression is regulated by numerous factors, such as the diurnal rhythm (Persson et al., 2010), insulin (Levenson et al., 2017), resistin (Macchi et al., 2020), thyroid hormone (Yildirim et al., 2021), diet (Krysa et al., 2017), exercise (Sponder et al., 2017), and various cholesterol-lowering drugs (Sahebkar et al., 2015). It seems that sex could modify the effects of extrinsic and intrinsic factors on the PCSK9 concentration. Even though a wealth of data exists regarding sex differences in CVD and their underlying risk factors, a comprehensive understanding is still lacking. Genetic mechanisms, based on the differences in sex chromosomes, sex hormones and their receptors, are speculated to play a major role. The effect of estrogens on lipid homeostasis and circulating levels of PCSK9 has received increasing attention. Postmenopausal women have higher PCSK9 concentrations than premenopausal women, which may be related to the decrease in estrogen during menopause (Ghosh et al., 2015). In men, no correlation has been found between serum testosterone and plasma PCSK9 levels, and testosterone replacement therapy does not have an effect on plasma PCSK9 levels (Ooi et al., 2015). In Ghosh M's study, females over 50 years of age (330 ng/ml) had higher PCSK9 levels than those below 50 years of age (276 ng/ml; $p < 0.05$), whereas the two groups of male participants had similar PCSK9 levels (279 vs. 270 ng/ml; $p > 0.05$) (Ghosh et al., 2015).

The regulating effects of estrogen on PCSK9 expression noted in recent studies are as follows: 1) PCSK9 levels increase in women after menopause, along with the sharp reduction in estrogen that occurs during this time period; however, PCSK9 levels do not increase in men during this time period (Ghosh et al., 2015). 2) PCSK9 levels change throughout the menstrual cycle, and an inverse relation exists between PCSK9 and estradiol in premenopausal women. The estradiol level is the highest at ovulation, while the PCSK9 level, on average, is 235 ng/ml in this phase, which is lower than that in the luteal and follicular phases (Ghosh et al., 2015). 3) The inverse relationship between PCSK9 and estradiol is also found in women preparing for *in vitro* fertilization. *In vitro* fertilization involves 2 treatment phases: Extreme suppression and strong stimulation of the endogenous estrogen levels. A comparison of PCSK9 levels in these two phases shows that PCSK9 levels are significantly reduced by 14% after the stimulation of estrogen synthesis, which indicates that high levels of endogenous estrogens reduce circulating PCSK9 levels (Persson et al., 2012).

A deep understanding of the mechanisms by which PCSK9 is regulated by estrogen could be beneficial for clarifying the sex difference in PCSK9 concentrations and its effects on atherosclerotic disease progression and cardiovascular outcomes. Estrogen is speculated to affect PCSK9 expression and function through a transcriptional and posttranscriptional mechanism (Figure 1). At the transcriptional level, estradiol and phytoestrogens suppress PCSK9 proximal promoter activities in human L02 hepatocytes through an estrogen receptor α (ERα)-mediated pathway (Jing et al., 2019). G-protein estrogen receptor (GPER), a well-recognized receptor activated by estrogens, has been increasingly found to mediate the physiological effects of estrogen. GPER activation can decrease PCSK9 mRNA and protein levels in human hepatic cell lines, thus suggesting its influence on the expression of PCSK9 (Hussain et al., 2015). *In vitro* studies have also found that estrogens could affect the PCSK9 functional state through a posttranscriptional mechanism. One of the possible mechanisms for the

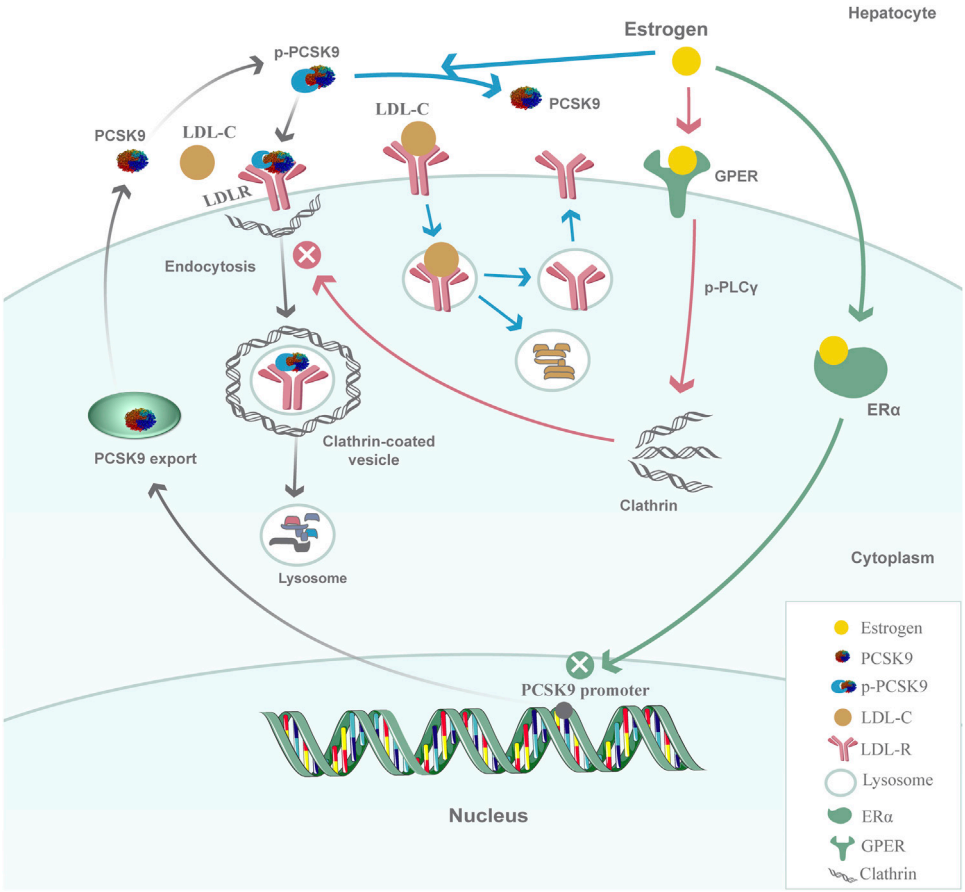

FIGURE 1
Model for the regulation of PCSK9 by estrogen in hepatic cells. At the transcriptional level, estrogen inhibits PCSK9 proximal promoter activities and decreases PCSK9 mRNA expression through the ERα-mediated pathway; at the posttranscriptional level, the activation of GPER in the membrane by estrogen rapidly initiates the phosphorylation of PLCγ and then alters clathrin distribution or influences the clathrin trafficking pathway to affect the internalization of the PCSK9-LDLR complex. Another possible mechanism is that estrogen could affect the PCSK9-LDLR interaction by inhibiting the phosphorylation of PCSK9 to protect LDLRs from degradation.

posttranscriptional inhibiting effect is that estradiol could block PCSK9 internalization in hepatic cells. The activation of GPER in the membrane by estradiol rapidly initiates the phosphorylation of phospholipase C-γ (PLC-γ), which in turn alters clathrin distribution or influences the clathrin trafficking pathway to affect the internalization of the PCSK9-LDLR complex in HepG2 cells (Fu et al., 2019). The other mechanism is that estradiol causes a functional switch in the PCSK9-LDLR interaction through phosphorylation. Starr's results showed a dynamic role of PCSK9 under estradiol conditioning at the protein level because estradiol treatment of HuH7 cells resulted in decreased phosphorylation of secreted PCSK9, which was associated with the protection of LDLRs (Starr et al., 2015). Taken together, these findings show that the regulation of estrogen and its receptors on PCSK9 inhibits PCSK9 function by suppressing PCSK9 proximal promoter activities, impairing PCSK9-LDLR complex internalization, and dephosphorylating secreted PCSK9 in hepatic cells, preventing it from escorting LDLRs to lysosomes for degradation. The upregulation of LDLRs by estradiol, at least in part, is likely to occur through PCSK9 downregulation, which in turn would lead to decreased circulating levels of LDL-C. Investigations into other possible mechanisms for the regulation of PCSK9 under the action of estrogen would be of great interest.

Clinical implications of sex difference in circulating PCSK9

Although men and women differ in many aspects, including genetic mechanisms and epigenetic mechanisms, estrogen is a recognized regulator that is significantly associated with the

discrepancy in circulating PCSK9 levels between men and women. The relations between elevated circulating PCSK9 levels and clinical conditions such as the severity and prognosis of CAD, the incidence of type 2 diabetes mellitus (T2DM), neurological damage after cardiac arrest, liver injury as well as inflammatory biomarkers and HDL-C are complex; moreover, the clinical implications of sex difference in PCSK9 levels need to be clarified.

Severity and prognosis of coronary artery disease

It is clear that PCSK9 contributes to every step of the molecular pathway of atherosclerosis. Recent studies have revealed that PCSK9 has various effects on the progression of atherosclerosis, including inflammation, foam cell formation, endothelial cell apoptosis, smooth muscle cell phenotypic switching, and platelet activation (Yurtseven et al., 2020; Puteri et al., 2022). Many clinical studies have tested the relation between circulating levels of PCSK9 and the presence and severity of CAD. The prevalence of coronary atherosclerotic lesions and the Gensini score increased as the circulating PCSK9 levels increased in patients with familial hypercholesterolemia (Cao et al., 2018a). In patients with CAD, circulating PCSK9 levels were found to be positively associated with severity scores (SYNTAX, Gensini, and Jeopardy) (Li et al., 2015a; Li et al., 2015b). In addition, PCSK9 levels were positively associated with the severity of coronary artery lesions independent of LDL-C concentrations in patients hospitalized for ACS (Cariou et al., 2017). However, a cross-sectional study in China explored associations of circulating PCSK9 levels and lipid parameters (LDL-C, non-HDL-C, apolipoprotein B, lipoprotein (a), etc.) with coronary artery lesion severity in non-lipid-lowering-drug-treated patients undergoing their first coronary angiography, and a positive association with the Gensini score was found in men but not in women (Li et al., 2017). A larger sample may be needed to confirm the lack of an association between PCSK9 levels and coronary artery lesion severity in women, as many CAD studies have included mostly men. Furthermore, the Gensini score has always been used as a surrogate marker of coronary artery lesion severity; however, it might not be fully representative of the anatomical and morphological features of severe coronary lesions.

Invasive and pathological evidence has suggested sex-specific differences in the pattern of compositional plaque progression: Men are more likely to have plaque rupture and occlusion that is associated with sudden onset symptoms than women, and women can present with plaque rupture as well as plaque erosion and an indolent course of anginal symptoms (Yahagi et al., 2015; Chandrasekhar and Mehran, 2016). Women suffer from higher rates of coronary microvascular dysfunction, possibly because they are particularly predisposed to mental stress and neuroendocrine dysfunction (Safdar et al., 2018). A positive association between circulating PCSK9 levels and the fraction of plaque consisting of necrotic core tissue (an index of plaque vulnerability) was documented by intravascular ultrasound (IVUS) in patients with stable CAD or ACS (Cheng et al., 2016). In addition, PCSK9 was demonstrated to be associated with aggravated microvascular obstruction. PCSK9 was found to aggravate microvascular obstruction and promote myocardial infarction (MI) expansion post-MI in MI mouse models, and a PCSK9 inhibitor weakened the enhanced platelet aggregation and ameliorated microvascular obstruction (Qi et al., 2021). The association between elevated circulating PCSK9 levels and coronary plaque morphology and coronary microvascular dysfunction may affect sex differences in the composition, progression and clinical presentation of coronary plaque.

In addition to the associations between PCSK9 levels and coronary artery lesion severity in women, knowledge of the relation of PCSK9 to CAD outcomes may also require further, more specific exploration. Although sex differences in CAD outcomes are not consistent among all reports, many studies have shown that female patients do not have more favorable outcomes than male patients; moreover, several studies have demonstrated an even worse prognosis in female patients than male patients. Women with stable angina and nonobstructive CAD were found to be 3 times more likely to experience a cardiac event within the first year of cardiac catheterization than men (Sedlak et al., 2013). Compared to men, women have a higher risk of death and adverse outcomes after primary PCI for STEMI (Kosmidou et al., 2017). A meta-analysis of the prognosis of young women compared with that of men demonstrated that young women with ACS may have a variety of nontraditional risk factors, and the in-hospital, short-term and long-term mortality rates of these female patients were higher than those of male patients (Ma et al., 2017).

The circulating PCSK9 level is independently predictive of major adverse cardiovascular events (MACEs) in patients with stable CAD (Li et al., 2015b). PCSK9 was shown to be independently associated with an increased number of ischemic MACEs in ACS patients undergoing PCI at the 1-year follow-up: The hazard ratio for upper vs. lower PCSK9-level tertiles was 2.62 ($p = 0.01$) (Navarese et al., 2017). A prospective, observational cohort study of 1,225 untreated patients with stable CAD showed that the group with high PCSK9 levels (≥234.52 ng/ml) had a significantly higher risk of MACEs than the group with low PCSK9 levels (<234.52 ng/ml) during a median of 3.3 years of follow-up, while patients in the group with high PCSK9 levels were more likely to be female (Peng et al., 2020). The same results were observed in another prospective study including 504 consecutive patients with stable CAD, the majority of whom were receiving statin treatment (Werner et al., 2014). Patients with higher PCSK9 levels had more primary adverse events, which included cardiovascular death and unplanned cardiovascular hospitalization, and women accounted for a

higher proportion of these patients. An investigation of serum PCSK9 levels in patients undergoing PCI also demonstrated that a higher serum PCSK9 level was independently associated with a higher rate of MACEs and all-cause death compared with a lower serum PCSK9 level, and the proportion of women was higher in the group with high PCSK9 levels (Choi et al., 2020). The sex differences in the outcomes of CAD may at least be partially related to the sex difference in circulating PCSK9 levels, which is related to specific coronary plaque features and coronary microvascular dysfunction. Therefore, a better understanding of the sex differences in the pathogenesis of coronary atherosclerosis and the role of PCSK9 could lead to the selection of appropriate preventive measures to improve both the quality of life and clinical outcomes in women.

Incidence of T2DM

The findings from the available clinical study on PCSK9 and T2DM suggest a trend toward a positive association between circulating PCSK9 levels and the incidence of T2DM in renal transplant recipients (Eisenga et al., 2017). Moreover, insulin and glycemic parameters of diabetes mellitus (DM), such as the homeostasis model assessment of insulin resistance (HOMA-IR) and glycated hemoglobin (HbA1c) level, are positively correlated with the circulating PCSK9 concentration (Peng et al., 2020; Hamamura et al., 2021). Nevertheless, these findings are not consistent among all reports (Ramin-Mangata et al., 2020). A population-based prospective study in China showed that the positive association between circulating PCSK9 levels and the risk of incident T2DM was found only in female participants with prediabetes; conversely, no significant association was observed among male prediabetic participants, which revealed the sex discrepancy in the relation between elevated circulating PCSK9 levels and the incidence of T2DM (Shi et al., 2020).

We suggest that gonadal hormones may be an important confounding factor for the relationship between circulating PCSK9 levels and the incidence of T2DM. Circulating PCSK9 levels change in women depending on their reproductive stage of life, and serum estrogen is inversely correlated with circulating PCSK9 levels, while in men, serum testosterone is not correlated with circulating PCSK9 levels (Ooi et al., 2015; Mauvais-Jarvis, 2018). In women, an early menopausal age (before the age of 45 years) is associated with an increased risk of diabetes compared to an older menopausal age (Shen et al., 2017), and the rapid and severe estrogen deficiency following surgical ovariectomy is also accompanied by an increased diabetes risk (Pandeya et al., 2018). The mechanisms for facilitating glucose homeostasis in women before menopause could be, at least in part, due to the beneficial effect of a physiological window of circulating estrogens. Sex hormones play a role in these sex differences in glucose homeostasis, prediabetic syndromes and diabetes and might affect the relation between circulating PCSK9 levels and the incidence of T2DM.

Neurological damage after cardiac arrest

Cardiac arrest causes significant morbidity and mortality, and women have been found to have worse outcomes despite improvements in prehospital and hospital care. Women were associated with a lower likelihood of good neurological outcomes at discharge and the 6-month follow-up in a multinational retrospective registry of patients who suffered out-of-hospital cardiac arrest (Vogelsong et al., 2021). However, data from the Cardiac Arrest Registry to Enhance Survival (CARES) indicate that men have lower rates of favorable neurological survival than women (Kotini-Shah et al., 2021). Several large Asian studies have found no sex differences in the rates of neurological survival between men and women (Ng et al., 2016; Goto et al., 2019). The reasons for these differences are complex and involve the pathophysiological features of the disease and its comorbidities, resuscitative care protocols, and the response to treatment (Jarman et al., 2019).

An extensive investigation of PCSK9 revealed its novel potential functions, including the regulation of neuronal development, apoptosis and differentiation, but the precise role of PCSK9 in brain physiology remained unclear (Mannarino et al., 2018). Moreover, high circulating PCSK9 levels were associated with unfavorable neurological function after resuscitation from out-of-hospital cardiac arrest (Merrelaar et al., 2020). The increase in PCSK9 levels was most likely caused by the inflammatory response and organ dysfunction after cardiopulmonary resuscitation (CPR). The favorable neurological outcomes in patients with low circulating PCSK9 levels may be attributed to a more rapid detoxification of bacterial lipids via higher LDL-R expression and a reduced inflammatory response. However, the sample size of the study was limited, and only 61 men and 18 women were enrolled. Thus, analyses in larger populations are needed to verify the role of PCSK9 in neurological outcomes after resuscitation and to explore the differences in neurological outcomes between women and men with different circulating PCSK9 levels.

Liver injury

PCSK9 has recently been shown to influence inflammatory responses in the liver. Circulating PCSK9 levels were associated with steatosis severity in patients who underwent liver biopsy for suspected nonalcoholic steatohepatitis (Ruscica et al., 2016). The mean PCSK9 levels in patients with end-stage liver disease and mixed disease etiology were much lower than those in healthy controls (Schlegel et al., 2017). Although PCSK9 expression differs in different stages of liver cirrhosis and different etiologies of liver injury, there is increasing evidence that PCSK9 contributes to the pathogenesis of nonalcoholic fatty liver disease (NAFLD). Mice that overexpressed PCSK9 with a high-fat diet had

increased hepatic steatosis, macrophage infiltration and fibrosis scores (Grimaudo et al., 2021).

PCSK9 inhibition seems to exert a protective effect against hepatic damage in NAFLD. A PCSK9 loss-of-function variant in humans was protective against liver steatosis and fibrosis in individuals with NAFLD (Grimaudo et al., 2021). The genetic deletion of PCSK9 improved liver inflammation and fibrosis in bile duct-ligated mice and reduced liver function markers such as alanine transaminase (ALT) and aspartate transaminase (AST) levels, suggesting that PCSK9 inhibition can rescue liver inflammation and hepatocyte injury (Zou et al., 2020). PCSK9-targeted therapies could be a potential therapeutic approach to ameliorate NAFLD, which is closely related to atherosclerotic disease and cardiovascular risk factors. However, one study including 202 hyperlipidemia patients found that there was a mean increase of 5.8 mg/dl and 6.2 mg/dl from baseline in ALT and AST levels, respectively, in patients who were taking PCSK9 inhibitors compared to those who were not taking PCSK9 inhibitors (Zafar et al., 2020). This study had a small sample size and no long-term follow-up, and no alcohol use or detailed liver comorbidities, such as NAFLD, were documented. To obtain a better understanding of the relation between plasma PCSK9 levels and NAFLD or other chronic liver diseases, more intensive studies are needed to estimate sex differences in the impact of PCSK9 inhibition in patients with metabolic liver diseases. In Ruscica M's study, circulating PCSK9 levels were not significantly associated with female sex in a multivariate analysis, and it was hypothesized that the induction of PCSK9 in NAFLD may overcome its regulation by sex hormones (Ruscica et al., 2016). This hypothesis also needs to be evaluated in larger studies.

Inflammatory biomarkers

The difference in vascular inflammation between men and women has recently become the focus of many studies (Shabbir et al., 2021). The proinflammatory role of PCSK9 in atherosclerosis has been supported by many studies. Higher levels of plasma PCSK9 were independently associated with inflammatory markers such as the white blood cell count (WBCC), fibrinogen levels, and high sensitivity C-reactive protein (hs-CRP) levels in patients with ACS and CAD (Li et al., 2015a). Moreover, PCSK9 has been found to enhance the production of proinflammatory cytokines; for example, the TLR4/NF-κB signaling pathway could be stimulated to mediate the PCSK9-induced increase in the inflammatory response (Tang et al., 2017). The effects of PCSK9 on CAD were found to be mediated partly by inflammation in addition to lipid metabolism. However, in the analysis performed based on sex, the relation between PCSK9 levels and the WBCC remained significant only in men (Li et al., 2014). Moreover, there was no differential effect of PCSK9 monoclonal antibody therapy on plasma hs-CRP concentrations, and no statistically significant relation between sex and hs-CRP changes was observed in Ye-Xuan Cao's meta-analysis (Cao et al., 2018b). Thus, there might be a different link between PCSK9 levels and inflammatory biomarkers according to sex, but recent data are still limited by sample size. Further studies are necessary to identify sex differences in the relation between PCSK9 levels and inflammatory markers.

High-density lipoprotein cholesterol

HDL-C is inversely associated with CVD across a wide range of concentrations. Indeed, different HDL subpopulations may have different functional properties since HDL particles are heterogeneous in size and biochemical composition. Numerous studies have shown that small- and medium-sized HDL particles are inversely related to cardiovascular risk (McGarrah et al., 2016; Duparc et al., 2020). On average, women have higher HDL-C levels than men, and the corresponding concentration of HDL-C associated with the lowest all-cause mortality for women (2.4 mmol/L) is also higher than that for men (1.9 mmol/L) (Madsen et al., 2017). PCSK9 monoclonal antibodies have been reported to cause not only a moderate increase in HDL-C levels but also an increase in medium-sized HDL particles (Zhang et al., 2015; Ingueneau et al., 2020). Plasma PCSK9 levels are positively correlated with small HDL particles; however, the relation of PCSK9 levels to HDL-C is complicated because the interaction between HDL particles and PCSK9 alters PCSK9 functionality (Burnap et al., 2021). HDL particles have been shown to promote the multimerization of PCSK9 and act as facilitators of PCSK9-driven LDLR degradation. In addition, PCSK9 binds to LDL particles, and LDL particles can inhibit the effects of PCSK9 on LDLRs (Kosenko et al., 2013); thus, lipoproteins dynamically alter PCSK9 function. Sex differences exist in the interaction between PCSK9 levels and HDL particles because PCSK9 is significantly enriched in HDL particles isolated from females (Burnap et al., 2021). Further exploration is needed to determine sex differences in PCSK9 activity and whether the role of sex in the HDL-PCSK9 relation might impact the efficacy of PCSK9 inhibition.

Sex difference in the clinical efficacy of PCSK9 inhibitor application

Despite the overwhelming evidence of cardiovascular benefits from trials with lipid-lowering medications, there is evidence that women are often undertreated in clinical practice (Bittner et al., 2015; Nanna et al., 2019). Moreover, women have been shown to experience more statin-associated side effects than men, and they may discontinue therapy because of their higher susceptibility to statin-associated adverse events (Karalis et al., 2016). However, in a recent analysis including a US nationwide sample of Medicare beneficiaries who were hospitalized for MI and had very high ASCVD risk, women were more likely to initiate treatment with PCSK9 inhibitors

(Colvin et al., 2021). Therefore, in light of the higher circulating PCSK9 levels in women, it is important to establish whether treatment with PCSK9 inhibitors, which produce substantial reductions in LDL-C, would confer consistent cardiovascular benefits in both sexes.

One concern related to PCSK9 inhibitors is whether they may increase the risk of impaired glucose metabolism and the development of new-onset diabetes; however, recent clinical trial data for PCSK9 monoclonal antibodies suggest that the application of alirocumab and evolocumab in the treatment of atherosclerotic disease does not increase the risk of new-onset diabetes or worsen glycemia. In addition, the inhibition of PCSK9 by polydatin, a natural antidiabetic product, could modify glucose metabolism disorders and thereby ameliorate diabetic complications by increasing the expression of liver glucokinase, a key enzyme in glucose metabolism (Wang et al., 2016). Nonetheless, it remains unclear whether treatment with PCSK9 inhibitors can exert a positive effect to alleviate glycemic parameters and whether there are sex differences in the effects of PCSK9 inhibitors on glucose metabolism in patients with DM.

In the FOURIER trial, the LDL-C reduction with evolocumab at 4 weeks was nominally greater in men than women, but the relative risk reductions in endpoint analysis were similar in women and men. The large size of the FOURIER trial population provides a robust evidence base that the absolute risk reductions of adverse events with evolocumab application were similar in both men and women, and no important safety issues were observed in either sex (Sever et al., 2021). Consistently, the preliminary results of the ODYSSEY OUTCOMES trial with alirocumab showed that the relative risk reductions for the primary composite endpoint were broadly similar in women and men (9 and 17%, respectively, P interaction = 0.35) (Schwartz et al., 2018). In conclusion, the benefits of PCSK9 monoclonal antibodies were found to be similar in both men and women with high ASCVD risk in recent studies.

The administration of PCSK9 monoclonal antibodies to patients with hyperlipidemia and CAD led to a 50–70% reduction in LDL-C levels (Sabatine et al., 2017; Sinnaeve et al., 2020). Small-molecule PCSK9-targeting agents have been found to be effective competitors for both PCSK9 monoclonal antibodies and siRNA (Salaheldin et al., 2022). P-21, considered the first oral small-molecule nanohepatic targeted anti-PCSK9/LDLR compound, seems to offer a more efficient, safer, and easier-to-administer treatment protocol. In a hypercholesterolemia mouse model, P-21 led to a reduction of more than 90% in LDL-C levels after 1 week of treatment, and toxicology studies in rats showed normal chemical biomarkers and normal histopathological findings, with no apparent toxic clinical signs (Salaheldin et al., 2022). The recent innovations in PCSK9 inhibitors have ushered in a new era in lipid-lowering therapy; however, more sex-specific subanalyses are necessary, and sex differences in their clinical efficacy should be estimated.

Conclusion

Although the overall mortality in patients with CAD has dramatically declined over recent decades as a result of preventive strategies, the decline has been less significant for women (Benjamin et al., 2017). The physiological roles of PCSK9 need to be further investigated because its functions are far more than the regulation of plasma LDL-C levels. Circulating PCSK9 levels are higher in women than in men, and postmenopausal women have higher PCSK9 concentrations than premenopausal women. Estrogen could affect circulating PCSK9 concentrations, probably through transcriptional and posttranscriptional mechanisms. The sex differences in circulating PCSK9 levels call for clinical attention and may represent a pharmacological target for the prevention and treatment of CVDs in women. The potential of PCSK9 in the prediction of ASCVD risk and MACEs based on sex differences requires further prospective investigation. Thus, sex-specific subanalyses may be warranted, and information regarding hormonal status should be taken into account, especially for women. This information might be taken into consideration when defining individual risk for cardiovascular events and/or refining PCSK9-lowering treatments.

Author contributions

CX and J-JL contributed to conception of the review. FJ wrote the first draft of the manuscript. S-FF and D-BT wrote sections of the manuscript. All authors contributed to manuscript revision, read, and approved the submitted version.

Funding

This work was Funding from Young Talent Development Plan of Changzhou Health Commission (2020-233) (CZQM2020054).

Conflict of interest

The authors declare that the research was conducted in the absence of any commercial or financial relationships that could be construed as a potential conflict of interest.

Publisher's note

References

An, L., Li, W., Shi, H., Zhou, X., Liu, X., Wang, H., et al. (2019). Gender difference of symptoms of acute coronary syndrome among Chinese patients: A cross-sectional study. *Eur. J. Cardiovasc. Nurs.* 18 (3), 179–184. doi:10.1177/1474515118820485

Bae, K. H., Kim, S. W., Choi, Y. K., Seo, J. B., Kim, N., Kim, C. Y., et al. (2018). Serum levels of PCSK9 are associated with coronary angiographic severity in patients with acute coronary syndrome. *Diabetes Metab. J.* 42 (3), 207–214. doi:10.4093/dmj.2017.0081

Bairey Merz, C. N., Shaw, L. J., Reis, S. E., Bittner, V., Kelsey, S. F., Olson, M., et al. (2006). Insights from the NHLBI-sponsored women's ischemia syndrome evaluation (WISE) study: Part II: Gender differences in presentation, diagnosis, and outcome with regard to gender-based pathophysiology of atherosclerosis and macrovascular and microvascular coronary disease. *J. Am. Coll. Cardiol.* 47, S21–S29. doi:10.1016/j.jacc.2004.12.084

Benjamin, E. J., Blaha, M. J., Chiuve, S. E., Cushman, M., Das, S. R., Deo, R., et al. (2017). Heart disease and stroke statistics-2017 update: A report from the American heart association. *Circulation* 135 (10), e146–e603. doi:10.1161/CIR.0000000000000485

Bittner, V., Deng, L., Rosenson, R. S., Taylor, B., Glasser, S. P., Kent, S. T., et al. (2015). Trends in the use of nonstatin lipid-lowering therapy among patients with coronary heart disease: A retrospective cohort study in the Medicare population 2007 to 2011. *J. Am. Coll. Cardiol.* 66 (17), 1864–1872. doi:10.1016/j.jacc.2015.08.042

Burnap, S. A., Sattler, K., Pechlaner, R., Duregotti, E., Lu, R., Theofilatos, K., et al. (2021). PCSK9 activity is potentiated through HDL binding. *Circ. Res.* 129 (11), 1039–1053. doi:10.1161/CIRCRESAHA.121.319272

Cao, Y. X., Li, S., Liu, H. H., and Li, J. J. (2018). Impact of PCSK9 monoclonal antibodies on circulating hs-CRP levels: A systematic review and meta-analysis of randomised controlled trials. *BMJ Open* 8 (9), e022348. doi:10.1136/bmjopen-2018-022348

Cao, Y. X., Liu, H. H., Sun, D., Jin, J. L., Xu, R. X., Guo, Y. L., et al. (2018). The different relations of PCSK9 and Lp(a) to the presence and severity of atherosclerotic lesions in patients with familial hypercholesterolemia. *Atherosclerosis* 277, 7–14. doi:10.1016/j.atherosclerosis.2018.07.030

Cariou, B., Guerin, P., Le May, C., Letocart, V., Arnaud, L., Guyomarch, B., et al. (2017). Circulating PCSK9 levels in acute coronary syndrome: Results from the PC-SCA-9 prospective study. *Diabetes Metab.* 43 (6), 529–535. doi:10.1016/j.diabet.2017.07.009

Chandrasekhar, J., and Mehran, R. (2016). Sex-based differences in acute coronary syndromes: Insights from invasive and noninvasive coronary technologies. *JACC. Cardiovasc. Imaging* 9 (4), 451–464. doi:10.1016/j.jcmg.2016.02.004

Cheng, J. M., Oemrawsingh, R. M., Garcia-Garcia, H. M., Boersma, E., van Geuns, R. J., Serruys, P. W., et al. (2016). PCSK9 in relation to coronary plaque inflammation: Results of the ATHEROREMO-IVUS study. *Atherosclerosis* 248, 117–122. doi:10.1016/j.atherosclerosis.2016.03.010

Choi, I. J., Lim, S., Lee, D., Lee, W. J., Lee, K. Y., Kim, M. J., et al. (2020). Relation of proprotein convertase subtilisin/kexin type 9 to cardiovascular outcomes in patients undergoing percutaneous coronary intervention. *Am. J. Cardiol.* 133, 54–60. doi:10.1016/j.amjcard.2020.07.032

Colvin, C. L., Poudel, B., Bress, A. P., Derington, C. G., King, J. B., Wen, Y., et al. (2021). Race/ethnic and sex differences in the initiation of non-statin lipid-lowering medication following myocardial infarction. *J. Clin. Lipidol.* 15 (5), 665–673. doi:10.1016/j.jacl.2021.08.001

DeFilippis, E. M., Collins, B. L., Singh, A., Biery, D. W., Fatima, A., Qamar, A., et al. (2020). Women who experience a myocardial infarction at a young age have worse outcomes compared with men: The mass general brigham YOUNG-MI registry. *Eur. Heart J.* 41 (42), 4127–4137. doi:10.1093/eurheartj/ehaa662

Ding, Z., Liu, S., Wang, X., Deng, X., Fan, Y., Sun, C., et al. (2015). Hemodynamic shear stress via ROS modulates PCSK9 expression in human vascular endothelial and smooth muscle cells and along the mouse aorta. *Antioxid. Redox Signal.* 22 (9), 760–771. doi:10.1089/ars.2014.6054

Duparc, T., Ruidavets, J. B., Genoux, A., Ingueneau, C., Najib, S., Ferrieres, J., et al. (2020). Serum level of HDL particles are independently associated with long-term prognosis in patients with coronary artery disease: The GENES study. *Sci. Rep.* 10 (1), 8138. doi:10.1038/s41598-020-65100-2

Eisenga, M. F., Zelle, D. M., Sloan, J. H., Gaillard, C., Bakker, S. J. L., and Dullaart, R. P. F. (2017). High serum PCSK9 is associated with increased risk of new-onset diabetes after transplantation in renal transplant recipients. *Diabetes Care* 40 (7), 894–901. doi:10.2337/dc16-2258

Ferri, N., Marchiano, S., Tibolla, G., Baetta, R., Dhyani, A., Ruscica, M., et al. (2016). PCSK9 knock-out mice are protected from neointimal formation in response to perivascular carotid collar placement. *Atherosclerosis* 253, 214–224. doi:10.1016/j.atherosclerosis.2016.07.910

Ferri, N., Ruscica, M., Coggi, D., Bonomi, A., Amato, M., Frigerio, B., et al. (2020). Sex-specific predictors of PCSK9 levels in a European population: The IMPROVE study. *Atherosclerosis* 309, 39–46. doi:10.1016/j.atherosclerosis.2020.07.014

Fu, W., Gao, X. P., Zhang, S., Dai, Y. P., Zou, W. J., and Yue, L. M. (2019). 17β-Estradiol inhibits PCSK9-mediated LDLR degradation through GPER/PLC activation in HepG2 cells. *Front. Endocrinol.* 10, 930. doi:10.3389/fendo.2019.00930

Gencer, B., Montecucco, F., Nanchen, D., Carbone, F., Klingenberg, R., Vuilleumier, N., et al. (2016). Prognostic value of PCSK9 levels in patients with acute coronary syndromes. *Eur. Heart J.* 37 (6), 546–553. doi:10.1093/eurheartj/ehv637

Gerdts, E., and Regitz-Zagrosek, V. (2019). Sex differences in cardiometabolic disorders. *Nat. Med.* 25 (11), 1657–1666. doi:10.1038/s41591-019-0643-8

Ghosh, M., Galman, C., Rudling, M., and Angelin, B. (2015). Influence of physiological changes in endogenous estrogen on circulating PCSK9 and LDL cholesterol. *J. Lipid Res.* 56 (2), 463–469. doi:10.1194/jlr.M055780

Goto, Y., Funada, A., Maeda, T., Okada, H., and Goto, Y. (2019). Sex-specific differences in survival after out-of-hospital cardiac arrest: A nationwide, population-based observational study. *Crit. Care* 23 (1), 263. doi:10.1186/s13054-019-2547-x

Grimaudo, S., Bartesaghi, S., Rametta, R., Marra, F., Margherita Mancina, R., Pihlajamaki, J., et al. (2021). PCSK9 rs11591147 R46L loss-of-function variant protects against liver damage in individuals with NAFLD. *Liver Int.* 41 (2), 321–332. doi:10.1111/liv.14711

Group, E. U. C. C. S., Regitz-Zagrosek, V., Oertelt-Prigione, S., Prescott, E., Franconi, F., Gerdts, E., et al. (2016). Gender in cardiovascular diseases: Impact on clinical manifestations, management, and outcomes. *Eur. Heart J.* 37 (1), 24–34. doi:10.1093/eurheartj/ehv598

Hamamura, H., Adachi, H., Enomoto, M., Fukami, A., Nakamura, S., Nohara, Y., et al. (2021). Serum proprotein convertase subtilisin/kexin type 9 (PCSK9) is independently associated with insulin resistance, triglycerides, lipoprotein(a) levels but not low-density lipoprotein cholesterol levels in a general population. *J. Atheroscler. Thromb.* 28 (4), 329–337. doi:10.5551/jat.56390

Hussain, Y., Ding, Q., Connelly, P. W., Brunt, J. H., Ban, M. R., McIntyre, A. D., et al. (2015). G-Protein estrogen receptor as a regulator of low-density lipoprotein cholesterol metabolism: Cellular and population genetic studies. *Arterioscler. Thromb. Vasc. Biol.* 35 (1), 213–221. doi:10.1161/ATVBAHA.114.304326

Ingueneau, C., Hollstein, T., Grenkowitz, T., Ruidavets, J. B., Kassner, U., Duparc, T., et al. (2020). Treatment with PCSK9 inhibitors induces a more anti-atherogenic HDL lipid profile in patients at high cardiovascular risk. *Vascul. Pharmacol.* 135, 106804. doi:10.1016/j.vph.2020.106804

Jarman, A. F., Mumma, B. E., Perman, S. M., Kotini-Shah, P., and McGregor, A. J. (2019). When the female heart stops: Sex and gender differences in out-of-hospital cardiac arrest epidemiology and resuscitation. *Clin. Ther.* 41 (6), 1013–1019. doi:10.1016/j.clinthera.2019.03.015

Jeenduang, N. (2019). Circulating PCSK9 concentrations are increased in postmenopausal women with the metabolic syndrome. *Clin. Chim. Acta.* 494, 151–156. doi:10.1016/j.cca.2019.04.067

Jing, Y., Hu, T., Lin, C., Xiong, Q., Liu, F., Yuan, J., et al. (2019). Resveratrol downregulates PCSK9 expression and attenuates steatosis through estrogen

receptor alpha-mediated pathway in L02cells. *Eur. J. Pharmacol.* 855, 216–226. doi:10.1016/j.ejphar.2019.05.019

Kajingulu, F. M., Lepira, F. B., Nkodila, A. N., Makulo, J. R., Mokoli, V. M., Ekulu, P. M., et al. (2022). Circulating Proprotein Convertase Subtilisin/Kexin type 9 level independently predicts incident cardiovascular events and all-cause mortality in hemodialysis black Africans patients. *BMC Nephrol.* 23 (1), 123. doi:10.1186/s12882-022-02748-0

Karalis, D. G., Wild, R. A., Maki, K. C., Gaskins, R., Jacobson, T. A., Sponseller, C. A., et al. (2016). Gender differences in side effects and attitudes regarding statin use in the Understanding Statin Use in America and Gaps in Patient Education (USAGE) study. *J. Clin. Lipidol.* 10 (4), 833–841. doi:10.1016/j.jacl.2016.02.016

Kenkre, T. S., Malhotra, P., Johnson, B. D., Handberg, E. M., Thompson, D. V., Marroquin, O. C., et al. (2017). Ten-year mortality in the WISE study (Women's Ischemia Syndrome Evaluation). *Circ. Cardiovasc. Qual. Outcomes* 10 (12), e003863. doi:10.1161/CIRCOUTCOMES.116.003863

Kosenko, T., Golder, M., Leblond, G., Weng, W., and Lagace, T. A. (2013). Low density lipoprotein binds to proprotein convertase subtilisin/kexin type-9 (PCSK9) in human plasma and inhibits PCSK9-mediated low density lipoprotein receptor degradation. *J. Biol. Chem.* 288 (12), 8279–8288. doi:10.1074/jbc.M112.421370

Kosmidou, I., Redfors, B., Selker, H. P., Thiele, H., Patel, M. R., Udelson, J. E., et al. (2017). Infarct size, left ventricular function, and prognosis in women compared to men after primary percutaneous coronary intervention in ST-segment elevation myocardial infarction: results from an individual patient-level pooled analysis of 10 randomized trials. *Eur. Heart J.* 38 (21), 1656–1663. doi:10.1093/eurheartj/ehx159

Kotini-Shah, P., Del Rios, M., Khosla, S., Pugach, O., Vellano, K., McNally, B., et al. (2021). Sex differences in outcomes for out-of-hospital cardiac arrest in the United States. *Resuscitation* 163, 6–13. doi:10.1016/j.resuscitation.2021.03.020

Krysa, J. A., Ooi, T. C., Proctor, S. D., and Vine, D. F. (2017). Nutritional and Lipid Modulation of PCSK9: Effects on Cardiometabolic Risk Factors. *J. Nutr.* 147 (4), 473–481. doi:10.3945/jn.116.235069

Levenson, A. E., Shah, A. S., Khoury, P. R., Kimball, T. R., Urbina, E. M., de Ferranti, S. D., et al. (2017). Obesity and type 2 diabetes are associated with elevated PCSK9 levels in young women. *Pediatr. Diabetes* 18 (8), 755–760. doi:10.1111/pedi.12490

Li, J. J., Li, S., Zhang, Y., Xu, R. X., Guo, Y. L., Zhu, C. G., et al. (2015). Proprotein Convertase Subtilisin/Kexin type 9, C-Reactive Protein, Coronary Severity, and Outcomes in Patients With Stable Coronary Artery Disease: A Prospective Observational Cohort Study. *Med. Baltim.* 94 (52), e2426. doi:10.1097/MD.0000000000002426

Li, S., Guo, Y. L., Xu, R. X., Zhang, Y., Zhu, C. G., Sun, J., et al. (2014). Association of plasma PCSK9 levels with white blood cell count and its subsets in patients with stable coronary artery disease. *Atherosclerosis* 234 (2), 441–445. doi:10.1016/j.atherosclerosis.2014.04.001

Li, S., Guo, Y. L., Zhao, X., Zhang, Y., Zhu, C. G., Wu, N. Q., et al. (2017). Novel and traditional lipid-related biomarkers and their combinations in predicting coronary severity. *Sci. Rep.* 7 (1), 360. doi:10.1038/s41598-017-00499-9

Li, S., Zhang, Y., Xu, R. X., Guo, Y. L., Zhu, C. G., Wu, N. Q., et al. (2015). Proprotein convertase subtilisin-kexin type 9 as a biomarker for the severity of coronary artery disease. *Ann. Med.* 47 (5), 386–393. doi:10.3109/07853890.2015.1042908

Liu, A., and Frostegard, J. (2018). PCSK9 plays a novel immunological role in oxidized LDL-induced dendritic cell maturation and activation of T cells from human blood and atherosclerotic plaque. *J. Intern. Med.* 284, 193–210. doi:10.1111/joim.12758

Liu, S., Deng, X., Zhang, P., Wang, X., Fan, Y., Zhou, S., et al. (2020). Blood flow patterns regulate PCSK9 secretion via MyD88-mediated pro-inflammatory cytokines. *Cardiovasc. Res.* 116 (10), 1721–1732. doi:10.1093/cvr/cvz262

Ma, Q., Wang, J., Jin, J., Gao, M., Liu, F., Zhou, S., et al. (2017). Clinical characteristics and prognosis of acute coronary syndrome in young women and men: A systematic review and meta-analysis of prospective studies. *Int. J. Cardiol.* 228, 837–843. doi:10.1016/j.ijcard.2016.11.148

Macchi, C., Greco, M. F., Botta, M., Sperandeo, P., Dongiovanni, P., Valenti, L., et al. (2020). Leptin, Resistin, and Proprotein Convertase Subtilisin/Kexin Type 9: The Role of STAT3. *Am. J. Pathol.* 190 (11), 2226–2236. doi:10.1016/j.ajpath.2020.07.016

Madsen, C. M., Varbo, A., and Nordestgaard, B. G. (2017). Extreme high high-density lipoprotein cholesterol is paradoxically associated with high mortality in men and women: two prospective cohort studies. *Eur. Heart J.* 38 (32), 2478–2486. doi:10.1093/eurheartj/ehx163

Mannarino, M. R., Sahebkar, A., Bianconi, V., Serban, M. C., Banach, M., and Pirro, M. (2018). PCSK9 and neurocognitive function: Should it be still an issue after FOURIER and EBBINGHAUS results? *J. Clin. Lipidol.* 12 (5), 1123–1132. doi:10.1016/j.jacl.2018.05.012

Mauvais-Jarvis, F. (2018). Gender differences in glucose homeostasis and diabetes. *Physiol. Behav.* 187, 20–23. doi:10.1016/j.physbeh.2017.08.016

McGarrah, R. W., Craig, D. M., Haynes, C., Dowdy, Z. E., Shah, S. H., and Kraus, W. E. (2016). High-density lipoprotein subclass measurements improve mortality risk prediction, discrimination and reclassification in a cardiac catheterization cohort. *Atherosclerosis* 246, 229–235. doi:10.1016/j.atherosclerosis.2016.01.012

Merrelaar, A., Buchtele, N., Schriefl, C., Clodi, C., Poppe, M., Ettl, F., et al. (2020). Low PCSK-9 levels Are Associated with Favorable Neurologic Function after Resuscitation from out of Hospital Cardiac Arrest. *J. Clin. Med.* 9 (8), E2606. doi:10.3390/jcm9082606

Nanna, M. G., Wang, T. Y., Xiang, Q., Goldberg, A. C., Robinson, J. G., Roger, V. L., et al. (2019). Sex Differences in the Use of Statins in Community Practice. *Circ. Cardiovasc. Qual. Outcomes* 12 (8), e005562. doi:10.1161/CIRCOUTCOMES.118.005562

Navarese, E. P., Kolodziejczak, M., Winter, M. P., Alimohammadi, A., Lang, I. M., Buffon, A., et al. (2017). Association of PCSK9 with platelet reactivity in patients with acute coronary syndrome treated with prasugrel or ticagrelor: The PCSK9-REACT study. *Int. J. Cardiol.* 227, 644–649. doi:10.1016/j.ijcard.2016.10.084

Ng, Y. Y., Wah, W., Liu, N., Zhou, S. A., Ho, A. F., Pek, P. P., et al. (2016). Associations between gender and cardiac arrest outcomes in Pan-Asian out-of-hospital cardiac arrest patients. *Resuscitation* 102, 116–121. doi:10.1016/j.resuscitation.2016.03.002

Ooi, T. C., Raymond, A., Cousins, M., Favreau, C., Taljaard, M., Gavin, C., et al. (2015). Relationship between testosterone, estradiol and circulating PCSK9: Cross-sectional and interventional studies in humans. *Clin. Chim. Acta.* 446, 97–104. doi:10.1016/j.cca.2015.03.036

Pagidipati, N. J., and Peterson, E. D. (2016). Acute coronary syndromes in women and men. *Nat. Rev. Cardiol.* 13 (8), 471–480. doi:10.1038/nrcardio.2016.89

Panahi, Y., Ghahrodi, M. S., Jamshir, M., Safarpour, M. A., Bianconi, V., Pirro, M., et al. (2019). PCSK9 and atherosclerosis burden in the coronary arteries of patients undergoing coronary angiography. *Clin. Biochem.* 74, 12–18. doi:10.1016/j.clinbiochem.2019.09.001

Pandeya, N., Huxley, R. R., Chung, H. F., Dobson, A. J., Kuh, D., Hardy, R., et al. (2018). Female reproductive history and risk of type 2 diabetes: A prospective analysis of 126 721 women. *Diabetes Obes. Metab.* 20 (9), 2103–2112. doi:10.1111/dom.13336

Peng, J., Liu, M. M., Jin, J. L., Cao, Y. X., Guo, Y. L., Wu, N. Q., et al. (2020). Association of circulating PCSK9 concentration with cardiovascular metabolic markers and outcomes in stable coronary artery disease patients with or without diabetes: a prospective, observational cohort study. *Cardiovasc. Diabetol.* 19 (1), 167. doi:10.1186/s12933-020-01142-0

Persson, L., Cao, G., Stahle, L., Sjoberg, B. G., Troutt, J. S., Konrad, R. J., et al. (2010). Circulating proprotein convertase subtilisin kexin type 9 has a diurnal rhythm synchronous with cholesterol synthesis and is reduced by fasting in humans. *Arterioscler. Thromb. Vasc. Biol.* 30 (12), 2666–2672. doi:10.1161/ATVBAHA.110.214130

Persson, L., Henriksson, P., Westerlund, E., Hovatta, O., Angelin, B., and Rudling, M. (2012). Endogenous estrogens lower plasma PCSK9 and LDL cholesterol but not Lp(a) or bile acid synthesis in women. *Arterioscler. Thromb. Vasc. Biol.* 32 (3), 810–814. doi:10.1161/ATVBAHA.111.242461

Puteri, M. U., Azmi, N. U., Kato, M., and Saputri, F. C. (2022). PCSK9 Promotes Cardiovascular Diseases: Recent Evidence about Its Association with Platelet Activation-Induced Myocardial Infarction. *Life (Basel, Switz.* 12 (2), 190. doi:10.3390/life12020190

Qi, Z., Hu, L., Zhang, J., Yang, W., Liu, X., Jia, D., et al. (2021). PCSK9 (Proprotein Convertase Subtilisin/Kexin 9) Enhances Platelet Activation, Thrombosis, and Myocardial Infarct Expansion by Binding to Platelet CD36. *Circulation* 143 (1), 45–61. doi:10.1161/CIRCULATIONAHA.120.046290

Ramin-Mangata, S., Wargny, M., Pichelin, M., Le May, C., Thédrez, A., Blanchard, V., et al. (2020). Circulating PCSK9 levels are not associated with the conversion to type 2 diabetes. *Atherosclerosis* 293, 49–56. doi:10.1016/j.atherosclerosis.2019.11.027

Rathod, K. S., Jones, D. A., Jain, A. K., Lim, P., MacCarthy, P. A., Rakhit, R., et al. (2021). The influence of biological age and sex on long-term outcome after percutaneous coronary intervention for ST-elevation myocardial infarction. *Am. J. Cardiovasc. Dis.* 11 (5), 659–678.

Robinson, J. G., Farnier, M., Krempf, M., Bergeron, J., Luc, G., Averna, M., et al. (2015). Efficacy and safety of alirocumab in reducing lipids and cardiovascular events. *N. Engl. J. Med.* 372 (16), 1489–1499. doi:10.1056/NEJMoa1501031

Robinson, J. G., Wallace, R., Limacher, M., Ren, H., Cochrane, B., Wassertheil-Smoller, S., et al. (2008). Cardiovascular risk in women with non-specific chest pain

(from the Women's Health Initiative Hormone Trials). *Am. J. Cardiol.* 102 (6), 693–699. doi:10.1016/j.amjcard.2007.12.044

Roubtsova, A., Chamberland, A., Marcinkiewicz, J., Essalmani, R., Fazel, A., Bergeron, J. J., et al. (2015). PCSK9 deficiency unmasks a sex- and tissue-specific subcellular distribution of the LDL and VLDL receptors in mice. *J. Lipid Res.* 56 (11), 2133–2142. doi:10.1194/jlr.M061952

Ruscica, M., Ferri, N., Macchi, C., Meroni, M., Lanti, C., Ricci, C., et al. (2016). Liver fat accumulation is associated with circulating PCSK9. *Ann. Med.* 48 (5), 384–391. doi:10.1080/07853890.2016.1188328

Sabatine, M. S., Giugliano, R. P., Keech, A. C., Honarpour, N., Wiviott, S. D., Murphy, S. A., et al. (2017). Evolocumab and Clinical Outcomes in Patients with Cardiovascular Disease. *N. Engl. J. Med.* 376 (18), 1713–1722. doi:10.1056/NEJMoa1615664

Safdar, B., Spatz, E. S., Dreyer, R. P., Beltrame, J. F., Lichtman, J. H., Spertus, J. A., et al. (2018). Presentation, Clinical Profile, and Prognosis of Young Patients With Myocardial Infarction With Nonobstructive Coronary Arteries (MINOCA): Results From the VIRGO Study. *J. Am. Heart Assoc.* 7 (13), e009174. doi:10.1161/JAHA.118.009174

Sahebkar, A., Simental-Mendia, L. E., Guerrero-Romero, F., Golledge, J., and Watts, G. F. (2015). Effect of statin therapy on plasma proprotein convertase subtilisin kexin 9 (PCSK9) concentrations: a systematic review and meta-analysis of clinical trials. *Diabetes Obes. Metab.* 17 (11), 1042–1055. doi:10.1111/dom.12536

Salaheldin, T. A., Godugu, K., Bharali, D. J., Fujioka, K., Elshourbagy, N., and Mousa, S. A. (2022). Novel oral nano-hepatic targeted anti-PCSK9 in hypercholesterolemia. *Nanomedicine.* 40, 102480. doi:10.1016/j.nano.2021.102480

Schlegel, V., Treuner-Kaueroff, T., Seehofer, D., Berg, T., Becker, S., Ceglarek, U., et al. (2017). Low PCSK9 levels are correlated with mortality in patients with end-stage liver disease. *PLoS One* 12 (7), e0181540. doi:10.1371/journal.pone.0181540

Schwartz, G. G., Steg, P. G., Szarek, M., Bhatt, D. L., Bittner, V. A., Diaz, R., et al. (2018). Alirocumab and Cardiovascular Outcomes after Acute Coronary Syndrome. *N. Engl. J. Med.* 379 (22), 2097–2107. doi:10.1056/NEJMoa1801174

Sedlak, T. L., Lee, M., Izadnegahdar, M., Merz, C. N., Gao, M., and Humphries, K. H. (2013). Sex differences in clinical outcomes in patients with stable angina and no obstructive coronary artery disease. *Am. Heart J.* 166 (1), 38–44. doi:10.1016/j.ahj.2013.03.015

Sever, P., Gouni-Berthold, I., Keech, A., Giugliano, R., Pedersen, T. R., Im, K., et al. (2021). LDL-cholesterol lowering with evolocumab, and outcomes according to age and sex in patients in the FOURIER Trial. *Eur. J. Prev. Cardiol.* 28 (8), 805–812. doi:10.1177/2047487320902750

Shabbir, A., Rathod, K. S., Khambata, R. S., and Ahluwalia, A. (2021). Sex Differences in the Inflammatory Response: Pharmacological Opportunities for Therapeutics for Coronary Artery Disease. *Annu. Rev. Pharmacol. Toxicol.* 61, 333–359. doi:10.1146/annurev-pharmtox-010919-023229

Shen, L., Song, L., Li, H., Liu, B., Zheng, X., Zhang, L., et al. (2017). Association between earlier age at natural menopause and risk of diabetes in middle-aged and older Chinese women: The Dongfeng-Tongji cohort study. *Diabetes Metab.* 43 (4), 345–350. doi:10.1016/j.diabet.2016.12.011

Shi, J., Zhang, W., Niu, Y., Lin, N., Li, X., Zhang, H., et al. (2020). Association of circulating proprotein convertase subtilisin/kexin type 9 levels and the risk of incident type 2 diabetes in subjects with prediabetes: a population-based cohort study. *Cardiovasc. Diabetol.* 19 (1), 209. doi:10.1186/s12933-020-01185-3

Simeone, P. G., Vadini, F., Tripaldi, R., Liani, R., Ciotti, S., Di Castelnuovo, A., et al. (2021). Sex-Specific Association of Endogenous PCSK9 With MemoryFunction in Elderly Subjects at High Cardiovascular Risk. *Front. Aging Neurosci.* 13, 632655. doi:10.3389/fnagi.2021.632655

Sinnaeve, P. R., Schwartz, G. G., Wojdyla, D. M., Alings, M., Bhatt, D. L., Bittner, V. A., et al. (2020). Effect of alirocumab on cardiovascular outcomes after acute coronary syndromes according to age: an ODYSSEY OUTCOMES trial analysis. *Eur. Heart J.* 41 (24), 2248–2258. doi:10.1093/eurheartj/ehz809

Sponder, M., Campean, I. A., Dalos, D., Emich, M., Fritzer-Szekeres, M., Litschauer, B., et al. (2017). Effect of long-term physical activity on PCSK9, high- and low-density lipoprotein cholesterol, and lipoprotein(a) levels: a prospective observational trial. *Pol. Arch. Intern. Med.* 127 (7-8), 506–511. doi:10.20452/pamw.4044

Starr, A. E., Lemieux, V., Noad, J., Moore, J. I., Dewpura, T., Raymond, A., et al. (2015). β-Estradiol results in a proprotein convertase subtilisin/kexin type 9-dependent increase in low-density lipoprotein receptor levels in human hepatic HuH7 cells. *FEBS J.* 282 (14), 2682–2696. doi:10.1111/febs.13309

Tang, Z. H., Peng, J., Ren, Z., Yang, J., Li, T. T., Li, T. H., et al. (2017). New role of PCSK9 in atherosclerotic inflammation promotion involving the TLR4/NF-κB pathway. *Atherosclerosis* 262, 113–122. doi:10.1016/j.atherosclerosis.2017.04.023

Vogelsong, M. A., May, T., Agarwal, S., Cronberg, T., Dankiewicz, J., Dupont, A., et al. (2021). Influence of sex on survival, neurologic outcomes, and neurodiagnostic testing after out-of-hospital cardiac arrest. *Resuscitation* 167, 66–75. doi:10.1016/j.resuscitation.2021.07.037

Waheed, N., Elias-Smale, S., Malas, W., Maas, A. H., Sedlak, T. L., Tremmel, J., et al. (2020). Sex differences in non-obstructive coronary artery disease. *Cardiovasc. Res.* 116 (4), 829–840. doi:10.1093/cvr/cvaa001

Wang, Y., Ye, J., Li, J., Chen, C., Huang, J., Liu, P., et al. (2016). Polydatin ameliorates lipid and glucose metabolism in type 2 diabetes mellitus by downregulating proprotein convertase subtilisin/kexin type 9 (PCSK9). *Cardiovasc. Diabetol.* 15, 19. doi:10.1186/s12933-015-0325-x

Werner, C., Hoffmann, M. M., Winkler, K., Bohm, M., and Laufs, U. (2014). Risk prediction with proprotein convertase subtilisin/kexin type 9 (PCSK9) in patients with stable coronary disease on statin treatment. *Vasc. Pharmacol.* 62 (2), 94–102. doi:10.1016/j.vph.2014.03.004

Xia, S., Du, X., Guo, L., Du, J., Arnott, C., Lam, C. S. P., et al. (2020). Sex Differences in Primary and Secondary Prevention of Cardiovascular Disease in China. *Circulation* 141 (7), 530–539. doi:10.1161/CIRCULATIONAHA.119.043731

Yahagi, K., Davis, H. R., Arbustini, E., and Virmani, R. (2015). Sex differences in coronary artery disease: pathological observations. *Atherosclerosis* 239 (1), 260–267. doi:10.1016/j.atherosclerosis.2015.01.017

Yildirim, A. M., Koca, A. O., Beyan, E., Dogan, O., Karakaya, S., Aksoz, Z., et al. (2021). Association of serum proprotein convertase Subtilisin/Kexin Type 9 (PCSK9) level with thyroid function disorders. *Eur. Rev. Med. Pharmacol. Sci.* 25 (17), 5511–5517. doi:10.26355/eurrev_202109_26662

Yurtseven, E., Ural, D., Baysal, K., and Tokgozoglu, L. (2020). An Update on the Role of PCSK9 in Atherosclerosis. *J. Atheroscler. Thromb.* 27 (9), 909–918. doi:10.5551/jat.55400

Zafar, Y., Sattar, Y., Ullah, W., Roomi, S., Rashid, M. U., Khan, M. S., et al. (2020). Proprotein convertase subtilisin/Kexin type-9 (PCSK-9) inhibitors induced liver injury - a retrospective analysis. *J. Community Hosp. Intern. Med. Perspect.* 10 (1), 32–37. doi:10.1080/20009666.2019.1710952

Zhang, X. L., Zhu, Q. Q., Zhu, L., Chen, J. Z., Chen, Q. H., Li, G. N., et al. (2015). Safety and efficacy of anti-PCSK9 antibodies: a meta-analysis of 25 randomized, controlled trials. *BMC Med.* 13, 123. doi:10.1186/s12916-015-0358-8

Zhang, Z., Wei, T. F., Zhao, B., Yin, Z., Shi, Q. X., Liu, P. L., et al. (2019). Sex Differences Associated With Circulating PCSK9 in Patients Presenting With Acute Myocardial Infarction. *Sci. Rep.* 9 (1), 3113. doi:10.1038/s41598-018-35773-x

Zou, Y., Li, S., Xu, B., Guo, H., Zhang, S., and Cai, Y. (2020). Inhibition of Proprotein Convertase Subtilisin/Kexin Type 9 Ameliorates Liver Fibrosis via Mitigation of Intestinal Endotoxemia. *Inflammation* 43 (1), 251–263. doi:10.1007/s10753-019-01114-x

frontiers | Frontiers in Pharmacology

TYPE Original Research
PUBLISHED 26 September 2022
DOI 10.3389/fphar.2022.933156

OPEN ACCESS

EDITED BY
Ahmed F,
Alexandria University, Egypt

REVIEWED BY
Hamid Nasiri,
Amirkabir University of Technology, Iran
Kun Liu,
Shenzhen Hospital, The University of Hong Kong, Hong Kong SAR, China

*CORRESPONDENCE
Hang Xu,
njglyyxh@126.com
Wei-Hong Ge,
6221230@sina.com

†These authors have contributed equally to this work and share first authorship

SPECIALTY SECTION
This article was submitted to Cardiovascular and Smooth Muscle Pharmacology, a section of the journal Frontiers in Pharmacology

RECEIVED 30 April 2022
ACCEPTED 30 August 2022
PUBLISHED 26 September 2022

CITATION
Dai M-F, Li S-Y, Zhang J-F, Wang B-Y, Zhou L, Yu F, Xu H and Ge W-H (2022), Warfarin anticoagulation management during the COVID-19 pandemic: The role of internet clinic and machine learning.
Front. Pharmacol. 13:933156.
doi: 10.3389/fphar.2022.933156

Warfarin anticoagulation management during the COVID-19 pandemic: The role of internet clinic and machine learning

Meng-Fei Dai[1,2†], Shu-Yue Li[2,3†], Ji-Fan Zhang[4], Bao-Yan Wang[1], Lin Zhou[1], Feng Yu[2], Hang Xu[1*] and Wei-Hong Ge[1*]

[1]Department of Pharmacy, Nanjing Drum Tower Hospital, The Affiliated Hospital of Nanjing University Medical School, Nanjing, China, [2]School of Basic Medicine and Clinical Pharmacy, China Pharmaceutical University, Nanjing, China, [3]Department of Pharmacy, Shanxi Province Cancer Hospital, Taiyuan, China, [4]Nanjing Foreign Language School, Nanjing, China

Background: Patients who received warfarin require constant monitoring by hospital staff. However, social distancing and stay-at-home orders, which were universally adopted strategies to avoid the spread of COVID-19, led to unprecedented challenges. This study aimed to optimize warfarin treatment during the COVID-19 pandemic by determining the role of the Internet clinic and developing a machine learning (ML) model to predict anticoagulation quality.

Methods: This retrospective study enrolled patients who received warfarin treatment in the hospital anticoagulation clinic (HAC) and "Internet + Anticoagulation clinic" (IAC) of the Nanjing Drum Tower Hospital between January 2020 and September 2021. The primary outcome was the anticoagulation quality of patients, which was evaluated by both the time in therapeutic range (TTR) and international normalized ratio (INR) variability. Anticoagulation quality and incidence of adverse events were compared between HAC and IAC. Furthermore, five ML algorithms were used to develop the anticoagulation quality prediction model, and the SHAP method was introduced to rank the feature importance.

Results: Totally, 241 patients were included, comprising 145 patients in the HAC group and 96 patients in the IAC group. In the HAC group and IAC group, 73.1 and 69.8% (p = 0.576) of patients achieved good anticoagulation quality, with the average TTR being 79.9 ± 20.0% and 80.6 ± 21.1%, respectively. There was no significant difference in the incidence of adverse events between the two groups. Evaluating the five ML models using the test set, the accuracy of the XGBoost model was 0.767, and the area under the receiver operating characteristic curve was 0.808, which showed the best performance. The results of the SHAP method revealed that age, education, hypertension, aspirin, and amiodarone were the top five important features associated with poor anticoagulation quality.

Conclusion: The IAC contributed to a novel management method for patients who received warfarin during the COVID-19 pandemic, as effective as HAC and with a low risk of virus transmission. The XGBoost model could accurately select patients at a high risk of poor anticoagulation quality, who could benefit from active intervention.

KEYWORDS

telemedicine, COVID-19, warfarin, internet, machine learning, anticoagulation quality

Introduction

Coronavirus disease 2019 (COVID-19) is a respiratory infection spreading around the world sharply, with a high rate of mortality (Wu and McGoogan, 2020). It has been recognized as a pandemic by the World Health Organization (World Health Organization, 2021). On 23 January 2020, China initiated the Level I response to public health incidents nationwide, which is the highest one (Jiang et al., 2022), and slowed the spread of COVID-19 effectively. However, social distancing and stay-at-home orders, which were adopted to avoid the spread of COVID-19, posed unique challenges for patients on medications, requiring continued monitoring by clinic staff, such as warfarin treatment (Kish and Lekic, 2021).

The vitamin K antagonist warfarin is an anticoagulant drug widely used in thromboprophylaxis and treatment. Warfarin has a narrow therapeutic window and wide variability in dose–response (Gu et al., 2018). It is necessary to frequently monitor the International Normalized Ratio (INR) and adjust the dosage accordingly to maintain the INR within the therapeutic range, which can ensure the effectiveness and safety of chronic warfarin treatment (Gu et al., 2019). Clinical pharmacists provide professional anticoagulation management services (AMSs) in hospital anticoagulation clinics (HACs) (Holbrook et al., 2012), including INR testing, dose adjustment, and medication education, which are associated with better anticoagulation quality than usual physician care (Ahmed et al., 2017; Manzoor et al., 2017). Unfortunately, the COVID-19 pandemic has made it difficult for patients to visit anticoagulation clinics to obtain AMSs (Gong et al., 2020; Zhang, 2020). Previous studies have shown a significant increase in adverse events of warfarin treatment during COVID-19 stringency measures (Vriz et al., 2021). Therefore, measures should be taken to improve the anticoagulation quality of patients during the COVID-19 pandemic.

For chronic disease management during the COVID-19 pandemic, telemedicine has been paid unprecedented attention, which can break through the barriers of medical attendance caused by COVID-19 (Zampino et al., 2021). "Internet + Anticoagulation clinic" (IAC) is a new approach for anticoagulation management, which is undoubtedly attractive to patients and clinical pharmacists, especially during the COVID-19 pandemic. To the best of our knowledge, only one previous study has investigated the effectiveness and safety of anticoagulation management provided by clinical pharmacists through the IAC during the COVID-19 pandemic (Jiang et al., 2022), with small sample size and short-term follow-ups, providing preliminary conclusions that IAC improved anticoagulation quality. Therefore, more studies are encouraged to provide crucial evidence for application of IAC during the COVID-19 pandemic.

More importantly, it is necessary for clinical pharmacists to accurately identify patients with poor anticoagulation quality and intervene early, which can improve their anticoagulation quality, and no studies have focused on the prediction of anticoagulation quality during the COVID-19 pandemic until now. The time in therapeutic range (TTR) calculates the time period in which the INR is controlled within the therapeutic range, which is commonly applied as a measure of anticoagulation quality (Rosendaal et al., 1993). However, the TTR cannot measure the degree of stability of INR control, and INR variability can (Numao et al., 2017). The previous study found that using both INR variability and TTR could distinguish patients with increased risk of adverse events more accurately than using a single item (Labaf et al., 2015). Therefore, we used both INR variability and TTR to measure the anticoagulation quality and for the first time proposed using machine learning (ML) technology to develop a model for anticoagulation quality prediction. ML can incorporate enormous numbers of variables, has been successfully applied in the medical field, and has shown excellent performance.

This study aimed to investigate the role of IAC in warfarin treatment and develop an ML model for anticoagulation quality prediction to optimize anticoagulation treatment during the COVID-19 pandemic.

Methods

Study design and participants

This was a retrospective, observational study. Patients who received warfarin at the Nanjing Drum Tower Hospital from January 2020 to September 2021 (a period of the COVID-19 pandemic in China) were enrolled and analyzed. The study protocol was approved by the Ethics Committee of the

Nanjing Drum Tower Hospital (No. 2020-029). The inclusion criteria were as follows: 1) patients who had been taking warfarin for 3 weeks for thromboprophylaxis of conditions such as atrial fibrillation (AF), deep venous thrombosis (DVT), pulmonary embolism (PE), and valvular heart disease (VHD); 2) age ≥18 years; and 3) had at least four eligible INR values, and the total follow-up time was more than 30 days. The exclusion criteria were as follows: 1) patients whose interval between any two adjacent INR was >120 days and who were considered lost to follow-up; 2) patients who had to discontinue warfarin therapy due to surgery or other reasons during the study period; and 3) patients with pregnancy, malignant tumor, or hemodialysis treatment.

Patients could choose anticoagulation management modes according to their conditions and were divided into two groups: the HAC group comprising patients who obtain AMSs through the hospital anticoagulation clinic, and the IAC group comprising patients who obtain AMSs through the "Internet + Anticoagulation clinic". For patients in the HAC group, the INR results were derived from blood analysis at the Drum Tower Hospital. For patients in the IAC group, the INR results were derived from blood analysis at local hospitals or point-of-care test (POCT).

Anticoagulation management modes

Specialist anticoagulation pharmacists provided AMSs through HAC and IAC for patients with chronic warfarin treatment. In order to eliminate biases from management content, both modes followed a standard interview with the same structure. Pharmacists collected relative information, including demographic characteristics, comorbidities, patient compliance, INR values, previous warfarin doses, concomitant medication, and adverse events. Then, pharmacists informed patients of warfarin dosing decisions and follow-up plans and conducted detailed medication education.

The IAC was a virtual clinic powered by the Internet and a mobile phone application (APP). Patients needed to fill in basic information when logging in to the APP and then upload photos of the INR test and answer questions about compliance, adverse events, and changes in concomitant medication since the previous test. Pharmacists would communicate with the patients through the APP conversation window and inform patients with medication education the dose of warfarin and follow-up plans.

Data collection

Data were collected from the hospital information system and standardized anticoagulation record database administered by pharmacists. Basic information was recorded for each patient, including demographic characteristics, indications for warfarin, and location. INR values, warfarin dose, adverse events, concomitant medication, and test date were recorded at each encounter in a standardized anticoagulation record database.

Study outcomes

The primary outcome was anticoagulation quality. Patients were considered to have good anticoagulation quality (the INR value was within the therapeutic range stably) only when they met both the criteria: TTR ≥60% and INR variability <0.65. Secondary outcomes were the incidence of adverse events, including thromboembolic and bleeding events.

The TTR was calculated using a linear interpolation method recommended by Rosendaal et al. (1993). Referring to the prevailing antithrombotic guidelines in China, the recommended therapeutic range of the INR was 2.0–3.0 for patients with AF, PE, and DVT and 1.5–2.5 for patients with VHD (diseases, 2018). INR variability was calculated using the method described by Fihn et al. (Fihn et al., 2003; van Leeuwen et al., 2008). INR_i is the INR value of each test, and τ_i is the time interval between two INR tests (van Leeuwen et al., 2008). INR variability measured the stability of INR control by calculating the time-weighted INR variance. The study conducted by Labaf et al. (2015) confirmed that when the INR variability was ≥0.65, the risk of thromboembolism and major bleeding was significantly increased. Therefore, the patients were divided into two groups: the good anticoagulation quality group comprised patients who met both TTR ≥60% and INR variability <0.65, and the other patients were found in the poor anticoagulation quality group.

$$\sigma^2 = \frac{1}{n-1}\sum_{i=2}^{n}\frac{(INR_i - INR_{i-1})^2}{\tau_i}, \tau = \tau_i - \tau_{i-1} \quad (1)$$

Secondary outcomes were thromboembolism and bleeding events. Thromboembolism included DVT, PE, systemic embolism (SE), stroke, and transient ischemic attack (TIA) (Wallentin et al., 2010). Referring to the recommendations of the International Society of Thrombosis and Hemostasis (ISTH), bleeding events included major bleeding and clinically relevant non-major bleeding (CRNMB) (Schulman et al., 2010).

Machine learning model development

The whole dataset was randomly assigned to a training set for training the model and a test set for evaluating the model (7:3), meaning that the ratio of patients with poor anticoagulation quality was maintained across both sets. The correlations of categorical and continuous variables with the anticoagulation quality were assessed using the chi-square test and the

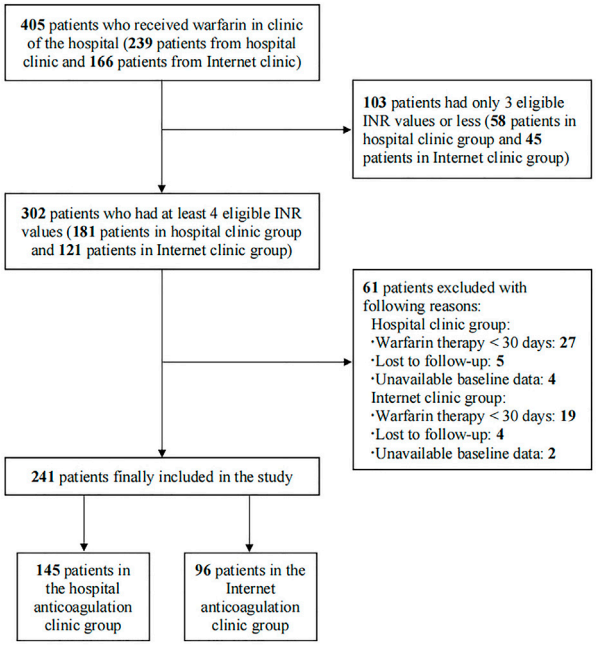

FIGURE 1
Flow diagram of the selection of patients.

Wilcoxon–Mann–Whitney test, respectively (Morang'a et al., 2020). The variables with $p < 0.05$ were considered statistically significant and were included in machine learning to avoid the inference of irrelevant features (Liu et al., 2021).

To select the ML algorithm that exhibits the best predictive ability, five well-accepted ML classifiers, K-nearest neighbors (KNN), support vector machine (SVM), random forest classifier (RFC), eXtreme Gradient Boosting (XGBoost), and Light Gradient Boosting Machine (LightGBM), were implemented for model construction to predict anticoagulation quality. The synthetic minority oversampling technique (SMOTE) (Blagus and Lusa, 2013) was used to balance the unbalanced data in the training set, and then the training set was learned by five ML algorithms to construct the model with 5-fold cross-validation, and the optimal value of the hyperparameters was determined using a grid search algorithm.

The receiver operating characteristic curve (ROC) and area under the curve (AUC), sensitivity, specificity, and accuracy in the test set were calculated to evaluate the predictive performance of five ML models. Then, the Shapley Additive exPlanations (SHAP) method, a visualized approach based on game theory, was used to interpret the individual variable impacts on the ML models (Lundberg and Lee, 2017).

Statistical analyses

Continuous variables were reported as median value and interquartile range (IQR) and were compared using the Wilcoxon–Mann–Whitney test. Categorical data were expressed as frequencies and percentages and were compared by the chi-square test or Fisher test. $p < 0.05$ was considered statistically significant. The ML algorithms were performed using *Python* 3.8 (https://www.python.org/) and the scikit-learn framework (https://www.scikit-learn.org/stable/). All statistical analyses were conducted using SPSS (version 22.0).

Results

Patient characteristics

A total of 405 patients who received warfarin were reviewed initially between January 2020 and September 2021, and the process of patient selection is presented in Figure 1. Finally, 241 patients were included in this study, 145 patients in the HAC group and 96 in the IAC group. Table 1 presented the demographics and characteristics of the patients. The median age of the patients was 57 years, 128 (53.1%) patients were male, and the main indication for warfarin treatment was VHD (93.8%). Hypertension (37.8%) and pulmonary arterial hypertension (39.0%) were the most common comorbidities. Beta-blockers (60.2%) were the most common concomitant medication. No significant difference was observed in baseline characteristics between the HAC and IAC groups.

Anticoagulation quality of patients in HAC and IAC

The TTR, INR variability, and adverse events of 241 patients with 1652 INR values were calculated (Table 2). 106 (73.1%) and 67 (69.8%) patients had good anticoagulation quality in the HAC group and the IAC group, and the average TTR was 79.9 ± 20.0% and 80.6 ± 21.1%, respectively. The average TTR of the 241 patients included in this study was 80.2 ± 20.4%. During the follow-up period, five patients (2.07%) experienced thromboembolic or major bleeding events and needed hospital admission care, and the remaining suffered only minor bleeding. No significant difference in the incidences of major bleeding (0.69 vs. 1.0%, $p = 1.000$), CRNMB (39.3 vs. 40.6%, $p = 0.838$), and thromboembolic (1.4 vs. 1.0%, $p = 1.000$) was detected between patients in the HAC group and the IAC group.

TABLE 1 Demographics and characteristics of patients classified by anticoagulation management mode.

Characteristics	All patients (n = 241)	Hospital anticoagulation clinic (n = 145)	Internet anticoagulation clinic (n = 96)	p value
Age, years	57 (47, 66)	57 (46, 66)	56 (48, 66)	0.848
Male, n (%)	128 (53.1)	78 (53.8)	50 (52.1)	0.795
BMI (kg/m^2)	22.9 (20.5, 25.2)	23.2 (20.8, 25.8)	22.0 (20.3, 24.8)	0.061
INR therapeutic range, n (%)				
1.5–2.5	226 (93.8)	135 (93.1)	91 (94.8)	0.595
2.0–3.0	15 (6.2)	10 (6.9)	5 (5.2)	
Education, n (%)				0.280
Primary school and below	78 (32.4)	42 (29.0)	36 (37.5)	
Middle school and above	163 (67.6)	103 (71.0)	60 (62.5)	
Comorbidities, n (%)				
Hypertension	91 (37.8)	54 (37.2)	37 (38.5)	0.838
Diabetes	13 (5.4)	8 (5.5)	5 (5.2)	0.917
Coronary artery disease	34 (14.1)	19 (13.1)	15 (15.6)	0.582
Pulmonary arterial hypertension	94 (39.0)	52 (35.9)	42 (43.8)	0.219
Renal insufficiency	18 (7.5)	8 (5.5)	10 (10.4)	0.157
History of thromboembolism	7 (2.9)	4 (2.8)	3 (3.1)	1.000
History of stroke	23 (9.5)	14 (9.7)	9 (9.4)	0.942
History of hemorrhage	3 (1.2)	1 (0.7)	2 (2.1)	0.717
Medications, n (%)				
Aspirin	23 (9.5)	15 (10.3)	8 (8.3)	0.603
Amiodarone	22 (9.1)	11 (7.6)	11 (11.5)	0.307
Digoxin	46 (19.1)	25 (17.2)	21 (21.9)	0.370
ACEI/ARB	28 (11.6)	15 (10.3)	13 (13.5)	0.448
Beta-blockers	145 (60.2)	91 (62.8)	54 (56.3)	0.312
Statins	44 (18.3)	32 (22.1)	12 (12.5)	0.060

BMI, body mass index; INR, international normalized ratio; ACEI, angiotensin-converting enzyme inhibitors; ARB, angiotensin receptor blocker.

Machine learning models for anticoagulation quality prediction

The 241 patients were classified according to anticoagulation quality (good anticoagulation quality group and poor anticoagulation quality group). The baseline characteristics of the two groups are shown in Table 3. The whole dataset was randomly assigned to a training set and a test set, and the baselines of the two sets were relatively balanced (Supplementary Table S1). According to variable selection, seven variables were significantly correlated with the chronic anticoagulation quality in the training set, including age, education, hypertension, renal insufficiency, and combined use of aspirin, amiodarone, and statins (Supplementary Table S2). Heatmap visualization of the correlations between the anticoagulation quality and the variables in the training set is shown in Supplementary Figure S1.

Five ML models were developed using seven selected variables on the training set to predict anticoagulation quality. The optimal value for the hyperparameters with a grid search algorithm is shown in Supplementary Table S3, and the results for five folds are shown in Supplementary Table S4. Then, the test set was used to test the predictive performance of each model, and the results are shown in Table 4 and Figure 2. Although the RFC model has the best specificity among the five models, the high sensitivity is particularly critical given that model is designed to recognize more patients with poor anticoagulation quality, and the XGBoost model is the optimum model with the consideration of the best sensitivity (76.7%), AUC (0.808), and accuracy (0.767).

The SHAP method was used to interpret the optimum ML model (XGBoost) and provided a direct visual understanding of feature contributions. The results suggested that age, education, hypertension, aspirin, and amiodarone were the top five important features, as shown in Figure 3. Poor anticoagulation quality was a high probability with patients of older age, low education, hypertension, aspirin, and amiodarone.

TABLE 2 Comparison of clinical outcomes of Hospital anticoagulation clinic vs. Internet anticoagulation clinic.

Clinical outcomes	All patients (n = 241)	Hospital anticoagulation clinic (n = 145)	Internet anticoagulation clinic (n = 96)	p value
Good anticoagulation quality	173 (71.8)	106 (73.1)	67 (69.8)	0.576
TTR (%)	80.2 ± 20.4	79.9 ± 20.0	80.6 ± 21.1	0.644
TTR ≥60%, n (%)	203 (84.2)	122 (84.1)	81 (84.4)	0.961
INR variability ≥0.65	46 (19.1)	26 (17.9)	20 (20.8)	0.575
Major bleeding, n (%)	2 (0.83)	1 (0.69)	1 (1.0)	1.000
CRNMB, n (%)	96 (39.8)	57 (39.3)	39 (40.6)	0.838
Oral hemorrhage	40 (16.6)	22 (15.2)	18 (18.8)	0.465
Epistaxis	20 (8.3)	15 (10.3)	5 (5.2)	0.157
Subconjunctival bleeding	10 (4.1)	6 (4.1)	4 (4.2)	1.000
Subcutaneous bleeding	12 (5.0)	4 (2.8)	8 (8.3)	0.100
Gastrointestinal bleeding	7 (2.9)	6 (4.1)	1 (1.0)	0.313
Hematuria	5 (2.1)	3 (2.1)	2 (2.1)	1.000
Metrorrhagia	2 (0.83)	1 (0.69)	1 (1.0)	1.000
Thromboembolic events, n (%)	3 (1.2)	2 (1.4)	1 (1.0)	1.000
Peripheral artery thrombosis	1 (0.4)	0 (0.0)	1 (1.0)	0.398
Valve thrombosis	1 (0.4)	1 (0.69)	0 (0.0)	1.000
Stroke	1 (0.4)	1 (0.69)	0 (0.0)	1.000

INR, international normalized ratio; TTR, time in therapeutic range; CRNMB, clinically relevant non-major bleeding.

TABLE 3 Demographics and characteristics of patients classified by anticoagulation quality.

Characteristics	Good anticoagulation quality (n = 173)	Poor anticoagulation quality (n = 68)	p value
Age, years	54 (42.5, 63)	65 (55.3, 71)	0.000*
Male, n (%)	93 (53.8)	35 (51.5)	0.749
BMI (kg/m^2)	22.8 (20.3, 25.3)	23.1 (21.1, 25.1)	0.454
Education, n (%)			0.000*
Primary school and below	41 (23.7)	37 (54.4)	
Middle school and above	132 (76.3)	31 (45.6)	
Comorbidities, n (%)			
Hypertension	57 (32.9)	34 (50.0)	0.014*
Diabetes	6 (3.5)	7 (10.3)	0.073
Coronary artery disease	23 (13.3)	11 (16.2)	0.563
Renal insufficiency	8 (4.6)	10 (14.7)	0.007*
Pulmonary arterial hypertension	64 (37.0)	30 (44.1)	0.308
History of thromboembolism	4 (2.3)	3 (4.4)	0.655
History of stroke	16 (9.2)	7 (10.3)	0.804
History of hemorrhage	1 (0.6)	2 (2.9)	0.193
Medications, n (%)			
Aspirin	10 (5.8)	13 (19.1)	0.002*
Amiodarone	9 (5.2)	13 (19.1)	0.001*
Digoxin	29 (16.8)	17 (25.0)	0.143
ACEI/ARB	17 (9.8)	11 (16.2)	0.166
Beta-blockers	107 (61.8)	38 (55.9)	0.394
Statins	26 (15.0)	18 (26.5)	0.039*

*Univariate analysis showed significant difference between the two group.
BMI, body mass index; INR, international normalized ratio; ACEI, angiotensin-converting enzyme inhibitors; ARB, angiotensin receptor blocker.

TABLE 4 Prediction performance of the five machine learning models on the test set.

Machine learning model	AUC	Sensitivity	Specificity	Accuracy
KNN	0.617	0.6316	0.5185	0.548
SVM	0.801	0.790	0.593	0.644
RFC	0.786	0.737	0.778	0.767
XGBoost	0.808	0.790	0.759	0.767
LightGBM	0.795	0.737	0.685	0.699

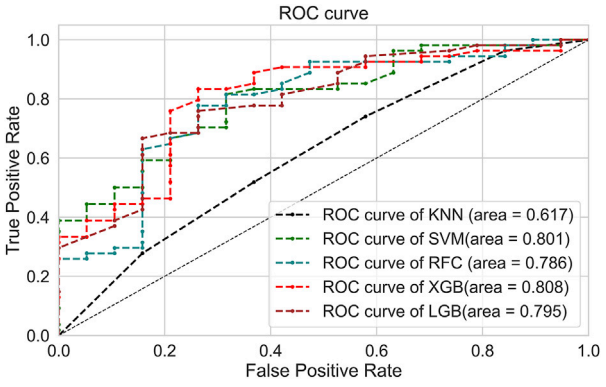

FIGURE 2
Receiver operating characteristic curve of the ML models.

Discussion

In this study, the Internet and machine learning techniques were used for the first time to optimize warfarin anticoagulation management during the COVID-19 pandemic in China. The role of the IAC in the care of patients who received warfarin during the COVID-19 pandemic was proven, and no significant difference in anticoagulation quality and incidence of adverse events was detected between patients in the IAC and HAC groups. The IAC could break the difficulties of medical treatment due to COVID-19-induced lockdowns, which was an important healthcare approach during the COVID-19 pandemic. Furthermore, we used both INR variability and TTR to measure the anticoagulation quality and for the first time developed an ML model (XGBoost) to predict anticoagulation quality and make individual decisions regarding who could benefit from active intervention.

The universally adopted strategy of reducing social interaction during the COVID-19 pandemic has led to unprecedented difficulties in the ongoing healthcare of chronically ill patients (Kow et al., 2020; Prem et al., 2020). A new approach to patient care was demanded. In this study, patients in the IAC group had a similar anticoagulation quality to those in the HAC group, and both groups had good anticoagulation quality. The average TTR of patients in the two groups was 79.9 ± 20.0% and 80.6 ± 21.1%, respectively. A meta-analysis pooling 95 studies worldwide reported that the patients were only 61% of the time in the therapeutic range (Mearns et al., 2014), and the TTR of patients managed in our institution was better than this level. It was interesting to note that patients in the HAC group achieved good anticoagulation quality even during the COVID-19 pandemic, which was consistent with the study conducted by Cope et al. (2021). However, patients in the HAC group needed to pay more time and money to obtain AMSs than before the COVID-19 pandemic and were at risk of exposure to COVID-19. The use of telemedicine for patient care, such as IAC, ensured social distancing and reduced person-to-person contact. It provided convenient access to routine care with low risk of virus transmission (Al Ammari et al., 2021).

High-quality anticoagulation was the key to ensure efficacy and safety of warfarin administration (Singer et al., 2013). Therefore, it is important for clinical pharmacists to identify patients with poor anticoagulation quality accurately and carry out interventions for these patients early, especially during the COVID-19 pandemic. We applied an ML algorithm to develop a prediction model of warfarin anticoagulation quality in the Chinese population for the first time. The XGBoost is an ensemble algorithm based on a tree-like structure, which combines multiple individual weak prediction models to produce a robust predictive estimator (Huang et al., 2021) and showed good predictive performance in this study, with AUC = 0.808 and accuracy = 0.767. Several studies have been conducted, such as the SAME-TT$_2$R$_2$ score (Apostolakis et al., 2013) and the Nomogram model established by Wang et al. (2021), both of which were used to predict the anticoagulation quality in AF patients, with a moderate predictive ability (c-index of SAME-TT$_2$R$_2$ = 0.72; c-index of the Nomogram model = 0.718). However, a single TTR value was used in both studies to evaluate the anticoagulation quality, and TTR could not measure the degree of stability of INR control, resulting in the limitation of anticoagulation quality evaluation (Wang et al., 2021). Even if the patient had a high TTR, the unstable anticoagulation intensity would lead to poor prognosis, and INR variability could compensate for this deficiency. Therefore, patients with a high TTR and low INR variability were defined as those with good anticoagulation quality in this study, whose INR value remained stable within the therapeutic range. The better anticoagulation quality standard and more

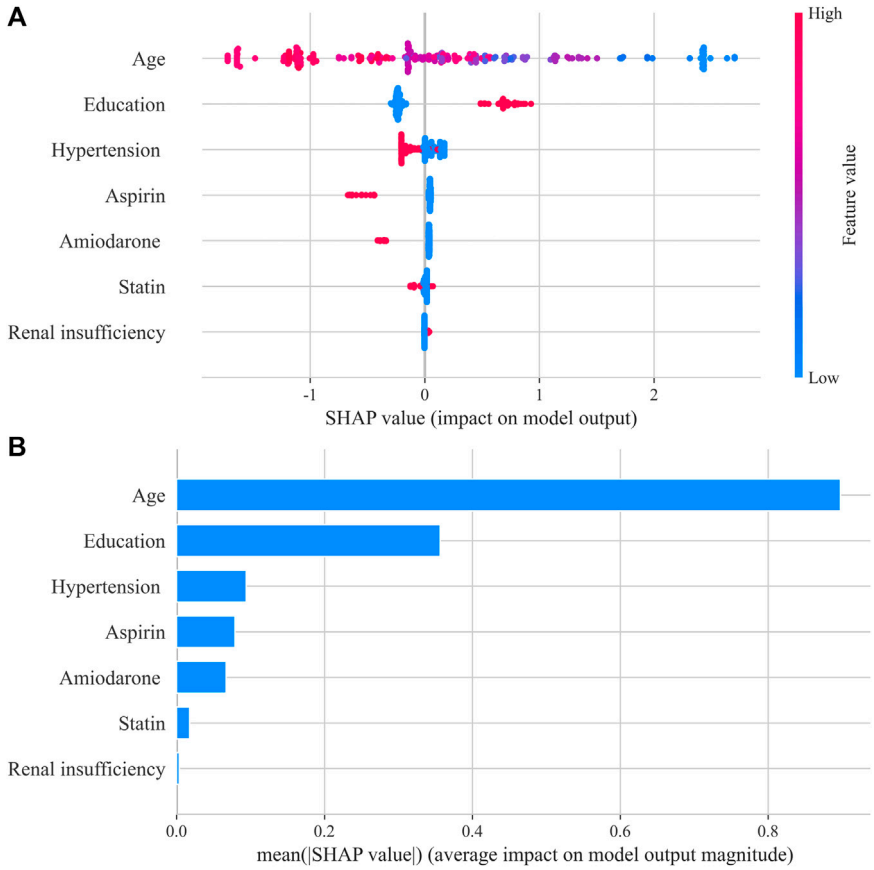

FIGURE 3
Shapley Additive exPlanations (SHAP) summary plot in the XGBoost model. **(A)** SHAP beeswarm plot showed the distribution of SHAP values of each feature. Red represents higher feature values, and blue represents lower feature values. **(B)** Typical bar chart of feature importance was shown based on the mean absolute SHAP value of each feature.

accurate prediction ability than that of the SAMe-TT$_2$R$_2$ score and the Nomogram model gave the XGBoost model considerable value for clinical application.

It is crucial for medical staff to understand how the model predicts risk for patients (Zheng et al., 2022). In this study, the risk factors associated with poor anticoagulation quality were ranked and provided a visual interpretation by the SHAP method. Age was the driving predictor of poor anticoagulation quality, which was also an important predictor of the SAME-TT$_2$R$_2$ model (Apostolakis et al., 2013) and the nomogram model (Wang et al., 2021). In elderly patients, the decline in self-management ability, multiple additional complications, and multiple medications was common, which would inevitably impact the efficacy of warfarin (Qiu et al., 2020). In addition, patients with low educational background were associated with poor anticoagulation quality and had insufficient understanding of the importance of warfarin therapy and insufficient knowledge of anticoagulation, resulting in a lack of self-management ability (Rodriguez et al., 2013). Therefore, medication education was crucial for these patients, which should be focused on by clinical pharmacists in clinical work. Hypertension and renal insufficiency were also associated with the poor quality of anticoagulation, which has been interpreted in previous studies. Renal insufficiency was associated with poor anticoagulation quality in Americans (Pokorney et al., 2015), and hypertension contributed to poor anticoagulation quality in African patients (Mwita et al., 2018). In addition, concomitant medications, such as amiodarone and aspirin, were found to be indicators of poor INR control. Amiodarone competes with warfarin for cytochrome P450 2C9, which is the major enzyme of warfarin metabolism, leading to fluctuations in anticoagulation intensity and even major bleeding events (Holm et al., 2017). Interactions of aspirin and warfarin on different components of the coagulation pathway can increase the risk of bleeding (Proietti and Lip, 2018). Although some factors are the inherent diseases and necessary drug treatment of patients which are hard to change, measures such as strengthening medication education can effectively improve the anticoagulation quality of patients. Previous studies showed that standardized medication education by pharmacists could significantly improve the quality of anticoagulation and also reduced the number of emergency admission (Verret et al., 2012; Neshewat et al., 2021).

Overall, the XGBoost model is expected to be applied in practice to select patients who could benefit from active intervention to improve warfarin treatment during the COVID-19 pandemic.

Limitations

There are several limitations to this study. First, this was a retrospective, observational study that might introduce selection bias. Second, patients in the IAC group were allowed to get the INR results from blood analysis at local hospitals, although patients could simplify the process of medical care in the local hospital, person-to-person contact could not be completely avoided, and POCT is a novel method for anticoagulation management during the COVID-19 pandemic. Third, some variables have not been collected, such as the patients' smoking or alcohol intake and patient genotypes (VKORC1 and CYP2C9), which limited the analysis, although patients with smoking and alcohol abuse are rare in our clinical practice. Finally, although the current study supports to apply machine learning models to predict anticoagulation quality as a decision-support technology, external validations are necessary.

Conclusion

In the real-world setting of our hospital, "Internet + Anticoagulation clinic" played a positive role in warfarin treatment during the COVID-19 pandemic, which ensured good anticoagulation quality and decreased person-to-person contact, with a low risk of virus transmission. Furthermore, the ML model offers a new avenue to select patients at high risk of poor anticoagulation quality, which can improve the warfarin therapy decision-making during the COVID-19 pandemic.

Data availability statement

The data that support the finding of this study is available on request from the corresponding author. The data are not publicly available due to ethical restrictions.

Ethics statement

The studies involving human participants were reviewed and approved by the Ethics Committee of the Nanjing Drum Tower Hospital (No.2020-029). Written informed consent for participation was not required for this study in accordance with the national legislation and the institutional requirements.

Author contributions

HX and GW-H are the guarantors of the entire manuscript. DM-F, LS-Y, and J-FZ contributed to the study conception and design; data acquisition, analysis, and interpretation; drafting of the manuscript; and critical revision of the manuscript for important intellectual content. B-YW, ZL, and YF contributed to the data acquisition, analysis, and interpretation. All authors contributed to the article and approved the submitted version.

Funding

The authors disclosed receipt of the following financial support for the research, authorship, and/or publication of this article: This study was funded by the Nanjing Medical Science and Technology Development Fund (QRX17060) and Jiangsu Pharmaceutical Association Shire Biopharmaceutical Fund (S201606).

Acknowledgments

We would like to show our gratitude to Dong-Jin Wang, the head of cardiothoracic Surgery Department of Drum Tower Hospital affiliated to Nanjing University Medical School, for support of the research.

Conflict of interest

The authors declare that the research was conducted in the absence of any commercial or financial relationships that could be construed as a potential conflict of interest.

Publisher's note

Supplementary material

The Supplementary Material for this article can be found online at: https://www.frontiersin.org/articles/10.3389/fphar.2022.933156/full#supplementary-material

References

Ahmed, N. O., Osman, B., Abdelhai, Y. M., and El-Hadiyah, T. M. H. (2017). Impact of clinical pharmacist intervention in anticoagulation clinic in Sudan. *Int. J. Clin. Pharm.* 39 (4), 769–773. doi:10.1007/s11096-017-0475-x

Al Ammari, M., AlThiab, K., AlJohani, M., Sultana, K., Maklhafi, N., AlOnazi, H., et al. (2021). Tele-pharmacy anticoagulation clinic during COVID-19 pandemic: Patient outcomes. *Front. Pharmacol.* 12, 652482. doi:10.3389/fphar.2021.652482

Apostolakis, S., Sullivan, R. M., Olshansky, B., and Lip, G. Y. H. (2013). Factors affecting quality of anticoagulation control among patients with atrial fibrillation on warfarin: The SAMe-tt2r$_2$ score. *Chest* 144 (5), 1555–1563. doi:10.1378/chest.13-0054

Blagus, R., and Lusa, L. (2013). SMOTE for high-dimensional class-imbalanced data. *BMC Bioinforma.* 14, 106. doi:10.1186/1471-2105-14-106

Cope, R., Fischetti, B., Eladghm, N., Elaskandrany, M., and Karam, N. (2021). Outpatient management of chronic warfarin therapy at a pharmacist-run anticoagulation clinic during the COVID-19 pandemic. *J. Thromb. Thrombolysis* 52 (3), 754–758. doi:10.1007/s11239-021-02410-w

diseases, E. C. (2018). Chinese guidelines for the prevention and treatment of thrombotic diseases. *Chin. Med. J.* 98, 2861–2888.

Fihn, S. D., Gadisseur, A. A., Pasterkamp, E., van der Meer, F. J., Breukink-Engbers, W. G., Geven-Boere, L. M., et al. (2003). Comparison of control and stability of oral anticoagulant therapy using acenocoumarol versus phenprocoumon. *Thromb. Haemost.* 90 (2), 260–266. doi:10.1160/th02-10-0179

Gong, K., Xu, Z., Cai, Z., Chen, Y., and Wang, Z. (2020). Internet hospitals help prevent and control the epidemic of COVID-19 in China: Multicenter user profiling study. *J. Med. Internet Res.* 22 (4), e18908. doi:10.2196/18908

Gu, Z. C., Kong, L. C., Yang, S. F., Wei, A. H., Wang, N., Ding, Z., et al. (2019). Net clinical benefit of non-vitamin K antagonist oral anticoagulants in atrial fibrillation and chronic kidney disease: A trade-off analysis from four phase III clinical trials. *Cardiovasc. Diagn. Ther.* 9 (5), 410–419. doi:10.21037/cdt.2019.07.09

Gu, Z. C., Zhou, L. Y., Shen, L., Zhang, C., Pu, J., Lin, H. W., et al. (2018). Non-vitamin K antagonist oral anticoagulants vs. Warfarin at risk of fractures: A systematic review and meta-analysis of randomized controlled trials. *Front. Pharmacol.* 9, 348. doi:10.3389/fphar.2018.00348

Holbrook, A., Schulman, S., Witt, D. M., Vandvik, P. O., Fish, J., Kovacs, M. J., et al. (2012). Evidence-based management of anticoagulant therapy: Antithrombotic therapy and prevention of thrombosis, 9th ed: American college of chest physicians evidence-based clinical practice guidelines. *Chest* 141 (2), e152S–e184S. doi:10.1378/chest.11-2295

Holm, J., Lindh, J. D., Andersson, M. L., and Mannheimer, B. (2017). The effect of amiodarone on warfarin anticoagulation: A register-based nationwide cohort study involving the Swedish population. *J. Thromb. Haemost.* 15 (3), 446–453. doi:10.1111/jth.13614

Huang, X., Yu, Z., Wei, X., Shi, J., Wang, Y., Wang, Z., et al. (2021). Prediction of vancomycin dose on high-dimensional data using machine learning techniques. *Expert Rev. Clin. Pharmacol.* 14 (6), 761–771. doi:10.1080/17512433.2021.1911642

Jiang, S., Lv, M., Zeng, Z., Fang, Z., Chen, M., Qian, J., et al. (2022). Efficacy and safety of app-based remote warfarin management during COVID-19-related lockdown: A retrospective cohort study. *J. Thromb. Thrombolysis* 54, 20–28. doi:10.1007/s11239-021-02630-0

Kish, K., and Lekic, S. (2021). Implementation of warfarin to direct oral anticoagulant conversion initiative in pharmacist-run anticoagulation clinics during COVID-19 pandemic. *J. Am. Coll. Clin. Pharm.* 4, 1154–1160. doi:10.1002/jac5.1470

Kow, C. S., Sunter, W., Bain, A., Zaidi, S. T. R., and Hasan, S. S. (2020). Management of outpatient warfarin therapy amid COVID-19 pandemic: A practical guide. *Am. J. Cardiovasc. Drugs* 20 (4), 301–309. doi:10.1007/s40256-020-00415-z

Labaf, A., Själander, A., Stagmo, M., and Svensson, P. J. (2015). INR variability and outcomes in patients with mechanical heart valve prosthesis. *Thromb. Res.* 136 (6), 1211–1215. doi:10.1016/j.thromres.2015.10.044

Liu, Y., Chen, J., You, Y., Xu, A., Li, P., Wang, Y., et al. (2021). An ensemble learning based framework to estimate warfarin maintenance dose with cross-over variables exploration on incomplete data set. *Comput. Biol. Med.* 131, 104242. doi:10.1016/j.compbiomed.2021.104242

Lundberg, S. M., and Lee, S. I. (2017). "A unified approach to interpreting model predictions," in *Advances in neural information processing systems* (Long Beach, CA: Neural Information Processing Systems), 4765–4774.

Manzoor, B. S., Cheng, W. H., Lee, J. C., Uppuluri, E. M., and Nutescu, E. A. (2017). Quality of pharmacist-managed anticoagulation therapy in long-term ambulatory settings: A systematic review. *Ann. Pharmacother.* 51 (12), 1122–1137. doi:10.1177/1060028017721241

Mearns, E. S., White, C. M., Kohn, C. G., Hawthorne, J., Song, J. S., Meng, J., et al. (2014). Quality of vitamin K antagonist control and outcomes in atrial fibrillation patients: A meta-analysis and meta-regression. *Thromb. J.* 12, 14. doi:10.1186/1477-9560-12-14

Morang'a, C. M., Amenga-Etego, L., Bah, S. Y., Appiah, V., Amuzu, D. S. Y., Amoako, N., et al. (2020). Machine learning approaches classify clinical malaria outcomes based on haematological parameters. *BMC Med.* 18 (1), 375. doi:10.1186/s12916-020-01823-3

Mwita, J. C., Francis, J. M., Oyekunle, A. A., Gaenamong, M., Goepamang, M., and Magafu, M. (2018). Quality of anticoagulation with warfarin at a tertiary hospital in Botswana. *Clin. Appl. Thromb. Hemost.* 24 (4), 596–601. doi:10.1177/1076029617747413

Neshewat, J., Wasserman, A., Alexandris-Souphis, C., Haymart, B., Feldeisen, D., Kong, X., et al. (2021). Reduction in epistaxis and emergency department visits in patients taking warfarin after implementation of an education program. *Thromb. Res.* 199, 119–122. doi:10.1016/j.thromres.2021.01.007

Numao, Y., Suzuki, S., Arita, T., Yagi, N., Otsuka, T., Sagara, K., et al. (2017). Predictors of international normalized ratio variability in patients with atrial fibrillation under warfarin therapy. *Circ. J.* 82 (1), 39–45. doi:10.1253/circj.CJ-16-1217

Pokorney, S. D., Simon, D. N., Thomas, L., Fonarow, G. C., Kowey, P. R., Chang, P., et al. (2015). Patients' time in therapeutic range on warfarin among US patients with atrial fibrillation: Results from ORBIT-AF registry. *Am. Heart J.* 170 (1), 141–148. doi:10.1016/j.ahj.2015.03.017

Prem, K., Liu, Y., Russell, T. W., Kucharski, A. J., Eggo, R. M., Davies, N., et al. (2020). The effect of control strategies to reduce social mixing on outcomes of the COVID-19 epidemic in wuhan, China: A modelling study. *Lancet. Public Health* 5 (5), e261–e270. doi:10.1016/s2468-2667(20)30073-6

Proietti, M., and Lip, G. Y. H. (2018). Impact of quality of anticoagulation control on outcomes in patients with atrial fibrillation taking aspirin: An analysis from the SPORTIF trials. *Int. J. Cardiol.* 252, 96–100. doi:10.1016/j.ijcard.2017.10.091

Qiu, S., Wang, N., Zhang, C., Gu, Z. C., and Qian, Y. (2020). Anticoagulation quality of warfarin and the role of physician-pharmacist collaborative clinics in the treatment of patients receiving warfarin: A retrospective, observational, single-center study. *Front. Pharmacol.* 11, 605353. doi:10.3389/fphar.2020.605353

Rodriguez, F., Hong, C., Chang, Y., Oertel, L. B., Singer, D. E., Green, A. R., et al. (2013). Limited English proficient patients and time spent in therapeutic range in a warfarin anticoagulation clinic. *J. Am. Heart Assoc.* 2 (4), e000170. doi:10.1161/jaha.113.000170

Rosendaal, F. R., Cannegieter, S. C., van der Meer, F. J., and Briët, E. (1993). A method to determine the optimal intensity of oral anticoagulant therapy. *Thromb. Haemost.* 69 (3), 236–239. doi:10.1055/s-0038-1651587

Schulman, S., Angerås, U., Bergqvist, D., Eriksson, B., Lassen, M. R., Fisher, W., et al. (2010). Definition of major bleeding in clinical investigations of antihemostatic medicinal products in surgical patients. *J. Thromb. Haemost.* 8 (1), 202–204. doi:10.1111/j.1538-7836.2009.03678.x

Singer, D. E., Hellkamp, A. S., Piccini, J. P., Mahaffey, K. W., Lokhnygina, Y., Pan, G., et al. (2013). Impact of global geographic region on time in therapeutic range on warfarin anticoagulant therapy: Data from the ROCKET AF clinical trial. *J. Am. Heart Assoc.* 2 (1), e000067. doi:10.1161/jaha.112.000067

van Leeuwen, Y., Rosendaal, F. R., and Cannegieter, S. C. (2008). Prediction of hemorrhagic and thrombotic events in patients with mechanical heart valve prostheses treated with oral anticoagulants. *J. Thromb. Haemost.* 6 (3), 451–456. doi:10.1111/j.1538-7836.2007.02874.x

Verret, L., Couturier, J., Rozon, A., Saudrais-Janecek, S., St-Onge, A., Nguyen, A., et al. (2012). Impact of a pharmacist-led warfarin self-management program on quality of life and anticoagulation control: A randomized trial. *Pharmacotherapy* 32 (10), 871–879. doi:10.1002/j.1875-9114.2012.01116

Vriz, O., Rossi Zadra, A., Eltayeb, A., Asiri, F., Pragliola, C., Fawzy, N., et al. (2021). Loss of engagement in controlling chronic anticoagulation therapy during Covid-19 stringency measures. A single center experience of disproportioned increase of stuck mechanical valves. *Monaldi Arch. Chest Dis.* 92. doi:10.4081/monaldi.2021.2065

Wallentin, L., Yusuf, S., Ezekowitz, M. D., Alings, M., Flather, M., Franzosi, M. G., et al. (2010). Efficacy and safety of dabigatran compared with warfarin at different levels of international normalised ratio control for stroke prevention in atrial fibrillation: An analysis of the RE-LY trial. *Lancet* 376 (9745), 975–983. doi:10.1016/s0140-6736(10)61194-4

Wang, N., Qiu, S., Yang, Y., Zhang, C., Gu, Z. C., and Qian, Y. (2021). Physician-Pharmacist collaborative clinic model to improve anticoagulation quality in atrial fibrillation patients receiving warfarin: An analysis of time in therapeutic range and a Nomogram development. *Front. Pharmacol.* 12, 673302. doi:10.3389/fphar.2021.673302

World Health Organization (2021). WHO announces COVID-19 outbreak a pandemic. OnlineAvailable at: https://www.euro.who.int/en/health-topics/health-emergencies/coronavirus-covid-19/news/news/2020/3/who-announces-covid-19-outbreak-a-pandemic (Accessed April 9, 2022).

Wu, Z., and McGoogan, J. M. (2020). Characteristics of and important lessons from the coronavirus disease 2019 (COVID-19) outbreak in China: Summary of a report of 72 314 cases from the Chinese center for disease control and prevention. *Jama* 323 (13), 1239–1242. doi:10.1001/jama.2020.2648

Zampino, R., Vitrone, M., Spiezia, S., Albisinni, R., and Durante-Mangoni, E. (2021). Remote outpatient management during COVID-19 lockdown: Patient-derived quality assessment. *Qual. Manag. Health Care* 30 (1), 76–77. doi:10.1097/qmh.0000000000000296

Zhang, H. (2020). Early lessons from the frontline of the 2019-nCoV outbreak. *Lancet* 395 (10225), 687. doi:10.1016/s0140-6736(20)30356-1

Zheng, X., Wang, F., Zhang, J., Cui, X., Jiang, F., Chen, N., et al. (2022). Using machine learning to predict atrial fibrillation diagnosed after ischemic stroke. *Int. J. Cardiol.* 347, 21–27. doi:10.1016/j.ijcard.2021.11.005

frontiers | Frontiers in Pharmacology

TYPE Original Research
PUBLISHED 05 October 2022
DOI 10.3389/fphar.2022.946445

OPEN ACCESS

EDITED BY
Fouad Antoine Zouein,
American University of Beirut, Lebanon

REVIEWED BY
Immanuel Selvaraj C,
VIT University, India
Duangjai Tungmunnithum,
Mahidol University, Thailand

*CORRESPONDENCE
Qing-Kun Shen,
qkshen@ybu.edu.cn
Li-Hua Cao,
lhcao@ybu.edu.cn

†These authors have contributed equally to this work

SPECIALTY SECTION
This article was submitted to Cardiovascular and Smooth Muscle Pharmacology, a section of the journal Frontiers in Pharmacology

RECEIVED 17 May 2022
ACCEPTED 24 August 2022
PUBLISHED 05 October 2022

CITATION
Deng H, Xu Q, Sang X-T, Huang X, Jin L-L, Chen F-E, Shen Q-K, Quan Z-S and Cao L-H (2022), Study on the vasodilatory activity of lotus leaf extract and its representative substance nuciferine on thoracic aorta in rats. *Front. Pharmacol.* 13:946445. doi: 10.3389/fphar.2022.946445

Study on the vasodilatory activity of lotus leaf extract and its representative substance nuciferine on thoracic aorta in rats

Hao Deng[1†], Qian Xu[1†], Xiao-Tong Sang[1], Xing Huang[1], Li-Li Jin[1], Fen-Er Chen[1,2], Qing-Kun Shen[1*], Zhe-Shan Quan[1] and Li-Hua Cao[3*]

[1]Key Laboratory of Natural Medicines of the Changbai Mountain, Ministry of Education, College of Pharmacy, Yanbian University, Yanji, China, [2]Shanghai Engineering Center of Industrial Asymmetric Catalysis for Chiral Drugs, Shanghai, China, [3]College of Medical, Yanbian University, Yanji, China

Lotus (*Nelumbo nucifera*) leaves are widely used for both edible and medicinal applications. For its further utilization, we studied the vasodilatory activity of lotus leaf extract for the first time. In this study, we obtained the extracts using different ratios of water and ethanol, which was followed by polarity-dependent extraction. We found that the CH_2Cl_2 layer exhibited better vasodilatory activity (EC_{50} = 1.21 ± 0.10 μg/ml). HPLC and ESI-HRMS analysis of the CH_2Cl_2 layer using the standard product as a control revealed that nuciferine (E_{max} = 97.95 ± 0.76%, EC_{50} = 0.36 ± 0.02 μM) was the main component in this layer. Further research revealed that nuciferine exerts a multi-target synergistic effect to promote vasodilation, via the NO signaling pathway, K^+ channel, Ca^{2+} channel, intracellular Ca^{2+} release, α and β receptors, etc. Nuciferine exhibits good vasodilatory activity, and it exhibits the potential to be utilized as a lead compound.

KEYWORDS

lotus leaves, nuciferine, vasodilation, thoracic aorta, HUVECs

Abbreviations: Ach, acetylcholine chloride; PhE, phenylephrine HCl; MS, mass spectrometry; HPLC, high-performance liquid chromatography; PE, petroleum ether; CH_2Cl_2, dichloromethane; EA, ethyl acetate; PGI_2, prostacyclin; NO, nitric oxide; SNP, sodium nitroprusside; IBMX, 3-isobutyl-1-methylxanthine; cGMP, guanosine 3′,5′-cyclic monophosphate; AA, arachidonic acid; COX, cyclooxygenase; VDCCs, voltage-dependent Ca^{2+} channels; ROCCs, receptor-operated Ca^{2+} channels; TNF-α, tumor necrosis factor-α; Modulators (Table 3).

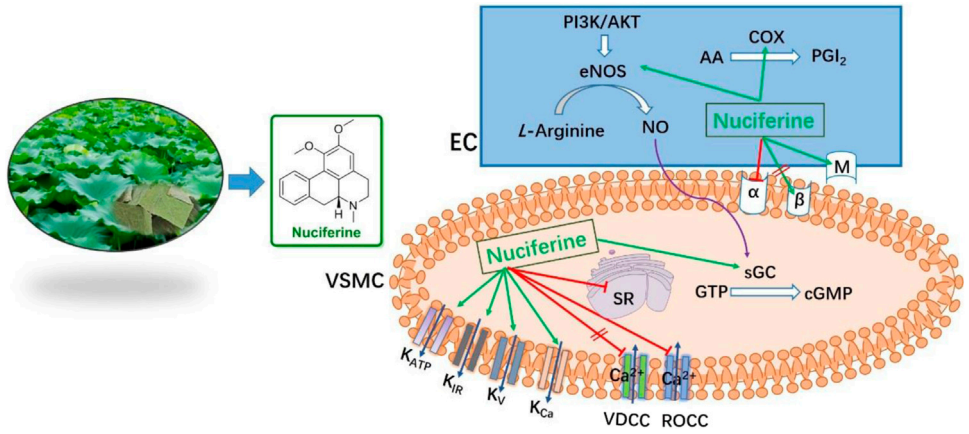

GRAPHICAL ABSTRACT

1 Introduction

Hypertension is a common chronic disease encountered in clinical practice. Based on the related complications, the mortality and disability rate are at the forefront of human diseases, which causes great harm to human health (Wang et al., 2014; Navaneethabalakrishnan et al., 2020). At present, most blood pressure-lowering drugs in clinical use are chemically synthesized. They exhibit several limitations, such as dependence, high toxicity, side effects, and large fluctuations in blood pressure during blood pressure reduction. Traditional Chinese medicine is known to exhibit less toxicity and side effects can exert an antihypertensive effect through multiple channels and targets, is rich in resources, and has broad development and application prospects. In recent years, the discovery of new active ingredients or lead compounds from natural products for the development of new drugs has gained attention for resolving global concerns and in research.

Lotus leaves are the dried leaves of *Nelumbo nucifera* Geartn., a plant belonging to the Nymphaeaceae family (Liu and Fan, 2014). In recent years, more attention has been paid to the research on elucidating the composition and function of lotus leaves. Its main ingredients include alkaloids, volatile oils, organic acids, and flavonoids (Nguyen and Pham, 1998; Ma et al., 2010; Chen and Qi, 2015; Tungmunnithum et al., 2018; Ye et al., 2018). It has various pharmacological activities, such as regulating fat and weight loss (Ma et al., 2015), anti-inflammatory (Wang M. X. et al., 2015), lowering blood pressure (Ye et al., 2014), anti-oxidation (Chen and Zeng, 2001; Chai et al., 2016; Guo et al., 2020), anti-bacterial (Wang et al., 2007; Yuan et al., 2014), anti-spasmodic (Yang et al., 2018), hemostasis (Chen et al., 2020), and hepatoprotective effects (Guo et al., 2013; Qiu et al., 2020; Wang et al., 2020).

Lotus leaves are widely distributed, rich in resources, and inexpensive. They exert the effect of lowering blood pressure, and their alkaloids have been reported to be involved in relaxation (Wang X. et al., 2015; Yang et al., 2018). However, there has been no systematic research on the active ingredients present in lotus leaves. In this study, we aimed to fill in the knowledge gap on lotus leaf and identify the main components of vasodilatory activity, to ensure more effective use of lotus leaves and provide a basis for its future clinical applications.

2 Materials and methods

2.1 Materials

Lotus leaf (*Nelumbo nucifera*) was purchased from Hunan Kang Biotech Co. Ltd. and identified taxonomically by Prof. Chang-hao Zhang (College of Pharmacy, Yanbian University). Acetylcholine chloride (Ach), Phenylephrine HCl (PhE), Modulators were purchased from Sigma Chemical Co (St. Louis, MO, United States).

2.2 Apparatus

Mass spectrometry (MS) was performed on LTQ Orbitrap XL (Thermo Scientific, United States) in electrospray ionization mode. High-performance liquid chromatography (HPLC) was undertaken on an Ultimate 3,000 (ThermoScientific) system.

2.3 Extraction procedures

The purchased lotus leaves were ground into powder. This 10 g of powder was added to a single-necked round-bottomed flask and then 300 ml of various solvents (H_2O; 25% Ethanol; 50% Ethanol; 75% Ethanol; Ethanol) was added to hot melt at

70°C for 6 h. Extracts were passed through a sand-core filter funnel and evaporated under reduced pressure until dry using a rotary evaporator. All dried extracts were weighed and stored at −20°C until use. The yield was calculated as % yield = (weight of dry extract/initial weight of dry sample) × 100.

2.4 Animals and tissues

Animals were strictly handled in accordance with the National Institutes of Health Guidelines for the Care and Use of Laboratory Animals (NIH Publication No. 85–23, revised 1996) and the study was approved by the Institutional Animal Care and Utilization Committee of Yanbian University. Male Sprague-Dawley (SD) rats weighing 250–300 g were used for all experiments, random grouping, 6-8 animals per group. For example, in the intact endothelium experiment, animals were randomly divided into 7 groups with 8 animals in each group (control group, +endo group, Prop group, Atrop group, Indo group, L-NAME group, ODQ group); the experimental results are as follows Figures 6–9. Other animal grouping information was detailed in the Supplementary Information.

SD rats were killed by cervical dislocation. A 3–4 mm long annular segment of the aorta was carefully removed and transferred promptly into ice-cold Krebs solution (NaCl 118.0 mM, KCl 4.7 mm, $MgSO_4$ 1.1 mm, KH_2PO_4 1.2 mm, $CaCl_2$ 1.5 mm, $NaHCO_3$ 25 mm, and glucose 10.0 mm in water, pH 7.4). In some aortic rings, the endothelium was mechanically removed by gently rubbing the surface of the ring back and forth with a plastic tube. Endothelial integrity or functional removal of the constricted blood vessels was confirmed by the presence of relaxation response (over 80%) or its absence (less than 10%) following the treatment with PhE (1 μM) and Ach (1 μM), respectively.

2.5 Isometric vascular tone record

The aortic rings were continuously suspended in a tissue bath containing Krebs solution (pH 7.4) and bubbling 95% O_2–5% CO_2 at 37°C by inserting 2 stainless steel wires into the lumen of the tube. After an equilibration period of 60 min, under a basal tension of 1 g, the force-displacement sensor (JH-2, Institute of Space Medical Engineering, Beijing, China), connected to the biological laboratory system (Model BL-420S, Cheng-du TME Technology Co., Ltd., Chengdu, China), was used to record changes in isometric tension.

2.6 Measurement of the activity of extracts

The contraction of aortic rings was achieved by PhE (1 μM). When the contraction reached a plateau, extracts were added cumulatively (100 μg/ml) to rings with intact endothelium. The relaxation effect was calculated as the percentage of the contraction in response to PhE.

2.7 Different solvent extraction and activity detection

The best solvent extract for vasodilation was extracted with PE, CH_2Cl_2, EA and *n*-butanol in sequence according to polarity.

2.8 HPLC

TSKgel ODS-100V column (C_{18}, 3 μm particle size, 4.6 mm I.D × 15 cm) was employed to separate components in CH_2Cl_2 extracts. The mobile phase was 0.1% trifluoroacetic acid in acetonitrile (HPLC grade) (A) and water (B) gradient elution (10:90–95:5). The run time was 35 min, the flow rate was 1.0 ml/min, and the detection wavelength was 273 nm. We diluted extract with acetonitrile to give a concentration of 5 mg/ml (Standard nuciferine, 0.5 mg/ml, 2 μL), which was passed through a 0.45-μm filter. The injection volume was 10 μL.

2.9 Vascular reactivity assessment

2.9.1 The effect of nuciferine on rat thoracic aorta

To observe the direct effect of nuciferine on the isolated rat aorta, the cumulative concentrations of nuciferine were applied when the tension of thoracic aorta strips was stable, and the vehicle was applied in the control group (Hu et al., 2018).

2.9.2 Vasorelaxant effect of nuciferine on the rat thoracic aorta pre-contracted with PhE

To check the vasorelaxation of nuciferine on the aortic strips with intact or denuded endothelium, after the strips were contracted with PhE (1 μM), a cumulative concentration of nuciferine was added successively into the bath and the changes in the tension were recorded. The percentage of tension change (diastolic ratio) after using nuciferine was calculated as (tension by PhE − tension by nuciferine)/tension by PhE × 100%.

2.9.3 Examination of α_1-receptor activities

To evaluate whether nuciferine acts as an α_1-receptor blockade, endothelium-denuded rings were incubated with the nuciferine (0.3, 0.6,1.2 and 2.4 μM) for 20 min before exposing them to PhE (0.1 nM–10 μM), which was added cumulatively. The obtained results are shown as percentages of contraction, and a comparison was done between the results obtained in the

TABLE 1 Extraction yields, and relaxation of Lotus leaf with different extraction solvents.

Extracting solvents	Yields (%, w/w)	Relaxation (10 μg/ml, %)
H_2O	20.53 ± 0.97	19.65 ± 0.19***
25% Ethanol	19.64 ± 1.74	54.50 ± 4.72***
50% Ethanol	21.21 ± 1.61	78.40 ± 3.25*
75% Ethanol	22.38 ± 1.64	90.63 ± 1.82
Ethanol	8.94 ± 0.96	75.52 ± 6.55*

*Mean $p < 0.05$.
***Mean $p < 0.001$ compared with 75% Ethanol group.
Yield was calculated as % yield = (weight of dry extract/initial weight of dry sample).

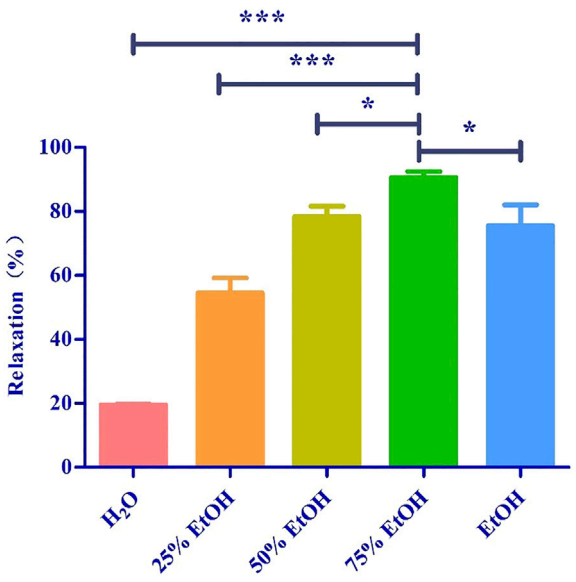

FIGURE 1
Relaxtion of Lotus leaf with different extraction solvents. The data are expressed as the means ± SD of 3 rats ($n = 3$). (* mean $p < 0.05$; *** mean $p < 0.001$ vs. 75% Ethanol group).

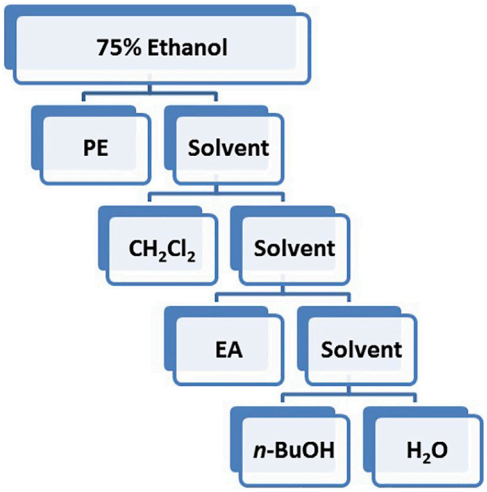

FIGURE 2
Flow chart of different solvent extraction.

absence (control) and the presence of the nuciferine (Cao et al., 2020).

2.9.4 Examination of β and M receptor activities

To assess whether the vasorelaxation induced by nuciferine is associated with β and M receptors, the aortic rings were pre-treated with 1 μM of propranolol or 1 μM of atropine for 20 min before the addition of 1 μM of PhE. The nuciferine (0.03–2.4 μM) was then added cumulatively.

2.9.5 Effects of PGI_2 on nuciferine-induced relaxation

To explore the possible participation of endothelium-derived prostacyclin (PGI_2) pathways, the endothelium-intact strips were firstly incubated with 10 μM of Indo, then contracted by PhE (1 μM) and finally a cumulative concentration of nuciferine (0.03–2.4 μM) was added to observe its vasorelaxation (Yang et al., 2020).

2.9.6 Effects of eNOS/sGC/cGMP signaling pathways

To explore the possible participation of endothelium-derived nitric oxide (NO) pathways, the endothelium-intact strips were firstly incubated with *L*-NAME (100 μM) or ODQ (10 μM) or, then, contracted by PhE (1 μM), and finally a cumulative concentration of nuciferine (0.03–2.4 μM) was added to observe its vasorelaxation PhE (1 μM) was precontracted to endothelium-denuded aortic ring and treated with drugs; SNP was used as a positive control. After the experiment, liquid nitrogen quickly freezes the vascular ring. The experimental operations were performed in the presence of the non-specific phosphodiesterase inhibitor IBMX, 10 μM. The frozen aorta was ground in a stainless

TABLE 2 Extraction yields, and relaxation of different solvent extraction.

Extracting solvents	Yields (%, w/w)	Relaxation (10 μg/ml, %)	EC_{50} μg/mL
PE	11.03 ± 1.41	22.20 ± 3.44***	Na
CH_2Cl_2	11.79 ± 2.12	98.22 ± 1.01	1.21 ± 0.10
EA	9.60 ± 0.64	18.44 ± 2.27***	Na
n-BuOH	26.40 ± 1.36	68.43 ± 7.76***	Na
H_2O	35.14 ± 1.13	16.55 ± 0.44***	Na

***Mean $p < 0.001$ compared with 75% Ethanol group.

TABLE 3 Modulators used for the vasorelaxative effect.

Modulator	Abbreviation	Inhibitory
Atropine	Atrop	Muscarinic receptor (M receptor)
Propranolol	Prop	β-Adrenergic receptor (β receptor)
Indomethacin	Indo	Cyclooxygenase (COX)
N^G-nitro-*L*-arginine methylester	*L*-NAME	nitric oxide synthase (NOS)
1*H*-[1,2,4]-oxadia-zolo-[4,3-a]-quinoxalin-1-one	ODQ	soluble guanylate cyclase (sGC)
Tetraethylammonium	TEA	Ca^{2+}-activated K^+ (K_{Ca}) channels
Glibenclamide	Gli	ATP-sensitive K^+ (K_{ATP}) channels
4-Aminopyridine	4-AP	Voltage-dependent K^+ (K_V) channels
Barium chloride	$BaCl_2$	Inward rectifier K^+ (K_{IR})channels

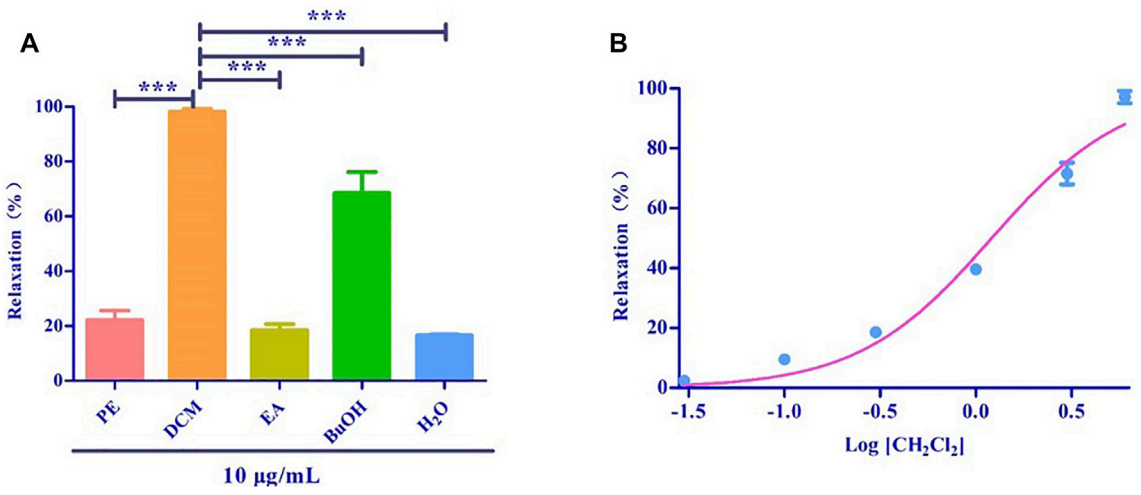

FIGURE 3
(A) Relaxation of different solvent extraction. **(B)** The cumulative concentration-response curve of the effect of CH_2Cl_2 (0.03 μg/ml to 6 μg/ml) on isolated rat aortic rings pre-contracted with PhE (1 μM). (*** mean $p < 0.001$ vs. CH_2Cl_2 group).

steel mortar, and the operation was carried out in the presence of liquid nitrogen. Weigh the tissue and add 0.1 M HCl (w/v: 1: 10) to homogenize and centrifuge at 1500 g for 15 min, take the supernatant. cGMP level is determined by enzyme immunoassay using acetylation procedure and direct cyclic GMP ELISA kit ADI-900–014 (Kubacka et al., 2018).

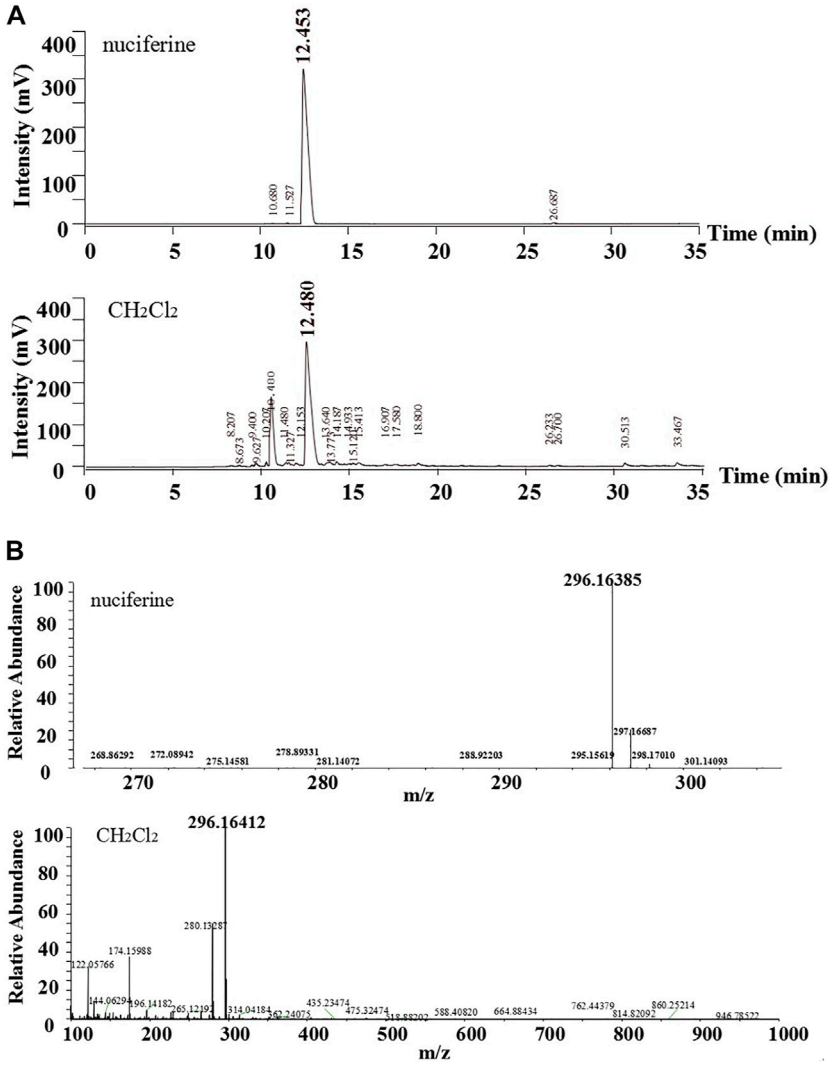

FIGURE 4
Comparative analysis of nuciferine standard substance and CH_2Cl_2 layer **(A)**HPLC; **(B)**ESI-HRMS.

2.9.7 Examination of K^+ channel effect

In order to determine whether nuciferine-induced relaxation was related to the activation of K^+ channels, we selected four types of K^+ channel blockers to inhibit the different K^+ channels, $BaCl_2$ (100 μM) for K_{IR}, 4-AP (1 mm) for K_V, TEA (1 mm) for K_{Ca}, and Gli (100 μM) for K_{ATP}.

2.9.8 Observation of intracellular calcium release

Endothelium-denuded rat thoracic aorta strips were incubated in Ca^{2+} free KBS solution, and then PhE (1 μM) was added to produce the first transient contraction (T_1). Subsequently, the strips were rinsed with KBS solution 4 times to supplement the intracellular Ca^{2+} loss and with Ca^{2+} free KBS solution for 2 times in succession. Followed that, nuciferine (0.1, 0.3, 0.6 μM) was added and incubated for 10 min and PhE (1 μM) was added again to produce the second transient vasocontraction (T_2). $T_2/T_1 \times 100\%$ was calculated as contraction (Qu et al., 2015; Hu et al., 2018; Kim et al., 2019).

2.9.9 Observation of extracellular calcium influx

Endothelium-denuded rat thoracic aorta strips were also employed and incubated in Ca^{2+}-free KBS. Then 1 μM PhE or 60 mm KCl was added to produce a basic contraction, and 0.01–10 mM of $CaCl_2$ were added in sequence to obtain a concentration–response curve. In order to examine the relation of nuciferine-induced vasorelaxation to the

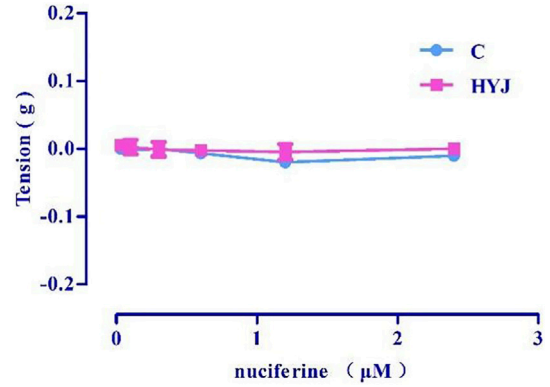

FIGURE 5
The effect of concentration-dependent addition of nuciferine on blood vessels. The data are expressed as the means ± SD of 6–8 rats (n = 6–8).

contractions by PhE or KCl, nuciferine was pre-incubated for 10 min after adding PhE or KCl. The contraction produced by highest concentration of $CaCl_2$ (10 mm) was taken as 100%, and then, based on which, the inhibitory rate of nuciferine could be calculated (Qu et al., 2015; Hu et al., 2018; Kim et al., 2019).

2.10 Cell culture

HUVECs were cultured at 37°C on gelatin-coated plates in the basal nutrient media DMEM supplemented with 10% fetal bovine serum, 100 U/ml penicillin, 100 μg/ml streptomycin.

2.11 Cell viability assay

Cell viability was determined by a standard MTT (3-(4,5-dimethyl-2-thiazolyl)-2,5.

-diphenyl-2-H-tetrazolium bromide) assay. Briefly, HUVECs were seeded in a 96-well plate at 1 cells/well × 10^4 cells/well (200 μL). 1, 3, 10, 30 or 100 μM nuciferine treatment for 24 h. MTT solution was added to each well. After 4 h incubation, 150 μL of DMSO was added to dissolve the formazan crystals. Cell viability was reflected by absorbance, which was measured at 492 nm using a microplate reader after

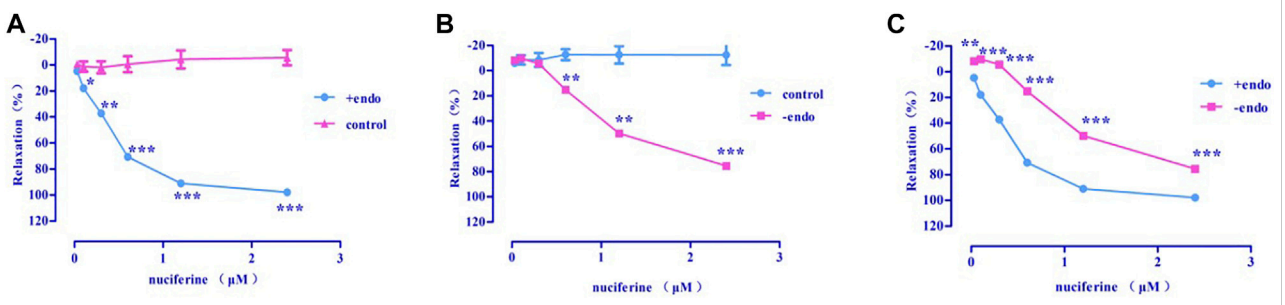

FIGURE 6
The vasodilation effect of nuciferine **(A)** Intact endothelium (+endo); **(B)**. Endothelium-denuded (-endo); **(C)** ±endo. The data are expressed as the means ± SD. of 6–8 rats (n = 6–8). (*p < 0.05; **p < 0.01 and ***p < 0.001 vs. control group).

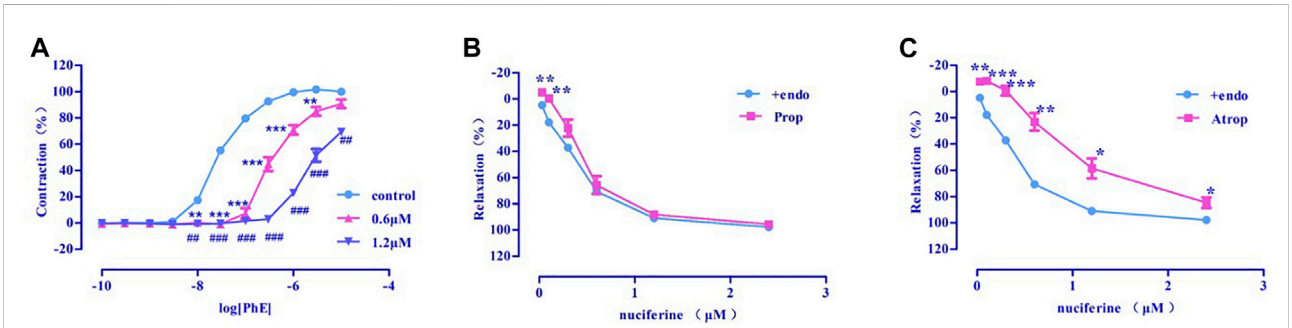

FIGURE 7
(A) α-receptor. **(B)** β receptor. **(C)** M receptor. The data are expressed as the means ± SD of 6–8 rats (n = 6–8). (*p < 0.05, **p < 0.01 and ***p < 0.001 vs. control group; $^{\#}p$ < 0.05, $^{\#\#}p$ < 0.01 and $^{\#\#\#}p$ < 0.001 vs. control group).

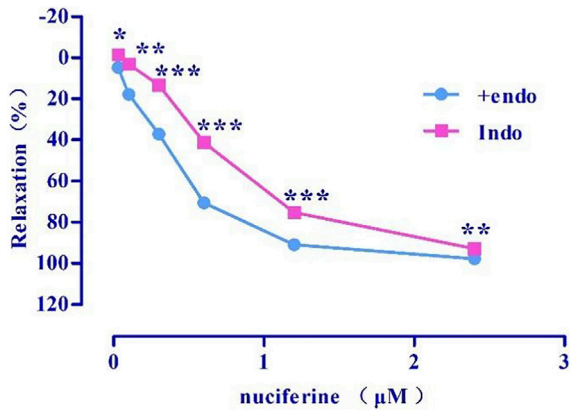

FIGURE 8
Effect of Indo on nuciferine induced vasorelaxation. The data are expressed as the means ± SD of 6–8 rats (n = 6–8). (*p < 0.05, **p < 0.01 and ***p < 0.001 vs. control group).

10 min of shaking. Cell viability was expressed as a percentage of the control value. Each experiment was performed in quintuplicate using three independent cultures.

2.12 Western blot Analysis

HUVECs were purchased from lonza (Switzerland). HUVECs were pre-incubated with nuciferine, then exposured to TNF-α (10 ng/ml) (Cao et al., 2020). Total cellular proteins were extracted, followed by protein concentration determination using a BCA kit. Followed by protein denaturation, electrophoresis, transferred to a membrane; the membrane was then blocked with a 5% non-fat skim milk solution for 1–2 h. Then incubated with primary and secondary antibodies. Tris-buffered saline and Tween 20 (TBST) was used to wash the membranes for 5 min, which was repeated three times. Densitometry analysis of the protein bands was performed using the ImageJ software.

2.13 Statistical analysis

GraphPad Prism 5 software was used for the statistical analysis. All values were expressed as mean ± SD of three independent experiments. When the data were normally distributed, they were analysed by unpaired two-tailed Student's t-tests and multiple groups were analysed by one-way analysis of variance (ANOVA). A p value <0.05 was considered significant.

3 Results

3.1 Yield of various solvent extracts

We investigated the yield of lotus leaf extracts in different solvents. The yield of the H_2O, 25% ethanol, 50% ethanol, 75% ethanol, and ethanol extracts ranged from 8.94 ± 0.96 to 22.38 ± 1.64% (Table 1). The vasodilatory activity of the H_2O, 25% ethanol, 50% ethanol, 75% ethanol, and ethanol extracts ranged from 19.65 ± 0.19 to 90.63 ± 1.82% (Table 1 and Figure 1). Based on the yield and vasodilatory activity, 75% ethanol was selected as the most suitable extraction solution.

3.2 Different solvent extractions

Based on the polarity, the extract obtained using 75% ethanol was further extracted using different solvents

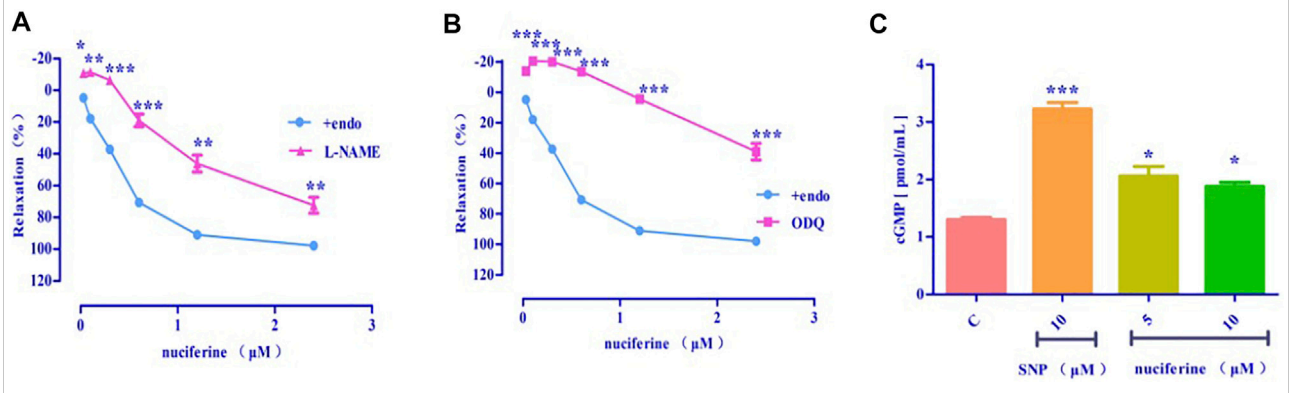

FIGURE 9
Effect of eNOS/sGC/cGMP on nuciferine-induced relaxation **(A)** L-NAME blocking effect; **(B)** ODQ blocking effect; **(C)** Detection of cGMP content. The data are expressed as the means ± SD of 6–8 rats (n = 6–8). (*p < 0.05, **p < 0.01 and ***p < 0.001 vs. control group).

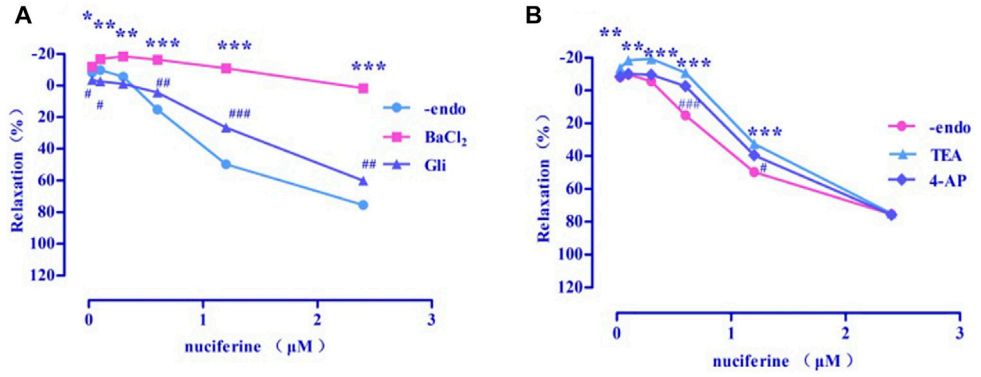

FIGURE 10
Effects of K^+ channel blockers on nuciferine induced vasorelaxation. The data are expressed as the means ± SD of 6–8 rats (n = 6–8). (*p < 0.05, **p < 0.01 and ***p < 0.001 vs. control group; $^{\#}p$ < 0.05, $^{\#\#}p$ < 0.01 and $^{\#\#\#}p$ < 0.001 vs. control group).

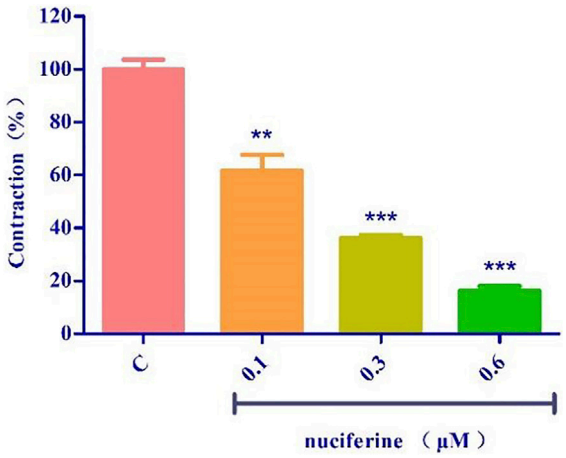

FIGURE 11
Effects of SR calcium release on nuciferine induced vasorelaxation. The data are expressed as the means ± SD of 6–8 rats (n = 6–8). (**p < 0.01 and ***p < 0.001 vs. control group).

(Figure 2). The CH_2Cl_2 layer exhibited the best vasodilatory activity (98.22 ± 1.01%) (Table 2 and Figure 3). The vasodilatory activity was concentration-dependent (EC_{50} = 1.21 ± 0.10 μg/ml) (Table 3).

3.3 HPLC and ESI-HRMS analyses

The standard nuciferine product peak appeared at **12.453** min. The component in the CH_2Cl_2 layer exhibited a peak at 12.480 min (Figure 4A). The peak shape and time were basically the same. Calculated ESI-HRMS value for nuciferine ($[M + H]^+$) was 296.16451, and it was found to be 296.16385. The found ESI-HRMS value of the component in the CH_2Cl_2 layer ($[M + H]^+$) was 296.16412 (Figure 4B).

3.4 Vascular reactivity assessment

3.4.1 Effect of nuciferine on rat thoracic aorta

Accumulation of nuciferine (0.03–2.4 μM) had no obvious effects on basal tension in rat thoracic aortic rings when compared to the vehicle control group (Figure 5).

3.4.2 Nuciferine relaxes the pre-contracted PhE in rat thoracic aorta

Nuciferine exerted concentration-dependent vasorelaxant effect on PhE induced contraction in both endothelium-intact (E_{max} = 97.95 ± 0.76%, EC_{50} = 0.36 ± 0.02 μM) (Figure 6A) and endothelium-denuded (E_{max} = 75.42 ± 1.83%, EC_{50} = 1.30 ± 0.03 μM) (Figure 6B) arteries. Therefore, the vasodilatory activity of nuciferine is thought to be related to the endothelium (Figure 6C).

3.4.3 Examination of α-, β-, and M-receptor activities

3.4.3.1 Examination of α-receptor activity

Pre-incubation with various concentrations of nuciferine (0.6, 1.2 μM) significantly inhibited the concentration-response contraction induced by PhE (0.1 nm–10 μM), and suppressed its maximal contraction (E_{max}) to 90.73 ± 3.26% and 69.39 ± 1.59%, respectively (vs. control group E_{max} = 100%) (Figure 7A). The vasodilatory activity of nuciferine is thought to be related to the α-receptor activity.

3.4.3.2 Examination of β- and M-receptor activities

There was no significant difference between propranolol pre-incubated vascular ring (E_{max} = 95.66 ± 1.30%, EC_{50} = 0.48 ± 0.02 μM) (Figure 7B) and the control group (E_{max} = 97.95 ±

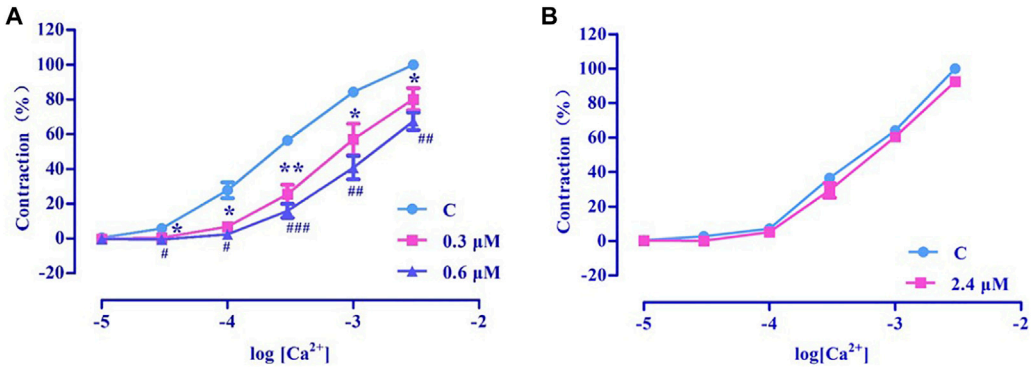

FIGURE 12
Effects of extracellular Ca^{2+} influx on nuciferine induced vasorelaxation. The data are expressed as the means ± SD of 6–8 rats (n = 6–8). (*p < 0.05 and **p < 0.01 vs. control group; $^{\#}p$ < 0.05, $^{\#\#}p$ < 0.01 and $^{\#\#\#}p$ < 0.001 vs. control group).

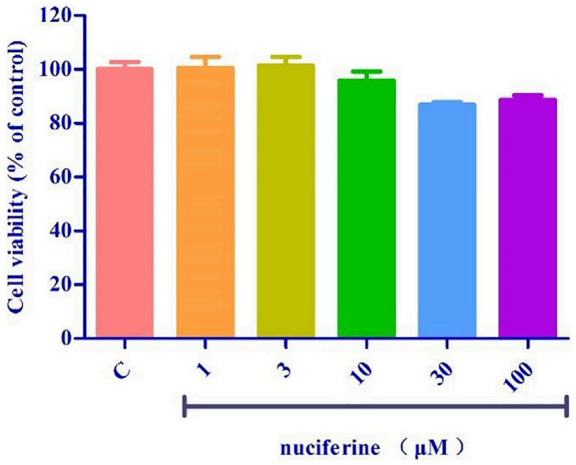

FIGURE 13
Toxicity test of nuciferine on HUVECs.

0.76%, EC_{50} = 0.36 ± 0.02 μM). The vasorelaxation induced by nuciferine is thought to be associated with M-receptor activity (E_{max} = 84.67 ± 4.06%, EC_{50} = 1.05 ± 0.03 μM) (Figure 7C).

3.4.4 Effects of PGI_2 on nuciferine-induced relaxation

Indo (E_{max} = 92.98 ± 0.31%, EC_{50} = 0.71 ± 0.01 μM) (Figure 8) pretreatment weakened the relaxing effect of nuciferine. Therefore, the vasodilatory effect of nuciferine may be related to PGI_2.

3.4.5 Effect of eNOS/sGC/cGMP on nuciferine-induced relaxation

After pretreatment with eNOS inhibitor *L*-NAME (E_{max} = 72.43 ± 5.00%, EC_{50} = 1.36 ± 0.04 μM) (Figure 9A) and sGC inhibitor ODQ (E_{max} = 39.01 ± 5.44%) (Figure 9B), the vasodilatory effect of nuciferine was found to be significantly reduced. The inhibitory effect of ODQ is stronger than that of *L*-NAME, and it is suspected that nuciferine can directly act on smooth muscle cells. The endothelium was pretreated with lotus leaf alkaline extract to remove the blood vessels, and then, the cGMP content was assessed. The results revealed that there were significant differences between the nuciferine group (5 μM, 2.06 ± 0.24 pmol/ml; 10 μM, 1.88 ± 0.10 pmol/ml) and the control group (1.30 ± 0.05 pmol/ml). The cGMP content of the positive control SNP was 3.23 ± 0.16 pmol/ml (10 μM) (Figure 9C). The vasodilatory effect of nuciferine is thought to be related to the eNOS/sGC/cGMP signaling pathway. The cGMP results also proved that lotus leaf can directly activate sGC in smooth muscle cells to increase the production of cGMP.

3.4.6 Examination of K^+ channel effect

Four types of selective K^+ channel blockers, including $BaCl_2$ (E_{max} = 1.73 ± 2.48%), Gli (E_{max} = 60.23 ± 2.30%, EC_{50} = 1.97 ± 0.01 μM), TEA (E_{max} = 74.93 ± 0.47%, EC_{50} = 1.63 ± 0.04 μM), and 4-AP (E_{max} = 75.80 ± 1.60%, EC_{50} = 1.50 ± 0.02 μM) were added into the incubation solution to obtain endothelium-denuded strips (E_{max} = 75.42 ± 1.83%, EC_{50} = 1.30 ± 0.03 μM) separately. The results revealed that all these K^+ channel blockers affected the nuciferine-induced relaxation (Figures 10A,B), especially $BaCl_2$.

3.4.7 Effect of sarcoplasmic reticulum calcium release

The endothelium-denuded strips were incubated in a Ca^{2+}-free solution and contracted by PhE, which promoted calcium release from the SR. The pre-treatment with nuciferine (0.1, 0.3, and 0.6 μM) significantly affected the PE-mediated vasocontraction (Figure 11). This result suggested that nuciferine interferes with SR Ca^{2+} release for its vasodilation upon considering the control group as 100%.

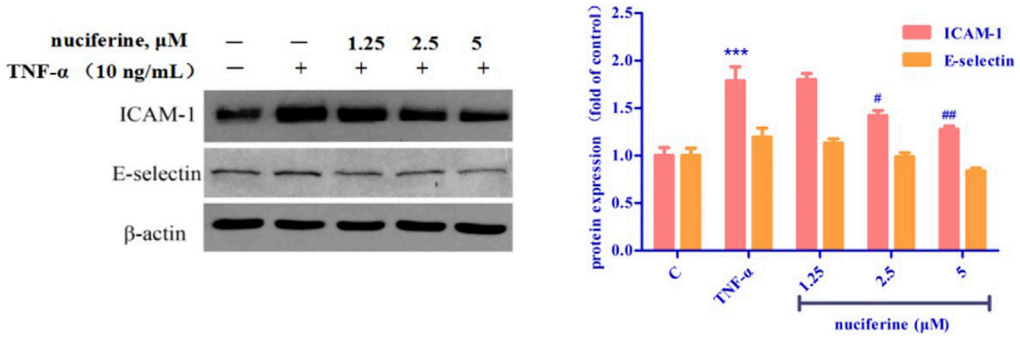

FIGURE 14
Effect of nuciferine on TNF-α-induced expression of adhesion molecules in HUVECs. (*$p < 0.01$ and ***$p < 0.001$ vs. control group).

3.4.8 Effect of extracellular Ca^{2+} influx on vasorelaxation by nuciferine

3.4.8.1 Examination of ROCCs effect

PhE promotes Ca^{2+} influx via ROCCs. The results revealed that nuciferine (0.3 and 0.6 μM) affected the contraction induced by $CaCl_2$ + PhE (Figure 12A), suggesting that the relaxation by nuciferine might be related to the ROCCs.

3.4.8.2 Examination of VDCCs effect

High concentration of KCl promoted Ca^{2+} influx via VDCCs. The results revealed that 2.4 μM nuciferine did not affect the contraction induced by $CaCl_2$ + KCl (E_{max} = 91.68 ± 1.01%) (Figure 12B), thereby suggesting that the relaxation by nuciferine might not be related to VDCCs.

3.5 Cell viability assay

Pretreatment with nuciferine (1–100 μM) for 24 h did not result in significant difference between the control group (Figure 13).

3.6 Vascular protection effect of nuciferine

TNF-α treatment increased the expression of cell adhesion molecules, such as ICAM-1 and E-selectin. Interestingly, pretreatment with nuciferine attenuated TNF-α-mediated cell adhesion molecules (Figure 14). Our results revealed that nuciferine may exert a vascular protective effect.

4 Discussion

Lotus leaves contain alkaloids, flavonoids, polysaccharides, and other ingredients (Nguyen and Pham, 1998; Ma et al., 2010; Chen and Qi, 2015; Tungmunnithum et al., 2018; Ye et al., 2018). Different ratios of water and ethanol were used to obtain the extracts, and the 75% ethanol extract was found to exert a strong vasodilator effect. The 75% ethanol extract was further subjected to polarity-dependent extraction, and it was found that the CH_2Cl_2 layer exhibited the highest vasodilatory activity. Therefore, the component analysis of the CH_2Cl_2 layer was carried out, and the components that accounted for about half of the entire peak area in the liquid phase analysis were separated by preparative liquid phase. The chromatographic characterization and the comparative analysis of liquid phase/mass spectrometry confirmed that the substance was nuciferine, which was consistent with previous research results that most of the alkaloids were dissolved in the dichloromethane layer (Wang et al., 2008) and nuciferine was the most abundant alkaloid in lotus leaf (Ma et al., 2010). Before this, some scholars have studied the relaxation mechanism of nuciferine on mesenteric arteries (Wang X. et al., 2015) and trachea (Yang et al., 2018). With this, we believe that nuciferine is the main component present in lotus leaves with vasodilator activity. Therefore, the thoracic aorta activity of nuciferine was further studied. In this study, we aimed to provide a basis for future studies on the vasodilatory activity of lotus leaf extracts.

As shown in Figure 6, nuciferine was found to directly act on the rat thoracic aorta without pretreatment, and there was no significant effect. The vasodilatory effect of nuciferine is more related to the endothelium. The vascular endothelium produces vasodilatory factors, such as NO and PGI_2 (Yam et al., 2016). When eNOS is activated, *L*-arginine is converted into NO in vascular endothelial cells. NO penetrates the endothelium and enters the smooth muscle cells, and then, activates the soluble guanylate cyclase, thereby increasing the intracellular levels of cGMP, which is synthesized from guanosine triphosphate (Qu et al., 2015; Kubacka et al., 2018). The thoracic aortic vasorelaxant effect of nuciferine was also blocked in the *L*-NAME and ODQ experiments, which is consistent with the trend of nuciferine to relax rat mesenteric arteries (Wang X. et al., 2015). But in the thoracic aorta experiment, the blocking effect of ODQ was more

obvious. Based on the above phenomenon, nuciferine may directly activate sGCs in smooth muscle cells to promote cGMP production. The nitric oxide donor SNP was selected as a positive control, and nuciferine directly treated smooth muscle cells. The detection of cGMP content in vessels found that nuciferine could directly act on smooth muscle cells, then relate vessels. In conclusion, the vasodilatory effect of nuciferine may be related to the NO signaling pathway.

As another endogenous vasodilator prostacyclin (PGI_2) synthesized and released by endothelial cells, both PGI_2 and NO act directly on smooth muscle cells. However, the mechanism of action of the two is slightly different. PGI_2 binds to smooth muscle cell membrane receptors and promotes the production of cAMP to relax vessels (Moncada et al., 1976; Gomberg-Maitland and Olschewski, 2008). Arachidonic acid (AA) is converted to PGI_2 by COX (Yam et al., 2016). In the present study, Indo was found to partially inhibit the relaxation effect of nuciferine. This is different from previous findings that the relaxation of mesenteric arteries by nuciferine is independent of PGI_2 (Wang X. et al., 2015). This suggested that the relaxation mechanism of nuciferine in the thoracic aorta and mesenteric arteries was different, and proved that the relaxation of the thoracic aorta by nuciferine may be related to the PGI_2 signaling pathway.

Ions play an important role in maintaining blood vessel homeostasis (Qu et al., 2015; Hu et al., 2018). We found that four different types of potassium channels are related to the vasodilatory effect of nuciferine, especially the inwardly rectifying potassium channels. In most cases, the contraction of the vascular smooth muscle is related to an increase in [Ca^{2+}] ions through the influx of extracellular Ca^{2+} and the release of intracellular Ca^{2+}. The influx of extracellular calcium is mainly through the VDCCs and ROCCs located in the cell membrane. The KCl-induced contraction is mainly caused by the depolarization and opening of the VDCCs membrane, which drives the influx of extracellular Ca^{2+}. PhE leads to the contractions in response to the extracellular Ca^{2+} influx upon direct activation of ROCCs. We found that the vasodilatory effect of nuciferine is related to the ROCCs pathway of intracellular calcium release and extracellular calcium influx (Kim et al., 2015; Lee et al., 2015; Kim et al., 2019).

Nuciferine relaxes the thoracic aorta through endothelium-dependent and -independent mechanisms. Therefore, nuciferine may act directly on endothelial cells and smooth muscle cells. α- and β-receptors are widely distributed in vascular smooth muscle cells, and muscarinic (M) receptors are distributed in the vascular endothelium. Stimulation of α-receptor results in vasoconstriction, and M- and β-adrenergic receptors are involved in vasodilation (Chiu et al., 2004; Yam et al., 2016). β-adrenergic receptors were not involved in the vasodilatory effect of nuciferine, which was consistent with mesenteric arteries findings (Wang X. et al., 2015). The present study demonstrates that the vasodilatory effects of nuciferine are associated with α- and M-receptors.

A variety of cardiovascular diseases such as hypertension, atherosclerosis and heart failure are often accompanied by endothelial dysfunction (Vanhoutte, 1996). TNF-α is reported to trigger the interaction between monocytes and vascular endothelial cells, enhance the expression of adhesion molecules, such as VCAM-1, ICAM-1, and E-selectin, and finally induce endothelial dysfunction (Yao et al., 2015; Zhou et al., 2017). Nuciferine did not show cytotoxicity at the concentration of 0–100 μM, and the results of western blot experiments showed that nuciferine inhibits the production of vascular adhesion factors in a concentration-dependent manner and protects vessels.

In summary, nuciferine was the main substance with a vasodilatory effect in the lotus leaf extract. The vasodilatory effects of nuciferine were mediated by multiple pathways, multiple-targets and had both endothelium-dependent and -independent mechanisms. Nuciferine mainly mediated the NO/cGMP signaling pathway, activated the K_{IR} channel, and inhibited ROCCs and SR Ca^{2+} release to relax thoracic aorta. Notably, Nuciferine has low cytotoxicity and endothelial protective effect, which was worth further development and research. This study provides a new research direction for the development and application of lotus leaf extract.

Data availability statement

The original contributions presented in the study are included in the article/Supplementary Material, further inquiries can be directed to the corresponding authors.

Ethics statement

The animal study was reviewed and approved by the Animals were strictly handled in accordance with the National Institutes of Health Guidelines for the Care and Use of Laboratory Animals (NIH Publication No. 85-3, revised 1996) and the study was approved by the Institutional Animal Care and Utilization Committee of Yanbian University.

Author contributions

Z-SQ, HD, and L-HC designed the study. HD, QX, XH, and X-TS performed the experiments. L-LJ, F-EC, and Q-KS analyzed and interpreted the results. DH and XQ wrote the manuscript.

Funding

This work was financially supported by the Higher Education Discipline Innovation Project (111 Project, D18012), National Natural Science Foundation of China (No.81960626, 82060628), Jilin Provincial Education Department of China (JJKH20191156KJ), Doctoral Research Startup Fundation of

Yanbian University (No. 602020087) and the Natural Science Foundation of Jilin Province (No.20210101242JC).

Acknowledgments

All authors approved the final manuscript. We would like to thank Editage (www.editage.cn) for English language editing.

Conflict of interest

The authors declare that the research was conducted in the absence of any commercial or financial relationships that could be construed as a potential conflict of interest.

Publisher's note

Supplementary material

The Supplementary Material for this article can be found online at: https://www.frontiersin.org/articles/10.3389/fphar.2022.946445/full#supplementary-material

References

Cao, L. H., Lee, H. S., Lee, Y. J., Lee, H. S., Lee, Y. J., Quan, Z. S., et al. (2020). Vascular protective effects of xanthotoxin and its action mechanism in rat aorta and human vascular endothelial cells. *J. Vasc. Res.* 57 (6), 313–324. doi:10.1159/000509112

Chai, J. Z., Jiang, L., Wei, J. Q., and Yin, G. L. (2016). Research progress of hypolipidemic and antioxidation effect of the lotus leaf. *Shipin Yanjiu Yu Kaifa* 37 (8), 209–212. doi:10.3969/j.issn.1005-6521.2016.08.049

Chen, H., and Zeng, Q. (2001). Extraction of functional component from lotus leaves and effect on scavenging of oxygen free radicals. *Shipin Yu Fajiao Gongye* 27, 34–38. doi:10.13995/j.cnki.11-1802/ts.2001.10.008

Chen, X., and Qi, J. (2015). Flavonoids and alkaloids in lotus leaves. *Zhongguo Shiyan Fangjixue Zazhi* 21 (18), 211–214. doi:10.13422/j.cnki.syfjx.2015180211

Chen, Y., Chen, Q., Wang, X., Sun, F., Fan, Y., Liu, X., et al. (2020). Hemostatic action of lotus leaf charcoal is probably due to transformation of flavonol aglycons from flavonol glycosides in traditional Chinses medicine. *J. Ethnopharmacol.* 249, 112364. doi:10.1016/j.jep.2019.112364

Chiu, C. C., Wu, J. R., Lee, C. H., Liou, S. F., Dai, Z. K., Chen, I. J., et al. (2004). Anti-hypertension effect of vanylidilol: A phenylaldehyde alpha/beta-adrenoceptor blocker with endothelium-dependent and K+ channels opening-associated vasorelaxant activities. *Pharmacology* 70 (3), 140–151. doi:10.1159/000074977

Gomberg-Maitland, M., and Olschewski, H. (2008). Prostacyclin therapies for the treatment of pulmonary arterial hypertension. *Eur. Respir. J.* 31 (4), 891–901. doi:10.1183/09031936.00097107

Guo, C., Zhang, N., Liu, C., Xue, J., Chu, J., and Yao, X. (2020). Qualities and antioxidant activities of lotus leaf affected by different drying methods. *Acta Physiol. Plant.* 42 (2), 14–18. doi:10.1007/s11738-019-2992-9

Guo, F., Yang, X., Li, X., Feng, R., Guan, C., Wang, Y., et al. (2013). Nuciferine prevents hepatic steatosis and injury induced by a high-fat diet in hamsters. *PLoS One* 8 (5), e63770. doi:10.1371/journal.pone.0063770

Hu, G. Y., Peng, C., Xie, X. F., Xiong, L., Cao, X. Y., and Zhang, S. Y. (2018). Patchouli alcohol isolated from Pogostemon cablin mediates endothelium-independent vasorelaxation by blockade of Ca2+ channels in rat isolated thoracic aorta. *J. Ethnopharmacol.* 220, 188–196. doi:10.1016/j.jep.2017.09.036

Kim, B., Lee, K., Chinannai, K. S., Ham, I., Bu, Y., Kim, H., et al. (2015). Endothelium-independent vasorelaxant effect of Ligusticum jeholense root and rhizoma on rat thoracic aorta. *Molecules* 20 (6), 10721–10733. doi:10.3390/molecules200610721

Kim, B., Ma, S. S., Jo, C., Lee, S., Choi, H., Lee, K., et al. (2019). Vasorelaxant effect of the ethanol extract from Valeriana fauriei briquet root and rhizome on rat thoracic aorta. *Pharmacogn. Mag.* 14 (60), 59–65. doi:10.4103/pm.pm_152_18

Kubacka, M., Kotanska, M., Kazek, G., Waszkielewicz, A. M., Marona, H., Filipek, B., et al. (2018). Involvement of the NO/sGC/cGMP/K+ channels pathway in vascular relaxation evoked by two non-quinazoline α1-adrenoceptor antagonists. *Biomed. Pharmacother.* 103, 157–166. doi:10.1016/j.biopha.2018.04.034

Lee, K., Shin, M. S., Ham, I., and Choi, H. Y. (2015). Investigation of the mechanisms of Angelica dahurica root extract-induced vasorelaxation in isolated rat aortic rings. *BMC Complement. Altern. Med.* 15, 395–398. doi:10.1186/s12906-015-0889-8

Liu, W. J., and Fan, L. P. (2014). Comparison of different extraction technology of lotus leaf tea. *Shipin Gongye Keji* 35 (14), 305314–306308.

Ma, C., Li, G., He, Y., Xu, B., Mi, X., Wang, H., et al. (2015). Pronuciferine and nuciferine inhibit lipogenesis in 3T3-L1 adipocytes by activating the AMPK signaling pathway. *Life Sci.* 136, 120–125. doi:10.1016/j.lfs.2015.07.001

Ma, W., Lu, Y., Hu, R., Chen, J., Zhang, Z., and Pan, Y. (2010). Application of ionic liquids based microwave-assisted extraction of three alkaloids N-nornuciferine, O-nornuciferine, and nuciferine from lotus leaf. *Talanta* 80 (3), 1292–1297. doi:10.1016/j.talanta.2009.09.027

Moncada, S., Gryglewski, R., Bunting, S., and Vane, J. R. (1976). An enzyme isolated from arteries transforms prostaglandin endoperoxides to an unstable substance that inhibits platelet aggregation. *Nature* 263 (5579), 663–665. doi:10.1038/263663a0

Navaneethabalakrishnan, S., Goodlett, B. L., Lopez, A. H., Rutkowski, J. M., and Mitchell, B. M. (2020). Hypertension and reproductive dysfunction: A possible role of inflammation and inflammation-associated lymphangiogenesis in gonads. *Clin. Sci.* 134 (24), 3237–3257. doi:10.1042/CS20201023

Nguyen, T., and Pham, T. K. (1998). Study on chemical constituents in leaves of *Nelumbo nucifera* Gaertn. *Pharm. J.* 272 (12), 13–18.

Qiu, M., Xiao, F., Wang, T., Zhao, W., Shao, S., Piao, S., et al. (2020). Protective effect of Hedansanqi Tiaozhi Tang against non-alcoholic fatty liver disease *in vitro* and *in vivo* through activating Nrf2/HO-1 antioxidant signaling pathway. *Phytomedicine* 67, 153140. doi:10.1016/j.phymed.2019.153140

Qu, Z., Zhang, J., Huo, L., Chen, H., Li, H., Fan, Y., et al. (2015). Antihypertensive and vasorelaxant effects of Rhizoma corydalis and its active component tetrahydropalmatine via NO/cGMP pathway and calcium channel blockade in isolated rat thoracic aorta. *RSC Adv.* 5 (114), 94130–94143. doi:10.1039/c5ra17756a

Tungmunnithum, D., Pinthong, D., Hano, C., and Hano, C. (2018). Flavonoids from *Nelumbo nucifera* gaertn., a medicinal plant: Uses in traditional medicine, phytochemistry and pharmacological activities. *Med. (Basel)* 5 (4), 127. doi:10.3390/medicines5040127

Vanhoutte, P. M. (1996). Endothelium-dependent responses and inhibition of angiotensin-converting enzyme. *Clin. Exp. Pharmacol. Physiol.* 23 (8), 23–29. doi:10.1111/j.1440-1681.1996.tb03037.x

Wang, G., Liu, K., Li, Y., Yi, W., Yang, Y., Zhao, D., et al. (2014). Endoplasmic reticulum stress mediates the anti-inflammatory effect of ethyl pyruvate in endothelial cells. *PLoS One* 9 (12), e113983. doi:10.1371/journal.pone.0113983

Wang, G., Zhang, B., Nie, Q., Li, H., and Zang, C. (2008). Optimal extraction of nuciferine and flavone from lotus leaf based on central composite design and response surface methodology. *Zhongguo Zhongyao Zazhi* 33 (20), 2332–2335.

Wang, J. T., Kong, Z., Yan, Y. M., Qin, M., Gao, G. L., Yu, X. M., et al. (2007). Study on the antibacterial activity of isoquinoline alkaloids by microcalorimetry. *Huaxue Shijie* 48, 460–463. doi:10.19500/j.cnki.0367-6358.2007.08.004

Wang, M. X., Liu, Y. L., Yang, Y., Zhang, D. M., and Kong, L. D. (2015). Nuciferine restores potassium oxonate-induced hyperuricemia and kidney inflammation in mice. *Eur. J. Pharmacol.* 747, 59–70. doi:10.1016/j.ejphar.2014.11.035

Wang, X., Cheang, W. S., Yang, H., Xiao, L., Lai, B., Zhang, M., et al. (2015). Nuciferine relaxes rat mesenteric arteries through endothelium-dependent and -independent mechanisms. *Br. J. Pharmacol.* 172 (23), 5609–5618. doi:10.1111/bph.13021

Wang, Z., Zhao, P., Zhang, Y., Shi, S., and Chen, X. (2020). The hepatoprotective effect and mechanism of lotus leaf on liver injury induced by Genkwa Flos. *J. Pharm. Pharmacol.* 72 (12), 1909–1920. doi:10.1111/jphp.13355

Yam, M. F., Tan, C. S., Ahmad, M., and Ruan, S. (2016). Mechanism of vasorelaxation induced by eupatorin in the rats aortic ring. *Eur. J. Pharmacol.* 789, 27–36. doi:10.1016/j.ejphar.2016.06.047

Yang, S., Xu, Z., Lin, C., Li, H., Sun, J., Chen, J., et al. (2020). Schisantherin A causes endothelium-dependent and -independent vasorelaxation in isolated rat thoracic aorta. *Life Sci.* 245, 117357. doi:10.1016/j.lfs.2020.117357

Yang, X., Yu, M. F., Lei, J., Peng, Y. B., Zhao, P., Xue, L., et al. (2018). Nuciferine relaxes tracheal rings via the blockade of VDLCC and NSCC channels. *Planta Med.* 84 (2), 83–90. doi:10.1055/s-0043-118178

Yao, W., Gu, C., Shao, H., Meng, G., Wang, H., Jing, X., et al. (2015). Tetrahydroxystilbene glucoside improves TNF-α-induced endothelial dysfunction: Involvement of tgfβ/smad pathway and inhibition of vimentin expression. *Am. J. Chin. Med.* 43 (1), 183–198. doi:10.1142/S0192415X15500123

Ye, L. H., He, X. X., Kong, L. T., Liao, Y. H., Pan, R. L., Xiao, B. X., et al. (2014). Identification and characterization of potent CYP2D6 inhibitors in lotus leaves. *J. Ethnopharmacol.* 153 (1), 190–196. doi:10.1016/j.jep.2014.02.014

Ye, L. H., He, X. X., Tao, X., Wang, L. S., Zhang, M. D., Zhou, Y. F., et al. (2018). Pharmacokinetics of nuciferine and N-nornuciferine, two major alkaloids from *Nelumbo nucifera* leaves, in rat plasma and the brain. *Front. Pharmacol.* 9, 902. doi:10.3389/fphar.2018.00902

Yuan, P. L., Chen, L., Liu, X. Y., Yu, B. W., Huang, Q., Chen, K. X., et al. (2014). Alkaloids from lotus leaf and their bioactivities. *Zhongchengyao* 36 (11), 2330–2333. doi:10.3969/j.issn.1001-1528.2014.11.024

Zhou, P., Lu, S., Luo, Y., Wang, S., Yang, K., Zhai, Y., et al. (2017). Attenuation of TNF-α-Induced inflammatory injury in endothelial cells by ginsenoside Rb1 via inhibiting NF-κB, JNK and p38 signaling pathways. *Front. Pharmacol.* 8, 464. doi:10.3389/fphar.2017.00464

frontiers | Frontiers in Pharmacology

TYPE Mini Review
PUBLISHED 10 October 2022
DOI 10.3389/fphar.2022.982185

OPEN ACCESS

EDITED BY
Ali H. Eid,
Qatar University, Qatar

REVIEWED BY
Tim Murphy,
University of New South Wales, Australia
Mohamed Noureldein,
Michigan Medicine, University of Michigan, United States

*CORRESPONDENCE
Isra Marei,
iym2001@qatar-med.cornell.edu
Chris R. Triggle,
cht2011@qatar-med.cornell.edu

SPECIALTY SECTION
This article was submitted to Cardiovascular and Smooth Muscle Pharmacology, a section of the journal Frontiers in Pharmacology

RECEIVED 30 June 2022
ACCEPTED 31 August 2022
PUBLISHED 10 October 2022

CITATION
Marei I, Ahmetaj-Shala B and Triggle CR (2022), Biofunctionalization of cardiovascular stents to induce endothelialization: Implications for in-stent thrombosis in diabetes. *Front. Pharmacol.* 13:982185. doi: 10.3389/fphar.2022.982185

Biofunctionalization of cardiovascular stents to induce endothelialization: Implications for in- stent thrombosis in diabetes

Isra Marei[1,2]*, Blerina Ahmetaj-Shala[2] and Chris R. Triggle[1]*

[1]Department of Pharmacology, Weill Cornell Medicine- Qatar, Doha, Qatar, [2]National Heart and Lung Institute, Imperial College London, London, United Kingdom

Stent thrombosis remains one of the main causes that lead to vascular stent failure in patients undergoing percutaneous coronary intervention (PCI). Type 2 diabetes mellitus is accompanied by endothelial dysfunction and platelet hyperactivity and is associated with suboptimal outcomes following PCI, and an increase in the incidence of late stent thrombosis. Evidence suggests that late stent thrombosis is caused by the delayed and impaired endothelialization of the lumen of the stent. The endothelium has a key role in modulating inflammation and thrombosis and maintaining homeostasis, thus restoring a functional endothelial cell layer is an important target for the prevention of stent thrombosis. Modifications using specific molecules to induce endothelial cell adhesion, proliferation and function can improve stents endothelialization and prevent thrombosis. Blood endothelial progenitor cells (EPCs) represent a potential cell source for the in situ-endothelialization of vascular conduits and stents. We aim in this review to summarize the main biofunctionalization strategies to induce the *in-situ* endothelialization of coronary artery stents using circulating endothelial stem cells.

KEYWORDS

in-stent thrombosis, diabetes, cellular dysfunction, endothelialization, endothelial progenitor cells, biofunctionalization, cell capture

Introduction

Cardiovascular diseases are the most prevalent non-communicable diseases worldwide, accounting for 31% of all deaths (WHO, 2017). Coronary artery disease (CAD) is the most common type of cardiovascular disease, causing the majority of cardiovascular-related deaths worldwide (Okrainec et al., 2004). The main cause of CAD is the accumulation of fatty and fibrous materials in the wall of the coronary artery forming an atherosclerotic lesion, which eventually leads to arterial occlusion (Ross, 1993). The growing size of the formed lesion can be sufficient to block the blood flow, however most clinical complications result from thrombus formation. A thrombus

obstructs blood flow to the heart muscle leading to myocardial ischemia and infarction (Lusis, 2000).

Percutaneous coronary intervention (PCI) is a non-surgical revascularization technique used to treat obstructive coronary arteries. PCI has become the treatment of choice for CAD. The implantation of intracoronary stents is one of the major PCI techniques used to relive the narrowing of coronary arteries (Smith et al., 2001). Although stenting have improved the acute outcomes of PCI, the long-term outcomes are still hindered by other factors such as age and other comorbidities (Smith et al., 2001). Stent thrombosis and restenosis remain the main causes that lead to vascular stent failure in patients undergoing PCI (Seabra-Gomes, 2006; Chaabane et al., 2013). Stent implantation causes mechanical vascular injury characterized by endothelial denudation and platelet activation, leading to thrombosis and stenosis (Kipshidze et al., 2004; Otsuka et al., 2012; Chaabane et al., 2013).

Evidence suggests that type 2 diabetes mellitus is associated with suboptimal outcomes following PCI or revascularization (Seabra-Gomes, 2006; Bittl, 2015; Koskinas et al., 2016). Type 2 diabetes mellitus is characterized by hyperglycemia and insulin resistance leading to endothelial dysfunction. The abnormal reactivity of diabetic endothelial cells is associated with an increased rate of cardiovascular events (Seabra-Gomes, 2006). In addition, patients with diabetes are at higher risk to develop coronary lesions in stented vessels and are presented with higher rates of completely occlusive restenosis following PCI (Seabra-Gomes, 2006). Diabetes also results in platelet dysfunction and hypo-responsiveness to antiplatelet treatments, increasing the risk of stent thrombosis (Gum et al., 2003; Watala et al., 2004; Angiolillo et al., 2005).

It has been suggested that inducing the rapid endothelialization of stents might improve the outcomes of PCI (Finn et al., 2007). Rapid endothelialization of blood-contacting devices and surfaces is desired due to the anti-thrombotic and anti-adhesive properties of endothelial cells, thus preventing the recruitment and adhesion of platelets and leukocytes to the stented area (Sousa et al., 2003). Establishing a functional endothelial cell layer rapidly after stent implantation might prevent stent thrombosis (Kong et al., 2004). Thus, in this review, we highlight the role of endothelial cells in protecting from stent thrombosis in the context of diabetes, and summarize the main studies that investigated biofunctionalization strategies to induce the *in-situ* endothelialization of coronary artery stents using circulating endothelial stem cells.

Pathogenesis of stent thrombosis: Role of endothelial cells

Coronary stents are prosthetic cylindrical meshes inserted into the coronary artery using a catheter to relieve the narrowing of the artery and improve blood flow to the heart muscle (Meads et al., 2000). Stents provide a permanent scaffolding for the vessel wall, thus inhibiting the arterial recoil and restenosis associated with plain old balloon angioplasty (Meads et al., 2000; Garcia-Garcia et al., 2006; Seabra-Gomes, 2006). To improve the outcomes of PCI, stents have evolved in terms of design and composition, from bare metal stents (BMS), to drug eluting stents (DES) and bioresorbable vascular scaffolds (BRS). We refer the reader to these reviews on the evolution of stents types, designs and materials (O'Brien and Carroll, 2009; Borhani et al., 2018; Torii et al., 2020; Scafa Udriște et al., 2021).

Stent thrombosis is the occlusion of a coronary artery stent by a thrombus. Standard definitions and classifications of stent thrombosis has been proposed by the Academic Research Consortium (ARC) (Garcia-Garcia et al., 2018). Stent thrombosis is classified into early, late or very late thrombosis according to the elapsed time from stent implantation, and could also be defined according to the degree of certainty as definitive, probable, or silent occlusion (Garcia-Garcia et al., 2018). The reported incidence of stent thrombosis was< 1% for early stent thrombosis (D'Ascenzo et al., 2013), 0.5–1% for late stent thrombosis (D'Ascenzo et al., 2013) and 0.2–0.4% per year for very late stent thrombosis with second generation DES while 2% was reported with 1st generation DES (Biondi-Zoccai et al., 2006). Although stent thrombosis incidence remains low, it constitutes a significant public health issue due to the high number of implanted stents worldwide and the major consequences of thrombotic events (Gori et al., 2019). The mortality caused by stent thrombosis has been reported to be as high as 45% (Biondi-Zoccai et al., 2006). Additionally, stent thrombosis was shown to be accountable for 20% of all myocardial infarction cases following PCI (Gori et al., 2019). Four factors have been identified to influence stent thrombosis including the used device, implantation procedure, patient status, and type of lesion.

The pathophysiological response to stent implantation involves wound healing processes including thrombosis, inflammation, and remodeling (Chaabane et al., 2013). The stenting process leads to a partial or complete denudation of the endothelial cell layer, stretching of the artery, and mechanical vascular injury. This induces platelet activation and adhesion, and the deposition of fibrin on the site of injury. The activated platelets express adhesion molecules, such as P-selectin, which leads to the recruitment of inflammatory cells (Costa and Simon, 2005). The recruited platelets and leukocytes respond by releasing growth factors and cytokines that induce smooth muscle cell proliferation, migration, and deposition of extracellular matrix proteins in the intima of the artery, leading to in-stent restenosis (Chaabane et al., 2013).

Endothelial cells play an important role in protecting from thrombosis and inflammation and maintaining blood fluidity.

The release of vasoprotective and thromboresistant agents such as Nitric oxide (NO) and prostacyclin prevents platelet activation and thrombus formation. Von Willebrand factor secretion is also an important factor that modulates platelets adhesion and aggregation under shear conditions (van Hinsbergh, 2012). Additionally, the normal endothelium activates fibrinolysis through the secretion of tissue plasminogen activator; an important mechanism for the resolution of thrombi (Oliver James et al., 2005). Endothelial injury leads to a disturbed production of these protective molecules, and an increase in the expression of adhesion molecules leading to thrombosis, leukocyte recruitment and smooth muscle cell dysregulation (van Hinsbergh, 2012).

The vascular endothelium is also an important interface between the vascular wall and the blood components, and its absence leads to the exposure of the subendothelial elements. The direct interaction of the blood with the subendothelial elements might trigger platelet adhesion leading to thrombosis (Palmaz, 1992). Additionally, implanted stent strut or coating material may induce stent thrombosis (Palmaz, 1992; Jaffer et al., 2015; Georgiadou and Voudris, 2017). It has been determined that the degree of stent coverage with endothelial cells is "the most powerful histological predictor" of stent thrombosis (Finn et al., 2007; Georgiadou and Voudris, 2017). Additionally, the degree of neointima formation following mechanical injury was found to be correlated with the rate of re-endothelialization (Douglas et al., 2013). The delayed stent coverage with endothelial cells in addition to the constant fibrin deposition and inflammation are associated with late and very late stent thrombosis, and the risk is greatly increased in stents with more than 30% uncovered struts (Finn et al., 2007; Claessen et al., 2014).

The stent design and composition are of the main factors that influence stent endothelialization and endothelial cell recovery following PCI (Cornelissen and Vogt, 2019). The surface topography of the stent affects cell adhesion and alignment. It has been shown that a topography resulting in elongated and aligned cells could accelerate the development of a healthy endothelium layer (Claessen et al., 2014). Additionally, the non-physiological nature of the stent material could affect the migration and adhesion of endothelial cells and thus biocompatibility is a key factor in improving endothelialization (Van der Heiden et al., 2013). Endothelialization is also influenced by the thickness of the strut and was shown to be improved in stents with thinner struts (Cornelissen and Vogt, 2019). Additionally, the types of drugs and polymers used in the stent affect cell adhesion and proliferation. While the antiproliferative drugs used in DES reduce neointima formation and in-stent restenosis, they also delay the endothelization of the stent leading to late stent thrombosis (Finn et al., 2007). The incidence of thrombosis in BMS and DES was not shown to be different, and the polymers used in BRS were shown to induce thrombosis (Buchanan et al., 2012). To reduce the occurrence of thrombotic events, dual anti-platelet therapy (aspirin and a P2Y12 inhibitor) is given to patients following PCI (Seabra-Gomes, 2006).

Stent thrombosis and diabetes

In diabetes mellitus, patients usually present with platelet dysfunction, hyperactivity or hypo-responsiveness, increasing their risk of stent thrombosis (Yuan and Xu, 2018). Additionally, the vascular endothelium is dysfunctional in response to hyperglycemia, and the proliferation and wound healing responses are impaired in this subgroup of patients (Triggle et al., 2020). Hyperglycemia results in the impairment of endothelial cells, reducing the generation of the vasodilator NO, thus favoring a vasoconstrictive state through the increase in vasoconstrictors and pro-thrombotic mediators, endothelin-1 (ET-1) and thromboxane A2 (TXA2). This imbalance disturbs the vascular tone and results in an increase in smooth muscle proliferation and migration, accompanied by an increased secretion of inflammatory cytokines and prothrombotic factors. The reduction in NO, and the increase of ET-1 and TXA2 induces platelet activation and thrombosis with the potential contribution of an elevated generation of prostacyclin that activates TXA2 receptors (Beckman et al., 2002; Seabra-Gomes, 2006; Vanhoutte and Tang, 2008). These conditions promote thrombus formation (Figure 1A). The incidence of stent thrombosis in patients with diabetes was found to be double that for patients without diabetes (Wiviott et al., 2008). Additionally, insulin was found to play a major role in influencing thrombosis. The chronic activation of endothelial cells by insulin might affect the production of vasoprotective and antithrombotic factors, activating a prothrombotic and proinflammatory status (Wu and Thiagarajan, 1996; Angiolillo et al., 2005). The prothrombotic status in these patients decreases their response to anti-platelet agents. The dysfunctional platelets in patients with diabetes are less sensitive to aspirin increasing their risk of ischemic events (Gum et al., 2003; Watala et al., 2004; Angiolillo et al., 2005). There is also evidence of the negative effect of the common anti-diabetes drug, metformin, on endothelial proliferation on stents releasing mTOR inhibitors, as was shown *in vitro* and in rabbit model (Habib et al., 2013a; Habib et al., 2013b). In terms of the time of occurrence, a meta-analysis of stent thrombosis in patients with and without diabetes have shown that both subgroups had a similar rate of early stent thrombosis following PCI with DES, however, diabetes was associated with an increase in the incidence of late stent thrombosis (Yuan and Xu, 2018).

Given the important role of the endothelium in the protection from thrombosis, re-endothelialization is a key therapeutic target to improve the outcomes of stent implantation in patients with diabetes, and to maintain an antithrombotic and anti-inflammatory status at the site of implantation (Douglas et al.,

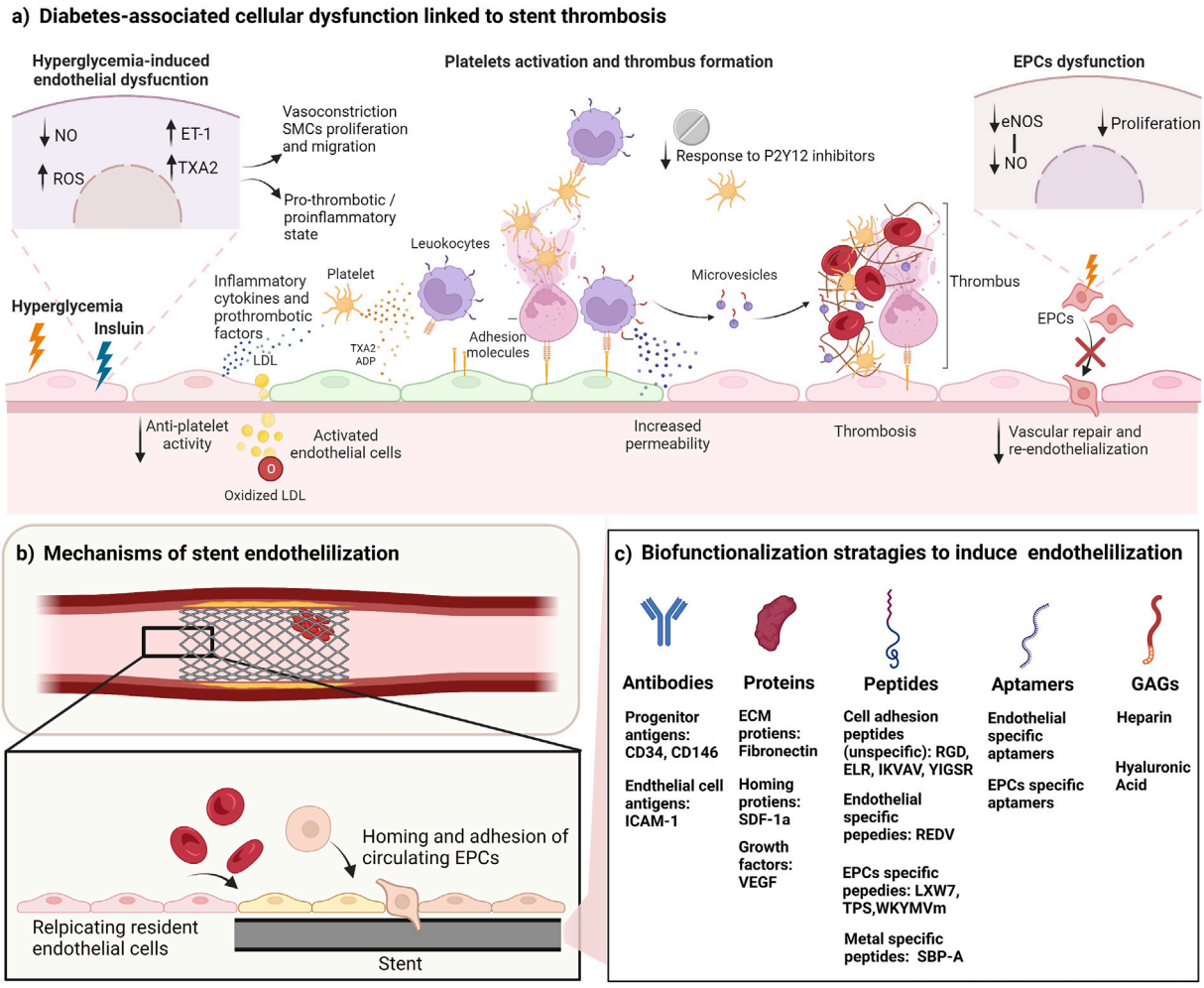

FIGURE 1
Biofunctionalization of stents to improve endothelialization and reduce thrombosis. **(A)** Cellular dysfunction in diabetes leads to high risk of stent thrombosis. Hyperglycemia results in vascular dysfunction characterized by reduced generation of NO, and induced synthesis of ET-1 and TXA2, resulting in a proinflammatory, pro-thrombotic and vasoconstrictive state. In addition, the chronic activation of endothelial cells by insulin affects the production of vasoprotective and antithrombotic factors. Diabetes also causes platelet hyperactivity, and hypo-responsiveness to anti-platelets drugs. Activated platelets bind to the vascular endothelium directly through adhesion molecules and stimulate an inflammatory response. Platelets also deposit chemokines into the surface of endothelial cells leading to leukocyte recruitment, and platelets can bind to leukocytes that adhere to the endothelial layer. Platelets also can influence endothelial cells by their secretion of vasoactive molecules (such as ADP, serotonin and TXA2) from their granules. The regenerative mechanisms by EPCs are also impaired due to EPCs dysfunction characterized by reduced EPC proliferation, and impaired eNOS and NO production. **(B)** Endothelialization of stents can reduce stent thrombosis. Stent endothelialization happens through 2 mechanisms: resident cell replication and EPC recruitment. Both mechanisms are impaired in diabetes. Targeting these mechanisms can enhance the endothelialization rate. **(C)** Biofunctionalization strategies to promote stent endothelialization. Surface biofunctionalization with mimicry factors aims to induce EPCs mobilization, capture, adhesion, and proliferation. Some of the listed factors also induce the proliferation of resident endothelial cells. NO, nitric oxide; eNOS, endothelial nitric oxide synthase; ROS, reactive oxygen species; TAX2, thromboxane A2; ET-1, endothelin-1; ADP, Adenosine diphosphate; LDL, low density lipoprotein; SMCs, smooth muscle cells; EPCs, endothelial progenitor cells; ICAM-1, intercellular adhesion molecule 1; ECM, extracellular matrix; SDF-1a, stromal cell-derived factor 1; VEGF, vascular endothelial growth factor; GAGs, glycosaminoglycans. Figure was created by BioRender.com.

2013). The gradual endothelialization of stents protects from the thrombotic events, however, this process is slow in BMS, and the drugs used in DES inhibit endothelial cell proliferation and complete coverage. Thus, there is a need for a modulation in the composition of the stents to induce rapid endothelial cell adhesion and proliferation and full stent coverage soon after implantation.

Stent biofunctionalization to induce endothelialization with circulating endothelial progenitor cells

Endothelialization of stents happens through two main mechanisms: (I) the proliferation and migration of the

resident cells at the site of injury, and (II) the homing and adhesion of circulating endothelial progenitor cells (EPCs) (Ong et al., 2005) (Figure 1B). Mature endothelial cells have a low proliferation and replication capacity, thus their participation in the endothelialization process is slow and limited. It is hypothesized that EPCs play a major role in the endothelialization process. EPCs are progenitors that circulate in the blood and have the ability to differentiate to mature endothelial cells and to participate in angiogenesis and neovascularization processes (Medina et al., 2017). Since their discovery by Asahara et al. (1997) in 1997, many attempts have been made to isolate EPCs using varying methods, which resulted in the identification of multiple cell populations that have been categorized under the EPC terminology (Medina et al., 2017). The main identified sub-populations are early EPCs (expressing CD31, CD45 and CD14, and lack expression of CD133) and late EPCs (expressing CD34, CD31 and CD133 and lack expression of the hematopoietic markers CD45, CD14, and CD115) (Tura et al., 2013; O'Neill TJtWamhoff et al., 2005; Zentilin et al., 2006). The late EPCs have been recently recognized to be the "true EPCs" due to their ability to differentiate into a stable mature endothelial phenotype, and to participate directly in the neovascularization process by incorporating into the vasculature (Yoder et al., 2007; Medina et al., 2010a; Keighron et al., 2018). A recent study used single-cell RNA-sequencing analysis (scRNA-seq) to identify specific markers in late EPCs, and found that this subpopulation expressed high levels of bone morphogenetic protein 2 and 4 (BMP 2 and 4) and ephrin B2 (EFNB2) when compared to other types of endothelial cells (Abdelgawad et al., 2021). BMP 2 and 4 were also found to be selectively expressed by late, but not, early EPCs, and to regulate EPC commitment and angiogenic potential (Smadja et al., 2008). Late EPCs and HUVECs share high expression of neuropilin 1 (NRP1) and Vascular endothelial growth factor (VEGF-C) (Abdelgawad et al., 2021), both important factors for the differentiation of endothelial precursors (Cimato et al., 2009; Zhang et al., 2019; Abdelgawad et al., 2021). This expression pattern could be used for the identification and differentiation between subpopulations of EPCs. We refer the reader to these reviews on the detailed differences between these subtypes and their therapeutic potential in many settings including diabetes (Medina et al., 2010b; Yoder, 2012; Pelliccia et al., 2022a; Triggle et al., 2022a).

Biofunctionalization of blood contacting implants and stents using attracting molecules (such as antibodies, proteins, glycosaminoglycan (GAGs), peptides and aptamers) have been proposed to induce endothelialization (Figure 1C). Other delivery approaches have been investigated such as nanoparticles and magnetic molecules. These modifications provide mimicry factors that aim to induce cell capture, adhesion, and proliferation of endothelial progenitors and/or influence their mobilization, taking advantage of their ability to migrate to the site of injury during vascular repair processes. Table 1 summarized some of the recent studies investigating the use of these factors to induce stent endothelialization. We also refer the reader to a comprehensive review on the chemistry aspect of biofunctionalization to incorporate these molecules into the surfaces of medical devices (Spicer et al., 2018).

To this date, the main clinically applied biofunctionalization strategy to induce EPCs capture and stent endothelization is the use of monoclonal antibodies against CD34, represented by the Genous™ EPC capture stent and the COMBO bio-engineered stent (OrbusNeich, Florida, United States) (Klomp et al., 2009; Tomasevic et al., 2019) (Table 1). CD34 biofunctionalized stents showed a great promise in early *in vivo* models, as they resulted in the rapid endothelialization of stents in a murine model (Kutryk and Kuliszewski, 2003). Also, early *ex-vivo* and clinical studies showed the rapid endothelialization of BMS (Larsen et al., 2012) and DES (Granada et al., 2010; Nakazawa et al., 2010), and for that it was hypothesized that these stents will protect from stent thrombosis. Despite their initial promise, recent clinical studies comparing the performance of the Genous™ EPC capture stent with DES didn't show superior results in terms of their protection from lumen loss and restenosis. Studies including the TRIAS-HR (71), HEALING and HEALING II (Duckers et al., 2007) showed that the Genous stent was associated with a trend towards increase in target vessel failure. In light of these findings, it was thought that combining the CD34 capture antibody with an anti-proliferative drug will improve these outcomes, thus the novel COMBO bio-engineered stent was developed.

The COMBO bio-engineered stent (OrbusNeich, Florida, United States), is a new generation DES which contains a sirolimus-releasing resorbable polymer matrix to reduce restenosis, in addition to the CD34 coating to induce endothelization. Although comparative clinical trials have shown that COMBO stents were non-inferior to other DESs including TaxusLiberte™ (REMEDEE randomized study) (Haude et al., 2013), and Xience™ (HARMONEE randomized study) (Saito et al., 2018), the COMBO stents were associated with a trend towards increase in the rates of target vessel failure at 12 months (Saito et al., 2018; Jakobsen et al., 2021). Additionally, a recent systematic review including a total of 3961 patients and comparing the COMBO EPC-capturing DES against standard DES from 4 randomized controlled trials, showed no difference in 1-year cardiac death when compared to standard DESs. However, COMBO stent was associated with higher rates of target lesion revascularization and target vessel failure (Pelliccia et al., 2022b). Thus the benefit of these stents in inducing rapid endothelization should be weighed against the possible risk of induced hyperplastic reactions and their consequences (Pelliccia et al., 2022b).

The use of CD34 antibody to capture EPCs has also been proposed for other medical devices, vascular grafts and tissue engineering scaffolds. Nevertheless, because CD34 is not specific

TABLE 1 Summary of the recent studies investigating the use of biomolecules to induce stent endothelialization.

	Stent type/ Material	Bioactive molecule	Biofunctionalization strategy	Outcomes	References
Clinical studies	Genous™ EPC capture stent (OrbusNeich, Florida, United States), stainless steel 316L	Murine monoclonal Anti-human CD34+ antibody	Covalently coupled poly-saccharide intermediate matrix coating, immobilized with anti-human CD34+ antibodies.	- Anti CD34 coated stents resulted in rapid endothelialization of stents in murine model (Kutryk and Kuliszewski, 2003). - Clinical studies: TRIAS-HR (Klomp et al., 2011), HEALING (Aoki et al., 2005) and HEALING II (Henricus Eric et al., 2007) showed that the Genous stent was associated with a trend towards increase in target vessel failure. HEALING IIB showed that although statins induced EPC recruitment, combining statin therapy with Genous stent didn't reduced in-stent restenosis.	(Kutryk and Kuliszewski, 2003; Klomp et al., 2011; Henricus Eric et al., 2007; Klomp et al., 2011; Aoki et al., 2005)
	COMBO bio-engineered stent (OrbusNeich, Florida, United States), stainless steel 316L	Sirolimus and murine monoclonal Anti-human CD34+ antibody	Sirolimus-releasing resorbable polymer matrix (SynBiosys™ urethane-linked multi-block copolymer composed of lactide/ glycolide/ caprolactone/ polyethylenglycol (PEG)) combined with anti CD34+ antibodies.	- COMBO stents were non-inferior to TaxusLiberte™ (REMEDEE randomized study) (Haude et al., 2013), and Xience™ (HARMONEE randomized study) (Saito et al., 2018) - Associated with a trend towards increase in the rates of target vessel failure at 12 months (Saito et al., 2018; Jakobsen et al., 2021). - No difference in 1-year cardiac death when compared to standard DESs. Showed higher rates of target lesion revascularization and target vessel failure (Pelliccia et al., 2022).	(Haude et al., 2013; Saito et al., 2018; Jakobsen et al., 2021; Pelliccia et al., 2022)
	Cobra PzF stent (CeloNova BioSiences, San Antonio, Texas), Cobalt chromium (CoCr)	Fluorinated Polyzene-F (PzF) polymer	Coated with a thin nano-layer of fluorinated Polyzene-F (PzF) polymer, and a layer of poly (bis [trifluoroethoxy]phosphazene).	- PzF previously showed reduced intimal hyperplasia, anti- thrombotic, and anti-inflammatory properties (Koppara et al., 2016) and had superior healing when compared to bioabsorbable polymer DES in porcine and rabbit models (Hiroyuki et al., 2019). - Clinical studies: 1-year follow up showed that the stent performance is satisfactory and confirmed clinical efficacy and safety (Maillard et al., 2021). - 5 years follow up showed low incidence of major adverse clinical events, with no reported stent thrombosis throughout the 5 years. Target vessel failure increased form 11.5% at 9 months to 17.4% at 5 years (Cutlip et al., 2022).	(Koppara et al., 2016; Hiroyuki et al., 2019; Maillard et al., 2021; Cutlip et al., 2022; Cornelissen et al., 2022)
In vivo studies	CoCr	A homing peptide for endothelial colony forming cell (WKYMVm)	Stents were coated with dopamine, and the peptide was conjugated to dopamine using N-hydroxysuccinimide (NHS) and 1-Ethyl-3-(3-dimethylaminopropyl) carbodiimide (EDC) to activate the carboxyl group of the peptide.	- *In vitro:* The modified stent improved the proliferation of HUVECs at day 7 of culture in comparison to BMS. - *In vivo:* peptide delivery to vessels was studied in rabbit iliac arteries, and peptide coating was observed up to 7 days, and diminished gradually.	(Bae et al., 2020)
	Stainless Steel	Murine monoclonal antihuman endoglin antibody	Commercially available stents: murine monoclonal antihuman endoglin antibody (ENDs) (Beijing Lepu Medical Technology limited corporation, China), in comparison to sirolimus eluting stents (SESs) (Johnson & Johnson, United States), and BMS (Abbott, United States).	Animal model: juvenile pigs. Findings: Mean neointima area and percent area stenosis were lower in ENDs and SESs when compared to BMSs at 14 days of implantation. Endothelial coverage of ENDs was significantly higher than that of SESs and BMSs at days 7 and 14, indicating induced endothelialization.	(Cui et al., 2014)
			Stainless steel stents coated with murine monoclonal ENDs and CD34s (Beijing Lepu Medical Technology limited corporation, China), and SESs (Johnson & Johnson, United States).	Animal model: pigs. Findings: mean neointima area and ENDs, SESs and CD34s were lower in ENDs, SESs and CD34s when compared to DES at day 14 of implantation. Endothelial coverage was induced in ENDs and CD34 when compared to SESs and BMSs at days 7 and 14.	(Cui et al., 2015)
	CoCr	Anti CD146 antibody and silicone (si) nanofilaments	Polished surfaces were coated with si nanofilments. Surfaces were treated with O2 plasma, followed by immersion in toluene dissolved in 3-aminopropyltriethoxysilane (APTES) to introduce amine groups. Antibodies were immobilized in the presence EDC and NHS.	- *In vitro*: both si nanofilaments and CD146 induced EPCs and MSCs capture under dynamic conditions (15 dyne/cm^2) in a perfusion pump system. Cell adhesion and spreading was improved on modified surfaces. - *In vivo*: stents were implanted into porcine coronary arteries for 1 week, and showed enhanced endothelial coverage in stents coated with both si nanofilaments and CD146 antibody. The modified stents reduced restenosis when compared to BMS.	(Park et al., 2020)
	Stainless steel 316L	Recombinant antibody fragments (scFv) specific for vascular endothelial growth factor receptor-2 (VEGFR2)	Surfaces were coated with titanium precursor followed by functionalization with amino groups and immobilization of oxidized glycosylated scFv molecules.	- *In vitro*: The modification didn't affect the metabolic activity or induce cytotoxicity of HUVECs. Adhesion of HUVECs was increased on VEGFR2 scFv surfaces. - *In vivo*: stents were implanted into porcine arteries for 5 and 30-days. There was no evidence of restenosis, thrombosis, or myocardial infarction at both time points. Stent coverage was significantly higher in modified stents when compared to BMS at 5 days. No significant difference was detected at 30 days. Histological sections showed coverage with a cell layer (80 μm) by day 30.	(Wawrzyńska et al., 2020)
	Nitinol	RGD peptide and CXCL1	Stents were coated with star-shaped polyethylenglycole (PEG), followed by immobilization of RGD alone or RGD/CXCL1.	- *In vitro*: increased adhesion of EOC and HUVEC to RGD and RGD/CXCL1 surfaces compared to BMS and star-PEG modified surfaces. Smooth muscle cells (SMCs) proliferation was not affected in RGD/CXCL1 and was reduced in star-PEG surfaces. - *In vivo*: stents were implanted in apoE-/- mice for one week, and showed reduced stenosis and thrombosis in	(Simsekyilmaz et al., 2016)

(Continued on following page)

TABLE 1 (*Continued*) Summary of the recent studies investigating the use of biomolecules to induce stent endothelialization.

	Stent type/ Material	Bioactive molecule	Biofunctionalization strategy	Outcomes	References
				RGD and RGD/CXCL1 stents. Star-PEG stents resulted in induced thrombosis. Endothelialization was increased in RGD/CXCL1 stents.	
	Stainless Steel	Vascular endothelial cadherin (VE-Cad) antibody	VE-Cad antibodies were immobilized on stainless steal stents grafted with sulfonamide zwitterionic and acrylic acid.	- *In vitro:* the modified stent with the co-polymer didn't cause blood cell or platelet adhesion or activation. Stents containing VE-Cad antibody resulted in induced EPCs adhesion and coverage, while small numbers were adhered to BMS and stents with the co-polymer alone. - *In vivo*: stents were implanted into rabbit carotid artery, and showed no signs of thrombosis or stenosis following 1 month of implantation. Modified stents were completely covered with endothelial cells.	(Chen et al., 2017)
	Titanium (Ti)	heparin/poly L-lysine nanoparticles	The nanoparticles were immobilized into dopamine coated Ti surfaces. Ti disks were coated with dopamine (2 mg/ml in Tris buffer, pH 8.5) for 12 h, followed by sonication in water. The process was repeated three times to coat with three layers, followed by incubation with nanoparticle suspension at 37°C for 24 h.	Ti modified samples were implanted into dog femoral arteries for 4 weeks. Ti surfaces showed severe thrombus formation and thick neo-intimal formation, whereas Ti modified surfaces showed no thrombosis or neointimal thickening. The Ti modified surfaces were also covered with a confluent layer of endothelial cells.	(Liu et al., 2014)
	Stainless Steel	Vildagliptin	Electrospinning of poly (D,L)-lactide-co-glycolide (PLGA), in combination with vildagliptin (240 mg/ 40 mg or 260 mg/20 mg) and hexafluoro isopropanol (HFIP). The nanofibrous sheets were mounted on commercially available BMSs (Gazelle BMS, Biosensors International, Switzerland) followed by vacuum drying.	- *In vitro:* Migration of HUVECs in transwells was enhanced in presence of vildagliptin eluents. - *In vivo: P*ure PLGA stents and vildagliptin eluting stents (low and high dose loading) were implanted into mechanically-denuded abdominal aorta of alloxan-induced-diabetic rabbits. Vildagliptin stents resulted in superior coverage with endothelial cells following 2 months of implantation when compared to pure PLGA stents. Nanofibrous stents induced the alignment of cells and insured cell-cell contact, unlike the pure PGLA stents. Endothelium- dependent vasodilation response to acetylcholine was higher in vildagliptin stents.	(Lee et al., 2019)
In vitro studies	CoCr	Elastin-like recombinamers (ELR) genetically modified with an REDV sequence	Plasma activation and etching using sodium hydroxide (NaOH) followed by silanization with 3-chloropropyltriethoxysilane and functionalized with the ELR	HUVEC cell adhesion response time was directly correlated to the amount of immobilized ELR on the surface. Surfaces activated with NaOH showed better adhesion and spreading of HUVECs.	(Castellanos et al., 2015)
	Stainless Steel 316L	Phage identified SUS316L-binding peptide (SBP-A, VQHNTKYSVVIR), followed by anti ICAM-1 antibody modification	The SBP-A peptide was used as a linker to immobilize ICAM-1 antibody. N-terminal streptavidin-modified anti-ICAM antibody was added to SBP-A-modified SUS316L disks.	The identified peptide (SBP-A) was not toxic to HUVECs. The described modification with SBP-A and anti ICAM-1 antibody influenced HUVECs adhesion and showed higher selectivity to HUVECs over SMCs.	(Sakaguchi-Mikami et al., 2020)
	CoCr	Endothelial specific oligonucleotide: 5' -GGG AGC TCA GAA TAA ACG CTC AAC AAC CCG TCA ACG AAC CGG AGT GTG GCA GGT TCG ACA TGA GGC CCG GAT C-3'	Aminosilanization using (3-Aminopropyl) triethoxysilane (APTES), followed by immobilization of of 3'-thiol modified oligonucliotide.	Porcine EPCs showed enhanced adhesion to modified surfaces and were able to proliferate and reached confluence in 4 days of culture.	(Barsotti et al., 2015)
	Ti	Ti oxide (TiO_2) nanotubes and fibronectin	TiO_2 surfaces were anodized to create TiO_2 nanotubes. Fibronectin was immobilized on TiO_2 nanotubes using polydopamine	Fibronectin functionalized TiO_2 nanotubes enhanced the adhesion, spreading, proliferation and secretion of nitric oxide and prostacyclin in HUVECs. The nanotube size had an inverse relationship with cytocompatibility.	(Jin et al., 2018)
	Ti	Ti nanotubes	Anodic oxidation	Ti nanotubes induced VEGF production by macrophages. Also, they inhibited glycolysis of macrophages by activating AMPK signaling, leading to reduced macrophage release of inflammatory factors and induced polarization, accelerating endothelialization.	(Yu et al., 2021)
	Nitinol	Semi-interpenetrating network (IPN) hydrogel consisting of Polyacrylamide (PAAm), polymethyl methacrylate (PMMA), polyurethane and polydopamine	Cast molding of stents in semi IPN hydrogel through free radical polymerization	Induced adhesion, proliferation, and migration of HUVECs. Reduced adhesion and proliferation of SMCs.	(Obiweluozor et al., 2019)
	Stainless steel 316L	Recombinant antibody fragments (scFv)	Incorporating hydroxyl groups through coating with titania, followed by silanization using APTES, and immobilization of glycosylated scFv.	The modification was nontoxic to the EPC line 55.1 (HucPEC-55.1) and maintained their viability on modified steal.	(Foerster et al., 2016)
	bio-absorbable magnesium alloy MgZnYNd	Arginine-leucine based poly (ester urea urethane)s (Arg-Leu-PEUUs) in comparison to poly (glycolide-co-lactide) (PLGA) coating	Spinning coating of disks with the polymers (Arg-Leu-PEUU in N,N-Dimethylformamide (DMF) or PLGA in Dichloromethane CH_2Cl_2) followed by solvent evaporation and heating.	Enhanced HUVECs viability, which was proportionally related to Arg ratio. HUVECs increased NO production. Viability of SMCs was not affected by the peptide.	(Liu et al., 2017; Liu et al., 2017)
	Ti	Heparin-VEGF-fibronectin	Layer-by-layer coating	The modification resulted in reduced platelet adhesion and aggregation and prolonged partial thrombin and prothrombin time, compared to unmodified Ti. HUVECs adhesion and proliferation were induced on modified surfaces	(Wang et al., 2013)
	PEG-diacrylate (PEGDA) hydrogel	REDV-containing peptides	Peptides that target α4β1 and α5β1 were coupled to PEGDA hydrogel using these combinations: RGDS+ REDV CRRETAWAC(cyclic)+REDV, P_RGDS+ KSSP_REDV, P_RGDS+ P_RDEV P_RGDS+ P_REDV	CRRETAWAC(cyclic)+REDV, P_RGDS+KSSP_REDV, and P_RGDS+P_REDV induced late EPCs capture under dynamic conditions in a parallel plate flow chamber system at 20 s^{-1}, and resulted in high tether percentages and velocity fluctuation	(Tian et al., 2022)

to EPCs, it has been suggested that other CD34 positive cells in the blood will compete with EPCs to adhere to the immobilized antibody (Sidney et al., 2014). This could be a contributing factor to the hyperplasia observed in the CD34 biofunctionalized stents. The use of other antibodies against CD133, and VE-Cadherin, amongst other antigens, have been reported to influence EPCs capture, however these stents have met mixed success *in vivo* (Sedaghat et al., 2013; Van der Heiden et al., 2013). Therefore, there is a need to incorporate other specific bioactive moieties to induce the specific recruitment of EPCs without inducing hyperplasia and restenosis.

Other EPC capturing strategies have been investigated *in vitro* and *in vivo,* however these approaches are yet to be validated and translated to clinical use (Table 1 respectively). Growth factors such as vascular endothelial growth factor (VEGF) have been used to induce EPCs adhesion and growth (Van der Heiden et al., 2013). Mobilization of stem cells using chemokines such as stromal cell derived factor 1a (SDF-1a) have also been investigated (Zhang et al., 2011). However, these factors are not specific to EPCs and might result in similar outcomes to what has been observed in CD34 coated stents.

A more specific approach to capture EPCs is the use of specific short peptide ligands and aptamers. These ligands provide an advantage over large biomolecules, because controlling the configuration and folding of large biomolecules is challenging during the biofunctionalization process. The literature describes the use of peptides with different specificities: (i) metal-binding peptides, (ii) non-specific cell adhesion peptides, (iii) endothelial cell-specific peptides and (iv) EPC-specific peptides. Metal-binding peptides are used as linkers to allow further modifications of the stent surface. Examples include the stainless-steel specific peptide SBP-A (Sakaguchi-Mikami et al., 2020).

One of the commonly used peptides that has shown enhanced cell biocompatibility is RGD (Arginyl-glycyl-aspartic acid) peptide, which is the principle ligand responsible for cell binding to the ECM (Bellis, 2011). Other peptides have been investigated such as the laminin derived sequences IKVAV (isoleucine-lysine-valine-alanine-valine) and YIGSR (Tyrosine-Isoleucine-Glycine-Serine-Arginine) (Massia and Hubbell, 1991; Grant et al., 1992). These peptides enhance the non-specific adhesion of cells to biofunctionalized surfaces. Peptides targeting endothelial cells have also been investigated, including REDV (Arginine-Glutamate-Aspartate-Valine) (Hubbell et al., 1991). Specific peptides to EPCs have been identified such as the disulfide cyclic octa-peptide (cGRGDdvc, also known as LXW7) (Hao et al., 2017), TPS (Threonine-Proline-Serine-Leucine-Glutamate-Glutamine-Arginine-Threonine-Valine-Tyrosine-Alanine-Lysine) (Veleva et al., 2007), and WKYMVm (Trp-Lys-Tyr-Met-Val-D-Met) (Bae et al., 2020a). These peptides interact with the integrins -which are adhesion receptors on the cells - and activate them, resulting in enhanced cell adhesion and binding. EPCs specific aptamers or oligonucleotides have been also tested (Barsotti et al., 2015). These bioactive molecules hold a great promise for the biofunctionalization of stents due to their specificity and ease of incorporation.

Challenges facing stent endothelialization with EPCs

One of the main challenges facing the *in situ* endothelialization with circulating EPCs is their low numbers in the blood (Yoder, 2012). These numbers were also shown to be reduced in disease states such as diabetes. Thus, strategies to boost the numbers of EPCs might be required. One example is the use of pharmacological induction using agents with known effects on EPCs such as statins. It was observed during the HEALING IIB study that statin therapy has increased the numbers of EPCs by 5.6-fold, and that the combination of statin therapy with EPC capturing stents resulted in optimal coverage of the stents (den Dekker et al., 2011). EPCs numbers could be boosted by other strategies such as combining more than one capturing molecule or incorporating chemokine or growth-factor-releasing nanoparticles within the coating of the stent. Additionally, local or systematic injection of autologous EPCs could help to boost the endothelialization of the stent.

Another limitation of stent endothelialization with EPCs is the variability in the intrinsic regenerative potential between patients, which might be affected by diabetes, cardiovascular diseases or other comorbidities (Emmert and Hoerstrup, 2016). This is important to consider particularly because the whole concept of *in situ* endothelialization depends on the intrinsic regenerative potential, and any impairment of this potential will affect the rate of endothelialization (Stassen et al., 2017). It was shown that EPCs function and regenerative ability is impaired in diabetes (Triggle et al., 2022b). This, in addition to vascular endothelial dysfunction, reduces the potential of stent coverage. Thus, enhancing endothelial and EPC function in these patients should be a target to improve endothelialization, in combination with stent biofunctionalization. Antidiabetic drugs with endothelial and cardioprotective effects (such as vildagliptin) (Lee et al., 2019) could be investigated in combination with the biofunctionalized stents.

In conclusion, stent endothelialization represents a potential target to reduce in-stent thrombosis following PCI. Specific biofunctionalization of stents is required to induce endothelialization without evoking restenosis. Targeting EPC and endothelial dysfunction in diabetes are key strategies to aid in the endothelialization process.

Author contributions

IM and CT developed the theoretical framework of the manuscript. IM wrote the manuscript. IM, CT, and BA-S reviewed and edited the manuscript.

Funding

This work was made possible by an Early Career Researcher Award ECRA02-007-3-006 from the Qatar National Research Fund (a member of The Qatar Foundation). IM is supported by the L'Oréal-UNESCO For Women in Science Young Talents Program/Middle East, 2020. The statements made herein are solely the responsibility of the authors. BA-S is funded by the British Heart Foundation Imperial Centre of Research Excellence Award—RE/18/4/34215.

Acknowledgments

Figure 1 was created using BioRender.com.

Conflict of interest

The authors declare that the research was conducted in the absence of any commercial or financial relationships that could be construed as a potential conflict of interest.

Publisher's note

All claims expressed in this article are solely those of the authors and do not necessarily represent those of their affiliated organizations, or those of the publisher, the editors and the reviewers. Any product that may be evaluated in this article, or claim that may be made by its manufacturer, is not guaranteed or endorsed by the publisher.

References

Abdelgawad, M. E., Desterke, C., Uzan, G., and Naserian, S. (2021). Single-cell transcriptomic profiling and characterization of endothelial progenitor cells: new approach for finding novel markers. *Stem Cell Res. Ther.* 12 (1), 145. doi:10.1186/s13287-021-02185-0

Angiolillo, D. J., Fernandez-Ortiz, A., Bernardo, E., Ramirez, C., Sabate, M., Jimenez-Quevedo, P., et al. (2005). Platelet function profiles in patients with type 2 diabetes and coronary artery disease on combined aspirin and clopidogrel treatment. *Diabetes* 54 (8), 2430–2435. doi:10.2337/diabetes.54.8.2430

Aoki, J., Serruys, P. W., van Beusekom, H., Ong, A. T., McFadden, E. P., Sianos, G., et al. (2005). Endothelial progenitor cell capture by stents coated with antibody against CD34: The HEALING-FIM (healthy endothelial accelerated lining inhibits neointimal growth-first in man) registry. *J. Am. Coll. Cardiol.* 45 (10), 1574–1579. doi:10.1016/j.jacc.2005.01.048

Asahara, T., Murohara, T., Sullivan, A., Silver, M., van der Zee, R., Li, T., et al. (1997). Isolation of putative progenitor endothelial cells for angiogenesis. *Sci. (New York, NY)* 275 (5302), 964–967. doi:10.1126/science.275.5302.964

Bae, I-H., Jeong, M. H., Park, D. S., Lim, K. S., Shim, J. W., Kim, M. K., et al. (2020). Mechanical and physio-biological properties of peptide-coated stent for re-endothelialization. *Biomater. Res.* 24, 4. doi:10.1186/s40824-020-0182-x

Bae, I-H., Jeong, M. H., Park, D. S., Lim, K. S., Shim, J. W., Kim, M. K., et al. (2020). Mechanical and physio-biological properties of peptide-coated stent for re-endothelialization. *Biomater. Res.* 24 (1), 4–9. doi:10.1186/s40824-020-0182-x

Barsotti, M. C., Al Kayal, T., Tedeschi, L., Dinucci, D., Losi, P., Sbrana, S., et al. (2015). Oligonucleotide biofunctionalization enhances endothelial progenitor cell adhesion on cobalt/chromium stents. *J. Biomed. Mat. Res. A* 103 (10), 3284–3292. doi:10.1002/jbm.a.35461

Beckman, J. A., Creager, M. A., and Libby, P. (2002). Diabetes and atherosclerosis: epidemiology, pathophysiology, and management. *JAMA* 287 (19), 2570–2581. doi:10.1001/jama.287.19.2570

Bellis, S. L. (2011). Advantages of RGD peptides for directing cell association with biomaterials. *Biomaterials* 32 (18), 4205–4210. doi:10.1016/j.biomaterials.2011.02.029

Biondi-Zoccai, G. G., Agostoni, P., Sangiorgi, G. M., Airoldi, F., Cosgrave, J., Chieffo, A., et al. (2006). Incidence, predictors, and outcomes of coronary dissections left untreated after drug-eluting stent implantation. *Eur. Heart J.* 27 (5), 540–546. doi:10.1093/eurheartj/ehi618

Bittl, J. A. (2015). Percutaneous coronary interventions in the diabetic patient: Where do we stand? *Circ. Cardiovasc. Interv.* 8 (4), e001944. doi:10.1161/CIRCINTERVENTIONS.114.001944

Borhani, S., Hassanajili, S., Ahmadi Tafti, S. H., and Rabbani, S. (2018). Cardiovascular stents: overview, evolution, and next generation. *Prog. Biomater.* 7 (3), 175–205. doi:10.1007/s40204-018-0097-y

Buchanan, G. L., Basavarajaiah, S., and Chieffo, A. (2012). Stent thrombosis: Incidence, predictors and new technologies. *Thrombosis* 2012, 956962. doi:10.1155/2012/956962

Castellanos, M. I., Zenses, A-S., Grau, A., Rodríguez-Cabello, J. C., Gil, F. J., Manero, J. M., et al. (2015). Biofunctionalization of REDV elastin-like recombinamers improves endothelialization on CoCr alloy surfaces for cardiovascular applications. *Colloids Surf. B Biointerfaces* 127, 22–32. doi:10.1016/j.colsurfb.2014.12.056

Chaabane, C., Otsuka, F., Virmani, R., and Bochaton-Piallat, M. L. (2013). Biological responses in stented arteries. *Cardiovasc. Res.* 99 (2), 353–363. doi:10.1093/cvr/cvt115

Chen, H., Wang, X., Zhou, Q., Xu, P., Liu, Y., Wan, M., et al. (2017). Preparation of vascular endothelial cadherin loaded-amphoteric copolymer decorated coronary stents for Anticoagulation and endothelialization. *Langmuir* 33 (46), 13430–13437. doi:10.1021/acs.langmuir.7b03064

Cimato, T., Beers, J., Ding, S., Ma, M., McCoy, J. P., Boehm, M., et al. (2009). Neuropilin-1 Identifies endothelial precursors in human and murine embryonic stem cells before CD34 expression. *Circulation* 119 (16), 2170–2178. doi:10.1161/CIRCULATIONAHA.109.849596

Claessen, B. E., Henriques, J. P., Jaffer, F. A., Mehran, R., Piek, J. J., and Dangas, G. D. (2014). Stent thrombosis: A clinical perspective. *JACC. Cardiovasc. Interv.* 7 (10), 1081–1092. doi:10.1016/j.jcin.2014.05.016

Cornelissen, A., Sakamoto, A., Sato, Y., Kawakami, R., Mori, M., Kawai, K., et al. (2022). COBRA PzF™ coronary stent in clinical and preclinical studies: setting the stage for new antithrombotic strategies? *Future Cardiol.* 18 (3), 207–217. doi:10.2217/fca-2021-0057

Cornelissen, A., and Vogt, F. J. (2019). The effects of stenting on coronary endothelium from a molecular biological view: time for improvement? *J. Cell. Mol. Med.* 23 (1), 39–46. doi:10.1111/jcmm.13936

Costa, M. A., and Simon, D. I. (2005). Molecular basis of restenosis and drug-eluting stents. *Circulation* 111 (17), 2257–2273. doi:10.1161/01.CIR.0000163587.36485.A7

Cui, S., Liu, J-H., Song, X-T., Ma, G-L., Du, B-J., Lv, S-Z., et al. (2014). A novel stent coated with antibodies to endoglin inhibits neointimal formation of porcine coronary arteries. *Biomed. Res. Int.* 2014, 428619. doi:10.1155/2014/428619

Cui, S., Song, X-T., Ding, C., Meng, L-J., Lv, S-Z., and Li, K. (2015). Comparison of reendothelialization and neointimal formation with stents coated with antibodies against endoglin and CD34 in a porcine model. *Drug Des. devel. Ther.* 9, 2249–2256. doi:10.2147/DDDT.S81257

Cutlip, D. E., Jauhar, R., Meraj, P., Garratt, K. N., Novack, V., Novack, L., et al. (2022). Five-year clinical outcomes of the cobra polyzene f nanocoated coronary stent system. *Cardiovasc. Revasc. Med.* 41, 76–80. doi:10.1016/j.carrev.2021.12.030

D'Ascenzo, F., Bollati, M., Clementi, F., Castagno, D., Lagerqvist, B., de la Torre Hernandez, J. M., et al. (2013). Incidence and predictors of coronary stent thrombosis: evidence from an international collaborative meta-analysis including 30 studies, 221, 066 patients, and 4276 thromboses. *Int. J. Cardiol.* 167 (2), 575–584. doi:10.1016/j.ijcard.2012.01.080

den Dekker, W. K., Houtgraaf, J. H., Onuma, Y., Benit, E., de Winter, R. J., Wijns, W., et al. (2011). Final results of the HEALING IIB trial to evaluate a bio-engineered

CD34 antibody coated stent (Genous™Stent) designed to promote vascular healing by capture of circulating endothelial progenitor cells in CAD patients. *Atherosclerosis* 219 (1), 245–252. doi:10.1016/j.atherosclerosis.2011.06.032

Douglas, G., Van Kampen, E., Hale, A. B., McNeill, E., Patel, J., Crabtree, M. J., et al. (2013). Endothelial cell repopulation after stenting determines in-stent neointima formation: Effects of bare-metal vs. drug-eluting stents and genetic endothelial cell modification. *Eur. Heart J.* 34 (43), 3378–3388. doi:10.1093/eurheartj/ehs240

Duckers, H. J., Silber, S., de Winter, R., den Heijer, P., Rensing, B., Rau, M., et al. (2007). Circulating endothelial progenitor cells predict angiographic and intravascular ultrasound outcome following percutaneous coronary interventions in the HEALING-II trial: evaluation of an endothelial progenitor cell capturing stent. *EuroIntervention* 3 (1), 67–75.

Emmert, M. Y., and Hoerstrup, S. P. (2016). Tissue engineered heart valves: moving towards clinical translation. *Expert Rev. Med. Devices* 13 (5), 417–419. doi:10.1586/17434440.2016.1171709

Finn, A. V., Joner, M., Nakazawa, G., Kolodgie, F., Newell, J., John, M. C., et al. (2007). Pathological correlates of late drug-eluting stent thrombosis: Strut coverage as a marker of endothelialization. *Circulation* 115 (18), 2435–2441. doi:10.1161/CIRCULATIONAHA.107.693739

Foerster, A., Hołowacz, I., Sunil Kumar, G., Anandakumar, S., Wall, J., Wawrzyńska, M., et al. (2016). Stainless steel surface functionalization for immobilization of antibody fragments for cardiovascular applications. *J. Biomed. Mat. Res. A* 104 (4), 821–832. doi:10.1002/jbm.a.35616

Garcia-Garcia, H. M., McFadden, E. P., Farb, A., Mehran, R., Stone, G. W., Spertus, J., et al. (2018). Standardized end point definitions for coronary intervention trials: the academic research consortium-2 consensus document. *Circulation* 137 (24), 2635–2650. doi:10.1161/CIRCULATIONAHA.117.029289

Garcia-Garcia, H. M., Vaina, S., Tsuchida, K., and Serruys, P. W. (2006). Drug-eluting stents. *Arch. Cardiol. Mex.* 76 (3), 297–319.

Georgiadou, P., and Voudris, V. (2017). Platelet activation and stent thrombosis. *Hell. J. Cardiol.* 58 (1), 49–50. doi:10.1016/j.hjc.2017.03.013

Gori, T., Polimeni, A., Indolfi, C., Räber, L., Adriaenssens, T., and Münzel, T. (2019). Predictors of stent thrombosis and their implications for clinical practice. *Nat. Rev. Cardiol.* 16 (4), 243–256. doi:10.1038/s41569-018-0118-5

Granada, J. F., Inami, S., Aboodi, M. S., Tellez, A., Milewski, K., Wallace-Bradley, D., et al. (2010). Development of a novel prohealing stent designed to deliver sirolimus from a biodegradable abluminal matrix. *Circ. Cardiovasc. Interv.* 3 (3), 257–266. doi:10.1161/CIRCINTERVENTIONS.109.919936

Grant, D. S., Kinsella, J. L., Fridman, R., Auerbach, R., Piasecki, B. A., Yamada, Y., et al. (1992). Interaction of endothelial cells with a laminin A chain peptide (SIKVAV) *in vitro* and induction of angiogenic behavior *in vivo*. *J. Cell. Physiol.* 153 (3), 614–625. doi:10.1002/jcp.1041530324

Gum, P. A., Kottke-Marchant, K., Welsh, P. A., White, J., and Topol, E. J. (2003). A prospective, blinded determination of the natural history of aspirin resistance among stable patients with cardiovascular disease. *J. Am. Coll. Cardiol.* 41 (6), 961–965. doi:10.1016/s0735-1097(02)03014-0

Habib, A., Karmali, V., Polavarapu, R., Akahori, H., Nakano, M., Yazdani, S., et al. (2013). Metformin impairs vascular endothelial recovery after stent placement in the setting of locally eluted mammalian target of rapamycin inhibitors via S6 kinase-dependent inhibition of cell proliferation. *J. Am. Coll. Cardiol.* 61 (9), 971–980. doi:10.1016/j.jacc.2012.12.018

Habib, A., Karmali, V., Polavarapu, R., Akahori, H., Pachura, K., and Finn, A. V. (2013). Metformin impairs endothelialization after placement of newer generation drug eluting stents. *Atherosclerosis* 229 (2), 385–387. doi:10.1016/j.atherosclerosis.2013.06.001

Hao, D., Xiao, W., Liu, R., Kumar, P., Li, Y., Zhou, P., et al. (2017). Discovery and characterization of a potent and specific peptide ligand targeting endothelial progenitor cells and endothelial cells for tissue regeneration. *ACS Chem. Biol.* 12 (4), 1075–1086. doi:10.1021/acschembio.7b00118

Haude, M., Lee, S. W., Worthley, S. G., Silber, S., Verheye, S., Erbs, S., et al. (2013). The REMEDEE trial: A randomized comparison of a combination sirolimus-eluting endothelial progenitor cell capture stent with a paclitaxel-eluting stent. *JACC. Cardiovasc. Interv.* 6 (4), 334–343. doi:10.1016/j.jcin.2012.10.018

Hiroyuki, J., Hiroyoshi, M., Qi, C., Matthew, K., Sho, T., Atsushi, S., et al. (2019). Thromboresistance and functional healing in the COBRA PzF stent versus competitor DES: Implications for dual antiplatelet therapy. *EuroIntervention* 15 (4), e342–e353. doi:10.4244/EIJ-D-18-00740

Hubbell, J. A., Massia, S. P., Desai, N. P., and Drumheller, P. D. (1991). Endothelial cell-selective materials for tissue engineering in the vascular graft via a new receptor. *Biotechnology.* 9 (6), 568–572. doi:10.1038/nbt0691-568

Jaffer, I. H., Fredenburgh, J. C., Hirsh, J., and Weitz, J. I. (2015). Medical device-induced thrombosis: what causes it and how can we prevent it? *J. Thromb. Haemost.* 1, s72–81. doi:10.1111/jth.12961

Jakobsen, L., Christiansen, E. H., Freeman, P., Kahlert, J., Veien, K., Maeng, M., et al. (2021). randomized clinical comparison of the dual-therapy cd34 antibody-covered sirolimus-eluting combo stent with the sirolimus-eluting orsiro stent in patients treated with percutaneous coronary intervention: the sort out x trial. *Circulation* 143 (22), 2155–2165. doi:10.1161/CIRCULATIONAHA.120.052766

Jin, Z., Yan, X., Liu, G., and Lai, M. (2018). Fibronectin modified TiO2 nanotubes modulate endothelial cell behavior. *J. Biomater. Appl.* 33 (1), 44–51. doi:10.1177/0885328218774512

Keighron, C., Lyons, C. J., Creane, M., O'Brien, T., and Liew, A. (2018). Recent advances in endothelial progenitor cells toward their use in clinical translation. *Front. Med.* 5, 354. doi:10.3389/fmed.2018.00354

Kipshidze, N., Dangas, G., Tsapenko, M., Moses, J., Leon, M. B., Kutryk, M., et al. (2004). Role of the endothelium in modulating neointimal formation: vasculoprotective approaches to attenuate restenosis after percutaneous coronary interventions. *J. Am. Coll. Cardiol.* 44 (4), 733–739. doi:10.1016/j.jacc.2004.04.048

Klomp, M., Beijk, M. A., Varma, C., Koolen, J. J., Teiger, E., Richardt, G., et al. (2011). 1-year outcome of TRIAS HR (TRI-stent adjudication study-high risk of restenosis) a multicenter, randomized trial comparing genous endothelial progenitor cell capturing stents with drug-eluting stents. *JACC. Cardiovasc. Interv.* 4 (8), 896–904. doi:10.1016/j.jcin.2011.05.011

Klomp, M., Beijk, M. A., Varma, C., Koolen, J. J., Teiger, E., Richardt, G., et al. (2011). 1-Year outcome of trias hr (tri-stent adjudication study–high risk of restenosis): a multicenter, randomized trial comparing genous endothelial progenitor cell capturing stents with drug-eluting stents. *JACC. Cardiovasc. Interv.* 4 (8), 896–904. doi:10.1016/j.jcin.2011.05.011

Klomp, M., Beijk, M. A. M., and de Winter, R. J. (2009). Genous endothelial progenitor cell-capturing stent system: A novel stent technology. *Expert Rev. Med. Devices* 6 (4), 365–375. doi:10.1586/erd.09.16

Kong, D., Melo, L. G., Mangi, A. A., Zhang, L., Lopez-Ilasaca, M., Perrella, M. A., et al. (2004). Enhanced inhibition of neointimal hyperplasia by genetically engineered endothelial progenitor cells. *Circulation* 109 (14), 1769–1775. doi:10.1161/01.CIR.0000121732.85572.6F

Koppara, T., Sakakura, K., Pacheco, E., Cheng, Q., Zhao, X., Acampado, E., et al. (2016). Preclinical evaluation of a novel polyphosphazene surface modified stent. *Int. J. Cardiol.* 222, 217–225. doi:10.1016/j.ijcard.2016.07.181

Koskinas, K. C., Siontis, G. C., Piccolo, R., Franzone, A., Haynes, A., Rat-Wirtzler, J., et al. (2016). Impact of diabetic status on outcomes after revascularization with drug-eluting stents in relation to coronary artery disease complexity: patient-level pooled analysis of 6081 patients. *Circ. Cardiovasc. Interv.* 9 (2), e003255. doi:10.1161/CIRCINTERVENTIONS.115.003255

Kutryk, .M. J., and Kuliszewski, M. (2003). In vivo *endothelial progenitor cell seeding for the accelerated endothelialization of endovascular devices*. NEW YORK, NY 10011 USA: American Journal of Cardiology; 2003: EXCERPTA MEDICA INC 650 AVENUE OF THE AMERICAS.

Larsen, K., Cheng, C., Tempel, D., Parker, S., Yazdani, S., den Dekker, W. K., et al. (2012). Capture of circulatory endothelial progenitor cells and accelerated re-endothelialization of a bio-engineered stent in human *ex vivo* shunt and rabbit denudation model. *Eur. Heart J.* 33 (1), 120–128. doi:10.1093/eurheartj/ehr196

Lee, C. H., Hsieh, M. J., Chang, S. H., Hung, K. C., Wang, C. J., Hsu, M. Y., et al. (2019). Nanofibrous vildagliptin-eluting stents enhance re-endothelialization and reduce neointimal formation in diabetes: *In vitro* and *in vivo*. *Int. J. Nanomedicine* 14, 7503–7513. doi:10.2147/IJN.S211898

Liu, J., Wang, P., Chu, C-C., and Xi, T. (2017). A novel biodegradable and biologically functional arginine-based poly (ester urea urethane) coating for Mg–Zn–Y–Nd alloy: enhancement in corrosion resistance and biocompatibility. *J. Mat. Chem. B* 5 (9), 1787–1802. doi:10.1039/c6tb03147a

Liu, J., Wang, P., Chu, C-C., and Xi, T. (2017). Arginine-leucine based poly (ester urea urethane) coating for Mg-Zn-Y-Nd alloy in cardiovascular stent applications. *Colloids Surf. B Biointerfaces* 159, 78–88. doi:10.1016/j.colsurfb.2017.07.031

Liu, T., Zeng, Z., Liu, Y., Wang, J., Maitz, M. F., Wang, Y., et al. (2014). Surface modification with dopamine and heparin/poly-l-lysine nanoparticles provides a favorable release behavior for the healing of vascular stent lesions. *ACS Appl. Mat. Interfaces* 6 (11), 8729–8743. doi:10.1021/am5015309

Lusis, A. J. (2000). Atherosclerosis. *Nature* 407 (6801), 233–241. doi:10.1038/35025203

Maillard, L., de Labriolle, A., Brasselet, C., Faurie, B., Durel, N., de Poli, F., et al. (2021). Evaluation of the safety and efficacy of the cobra pzf nanocoated coronary stent in routine, consecutive, prospective, and high-risk patients: the e-cobra study. *Catheter. Cardiovasc. Interv.* 98 (1), 45–54. doi:10.1002/ccd.29065

Massia, S. P., and Hubbell, J. A. (1991). Human endothelial cell interactions with surface-coupled adhesion peptides on a nonadhesive glass substrate and two polymeric biomaterials. *J. Biomed. Mat. Res.* 25 (2), 223–242. doi:10.1002/jbm.820250209

Meads, C., Cummins, C., Jolly, K., Stevens, A., Burls, A., and Hyde, C. (2000). Coronary artery stents in the treatment of ischaemic heart disease: A rapid and systematic review. *Health Technol. Assess.* 4 (23), 1–153. doi:10.3310/hta4230

Medina, R. J., Barber, C. L., Sabatier, F., Dignat-George, F., Melero-Martin, J. M., Khosrotehrani, K., et al. (2017). Endothelial progenitors: A consensus statement on nomenclature. *Stem Cells Transl. Med.* 6 (5), 1316–1320. doi:10.1002/sctm.16-0360

Medina, R. J., O'Neill, C. L., Sweeney, M., Guduric-Fuchs, J., Gardiner, T. A., Simpson, D. A., et al. (2010). Molecular analysis of endothelial progenitor cell (EPC) subtypes reveals two distinct cell populations with different identities. *BMC Med. Genomics* 3, 18. doi:10.1186/1755-8794-3-18

Medina, R. J., O'Neill, C. L., Sweeney, M., Guduric-Fuchs, J., Gardiner, T. A., Simpson, D. A., et al. (2010). Molecular analysis of endothelial progenitor cell (EPC) subtypes reveals two distinct cell populations with different identities. *BMC Med. Genomics* 3, 18. doi:10.1186/1755-8794-3-18

Nakazawa, G., Granada, J. F., Alviar, C. L., Tellez, A., Kaluza, G. L., Guilhermier, M. Y., et al. (2010). Anti-CD34 antibodies immobilized on the surface of sirolimus-eluting stents enhance stent endothelialization. *JACC. Cardiovasc. Interv.* 3 (1), 68–75. doi:10.1016/j.jcin.2009.09.015

O'Neill TJtWamhoff, B. R., Owens, G. K., and Skalak, T. C. (2005). Mobilization of bone marrow-derived cells enhances the angiogenic response to hypoxia without transdifferentiation into endothelial cells. *Circ. Res.* 97 (10), 1027–1035. doi:10.1161/01.RES.0000189259.69645.25

Obiweluozor, F. O., Tiwari, A. P., Lee, J. H., Batgerel, T., Kim, J. Y., Lee, D., et al. (2019). Thromboresistant semi-IPN hydrogel coating: towards improvement of the hemocompatibility/biocompatibility of metallic stent implants. *Mat. Sci. Eng. C Mat. Biol. Appl.* 99, 1274–1288. doi:10.1016/j.msec.2019.02.054

O'Brien, B., and Carroll, W. (2009). The evolution of cardiovascular stent materials and surfaces in response to clinical drivers: A review. *Acta Biomater.* 5 (4), 945–958. doi:10.1016/j.actbio.2008.11.012

Okrainec, K., Banerjee, D. K., and Eisenberg, M. J. (2004). Coronary artery disease in the developing world. *Am. Heart J.* 148 (1), 7–15. doi:10.1016/j.ahj.2003.11.027

Oliver James, J., Webb David, J., and Newby David, E. (2005). Stimulated tissue plasminogen activator release as a marker of endothelial function in humans. *Arterioscler. Thromb. Vasc. Biol.* 25 (12), 2470–2479. doi:10.1161/01.ATV.0000189309.05924.88

Ong, A. T., Aoki, J., Kutryk, M. J., and Serruys, P. W. (2005). How to accelerate the endothelialization of stents. *Arch. Mal. Coeur Vaiss.* 98 (2), 123–126.

Otsuka, F., Finn, A. V., Yazdani, S. K., Nakano, M., Kolodgie, F. D., and Virmani, R. (2012). The importance of the endothelium in atherothrombosis and coronary stenting. *Nat. Rev. Cardiol.* 9 (8), 439–453. doi:10.1038/nrcardio.2012.64

Palmaz, J. C. (1992). Intravascular stenting: From basic research to clinical application. *Cardiovasc. Interv. Radiol.* 15 (5), 279–284. doi:10.1007/BF02733951

Park, K-S., Kang, S. N., Kim, D. H., Kim, H-B., Im, K. S., Park, W., et al. (2020). Late endothelial progenitor cell-capture stents with CD146 antibody and nanostructure reduce in-stent restenosis and thrombosis. *Acta Biomater.* 111, 91–101. doi:10.1016/j.actbio.2020.05.011

Pelliccia, F., Pasceri, V., Zimarino, M., De Luca, G., De Caterina, R., Mehran, R., et al. (2022). Endothelial progenitor cells in coronary atherosclerosis and percutaneous coronary intervention: A systematic review and meta-analysis. *Cardiovasc. Revascularization Med.* 42, 94–99. doi:10.1016/j.carrev.2022.02.025

Pelliccia, F., Zimarino, M., De Luca, G., Viceconte, N., Tanzilli, G., and De Caterina, R. (2022). Endothelial progenitor cells in coronary artery disease: from bench to bedside. *Stem Cells Transl. Med.* 11 (5), 451–460. doi:10.1093/stcltm/szac010

Ross, R. (1993). The pathogenesis of atherosclerosis: A perspective for the 1990s. *Nature* 362 (6423), 801–809. doi:10.1038/362801a0

Saito, S., Krucoff, M. W., Nakamura, S., Mehran, R., Maehara, A., Al-Khalidi, H. R., et al. (2018). Japan-united states of america harmonized assessment by randomized multicentre study of orbusneich's combo stent (japan-usa harmonee) study: primary results of the pivotal registration study of combined endothelial progenitor cell capture and drug-eluting stent in patients with ischaemic coronary disease and non-st-elevation acute coronary syndrome. *Eur. Heart J.* 39 (26), 2460–2468. doi:10.1093/eurheartj/ehy275

Sakaguchi-Mikami, A., Fujimoto, K., Taguchi, T., Isao, K., and Yamazaki, T. (2020). A novel biofunctionalizing peptide for metallic alloy. *Biotechnol. Lett.* 42 (5), 747–756. doi:10.1007/s10529-020-02832-1

Scafa Udriște, A., Niculescu, A-G., Grumezescu, A. M., and Bădilă, E. (2021). Cardiovascular stents: a review of past, current, and emerging devices. *Materials* 14 (10), 2498. doi:10.3390/ma14102498

Seabra-Gomes, R. (2006). Percutaneous coronary interventions with drug eluting stents for diabetic patients. *Heart* 92 (3), 410–419. doi:10.1136/hrt.2005.062992

Sedaghat, A., Sinning, J-M., Paul, K., Kirfel, G., Nickenig, G., and Werner, N. (2013). First *in vitro* and *in vivo* results of an anti-human CD133-antibody coated coronary stent in the porcine model. *Clin. Res. Cardiol.* 102 (6), 413–425. doi:10.1007/s00392-013-0547-4

Sidney, L. E., Branch, M. J., Dunphy, S. E., Dua, H. S., and Hopkinson, A. (2014). Concise review: evidence for CD34 as a common marker for diverse progenitors. *Stem Cells* 32 (6), 1380–1389. doi:10.1002/stem.1661

Simsekyilmaz, S., Liehn, E. A., Weinandy, S., Schreiber, F., Megens, R. T., Theelen, W., et al. (2016). Targeting in-stent-stenosis with RGD- and CXCL1-coated mini-stents in mice. *PLoS One* 11 (5), e0155829. doi:10.1371/journal.pone.0155829

Smadja, D. M., Bièche, I., Silvestre, J-S., Germain, S., Cornet, A., Laurendeau, I., et al. (2008). Bone morphogenetic proteins 2 and 4 are selectively expressed by late outgrowth endothelial progenitor cells and promote neoangiogenesis. *Arterioscler. Thromb. Vasc. Biol.* 28 (12), 2137–2143. doi:10.1161/ATVBAHA.108.168815

Smith, S. C., Jr., Dove, J. T., Jacobs, A. K., Kennedy, J. W., Kereiakes, D., Kern, M. J., et al. (2001). ACC/AHA guidelines for percutaneous coronary intervention (revision of the 1993 ptca guidelines)-executive summary: a report of the american college of cardiology/american heart association task force on practice guidelines (committee to revise the 1993 guidelines for percutaneous transluminal coronary angioplasty) endorsed by the society for cardiac angiography and interventions. *Circulation* 103 (24), 3019–3041. doi:10.1161/01.cir.103.24.3019

Sousa, J. E., Serruys, P. W., and Costa, M. A. (2003). New frontiers in cardiology: drug-eluting stents: Part I. *Circulation* 107 (17), 2274–2279. doi:10.1161/01.CIR.0000069330.41022.90

Spicer, C. D., Pashuck, E. T., and Stevens, M. M. (2018). Achieving controlled biomolecule–biomaterial conjugation. *Chem. Rev.* 118 (16), 7702–7743. doi:10.1021/acs.chemrev.8b00253

Stassen, O., Muylaert, D. E. P., Bouten, C. V. C., and Hjortnaes, J. (2017). Current challenges in translating tissue-engineered heart valves. *Curr. Treat. Options Cardiovasc. Med.* 19 (9), 71. doi:10.1007/s11936-017-0566-y

Tian, Y., Seeto, W. J., Páez-Arias, M. A., Hahn, M. S., and Lipke, E. A. (2022). Endothelial colony forming cell rolling and adhesion supported by peptide-grafted hydrogels. *Acta Biomater.* S1742 7061. 00523–532. doi:10.1016/j.actbio.2022.08.047

Tomasevic, M., Rakocevic, J., Dobric, M., Aleksandric, S., and Labudovic, M. (2019). Capturing endothelial cells by coronary stents - from histology to clinical outcomes. *Serbian J. Exp. Clin. Res.* 0 (0). doi:10.2478/sjecr-2019-0018

Torii, S., Jinnouchi, H., Sakamoto, A., Kutyna, M., Cornelissen, A., Kuntz, S., et al. (2020). Drug-eluting coronary stents: Insights from preclinical and pathology studies. *Nat. Rev. Cardiol.* 17 (1), 37–51. doi:10.1038/s41569-019-0234-x

Triggle, C. R., Ding, H., Marei, I., Anderson, T. J., and Hollenberg, M. D. (2020). Why the endothelium? The endothelium as a target to reduce diabetes-associated vascular disease. *Can. J. Physiol. Pharmacol.* 98 (7), 415–430. doi:10.1139/cjpp-2019-0677

Triggle, C. R., Marei, I., Ye, K., Ding, H., Anderson, T. J., Hollenberg, M. D., et al. (2022). Repurposing metformin for vascular disease. *Curr. Med. Chem.* 29. doi:10.2174/0929867329666220729154615

Triggle, C. R., Mohammed, I., Bshesh, K., Marei, I., Ye, K., Ding, H., et al. (2022). Metformin: Is it a drug for all reasons and diseases? *Metabolism.* 133, 155223. doi:10.1016/j.metabol.2022.155223

Tura, O., (2013) Skinner Em Fau - Barclay, G. R., Barclay Gr Fau - Samuel, K., Samuel, K., Fau - Gallagher, R. C. J., Gallagher Rc Fau - Brittan, M., et al. . Late outgrowth endothelial cells resemble mature endothelial cells and are not derived from bone marrow. *Stem Cells*. 338–348.doi:10.1002/stem.1280

Van der Heiden, K., Gijsen, F. J., Narracott, A., Hsiao, S., Halliday, I., Gunn, J., et al. (2013). The effects of stenting on shear stress: relevance to endothelial injury and repair. *Cardiovasc. Res.* 99 (2), 269–275. doi:10.1093/cvr/cvt090

van Hinsbergh, V. W. M. (2012). Endothelium--role in regulation of coagulation and inflammation. *Semin. Immunopathol.* 34 (1), 93–106. doi:10.1007/s00281-011-0285-5

Vanhoutte, P. M., and Tang, E. H. (2008). Endothelium-dependent contractions: when a good guy turns bad. *J. Physiol.* 586 (22), 5295–5304. doi:10.1113/jphysiol.2008.161430

Veleva, A. N., Cooper, S. L., and Patterson, C. (2007). Selection and initial characterization of novel peptide ligands that bind specifically to human blood outgrowth endothelial cells. *Biotechnol. Bioeng.* 98 (1), 306–312. doi:10.1002/bit.21420

Wang, H., Yin, T., Ge, S., Zhang, Q., Dong, Q., Lei, D., et al. (2013). Biofunctionalization of titanium surface with multilayer films modified by heparin-VEGF-fibronectin complex to improve endothelial cell proliferation and blood compatibility. *J. Biomed. Mat. Res. A* 101 (2), 413–420. doi:10.1002/jbm.a.34339

Watala, C., Golanski, J., Pluta, J., Boncler, M., Rozalski, M., Luzak, B., et al. (2004). Reduced sensitivity of platelets from type 2 diabetic patients to acetylsalicylic acid (aspirin)-its relation to metabolic control. *Thromb. Res.* 113 (2), 101–113. doi:10.1016/j.thromres.2003.12.016

Wawrzyńska, M., Kraskiewicz, H., Paprocka, M., Krawczenko, A., Bielawska-Pohl, A., Biały, D., et al. (2020). Functionalization with a VEGFR2-binding antibody fragment leads to enhanced endothelialization of a cardiovascular stent *in vitro* and *in vivo*. *J. Biomed. Mat. Res. B Appl. Biomater.* 108 (1), 213–224. doi:10.1002/jbm.b.34380

WHO (2017). *Cardiovascular diseases (CVDs) Fact Sheet*. Turkey,United Kingdom: WHO.

Wiviott, S. D., Braunwald, E., Angiolillo, D. J., Meisel, S., Dalby, A. J., Verheugt, F. W., et al. (2008). Greater clinical benefit of more intensive oral antiplatelet therapy with prasugrel in patients with diabetes mellitus in the trial to assess improvement in therapeutic outcomes by optimizing platelet inhibition with prasugrel-thrombolysis in myocardial Infarction 38. *Circulation* 118 (16), 1626–1636. doi:10.1161/CIRCULATIONAHA.108.791061

Wu, K. K., and Thiagarajan, P. (1996). Role of endothelium in thrombosis and hemostasis. *Annu. Rev. Med.* 47 (0066-4219), 315–331. doi:10.1146/annurev.med.47.1.315

Yoder, M. C. (2012). Human endothelial progenitor cells. *Cold Spring Harb. Perspect. Med.* 2 (7), a006692. doi:10.1101/cshperspect.a006692

Yoder, M. C., Mead, L. E., Prater, D., Krier, T. R., Mroueh, K. N., Li, F., et al. (2007). Redefining endothelial progenitor cells via clonal analysis and hematopoietic stem/progenitor cell principals. *Blood* 109 (5), 1801–1809. doi:10.1182/blood-2006-08-043471

Yu, W. P., Ding, J. L., Liu, X. L., Zhu, G. D., Lin, F., Xu, J. J., et al. (2021). Titanium dioxide nanotubes promote M2 polarization by inhibiting macrophage glycolysis and ultimately accelerate endothelialization. *Immun. Inflamm. Dis.* 9 (3), 746–757. doi:10.1002/iid3.429

Yuan, J., and Xu, G. M. (2018). Early and late stent thrombosis in patients with versus without diabetes mellitus following percutaneous coronary intervention with drug-eluting stents: A systematic review and meta-analysis. *Am. J. Cardiovasc. Drugs* 18 (6), 483–492. doi:10.1007/s40256-018-0295-y

Zentilin, L., Tafuro, S., Zacchigna, S., Arsic, N., Pattarini, L., Sinigaglia, M., et al. (2006). Bone marrow mononuclear cells are recruited to the sites of VEGF-induced neovascularization but are not incorporated into the newly formed vessels. *Blood* 107 (9), 3546–3554. doi:10.1182/blood-2005-08-3215

Zhang, H-f., Wang, Y-l., Tan, Y-z., Wang, H-j., Tao, P., and Zhou, P. (2019). Enhancement of cardiac lymphangiogenesis by transplantation of CD34+VEGFR-3+ endothelial progenitor cells and sustained release of VEGF-C. *Basic Res. Cardiol.* 114 (6), 43. doi:10.1007/s00395-019-0752-z

Zhang, L., Zhu, J., Du, R., Zhu, Z., Zhang, J., Han, W., et al. (2011). Effect of recombinant human SDF-1a on re-endothelialization after sirolimus-eluting stent implantation in rabbit aorta abdominalis. *Life Sci.* 89 (25 26), 926–930. doi:10.1016/j.lfs.2011.09.020

Advantages of publishing in Frontiers

OPEN ACCESS
Articles are free to read for greatest visibility and readership

FAST PUBLICATION
Around 90 days from submission to decision

HIGH QUALITY PEER-REVIEW
Rigorous, collaborative, and constructive peer-review

TRANSPARENT PEER-REVIEW
Editors and reviewers acknowledged by name on published articles

Frontiers
Avenue du Tribunal-Fédéral 34
1005 Lausanne | Switzerland

Visit us: www.frontiersin.org
Contact us: frontiersin.org/about/contact

REPRODUCIBILITY OF RESEARCH
Support open data and methods to enhance research reproducibility

DIGITAL PUBLISHING
Articles designed for optimal readership across devices

FOLLOW US
@frontiersin

IMPACT METRICS
Advanced article metrics track visibility across digital media

EXTENSIVE PROMOTION
Marketing and promotion of impactful research

LOOP RESEARCH NETWORK
Our network increases your article's readership